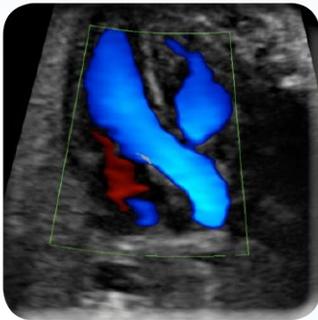# ULTRASOUND
in Obstetrics and Gynecology:
A Practical Approach

Editor
Alfred Abuhamad, MD

with contributions from
Rabih Chaoui, MD
Philippe Jeanty, MD
Dario Paladini, MD

Editorial Assistant
Emily Walsh, BA, MA

Forward by Professor John Hobbins, MD

FIRST EDITION

Ultrasound was introduced into the practice of Obstetrics and Gynecology over four decades ago, and along the way its impact has risen exponentially to a point where it is rare even for a low risk, uncomplicated, patient to make it through pregnancy without having at least two ultrasound examinations and a high risk patient to have less than four scans. Most important is the pivotal role ultrasound plays in our obstetrical decision-making and in GYN one rarely hangs one's hat on a diagnosis made by a pelvic exam alone.

While building a career in OB/GYN, residency represents, by far, the most impactful step. Recently, I asked graduating residents from around the country interested in our perinatal fellowship to rate their training in ultrasound (from 1 to 10). The average was 3. Only one of the twenty three individuals I interviewed rated their training as 9. Why? Because in resident training programs the importance of ultrasound is often downplayed in favor of other facets of the specialty, and enlightened faculty members interested in imparting ultrasound knowledge and skills are challenged by the woeful lack of resource material on the basics of obstetrical and gynecological ultrasound. Yes, students or program directors can easily find some directed texts on the fetal CNS, heart, skeletal dysplasias, and high risk pregnancy, in general, but locating a text that deals with the nitty- gritty of day-to-day scanning has been challenging. Until now!

Dr. Abuhamad and colleagues have come up with a resource that really fills the void perfectly. This text concisely covers the physics of ultrasound and how to exploit the features of today's equipment to optimize every image, while using methods to assure that the fetus is exposed to the lowest ultrasound energies. It tackles something as mundane as how to hold a transducer properly, as well as providing clever hints on how, for example, to insert the vaginal transducer into the umbilicus to better image the fetus in an obese patient. The authors outline beautifully what ultrasound will enable us to see in a normal first trimester, second trimester, and third trimester pregnancy, as well as in a non-pregnant uterus and adnexa – and they give tips along the way on how to cone in on the essential items to piece together a clinical picture. They also masterfully cover many of the common clinical surprises that a sonographer and sonologist might encounter. Most importantly, the text is embellished with some of the most beautiful ultrasound images I have seen in any textbook.

If you are an experienced sonographer or sonologist who wants a booster dose of ultrasound knowledge or a quasi-novice thrown suddenly into an ultrasound-heavy clinical practice, or ANY student wanting to learn more about OB/GYN ultrasound, this book will provide the necessary backdrop to help you become a more savvy and proficient practitioner.

I cannot wait to get this into the hands of every one of our residents and fellows.

- John C. Hobbins, MD

Alfred Abuhamad, MD

Dr. Alfred Abuhamad is Professor and Chairman of the Department of Obstetrics and Gynecology and Vice Dean for Clinical Affairs at Eastern Virginia Medical School, Norfolk, Virginia. Dr. Abuhamad is recognized internationally as a leading expert in imaging in Obstetrics & Gynecology and Fetal Echocardiography. He is the president elect of the Society of Ultrasound in Medical Education and immediate past-President of the American Institute of Ultrasound in Medicine. Dr. Abuhamad established the International Society of Ultrasound in Obstetrics and Gynecology Outreach Committee and led several ultrasound training activities in the developing world.

Emily Walsh

Emily Walsh has been working at Eastern Virginia Medical School for seven years, three of those years in the Department of Obstetrics and Gynecology. She holds a Bachelors of Arts and Masters of Arts in Communications, with a focus in Digital Media. Emily has been published in *Alberta Katherine Magazine* out of Jacksonville, Florida and was a contributing writer for Regent University's *The Daily Runner*. Emily is also the Co-Founder of LE Literary Services, which offers publishing and editorial assistance to authors.

Rabih Chaoui, MD

Dr. Rabih Chaoui is Co-Director of the Center of Prenatal Diagnosis and Human Genetics in Berlin, Germany. A leading international authority on fetal imaging, Dr. Chaoui has contributed extensively to the literature in obstetrical imaging and fetal echocardiography and played a major role in ultrasound education globally as the chairman of the International Society of Ultrasound in Obstetrics and Gynecology's Education Committee from 2009 - 2013.

Philippe Jeanty, MD

Dr. Philippe Jeanty is a world renowned radiologist with extensive expertise in women's imaging. He has published extensively and authored several books in ultrasound. He is the founder of The Fetus.net, an open access site that disseminates information on fetal ultrasound. Dr. Jeanty is considered an international expert in the field of ultrasound, he has mentored several fellows and led many ultrasound education and training courses in low-resource settings.

Dario Paladini, MD

Prof. Dario Paladini is Associate Professor in Obstetrics and Gynecology. He is currently the Director of the Fetal Medicine and Surgery Unit at Gaslini Children's Hospital in Genoa, Italy. Prof. Paladini is a leading international expert in fetal imaging, from 3D/4D ultrasound to fetal cardiology, and neurosonography to early assessment. He has authored more than 150 peer-review articles in fetal imaging and gynecological ultrasound (IOTA trials) and Gynecologic Oncology. Prof. Paladini is also co-author of *Ultrasound of Fetal Anomalies*, a prized textbook on fetal anomalies in its 2nd edition. Finally, he is deeply involved in OBGYN ultrasound education globally as the Chairman of the International Society of Ultrasound in Obstetrics and Gynecology's Education Committee (2004-2009) and Chairmen of the Italian Society of Ultrasound in OBGYN (SIEOG; 2010-2012).

"You give but little when you give of your possessions. It is when you give of yourself that you truly give". Khalil Gibran - The Prophet

I embarked on this journey with one focus in mind, to produce an educational resource designed to enhance the theoretical and practical knowledge of ultrasound with the goal of enhancing care for women around the world. Ultrasound has assumed an integral part of obstetrics and gynecology, whether in identifying a high-risk pregnancy or in assessing the non-pregnant uterus and adnexae. The proper application of ultrasound requires an in depth knowledge of the technology and practical skills for image acquisition, both of which are deficient in many parts of the world. This e-book is intended to fill this gap in all settings.

This e-book has three main sections; the first three chapters focus on the technical and practical use of ultrasound with a review of the physical principles of sound, the practical approach to the ultrasound equipment, and the technical aspect of performing the ultrasound examination. The second section, chapters four to ten, addresses the obstetric ultrasound examination and the third section, chapters eleven to fourteen, addresses the gynecologic ultrasound examination. The last chapter shows how to write an ultrasound report, a key component of the examination. Two chapters in particular, chapters ten and fourteen, present a stepwise-standardized approach to the basic obstetric and gynecologic ultrasound examinations respectively. The book is filled with descriptive figures, tables, and tips that the authors use in their daily ultrasound practice and have been accrued through many years of experience.

Many contributed to the success of this book, first and foremost, my friends and co-authors, Rabih Chaoui, Philippe Jeanty, and Dario Paladini who collectively possess an immense knowledge in ultrasound, are recognized as giants in this field, and provided book content and editorial review. Second, Ms. Emily Walsh, who helped design the book, organize the figures and tables, and produce the product that you see today. Her artistic abilities, time commitment, and focused approach made this project a reality. Third, the Marketing Department at Eastern Virginia Medical School, who coordinated the website to host and support the book. Last, but not least, my wife, Sharon, who was a great support and unselfishly allowed me to spend countless hours on this project.

A special thank you to the International Society of Ultrasound in Obstetrics and Gynecology (ISUOG) for the support they provide to ultrasound education in low-resource settings around the world and for many ISUOG volunteers who donated their time and expertise to this cause. It is primarily through these activities that I have seen first-hand the impact of ultrasound in women's healthcare.

Many women around the world approach pregnancy and delivery with fear of death or serious injury. If through this educational resource, we are able to impact a single life, then our efforts would have been justified.

-   Alfred Abuhamad, MD.

To Sharon,
For your unwavering support, dedication, and commitment to ultrasound
With love

CONTENTS

INTRODUCTION

The introduction of ultrasound to obstetrics and gynecology has made tremendous impact to patient care as it allowed imaging of the fetus and placenta in obstetrics and maternal internal organs in gynecology with such clarity to allow advanced diagnosis and also to guide various life saving interventions. Understanding the physical principles of ultrasound is essential for a basic knowledge of instrument control and also for understanding safety and bioeffects of this technology. In this chapter, we present the basic concepts of the physical principles of ultrasound, define important terminology, review the safety and bioeffects and report on ultrasound statements of national and international organizations.

PHYSICAL CHARACTERISTICS OF SOUND

Sound is a mechanical wave that travels in a medium in a longitudinal and straight-line fashion. When a sound travels through a medium, the molecules of that medium are alternately compressed (squeezed) and rarefied (stretched). Sound cannot travel in a vacuum; it requires a medium for transmission, as the sound wave is a mechanical energy that is transmitted from one molecule to another. It is important to note that the molecules do not move as the sound wave passes through them, they oscillate back and forth, forming zones of compression and rarefaction in the medium. Seven acoustic parameters describe the characteristics of a sound wave. **Table 1.1** lists these characteristics.

TABLE 1.1	Characteristics of Sound Waves
- Frequency - Period - Amplitude - Power - Intensity - Wavelength - Propagation speed	

Frequency of a sound wave is the number of cycles that occurs in one second (**Figure 1.1**). The unit Hertz is 1 cycle / second. *Frequency* is an important characteristic of sound in ultrasound imaging as it affects penetration of sound and image quality. *Period* of a sound wave is related to

the time that a wave takes to vibrate up and down and thus is reciprocally related to frequency. For instance, a sound wave with a frequency of 10 Hertz will have a period of 1/10 second. *Amplitude*, *power* and *intensity* are three wave characteristics that relate to the strength of a sound wave. *Amplitude* is defined by the difference between the peak (maximum) or trough (minimum) of the wave and the average value (**Figure 1.2**). The peak or crest, represents the zone of compression and the trough represents the zone of rarefaction (**Figure 1.2**). Units of amplitudes are expressed in pressure parameters (Pascals) and in clinical imaging in million Pascals (MPa). The *amplitude* of a sound wave diminishes as sound propagates through the body. *Power* is the rate of energy transferred through the sound wave and is expressed in Watts. *Power* is proportional to the amplitude squared of a sound wave. *Power* can be altered up or down by a control on the ultrasound machine. Intensity is the concentration of energy in a sound wave and thus is dependent on the power and the cross sectional area of the sound beam. The *intensity* of a sound beam is thus calculated by dividing the power of a sound beam (Watts) by its cross sectional area (cm^2), expressed in units of W/cm^2. The *wavelength* of a sound wave is the length of a wave and is defined as the distance of a complete cycle. It is designated by the symbol lambda (λ), is expressed in mm in clinical settings (**Figure 1.3**), and can be calculated by dividing the velocity of the wave by the frequency of the wave ($\lambda = v/f$). The *propagation speed* is the distance that a sound wave travels through a specified medium in 1 second.
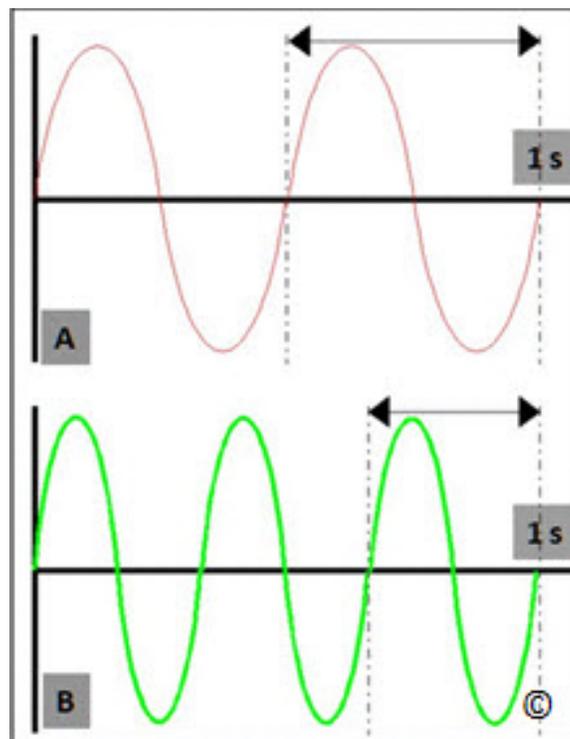

Figure 1.1: Frequency of sound is the number of cycles per second (s) and is expressed in Hertz (1 cycle / sec). In Wave A, the frequency is 2 cycles per sec or 2 Hertz and in wave B the frequency is 3 cycles per sec or 3 Hertz. The double arrows denote sound wavelengths, described in figure 1.3.
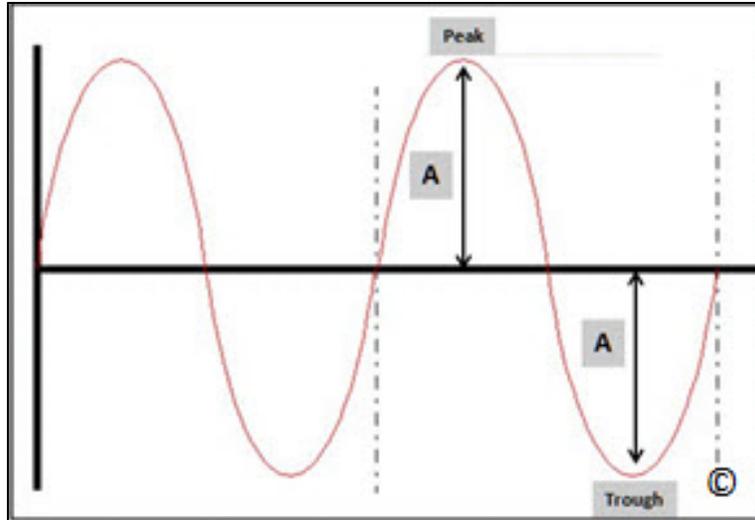
Figure 1.2: Amplitude (A) is defined by the difference between the peak (maximum) or trough (minimum) of the wave and the average value. Units of amplitude are expressed in million Pascals (MPa).
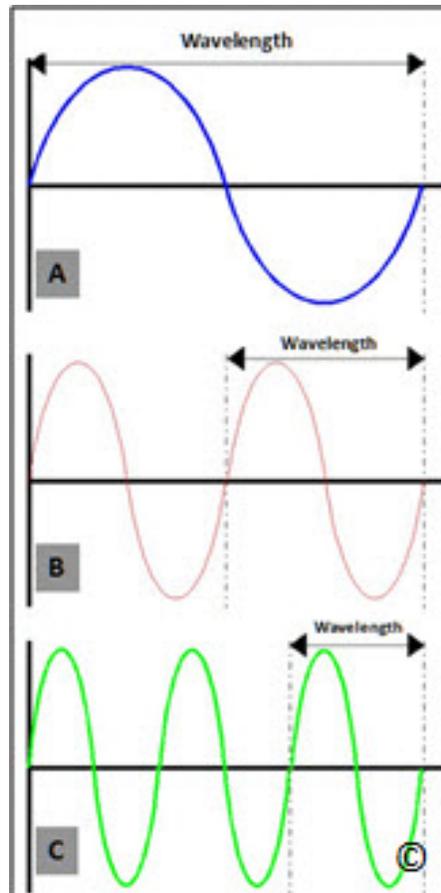

Figure 1.3: The wavelength of a sound wave is the length of a wave and is defined as the distance of a complete cycle. It is designated by the symbol lambda (λ), and is expressed in mm. In this schematic, 3 sound waveforms are shown with respectively shorter wavelengths from A to C.

TABLE 1.2	Speed of Sound in Various Media
Medium Type	**Speed (m/s)**
Air	330
Fat	1,450
Water	1,450
Soft Tissue	1,540
Bone	3,500
Metals	up to 7,000

The sound source, which is the ultrasound machine and/or the transducer, determines the frequency, period, amplitude, power and intensity of the sound. Wavelength is determined by both the sound source and the medium and the propagation speed is a function of the medium only. The propagation speed of sound in soft tissue is constant at 1,540 m/s. **Table 1.2** shows the propagation of sound in other biologic media and materials.

WHAT IS ULTRASOUND?

Sound is classified based upon the ability of the human ear to hear it. Sounds sensed by young healthy adult human ears are in the range of 20 cycles per second or Hertz, abbreviated as Hz, to 20,000 Hz, or 20 KHz (Kilo Hertz) termed audible sound (Range of 20 – 20,000 Hz). If the frequency of a sound is less than 20 Hz, it cannot be heard by humans and is defined as infrasonic or infrasound. If the frequency of sound is higher than 20 KHz, it cannot be heard by humans and is called ultrasonic or ultrasound, **Table 1.3**. Typical frequencies used in medical ultrasound are 2-10 MHz (mega, (million), Hertz). Ultrasound frequencies that are commonly used in obstetrics and gynecology are between 3 and 10 MHz.

TABLE 1.3	Frequency Spectrum of Sound
Sound Wave	**Frequency**
Ultrasound	Greater than 20 KHz
Audible Sound	20 Hz to 20 KHz
Infrasound	Less than 20 Hz

HOW IS ULTRASOUND GENERATED?

Ultrasound waves are generated from tiny piezoelectric crystals packed within the ultrasound transducers (**Figure 1.4**). When an alternate current is applied to these crystals, they contract and expand at the same frequency at which the current changes polarity and generate an ultrasound beam. The ultrasound beam traverses into the body at the same frequency generated. Conversely, when the ultrasound beam returns to the transducer, these crystals change in shape and this minor change in shape generate a tiny electric current that is amplified by the ultrasound machine to generate an ultrasound image on the monitor. The piezoelectric crystals within the transducer therefore transform electric energy into mechanical energy (ultrasound) and vice-versa. One crystal is not sufficient to produce an ultrasound beam for clinical imaging and modern transducers have large number of crystals arranged into parallel rows (**Figure 1.4**). Each crystal can nevertheless be stimulated individually. The crystals are protected by a rubber covering that helps decrease the resistance to sound transmission (impedance) from the crystals to the body. The high frequency sound generated by a transducer do not travel well through air, so in order to facilitate their transfer from the transducer to the skin of the patient, a watery gel is applied that couples the transducer to the skin and permits the sound to go back and forth. Ultrasound is therefore generated inside transducers by tiny crystals that convert electric current to ultrasound and convert returning ultrasound beams from the body into electric currents. Modern transducers have crystals made of synthetic plumbium zirconium titanate (PZT).
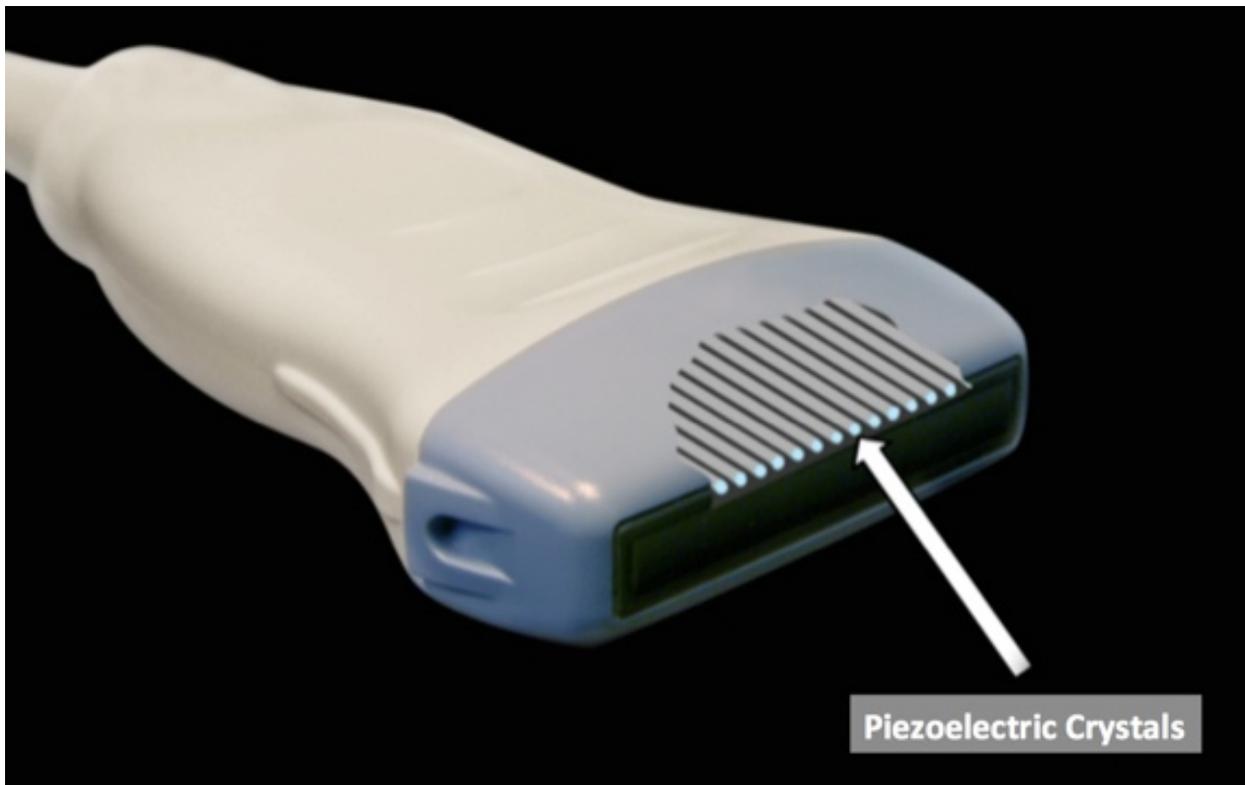

Figure 1.4: Piezoelectric crystals shown within a transducer. Note the symmetrical arrangement of the crystals. This figure is a diagrammatic representation, as the crystals are typically much smaller than shown. Figure 1.4 is modified with permission from the Society of Ultrasound in Medical Education (SUSME.org).

HOW IS AN ULTRASOUND IMAGE FORMED?

Modern ultrasound equipment create an ultrasound image by sending multiple sound pulses from the transducer at slightly different directions and analyzing returning echoes received by the crystals. Details of this process is beyond the scope of this book, but it is important to note that tissues that are strong reflectors of the ultrasound beam, such as bone or air will result in a strong electric current generated by the piezoelectric crystals which will appear as a hyperechoic image on the monitor (**Figure 1.5**). On the other hand, weak reflectors of ultrasound beam, such as fluid or soft tissue, will result in a weak current, which will appear as a hypoechoic or anechoic image on the monitor (**Figure 1.5**). The ultrasound image is thus created from a sophisticated analysis of returning echoes in a grey scale format. Given that the ultrasound beam travels in a longitudinal format, in order to get the best possible image, keep the angle of incidence of the ultrasound beam perpendicular to the object of interest, as the angle of incidence is equal to the angle of reflection (**Figure 1.6**).
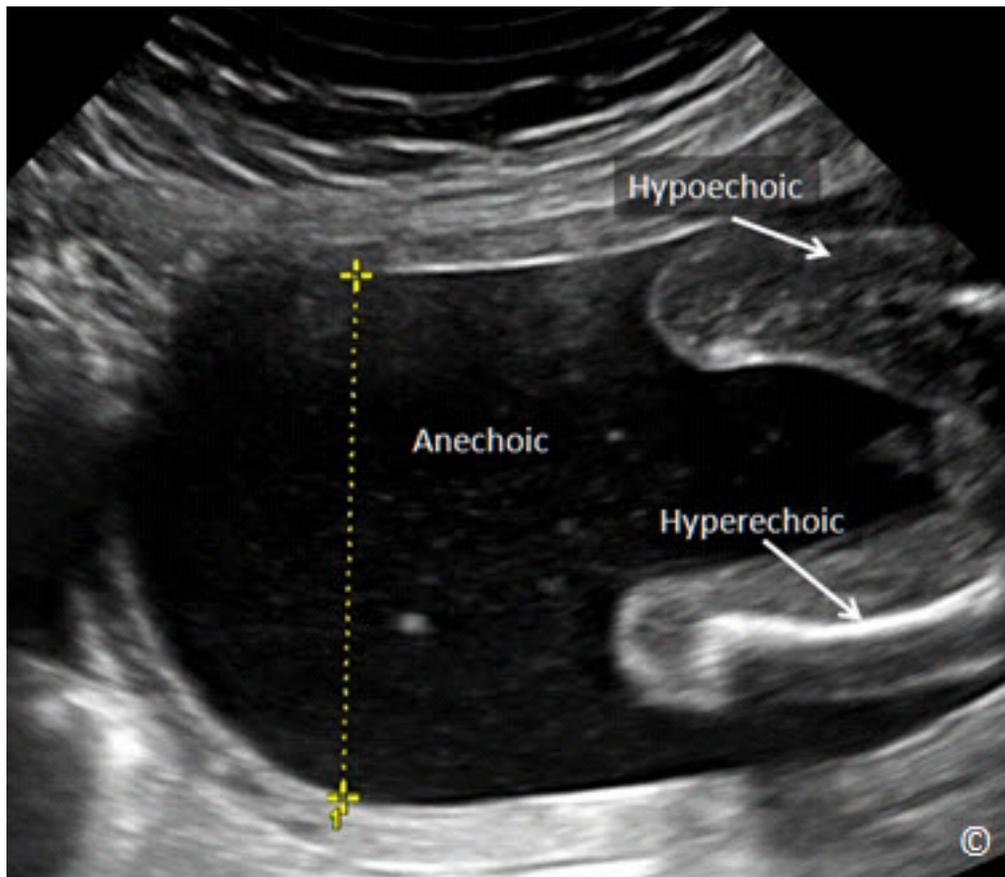

Figure 1.5: Ultrasound image of fetal extremities in the second trimester. Note the hyperechoic femur, the hypoechoic soft tissue in the thigh and anechoic amniotic fluid. Calipers measure the maximal vertical pocket of amniotic fluid (chapter 9).
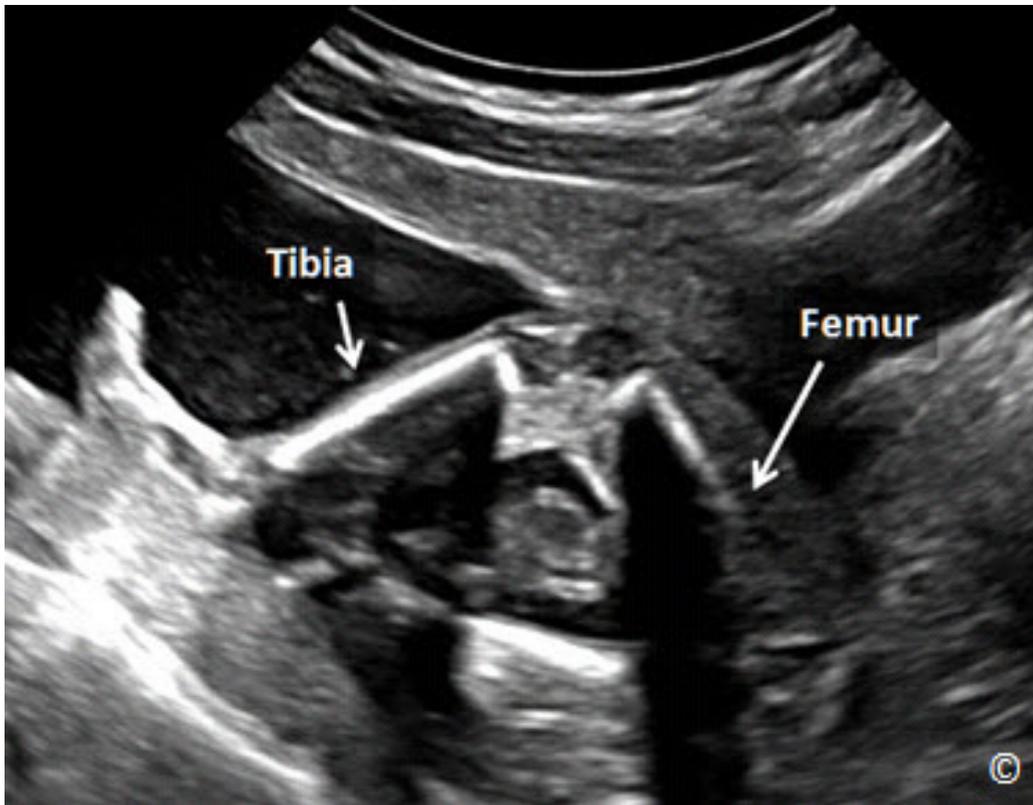
Figure 1.6: Ultrasound image of fetal lower extremity in the second trimester demonstrating the effect of the angle of insonation. Note how clearly the tibia is seen, as the angle of insonation is almost 90 degrees to it. The femur is barely seen, as the angle of insonation is almost parallel to it.

WHAT ARE DIFFERENT TYPES OF ULTRASOUND MODES?

A-mode, which stands for "Amplitude mode", is no longer used in clinical obstetric and gynecologic ultrasound imaging but was the basis of modern ultrasound imaging. In A-mode display, a graph shows returning ultrasound echoes with the x-axis representing depth in tissues and the y-axis representing amplitude of the returning beam. Historically, A-mode ultrasound was used in obstetrics in measuring biparietal diameters (**Figure 1.7**). B-mode display, which stands for "Brightness mode", known also as two-dimensional imaging, is commonly used to describe any form of grey scale display of an ultrasound image. The image is created based upon the intensity of the returning ultrasound beam, which is reflected in a variation of shades of grey that form the ultrasound image (**Figure 1.8**). It is important to note that B-mode is obtained in real-time, an important and fundamental characteristic of ultrasound imaging. **Table 1.4** shows various echogenicity of normal fetal tissue.
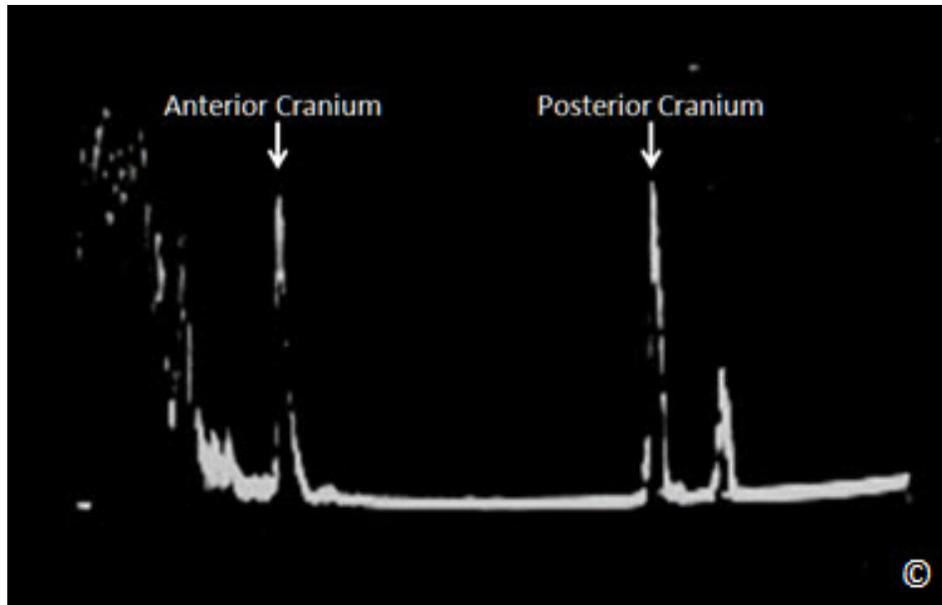
Figure 1.7: A-Mode ultrasound of fetal head. The first spike corresponds to the anterior cranium and the second spike corresponds to the posterior cranium. The biparietal diameter is the distance between these 2 spikes.
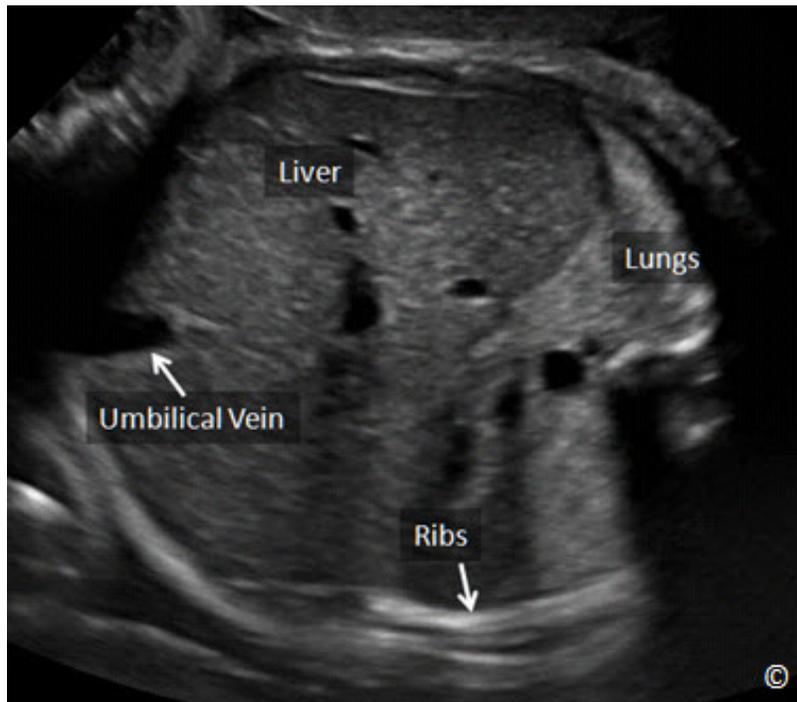

Figure 1.8: Variations in grey scale in a 2D ultrasound image of a fetal abdomen in the second trimester. Note the hyperechoic ribs and lung tissue, hypoechoic liver and anechoic umbilical vein. The intensity of the returning beam determines echogenicity.

TABLE 1.4	Various Ultrasound Echogenicity of Fetal Tissue			

Organ System	Anechoic	Slightly Echoic	More Echoic	Echogenic
Bone				√
Brain		√		
Lungs			√	
Stomach	√			
Liver		√		
Intestines			√	
Kidneys			√	
Bladder	√			
Placenta			√	
Amniotic Fluid	√			

M-mode display, which stands for "Motion mode" is a display that is infrequently used in current ultrasound imaging but is specifically used to assess the motion of the fetal cardiac chambers and valves in documentation of fetal viability and to assess certain fetal cardiac conditions such as arrhythmias and congenital heart disease. The M-mode originates from a single beam penetrating the body with a high pulse repetition frequency. The display on the monitor shows the time of the M-mode display on the x-axis and the depth on the y axis (**Figure 1.9**).
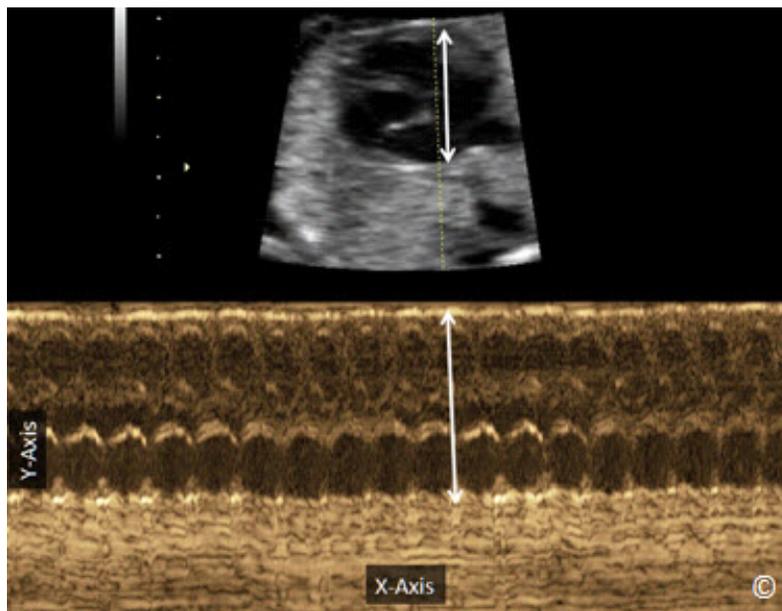

Figure 1.9: M-mode ultrasound of the fetal heart in the second trimester. The M-mode display (in sepia color) corresponds to the single ultrasound beam (dashed yellow line) with the X-axis displaying time and Y-axis displaying depth. Note the display of the heart on B-mode and corresponding M-mode shown by the double-headed arrows.

Color and spectral (pulsed) Doppler modes are dependent on the *Doppler principle (effect).* The Doppler principle describes the apparent variation in frequency of a light or a sound wave as the source of the wave approaches or moves away, relative to an observer. The traditional example that is given to describe this physical phenomenon is the apparent change in sound level of a train as the train approaches and then departs a station. The sound seems higher in pitch as the train approaches the station and seems lower in pitch as the train departs the station. This apparent change in sound pitch, or what is termed the frequency shift, is proportional to the speed of movement of the sound-emitting source, the train in this example. It is important to note that the actual sound of the train is not changing; it is the perception of change in sound to a stationary observer that determines the "Doppler effect". In clinical applications, when ultrasound with a certain frequency (f_o) is used to insonate a certain blood vessel, the reflected frequency (f_d) or frequency shift is directly proportional to the speed with which the red blood cells are moving (blood flow velocity) within that particular vessel. This frequency shift of the returning signal is displayed in a graphic form as a time-dependent plot. In this display, the vertical axis represents the frequency shift and the horizontal axis represents the temporal change of this frequency shift as it relays to the events of the cardiac cycle (**Figure 1.10**). This frequency shift is highest during systole, when the blood flow is fastest and lowest during end diastole, when the blood flow is slowest in the peripheral circulation (**Figure 1.10**). Given that the velocity of flow in a particular vascular bed is inversely proportional to the downstream impedance to flow, the frequency shift therefore derives information on the downstream impedance to flow of the vascular bed under study. The frequency shift is also dependent on the cosine of the angle that the ultrasound beam makes with the targeted blood vessel (see formula in **Figure 1.10**). Given that the insonating angle (angle of incidence) is difficult to measure in clinical practice, indices that rely on ratios of frequency shifts were developed to quantitate Doppler waveforms. By relying on ratios of frequency shifts, these Doppler indices are thus independent of the effects of the insonating angle of the ultrasound beam. Doppler indices that are commonly used in obstetric and gynecologic practice are shown in (**Figure 1.11**).
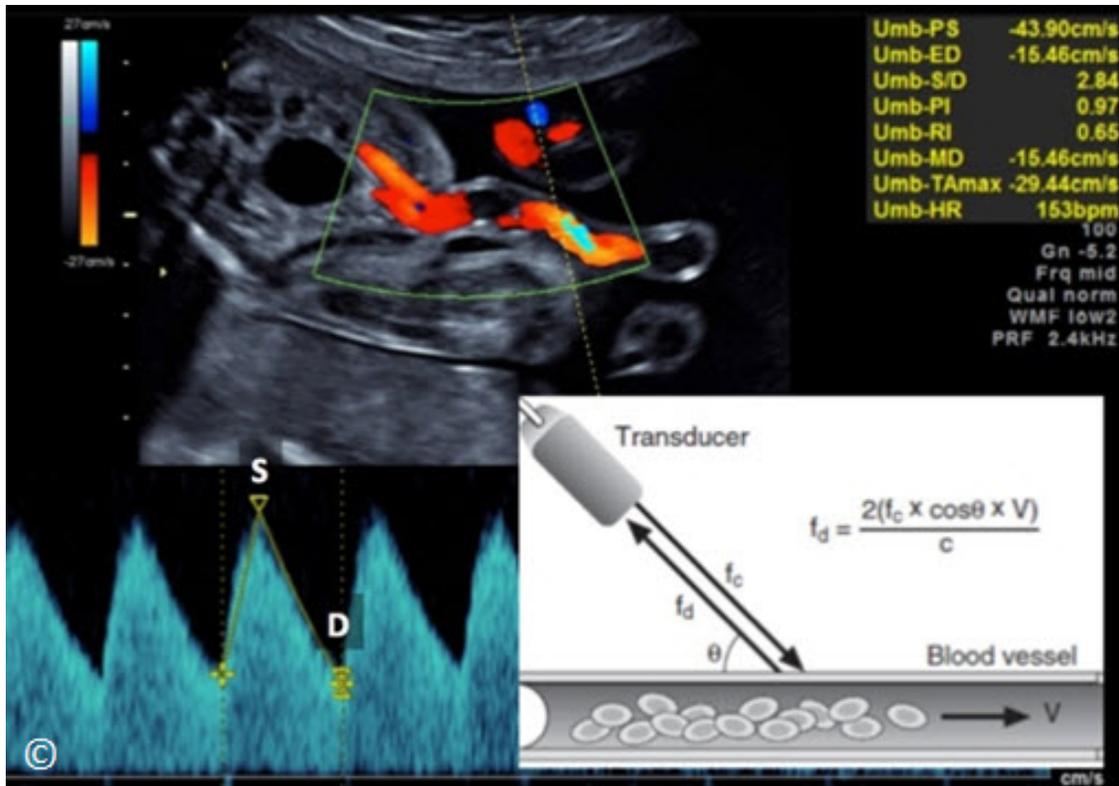
Figure 1.10: Doppler velocimetry of the umbilical artery at the abdominal cord insertion. "S" corresponds to the frequency shift during peak systole and "D" corresponds to the frequency shift during end diastole. The Doppler effect formula is also shown in white background. (Schematic of Doppler formula modified with permission from *A Practical Guide to Fetal Echocardiography Normal and Abnormal Hearts* – Abuhamad, Chaoui, second edition – Wolters Kluwer.
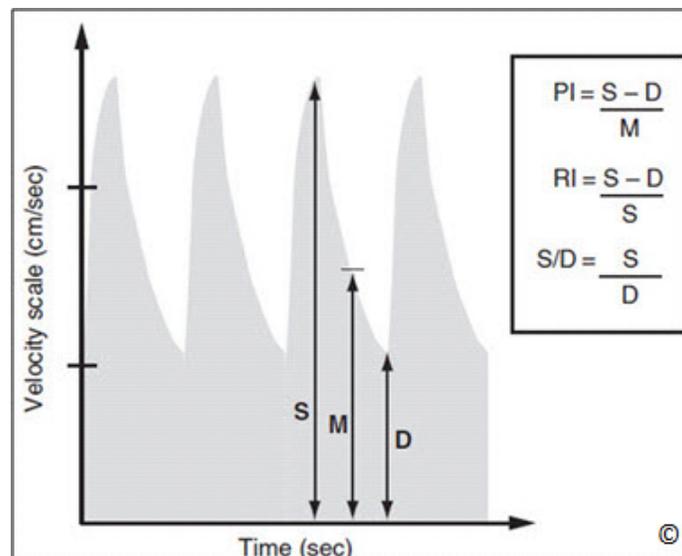

Figure 1.11: Doppler waveforms formulas that are commonly used in obstetrics and gynecology. PI = pulsatility index, RI = resistive index, S = peak systolic frequency shift, D = end diastolic frequency shift and M = mean frequency shift. Reproduced with permission from *A Practical Guide to Fetal Echocardiography: Normal and Abnormal Hearts* – Abuhamad, Chaoui, second edition – Wolters Kluwer.
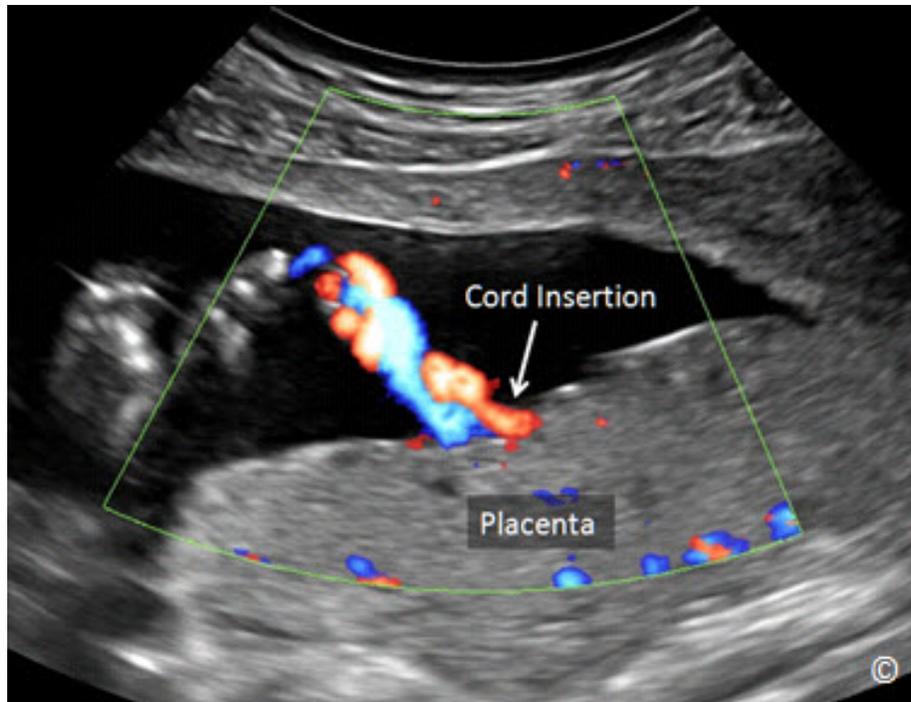
Figure 1.12: Color Doppler mode of the cord insertion into a posterior placenta. Blood in the umbilical vein is colored red (towards the transducer) and blood in the umbilical arteries is colored blue (away from the transducer).

Color Doppler mode or Color flow mode is a mode that is superimposed on the real-time B-mode image. This mode is used to detect the presence of vascular flow within the tissue being insonated (**Figure 1.12**). By convention, if the flow is towards the transducer it is colored red and if the flow is away from the transducer it is colored blue. The operator controls various parameters of color Doppler such as the velocity scale or pulse repetition frequency (PRF), wall filter, size of the area within the field of B-mode and the angle of incidence that the ultrasound beam makes with the direction of blood flow. Low velocity scales and filters are reserved for low impedance vascular beds such as ovarian flow in gynecology (**Figure 1.13**) and high velocity scales and filters are reserved for high impedance circulation such as cardiac outflow tracts (**Figure 1.14**). In order to optimize the display of color Doppler, the angle of insonation should be as parallel to the direction of blood flow as possible. If the angle of insonation approaches ninety degrees, no color flow will be displayed given that the "Doppler effect" is dependent on the cosine of the angle of insonation, and cosine of 90 degrees is equal to zero (**Figure 1.15**).
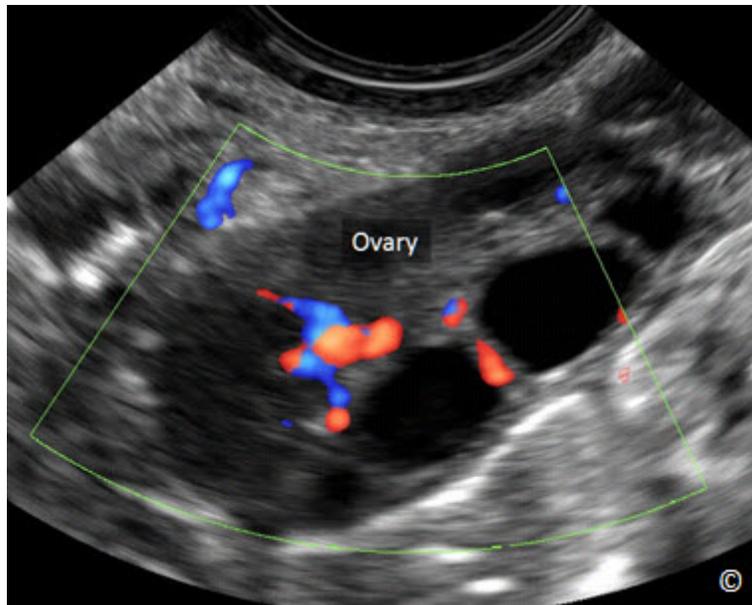
Figure 1.13: Color Doppler mode of blood flow within the ovary (labeled). Typically ovarian flow is low impedance and detected on low velocity scale with low filter setting.
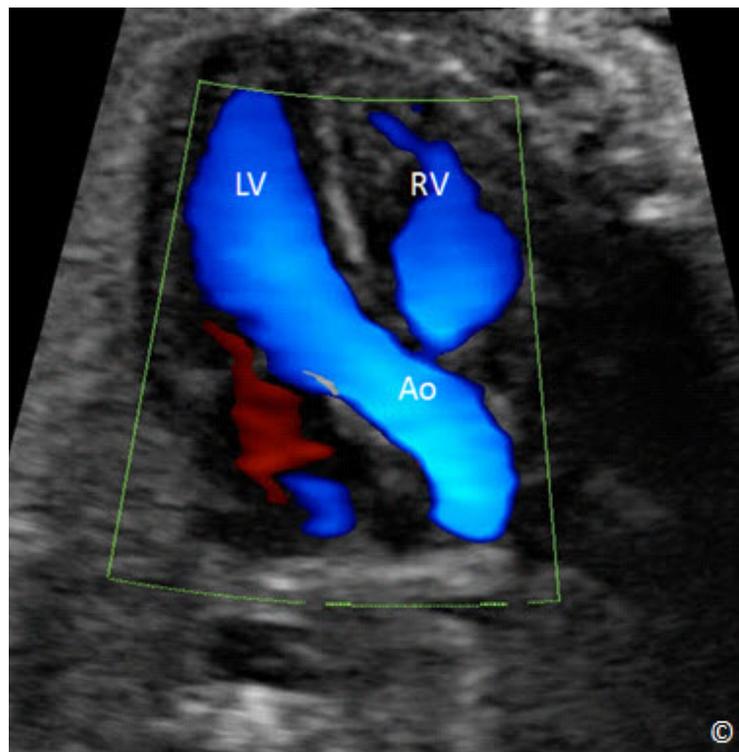

Figure 1.14: Color Doppler mode of left ventricular outflow in the fetal heart. Blood flow in the fetal heart has high velocity and thus is detected on high velocity scale. LV=left ventricle, RV=right ventricle, Ao=aorta.
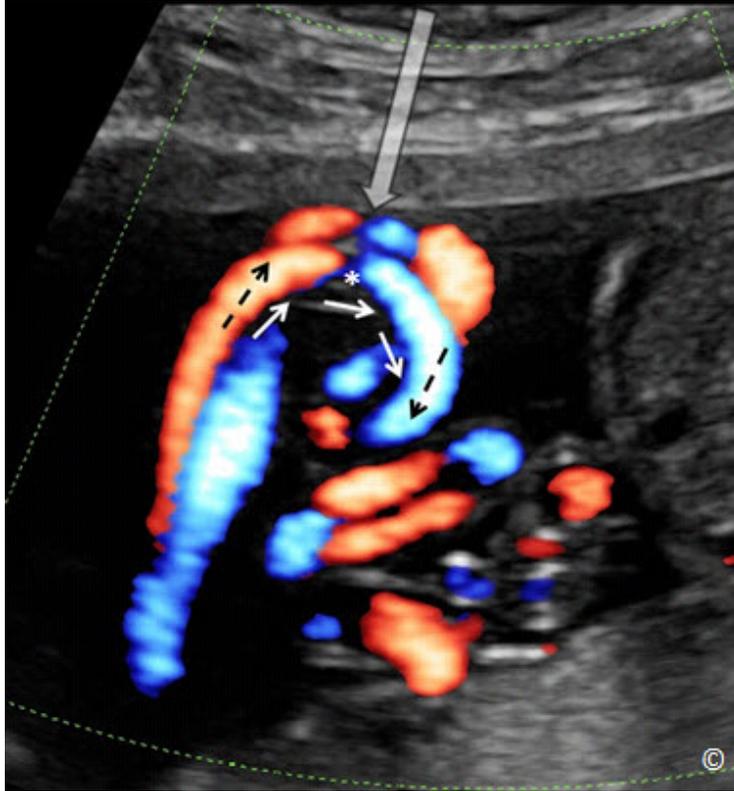
Figure 1.15: Blood flow in an umbilical cord showing the Doppler Effect. White arrows show the direction of blood flow. Note the absence of blood flow on color Doppler (asterisk) where the ultrasound beam (grey arrow) images the cord with an angle of insonation equal to 90 degrees. The black arrows represent blood flow with an angle of insonation almost parallel to the ultrasound beam and thus display the brightest color corresponding to the highest velocities.

In the spectral Doppler mode, or pulsed Doppler mode, quantitative assessment of vascular flow can be obtained at any point within a blood vessel by placing a sample volume or the gate within the vessel **(Figure 1.16)**. Similar to color Doppler, the operator controls the velocity scale, wall filter and the angle of incidence. Flow towards the transducer is displayed above the baseline and flow away from the transducer is displayed below the baseline. In spectral Doppler mode, only one crystal is typically necessary and it alternates between sending and receiving ultrasound pulses.
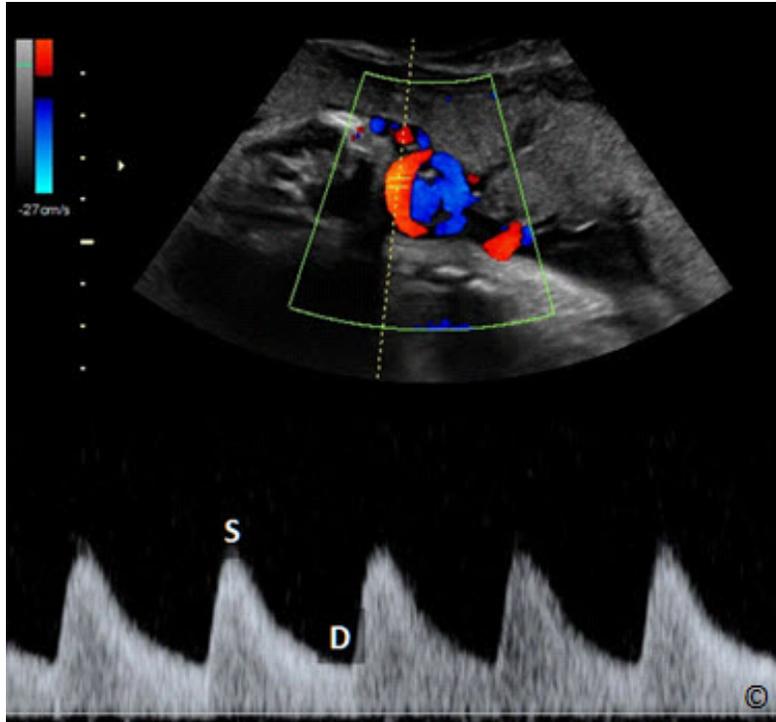
Figure 1.16: Pulsed Doppler mode of the umbilical artery. S corresponds to the frequency shift during peak systole and D corresponds to the frequency shift at end diastole.

Doppler mode, or Energy mode, or High Definition Doppler mode is a sensitive mode of Doppler that is available on some high-end ultrasound equipment and is helpful in the detection of low velocity flow **(Figure 1.17)**. The strength (amplitude) of the reflected signal is primarily processed. Power Doppler mode is less affected by the angle of insonation than the traditional color or spectral Doppler.
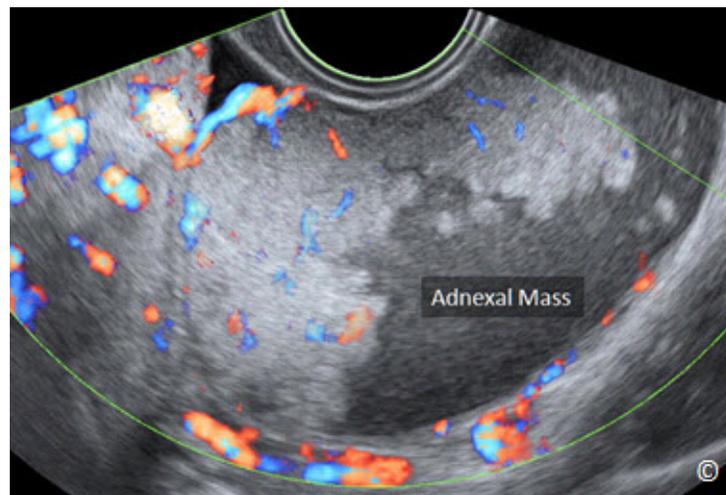

Figure 1.17: Power Doppler mode showing vascularity within a borderline ovarian tumor. Power Doppler mode is helpful in the detection of low velocity flow.

WHAT ARE THE BIOEFFECTS OF ULTRASOUND?

Ultrasound is a form of mechanical energy and its output varies based upon the mode applied. In general B-mode has the lowest energy and pulsed Doppler has the highest energy. Given the presence of a theoretical and potential harm of ultrasound, the benefit to the patient must always outweigh the risk. In general, ultrasound is considered to be a safe imaging modality as compared to other imaging modalities that have ionizing radiation like X-ray and Computed Tomography (CT). There are 2 important indices for measurement of bioeffects of ultrasound; the Thermal Index (TI) and the Mechanical Index (MI). The Thermal Index is a predictor of maximum temperature increase under clinically relevant conditions and is defined as the ratio of the power used over the power required to produce a temperature rise of 1° C. The TI is reported in three forms; TIS or Thermal index Soft tissue, assumes that sound is traveling in soft tissue, TIB or Thermal index Bone, assumes that sound is at or near bone, TIC, or Thermal index Cranial assumes that the cranial bone is in the sound beam's near field. The Mechanical index (MI) gives an estimation of the cavitation effect of ultrasound, which results from the interaction of sound waves with microscopic, stabilized gas bubbles in the tissues. Other effects included in this category are physical (shock wave) and chemical (release of free radicals) effects of ultrasound on tissue.

In 1992, the Output Display Standard (ODS) was mandated for all diagnostic ultrasound devices. In this ODS, the manufacturers are required to display in real time, the TI and the MI on the ultrasound screen with the intent of making the user aware of bioeffects of the ultrasound examination (**Figure 1.18**). The user has to be aware of the power output and make sure that reasonable levels are maintained. Despite the lack of scientific reports of confirmed harmful bioeffect from exposure to diagnostic ultrasound, the potential benefit and risk of the ultrasound examination should be assessed and the principle of ALARA should be always followed. The ALARA principle stands for As Low As Reasonably Achievable when adjusting controls of the ultrasound equipment in order to minimize the risk. Always keep track of the TI and MI values on the ultrasound screen, and keep the TI below 1 and MI below 1 for obstetrical ultrasound imaging.

Figure 1.18: An ultrasound examination of the fetal abdomen in the third trimester of pregnancy. Note the display of MI and TIb in white rectangle. MI= Mechanical Index and TIb=Thermal Index bone.

WHAT ARE SOME RELEVANT OFFICIAL STATEMENTS FROM ULTRASOUND SOCIETIES?

Several national and international societies have official statements that relates to the use of medical ultrasound in obstetrics and gynecology. We have assembled in this chapter some of the relevant official statements along with the Internet link to their source. It is important to note that official societal statements tend to be updated from time to time and the reader should consult with the society's website for the most recent version.

International Society of Ultrasound in Obstetrics and Gynecology (ISUOG) (www.ISUOG.org)

ISUOG- Statement on the safe use of Doppler in the 11 to 13+6-week fetal ultrasound examination (1):

1) Pulsed Doppler (spectral, power and color flow imaging) ultrasound should not be used routinely.
2) Pulsed Doppler ultrasound may be used for clinical indications such as to refine risks for trisomies.

3) When performing Doppler ultrasound, the displayed thermal index (TI) should be ≤1.0 and exposure time should be kept as short as possible (usually no longer than 5–10 min) and should not exceed 60 min.
4) When using Doppler ultrasound for research, teaching and training purposes, the displayed TI should be ≤1.0 and exposure time should be kept as short as possible (usually no longer than 5–10 min) and should not exceed 60 min. Informed consent should be obtained.
5) In educational settings, discussion of first-trimester pulsed or color Doppler should be accompanied by information on safety and bioeffects (e.g. TI, exposure times and how to reduce output power)
6) When scanning maternal uterine arteries in the first trimester, there are unlikely to be any fetal safety implications as long as the embryo/fetus lies outside the Doppler ultrasound beam.

ISUOG- Safety Statement, 2000 (reconfirmed 2003) (2):

The thermal index (TI) and the mechanical index (MI) are not perfect indicators of the risks of thermal and nonthermal bioeffects, but currently they should be accepted as the most practical and understandable methods of estimating the potential for such risks.

B-mode and M-mode
Acoustic outputs are generally not high enough to produce deleterious effects. Their use therefore appears to be safe, for all stages of pregnancy.

Doppler Ultrasound
Significant temperature increase may be generated by spectral Doppler mode, particularly in the vicinity of bone. This should not prevent use of this mode when clinically indicated, provided the user has adequate knowledge of the instrument's acoustic output, or has access to the relevant TI. Caution is recommended when using color Doppler mode with a very small region of interest, since this mode produces the highest potential for bioeffects. When ultrasound examination is clinically indicated, there is no reason to withhold the use of scanners that have received current Food and Drug Administration clearance in tissues, which have no identifiable gas bodies. Since ultrasound contrast agents are mostly gas-carriers, the risk of induction and sustenance of inertial cavitation is higher in circumstances when these agents are employed.

Pregnancy
Based on evidence currently available, routine clinical scanning of every woman during pregnancy using realtime B-mode imaging is not contraindicated. The risk of damage to the fetus by teratogenic agents is particularly great in the first trimester. One has to remember that heat is generated at the transducer surface when using the transvaginal approach. Spectral and color Doppler may produce high intensities and routine examination by this modality during the embryonic period is rarely indicated. In addition, because of high acoustic absorption by bone, the potential for heating adjacent tissues must also be kept in mind. Exposure time and acoustic output should be kept to the lowest levels consistent with obtaining diagnostic information and limited to medically indicated procedures, rather than for purely entertainment purposes.

Education

Education of ultrasound operators is of the utmost importance since the responsibility for the safe use of ultrasound devices is now shared between the users and the manufacturers, who should ensure the accuracy of the output display.

ISUOG-Statement on the non-medical use of ultrasound (2009) (3):

The International Society of Ultrasound in Obstetrics and Gynecology (ISUOG) and World Federation of Ultrasound in Medicine and Biology (WFUMB) disapprove of the use of ultrasound for the sole purpose of providing souvenir images of the fetus. There have been no reported incidents of human fetal harm in over 40 years of extensive use of medically indicated and supervised diagnostic ultrasound. Nevertheless, ultrasound involves exposure to a form of energy, so there is the potential to initiate biological effects. Some of these effects might, under certain circumstances, be detrimental to the developing fetus. Therefore, the uncontrolled use of ultrasound without medical benefit should be avoided. Furthermore, ultrasound should be employed only by health professionals who are trained and updated in the clinical usage and bioeffects of ultrasound.

American Institute of Ultrasound in Medicine (AIUM) (www.AIUM.org)

AIUM-As Low As Reasonably Achievable (ALARA) Principle (2008) (4):

The potential benefits and risks of each examination should be considered. The ALARA (As Low As Reasonably Achievable) Principle should be observed when adjusting controls that affect the acoustical output and by considering transducer dwell times. Further details on ALARA may be found in the AIUM publication "Medical Ultrasound Safety.

AIUM-Conclusions Regarding Epidemiology for Obstetric Ultrasound (2010) (5):

Based on the epidemiologic data available and on current knowledge of interactive mechanisms, there is insufficient justification to warrant conclusion of a causal relationship between diagnostic ultrasound and recognized adverse effects in humans. Some studies have reported effects of exposure to diagnostic ultrasound during pregnancy, such as low birth weight, delayed speech, dyslexia and non-right-handedness. Other studies have not demonstrated such effects. The epidemiologic evidence is based primarily on exposure conditions prior to 1992, the year in which acoustic limits of ultrasound machines were substantially increased for fetal/obstetric applications

AIUM-Prudent Use and Clinical Safety (2012) (6):

Diagnostic ultrasound has been in use since the late 1950s. Given its known benefits and recognized efficacy for medical diagnosis, including use during human pregnancy, the American Institute of Ultrasound in Medicine herein addresses the clinical safety of such use:

No independently confirmed adverse effects caused by exposure from present diagnostic ultrasound instruments have been reported in human patients in the absence of contrast agents. Biological effects (such as localized pulmonary bleeding) have been reported in mammalian systems at diagnostically relevant exposures but the clinical significance of such effects is not yet known. Ultrasound should be used by qualified health professionals to provide medical benefit to the patient. Ultrasound exposures during examinations should be as low as reasonably achievable (ALARA).

AIUM-Prudent Use in Pregnancy (2012) (7):

The AIUM advocates the responsible use of diagnostic ultrasound and strongly discourages the non-medical use of ultrasound for entertainment purposes. The use of ultrasound without a medical indication to view the fetus, obtain images of the fetus, or determine the fetal gender is inappropriate and contrary to responsible medical practice. Ultrasound should be used by qualified health professionals to provide medical benefit to the patient.

AIUM-Statement on Measurement of Fetal Heart Rate (2011) (8):

When attempting to obtain fetal heart rate with a diagnostic ultrasound system, AIUM recommends using M-mode at first, because the time-averaged acoustic intensity delivered to the fetus is lower with M-mode than with spectral Doppler. If this is unsuccessful, spectral Doppler ultrasound may be used with the following guidelines: use spectral Doppler only briefly (e.g. 4-5 heart beats) and keep the thermal index (TIS for soft tissues in the first trimester, TIB for bones in second and third trimesters) as low as possible, preferably below 1 in accordance with the ALARA principle.

References:

1) International Society of Ultrasound in Obstetrics and Gynecology official statement on the Safe use of Doppler in the 11 to 13+6 week fetal ultrasound examination. UOG: Volume 37, Issue 6, Date: June 2011, Page: 628
2) International Society of Ultrasound in Obstetrics and Gynecology official statement on Safety. UOG: Volume 21, Issue 1, Date: January 2003, Page: 100
3) International Society of Ultrasound in Obstetrics and Gynecology official statement on Non-Medical use of ultrasound. UOG: Volume 33, Issue 5, Date: May 2009, Page: 617
4) American Institute of Ultrasound in Medicine official statement on http://www.aium.org/officialStatements/39
5) American Institute of Ultrasound in Medicine official statement on As Low As Reasonably Achievable principal; 2008. http://www.aium.org/officialStatements/16
6) American Institute of Ultrasound in Medicine official statement on Conclusions regarding epidemiology for obstetric ultrasound; 2010 http://www.aium.org/officialStatements/34

7) American Institute of Ultrasound in Medicine official statement on Prudent use in pregnancy; 2012. http://www.aium.org/officialStatements/33

8) American Institute of Ultrasound in Medicine official statement on Measurement of fetal heart rate; 2011. http://www.aium.org/officialStatements/43

INTRODUCTION

Performing and successfully completing an ultrasound examination requires multitude of skills that include the medical knowledge, the technical dexterity, and the know-how to navigate the various knobs of the ultrasound equipment. Today's ultrasound machines are complex and quite advanced in electronics and in post-processing capabilities. Being able to optimize the ultrasound image is much dependent on the understanding of the basic functionality of the ultrasound equipment. This chapter will focus on the review of various components of the ultrasound equipment and the basic elements of image optimization. The following chapter (chapter 3) will introduce some helpful scanning techniques.

THE ULTRASOUND EQUIPMENT

Ultrasound technology has changed drastically over the past decade allowing for significant miniaturization in the design and manufacturing of ultrasound equipment. The spectrum of ultrasound equipment today includes machines that can fit in the palm of one's hand and high-end machines that can perform very sophisticated ultrasound studies. It is important to note that before you acquire ultrasound equipment, you should have an understanding of who will be using the equipment, for which medical purpose it is intended to be used, in which environment it will be used and how will it be serviced. The answer to these important questions will help in guiding you to the appropriate type of ultrasound equipment for the right setting. For instance, ultrasound equipment destined for low-resource (outreach) settings should have special characteristics such as portability, sturdiness and a back-up battery in order to adjust to fluctuation in electricity. Furthermore, ultrasound equipment designed for the low-resource (outreach) setting should be easily shipped for repairs and service.

Ultrasound Transducers

Ultrasound transducers are made of a transducer head, a connecting wire or cable and a connector, or a device that connects the transducer to the ultrasound machine. The transducer head has a footprint region (**Figure 2.1**) where the sound waves leave and return to the transducer. It is this footprint region of the transducer that needs to remain in contact with the body in order to transmit and receive ultrasound waves. A gel is applied to the skin/mucosa surface of the body to facilitate transmission of ultrasound waves given that sound waves do not transmit well in air. Each transducer also has a transducer (probe) marker located next to the head of the transducer in order to help identify its orientation (**Figure 2.2**). This probe marker

can be a notch, a dot or a light on the probe's head. The use of this probe marker in handling the transducer and its orientation will be further discussed in the following chapter (Chapter 3).

Figure 2.1: Footprint of a curvilinear abdominal transducer. The footprint region is where the sound waves leave and return to the transducer.
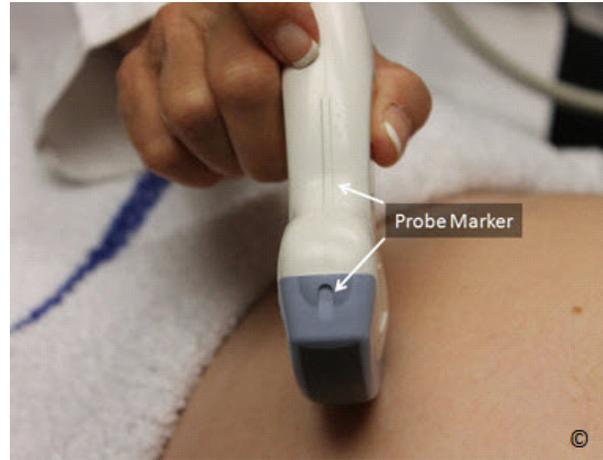

Figure 2.2: Probe marker of a curvilinear abdominal transducer. The probe marker is essential in the proper handling and orientation of the transducer (discussed in chapter 3).

Transducers are produced in an array of shapes, sizes and frequencies and are adapted for specific clinical applications. In general, transducers for cardiac applications have small footprints. Vascular transducers have high frequencies and are linear in shape and obstetric and abdominal transducers are curvilinear in footprint shape in order to conform to the shape of the abdomen (**Figure 2.3**).

Figure 2.3: Abdominal transducer used for obstetric applications. Note the curvilinear shape of the footprint, which helps to conform to the abdominal curvature.

Linear transducers produce sound waves that are parallel to each others with a corresponding rectangular image on the screen. The width of the image and number of scan lines is uniform throughout all tissue levels (**Figure 2.4**). This has the advantage of good near field resolution. Linear transducers are not well suited for curved parts of the body as air gaps are created between the skin and transducer (**Figure 2.5**).

Figure 2.5: Linear transducer used for obstetric scanning in the late second trimester of pregnancy. Note the gap produced between the transducer footprint and the abdominal wall (white arrows). This can be eliminated by simply applying gentle pressure on the abdomen.

Figure 2.4: Transverse plane of the fetal chest in the second trimester of pregnancy using a linear transducer. Note the rectangular screen image and a good near-field resolution.

Sector transducers produce a fan like image that is narrow near the transducer and increase in width with deeper penetration. Sector transducers are useful when scanning in small anatomic sites, such as between the ribs as it fits in the intercostal space, or in the fontanel of the newborn (**Figure 2.6**). Disadvantages of the sector transducer include its poor near field resolution and somewhat difficult manipulation.

Figure 2.6: Sector transducer; note the small footprint, which allows for imaging in narrow anatomic locations such as the intercostal spaces or the neonatal fontanels.

Curvilinear transducers are perfectly adapted for the abdominal scanning due to the curvature of the abdominal wall (**Figure 2.3**). The frequency of the curvilinear transducers ranges between 2 and 7 MHz. The density of the scan lines decreases with increasing distance from the transducer and the image produced on the screen is a curvilinear image, which allows for a wide field of view (**Figure 2.7**).
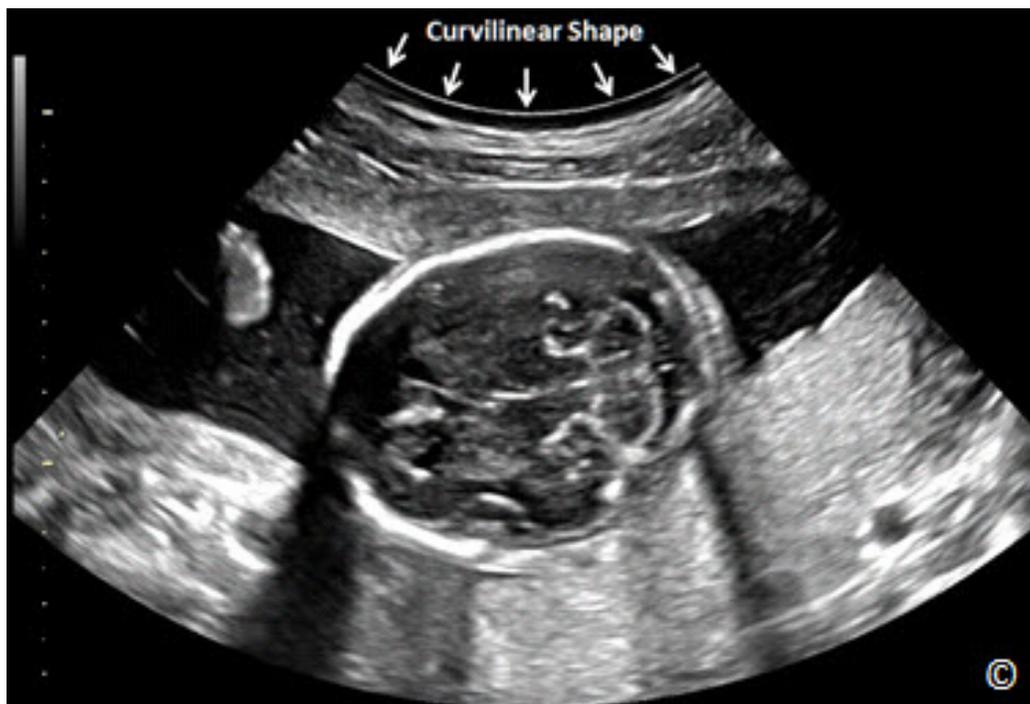
Figure 2.7: Ultrasound image of the fetal head using a curvilinear transducer. Note that the image is curvilinear in shape (arrows) and has a wide field of view.

Transvaginal transducers, like other endocavitary transducers, have a small footprint and their frequencies are typically in the range of 5-12 MHz (**Figure 2.8**). They are designed to fit in small endocavitary spaces with the footprint at the top of the transducer (transvaginal) or at the dorsal aspect of the transducer (rectal). When performing a transvaginal ultrasound examination, a clean condom, or the digit of a surgical rubber glove, should cover the transvaginal transducer. Ultrasound gel should be placed inside and outside the protective cover in order to facilitate the transmission of sound.
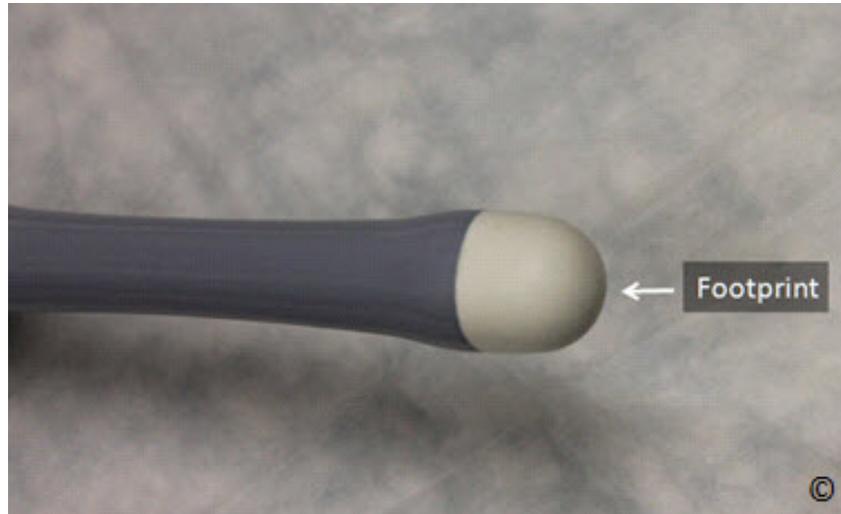
Figure 2.8: The head of a transvaginal transducer; note the small footprint (labeled) at the top of the transducer.

Protocols for ultrasound transducer cleaning should be adhered to in order to reduce the spread of infectious agents. Both the transabdominal and the transvaginal transducers should be wiped between ultrasound examinations and disinfection of the transvaginal transducer should be performed according to national or manufacturer guidelines (1).

Controls of the Ultrasound Equipment

Ultrasound equipment has a wide array of options and features. These features are typically operated from either the console of the ultrasound equipment, a touch screen monitor or a combination of both (**Figure 2.9**). The basic controls that you need to familiarize yourself in the early stages of ultrasound scanning are the following:

Figure 2.9: Ultrasound equipment showing a wide array of knobs for control of various features. Most ultrasound equipment have a keyboard and a trackball on their consoles.

Power or Output Control: This controls the strength of the electrical voltage applied to the transducer crystal at pulse emission. Increasing the power output increases the intensity of the ultrasound beam emitting and returning to the transducer, thus resulting in increase in signal to noise ratio. Increasing the power results in an increase in ultrasound energy delivered to the patient. It is therefore best practice to operate on the minimum power possible for the type of study needed. Resorting to lower frequency transducers can help achieve more depth while minimizing power output.

Depth: The depth knob allows you to increase or decrease the depth of the field of view on the monitor. It is important to always maximize the area of interest on your monitor and decrease the depth of your field of view, which enlarges the target anatomic organs under view. **Figures 2.10 A and B** show the importance of depth control in obstetrical scanning.

Gain: The gain knob adjusts the overall brightness of the image by amplifying the strength of the returning ultrasound echo. The overall brightness of the image can be increased or decreased by turning the gain knob clockwise or counterclockwise respectively. **Figures 2.11 A and B** show the same ultrasound image under low and high gain settings.
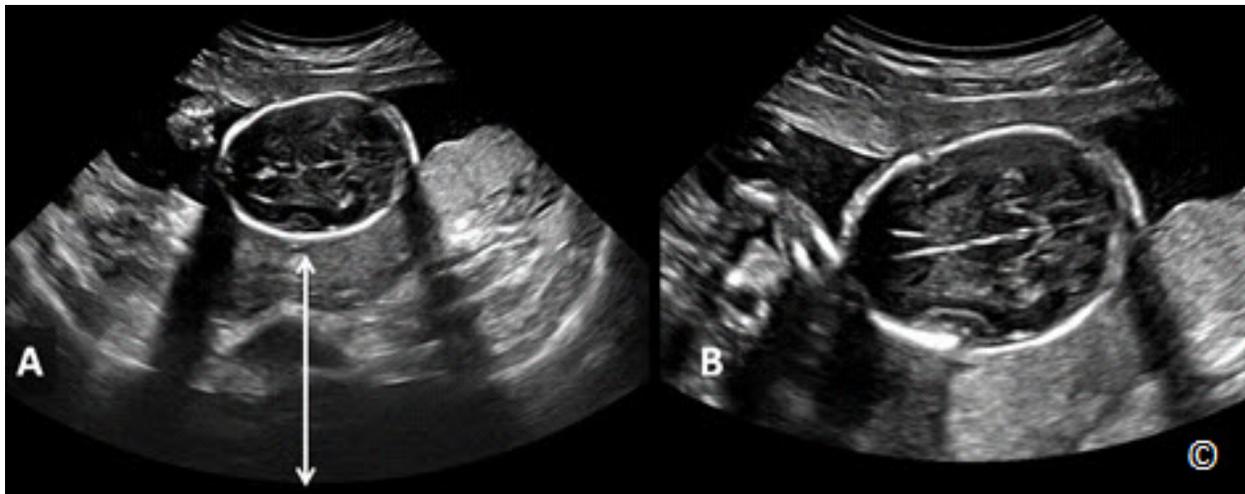
Figure 2.10 A and B: Figures A and B represent transverse view of the same fetal head at the level of the biparietal diameter. In A, the depth (white double arrow) is increased, resulting in a small head, whose anatomic details are consequently difficult to see. In B, the depth is reduced, which allows for a larger head thus improving visualization.

Figure 2.11 A and B: Figures A and B represent transverse view of the same fetal head at the level of the cerebellum. In A, the gain is too low and in B, the gain is adequate. Note better visualization of intracranial anatomy with a higher gain (B). Adjusting the gain to the correct level comes with experience.

Time Gain Compensation (TGC): The Time Gain Compensation (TGC) allows adjustment of brightness at a specific depth of the image. The upper knobs increase or decrease brightness closer to the transducer footprint and the lower knobs increase or decrease brightness farthest from the transducer footprint. **Figure 2.12** shows the TGC location on one of the ultrasound machine console. As a general rule, in transabdominal ultrasound, the upper field gain knobs should be kept slightly to the left than lower field ones (in this way the eye of the operator can focus on the deeper part of the screen where the fetus is). The reverse is true with transvaginal ultrasound, where the region of interest is often in the near field.

Figure 2.12: Time Gain Compensation (TGC) on an ultrasound consol. The upper and lower knobs adjust brightness in the upper and lower fields respectively (labeled). The overall knob (labeled) adjusts brightness in the whole image.

Focal Zones: The focal zones should always be placed at the depth of interest on the ultrasound image in order to ensure the best possible lateral resolution. Multiple focal zones can be used to maximize lateral resolution over depth; however this will result in a slower frame rate and is thus less desirable when scanning moving structures such as in obstetrics or the fetal heart specifically.

Freeze: The freeze knob allows the image to be held (frozen) on the screen. While the image is frozen measurements can then be taken and organ annotations can be applied to the image before saving it. Furthermore, the option to "cineloop" (scroll) back to previous time frames is an option that is available on most ultrasound equipment. This is a very important function in obstetric ultrasound imaging, as it assists in capturing frames during fetal movements, such as measurement of long bones.

Trackball: The Trackball or Mouse pad is used for moving objects on the monitor and for scrolling back in freeze mode. It has a multi-function and can be used in conjunction with caliper placement, screen annotation, or moving the zoom or Doppler boxes to the desired location.

Res or Zoom: Some ultrasound equipment has this function, which allows magnification of areas of the ultrasound image displayed on the monitor in real time. The trackball is used in conjunction with the Res/Zoom knob to choose the area for magnification.

2-D: The 2-D knob stands for the 2-D mode of scanning or the traditional B-mode imaging. B stands for brightness (mode). In this mode, the image is displayed in grey scale and is comprised of pixels arranged in a sector or linear fashion with various shades of grey thus representing the

intensity of the returning signal (**Figure 2.13**). When the operator presses this knob, the traditional 2-D image is activated. This knob is also used to get back to grey scale imaging from color Doppler and/or Pulsed Wave Doppler.
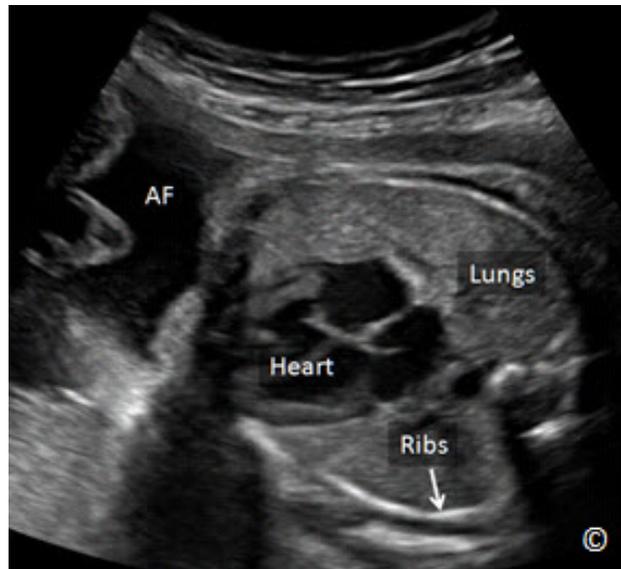

Figure 2.13: Two-dimensional ultrasound image of the fetal chest at the level of the four-chamber view. Note the various gradation of grey with the ribs being the brightest (echogenic) followed by the lungs and heart (labeled). The amniotic fluid (AF) is black in color (anechoic) reflecting a weak intensity of the returning echo.

M-Mode: The M-Mode knob activates the M-Mode function of the ultrasound machine. M-Mode stands for Motion mode and in this function an M-Mode cursor line appears on the upper section of the image with an M-Mode display on the lower part of the image (**Figure 2.14**). The M-Mode display corresponds to the anatomic components that the M-Mode cursor intersects. The M-Mode is used primarily to document motion, such as cardiac activity of the fetus in early gestation (**Figure 2.15**).
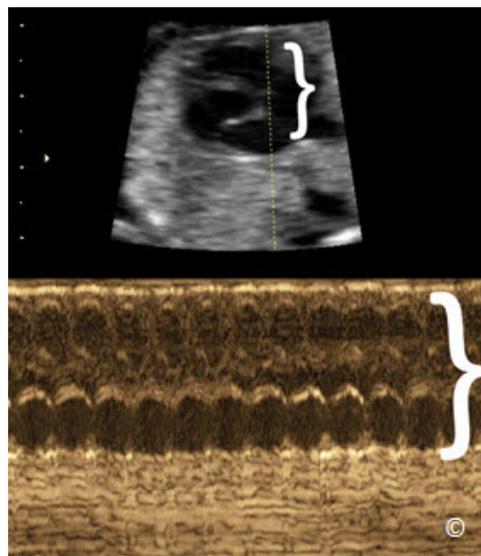
Figure 2.14: M-Mode cursor line (dashed line) is shown through the fetal heart (small bracket) in the upper image. Note the corresponding M-Mode display (large bracket) in the lower image showing cardiac motion.
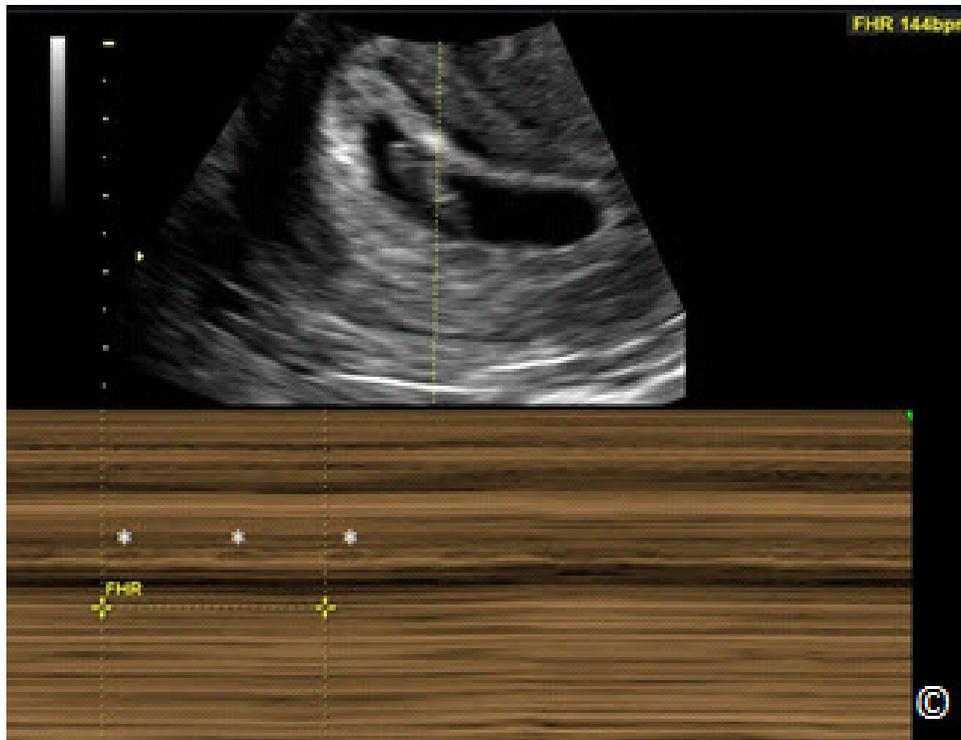
Figure 2.15: M-Mode applied in the first trimester for documentation of fetal heart activity. Reflections in the M-Mode tracing (asterisks) represent cardiac motion. Calipers are measuring fetal heart rate (FHR) at 144 beats per minute (bpm).

Color Flow: The color flow knob activates color flow or color Doppler, which adds a box superimposed on the 2-D real-time image on the screen. The operator can control the size and location of the color box on the 2-D image. Color flow or color Doppler detects blood flow in the insonated tissue and assigns color to the blood flow based upon the direction of blood flow. By convention, red is assigned for blood flow moving in the direction of the transducer (up) and blue is assigned for blood moving in the direction away from the transducer (down). The operator can also control the velocity scale of blood flow (pulse repetition frequency) and the filter or threshold of flow. These parameters are important in assessing various vascular beds. Note that the display of color flow follows the physical principles of Doppler flow and thus if the ultrasound beam is perpendicular to the direction of flow, color Doppler information will not be displayed on the monitor (see chapter 1 for details). Newer ultrasound equipment tries to overcome this limitation by providing other means for display of blood flow such as **Power Doppler** which primarily relies on wave amplitude and **B-flow** (not to be confused with B-Mode) both of which are relatively angle independent.

Pulsed Wave Doppler: The pulse wave Doppler (Pulsed Doppler) or **Spectral Doppler** knob activates the pulse Doppler display. In this display a cursor line with a gate appears in the upper half of the screen and a pulse or spectral Doppler display appears in the lower half of the screen **(Figure 2.16)**. The pulsed wave Doppler gate can be moved by the operator and placed within a vessel as imaged by color Doppler. Typically, this mode is activated when a vessel is first identified or suspected and after color flow Doppler is activated. Pulsed Doppler allows obtaining specific quantitative information about a vessel such as S/D ratio of the umbilical

artery (**Figure 2.17**). Flow towards the transducer is displayed above the baseline and flow away from the transducer is displayed below the baseline. The operator has the option to invert the display of the Doppler spectrum in order to display the waveforms above the line **(Figure 2.16)**. See chapter 1 for more details.
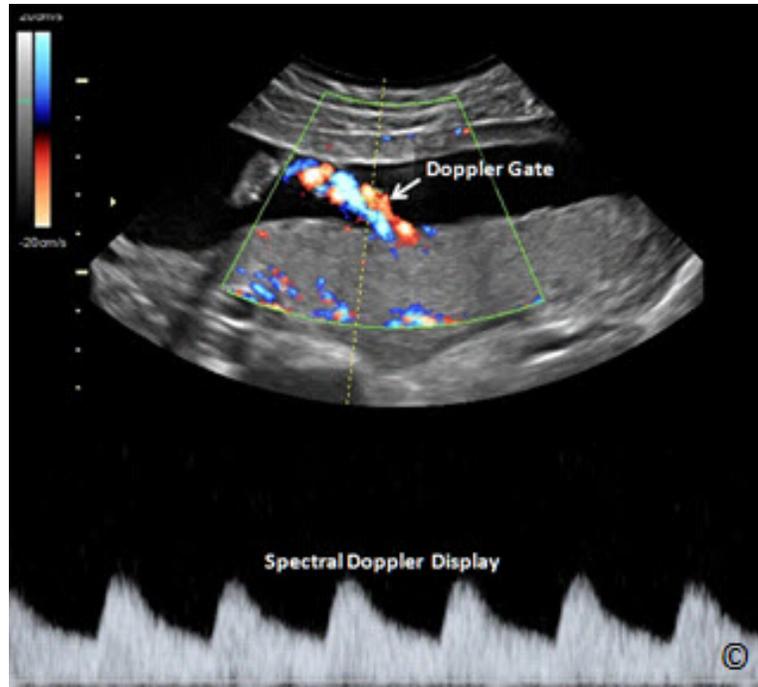

Figure 2.16: Pulsed wave Doppler of the umbilical artery. Note that the Doppler gate is placed within the umbilical artery as seen in the upper part of the image and the spectral Doppler waveform is displayed in the lower part of the image. The spectral Doppler is inverted to display the waveforms above the line.
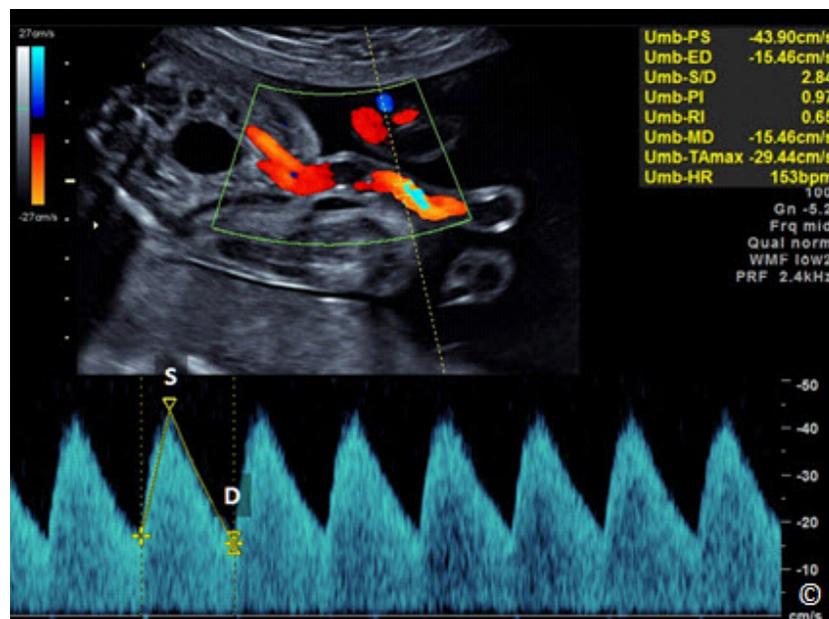
Figure 2.17: Pulsed wave Doppler of the umbilical artery at the abdominal insertion. Doppler waveforms are shown in blue color. S stands for flow at peak systole and D stands for flow at end diastole. Note the Doppler indices in the right upper corner of the image (yellow). For more details, refer to Chapter 1.

Measurement: The measurement function or knob can also be displayed as Measure or Cal (Calculation) on the ultrasound console. This function allows the operator to measure, in different formats, various objects on the screen. When the measure button is pressed, a caliper appears on the screen. Use the trackball to move the caliper to the desired location and set it. Once set, a second caliper appears, which can be set in similar fashion. Stored normograms within the ultrasound equipment allow for determination of gestational age and estimation of fetal weight when various fetal biometric parameters are measured.

STARTING AN EXAMINATION

Before starting an ultrasound examination, it is important to ensure that essential information about the patient is entered into the ultrasound equipment in order to be able to save ultrasound images on the hard drive of the ultrasound machine, accurately calculate gestational age in pregnancy and print ultrasound images for documentation purposes. Minimal relevant information that is required to be entered includes the patient's name, date of birth and first day of the last menstrual period. On many ultrasound equipment, a knob identified as "Patient or Start" leads you to this screen where this information can be entered (**Figure 2.18**). If you do not enter this information or any other patient identifier at the initiation of your examination (patient name); most ultrasound systems will not allow you to print or save an image from your examination.

Figure 2.18: Consol of an Ultrasound equipment showing the knob identified as "Patient" (white circle), which leads you to a screen on the monitor (not shown) where patient identifiers are entered before initiating the ultrasound examination.

When a patient returns for a follow-up examination, modern ultrasound equipment allows you to retrieve the patient information automatically without a need to reenter the data.

DOCUMENTING AN EXAMINATION

An ultrasound report is required at the conclusion of the ultrasound examination. Chapter 15 details the parameters of an ultrasound report in obstetrics and gynecology. It is important to know that image documentation is an essential component of the ultrasound examination and report. Images can be produced in paper format or stored digitally on the ultrasound equipment. Several ultrasound systems have knobs for images, which can be formatted to allow for printing on a thermal printer and for saving a digital copy in a DICOM format on the equipment hard drive. The operator also has the option of downloading and saving a study on an external hard drive or a USB jump drive. This is an important function in the low-resource setting as it allows for exchange of cases for educational and consultative function. Typically these knobs can be formatted for these functions, such as for thermal paper printer, for saving on the hard drive and for downloading to the USB outlet. A permanent copy of the ultrasound report, including ultrasound images, should be kept and stored in accordance with national regulations.

References:

1) American Institute of Ultrasound in Medicine (AIUM) Guidelines for Cleaning and Preparing Endocavitary Ultrasound Transducers Between Patients (Approved 6/4/2003) – http://www.aium.org/officialStatements/27

INTRODUCTION

Ultrasound is an operator dependent imaging modality, and thus the quality of the ultrasound examination is dependent in large part on the skills of the operator. The technical aspects of the ultrasound examination in obstetrics and gynecology are not standardized, and the operators develop their own ultrasound skills and approach to the ultrasound examination based upon their own experience and habits. Understanding some basic principles and technical aspects of the ultrasound examination will undoubtedly improve the quality of the examination and reduce repetitive stress injuries. In this chapter, we present the technical aspects of the ultrasound examination with a focus on obstetrics. The approach to the performance of the transvaginal pelvic ultrasound examination is discussed in details in Chapters 11 and 14 and a standardized approach to the performance of the basic obstetric ultrasound examination is presented in chapter 10.

PREPARING THE PATIENT

The obstetric ultrasound examination is best performed with the patient on a comfortable scanning (ultrasound) table or stretcher with the patient's upper torso slightly inclined upward and the head supported by a soft pillow for comfort (**Figure 3.1**). If the ultrasound table does not incline, placing a pillow behind the patient's upper chest will improve comfort. Typically ultrasound tables have a retractable section beneath the legs with stirrups, which allow for the performance of a transvaginal ultrasound examination if needed (**Figure 3.2**). If a retractable portion and/or stirrups are not available, elevating the patient's buttocks with pillows or an inverted bedpan allows for the performance of the transvaginal ultrasound examination when needed (**Figure 3.3**). It is important to place the patient closer to the side of the table where the ultrasound machine is located (typically to the right side of the patient) as this will minimize reaching-over by the operator's arm, which improves ergonomics. Having a support pillow at the edge of the table where the operator's elbow rests will minimize tension on the operator's arm and shoulder and thus reduce the likelihood of repetitive stress injuries during the ultrasound examination (**Figure 3.4**). An alternate approach is to rest the operator's elbow on the patient's right thigh during the ultrasound examination (**Figure 3.5**).

Figure 3.1: The optimal position of the patient on the examination table. Note that the patient's upper torso is slightly inclined upward (arrow) for comfort.
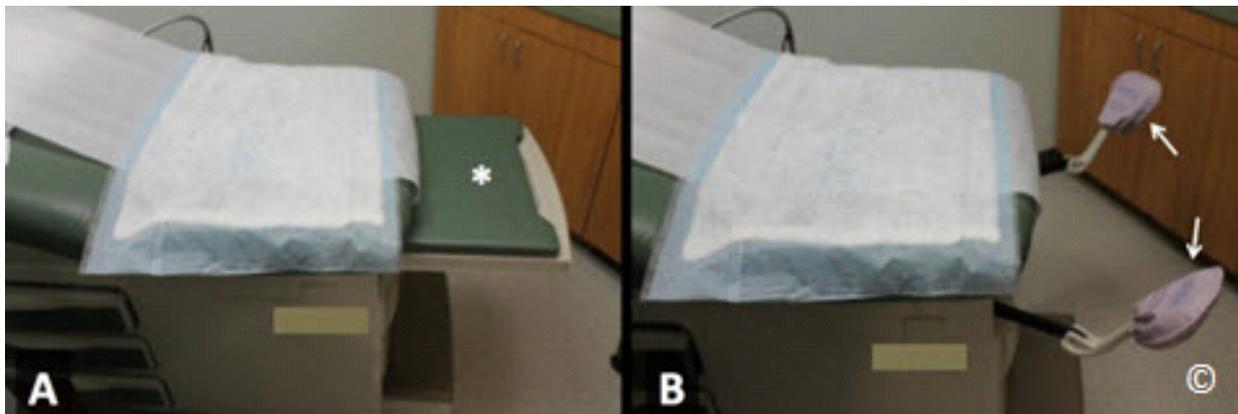
Figure 3.2: Ultrasound examination table showing a retractable section in A (asterisk), and the stirrups in B (arrows) that allow for the performance of a transvaginal ultrasound examination if needed.

Figure 3.3: A folded bed sheet is placed to elevate the patient's (mannequin in this figure) buttocks (arrows) for a transvaginal ultrasound examination if an ultrasound table's retractable portion and/or stirrups are not available.

Support Pillow

Figure 3.4: Note the support pillow (labeled) at the edge of the table (asterisk) for support of the operator's elbow during ultrasound examination.

Figure 3.5: Note the ultrasound operator's elbow resting on the patient's thigh (arrows). This provides support and minimizes repetitive stress injuries.

Patients do not need to wear a special gown for the ultrasound examination but they should be provided with a towel (paper or linen) or a sheet to protect their clothes and for modesty (**Figure 3.6**). In some low-resource settings, patients may bring their own towels to the ultrasound examination. The ultrasound gel is water-based and typically does not stain, but it does wet clothes, which is unpleasant. Asking the patient to have a full bladder is generally not required anymore with modern ultrasound equipment. If the uterus is deep in the pelvis, in the first and early second trimester, and/or is obstructed by bowel gas, a transvaginal ultrasound should be performed when feasible for better visualization of gestational sac and adnexae.
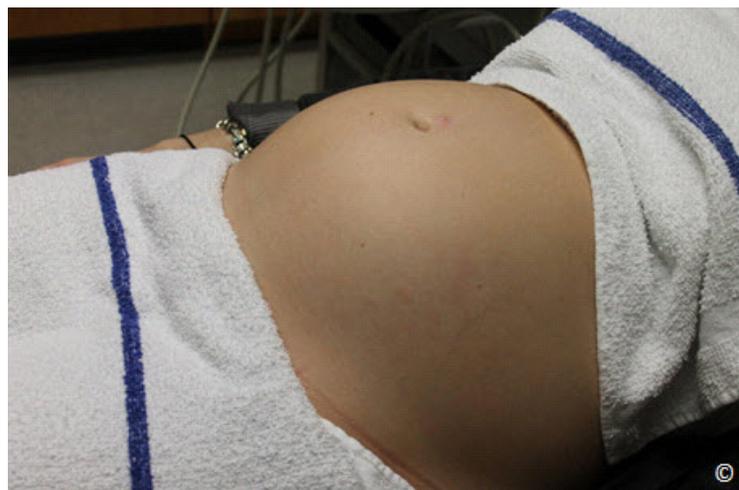
Figure 3.6: Patient preparation for an ultrasound examination. Note the placement of towels to protect the patient's clothes and for modesty.

APPLYING THE COUPLING AGENT

The coupling agent, either a gel or oil, eliminates the air interface between the transducer and the patient's skin (see chapter 1) . Gels are more convenient than oil, because the latter tends to stain and is more difficult to wipe off. But in low-resource countries where obtaining ultrasound gel is either expensive or impractical, regular cooking oil does an excellent job. When applying the gel, remember to use as little as possible, as scanning through a thick layer of gel tends to degrade the quality of the image by interposing numerous micro bubbles that are contained within the gel. All brands of gel are equally suited for sound transmission, but if you make lengthy examinations, try to select one that does not dry too fast. Other products that can degrade the ultrasound image include creams that the patient may have applied on her abdomen before the ultrasound examination. For instance, anti-stretchmark creams may contain chemicals that deteriorate sound transmission. Manufacturers market gel heaters for the purpose of easing patient discomfort, but an inexpensive baby bottle warmer will do as well.

POSITIONING THE OPERATOR/EQUIPMENT

There are 2 main operator positions for the performance of the obstetric ultrasound examination: standing or sitting. The standing position (**Figure 3.7**) minimizes pressure on the operator's shoulder and elbow and maintains the shoulder joint in an adducted position. Although this position minimizes repetitive stress injuries, it is somewhat uncomfortable for long examinations. The sitting position (**Figure 3.8**) allows for more comfort during the examination and is also a better station from which to manipulate the keyboard of the machine. In the sitting position, it is critical to ensure that the chair is high enough and the table is at a lower level in order to minimize reaching over with the transducer and to allow for minimal abduction of the operator's shoulder joint during scanning **(Figure 3.8)**. When performing an ultrasound examination, face the screen as perpendicularly as possible in order to avoid perception and distortion artifacts, especially with newer ultrasound monitors. For example, a biparietal diameter can be difficult to measure when you look at the screen obliquely. Work in dim light to help avoid reflections on the screen.

Figure 3.7: The standing position minimizes pressure on the operator's shoulder and elbow and maintains the shoulder joint in an adducted position.

Figure 3.8: The sitting position allows for more comfort during the examination and is also a better station from which to manipulate the keys of the machine.

MINIMIZING REPETITIVE STRESS INJURIES

Repetitive stress injuries affecting the neck, shoulder, elbow and wrist are common in busy ultrasound practitioners. To avoid repetitive stress injuries pay attention to the following factors:

Posture

Position your ultrasound equipment and the patient such that the posture you hold is comfortable. Do not lean or bend over the patient and, avoid reaching over, especially in obese patients, during transabdominal (**Figure 3.9**) or transvaginal ultrasound examinations. Stand close to the patient and if not sitting, use the bed as a support to lean onto. If you are sitting, use a chair high enough, with a footrest. Position the patient close to the side of the table next to the ultrasound equipment which should be close enough to allow you to rest your "keyboard-hand" on the ultrasound console, instead of having to reach out each time. It is also important to place your non-scanning hand (typically left hand) on the freeze knob in order to freeze the image immediately when the desired target anatomy is viewed. Support your elbow of your scanning arm during the examination with a support pillow placed on the edge of the table or on the patient's thigh as shown in **Figures 3.4 and 3.5**.
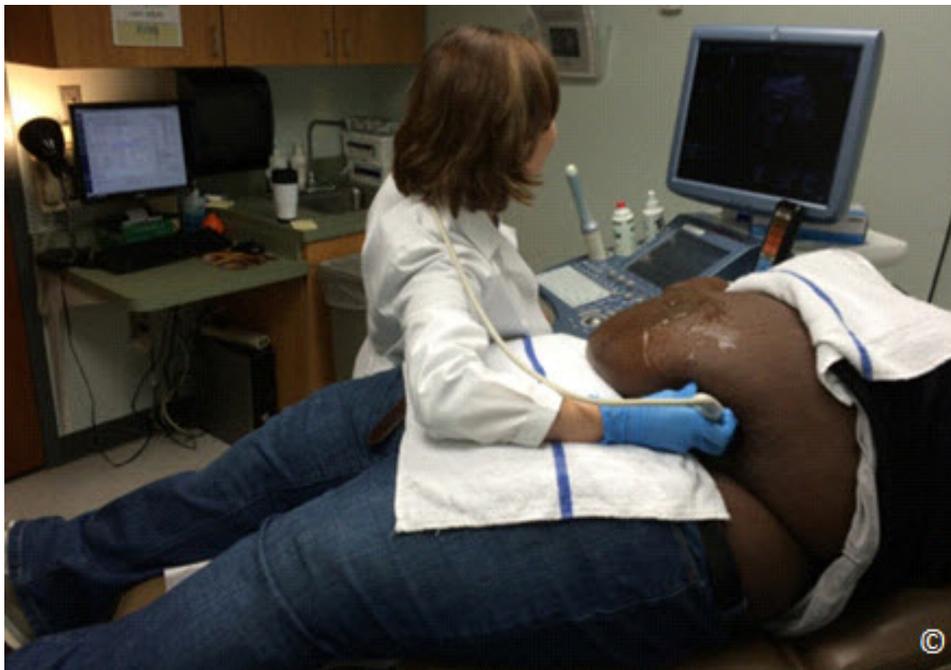
Figure 3.9: Reaching over the abdomen for an ultrasound examination in an obese woman. This should be avoided in order to minimize repetitive stress injury.

Ambient Light

Dim the ambient light so that there is no glare on the screen, yet enough light to find the keys on the keyboard easily. Diming the ambient light is also important to allow you to optimize the ultrasound gain. In bright light, users tend to "over gain" the images and this "washes away" the subtle signals in the lighter part of the screen.

The Monitor

Position the monitor of the ultrasound equipment such that its display is at eye-level and perpendicular to your line of sight. Newer ultrasound equipment have flat panels for monitors, which are commonly on adjustable arms. It is usually simple to add a second monitor for the patient to view the examination. This will also avoid having the patient twist on the ultrasound table to look at the monitor on the ultrasound machine, as this may tense abdominal musculature and impair the examination. The second monitor may be connected either from a video port or a digital port.

HOLDING THE TRANSDUCER AND IMAGE ORIENTATION

Abdominal ultrasound transducers come in various shapes and sizes and are customized to specific study types and indications (see chapter 2 for details). In general, the curvilinear transducers are best adapted to obstetric scanning as they conform to the abdominal curvature in pregnancy (**Figure 3.10**). Larger transducers are harder to manipulate then smaller ones, but when they provide special functions such as 3D, our experience has been that users will tolerate the added bulk.

Figure 3.10: Curvilinear transducer being used in obstetrical scanning.

Figure 3.11 shows our preferred way of holding the transducer. The transducer should be held in the operator's scanning hand in a comfortable way and with minimal pressure on the wrist and phalangeal joints. It is important that the transducer rests (fills) the palm of the hand and the fingers hug the body of the transducer with minimal pressure (**Figure 3.11**). In this position, the thumb and fingers allow for the greatest precision of movements, such as sliding, rotating or angling, with minimal tension on the wrist. Note that the transducer is held very close to its footprint. Holding the transducer with the thumb and fingers at mid-body (**Figure 3.12**) forces the operator to use wrist motion, which increases the chance of repetitive stress injury and does not allow for fine transducer manipulation. Finally, holding the transducer near its cable end (**Figure 3.13**) is least effective as it requires elbow and shoulder motions and thus results in significant fatigue.

Figure 3.11: Our preferred way of holding a transducer. The transducer is held in the palm of the hand with minimal pressure on the wrist and phalangeal joints

Figure 3.12: Holding the transducer with the thumb and fingers at mid-body should be avoided, as it involves wrist motion for manipulation and thus may result in repetitive stress injury.

Figure 3.13: Holding the transducer with the thumb and fingers near its cable end is least effective as it involves elbow and shoulder motion for manipulation and thus may result in repetitive stress injury.

All transducers have a mark/notch that distinguishes one side from the other. In holding the transducer transversely, the mark on the transducer should be to the patient's right side (**Figure 3.14**) and if the transducer is held in a longitudinal orientation, the mark should be towards the uterine fundus (patient's head) (**Figure 3.15**). This orientation allows for the display of the right side of the patient's abdomen in transverse scanning and the upper part of the patient's abdomen in longitudinal scanning on the right side of the monitor (left side of the operator facing the monitor). Besides facilitating interpretation of your ultrasound images by others, there are advantages to sticking to these simple rules: The position of the fetus and placenta can be evaluated with a quick glance at the ultrasound images and spatial orientation is greatly facilitated.

Figure 3.14: When holding the transducer transversely, the mark on the transducer (labeled) should be to the patient's right side (labeled).

Figure 3.15: When holding the transducer longitudinally, the transducer mark (labeled) should be towards the uterine fundus (patient's head) (labeled).

The transducer cable should be supported in order to provide minimal pull (eliminate drag) during scanning. On many occasions, the cable can be supported in the transducer holder during scanning (**Figure 3.16**). Check that the cable is not too rigid, which may interfere with the ease of transducer manipulation. The transducer should be placed gently on the patient's abdomen with minimal pressure. Applying abdominal pressure with the transducer will not improve image quality and is uncomfortable for the patient and for the operator. Furthermore, transducer pressure on the abdomen may result in fetal bradycardia in some instances. The only instance where "digging" the transducer is justified is in late pregnancy, when the fetal head is low in the pelvis and evaluation of head anatomy and biometry is difficult.

Figure 3.16: In order to minimize pull on the transducer, the transducer cable should be supported as shown in this figure (labeled).

ULTRASOUND SCANNING TECHNIQUES

Understanding that ultrasound is an operator dependent imaging modality, there are some scanning techniques that can improve your image and maximize visualization of fetal anatomy and adnexal structures. We have selected here some scanning techniques that the authors use on a daily basis in their busy practice.

Select the appropriate ultrasound transducer and settings

It is important to start your ultrasound examination by selecting the appropriate ultrasound transducer and "presets" for the study. Transducers have various footprint sizes and Megahertz (MHz) ranges. Some are adapted for the first trimester and others for the third trimester when depth is critical. For more details on properties of transducers, see chapter 2. Furthermore, ultrasound machines have manufacturer-established presets that optimize resolution and frame rate for various types of study. It is important that you familiarize yourself with the presets and choose the right preset for the right study. It is advisable to have a session with the ultrasound company's application specialist when a new ultrasound machine is bought in order to customize yourself with the manufacturer's presets and the functionality of the equipment.

Apply minimal pressure on the abdomen

Learn to scan while applying minimal pressure on the patient's abdomen. There are several advantages to this technique including minimizing the patient's discomfort and reducing possibility of stress injury on the operator's wrist and elbow. Furthermore, applying minimal pressure will allow for a film of amniotic fluid between the anterior uterine wall and the target organ, which enhances visualization (**Figures 3.17 A and B**). The only pressure that is needed is to allow full contact between the ultrasound transducer's footprint and the patient's skin.
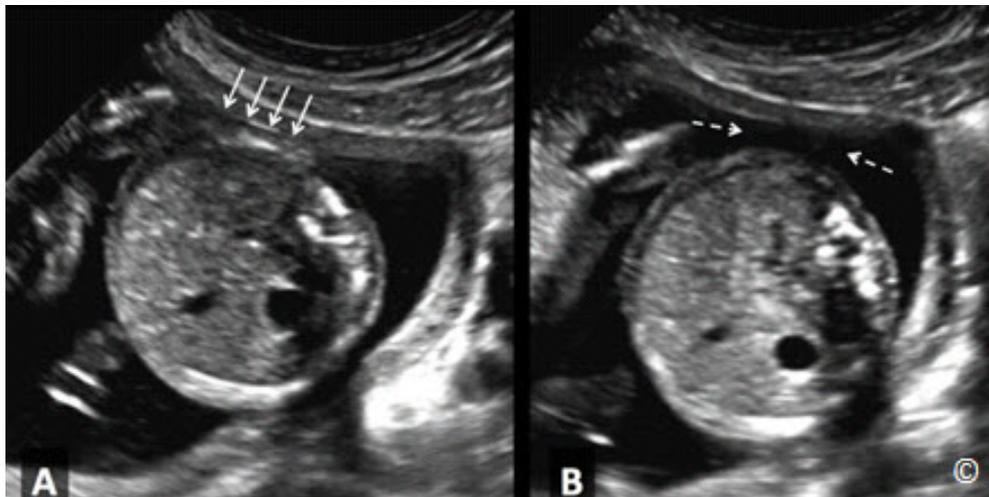
Figure 3.17 A and B: Transverse plane of the fetal abdomen in the second trimester of pregnancy. In A, increased pressure is applied on maternal abdomen resulting in compression of the fetal abdomen (arrows). Minimal optimal pressure is applied in B resulting in improved imaging with a film of amniotic fluid between the uterine wall and the fetal abdomen (broken arrows). Furthermore, minimal pressure results in no deformity of the abdominal perimeter, which improves abdominal circumference measurement (in B).

Reduce depth to a minimum

In order to optimize the performance of ultrasound, especially in obstetrics, it is important to minimize the amount of depth on your ultrasound screen (**Figures 3.18 A and B**). This will enhance resolution and frame rate. An image with greater depth requires more processing from the ultrasound equipment, which results in slower frame rate and reduced resolution.
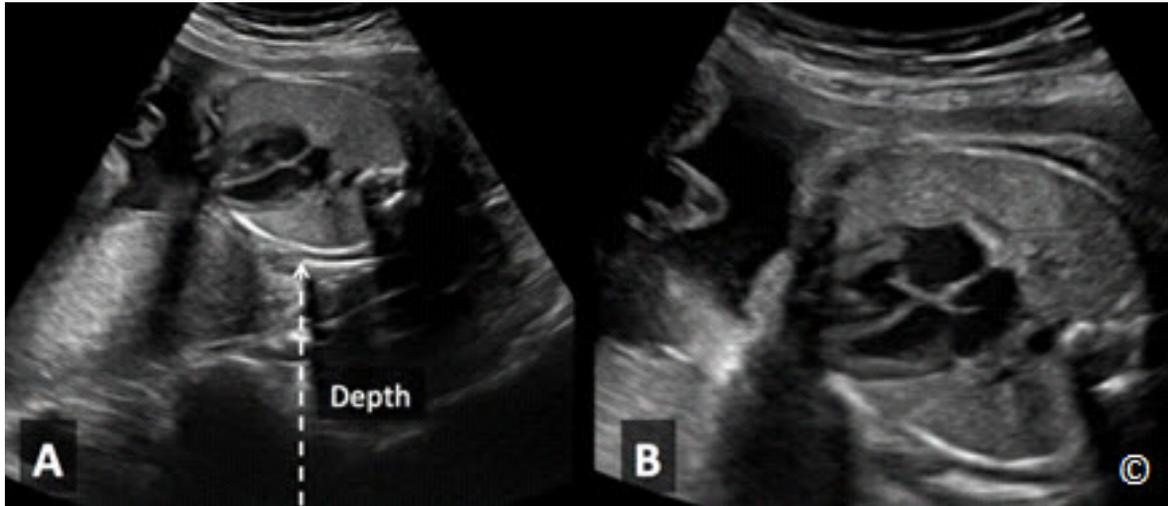

Figure 3.18 A and B: Ultrasound image of the four-chamber view in the second trimester of pregnancy. Note how small the fetal heart is in A, as the depth of the image is not adjusted (arrow). The depth is minimized in B (same fetus) resulting in image magnification. Minimizing depth also improves frame rate (not shown).

Minimize the sector width

Most ultrasound machines have the ability to adjust the sector width on the ultrasound screen. It is important to start your examination with a wide sector width (**Figure 3.19**) and once the target organ is under view, reduce the sector width as much as possible around the target organ (**Figure 3.20**).

Figure 3.19: Transverse view of the fetal head in the second trimester of pregnancy. This shows a wide sector width (arrow), which is the initial approach to image optimization. Once the target organ is under view, reduce the sector width (See **Figure 3.20**).

Figure 3.20: Transverse view of the fetal head of the same fetus shown in figure 3.19. Adequate sector width is applied (arrow). This maneuver optimizes imaging and increases frame rate.

Adjust focal zones

Focal zones should be adjusted to the level of the target organ at study (**Figure 3.21 A and B**). Using multiple focal zones tend to reduce frame rate and thus should be avoided in obstetrical scanning.
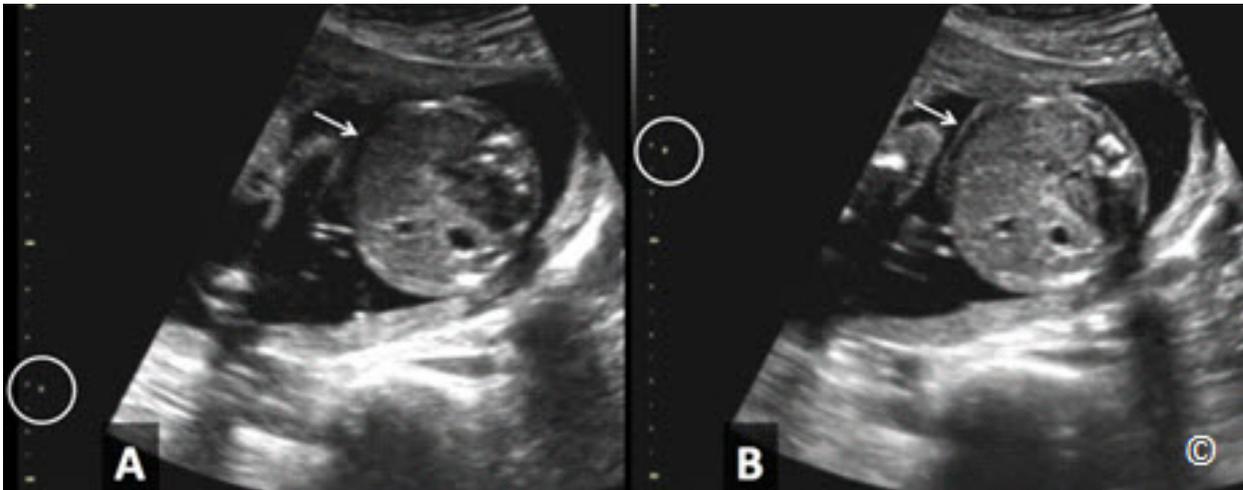
Figure 3.21 A and B: Ultrasound of the transverse plane of the fetal abdomen. In A, the focal zone is erroneously applied below the target organ (circle). Note the improved lateral resolution (arrows – compare A to B) of the target organ (abdomen) in B where the focal zone is accurately applied (circle).

Zoom area of interest

Once you have adjusted the depth, sector width, and focal zone, magnify the area of interest by selecting the "zoom" option on the ultrasound machine (**Figure 3.22 A and B**). This can be achieved by zooming the whole image, or selecting an area of interest from the image to magnify. It is important to learn to scan with this feature, which allows for the identification of details within target organs. This is especially critical when you are scanning the fetal heart given its complex anatomy and small size (**Figure 3.22-B**).

Note that for many machines there are 2 forms of zoom. One is simply a button that is "rotate" right or left and makes the image bigger or small. The other zoom (often a box that you can position and size over and area) is a "write-zoom", that reconfigures the machine to concentrate more data on that area. Familiarize yourself with both options if available on your ultrasound equipment.
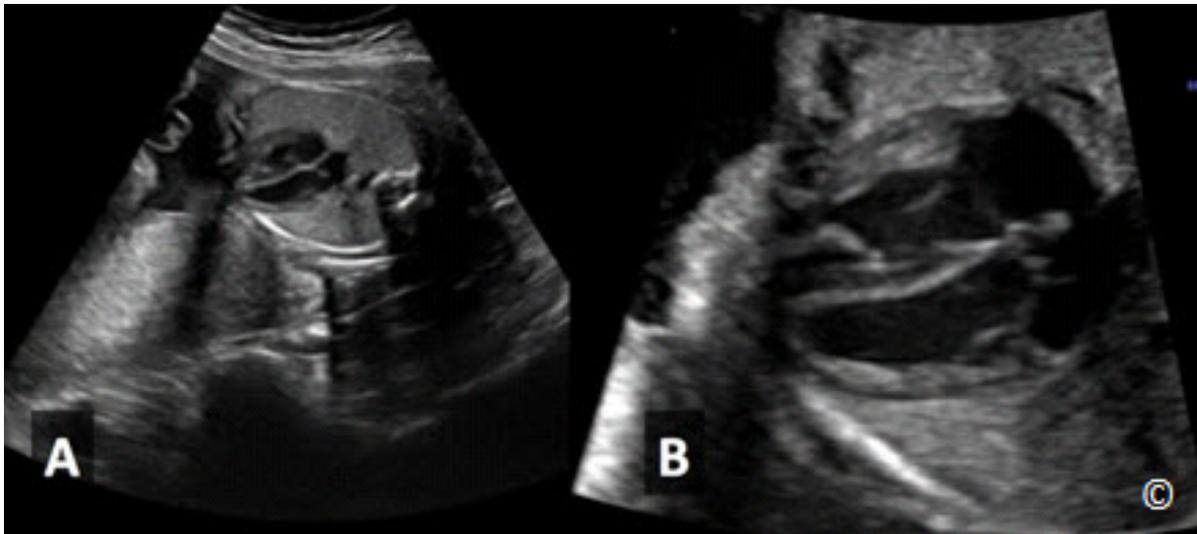
Figure 3.22 A and B: Four-chamber view of the fetal heart without (A) and with (B) magnification in the same fetus. The detailed anatomic features of the heart can be easily recognized in B when compared to A. Image magnification and zoom are important features in cardiac imaging.

Maintain the target anatomic area in the center of the screen

It is important to keep the area of interest in the center of your screen in order to minimize the effect of lateral resolution as the ultrasound resolution decreases significantly from the central area of the image towards each lateral side. Furthermore, this technique allows for the ultrasound beam to insonate the target area in a perpendicular orientation, which enhances visualization (**Figure 3.23 A and B**). The "slide technique", which has not been previously described to our knowledge, allows you to move a target area from the lateral aspect of the image into the center without losing orientation. The slide technique involves sliding the transducer along its long axis as shown in **Clip 3.1 A**. This brings target anatomy from the lateral to the center of the screen while maintaining the same anatomic view and orientation of the target image. **Clip 3.1B** shows the corresponding ultrasound cineloop.
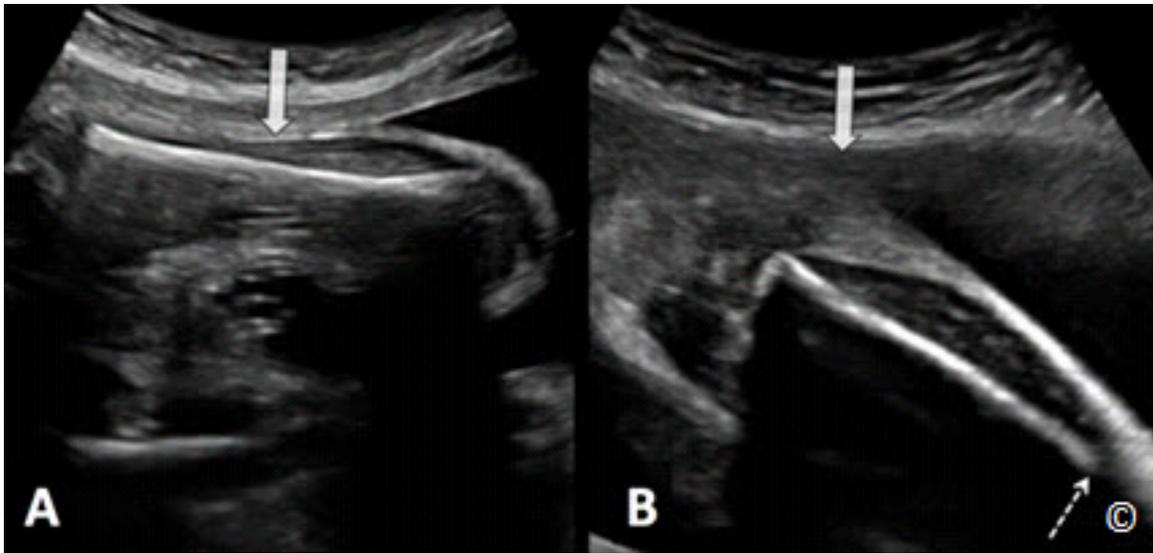
Figure 3.23 A and B: Ultrasound image of a femur in longitudinal view. In A, the femur is in the center of the image allowing for optimal imaging of its borders and thus measurements. In B, the distal portion of the femur is in the lateral aspect of the image resulting in reduced resolution (broken arrow). The solid arrow in A and B shows the direction of the ultrasound beam.

ULTRASOUND SCANNING TECHNIQUES FOR THE OBESE PREGNANT PATIENT

The prevalence of obesity continues to be on the rise, with the most recent estimates reporting obesity in about one-third of the adult population (1), and in more than one half of pregnant women in the United States (2). Obese women are at increased risk for complications during pregnancy, including gestational diabetes, hypertension, and cesarean delivery (3). In addition to maternal complications, obesity also poses risks to the fetus including an increased risk of prematurity, stillbirth, macrosomia, and a higher rate of congenital anomalies (4). Although sonographic screening during pregnancy is recommended for all women, it is particularly relevant in the obese population due to higher rates of structural abnormalities, specifically neural tube defects, heart defects, and abdominal wall defects (5).

Sonographic assessment of fetal anatomy in the obese population is challenging with multiple studies confirming that maternal obesity significantly reduces the likelihood of completion of the anatomic survey, and ultrasound screening is associated with lower detection rates of fetal anomalies (6-9). A recent fetal imaging consensus meeting in the United States, sponsored by multiple societies including the Eunice Kennedy Shriver National Institute of Child Health and Development (NICHD), made specific recommendations for the pregnant obese population, including a targeted ultrasound at 20-22 weeks gestation (approximately 2 weeks later than the usual time period for anatomy survey in the non-obese patients), and a follow up ultrasound exam in 2 to 4 weeks if fetal anatomy could not be completely assessed (10).

The main difficulty that arises when scanning obese pregnant women is the size of the panniculus, which not only significantly increases the distance between the transducer and the fetal target organs, but also scatters the ultrasound beam and thus degrades resolution (**Figure 3.24**). Several ultrasound-scanning techniques, which attempt to reduce the distance between the patient's skin and the fetus, can be utilized to help improve imaging in obese patients (11). The following is a list of techniques commonly used in ultrasound examinations of obese pregnant women:
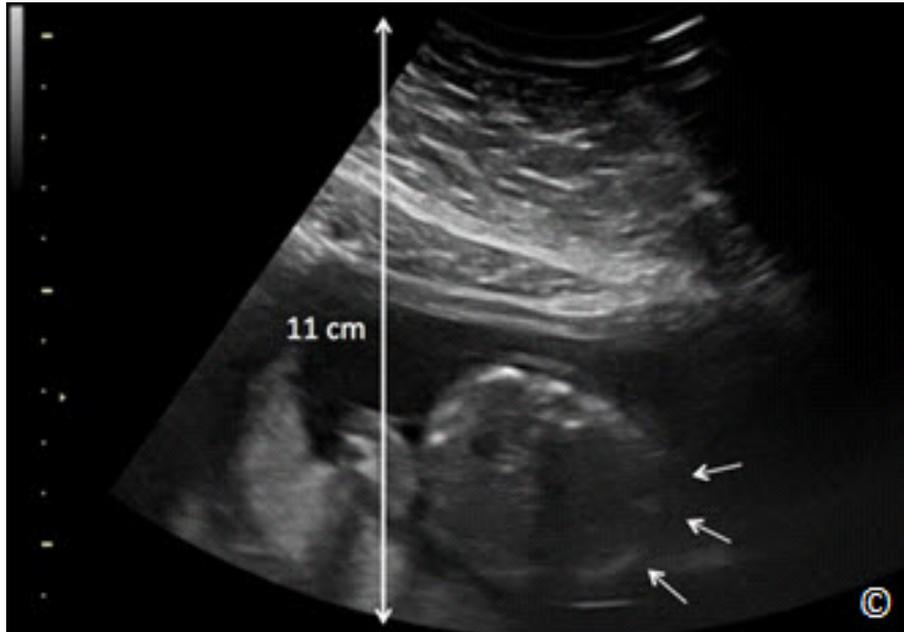
Figure 3.24: Ultrasound image of the fetal abdomen at a depth of 11 cm in an obese pregnant woman. Note the sub-optimal resolution of the right lateral fetal abdomen (small arrows).

Transvaginal ultrasound in early gestation

Ultrasound performed transvaginally between 13 and 15 weeks' gestation may prove to be the most optimal time for imaging of the fetus in obese women with high body-mass index (BMI). Several studies have shown the ability of the "early" ultrasound in documenting fetal anatomy in the general population (12-14) and this approach should be adapted to the obese pregnant women especially those with a high BMI. Further studies however are needed to confirm the feasibility of this approach in the obese population.

Scanning underneath the panniculus

The operator can lift the panniculus with the left hand and scan underneath it with the right hand. This maneuver is tiring however and should not be employed for long scanning time. Alternatively, you can ask an assistant or the patient to hold the panniculus up, as this will reduce the patient's skin to fetus distance in most instances (**Figure 3.25**).

Figure 3.25: Scanning under the panniculus in an obese pregnant woman. In this figure, the patient is holding the panniculus up (arrow) during the examination.

Scanning above the panniculus

The ultrasound examination can be performed above the panniculus in the region of the mid-abdomen while pushing the panniculus down, which may shorten the distance between the skin surface and the fetus (**Figure 3.26**). This maneuver may be improved by filling the patient's bladder, which displaces the uterus cephalad.

Figure 3.26: Scanning above the panniculus in an obese pregnant patient. In this figure, an assistant is pushing the panniculus down (arrow) during the examination.

Using the umbilicus as an acoustic window

The umbilicus can be used as an acoustic window by filling it with ultrasound gel and scanning through it. Alternatively, the transvaginal probe can be used through the umbilicus given its small footprint (**Figure 3.27**). This may allow you to see fetal anatomy more clearly in some obese patients.

Figure 3.27: Scanning through the umbilicus using the transvaginal transducer in an obese pregnant patient. This technique may improve imaging in some obese patients.

Placing the patient in the Sims position

The Sims position involves a position in which the patient lies on the left side with the knee and thighs drawn upward toward the chest. The chest and abdomen are allowed to fall forward. This approach for scanning allows the panniculus to be displaced to the left side. The operator places the transducer on the mother's right flank, groin and right lateral quadrants of the abdomen where the adipose tissue is thin (**Figure 3.28**).

Figure 3.28: Scanning a pregnant obese woman in the Sims position. Note that the woman's panniculus is shifted to the left side. Insonating the uterus from the right lateral quadrant may improve imaging given the presence of less adipose tissue.

CLIP 3.1

CLIP 3.2

References:

1) Center for Disease Control and Prevention; Adult Obesity Facts – http://www.cdc.gov/obesity/data/adult.html
2) Flegal KM, Carroll MD, Kit BK, Ogden CL. Prevalence of obesity and trends in the distribution of BMI among US adults 1999-2010. JAMA 2012; 307: 491-7.
3) Cedergren MI. Maternal morbid obesity and the risk of adverse pregnancy outcome. Obstet Gynecol 2004; 103:219-24.
4) Stothard KJ, Tennant PW, Bell R, Rankin J. Maternal overweight and obesity and the risk of congenital anomalies: a systematic review and meta-analysis. JAMA 2009; 301: 636-50.
5) Watkins ML, Rasmussen SA, Honein MA, Botto LD, Moore CA. Maternal obesity and risk for birth defects. Pediatrics 2003; 111:1152-8.
6) Dashe JS, McIntire DD, Twickler, DM. Effect of maternal obesity on the ultrasound detection of anomalous fetuses. American College of Obstetricians and Gynecologists 2009; 113: 1001-8.
7) Dashe, JS, McIntire DD, Twickler DM. Maternal obesity limits the ultrasound evaluation of fetal anatomy 2009; 28: 1025-30.
8) Fuchs F, Houllier M, Voulgaropoulos A, Levaillant JM, Colmant C, Bouyer J, Senat MV. Factors affecting feasibility and quality of second-trimester ultrasound scans in obese pregnant women. Ultrasound Obstetric Gynecology 2013; 41: 40-46.
9) Hershey D. Effect of maternal obesity on the ultrasound detection of anomalous fetuses, Obstetric Gynecology 2009; 114:694.
10) Reddy UM, Abuhamad AZ, Levine D, Saade GR. Fetal Imaging Executive Summary of a Joint Eunice Kennedy Shriver National Institute of Child Health and Human Development, Society for Maternal-Fetal Medicine, American Institute of Ultrasound in Medicine, American College of Obstetricians and Gynecologists, American College of Radiology, Society for Pediatric Radiology, and Society of Radiologists in Ultrasound Fetal Imaging Workshop. J Ultrasound Med 2014; 33:745–757.
11) Paladini D. Sonography in obese and overweight pregnant women: clinical, medicolegal and technical issues. *Ultrasound Obstetric Gynecology* 2009; 33: 720–729
12) Rossi AC, Prefumo F. Accuracy of ultrasonography at 11-14 weeks of gestation for detection of fetal structural anomalies: a systematic review. Obstet Gynecol. 2013 Dec; 122(6):1160-7.
13) Souka AP, Pilalis A, Kavalakis Y, Kosmas Y, Antsaklis P, Antsaklis A. Assessment of fetal anatomy at the 11-14-week ultrasound examination. Ultrasound Obstet Gynecol. 2004 Dec; 24(7):730-4.
14) Whitlow BJ, Economides DL. The optimal gestational age to examine fetal anatomy and measure nuchal translucency in the first trimester. Ultrasound Obstet Gynecol. 1998 Apr; 11(4):258-61.

INTRODUCTION

First trimester ultrasound is often done to assess pregnancy location and thus it overlaps between an obstetric and gynecologic ultrasound examination. Accurate performance of an ultrasound examination in the first trimester is important given its ability to confirm an intrauterine gestation, assess viability and number of embryo(s) and accurately date a pregnancy, all of which are critical for the course of pregnancy.

Main objectives of the first trimester ultrasound examination are listed in **Table 4.1**. These objectives may differ somewhat based upon the gestational age within the first trimester window, be it 6 weeks, 9 weeks, or 12 weeks, but the main goals are identical. In this chapter, the approach to the first trimester ultrasound examination will be first discussed followed by the indications to the ultrasound examination in early gestation. Chronologic sequence of the landmarks of the first trimester ultrasound in the normal pregnancy will be described and ultrasound findings of pregnancy failure will be presented. The chapter will also display some of the major fetal anomalies that can be recognized by ultrasound in the first trimester. Furthermore, given the importance of first trimester assignment of chorionicity in multiple pregnancies, this topic will also be addressed in this chapter.

TABLE 4.1	Main Objectives of Ultrasound Examination in the First Trimester

- Confirmation of pregnancy
- Intrauterine localization of gestational sac
- Confirmation of viability (cardiac activity in embryo/fetus)
- Detection of signs of early pregnancy failure
- Single vs. Multiple pregnancy (define chorionicity in multiples)
- Assessment of gestational age (pregnancy dating)
- Assessment of normal embryo and gestational sac before 10 weeks
- Assessment of basic anatomy after 11 week

TRANSVAGINAL ULTRASOUND EXAMINATION IN THE FIRST TRIMESTER

There is general consensus that, with rare exceptions, ultrasound examination in the first trimester of pregnancy should be performed transvaginally. The transvaginal transducers have higher resolution and are positioned closer to the uterus, the gestational sac and pelvic organs,

when compared to the abdominal transducers. The closer proximity and higher resolution of the transvaginal transducers allow for excellent anatomic details and recognition of first trimester anatomy (**Figure 4.1**). When inserted gently, the transvaginal ultrasound transducer is well tolerated by most women. **Table 4.2** lists recommended steps for the performance of the transvaginal ultrasound examination.
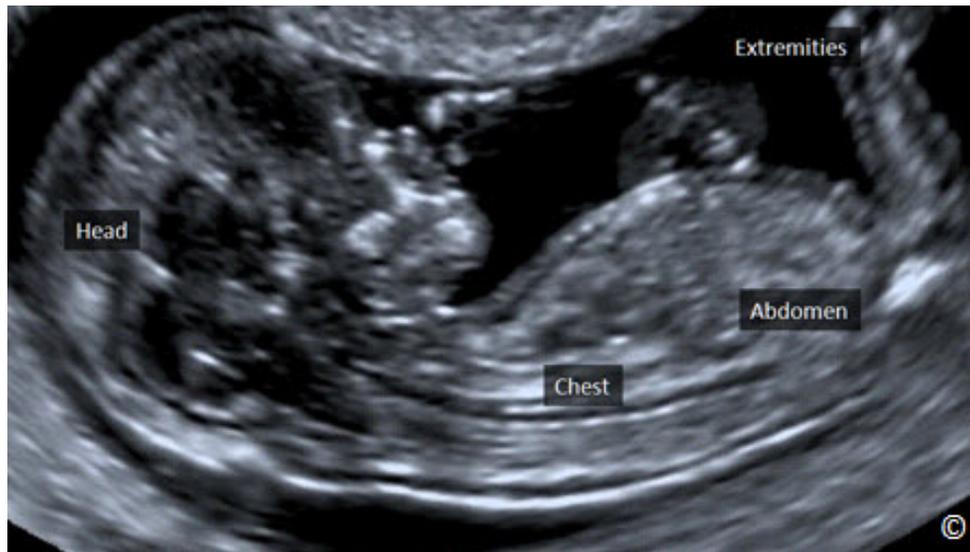
Figure 4.1: Transvaginal ultrasound of a fetus at 12 weeks' gestation in a midsagittal orientation. Note the high level of resolution, which allows for clear depiction of fetal anatomic structures (labeled).

TABLE 4.2	Steps for the Performance of the Transvaginal Ultrasound Examination

- The patient is informed and consented (orally) to the performance of the transvaginal ultrasound examination
- The patient emptied her bladder and is placed in a dorsal lithotomy position or in a supine position with the buttocks elevated by a cushion
- Cover sheet is applied to provide privacy and when possible it is recommended to have a third person (chaperon) present in the room in addition to the patient and examiner
- Check that the transvaginal transducer has been cleaned based upon recommended guidelines, is connected to the machine and is switched on before you start the examination
- Apply gel on the transducer tip, cover with a single-use condom (or latex glove) and apply gel on the outside of the condom, paying attention not to create air bubbles below the cover
- Insert the transducer gently and angle it inferiorly (towards rectum) during insertion into the vaginal canal as this reduces patient's discomfort
- Speak with the patient, explain what you are doing and ask about possible discomfort

The beginning of the examination should be performed in an overview without magnification, trying to visualize the uterus with its position, size, shape, content, as well as the neighboring organs, such as the left and right adnexa, the urinary bladder and the cul-de-sac. Following this overview, the region of interest, e.g. the pregnancy, should be magnified to get the best view and detailed assessment.

INDICATIONS FOR THE ULTRASOUND EXAMINATION IN THE FIRST TRIMESTER

In many parts of the world, first trimester ultrasound examination is often indication-driven (1) unlike the "routine" second trimester ultrasound examination that is commonly performed for fetal anatomic assessment. Indications for the first trimester ultrasound examination vary but typically are related to maternal symptoms. **Table 4.3** lists common indications for an ultrasound examination in the first trimester of pregnancy.

TABLE 4.3	Common Indications for Ultrasound in the First Trimester of Pregnancy
- Amenorrhea (patient does not know she is pregnant) - Pelvic pain - Vaginal bleeding - Unknown menstrual dates - Subjective feeling of pregnancy - Uterus greater or smaller than dates on clinical evaluation - Pregnancy test positive or increased Human Chorionic Gonadotropin (hCG) values - Nuchal translucency measurement	

SONOGRAPHIC LANDMARKS IN THE FIRST TRIMESTER

The normal intrauterine pregnancy undergoes significant and rapid change in early gestation, from a collection of undifferentiated cells to a fetus within an amniotic sac connected to a placenta and a yolk sac. All this change occurs within a span of 3-4 weeks. This significant progression can be seen on ultrasound from a chorionic sac: the first sonographic evidence of pregnancy, to the embryo with cardiac activity. Identifying the ultrasound landmarks of a normal pregnancy in the first trimester, and understanding their normal progression, helps to confirm pregnancy and assist in the diagnosis of pregnancy failure.

Gestational Sac

The gestational sac, also referred to as the chorionic cavity, is the first sonographic evidence of pregnancy. It is first located slightly paracentrically in the decidua and referred to as the "intradecidual sac sign", as the gestational sac is buried in the endometrium (**Figure 4.2**). The gestational sac should not be confused with a fluid accumulation (blood) between the decidual layers (**Figure 4.3 A and B**). This fluid collection in the decidua has been referred to as "pseudosac", especially in the presence of an ectopic pregnancy. The gestational sac on transvaginal ultrasound appears a few days after the menstrual period is missed and is first seen at 4 to 4.5 weeks from the first day of the last menstrual period (LMP). The first appearance of a gestational sac on ultrasound may be difficult to visualize but it has a rapid growth at about 1mm per day. When the gestational sac has a mean diameter of 2 - 4mm, its borders appear echogenic, which makes its demonstration easy (**Figure 4.4**). The echogenic ring of the gestational sac is an important ultrasound sign, which helps to differentiate it from an intrauterine fluid or blood collection. The shape of the gestational sac is first circular but with the appearance of the yolk sac and the embryo it becomes more ellipsoid (**Figure 4.5**). Size, growth and shape of the gestational sac can vary and the mean sac diameter (MSD) is calculated as the arithmetic mean of its greatest sagittal, transverse and coronal planes. A MSD cutoff of ≥25 mm with no embryo is diagnostic of failed pregnancy (**Figure 4.6**). This would yield a specificity and positive predictive value at (or as close as can be determined) to 100% (2). When the MSD is between 16 and 24 mm, the absence of an embryo is suspicious, though not diagnostic, for failed pregnancy (2).
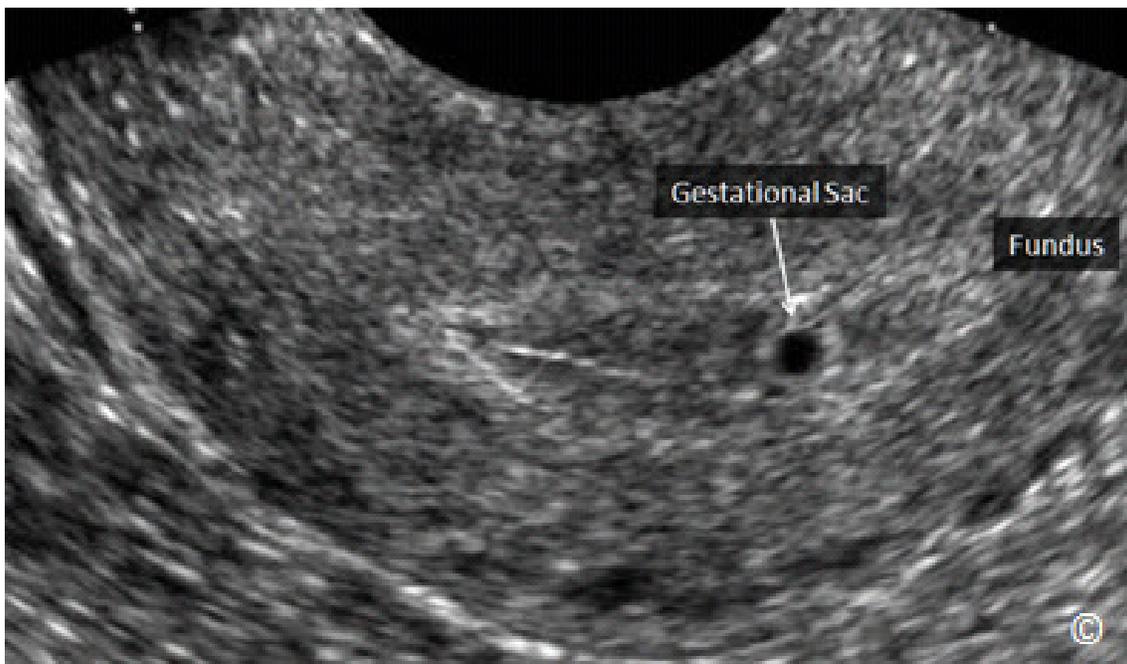
Figure 4.2: Mid-sagittal plane of the uterus showing a gestational sac at 5 weeks' gestation (labeled). Note the paracentric location of this gestational sac within the decidua. The uterine fundus is labeled for orientation.
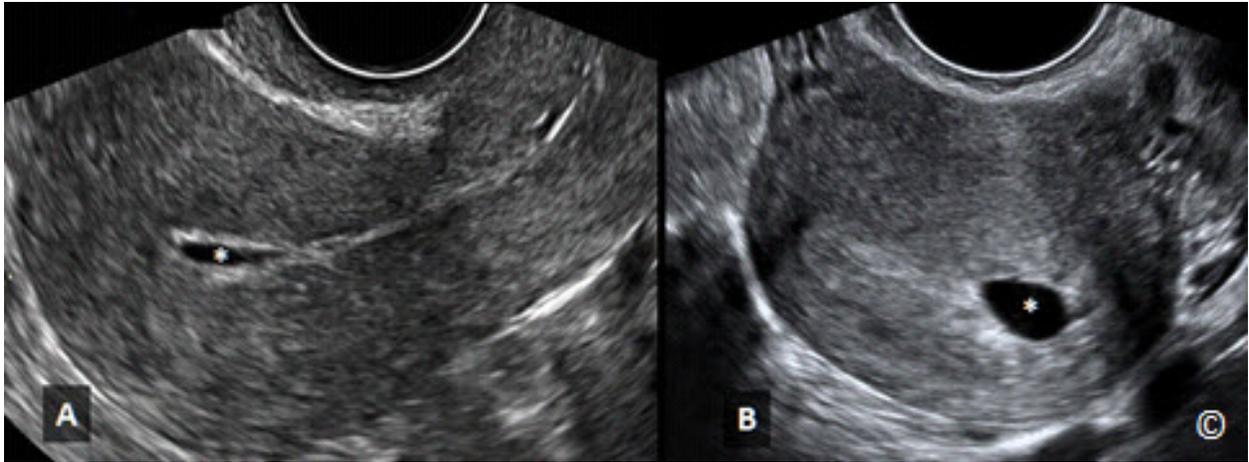
Figure 4.3 A & B: Mid-sagittal (A) and transverse (B) planes of two uteri showing fluid accumulation (asterisk) between the decidual layers (pseudosacs). This finding should not be confused with an intrauterine gestational sac. See text for details.
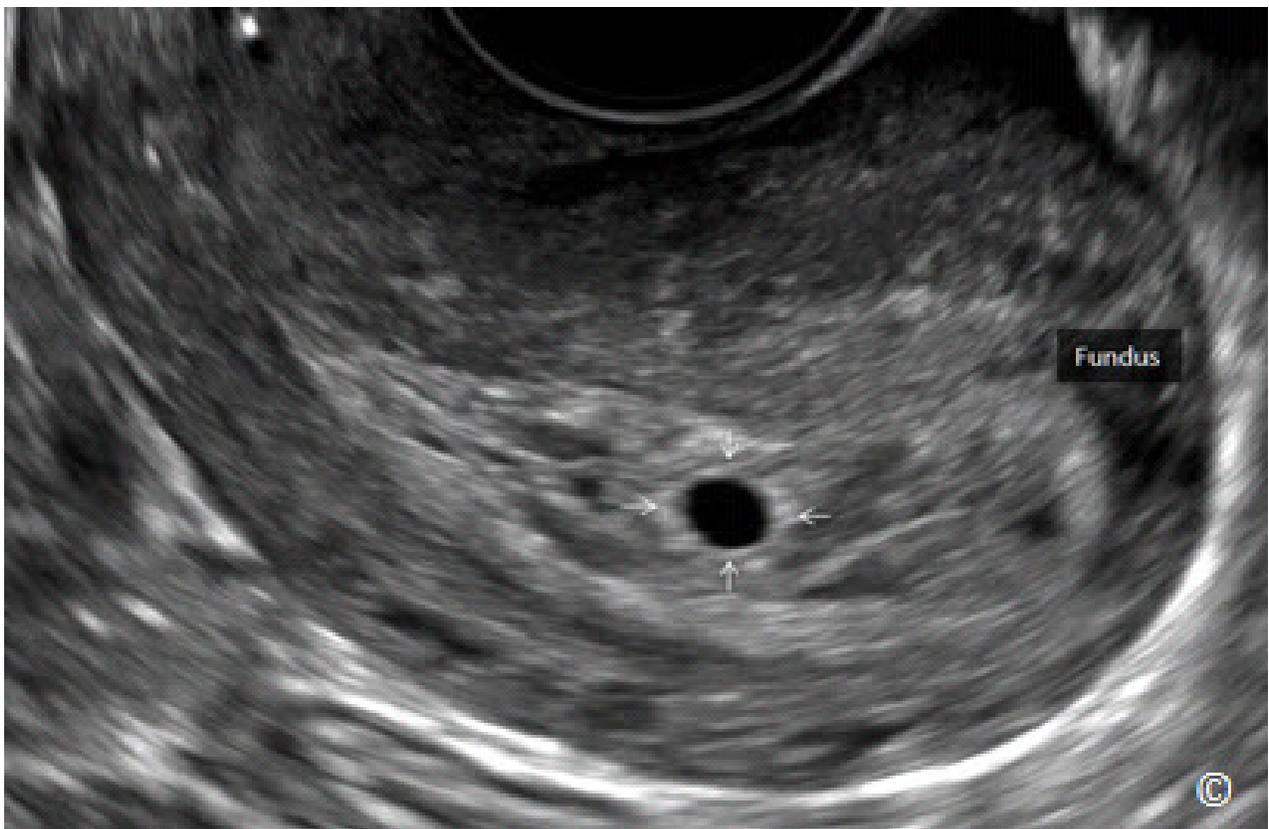
Figure 4.4: Sagittal plane of a uterus with a gestational sac at 4.5 weeks' gestation. Note the echogenic borders (arrows) of the gestational sac. The echogenic borders (ring) of the gestational sac help to differentiate it from an intrauterine fluid or blood collection.
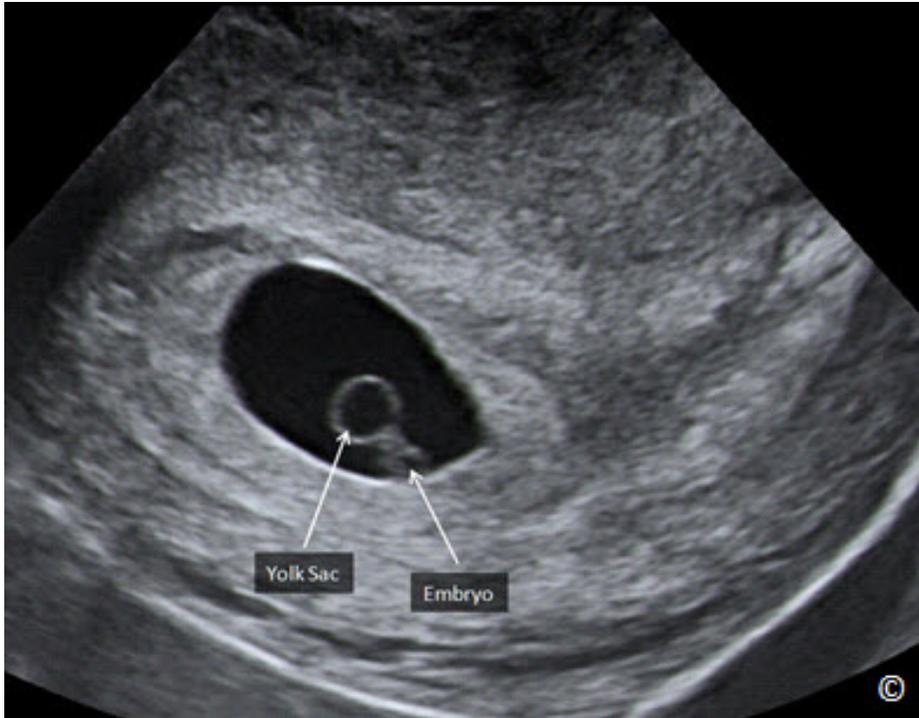
Figure 4.5: Mid-sagittal plane of a uterus with a gestational sac at 6 weeks' gestation. Note the presence of a yolk sac (labeled) and a small embryo (labeled). The shape of the gestational sac is more ellipsoid than circular.
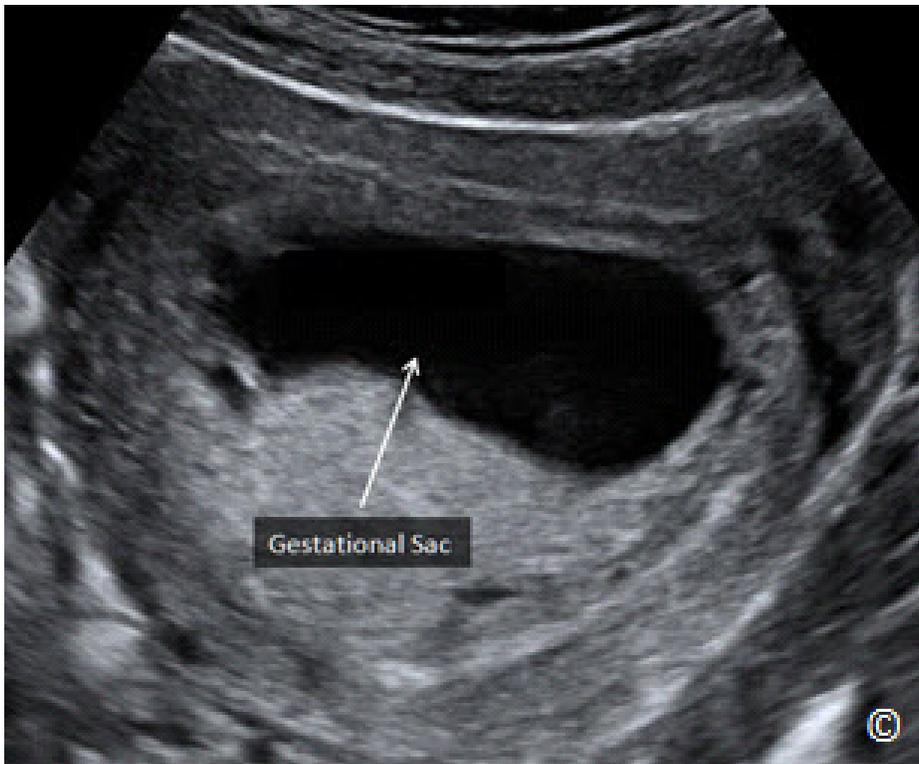
Figure 4.6: A large gestational sac (MSD > 25 mm) with no embryo seen. This is diagnostic of a failed pregnancy.

Yolk Sac

The yolk sac is seen at 5 weeks gestation (menstrual age) on transvaginal ultrasound, as a small ring within the gestational sac with highly echogenic borders (**Figure 4.7**). It is visible at 5 weeks + 5 days gestation. It has a diameter of around 2mm at 6 weeks and increases slowly to around 6mm at 12 weeks. The first detection of the embryo by ultrasound is noted in close proximity to the free wall of the yolk sac, since the yolk sac is connected to the embryo by the vitelline duct (**Figure 4.8**). A small yolk sac with a diameter less than 3mm between 6-10 weeks or a diameter of more than 7mm before 9 weeks are suspicious for an abnormal pregnancy and thus this observation requires a follow-up ultrasound examination to assess pregnancy viability (**Figure 4.9 A and B**).

Figure 4.7: A mid-sagittal plane of a uterus with a gestational sac at 5.5 weeks' gestation. Note the yolk sac seen within the gestational sac (labeled) with highly echogenic borders.
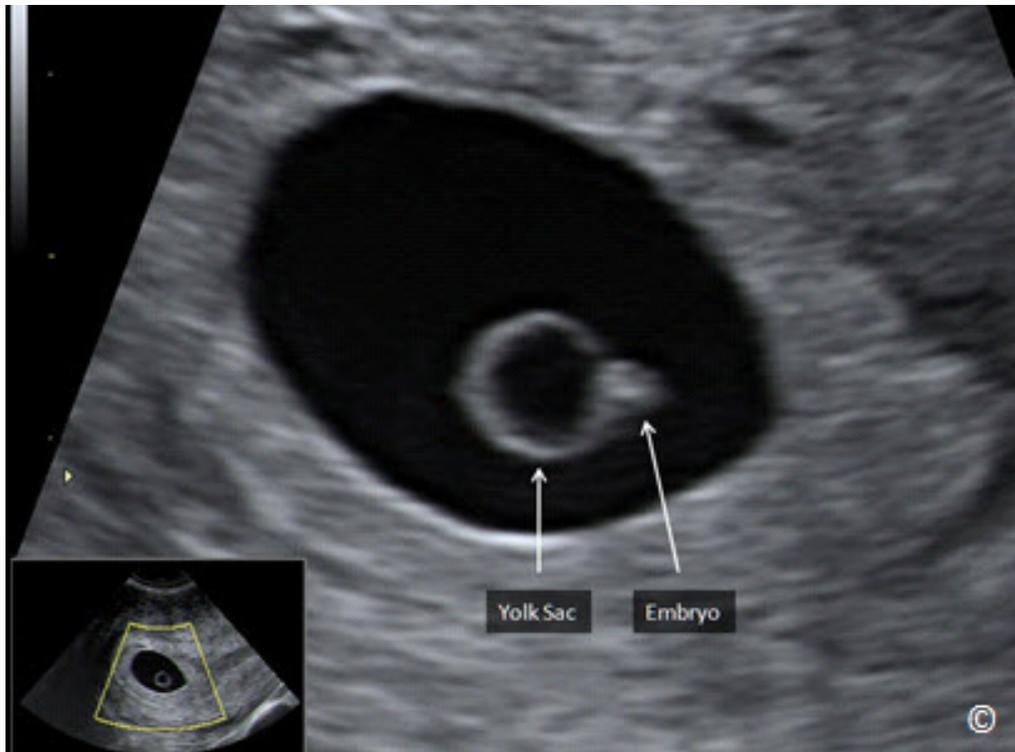
Figure 4.8: Gestational sac at 6 weeks. Note the location of the embryo (labeled) in close proximity to the free wall of the yolk sac (labeled). The embryo is attached to the yolk sac by the vitelline duct (not seen). The yolk sac and the embryo give the appearance of a diamond engagement ring at this gestation.
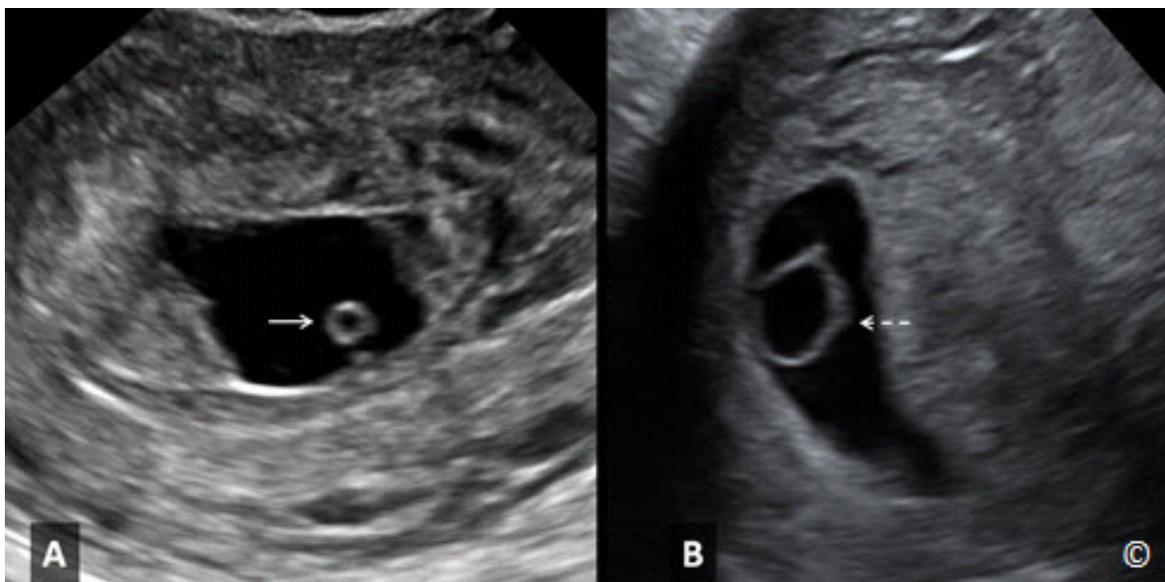
Figure 4.9 A & B: Figures 4.9 A and B show 2 gestational sacs with abnormal size yolk sacs: small in A - (solid arrow) and large in B (broken arrow). Abnormal size of yolk sacs is correlated with a suspicion for an abnormal pregnancy.

Amnion

The amniotic sac develops as a thin echogenic structure surrounding the embryo (**Figure 4.10**). The amniotic sac appears following the appearance of the yolk sac and just before the appearance of the embryo. Whereas the gestational sac shows variations in size and shape, the growth of the amniotic sac is closely related to that of the embryo between 6 and 10 weeks.
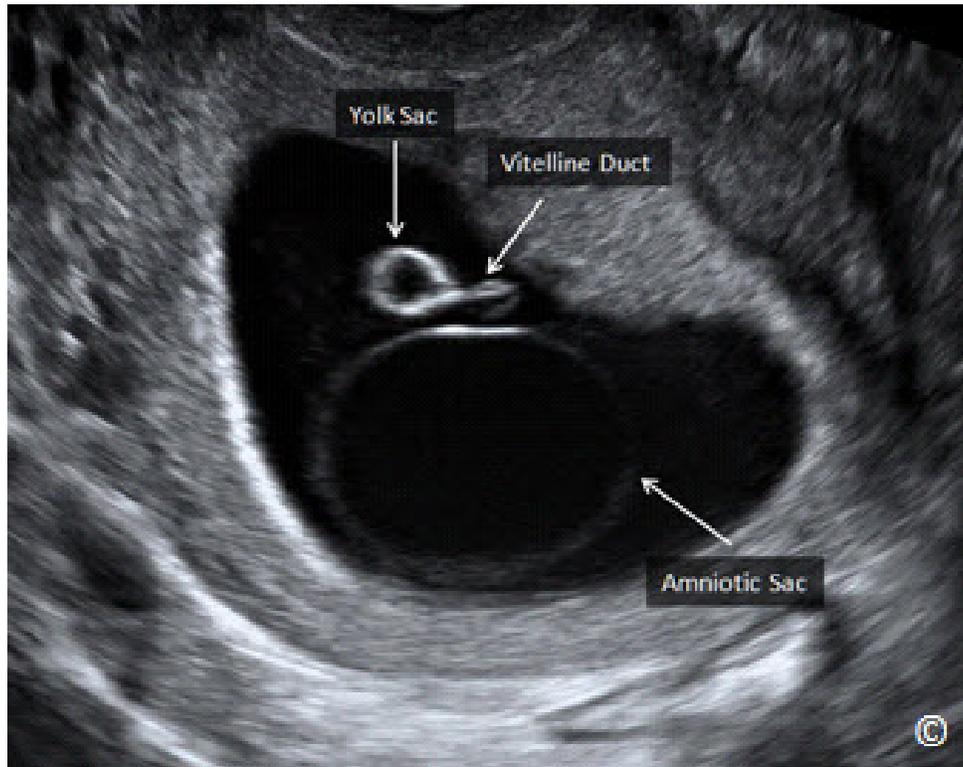
Figure 4.10: Gestational sac at 7 weeks gestation. The amniotic sac (labeled) is seen as a thin reflective circular membrane. The yolk sac and vitelline duct are seen as extra-amniotic structures (labeled).

Embryo

The embryo is first seen on transvaginal ultrasound as a focal thickening on top of the yolk sac, giving the appearance of a "diamond engagement ring" (**Figure 4.8**), at around the 5th menstrual week. First cardiac activity should be seen at 6 to 6.5 weeks. The embryo can be recognized by high resolution transvaginal ultrasound at the 2-3mm length size (**Figure 4.11**), but cardiac activity can be consistently seen when the embryo reaches a 5-7 mm in length or greater. Cardiac rhythm increases rapidly in early gestation being around 100-115 before 6 weeks, rising to 145-170 at 8 weeks and dropping down to a plateau of 137 to 144 after 9 weeks gestation. The size of the embryo increases rapidly by approximately 1mm per day in length. The measurement of the length of the embryo, referred to as the Crown-Rump-Length (CRL), is reported in millimeters.

It is the longest distance in a straight line from the cranial to the caudal end of the body and is the most accurate assessment for pregnancy dating. Recent studies suggest that it is prudent to use a cutoff of ≥7 mm (rather than ≥5 mm) for CRL with no cardiac activity for diagnosing failed pregnancy. This would yield a specificity and positive predictive value at (or as close as can be determined) to 100%. Since cardiac activity is usually visible as soon as an embryo is detectable, the finding of no heartbeat with a CRL <7 mm is suspicious, though not diagnostic, for failed pregnancy (2, 3).
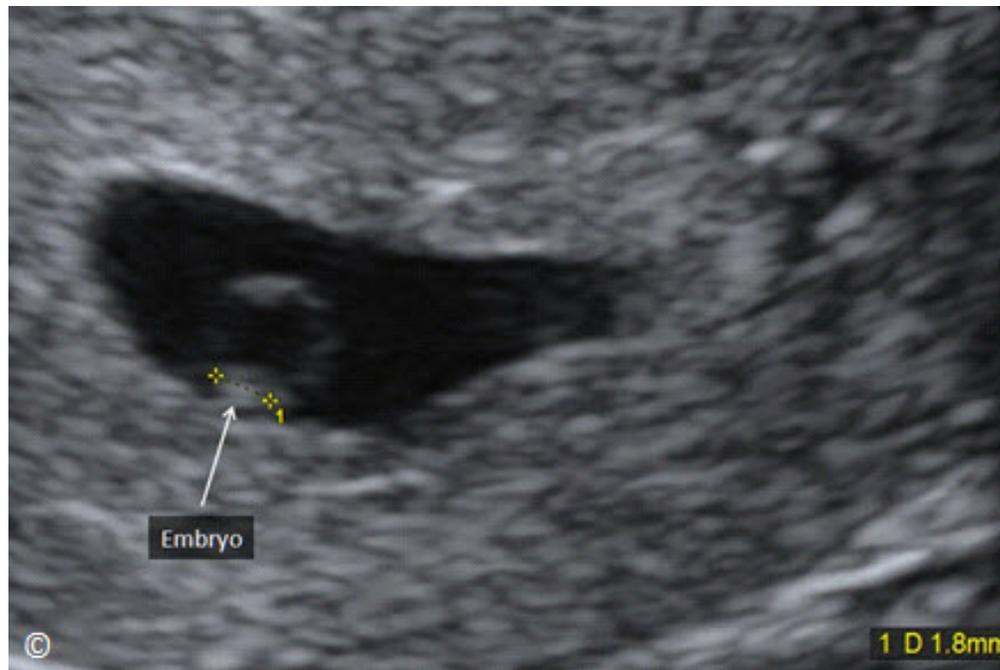
Figure 4.11: Transvaginal ultrasound of a gestational sac with an embryo (labeled) measuring 1.8 mm in size. Note the proximal location of the yolk sac (not labeled) to the embryo.

Note that the embryo develops within the amniotic cavity and is referred to as intraamniotic whereas the yolk sac is outside of the amniotic cavity and is referred to as extraamniotic (**Figure 4-10**). The fluid that the yolk sac in embedded into is the extraembryonic coelom.

The appearance of the embryo on ultrasound changes from 6 weeks to 12 weeks gestation. At 6 weeks gestation, the embryo appears as a thin cylinder with no discernible body parts "the grain of rice appearance" (**Figure 4.12**). As gestational age advances, the embryo develops body curvature and clear delineation on ultrasound of a head, chest, abdomen and extremities "the gummy-bear appearance" (**Figure 4.13, 4.14 and 4.1**). Close observation of anatomic details on transvaginal ultrasound at or beyond 12 weeks gestation may allow for the diagnosis of major fetal malformations. This requires extensive expertise and is beyond the scope of this book. We provide a table of major fetal malformations (**Table 4.4**) that can be diagnosed at 12 weeks or

beyond. **Figures 4.15 – 4.18** show examples of fetuses with major malformations at or before 12 weeks of gestation.
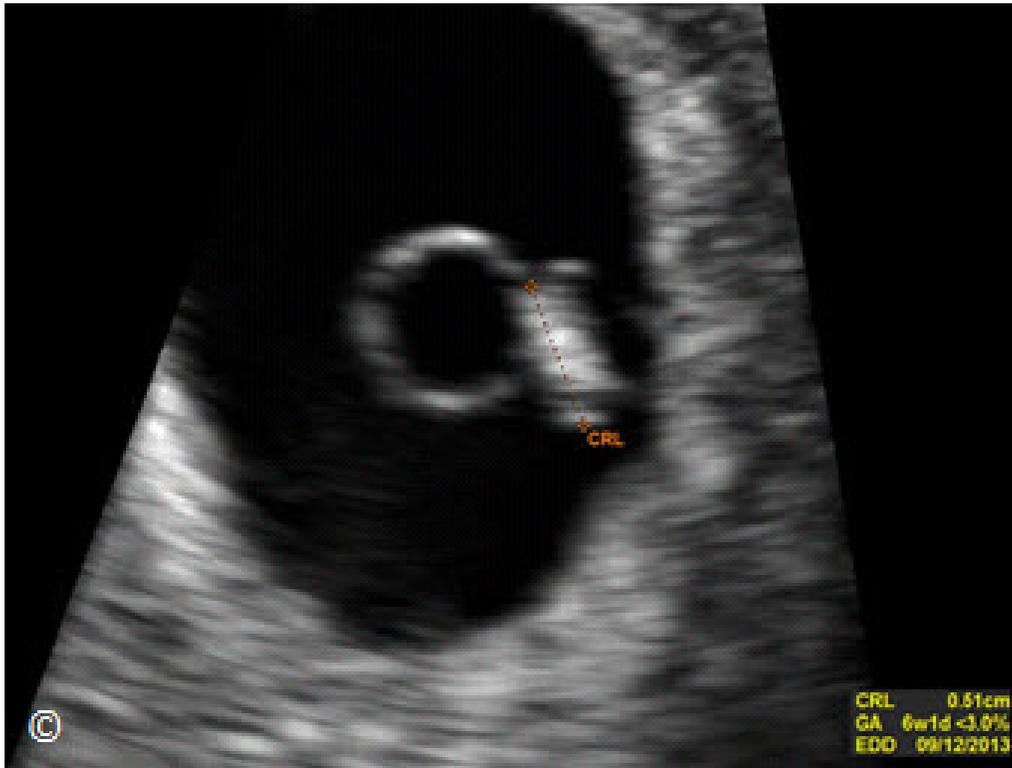
Figure 4.12: Gestational sac at 6 weeks with an embryo measuring 5.1 mm in Crown-Rump Length (CRL). Note the straight shape of the embryo, resembling a grain of rice.

Figure 4.13: Gestational sac with an embryo at 8 weeks. Note the appearance of body curvature of the embryo (labeled), resembling a gummy bear in shape. The yolk sac is also labeled.
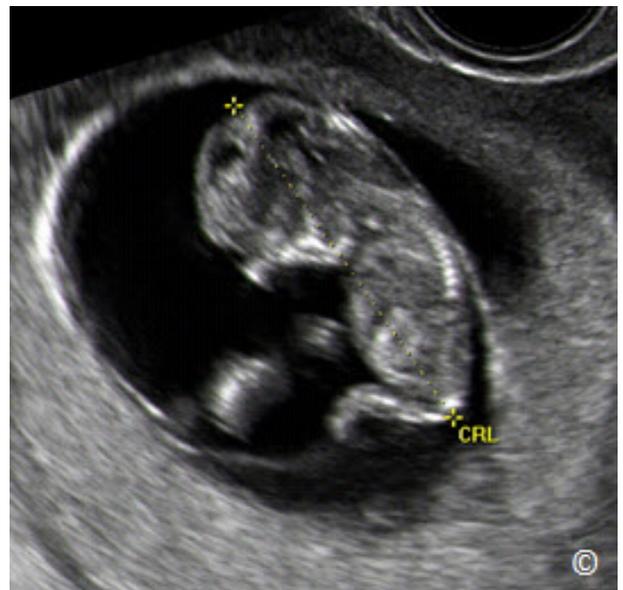
Figure 4.14: Gestational sac with an embryo at 10 weeks gestation. Note the clear delineation of a head, chest, abdomen and extremities. CRL=Crown-Rump Length.

TABLE 4.4	Major Fetal Malformation that can be Diagnosed in Early Gestation

- Anencephaly-exencephaly sequence
- Alobar and semilobar holoprosencephaly
- Large encephalocele
- Pentallogy of Cantrell (severe thoraco-abdominal wall defect with ectopia cordis and exomphalos)
- Gastroschisis
- Large omphalocele (watch-out for possible physiologic herniation of the bowel)
- Limb-body-wall complex (also known as body-stalk anomaly)
- Cystic hygroma
- Gross limb defects
- Frank hydrops

Figure 4.15: Mid-sagittal view of a fetus at 11 weeks gestation with anencephaly. Note the abnormally shaped head with absence of cranium (arrow).

Figure 4.16: Coronal view of a fetus at 10 weeks gestation with cystic hygroma. Note the generalized subcutaneous swelling (arrows). CRL = Crown-Rump Length.

Figure 4.17: A fetus with Pentalogy of Cantrell at 12 weeks gestation. Note the presence of a large abdominal and chest defect (arrow), with a protruding omphalocele.
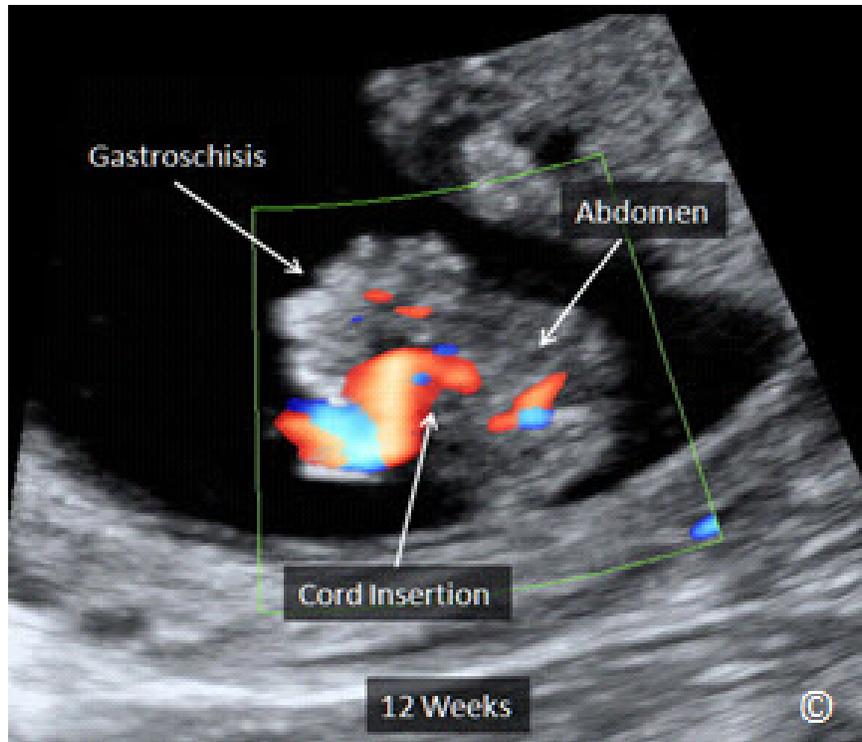
Figure 4.18: Gastroschisis (labeled) in a fetus at 12 weeks gestation demonstrated in a transverse view of the abdomen. Note the cord insertion (labeled) to the left of the defect.

MULTIPLE GESTATION AND CHORIONICITY

Chapter 7 describes in details ultrasound in multiple gestations. We will present here the role of the first trimester ultrasound in assigning chorionicity and amnionicity. Twins and higher order multiple gestations are easily diagnosed in early gestation. The first trimester is the most optimum time for the diagnosis of multiple gestations and for the assessment of chorionicity. In multiple gestations, first trimester ultrasound has also the essential role of assessing the type of chorionicity and recording it in the written ultrasound report. As pregnancy advances, it becomes more difficult to be certain of the chorionicity of multiple gestations.

We will focus on twins in this section as higher order multiple pregnancies is beyond the scope of this book and applies the same diagnostic principles as twins. The presence of a higher older multiple pregnancy should necessitate referral to an advanced imaging center. Twins can share one placenta and are thus referred to as monochorionic (MC). Twins can have two separate placentas and are then called dichorionic (DC). Dichorionic twins are two independent pregnancies within one uterus and with very rare exceptions have no shared placental vascular network between the twins. All dichorionic placentas, by definition, have 2 amniotic sacs and thus are diamniotic also. Dizygotic twins always have dichorionic placentation. Their placentas

may be separated or intimately fused. Dizygotic twins are more common than monozygotic twins, with a ratio of 3 to 1.

Most monozygotic twins have a placenta that is monochorionic – diamniotic (~75 %), some monozygotic twins have a dichorionic – diamniotic placenta (~25 %), and rarely, the placenta can be monochorionic- monoamniotic (~1%). Conjoined twins are monoamniotic and are less common still. These three entities of twinning are best diagnosed in early gestation after 8 weeks when yolk sac(s) are present and further management and follow up of gestation depends highly on the twin subgroup detected:

1) In dichorionic-diamniotic twins there are two gestational sacs with thick dividing membrane that includes chorionic tissue, separating both gestational sacs. The chorionic tissue separating the gestational sacs is referred to as "delta, lambda or twin-peak" sign and is diagnostic of a dichorionic gestation (**Figure 4.19**). In each sac we can find a yolk sac and an embryo.

2) In monochorionic- diamniotic twins, there is one gestational sac but each embryo has its own amniotic sac and yolk sac (**Figure 4.20**). The dividing membrane that separates the amniotic cavities is thin and inserts in a characteristic "T" configuration into the shared placenta (**Figure 4.21**).

3) In monochorionic-monoamniotic twins, there is one gestational sac, one amniotic sac, one yolk sac but two embryos. No separating/dividing membrane is noted (**Figure 4.22**).

4) Conjoined twins will have the same placental characteristics as a monochorionic-monoamniotic placenta with conjoined embryos (**Figure 4.23**). Note that the term "conjoined" is a misnomer as the twin has actually failed to separate completely instead of being conjoined. The terminology however is well accepted.

Further detailed discussion of multiple gestations is presented in Chapter 7.
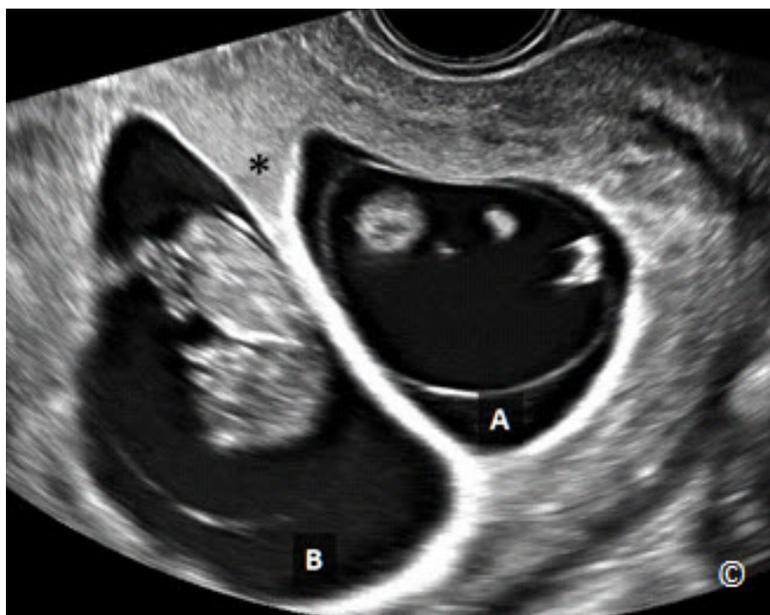
Figure 4.19: Dichorionic-diamniotic twin pregnancy. Note the thick dividing membrane separating both gestational sacs (A and B). Chorionic tissue (asterisk) is present at the attachment of the dividing membrane known as "delta or lamda" sign.

Figure 4.20: Monochorionic- diamniotic twins (A and B) at 8 weeks gestation. Note the presence of 2 yolk sacs (arrows). A thin separating membrane is not visible in this image.
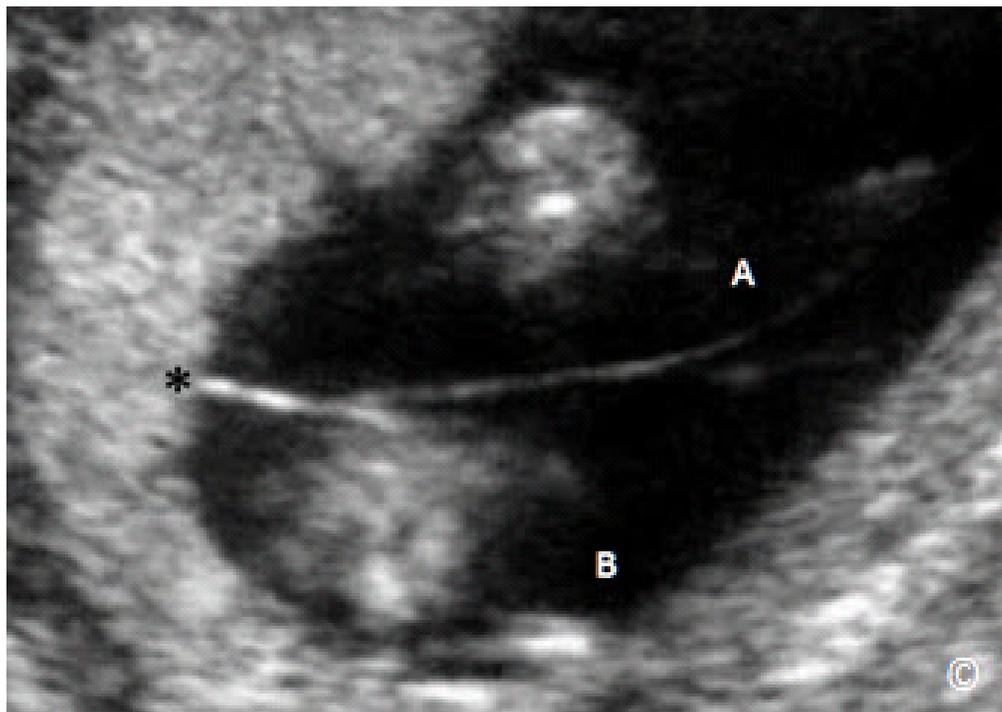
Figure 4.21: Monochorionic-Diamniotic twins. Note a thin dividing membrane that separates the amniotic cavities (A and B) and inserts in a characteristic "T" configuration (asterisk) into the shared placenta.
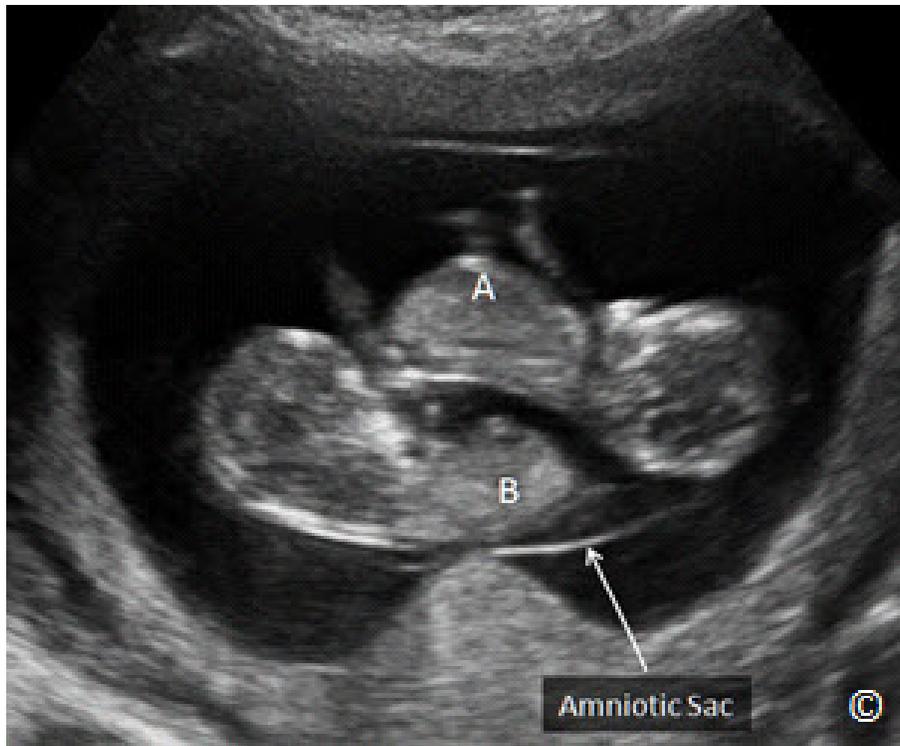
Figure 4.22: Monochorionic- monoamniotic twins (A and B). Note the presence of a single amniotic sac (labeled).
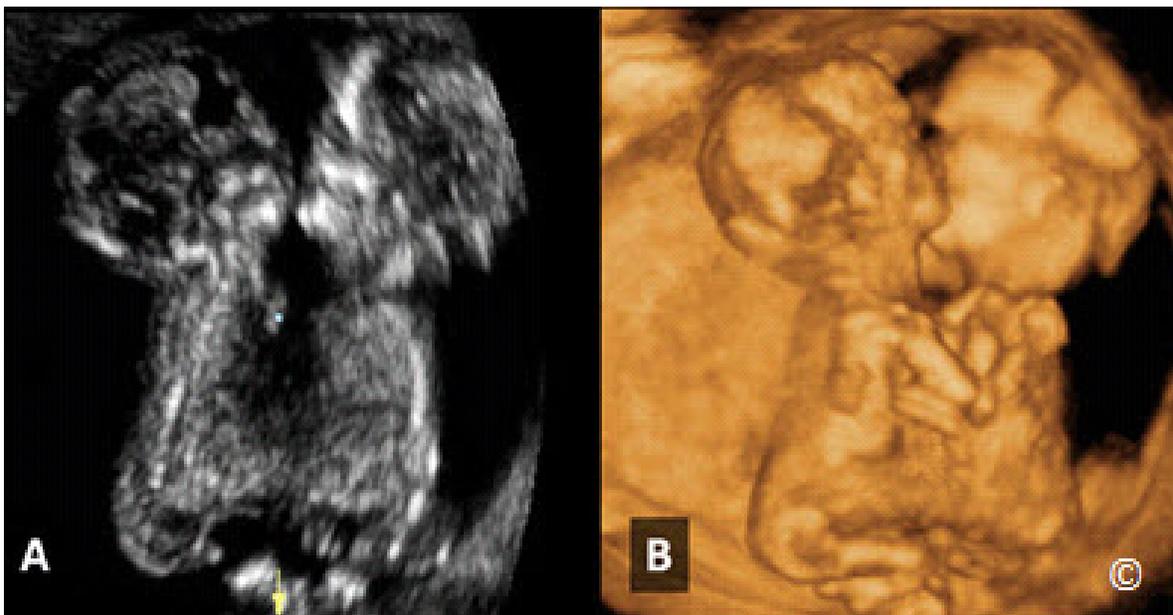
Figure 4.23 A & B: Conjoined twins at 12 weeks gestation on 2D (A) and 3D (B) ultrasound. Note that the twins are joined at the chest and abdomen. More detail on conjoined twins is presented in chapter 7.

PREGNANCY DATING IN THE FIRST TRIMETESTER

One of the most important aspects of obstetric ultrasound in the 1st trimester is dating of pregnancy; this is accomplished by performing few simple biometric measurements: 1) the gestational sac diameter, when no embryo is seen; 2) the length of the embryo, or Crown-Rump Length (CRL); 3) in the late 1st trimester (12-13 weeks), the Biparietal Diameter (BPD). The obtained values are to be compared with established reference ranges to provide an accurate dating. With an accurate ultrasound-derived gestational age in the first and second trimester of pregnancy, ultrasound can reliably date a pregnancy with unknown dates and establish an estimated date of delivery with accuracy.

In clinical medicine the age of an embryo or a fetus is expressed in *"weeks of gestation"* and not in months and these weeks are calculated from the first day of the last menstrual period (LMP), which corresponds to 2 additional weeks from the date of conception. Gestational age is therefore calculated from the first day of the last menstrual period (LMP) and roughly corresponds to the dates of conception plus about 14 days. An easy estimation of the date of delivery is the Naegle's rule, which is the first day of the LMP + 7 days and minus 3 months (use the next calendar year). In general most ultrasound equipment has an integrated calculator, which calculates the estimated date of delivery as the LMP is entered. **Table 4.5** lists some facts about gestational dating in the first trimester.

TABLE 4.5	Facts about Gestational Dating in the First Trimester
- Gestational age is calculated from date of onset of the last menstrual period (LMP) and not from time of conception - Date of delivery = first day of LMP + 280 days - Ultrasound equipment provide a calculator of gestational age - Measuring the embryo or the fetus or other structures before 14 weeks is the most reliable way to estimate gestational age by ultrasound	

In estimating gestational age by ultrasound, it is important to remember these critical points:

- Once an established date of delivery is assigned to a pregnancy following an ultrasound examination, irrespective whether the assigned established dates were those by ultrasound or by menstrual dates, these dates should not be changed during pregnancy.

- If a patient reports no menstrual dates, ultrasound in the first or second trimester should establish the estimated date of delivery.
- If the ultrasound biometric measurements vary from the menstrual dates by more than 5-7 days in the first trimester, than ultrasound should be used to establish the date of delivery (1).
- Ultrasound dating of pregnancy is most accurate in the first trimester.

BIOMETRIC MEASUREMENTS IN THE FIRST TRIMESTER

Biometric measurements for dating in the first trimester of pregnancy include the length of the embryo; referred to as the crown-rump length (CRL), mean gestational sac diameter (MSD), embryo/fetus biparietal diameter (greater than 11 weeks), and more rarely, the yolk sac and/or amnion sac diameters. The most accurate and reproducible biometric measurement is the CRL and should be the preferred measurement when feasible.

Crown-Rump Length

The CRL corresponds to the length of the embryo in millimeters. Although, the name implies a measurement from the crown to the rump of the embryo, the actual measurement corresponds to the longest "straight line" distance from the top of the head to the rump of the embryo/fetus (**Figure 4.24**), despite the noted body curvature. The CRL measurements are more accurate in the earlier parts of the first trimester. When measuring the CRL, the operator should use the mean of three discrete measurements, obtained in a mid-sagittal plane. It is recommended to follow the following parameters when dating a first trimester pregnancy (< 14 weeks) by CRL:

- For pregnancies at less than 9 weeks' gestation, a discrepancy of more than 5 days from LMP is an appropriate reason for changing the Expected Date of Delivery (EDD).
- For pregnancies between 9 and 13 6/7 weeks' gestation, a discrepancy of more than 7 days should result in a change in the EDD.

The CRL increases rapidly at a rate of approximately 1.1 mm per day. An approximate formula to calculate gestational age from the CRL is Gestational Age in days = CRL (mm) + 42, however this may not be needed since most ultrasound equipment have integrated software which allows gestational age determination upon measurement of CRL or other biometric data. **Table 4.6** shows gestational age and corresponding CRL in mm.

Figure 4.24: Crown-Rump Length (CRL) measurement of a fetus at 12 weeks gestation. Note that the CRL measurement corresponds to the longest straight line from the top of the head to the rump region.

TABLE 4.6	Gestational age and corresponding Crown Rump Length (mm)
Gestational Age (GA	Crown Rump Length (mm)
6 + 0 weeks	5
7 + 0 weeks	10
8 + 0 weeks	15
9 + 0 weeks	23
10 + 0 weeks	32
11 + 0 weeks	42

Mean Sac Diameter

Since the gestational sac is the first evidence of pregnancy on ultrasound and is first visualized within the endometrial cavity at 4 to 4.5 weeks after the LMP, its detection and measurement can be used to confirm and date a pregnancy. Its size at first appearance is around 2 to 4 mm in diameter, and is localized in the decidua, paracentrically with echogenic borders. The early demonstration of a gestational sac is best performed by transvaginal ultrasound. The biometric measurement for pregnancy dating uses the mean sac diameter (MSD) calculated as the arithmetic mean diameters derived from its greatest sagittal, transverse and coronal planes (**Figure 4.25 A and B**). Gestational sac confirms the presence of an intrauterine pregnancy but not the viability of the embryo. Therefore an empty gestational sac or with a yolk sac are signs

that the pregnancy is 5-6 weeks gestation, a follow in 7-14 days will demonstrate the presence of an embryo and confirms viability. It is not recommended to use the MSD for estimating the due date, as the CRL is a more precise dating method and should be the preferred choice.
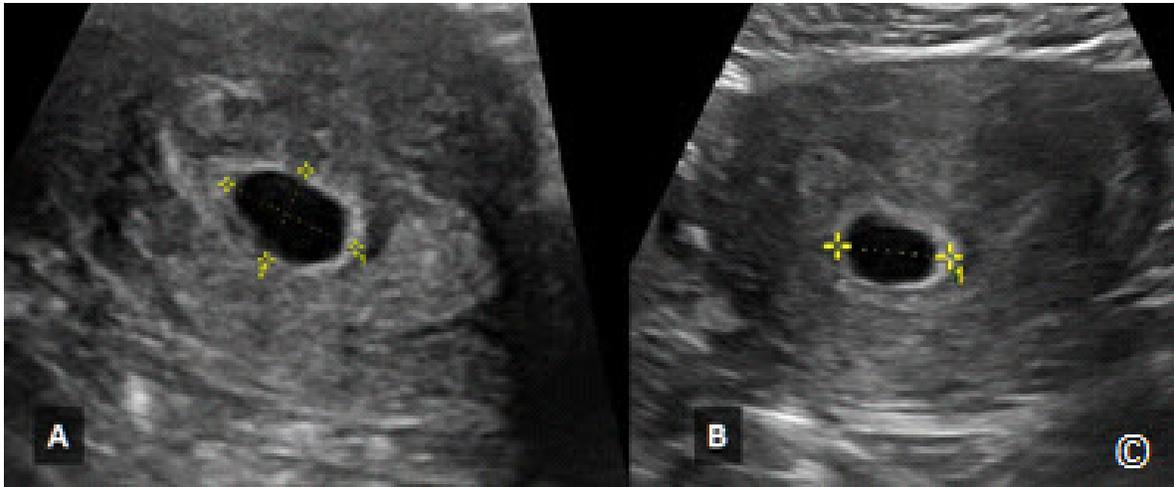
Figure 4.25 A & B: Mean sac diameter (MSD) of a gestational sac at 5 weeks calculated as the arithmetic mean diameters derived from its greatest sagittal (A1), transverse (A2) and coronal planes (B1).

Amniotic Sac / Yolk Sac

The amniotic sac develops around the embryo as a thin membrane that surrounds the embryo and is less echogenic than the yolk sac (**Figure 4.10**). Whereas the gestational sac shows variations in size and shape, the growth of the amniotic sac is closely related to the growing embryo.

Once an embryo with cardiac activity is seen on ultrasound, the MSD, the size of the amniotic cavity or yolk sac are not used for dating, but for documentation of normal development. Observation of abnormal measurements of these structures in association with a normal developing embryo are often not enough to diagnose a failed pregnancy, but close follow up is prudent.

NUCHAL TRANSLUCENCY

Nuchal translucency (NT) is a measurement of a collection of fluid under the skin behind the fetal neck in the first-trimester of pregnancy. NT is measured between 11weeks and 13 weeks and 6 days or a CRL of 45 – 84 mm. NT provides a risk assessment for chromosomal abnormalities and can be a marker of other fetal abnormalities. For efficiency in screening, NT is best combined with maternal age and maternal blood biochemical markers such as hCG and pregnancy-associated plasma protein (PAPP-A). In order to incorporate NT in clinical practice,

physicians and sonographers should get certified in NT measurement and an ongoing quality assurance program on NT measurement should be established. National and international NT quality assurance programs exist such as the Fetal Medicine Foundation (www.fetalmedicine.com) and the Nuchal Translucency Quality Review (www.ntqr.org). **Table 4.7** shows the technical aspects of NT measurement. **Figures 4.26 and 4.27** show 2 fetuses with a normal and large NT measurement respectively.

TABLE 4.7	Technical Aspects of Nuchal Translucency Measurement (NT) – From NTQR.org with Permission

1. Margins of NT edges clear
2. Fetus in the mid-sagittal plane
3. Fetus occupies the majority of the ultrasound image
4. Fetal head in the neutral position
5. Fetus observed away from the amnion
6. (+) Calipers used
7. The calipers horizontal crossbars are placed on the NT line
8. The calipers are placed perpendicular to the long axis of the fetus
9. The measurement is at the widest NT space
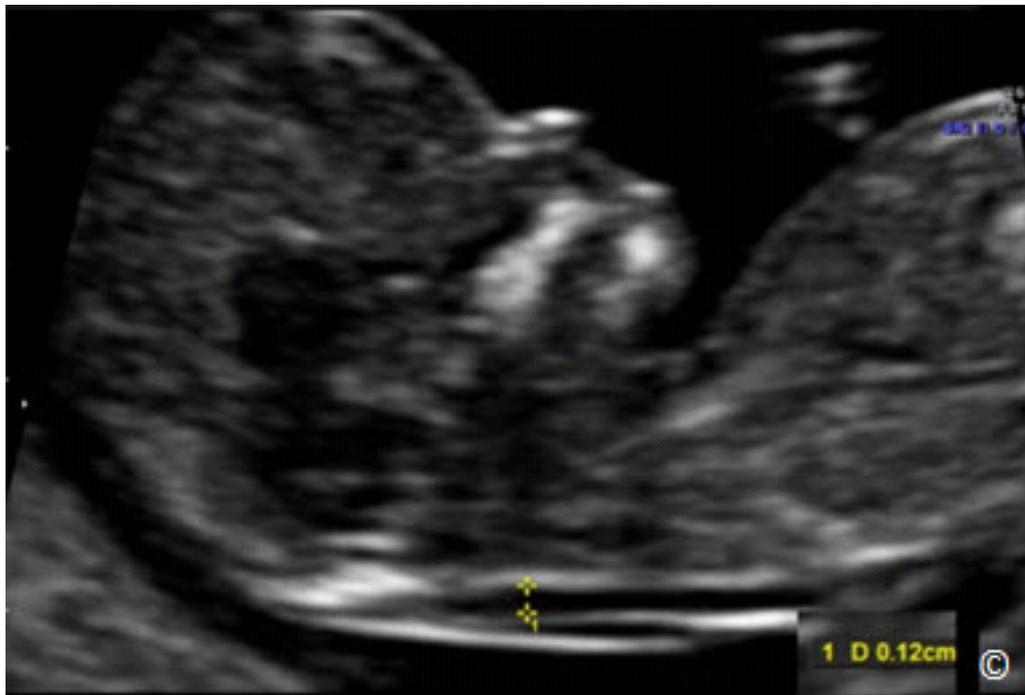
Figure 4.26: Mid-sagittal plane of a fetus in the first trimester of pregnancy with a normal nuchal translucency measurement (NT).

Figure 4.27: Mid-sagittal plane of a fetus in the first trimester of pregnancy with an enlarged nuchal translucency measurement (NT).

ELEMENTS OF PREGNANCY FAILURE

The examiner dealing with first trimester ultrasound is often confronted with the situation of a suspected or a confirmed early pregnancy failure. It should be known that during this stage, at least 10-15% of all pregnancies end as pregnancy failure and the diagnosis can often be made by ultrasound, typically before symptoms develop by patients. Depending on the gestational age of pregnancy, several scenarios can be expected:

- Pregnancy confirmed by a positive pregnancy test but no gestational sac is noted in the uterine cavity by ultrasound, suggesting the differential diagnosis of an incomplete abortion, an ectopic pregnancy or an early intrauterine pregnancy that is not yet recognizable by transvaginal ultrasound.
- Gestational sac noted by transvaginal ultrasound, but no signs of embryo or yolk sac within it.
- An embryo visualized on transvaginal ultrasound, but no cardiac activity detected.
- An embryo with cardiac activity detected, but various measurements are out of range (heart rate, size of yolk sac, embryo, amniotic sac etc.).
- Presence of subchorionic bleeding, with or without clinical signs of bleeding.
- Abnormal anatomic appearance of the embryo.

In many conditions if the health of the patient is not in danger (bleeding, pain etc.) and an ectopic pregnancy is not in the differential diagnosis, a follow-up ultrasound examination is helpful to assess for change in the ultrasound findings and in confirming the suspected diagnosis. Given that the developing gestational sac undergoes notable significant change on a weekly basis in the first trimester, follow-up ultrasound that fails to show a noticeable change after 1 week or more, casts a poor prognostic sign and can confirm the diagnosis of a suspected failed pregnancy. The presence of subchorionic bleeding is generally associated with a good outcome in the absence of other markers of pregnancy failure **(Figure 4.28 A & B)**. It is the opinion of the authors that in the absence of specific findings of failed pregnancy, conservative management with follow-up ultrasound examination is helpful in the evaluation of a suspected failed pregnancy in the first trimester. **Table 4.8** lists specific findings of failed pregnancy in the first trimester which when noted can establish the diagnosis without a need for a follow-up examination.
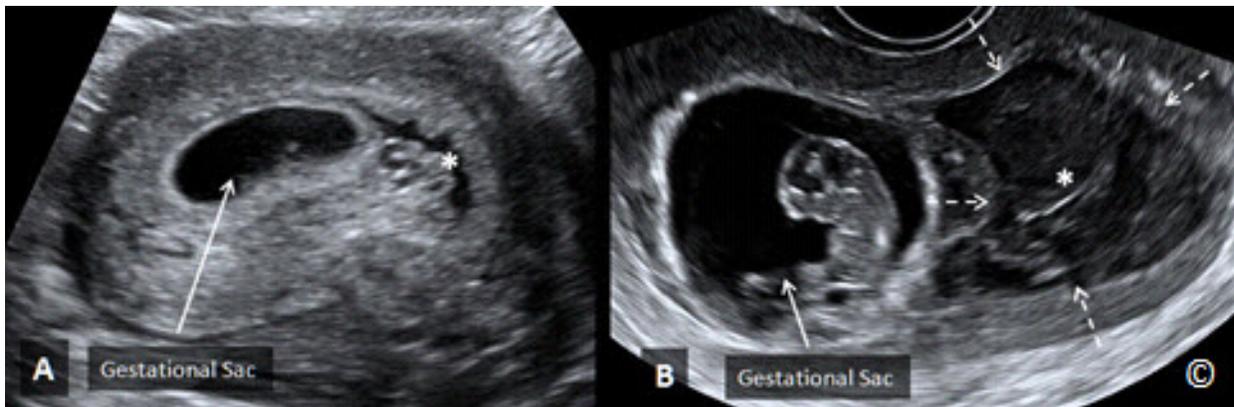
Figure 4.28 A & B: Small (A - asterisk) and large (B – asterisk and broken arrows) subchorionic bleeding in 2 pregnancies. Despite its size, the subchorionic bleeding in B was associated with a good pregnancy outcome.

TABLE 4.8	Diagnostic Signs of Early Pregnancy Failure in the First Trimester

- Crown-Rump length of equal to or greater than 7 mm without cardiac activity
- MSD of equal to or greater than 25 mm without an embryo
- Absence of embryo with heartbeat at 2 or more weeks after an ultrasound that showed a gestational sac without a yolk sac
- Absence of embryo with heartbeat at 11 days or more after an ultrasound that showed a gestational sac with a yolk sac

CONCLUSIONS

The ultrasound examination in the first trimester is an important step in the evaluation of the pregnancy as it allows for confirmation of an intrauterine gestation and for accurate pregnancy dating. It is of note that significant change occurs in the first trimester in the normal pregnancy and this change can be detected by transvaginal ultrasound examination. Sequential steps of the normal development of the pregnancy should be known in order to better compare the actual ultrasound findings with the corresponding gestational age. This is the basic knowledge that is needed in order to differentiate a normal from an abnormal gestation.

References:

1) Reddy UM, Abuhamad AZ, Levine D, Saade GR. Fetal Imaging Executive Summary of a Joint Eunice Kennedy Shriver National Institute of Child Health and Human Development, Society for Maternal-Fetal Medicine, American Institute of Ultrasound in Medicine, American College of Obstetricians and Gynecologists, American College of Radiology, Society for Pediatric Radiology, and Society of Radiologists in Ultrasound Fetal Imaging Workshop. J Ultrasound Med 2014; 33:745–757.
2) Doubilet PM, Benson CB, Bourne T, Blaivas M; Barnhart KT, Benacerraf BR, et al. Diagnostic criteria for nonviable pregnancy early in the first trimester. N Engl J Med. 2013 Oct 10; 369(15): 1443-51.
3) Abdallah Y, Daemen A, Kirk E, Pexsters A, Naji O, Stalder C, Gould D, Ahmed S, Guha S, Syed S, Bottomley C, Timmerman, Bourne T. Limitations of current definitions of miscarriage using mean gestational sac diameter and crown–rump length measurements: a multicenter observational study. Ultrasound Obstet Gynecol 2011; 38: 497-502.

ULTRASOUND IN THE SECOND TRIMESTER — 5

INTRODUCTION

The main objective of a second trimester ultrasound examination is to accurately date the pregnancy, evaluate fetal anatomy, and assess placental location and the adnexae. Second trimester components of the basic ultrasound examination are listed in **Table 5.1** and may vary based upon the level of support provided by the local health care system and national guidelines.

TABLE 5.1	Components of the Basic Second Trimester Ultrasound Examination
	- Fetal presentation and position - Cardiac activity - Fetal number (and chorionicity if multiple pregnancy) - Fetal age/size (biometry) - Amniotic fluid assessment - Placental appearance and location - Basic fetal anatomy - Assessment of the adnexae

TIMING OF THE SECOND TRIMESTER ULTRASOUND EXAMINATION

It is generally accepted that the "second trimester/mid-trimester" refers to the period of 14-28 weeks of gestation, but for the sake of this chapter, we are referring to the second trimester as an ultrasound performed within the gestational period of 18 – 22 weeks. In countries where access to ultrasound clinics is difficult or limited, this time period can be extended to 16-25 weeks of gestation, with same caveats. At 16 weeks, the basic anatomy survey is more challenging than later in gestation, especially when portable ultrasound equipment is used and/or in obese women. On the other hand, dating a pregnancy at 25 weeks or greater, in the absence of a previous ultrasound, is much less precise than earlier in gestation.

Who should perform the ultrasound examination?

The operator performing the ultrasound examination differs according to local rules and traditions. In some countries, sonographers do the ultrasound examination and doctors review them; in other countries, doctors primarily do the ultrasound examinations. In certain locations, midwives perform the basic ultrasound examinations, whereas the doctors perform the targeted ultrasound examinations. This last approach is most applicable to low-resource (outreach) countries, due to shortage of medical personnel. Based upon our experience in low-resource settings, where sonographers are typically not available and healthcare workers are in short demand, midwives, when trained appropriately in didactic and hands-on supervised courses with competency evaluation, can achieve a basic ultrasound skill that allows for limited ultrasound examinations. Irrespective of the model in place, it is critical to ensure that operators performing the ultrasound examinations are skilled and trained in the performance of these examinations.

In several countries, guidelines for the performance of the basic ultrasound examination and the qualifications of the healthcare workers to perform such examinations are established. Readers who wish to review these guidelines and qualifications are referred to the American Institute of Ultrasound in Medicine (www.AIUM.org) and the International Society of Ultrasound in Obstetrics and Gynecology (www.ISUOG.org) websites.

Preparation for the ultrasound examination

Before the ultrasound examination is initiated the operator should have a good understanding of the physical principles of ultrasound, the basic operations of the ultrasound equipment and basic technical skills for the performance of the ultrasound examination, details of which are provided in Chapters 1, 2 and 3. **Table 5.2** provides an itemized list that needs to be checked before the initiation of any obstetric mid-trimester ultrasound examination.

Table 5.2	Itemized List to be Checked Before Initiation of the Second Trimester Ultrasound
	- Ensure that the woman's position on the ultrasound bed is comfortable - Choose the obstetric setting on ultrasound machine - Enter the woman's name and other identifiers - Enter the woman's last menstrual period - Place gel on the abdomen - Adjust the gain settings - Adjust the depth and focal ranges - Use the correct orientation of the transducer when scanning

When performing an obstetric ultrasound examination in low-resource settings, the second trimester ultrasound examination can be simplified to six standardized steps, which are geared towards the identification of findings that have a direct impact on the wellbeing of the mother and fetus. These six steps are designed to assess fetal presentation and lie, the presence of fetal cardiac activity, the number of fetuses within the uterus, the adequacy of the amniotic fluid, the localization of the placenta and pregnancy dating. The technical aspects of five of these six steps are described and illustrated in Chapter 10. We will hereby describe the sixth step, which involves the biometric measurement of the fetus, including the biparietal diameter, the head circumference, the abdominal circumference and the femur length.

Fetal Biometry

Fetal biometry refers to *fetal age* and corresponds to the length of gestation (dating) while *size* refers to the fetal weight and will be discussed later. Caution! A pregnancy should not be re-dated if a prior appropriate ultrasound examination established pregnancy dates. Re-dating on the basis of 2nd trimester biometry should only be performed if the woman has not undergone any other earlier ultrasound in pregnancy in which dating was established. Although ultrasound dating in pregnancy is accurate in the second trimester, it is less precise than in the first trimester of pregnancy, when pregnancy is dated by crown-rump length measurement. We recommend the following parameters for pregnancy dating in the second trimester:

- For pregnancies between 14 0/7 weeks and 15 6/7 weeks gestation, a discrepancy of more than 7 days should result in a change in the Expected Date of Delivery (EDD).
- For pregnancies between 16 0/7 weeks and 21 6/7 weeks gestation, a discrepancy of more than 10 days should result in a change in the EDD.
- For pregnancies between 22 0/7 weeks and 27 6/7 weeks gestation, a discrepancy of more than 14 days should result in a change in the EDD.

Four fetal biometric measurements are required for dating and/or for estimating fetal weight including the Biparietal Diameter (BPD), the Head Circumference (HC), the Abdominal Circumference (AC) and the Femur Length (FL). In the following sections, measurement of each of these 4 biometric parameters is explained in details.

Biparietal Diameter

The Biparietal Diameter (BPD) (**Figures 5.1** and **5.2**) should be measured in a cross-sectional view of the fetal head at the level of the thalami. Sonographic landmarks identifying the correct BPD plane are listed in **Table 5.3** and the procedure to measure the BPD is shown in **Table 5.4**.

On occasions, especially in the third trimester when the fetal head is engaged, the BPD can be measured from a coronal plane of the head, if this is the only imaging option available.
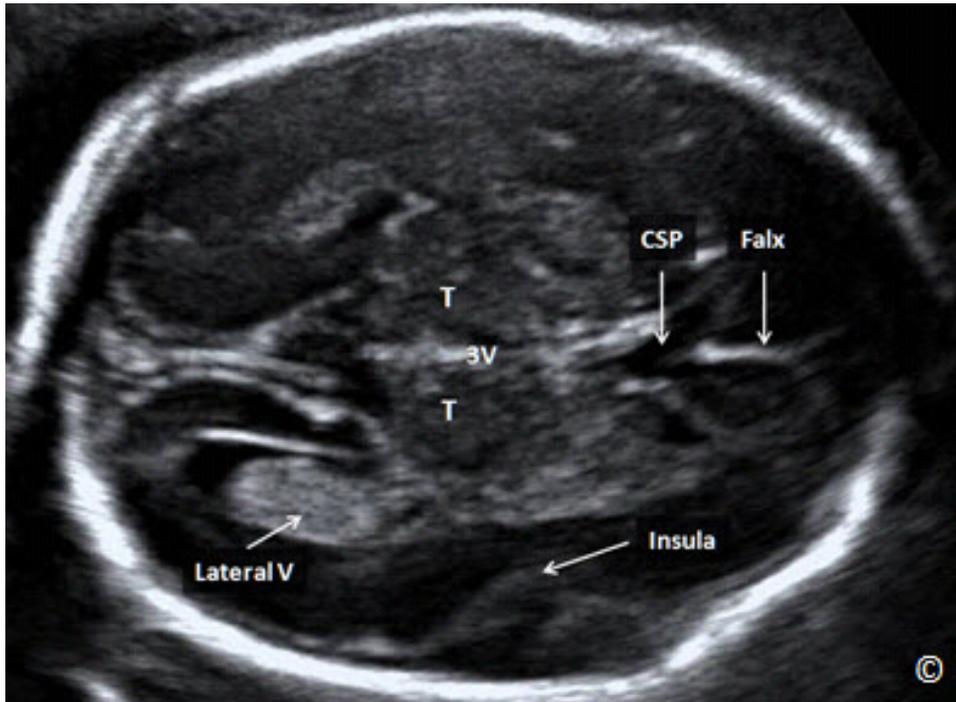
Figure 5.1: A transverse plane of the fetal head at the level of the biparietal diameter (BPD). In this plane, you should see the cavum septae pellucidi (CSP), the falx (labeled), the thalami (T), 3rd ventricle (3V) and the insula (labeled). A portion of the lateral ventricle is also seen (labeled).
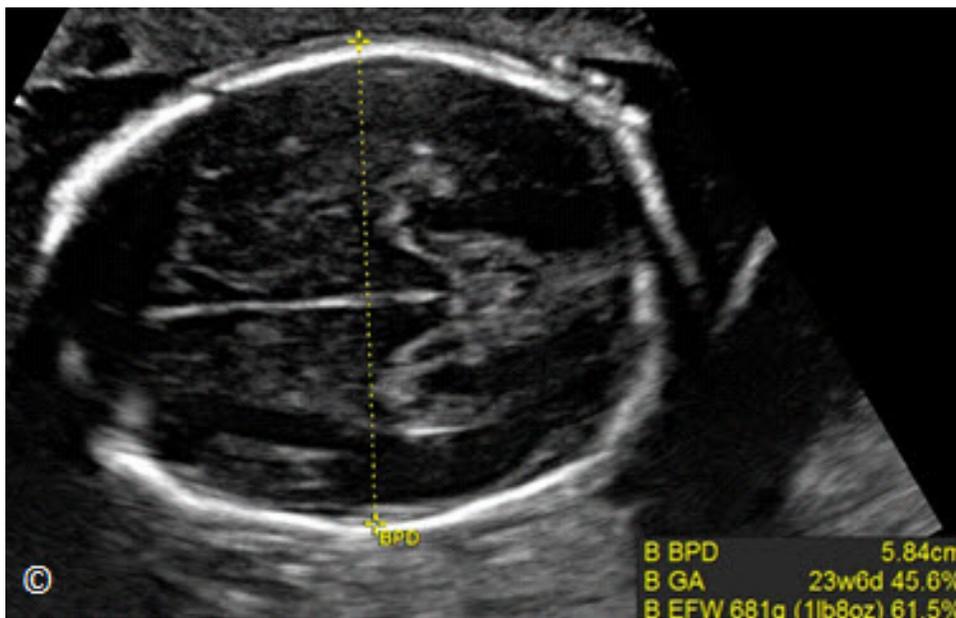
Figure 5.2: Transverse plane of the fetal head at the level of the biparietal diameter (BPD) showing correct caliper placement. Note that the upper and lower calipers are traditionally placed on the outer and inner edge(s) of the cranium respectively (GA = gestational age and EFW = estimated fetal weight).

Table 5.3	Sonographic Landmarks for the Measurement of the Biparietal Diameter Plane (BPD). See Figure 5.1

- Midline Falx
- Thalami
- Symmetrical appearance of both cerebral hemispheres
- No cerebellum visualized
- Cavum Septae Pellucidi
- Insula

Table 5.4	Procedure for the Measurement of the Biparietal Diameter (BPD). See Figure 5.2

- Activate the biometry software (calculate knob) on the console of the ultrasound equipment
- Select the BPD option, a caliper will appear on the monitor
- Position the caliper on the outer edge of the proximal parietal bone, roughly at the level of the thalami, where the head is wider, and set it
- Position the second caliper, symmetrically, on the inner edge of the distal parietal bone, in such a way that the line between the two calipers is at 90° with the midline falx, and set it.
- Ensure that the BPD measurement is the widest possible and is perpendicular to the midline falx.

Head Circumference

The Head Circumference (HC) is measured in the trans-thalamic view, which is the same plane as that for the BPD measurement (**Figure 5.1** and **5.2**). There are three options for the measurement of the HC on most ultrasound equipment; the ellipse method (**Figure 5.3**), the 2-diameter method and the trace method. The ellipse method allows the operator to expand an ellipse over the cranium, typically by initially fixing the BPD and occipito-frontal diameters (OFD). The 2-diameter method utilizes the 2 diameters (BPD and OFD) and calculates the HC from an ellipsoid formula. The tracing method simply traces the cranium as seen on the display monitor. Of the three methods that can be selected on most ultrasound equipment, the ellipse method is preferred as it has the least inherent error (**Figure 5.3**). The authors recommend that you perform the HC measurement following the BPD measurement. This approach allows the

operator to utilize the calipers placed for BPD measurement, which expedites the process. It is of note that when the HC is being measured, the lower caliper from the BPD diameter should be moved to the outer bony parietal edge (**Figure 5.4**). **Table 5.5** lists the steps for the measurement of the HC.

B OFD (HC)	7.89cm
B HC	22.05cm
B GA	24w1d 41.0%
B EFW	690g (1lb8oz) 65.4%
CI (BPD/OFD)	73%
FL/HC	19%
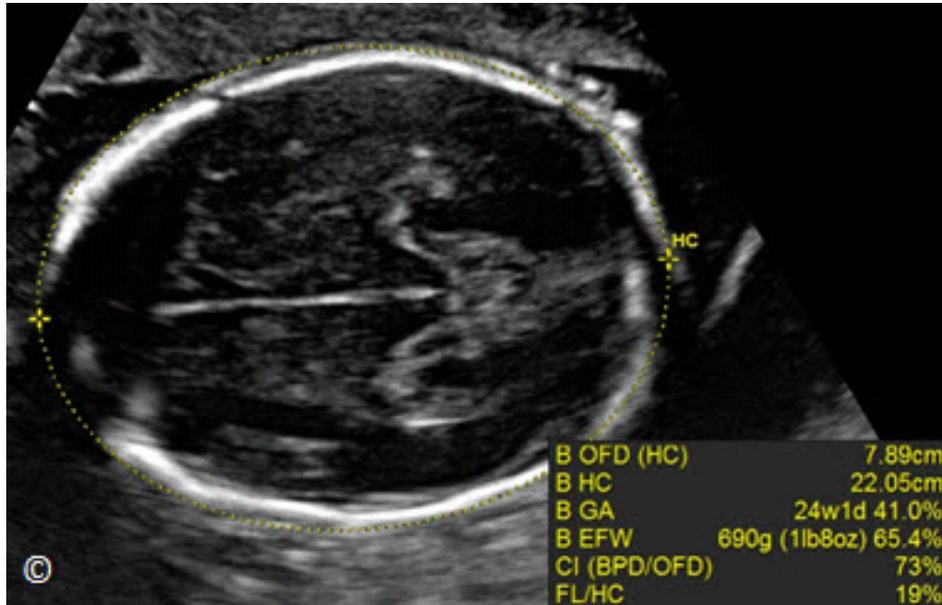
Figure 5.3: Transverse plane of the fetal head at the biparietal diameter (BPD) level. The head circumference (HC) is measured using the ellipse method. Note that the ellipse is tracing the outer edge of the fetal cranium. (OFD= occipito-frontal diameter, GA=gestational age, EFW=estimated fetal weight, CI=cephalic index and FL = femur length).

BPD	6.16cm
GA	25w0d 86.5%
OFD (HC)	7.87cm
HC	22.77cm
GA	24w6d 74.3%
CI (BPD/OFD)	78%
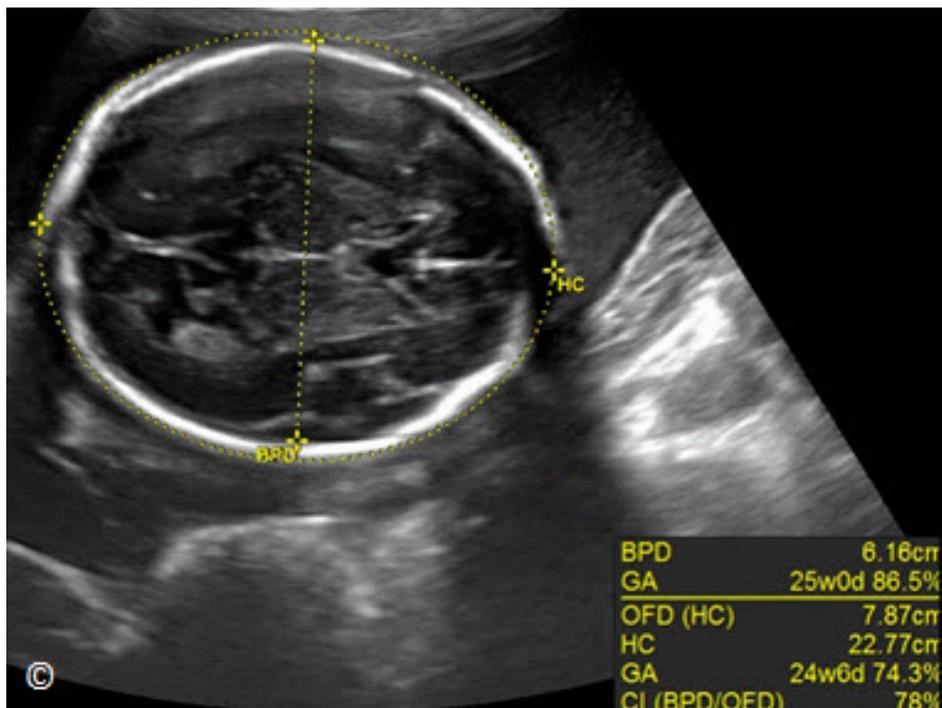
Figure 5.4: Transverse plane of the fetal head at the biparietal diameter (BPD) level. The head circumference (HC) is measured using the ellipse method. Note that the ellipse is tracing the outer edge of the fetal cranium, and the lower caliper for BPD measurement is placed at the inner edge of the parietal bone. (OFD= occipito-frontal diameter, GA=gestational age and CI=cephalic index).

TABLE 5.5	Procedures for the Measurement of the Head Circumference

- Activate the biometry software (Calculate knob) on the scanner console, select the HC and a caliper will appear on the screen
- Position the caliper on the outer edge of the proximal parietal bone, similar to the BPD measurement, and set it
- Position the second caliper, symmetrically, on the outer edge of the distal parietal bone, in such a way that the line between the two calipers is at 90° with the midline falx, and set it
- Open up the ellipse by rotating the trackball on the console sideways, until the ellipse is perfectly overlaid on the skull contour
- If the ellipse is not aligned with the ovoid of the fetal head, change the position of the two calipers, which act as hinges

Abdominal Circumference

The Abdominal Circumference (AC) is measured on a transverse section of the upper fetal abdomen. Sonographic landmarks identifying the correct plane for the AC measurement are listed in **Table 5.6** and **Figure 5.5**.

TABLE 5.6	Sonographic Landmarks for the Abdominal Circumference (AC)

- Circular cross section of the abdomen (as circular as possible)
- Spine seen on cross section
- Stomach bubble
- Intra-hepatic portion of the umbilical vein at the level of the portal sinus
- Large sections of fetal ribs seen on each side laterally
- Kidneys not be visualized in the image
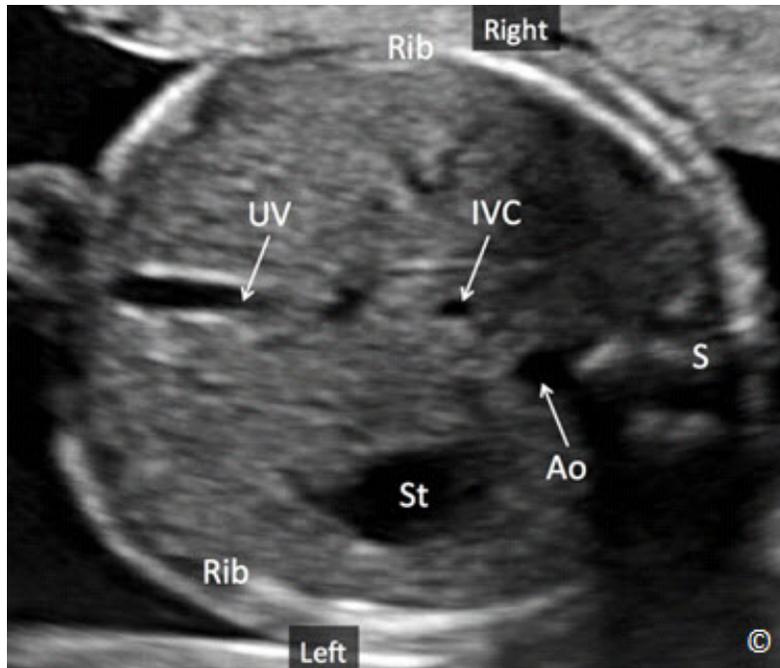
Figure 5.5: Transverse plane of the fetal abdomen at the anatomic level of the abdominal circumference. Note the anatomic landmarks that include the stomach bubble (St), the umbilical vein (UV), the descending aorta (Ao) and the inferior vena cava (IVC). The spine (S) is seen at 3 o'clock and one full rib (Rib) on each side.

Care should be taken to ensure that the cross-section of the abdomen is as circular as possible, in order to avoid errors in the measurement. This is easier in the 2nd than the 3rd trimester, when the fetal limbs or shadowing can indent the abdominal circumference (**Figure 5.6**). The AC is best measured with the fetal spine at 3 or 9 o'clock (**Figure 5.7 A and B**). Avoid measuring the AC if at all possible when the fetal spine is at 6 or 12 o'clock (**Figures 5.6 and 5.8 A and B**). The procedure to measure the AC is shown in **Table 5.7**.
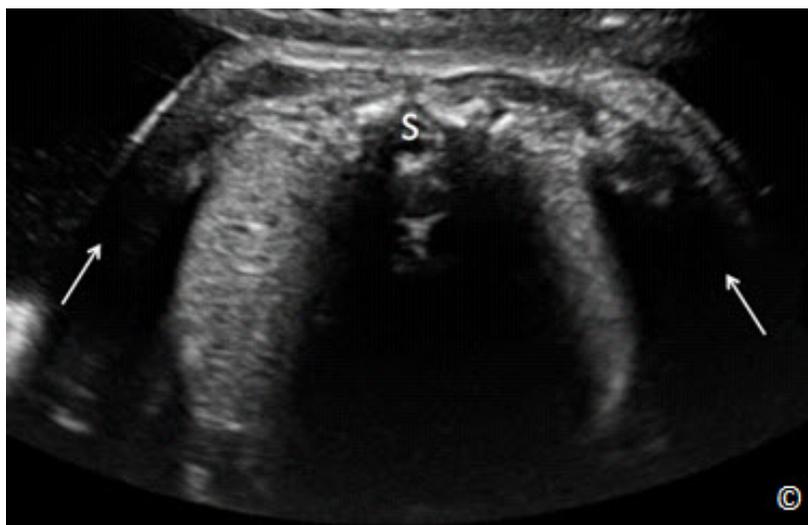
Figure 5.6: Transverse plane of the fetal abdomen at the level of the abdominal circumference (AC) in the third trimester of pregnancy. Note the shadowing (arrows) from upper extremity bones, obscuring the AC lateral borders. The spine (S) is at the 12 o'clock position, which makes optimal measurement of AC difficult.
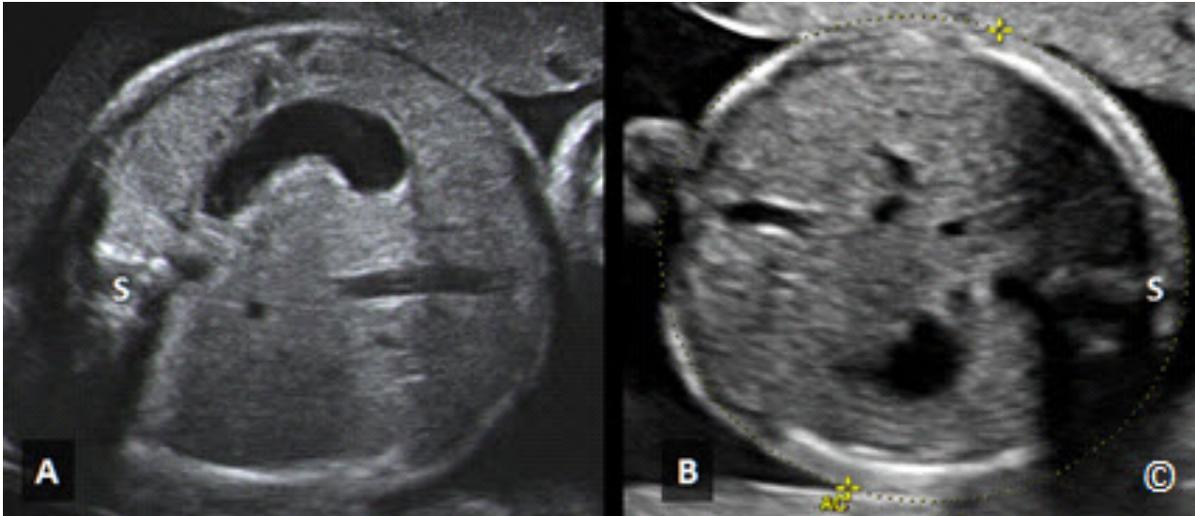
Figure 5.7 A and B: Transverse planes of the fetal abdomen at the level of the abdominal circumference (AC). The spine (S) is at the 9 o'clock position in A and at the 3 o'clock position in B. Spine positions at 9 or 3 o'clock are most optimal for AC measurement as it minimizes shadowing.
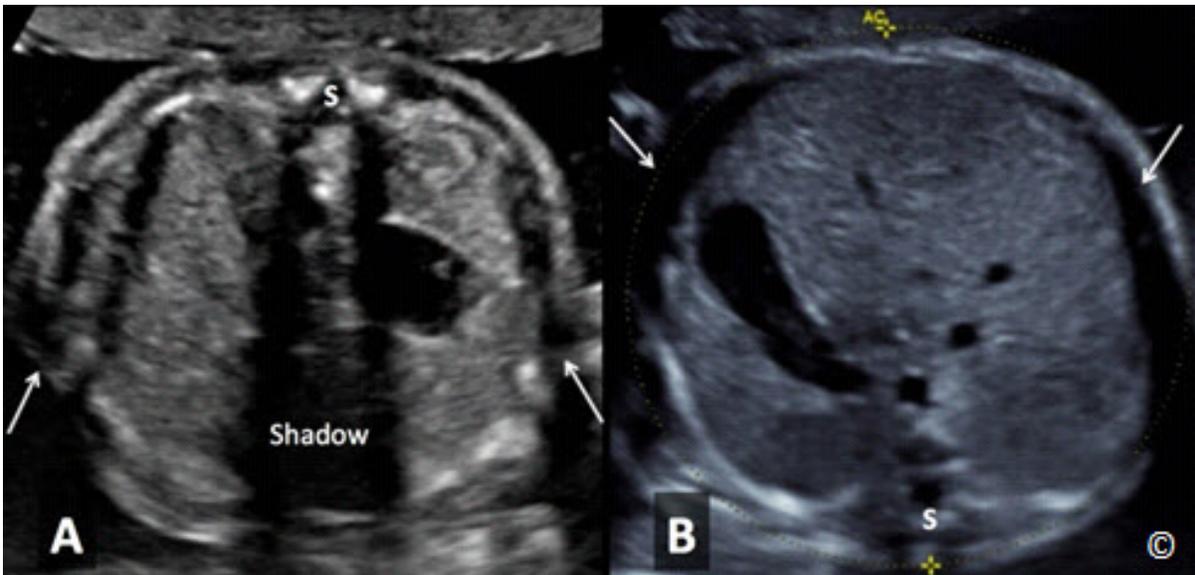
Figure 5.8 A and B: Transverse planes of the fetal abdomen at the level of the abdominal circumference (AC). The spine (S) is at the 12 o'clock position in A and at the 6 o'clock position in B. Spine position at 12 or 6 o'clock is the least optimal for AC measurement as it increases shadowing (A-labeled) and minimizes the ability to assess the lateral borders (arrows) (A and B) due to decrease in lateral resolution and rib shadowing.

TABLE 5.7	Procedures for the Measurement of the Abdominal Circumference (AC)

- Activate the biometry software on the scanner console (Calculate knob), select the AC and a caliper will appear on the screen
- Position the caliper on the outer surface of the skin line, on the proximal side of the fetal abdomen, roughly at the level of the rib end, and set it
- Position the second caliper, symmetrically, on the distal surface of the skin line, in such a way that the line between the two calipers is at 90° with the midline, and set it
- Open up the ellipse by rotating the trackball on the console sideways, until the ellipse is perfectly overlaid on the skin contour. Ensure to include the outer edge of the skin contour with the measurement
- If the ellipse is not aligned with the cutaneous outline of the abdomen, change the position of the two calipers, which act as hinges

Femur Length

In order to optimize the measurement of the Femur Length (FL), the whole femur diaphysis should be displayed on the screen, and the angle between the insonating beam and the shaft of the femur should be kept in the range of 45-90° in order to avoid underestimating the length of the femur due to ultrasound wave deflection (**Figure 5.9**). The longest visible diaphysis should be measured by placing each caliper at the end of the ossified diaphysis without including the distal femoral epiphysis, if visible (**Figure 5.10**). Femur measurement should exclude triangular spur artefacts that can falsely extend the diaphysis length (**Figure 5.10**).
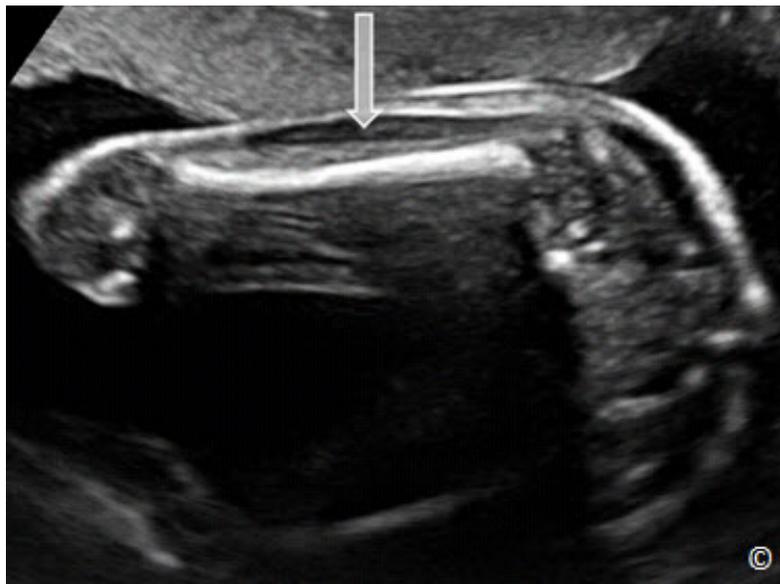
Figure 5.9: Optimal imaging of the femur for length measurement. Note that the whole femur diaphysis is seen and the angle between the insonating beam (arrow) and the shaft of the femur is almost 90 degrees.
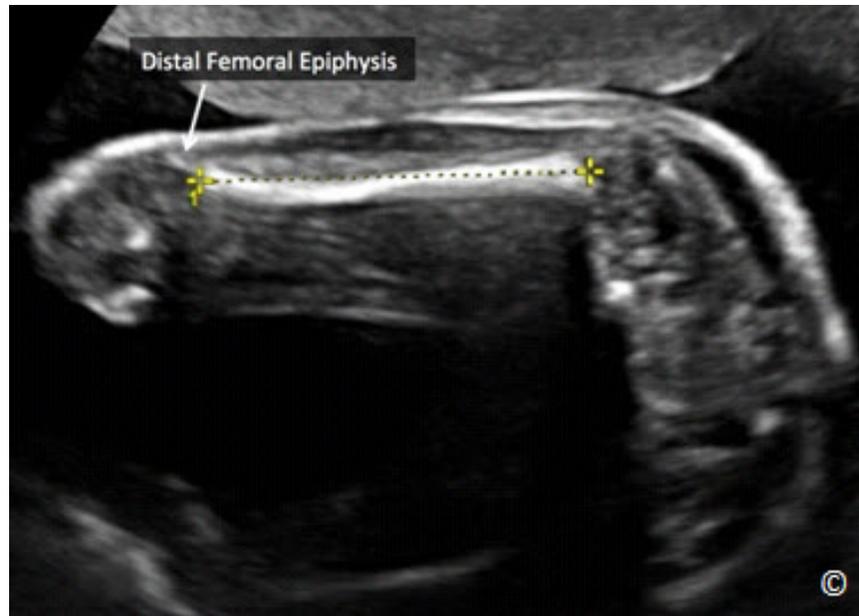
Figure 5.10: Femur length measurement. Note that the longest visible diaphysis is measured by placing each caliper at the end of the ossified diaphysis without including the distal femoral epiphysis (labeled).

It is important to note that imaging of the long axis of the femur can be more technically difficult than the BPD, HC and AC. Consideration should therefore be given to delay the introduction of the FL to the basic ultrasound examination, until more technical expertise is acquired by novice ultrasound operators. If this course is chosen, formula for EFW that does not utilize FL should be activated in the ultrasound equipment.

Estimating Fetal Weight

Once the four measurements described above have been calculated, the software of the ultrasound equipment derives the estimated fetal weight (EFW), using a mathematical formula. Hadlock et al is the formula that is most commonly used for EFW and was developed in the late 1980s (1). Calculating the EFW is more accurate in the second trimester than the third trimester but EFW is clearly of lesser clinical relevance in the second trimester. In the 3rd trimester, EFW is of crucial importance to detect fetal growth restriction or macrosomia. The estimation of macrosomia is not very accurate and the error can exceed 10% (2). Detailed discussion on estimation of fetal weight will be presented in the following chapter.

Basic Fetal Anatomy

Although fetal anatomy is part of the basic ultrasound examination as defined by national and international organizations (3, 4), in some low-resource (outreach) settings, the primary objective of the second trimester ultrasound is to identify high-risk pregnancies at increased risk for neonatal and maternal morbidity and mortality. To that end, review of basic fetal anatomy is typically not part of the basic ultrasound examination in that setting. Basic fetal anatomy is presented in this chapter for completeness sake and also as it is part of the basic ultrasound examination in the second and third trimester in many countries. Placental appearance, its location within the uterine cavity, amniotic fluid assessment and the adnexae are also part of the basic ultrasound examination. They are covered in separate chapters later in the book. **Table 5.8** shows a list of basic fetal anatomy for the second trimester ultrasound.

For more information on the practice guideline for the performance of the basic obstetric ultrasound examination, visit the American Institute of Ultrasound in Medicine (www.AIUM.org) and the International Society of Ultrasound in Obstetrics and Gynecology (www.ISUOG.org) websites (3, 4).

TABLE 5.8	List of Basic Fetal Anatomy in the Second Trimester of Pregnancy

- HEAD
    - o Lateral cerebral ventricles, Choroid plexus, Midline falx, Cavum septae pellucidi, Cerebellum, Cistern magna; and Upper lip and philtrum.
- CHEST
    - o Heart; Four-chamber view, Left ventricular outflow tract, Right ventricular outflow tract and Lung fields.
- ABDOMEN
    - o Stomach (presence, size, and situs), Kidneys, Urinary bladder, Umbilical cord insertion into the fetal abdomen, and Umbilical cord vessel number.
- SKELETAL
    - o Cervical, Thoracic, Lumbar, and Sacral spine.
- Extremities
    - o Legs and Arms
- PLACENTA
- AMNIOTIC FLUID
- ADNEXAE

Head anatomy

Three axial sonographic planes are needed to assess the head anatomy: the plane at the level of the lateral ventricles (**Figure 5.11**), the plane at the level of the BPD (**Figure 5.2**), and the plane at the level of the posterior fossa (**Figure 5.12**).
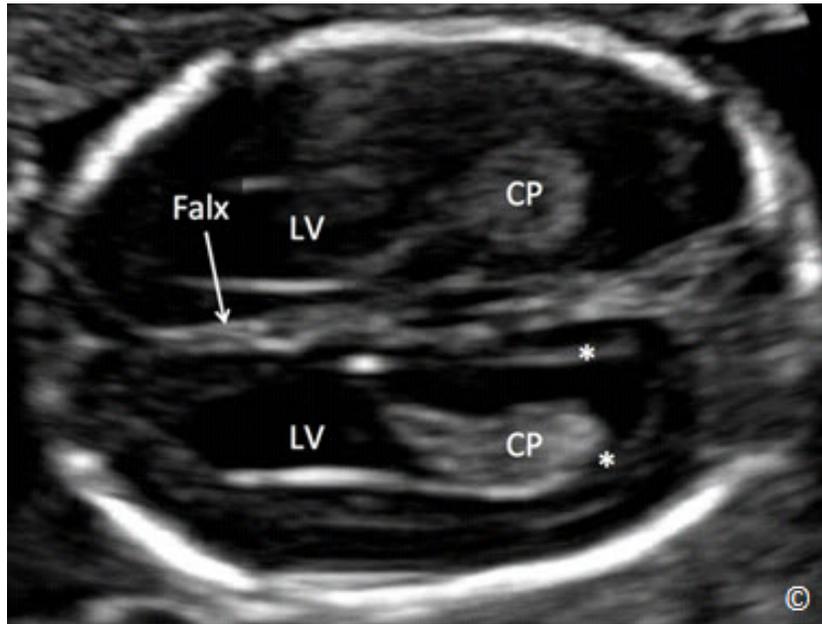
Figure 5.11: Transverse plane of the fetal head at the level of the lateral ventricles (LV). Sonographic landmarks for LV measurement include the LV, the cavum septae pellucidi and the midline falx (labeled). The LV is measured at the level of the atrium (asterisks). CP = Choroid Plexus.
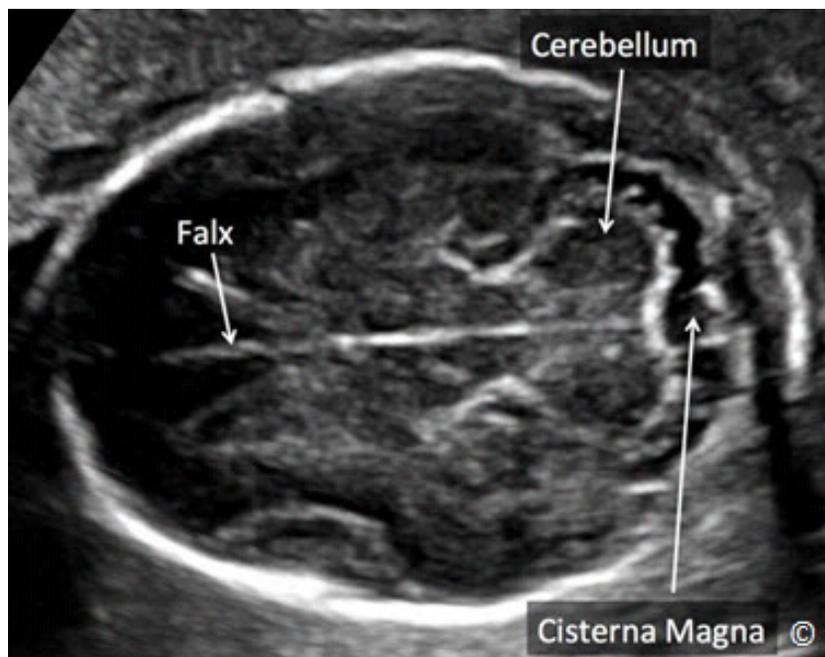
Figure 5.12: Transverse plane of the fetal head at the level of the posterior fossa. Sonographic landmarks include the cerebellum, cisterna magna and falx (labeled).

Plane at level of Lateral Ventricles

This represents an axial view of the fetal head, at the level of the lateral ventricles (**Figure 5.11**). Sonographic landmarks identifying the correct anatomic plane include the lateral ventricles, the cavum septae pellucidi and the midline falx (**Figure 5.11**). On this view, the width of the atrium of the distal lateral ventricle should be measured (**Figure 5.11**). Visualization of the proximal lateral ventricle is obscured by proximal parietal bone shadowing (**Figure 5.11**). The atrium of the lateral ventricle should be measured at the level shown in **Figure 5.11** and should be equal to or <10.0 mm. anytime in gestation. Ventriculomegaly is defined by a lateral ventricular measurement of greater than 10 mm and is the most common intracranial malformation (**Figure 5.13**) diagnosed prenatally. Ventriculomegaly is associated with many intracranial malformations and with fetal aneuploidy and its finding should therefore result in a targeted ultrasound examination of fetal anatomy and counselling for fetal aneuploidy testing. Holoprosencephaly, which results from failure of division of the prosencephalon during early embryogenesis into two lateral ventricles, can also be detected in this plane (**Figure 5.14 A and B**). Anencephaly (absence of brain tissue associated with absent calvarium) (**Figure 5.15 A and B**) and encephalocele (**Figure 5.16 A and B**), (localized defect of cranium – neural tube defect), can also be detected in this plane.
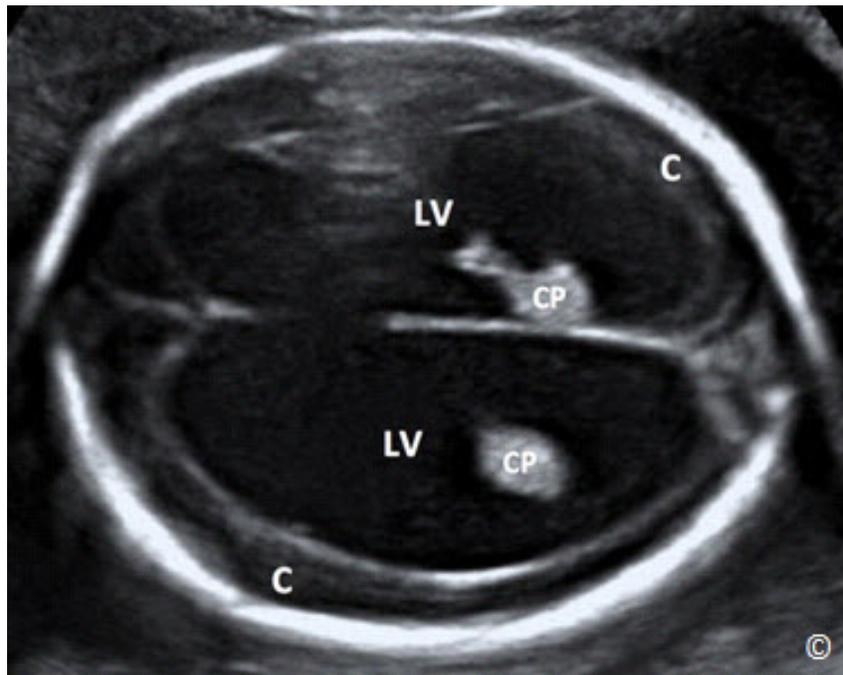
Figure 5.13: Transverse plane of the fetal head at the level of the lateral ventricles (LV) in a fetus with bilateral ventriculomegaly. Note the enlarged lateral ventricles (LV) and compressed cerebral cortex (C) and choroid plexus (CP).
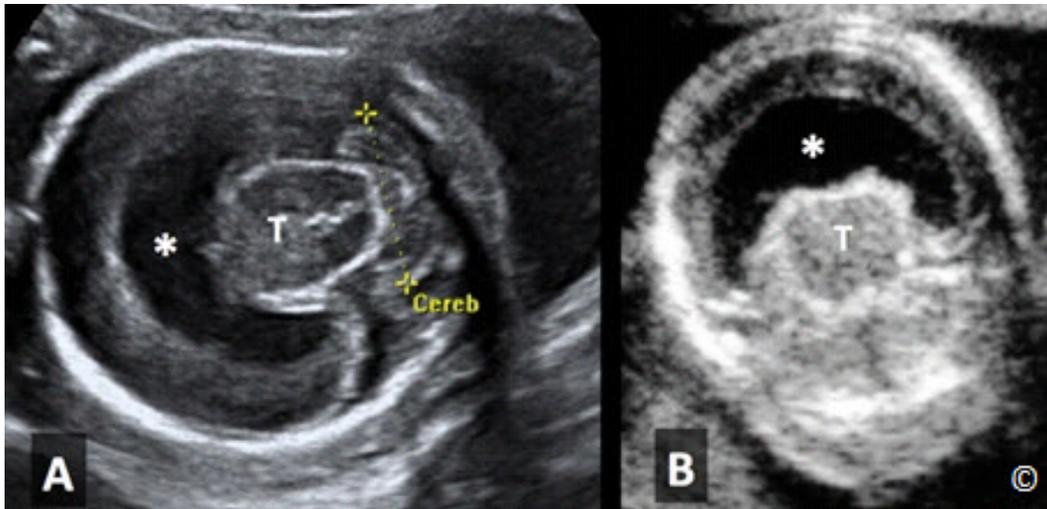
Figure 5.14 A and B: Holoprosencephaly in 2 fetuses shown in a transverse plane (A) and coronal plane (B) of the fetal head. A single ventricle is seen (asterisk) with fused thalami (T). Note a hypoplastic cerebellum (Cereb) in A (not typically a feature of holoprosencephaly).
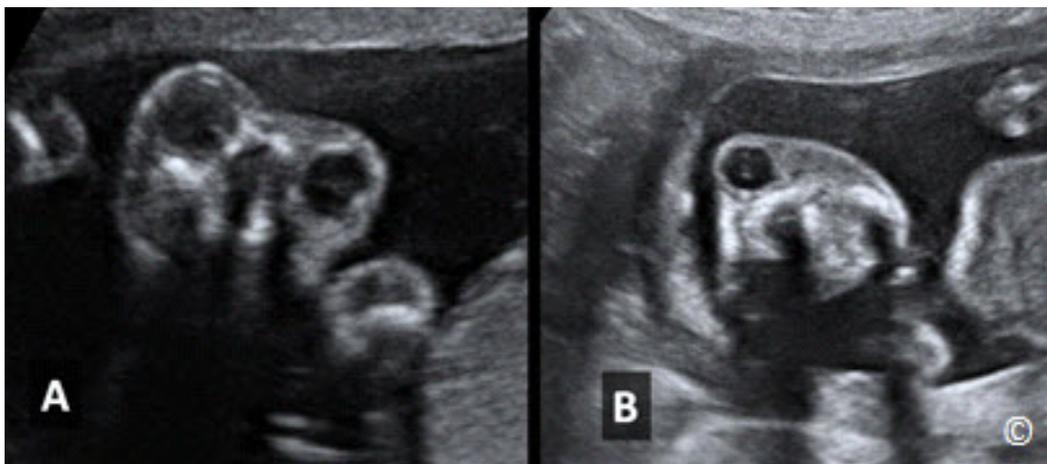
Figure 5.15 A and B: Imaging of the fetal head in 2 fetuses with anencephaly (A and B). Note the absence of fetal cranium and normal brain tissue.
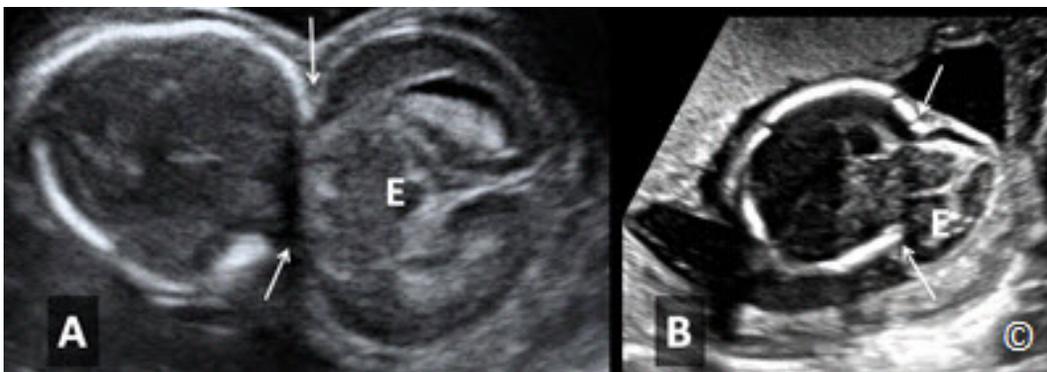
Figure 5.16 A and B: Transverse planes of the fetal head in 2 fetuses (A and B) with encephaloceles (E). Note the location of the cranial defect (arrows), in the occipital aspect of the cranium, which is the most common location for such defects. Brain tissue can be seen in both encephaloceles (E).

Plane at level of Posterior Fossa

The plane at the level of the posterior fossa, also known as the trans-cerebellar plane, is an axial (or slightly oblique) view at the level of the posterior fossa (**Figure 5.17**). In this plane you can see the cerebellum, the cisterna magna, and the 3rd and 4th ventricles (**Figure 5.17**). This plane is easily obtained by angling the ultrasound transducer posteriorly about 45 degrees from the BPD plane while avoiding shadowing from the cranial bone. The most common abnormalities detected in this view represent the Dandy-Walker malformation (**Figure 5.18**), cerebellar vermis dysgenesis (**Figure 5.19**) and the Chiari II malformation (**Figure 5.20**) (typical of spina bifida). Occasionally, posterior, small occipital encephaloceles may only become evident in this scanning plane. Spina bifida (with Chiari II malformation) (**Figure 5.20, 5.21 A and B**) requires neonatal surgery both to cover the spinal defect and to shunt the commonly associated obstructive ventriculomegaly.
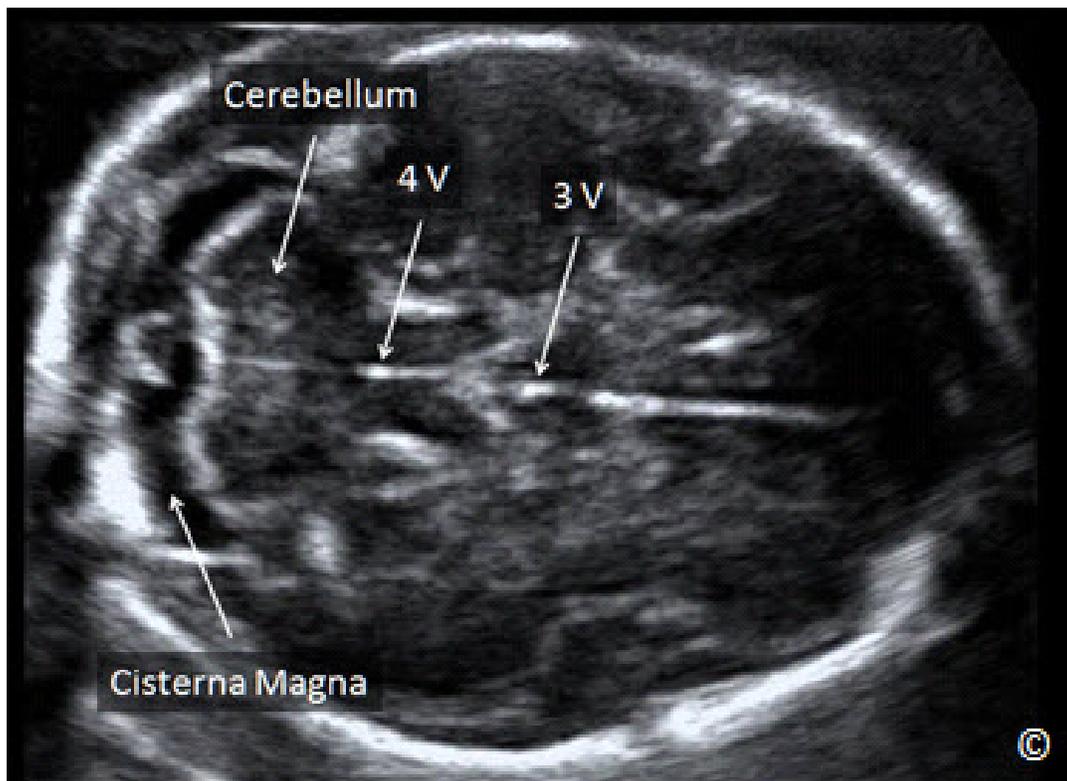
Figure 5.17: Transcerebellar plane of the fetal head (transverse – oblique). The posterior fossa contains the cerebellum and cisterna magna (labeled). The 4th and 3rd ventricles (4V and 3V) are seen in this plane.
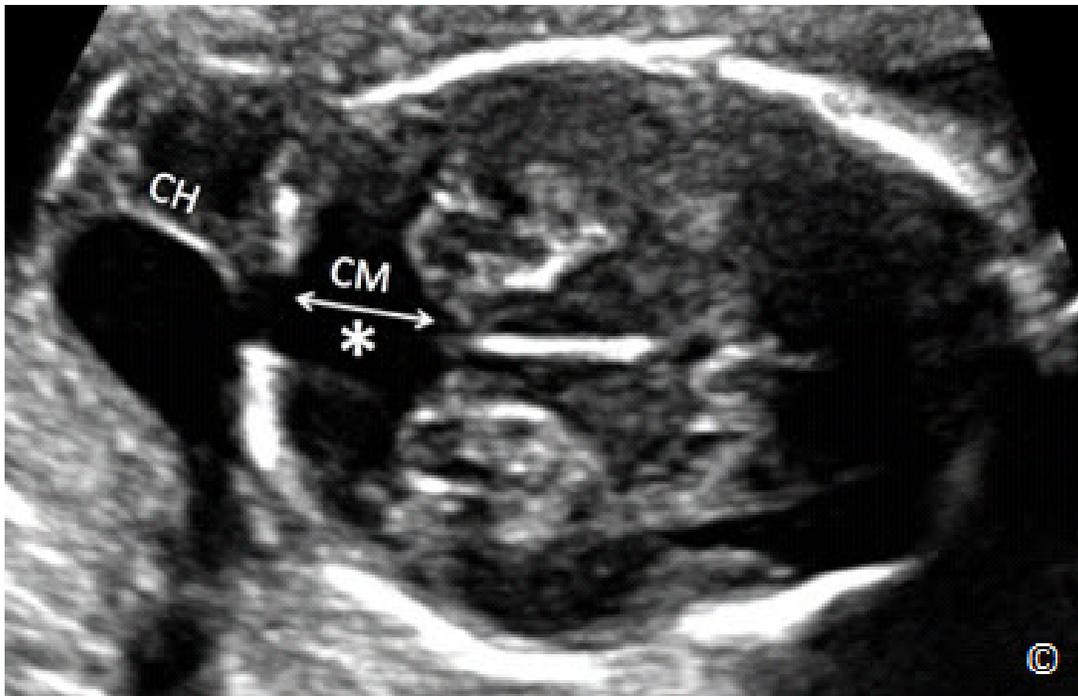
Figure 5.18: Transcerebellar plane of a fetus with Dandy Walker malformation (asterisk). Note the absence of the cerebellum and enlargement of cisterna magna (CM). Note the presence of a cystic hygroma (CH) in this fetus.

Figure 5.19: Transcerebellar plane of a fetus with cerebellar vermis dysgenesis (asterisk). Note the absence of the cerebellar vermis (CV) with enlargement of cisterna magna (asterisk).
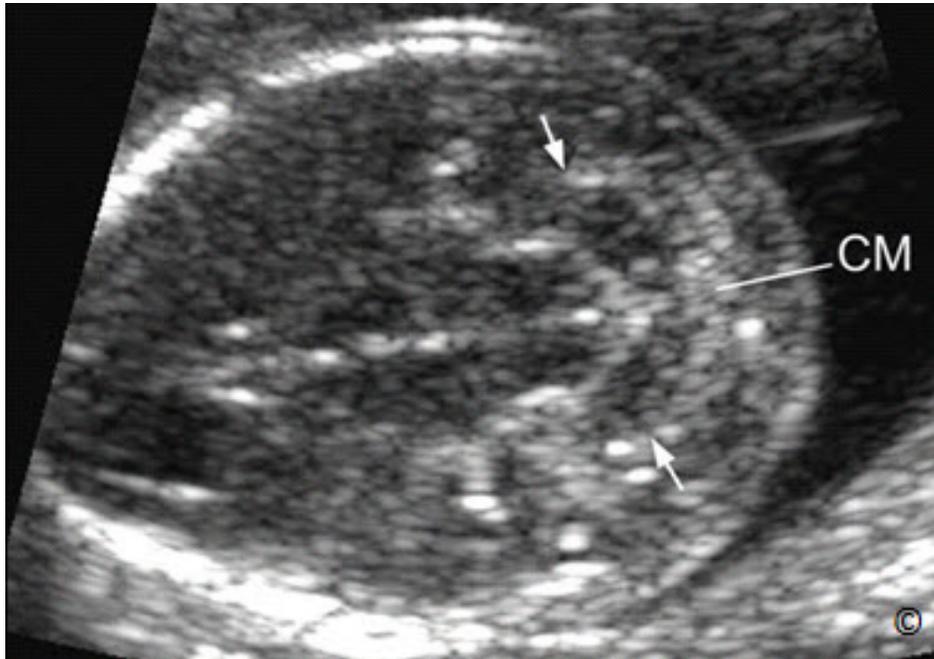
Figure 5.20: Transcerebellar plane of a fetus with spina bifida showing the posterior fossa changes (Chiari II). Note the obliteration of the cisterna magna (CM) and abnormal shape of the cerebellum (arrows).
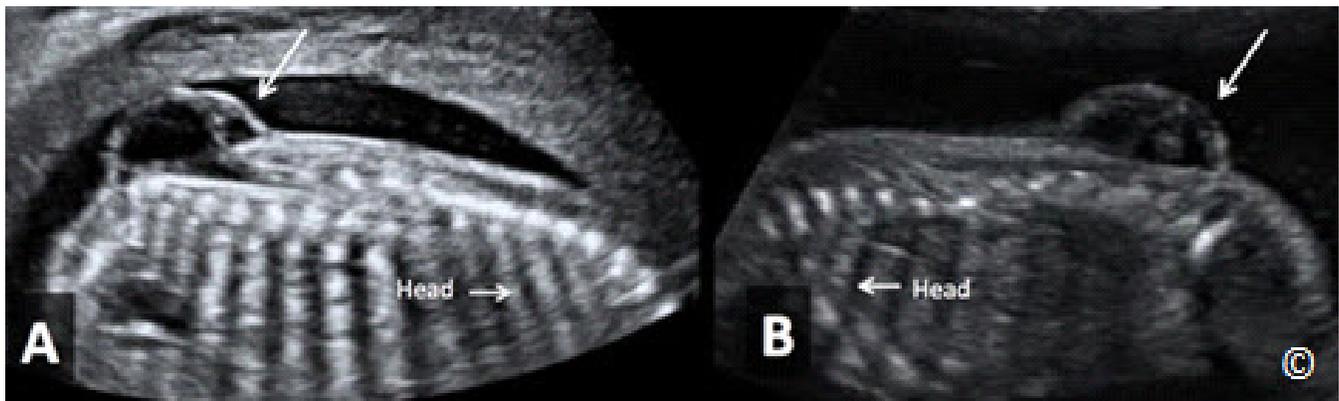
Figure 5.21 A and B: Longitudinal (Mid-sagittal) planes of the fetal spine in 2 fetuses (A and B) with spina bifida. Note the lumbo-sacral locations of the spinal defects (arrows).

Plane at level of Biparietal Diameter

The sonographic landmarks identifying the correct BPD plane have been previously described in this chapter (**Figure 5.2**) and include the midline falx, the cavum septae pellucidi and the thalami. Abnormalities detected in this plane include ventriculomegaly (**Figure 5.22 A and B**), holoprosencephaly (**Figure 5.14**), agenesis of the corpus callosum (**Figure 5.23**) and septo-optic dysplasia (**Figure 5.24**). Other rare intracranial abnormalities, such as tumors, can also be detected in this plane. Comprehensive evaluation of the fetal central nervous system requires

multiple views of the fetal brain from its sagittal, coronal and axial (transverse) views and through the abdominal and transvaginal (when feasible) approach.
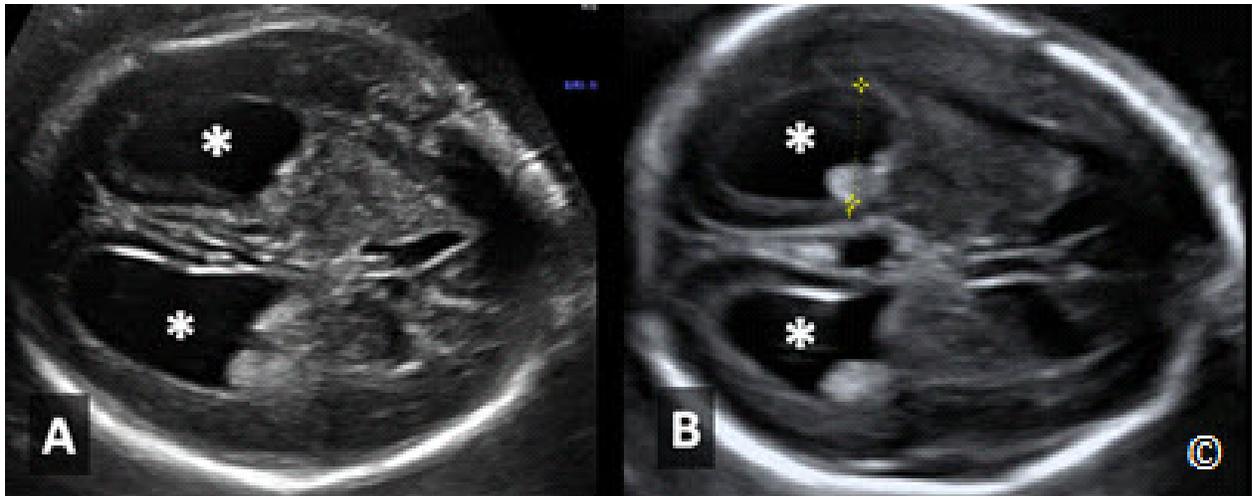
Figure 5.22 A and B: Transverse plane of the fetal head) in 2 fetuses with bilateral ventriculomegaly (asterisks). Note the enlarged lateral ventricles (asterisks).
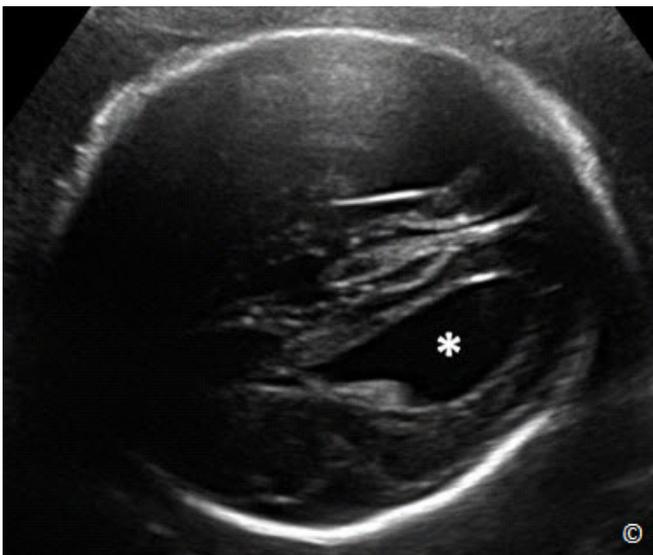
Figure 5.23: Transverse plane of the fetal head at the level of the lateral ventricles in a fetus with agenesis of the corpus callosum (ACC). Note the tear-shaped lateral ventricle (asterisk), a characteristic of ACC.
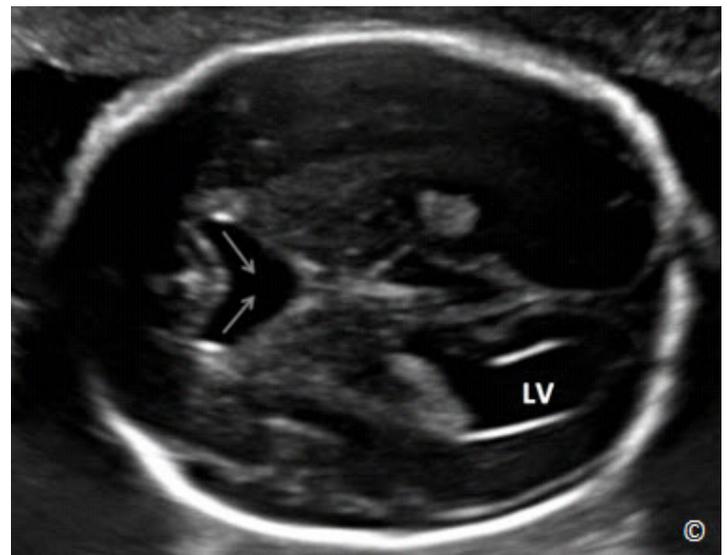
Figure 5.24: Transverse plane of the fetal head at the level of the BPD in a fetus with septo-optic dysplasia. Note the absence of cavum septae pellucidi and fusion of frontal horns of the lateral ventricles (arrows). LV= left ventricle.

Facial Anatomy

Basic sonographic anatomy of the face can be primarily achieved by the evaluation of the orbits and the upper lip and philtrum.

Plane at level of Fetal Face

The evaluation of the fetal face can be obtained by rotating the transducer 90 degrees from the BPD plane and sliding tangentially to view the two orbits and then the upper lip and philtrum. The bi-ocular plane is a tangential plane of the fetal head at the level of the orbits (**Figure 5.25**). The tangential view of the lips (**Figure 5.26**) allows for the detection of facial clefting (**Figure 5.27**). The mid-sagittal view of the facial profile (**Figure 5.28**) is important as it allows for evaluation of the fetal lower chin, is recognized by mothers and may play a role in maternal-fetal bonding.

Figure 5.25: Tangential plane of the fetal head at the level of the orbits. Outer (1) and inner (2) ocular diameters can be measured in this plane.

Figure 5.26: Tangential plane of the fetal face showing the soft tissue of the upper lip, philtrum and lower lip (labeled).
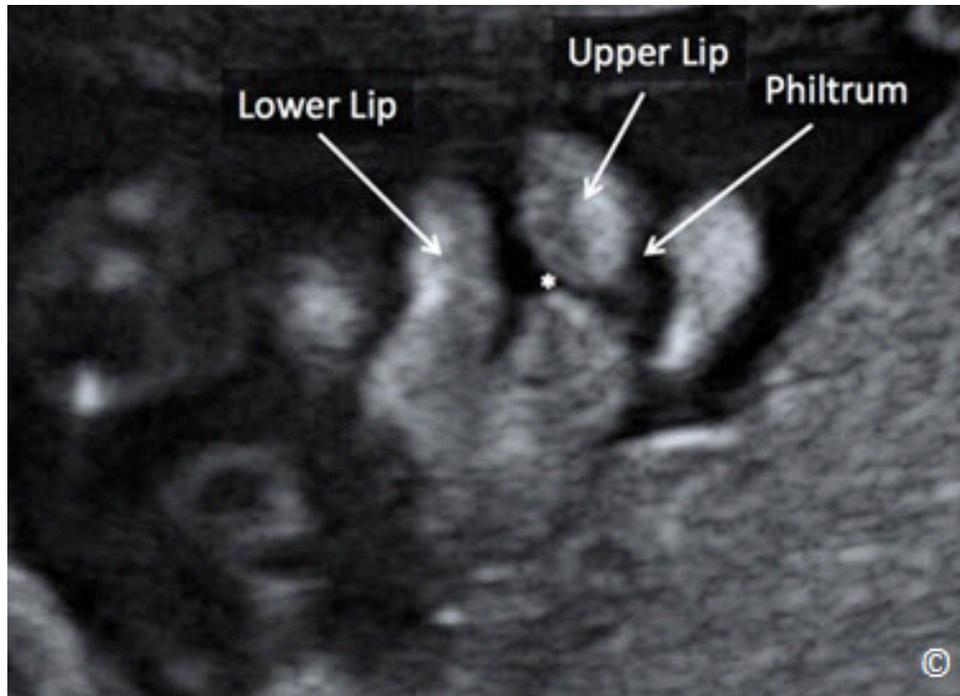
Figure 5.27: Tangential plane of the fetal face showing the soft tissues of the upper lip, philtrum and lower lip in a fetus with left cleft lip (asterisk).
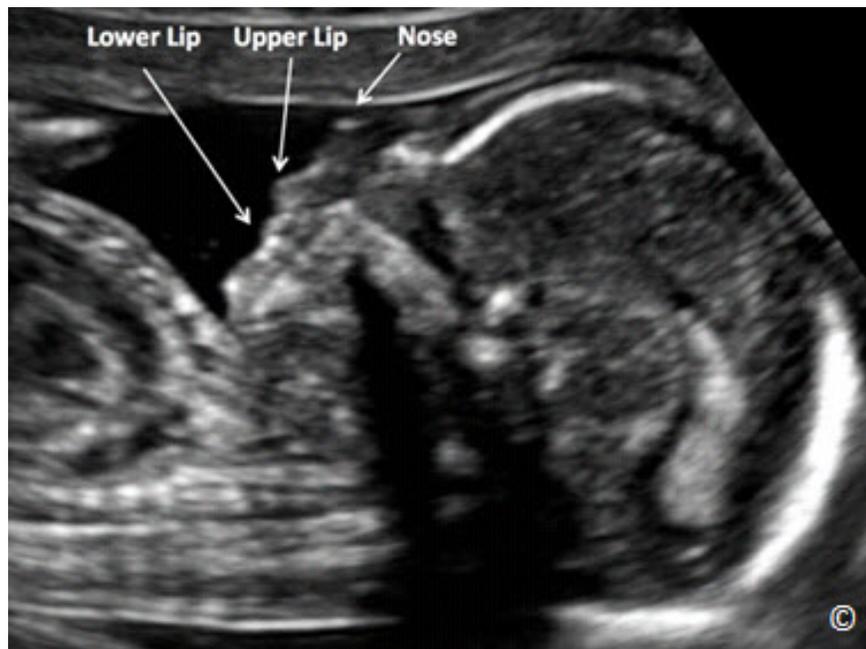
Figure 5.28: Midsagittal view of the fetal head and face. Note the recognizable fetal profile that includes the tip of the nose, the upper lip, and lower lip (labeled).

Chest Anatomy

The plane required to assess both the lungs and the heart is the 4-chamber view, which corresponds to an axial view of the chest at the level of the heart (**Figure 5.29**). **Table 5.9** lists the sonographic landmarks of the four-chamber view plane.
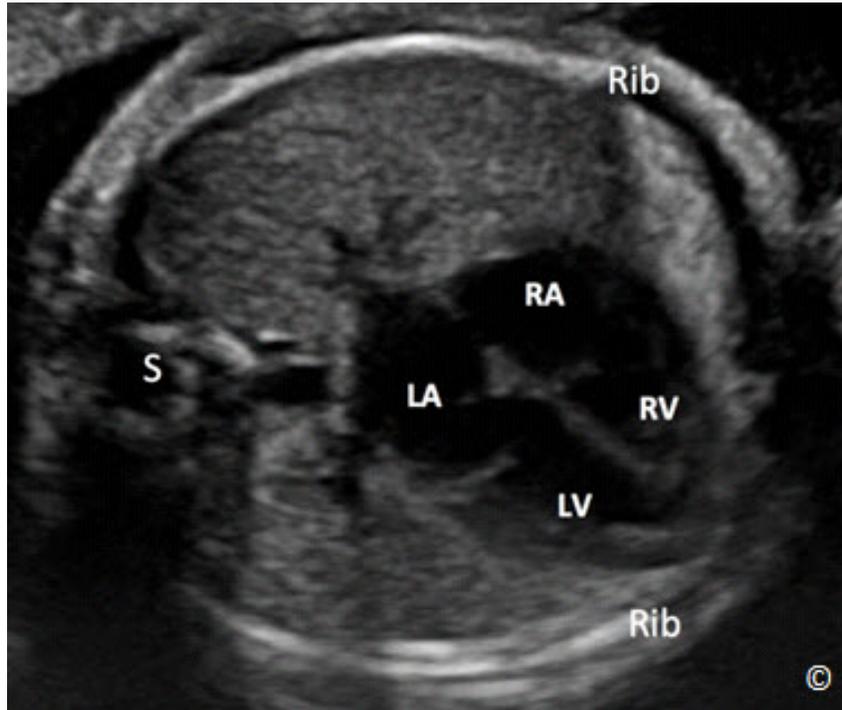
Figure 5.29: Axial (transverse) view of the fetal chest at the level of the four-chamber view. Note the presence of one full rib on each lateral border (Rib). S= spine, LA= left atrium, RA= right atrium, LV= left ventricle and RV= right ventricle.

TABLE 5.9	Sonographic Landmarks of the Four-Chamber View Plane

- One full rib on each side of the chest
- Four-chamber view
- Heart occupies 1/3 of thoracic area
- Heart rotated to left with cardiac axis at 45 +/-20°

In this plane, the cardiac chamber that is the most posterior is the left atrium, whereas the cardiac chamber just below the sternum is the right ventricle (**Figure 5.29**). Major anomalies that can be identified in this view include cardiac and pulmonary malformations. Common congenital heart abnormalities that can be detected on the 4-chamber view include ventricular hypoplasia (right or left) (**Figure 5.30**), large septal defects (atrio-ventricular septal defect) and severe outflow tract obstructions (pulmonary valvular atresia or critical aortic stenosis). Most of these cardiac defects require neonatal cardiac surgery because of ductus-dependency. Atrio-ventricular septal defect does not represent a neonatal emergency, but is associated with Down syndrome in up to 60% of the cases. Most common chest lesions include: diaphragmatic hernia (**Figure 5.31**); cystic and hyperechoic lesions of the lung, such as Congenital Cystic Adenomatoid Malformation (C-CAM, cystic or solid type) (**Figure 5.32**); extra-lobar sequestration (**Figure 5.33**); and pleural effusions (**Figure 5.34**). Some of these lesions are benign and often regress spontaneously by the time of birth. Pleural effusions, if in the context of non-immune hydrops fetalis, can lead to fetal or neonatal demise. Diaphragmatic hernia needs early post-natal surgery, with survival rates of roughly 50 - 70% in tertiary centers.
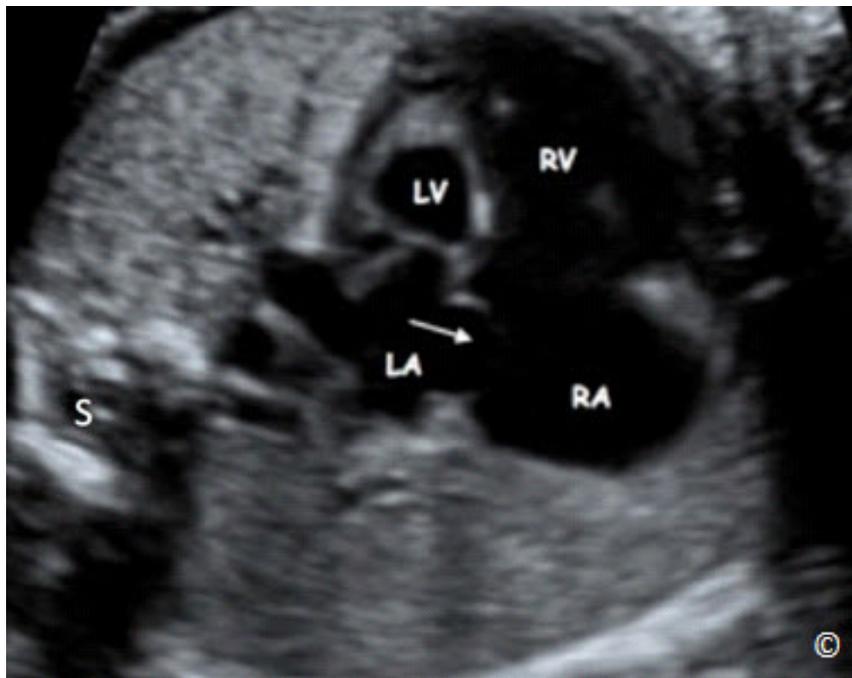
Figure 5.30: Four-chamber view plane of a fetus with hypoplastic left heart syndrome. Note the diminutive size of the left ventricle (LV). Arrow points to the foramen ovale that typically displays reverse flow in this condition. S = spine, LA= left atrium, RA= right atrium, and RV= right ventricle.
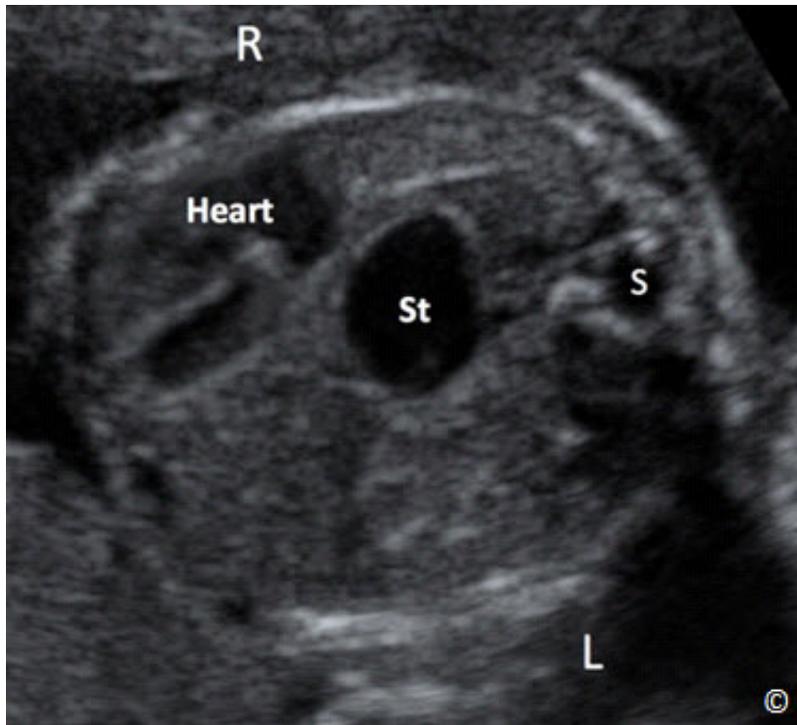
Figure 5.31: Transverse plane of the chest in a fetus with congenital diaphragmatic hernia. Note the upward displacement of the stomach (St) into the chest. The heart (labeled) is pushed into the right chest. S = spine, R=right, L=left.
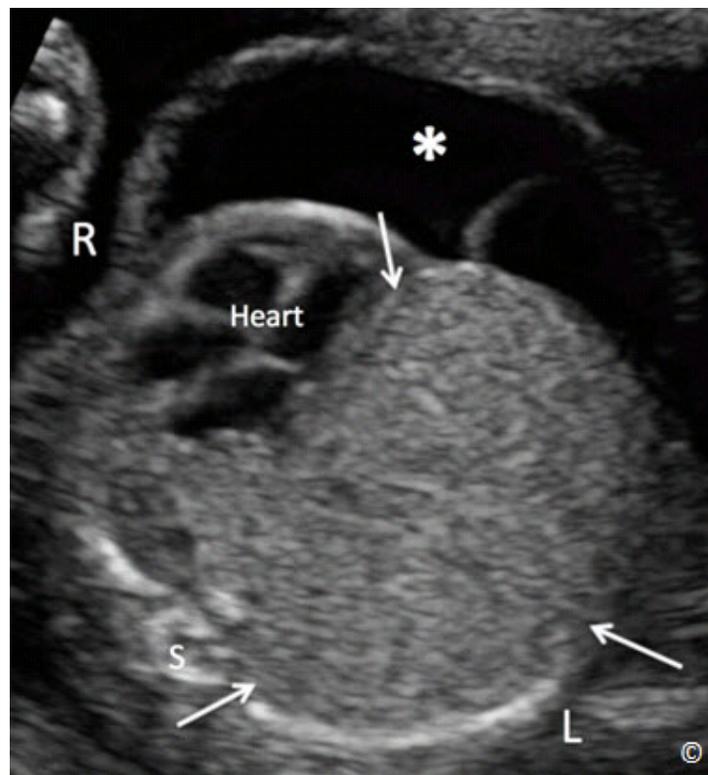
Figure 5.32: Transverse plane of the fetal chest at the level of the four-chamber view in a fetus with congenital cystic adenomatoid malformation of the left lung. Note the large echogenic lung mass (arrows) associated with fetal ascites (asterisk). The heart is shifted to the right chest. R = right, L = left and S = spine.
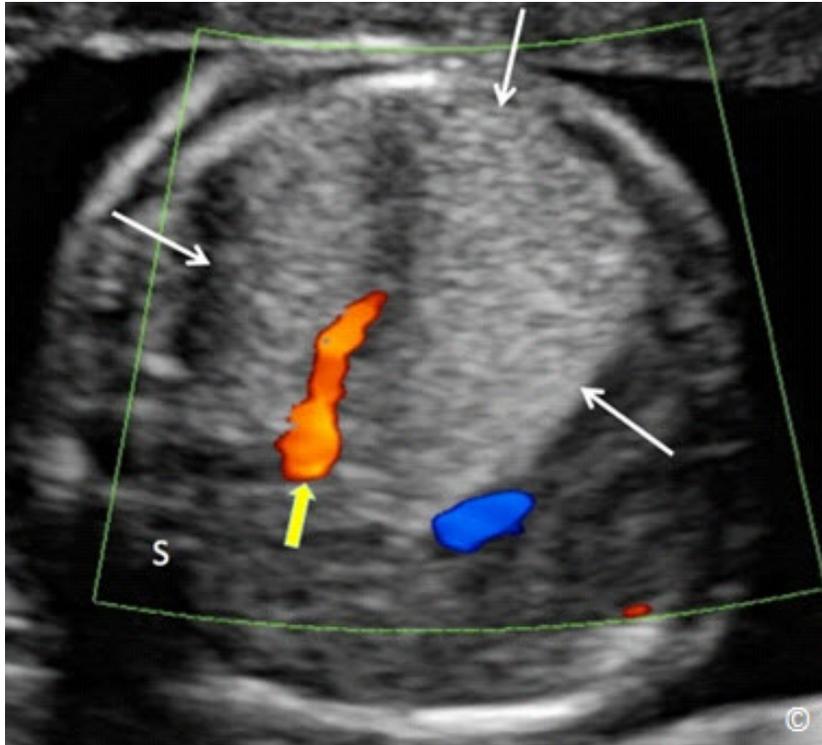
Figure 5.33: Transverse plane of the chest in 2D and color Doppler modes in a fetus with pulmonary sequestration (white arrows). Note the vascular supply (yellow arrow) that typically arises from the systemic circulation. S = spine
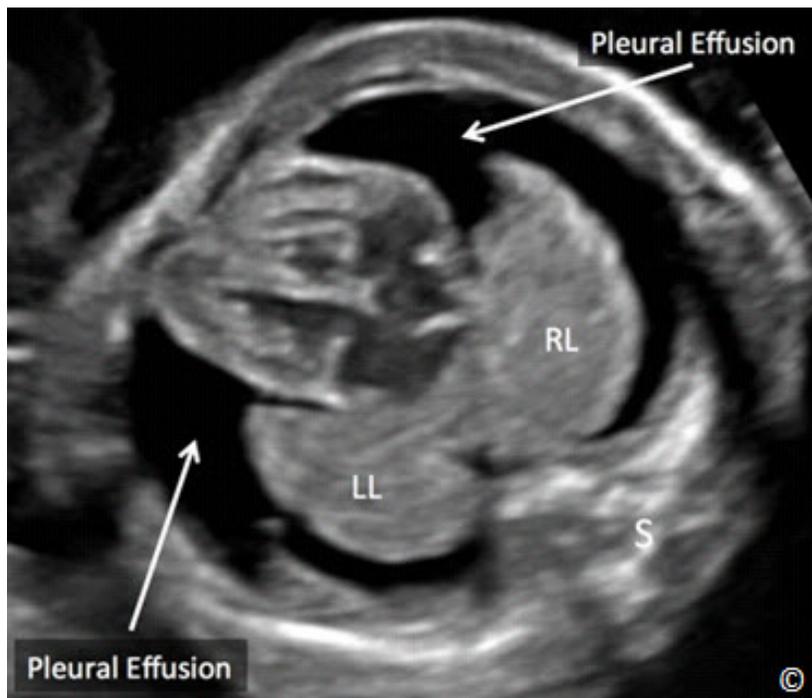
Figure 5.34: Transverse view of the fetal chest at 23 weeks' gestation showing bilateral pleural effusions (arrows). Pleural effusions regressed spontaneously and resolved in this fetus with follow-up ultrasound examinations. S = spine, RL = right lung, LL = left lung.

Abdominal Anatomy

The stomach is visualized on the transverse view in which the AC is measured. Persistent, non-visualization of the stomach is typically a sign of esophageal atresia, whereas double bubble is a sign of duodenal atresia (**Figure 5.35**). Wall abnormalities include exomphalos (omphalocele) (**Figure 5.36**) and gastroschisis (**Figure 5.37 A and B**). All these anomalies are usually non-life threatening, but require early neonatal surgery. Some major kidney anomalies are associated with significant decrease in amniotic fluid such as bilateral renal agenesis (**Figure 5.38 A and B**), infantile polycystic disease (**Figure 5.39 A - C**), and bladder outlet obstruction (**Figure 5.40 A and B**). Hydronephrosis, from reflux or pyelo-ureteral obstruction (**Figure 5.41**) is generally less severe.
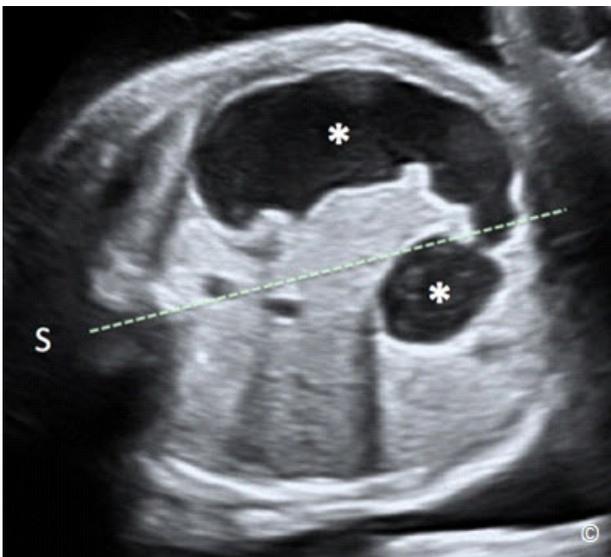
Figure 5.35: Transverse plane of the abdomen in a fetus with duodenal atresia. Note the enlarged stomach that crosses the midline (dashed line) and is shaped in a double bubble (asterisks). S = spine.
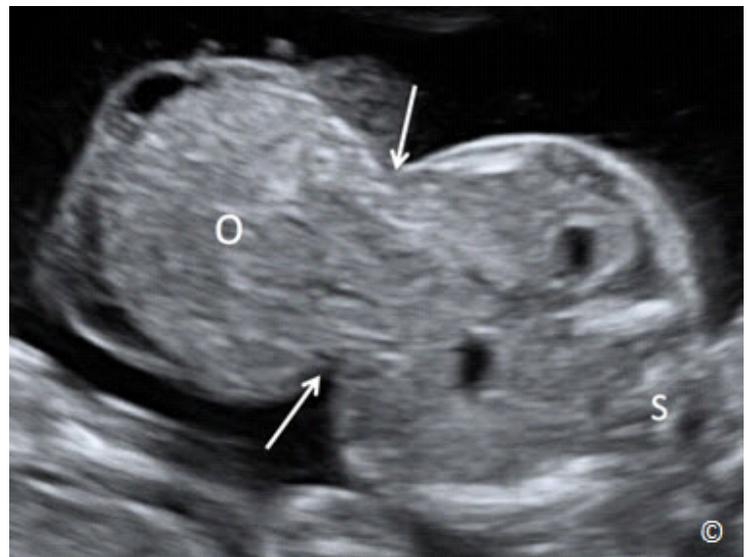
Figure 5.36: Transverse plane of the fetal abdomen in a fetus with an omphalocele (O). Note the central location of the defect in the abdomen (arrows). S = spine.
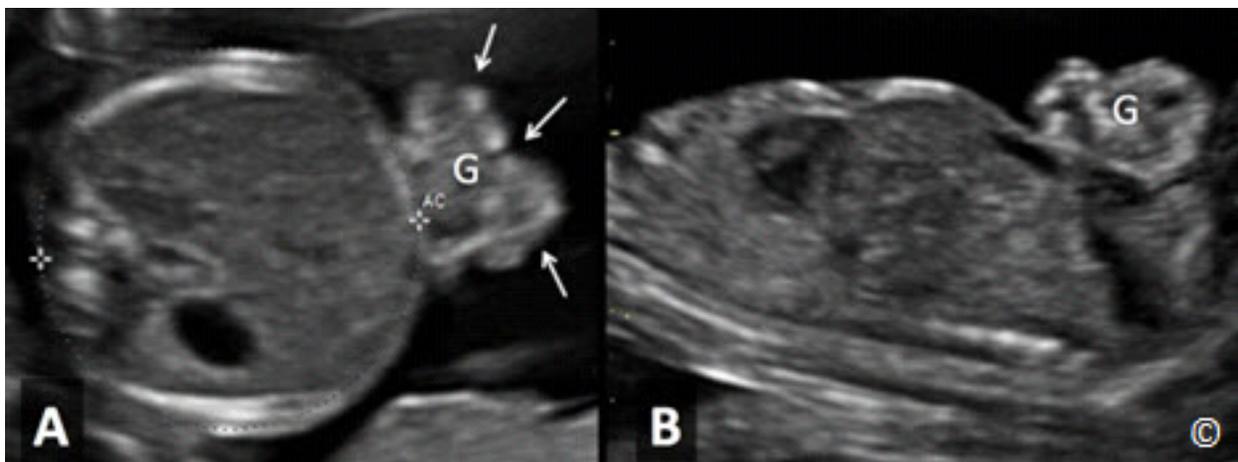
Figure 5.37 A and B: Transverse (A) and midsagittal (B) planes of a fetus with gastroschisis (G). Note the lack of a membrane cover of the gastroschisis (arrows). AC = Abdominal Circumference.
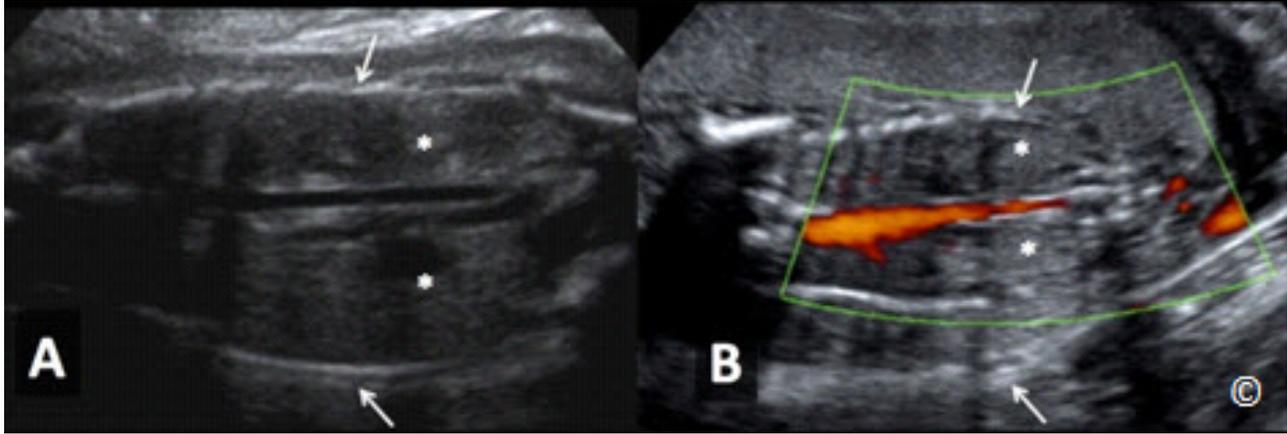
Figure 5.38 A and B: Coronal planes of the abdomen in 2D (A) and color Doppler (B) modes in a fetus with bilateral renal agenesis. Note the presence of anhydramnios (arrows) and absence of kidneys (asterisks) in the renal fossa. Note the absence of renal arteries on color Doppler (B).
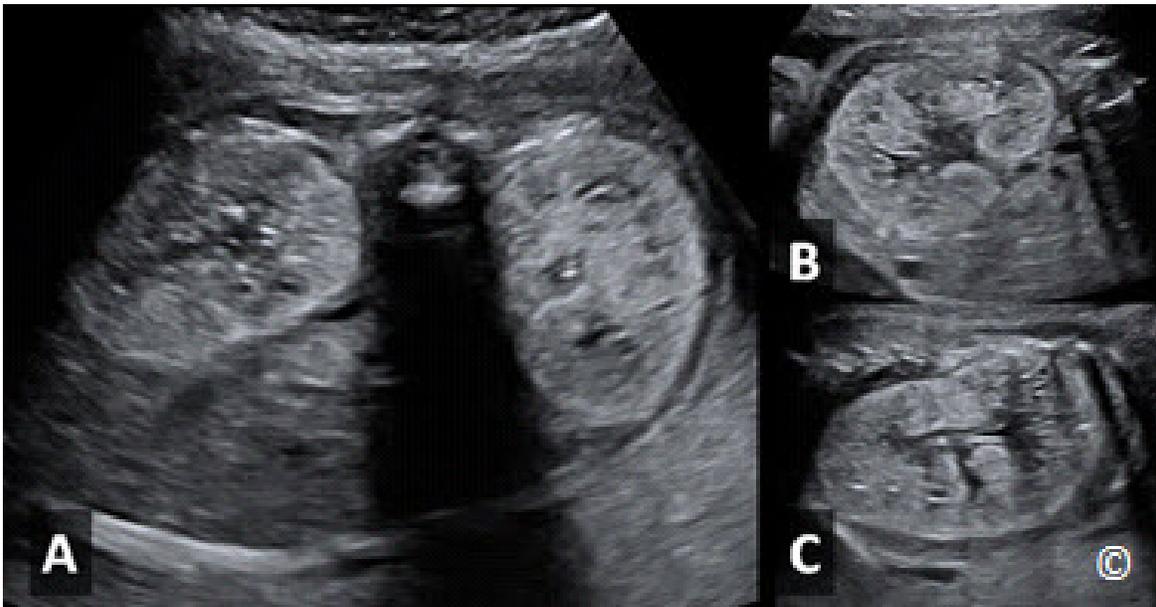
Figure 5.39 A, B, and C: Transverse (A) and longitudinal (B and C) views of the kidneys in a fetus with infantile polycystic kidney disease. Note the enlarged size of both kidneys and increase in echogenicity. There is also associated anhydramnios (not shown).
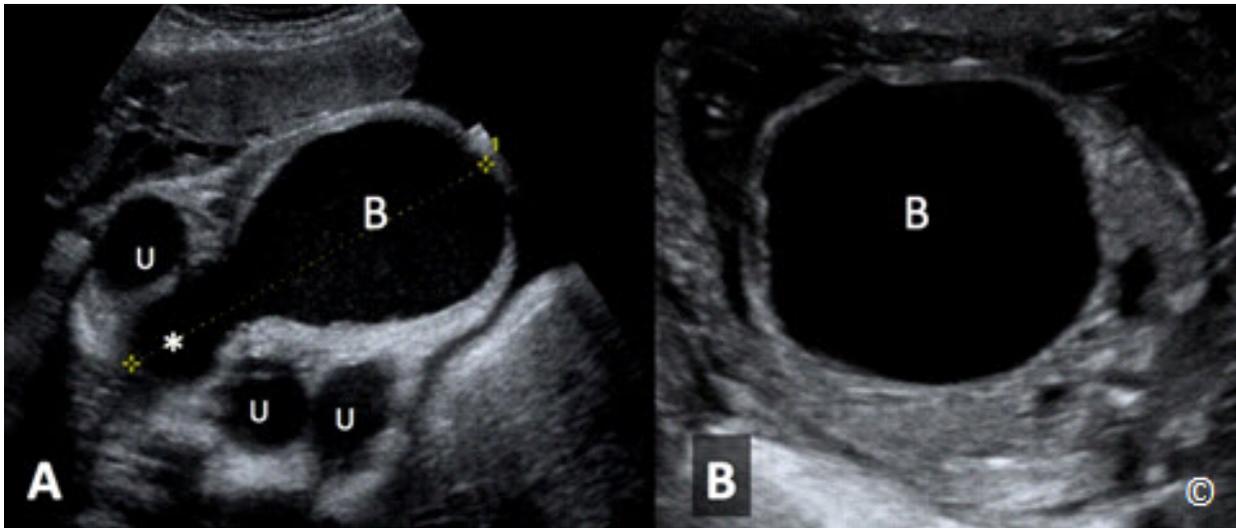
Figure 5.40 A and B: Transverse planes of the lower (A) and upper (B) pelvis in a fetus with posterior urethral valves. Note the distended bladder (B), dilated ureters, seen on cross section in A (U) and the characteristic keyhole appearance of the proximal urethra, seen in A (asterisk).
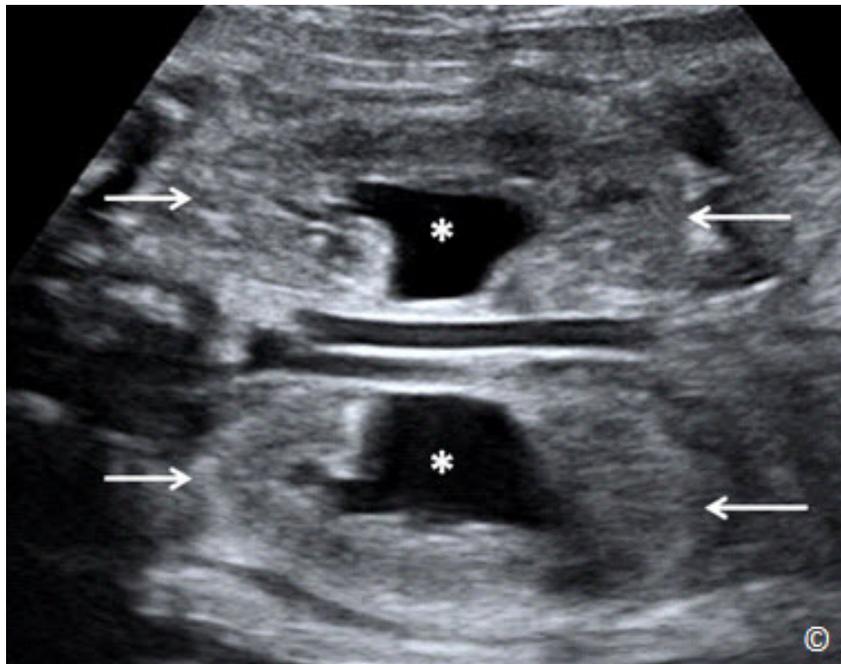
Figure 5.41: Coronal view of the abdomen in a fetus with bilateral uretero-pelvic obstruction. Note the dilated renal pelves (asterisks). The kidney borders are marked with arrows.

Skeletal Anatomy

The spine should be visualized and evaluated in sagittal, transverse or coronal planes, though the highest detection rate of spina bifida (**Figure 5.42 A - C**) is not reached through the direct assessment of the spine but through the recognition of the cranial signs ["*banana*" (**Figure 5.43**) and "*lemon*" (**Figure 5.44**) signs]. The long bones of the 4 limbs should be visualized as well, noting major abnormalities, such as severe shortening (micromelia) or bowing (**Figures 5.45 and 5.46**). An attempt to visualize both hands and feet should be made when feasible. Major abnormalities, such as transverse reduction defect, with absence of a hand or a foot, or aplasia radii can be diagnosed when such attempt is made. Of importance is also the assessment of fetal joint movement. Fixed joints in a fetus should suspect the presence of arthrogryposis.
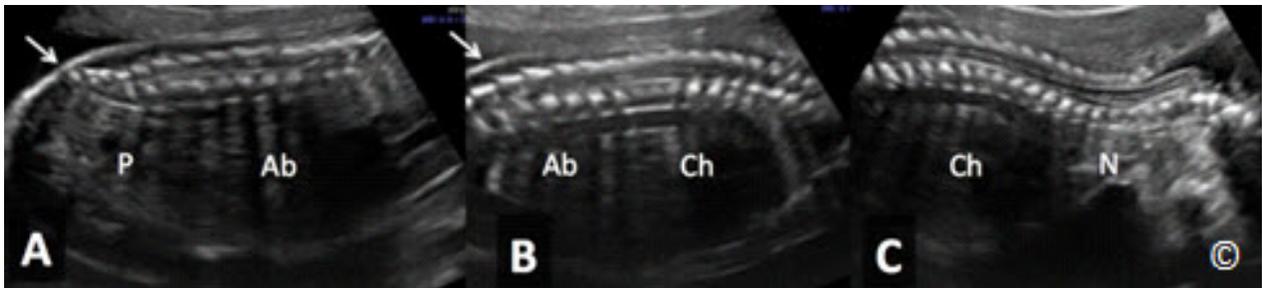
Figure 5.42 A, B, and C: Mid-sagittal planes of the fetal pelvis (P)(Figure A), abdomen (Ab)(Figure B), chest (Ch) and neck (N)(Figure C) showing longitudinal views of the spine. The intact overlying skin can be seen in planes A and B (arrows).
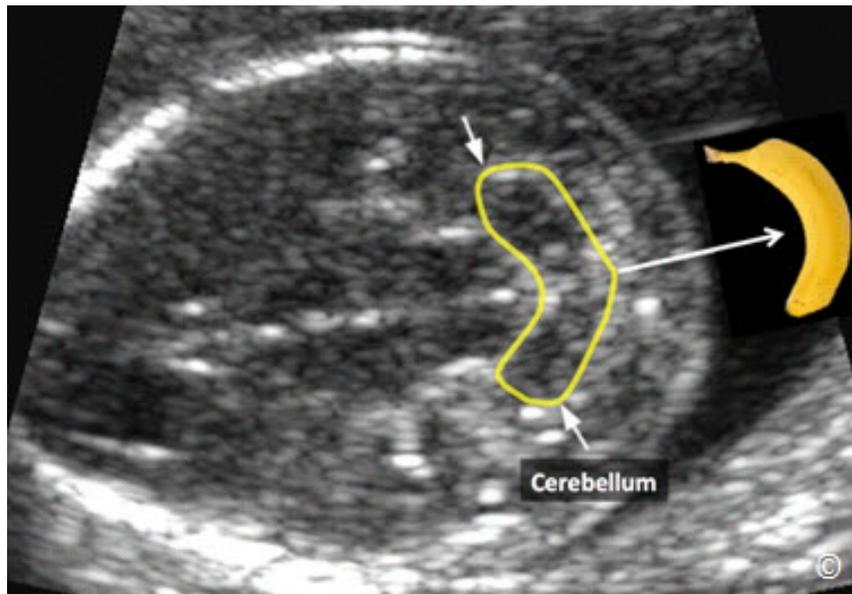
Figure 5.43: Transverse view of the fetal head at the level of the cerebellum (Transcerebellar) in a fetus with spinal neural tube defect. Note the "banana-shaped" cerebellum (arrows, yellow line), a central nervous system feature (Arnold Chiari) associated with open neural tube defect. See text for details.
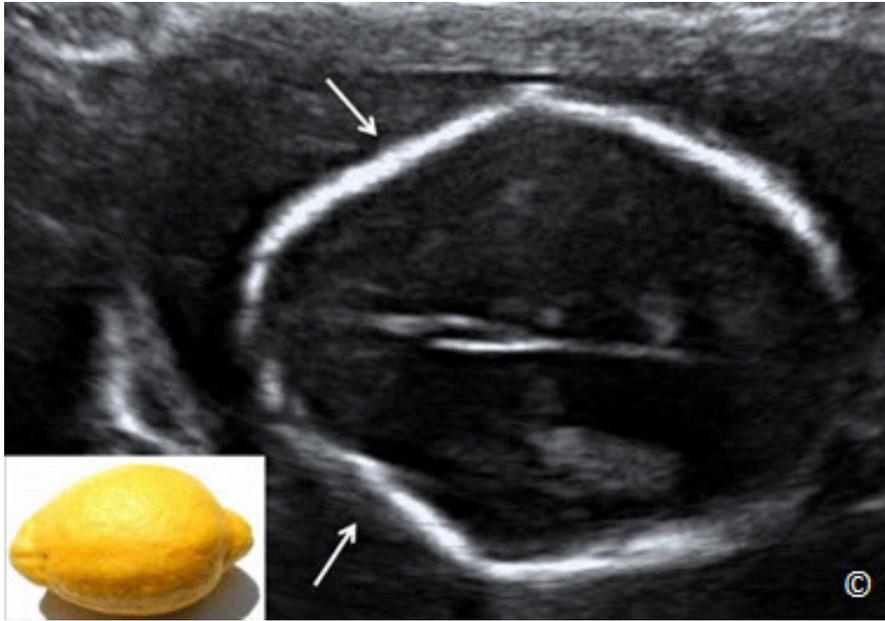
Figure 5.44: Transverse view of the fetal head at the level of the lateral ventricular plane in a fetus with spinal neural tube defect. Note the "lemon-shaped" cranium (arrows), a feature (Arnold Chiari) associated with open neural tube defect. See text for details.
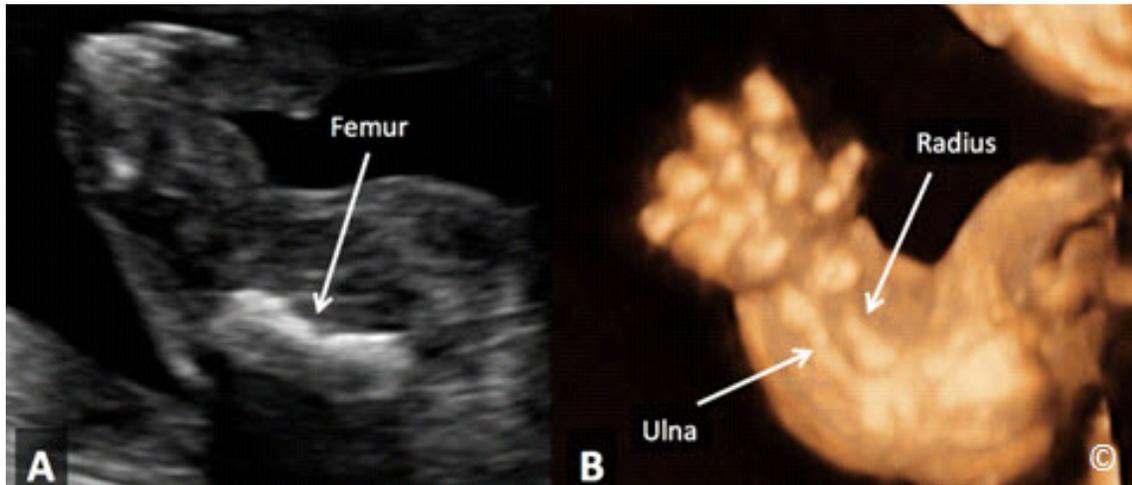

Figure 5.45: Longitudinal view of the femur in 2D mode (A), and the upper extremity in 3D ultrasound (B) of a fetus with lethal skeletal dysplasia. Note the severe shortening and bowing of the long bones.

Figure 5.46: Midsagittal view of a fetus with lethal skeletal dysplasia (same as in figure 5-45). Note the small chest (C) in comparison to the abdomen (A).

REFERENCES:

1) Hadlock FP, Harrist RB, Carpenter RJ, Deter RL, Park SK. Sonographic estimation of fetal weight. The value of femur length in addition to head and abdomen measurements. Radiology. 1984 Feb;150(2):535-40

2) Sandmire HF. Whither ultrasonic prediction of fetal macrosomia? Obstetric Gynecology 1993;82:860-862

3) L. J. Salomon, Z. Alfirevic, V. Berghella, C. Bilardo, E. Hernandez-andrade, S. L. Johnsen, K. Kalache, K.yY Leung, G. Malinger, H. Munoz, F. Prefumo, A. Toi and W. Lee on behalf of the ISUOG Clinical Standards Committee. Practice guidelines for performance of the routine mid-trimester fetal ultrasound scan. Ultrasound Obstetric Gynecology 2011; 37: 116–126.

4) ISUOG. Cardiac screening examination of the fetus: guidelines for performing the 'basic' and 'extended basic' cardiac scan. *Ultrasound Obstetric Gynecology* 2006; 27: 107–113.

5) ISUOG. Sonographic examination of the fetal central nervous system: guidelines for performing the 'basic examination' and the 'fetal neurosonogram'. *Ultrasound Obstetric Gynecology* 2007; 29: 109–116

6) American Institute of Ultrasound in Medicine practice guidelines on the performance of the obstetric ultrasound examination, 2013.
   http://www.aium.org/resources/guidelines/obstetric.pdf

INTRODUCTION

The main objective of a third trimester obstetrical ultrasound examination is to provide accurate diagnostic information in order to optimize antenatal care and improve outcome for the mother and the fetus. The primary objective of a third trimester ultrasound examination is typically focused on fetal growth, position of the placenta, and the assessment of amniotic fluid.

It is generally accepted that ultrasound examination performed beyond the 28th week of gestation is considered in the third trimester and the assessment of fetal growth is commonly initiated at or around 28 - 32 weeks in at-risk pregnancies. It is important to note that despite the fact that a pregnancy may have had a prior second trimester ultrasound examination that determined normal fetal anatomy, it is the opinion of the authors that with any ultrasound examination that is performed in pregnancy, a re-evaluation of fetal anatomy is recommended, as many fetal malformations may not appear until later in gestation and some abnormalities may have been missed on prior ultrasound examinations. **Table 6.1** lists the component of the third trimester ultrasound examination. Pregnancy dating in the third trimester (> 28 weeks) is less accurate than earlier in gestation. If the first ultrasound in the pregnancy is performed in the third trimester, a discrepancy of gestational dating of more than 21 days should reassign the Expected Date of Delivery (EDD). Careful consideration should be given however for pregnancy management based upon a third trimester ultrasound given the possibility of associated fetal growth abnormality.

Determining the location of the placenta, assessment of the adnexae and amniotic fluid volume and basic fetal anatomy are discussed in details in respective chapters in the book. Furthermore, chapter 10 describes a six-steps standardized approach to the performance of the basic ultrasound examination. In this chapter we report in details on ultrasound assessment of fetal weight and discuss the role of spectral Doppler in the growth-restricted fetus.

TABLE 6.1	Components of the Third Trimester Ultrasound Examination
	- Cardiac activity - Fetal size (biometry and estimation of fetal weight) - Fetal presentation and lie - Fetal anatomy - Placental localization - Amniotic fluid assessment - Evaluation of adnexae

ASSESSMENT OF FETAL WEIGHT

Pregnancy dating should not be performed in the third trimester given the inaccuracy of ultrasound in that gestational window, as the range is as wide as plus or minus 3 weeks. When faced with a pregnancy with unknown menstrual dates, presenting for an ultrasound in the third trimester, ultrasound dating in this scenario should be used for clinical management and if pregnancy induction is desired, consideration for documentation of fetal lung maturity should be performed.

Estimating fetal weight requires assessment of multiple biometric parameters, which typically include measuring the Biparietal Diameter (BPD), Head Circumference (HC), Abdominal Circumference (AC) and Femur Length (FL), and deriving the actual weight via a mathematical formula. Several formulas are currently available, but the one that is commonly preselected in the software of most ultrasound equipment is that developed by Hadlock et al (1). On-going studies will generate, in the near future, fetal weight formulas that are more contemporary. Details on the accurate measurement of the BPD, HC, AC and FL are described in chapter 5. Estimating fetal weight is more critical in the third trimester as it becomes important to detect fetal growth restriction or macrosomia. However, it should be considered that the assessment of fetal weight by ultrasound is more precise, the closer the fetal weight is to the mean. As the fetal weight falls outside the two standard deviations from the mean, the error in the ultrasound measurement increases. At both ends of the Gaussian curve (towards growth restriction and macrosomia), the fetal weight estimation becomes less precise and the measurement error commonly exceeds 10%. **Table 6.2** lists some important points related to estimating fetal weight by ultrasound.

TABLE 6.2	Ultrasound Estimation of Fetal Weight; Relevant Points

- BPD and HC are more precise biometric markers of gestational age than AC & FL.
- Transverse cerebellar diameter is the single biometric variable least affected by growth restriction and thus may be used in growth-restricted fetuses in which pregnancy dating is not established (2) (**Figure 6.1**).
- AC is the most accurate and sensitive predictor of fetal weight. It is typically the first biometric marker to be affected by growth abnormalities.
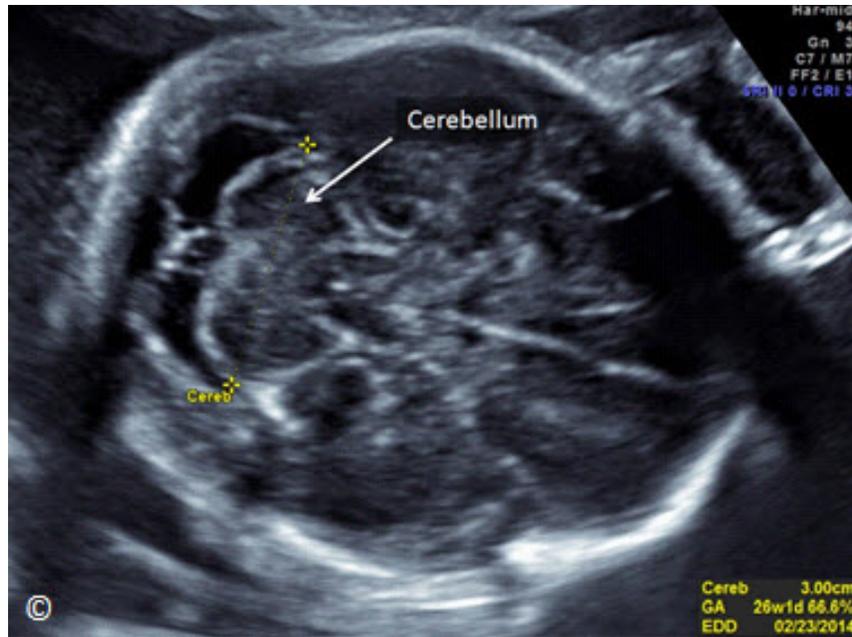- AC is a difficult biometric marker to measure with the fetal spine at 6 or 12 o'clock.

Figure 6.1: Transverse plane of the fetal head at the level of the posterior fossa showing the cerebellum. Measurement of transverse cerebellar diameter (shown) is least affected by fetal growth restriction.

INTRAUTERINE GROWTH RESTRICTION

Intrauterine growth restriction (IUGR) is defined by a sonographic estimated fetal weight below the 10th percentile for gestational age. It is a complex problem with various definitions, poor detection and limited preventive or treatment options. Evidence also link IUGR with impaired intellectual performance and diseases like hypertension and obesity in adulthood (3). It is important however to detect IUGR before birth as when IUGR is diagnosed prenatally and fetal surveillance is performed, pregnancy outcomes can be improved (4-6). IUGR has been classified as symmetrical or asymmetrical based upon whether the HC is affected or not. This classification differentiates early (symmetrical) versus late (asymmetrical) IUGR, with early IUGR being more commonly associated with chromosomal abnormalities or fetal infections. It is commonly agreed that the management is similar for both forms of IUGR and this distinction is no longer of real clinical value.

The first suspicion for the presence of IUGR may come from lagging fundal heights on prenatal visits. It is important to note that this screening method is effective when accurate fundal height measurements are obtained and when serial fundal height examinations are done (7). Once IUGR is diagnosed prenatally, a targeted ultrasound examination should be performed to exclude fetal malformations. Furthermore the assessment of amniotic fluid is an essential component of pregnancy evaluation and fetal surveillance. Fetal surveillance includes cardiotocography in the

form of non-stress testing and umbilical artery Doppler where available. Umbilical artery Doppler evaluation of IUGR has been shown to significantly reduce hospital admissions, duration of hospitalization, and perinatal mortality, without increasing the rate of unnecessary interventions (8). Doppler waveforms of the umbilical arteries can be obtained from any segment along the umbilical cord (**Figure 6.2**). In the same pregnancy, waveforms obtained near the placental end of the cord show more end-diastolic flow than waveforms obtained from the abdominal cord insertion (9). **Figure 6.3** shows umbilical artery Doppler waveforms obtained at the placental cord insertion. To optimize reproducibility, especially in multiple pregnancies, we recommend interrogating the umbilical artery at the abdominal cord insertion (**Figure 6.4**). The S/D ratio should be obtained in the absence of fetal breathing, and when the waveforms are uniform (**Figure 6.3** and **6.4**). Reversed end-diastolic velocity in the umbilical arterial circulation represents an advanced stage of placental compromise and has been associated with obliteration of more than 70% of arterioles in the placental tertiary villi (10, 11) (**Figure 6.5**). The presence of absent (**Figure 6.6**) or reversed end-diastolic flow in the umbilical artery is commonly associated with severe (birth weight below the 3rd percentile for gestational age) IUGR and oligohydramnios (12, 13). If Doppler surveillance is to be incorporated in clinical practice, the operators should undergo hands on training and should understand the physics of Doppler and the pathophysiology of placental insufficiency in fetal growth restriction.
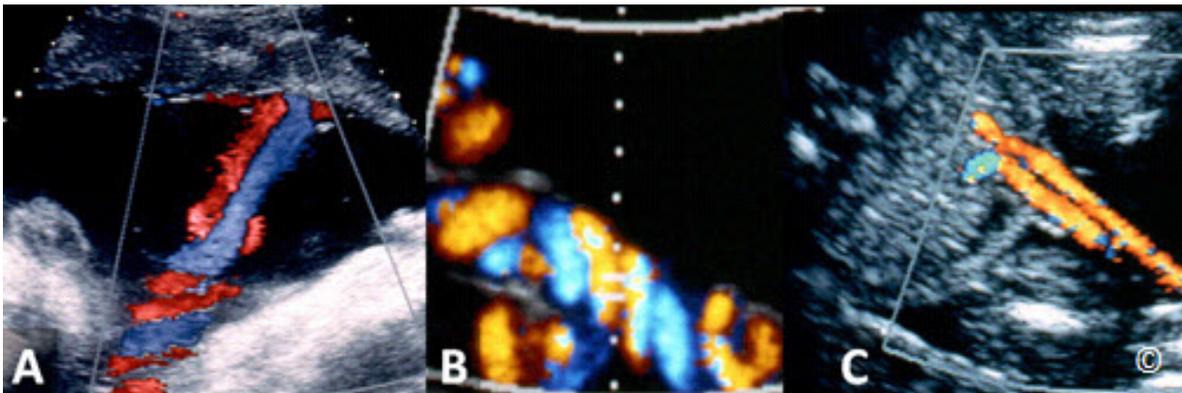
Figure 6.2: Color Doppler mode showing the umbilical cord at its placental insertion site (A), free loop in the amniotic cavity (B), and at the fetal abdominal insertion (C).
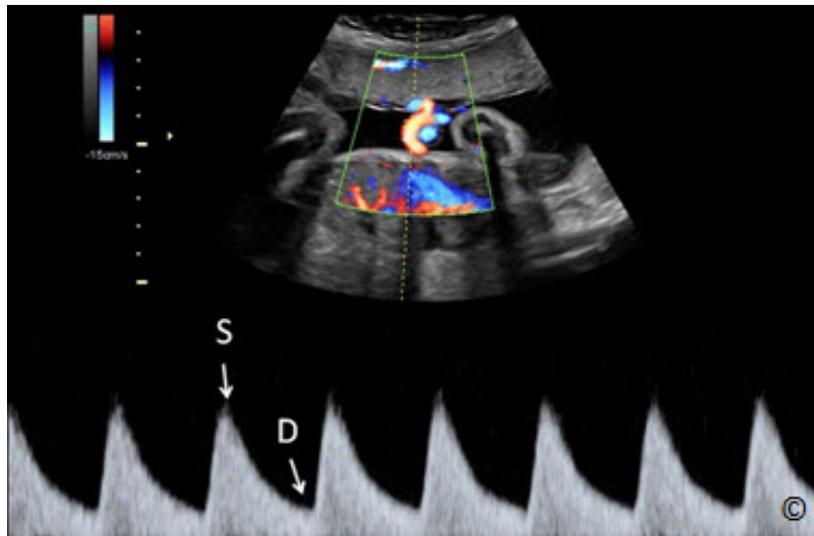
Figure 6.3: Spectral (Pulse) Doppler of the umbilical artery at the placental cord insertion. (S = Systole and D= Diastole). Note the uniformity of Doppler waveforms, implying absent fetal breathing.
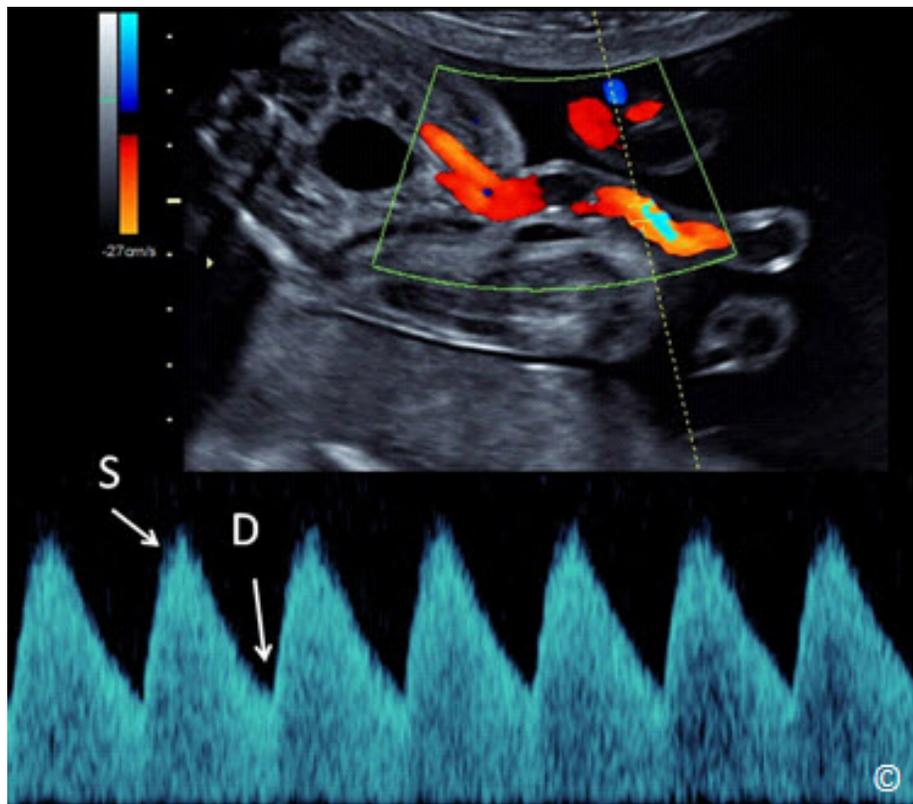

Figure 6.4: Spectral (Pulse) Doppler of the umbilical artery at the abdominal cord insertion. (S = Systole and D= Diastole).
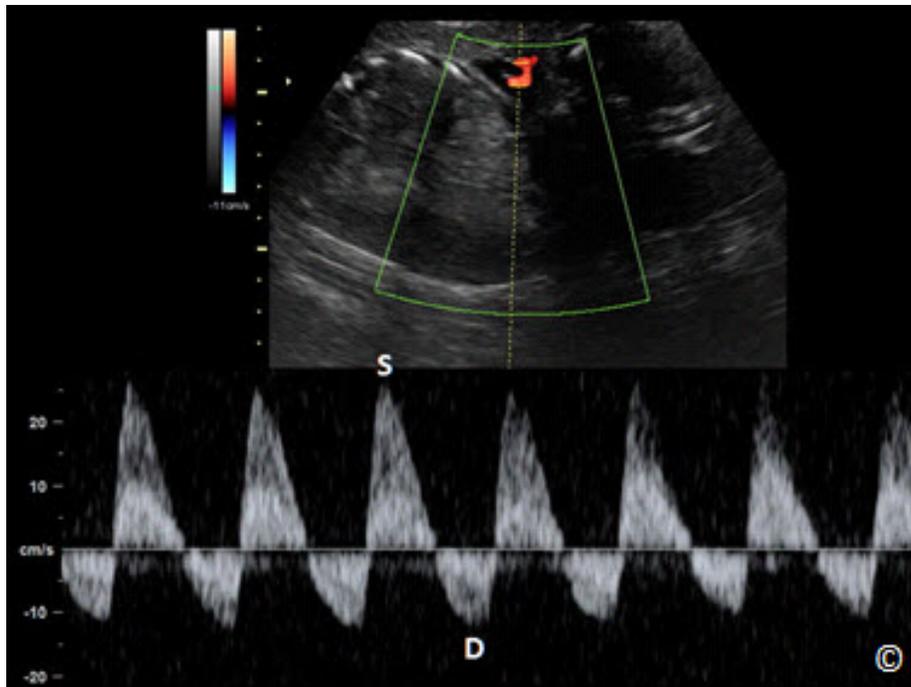
Figure 6.5: Spectral (Pulse) Doppler of the umbilical artery in a fetus with reversed end diastolic velocity (D). This pattern represents an advanced stage of fetal compromise (S = Systole).
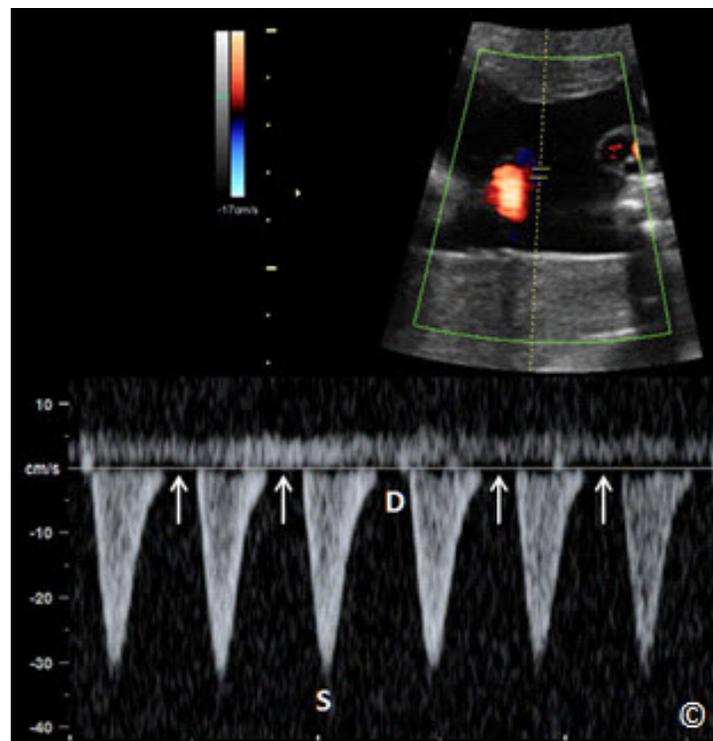
Figure 6.6: Spectral (Pulse) Doppler of the umbilical artery in a fetus with absent end diastolic velocity (arrows). (S = Systole and D = Diastole).

The middle cerebral artery has also been used in surveillance of the IUGR fetus, in combination with the umbilical artery. Under normal conditions, the middle cerebral artery shows a high impedance circulation with continuous forward flow present throughout the cardiac cycle (**Figure 6.7**) (14). The middle cerebral arteries, which carry more than 80% of the cerebral circulation, represent major branches of the circle of Willis and are the most accessible cerebral vessels for ultrasound imaging in the fetus (15). The middle cerebral artery can be imaged with color Doppler ultrasound in a transverse plane of the fetal head obtained at the base of the skull (**Figure 6.8**). In this transverse plane, the proximal and distal middle cerebral arteries are seen in their longitudinal view, with their course almost parallel to the ultrasound beam (**Figure 6.8**). In the presence of fetal hypoxemia, central redistribution of blood flow occurs, resulting in an increased blood flow to the brain, heart and adrenal glands, and a reduction in flow to the peripheral and placental circulations. This blood flow redistribution, known as the brain-sparing reflex, is reflected in a low pulsatility index (PI) in the middle cerebral artery (**Figure 6.9**) in IUGR hypoxemic fetuses and plays a major role in fetal adaptation to oxygen deprivation (14, 16). Middle cerebral artery Doppler has been found to identify a subset of IUGR fetuses at increased risk for cesarean delivery due to non-reassuring fetal heart rate patterns, and neonatal acidosis (17,18).
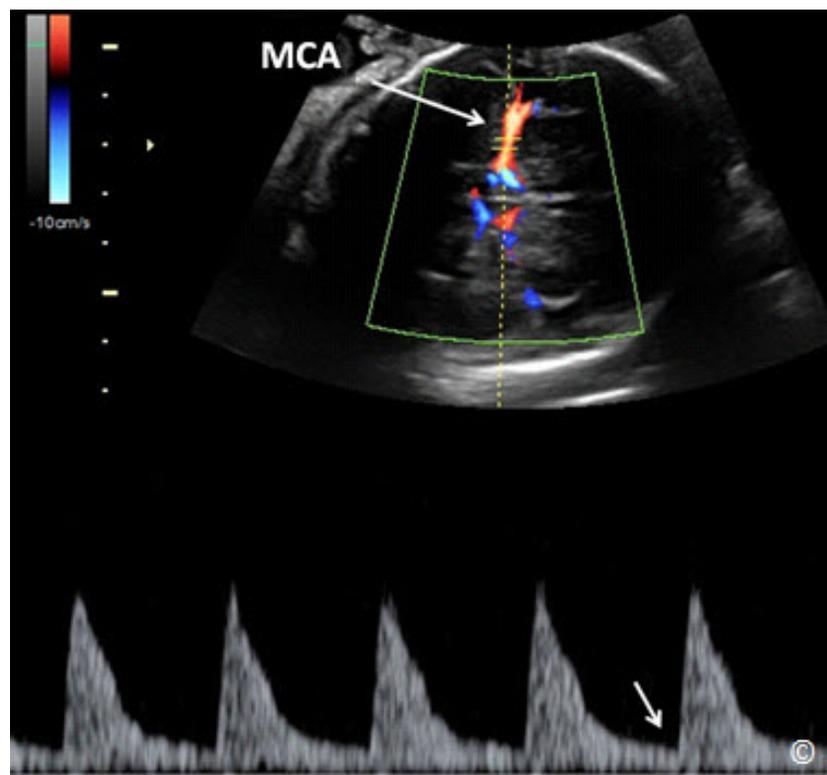

Figure 6.7: Spectral (Pulse) Doppler of the middle cerebral artery (MCA) in a normal fetus. Note that the MCA shows high impedance circulation with continuous forward flow during diastole (arrow).
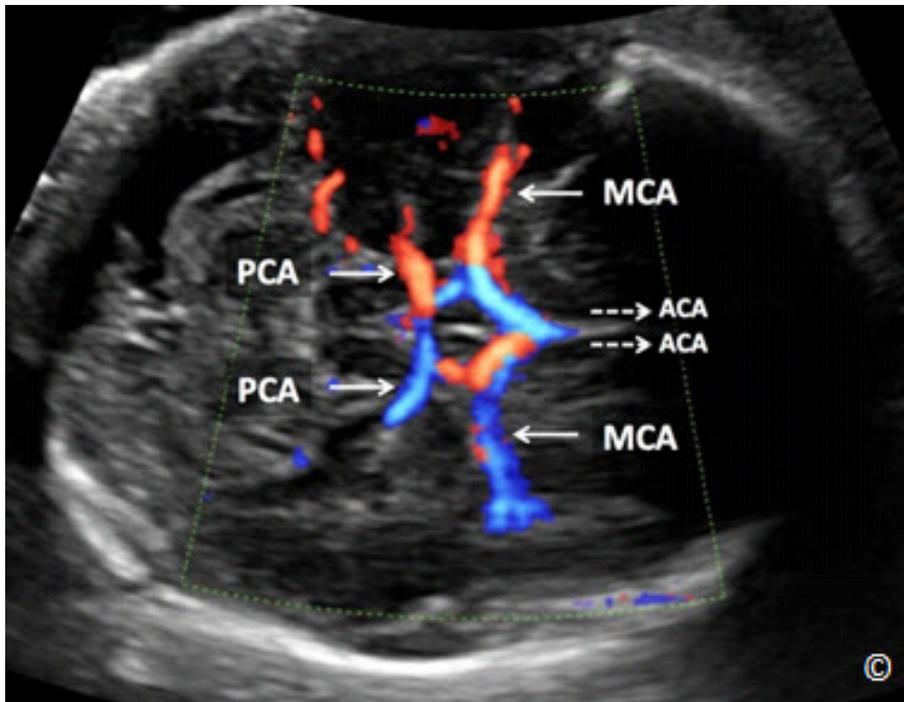
Figure 6.8: Transverse plane at the base of the fetal brain with color Doppler mode showing the circle of Willis. Note the course of the middle cerebral arteries (MCA) and posterior cerebral arteries (PCA). The anterior cerebral arteries (ACA) are not seen due to their course perpendicular to the ultrasound beam (dashed arrows).
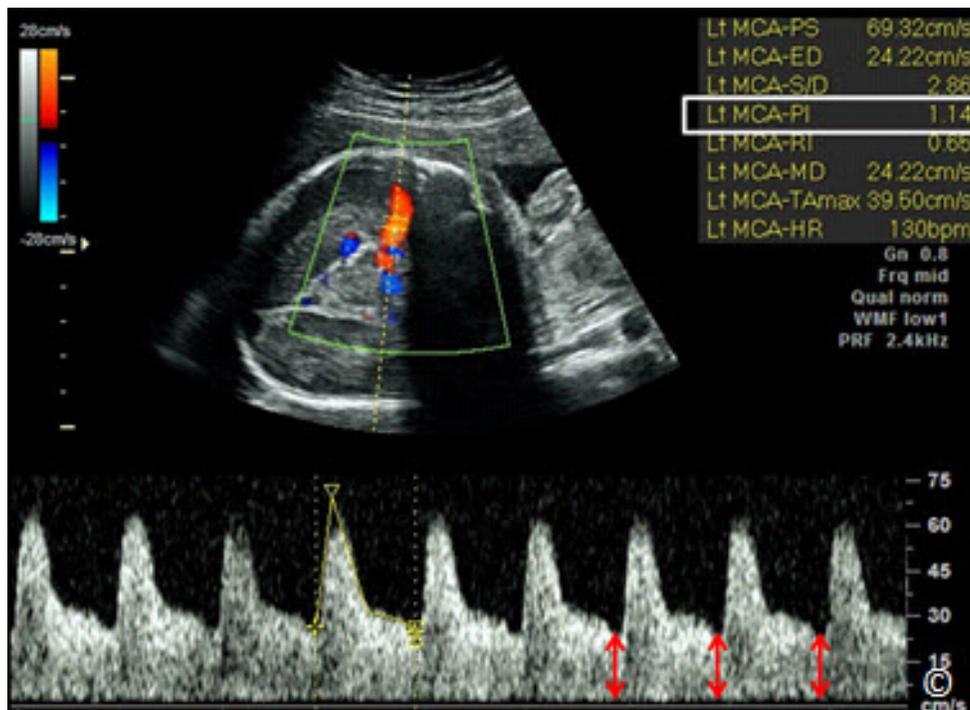

Figure 6.9: Spectral (Pulse) Doppler of the middle cerebral artery in a growth restricted fetus. Note the low impedance circulation (PI = 1.14) (white rectangle) with increased flow during diastole (red double arrows). This represents brain sparing.

FETAL MACROSOMIA

The term fetal macrosomia implies fetal obesity and has been traditionally defined by a fetal weight greater than 4000 or 4500 grams irrespective of gestational age (19). Large for gestational age is a term that is used for the neonatal period and is defined by a birth weight equal to or greater than the 90th percentile for a given gestational age (19). Although the risk of neonatal morbidity is increased at birth weights above the 4000 grams threshold, the neonatal risk is markedly increased above the 4500 grams threshold (20,21). It is for this reason that a threshold of 4500 grams is often used for defining fetal macrosomia.

The incidence of macrosomia can be as high as 10% of live births and a number of risk factors predispose for macrosomia; they are listed in **Table 6.3**.

TABLE 6.3	Predisposing Factors for Neonatal Macrosomia
- Pregestational or gestational diabetes - Prior history of macrosomia - Maternal obesity - Increased weight gain during pregnancy - Gestational age greater than 42 weeks - Increased maternal birth weight - Increased maternal height	

Macrosomia predisposes the mother and the newborn to significant complications including an increased risk for postpartum hemorrhage, birth canal lacerations and cesarean delivery. Fetal trauma includes an increased risk for shoulder dystocia, which may result in brachial plexus injury (Erb-Duchenne palsy).

Ultrasound has been shown to be inaccurate in predicting macrosomia (22,23). Using the Hadlock's formula to predict fetal weight, a mean absolute error of 13% for infants greater than 4,500 g is noted, compared with 8% for non-macrosomic infants (24). Among women without diabetes, ultrasound biometry used to detect macrosomia has a sensitivity of 22-44%, a specificity of 99%, a positive predictive value of 30-44%, and a negative predictive value of 97-99% (25,26). With birth weight exceeding 4,500 g, only 50% of fetuses weigh within 10% of the ultrasound-derived estimated weight (27), suggesting that the usefulness of ultrasonography for obtaining estimated weights is limited. These limitations are neither operator-dependent nor equipment-dependent (27). One study comparing ultrasound-estimated fetal weight, Leopold maneuvers-estimated weight, and maternal perception of fetal weight in post-term parous women found no statistical differences between the three groups (28).

On ultrasound examination, the macrosomic fetus will show an increased subcutaneous fat layer that is mostly evident in the abdominal circumference plane (**Figure 6.10**). The abdominal circumference is the most sensitive biometric marker of fetal macrosomia and the first to show such growth abnormality.
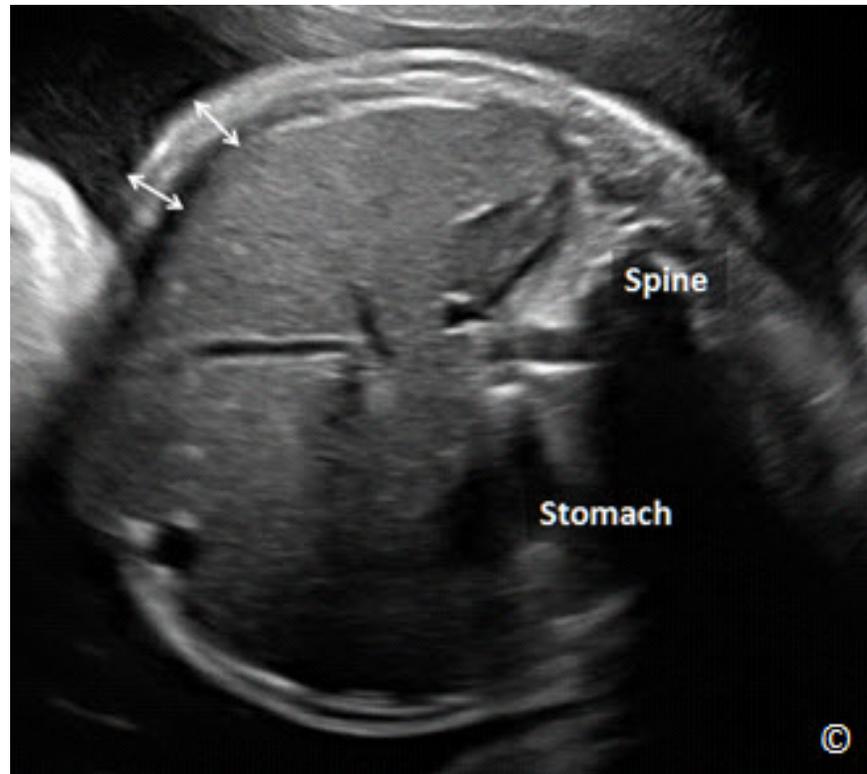

Figure 6.10: Transverse plane of the fetal abdomen at the level of the abdominal circumference in a macrosomic fetus. Note the increased subcutaneous fat (double arrows).

References:

1) Hadlock FP, Harrist RB, Carpenter RJ, Deter RL, Park SK. Sonographic estimation of fetal weight. The value of femur length in addition to head and abdomen measurements. Radiology. 1984 Feb;150(2):535-40

2) Chavez MR, Ananth CV, Smulian JC, Yeo L, Oyelese Y, Vintzileos AM. Fetal transcerebellar diameter measurement with particular emphasis in the third trimester: a reliable predictor of gestational age. Am J Obstet Gynecol. 2004 Sep;191(3):979-84

3) Demicheva E, Crispi F. Long-Term Follow-Up of Intrauterine Growth Restriction: Cardiovascular Disorders. Fetal Diagn Ther. 2013 Aug 14. [Epub ahead of print]

4) American College of Obstetricians and Gynecologists. Intrauterine growth restriction. Washington (DC): ACOG; 2000. ACOG Practice Bulletin No. 12.

5) Bilardo CM, Wolf H, Stigter RH, Ville Y, Baez E, Visser GH, Hecher K. Relationship between monitoring parameters and perinatal outcome in severe, early intrauterine growth restriction. Ultrasound Obstetric Gynecology 2004; 23(2):119-25.

6) Baschat AA. Arterial and venous Doppler in the diagnosis and management of early onset fetal growth restriction. Early Hum Dev 2005; 81(11):877-87.

7) Cnattingius S, Axelsson O, Lindmark G. Symphysis-fundus measurements and intrauterine growth retardation. Acta Obstet Gynecol Scand 1984;63:335-40

8) Alfirevic Z, Neilson P. Doppler ultrasonography in high-risk pregnancies: systematic review with meta-analysis. Am J Obstet Gynecol 1995; 172:1379-87.

9) Trudinger BJ. Doppler ultrasonography and fetal well being. In: Reece EA, Hobbins JC, Mahoney M, Petrie RH, eds. Medicine of the Fetus and Mother. Philadelphia: JB Lipincott Co.; 1992.

10) Kingdom JC, Burrell SJ, Kaufmann P. Pathology and clinical implications of abnormal umbilical artery Doppler waveforms. Ultrasound Obstet Gynecol 1997; 9(4):271-286.

11) Morrow RJ, Adamson SL, Bull SB, Ritchie JW. Effect of placental embolization on the umbilical artery velocity waveform in fetal sheep. Am J Obstet Gynecol 1989; 161(4):1055-1060.

12) McIntire DD, Bloom SL, Casey BM, Leveno KJ. Birth weight in relation to morbidity and mortality among newborn infants. N Engl J Med 1999; 340(16):1234-8.

13) Copel JA, Reed KL. Doppler ultrasound in Obstetrics and Gynecology. First edition, New York, New York: Raven Press; 1995:187-198.

14) Mari G, Deter RL. Middle cerebral artery flow velocity waveforms in normal and small-for-gestational age fetuses. Am J Obstet Gynecol 1992; 166:1262-1270.

15) Veille JC, Hanson R, Tatum K. Longitudinal quantitation of middle cerebral artery blood flow in normal human fetuses. Am J Obstet Gynecol 1993; 169(6):1393-1398.

16) Berman RE, Less MH, Peterson EN, Delannoy CW. Distribution of the circulation in the normal and asphyxiated fetal primate. Am J Obstet Gynecol 1970; 108:956-969.

17) Severi FM, Bocchi C, Visentin A, Falco P, Cobellis L, et al. Uterine and fetal cerebral Doppler predict the outcome of third trimester small-for-gestational age fetuses with normal umbilical artery Doppler. Ultrasound Obstet Gynecol 2002;19:225-228.

18) Cruz-Martinez R, Figueras F, Hernandez-Andrade E, Oros D, Gratacos E. Fetal brain Doppler to predict cesarean delivery for nonreassuring fetal status in term small-for-gestational-age fetuses. Obstet Gynecol 2011; 117(3):618-26.

19) American College of Obstetricians and Gynecologists. Fetal macrosomia. Washington (DC): ACOG; 2000. ACOG Practice Bulletin No. 22.

20) McFarland LV, Raskin M, Daling JR, Benedetti TJ. Erb Duchenne's palsy: a consequence of fetal macrosomia and method of delivery. Obstet Gynecol 1986;68:784-788

21) Gross TL, Sokol RJ, Williams T, Thompson K. Shoulder dystocia: a fetal-physician risk. Am J Obstet Gynecol 1987;156:1408-1418

22) Rossavik IK, Joslin GL. Macrosomatia and ultrasonography: what is the problem? South Med J 1993; 86:1129-1132

23) Sandmire HF. Whither ultrasonic prediction of fetal macrosomia? Obstet Gynecol 1993;82:860-862

24) Alsulyman OM, Ouzounian *lG,* Kjos SL. The accuracy of intrapartum ultrasonographic fetal weight estimation in diabetic pregnancies. Am J Obstet Gynecol 1997; 177: 503-506

25) Smith GC, Smith MF, McNay MB, Fleming IE. The relation between fetal abdominal circumference and birth weight: findings in 3512 pregnancies. Br J Obstet Gynaecol 1997;104:186-190

26) O'Reilly-Green CP, Divon MY. Receiver operating characteristic curves of sonographic estimated fetal weight for prediction of macrosomia in prolonged pregnancies. Ultrasound Obstet Gynecol 1997;9:403-408

27) Benacerraf BR, Gelman R, Frigoletto FD Jr. Sonographically estimated fetal weights: accuracy and limitation. Am *1* Obstet Gynecol 1988;159:1118-1121

28) Chauhan SP, Sullivan CA, Lutton TD, et al: Parous patients' estimate of birth weight in posterm pregnancy. J Perinatol 15:192,1995

INTRODUCTION

Since the early eighties and until 2009, there has been a steady and significant increase in the frequency of twins (1, 2). In the United States in 2011, twin birth rate was 33.2 per 1,000 total births and was essentially unchanged from 2009 and 2010 (3). The rate of twin births rose 76% from 1980 to 2009–2011, primarily due to increasing maternal age and widespread use of assisted reproductive technologies, but the pace of increase has slowed in recent years (3).

Infants born to twin pregnancies are generally born earlier and smaller than those in singleton pregnancies, and accordingly, are less likely to survive to their first birthday (4). In 2011, 11% of twins were delivered very preterm (less than 32 weeks of gestation), compared with less than 2% of singletons (3). Pregnancies with twins and higher order multiples are at increased risk for many maternal and fetal/child complications. **Table 7.1** lists the maternal and fetal/child complications of twin pregnancy.

TABLE 7.1	Maternal and Fetal/Child Complications of Twin Pregnancies

Maternal

- Preterm labor
- Preterm premature rupture of membranes
- Preeclampsia
- Placental abnormalities
- Pyelonephritis
- Postpartum hemorrhage

Fetal/Child

- Growth abnormalities
- Congenital malformations
- Admission to neonatal intensive care unit
- Cerebral palsy
- Perinatal death

Ultrasound is an integral part of the diagnosis and management of twin pregnancies. Ultrasound has indeed revolutionized the care of pregnancies with twins from the initial diagnosis to guiding the delivery of the neonates. In this chapter we review the utility of ultrasound in twin pregnancies. The role of ultrasound in the management of high-order multiple pregnancies is beyond the scope of this book. Furthermore, discussion of fetal congenital abnormalities in twins

is not covered here as it is presented in chapter 5. **Table 7.2** lists the benefits of ultrasound in twin pregnancies.

TABLE 7.2	Benefits of Ultrasound in Twin Pregnancies
	- Diagnosis of twins - Determining chorionicity of placenta(s) - Evaluation of fetal anatomy - Detection of fetal growth abnormalities and discordance - Fetal surveillance - Assessment for the presence of complications such as twin-twin transfusion syndrome and cord entanglement - Determining fetal presentation in labor - Guiding fetal interventions

ETIOLOGY AND PLACENTATION OF TWINS

Twins can be classified into 2 main categories; dizygotic and monozygotic, based upon the number of eggs fertilized at conception. Dizygotic twins occur when 2 eggs are fertilized with 2 separate sperms resulting in twins that are distinct genetically but share the same uterus. Dizygotic twins (also called fraternal) are almost always dichorionic / diamniotic, as each fetus has its own set of placenta and membranes. Several factors affect the rate of dizygotic twinning including maternal age, race, increasing parity, geographic area and presence of assisted reproduction (5). The rate of dizygotic twinning varies significantly around the world with the highest rate reported in Nigeria and the lowest rate in Japan (6).

Monozygotic twins (also referred to as identical) occur when 1 egg is fertilized by one sperm with division of the embryo into 2. These twins are therefore identical genetically. Unlike dizygotic twins, the rate of monozygotic twins is fairly constant throughout the world at 1/250 pregnancies (7) excluding pregnancies of assisted reproduction. Monozygotic twins are associated with higher perinatal morbidity and mortality than dizygotic twins. Monozygotic twins can have various types of placentation based upon the timing of the division of the fertilized egg. **Table 7.3** shows placentation in monozygotic twins in relation to the timing of cleavage.

TABLE 7.3	Placentation in Monozygotic Twins and Timing of Cleavage	
Time of Cleavage	**Placentation**	**Frequency**
0-3 Days	Dichorionic/Diamniotic	~ 25%
4-8 Days	Monochorionic/Diamniotic	~ 75%
9-12 Days	Monochorionic/Monoamniotic	~ 1%
13-15 Days	Conjoined	Rare

DETERMINING TWIN PLACENTATION BY ULTRASOUND

Ultrasound can determine the type of placentation in twins with high accuracy, especially in the first trimester of pregnancy (see chapter 4). When 2 separate and distinct chorionic sacs are seen in the endometrial cavity by the 5th week of gestation, the diagnosis of dichorionic/diamniotic placentation can be accurately made (**Figure 7.1**). Later on in the first trimester, when the 2 sacs are adjoining, the assessment of placentation requires attention to other details. Although in general, the number of yolk sacs correlates with the number of amnions, this rule has many exceptions, as monoamniotic twins can be associated with a single yolk sac, a partially divided yolk sac or two yolk sacs. The characteristic of the dividing membrane between the 2 gestational sacs, when present, is the most accurate way for determining chorionicity in twin gestation. If the placenta appears to fill the junction between the membranes at its insertion into the placenta, resulting in a thick wedge-shaped configuration (Lambda, Delta or twin-peak sign), this is diagnostic of dichorionic / diamniotic placentation (**Figure 7.2**). In monochorionic pregnancies, the membranes attach to the uterine wall in a thin T-shaped configuration without any placental tissue at its insertion site (**Figure 7.3**). Ultrasound in the first trimester of pregnancy is very accurate in determining chorionicity in twin pregnancies with rates approaching 100 % when correlated with pathology (8). The accuracy of ultrasound in determining chorionicity decreases with advancing gestation. It is therefore essential that a first trimester ultrasound be part of the management of twin gestation and that chorionicity is determined and reported at that time when feasible.
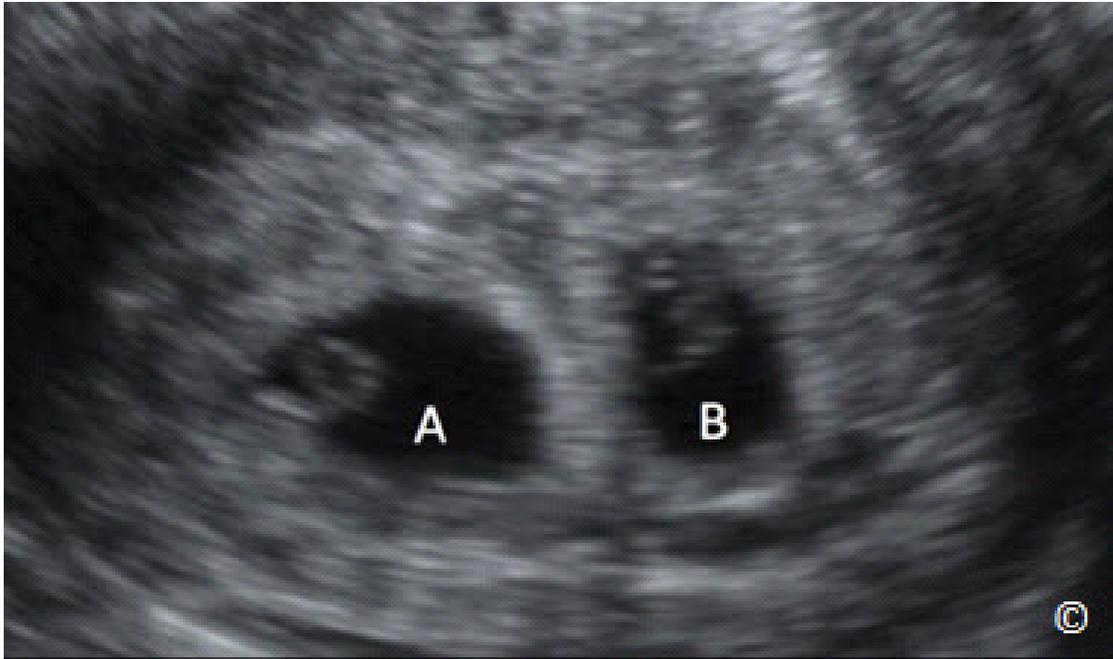
Figure 7.1: Sagittal plane of the uterus at 5 weeks gestation with 2 distinct chorionic sacs. The thick separation of the chorionic sacs suggests a dichorionic twin gestation.
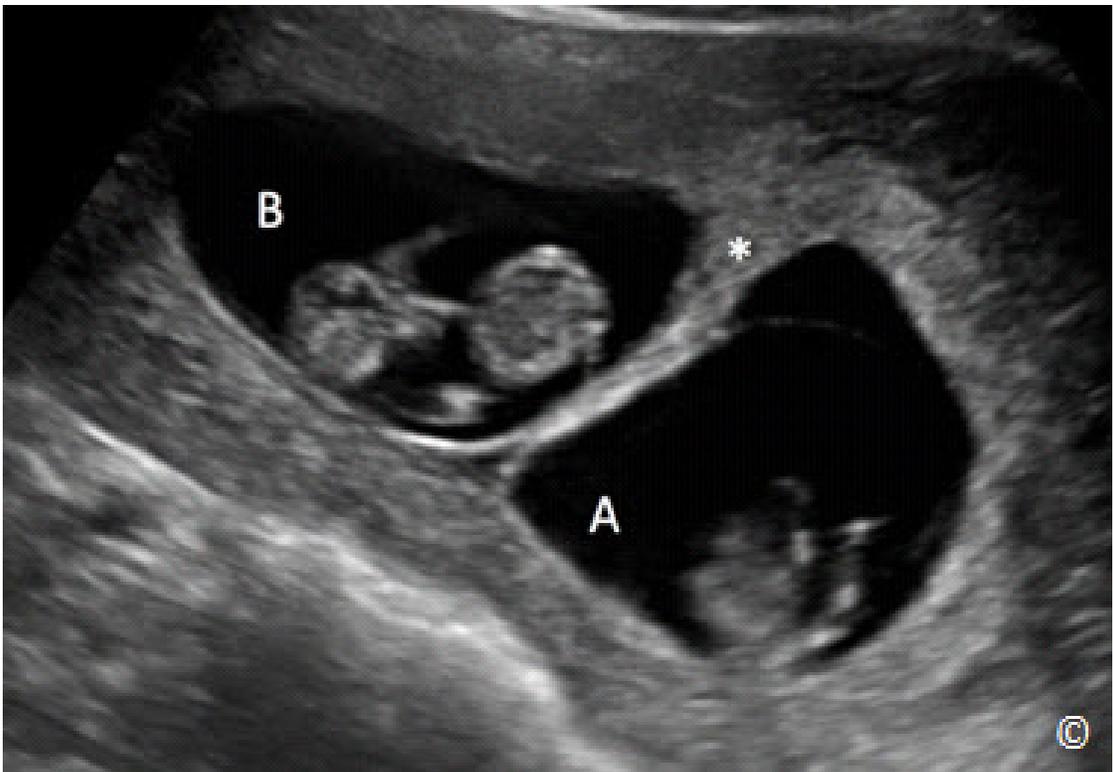

Figure 7.2: Dichorionic – diamniotic twin gestation (A and B). Note the thick dividing membrane with a twin-peak sign (asterisk) at placental insertion.
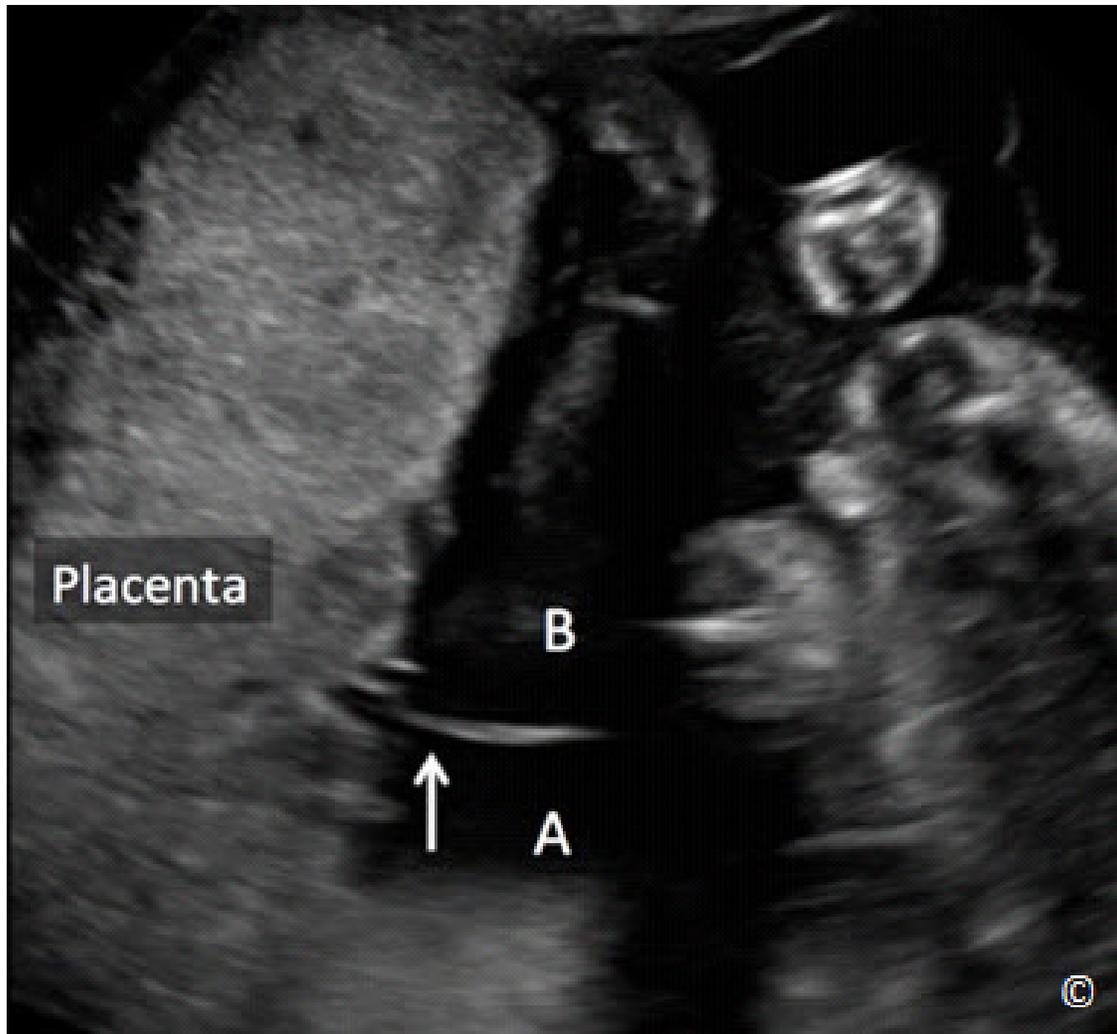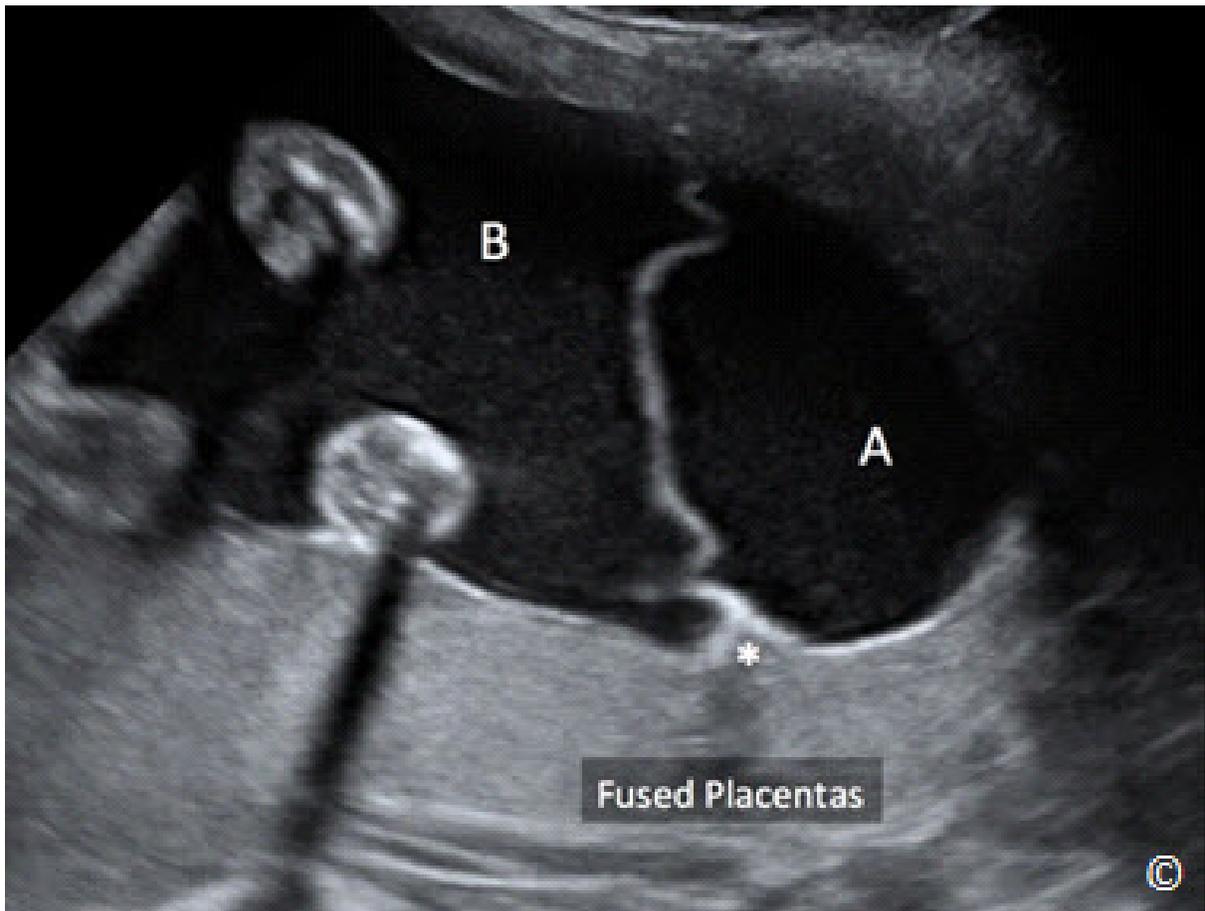
Figure 7.3: Monochorionic – diamniotic twin gestation (A and B). Note the thin dividing membrane with a T-shape (arrow) configuration at placental insertion.

During the second and third trimester, determining chorionicity and amnionicity is about 90 % accurate (9) and should follow this sequence:

1) Determine fetal gender, if the twins are of different gender, this in all likelihood indicates dichorionicity.
2) If the twins have the same gender, assess for the location and number of placental masses. The presence of separate placentas is an indication of dichorionic placentation. The presence of a single placental mass however requires further investigation (**Figure 7.4**)
3) Assess the thickness of the dividing membrane; in the setting of dichorionic/diamniotic placentation, the dividing membrane has 4 layers (2 layers of amnion and 2 layers of chorion) and thus it is thicker than the dividing membrane in a monochorionic twin,

which has only 2 layers of amnion. Some authors reported that a dividing membrane of less than 2 mm in thickness in the second and third trimester of pregnancy, predicts monochorionic twins with 90 % accuracy (9) (**Figure 7.5 A and B**). This method however has poor reproducibility.

4) Another method involves counting the layers of the dividing membrane after magnification. As stated earlier, the dividing membrane in a dichorionic twin pregnancy will have 4 layers whereas a monochorionic membrane has 2 layers (**Figure 7.6 A and B**). Although this method is reported to have high accuracy, it is in the authors' opinion that it requires expertise and optimal imaging and not easily reproducible.

5) Perhaps the most accurate and reliable method in the second and third trimester is the twin-peak, Delta or Lambda sign described in the first trimester evaluation. The twin-peak sign (**Figure 7.7**), when seen, has been shown to have 100 % accuracy in determining chorionicity in the second and third trimester of pregnancy (10).
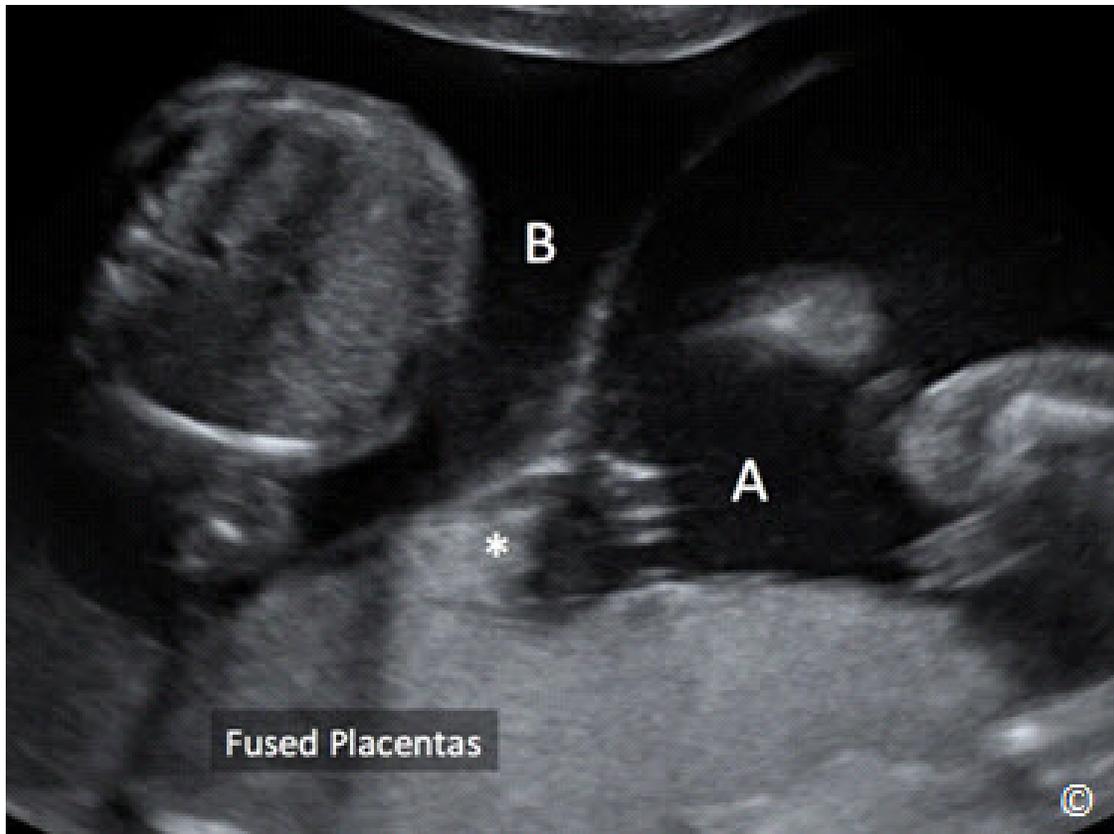

Figure 7.4: Dichorionic – diamniotic twin gestation (A and B) in the second trimester. Note the thick dividing membrane with a twin-peak sign (asterisk) at placental insertion. Note also the presence of fused placentas (labeled).
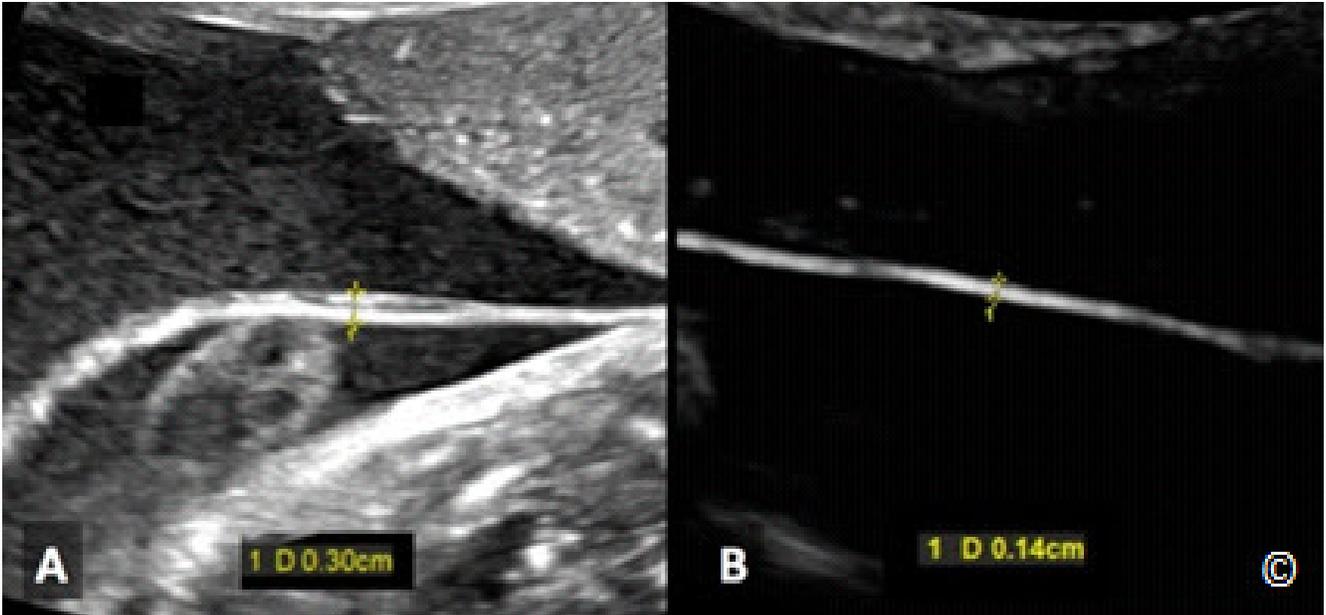
Figure 7.5: Membrane thickness as a predictor of chorionicity in twin gestation. Note a thick dividing membrane (> 2 mm) in a dichorionic twin gestation in A and a thin dividing membrane (< 2 mm) in a monochorionic twin gestation. See text for more details.
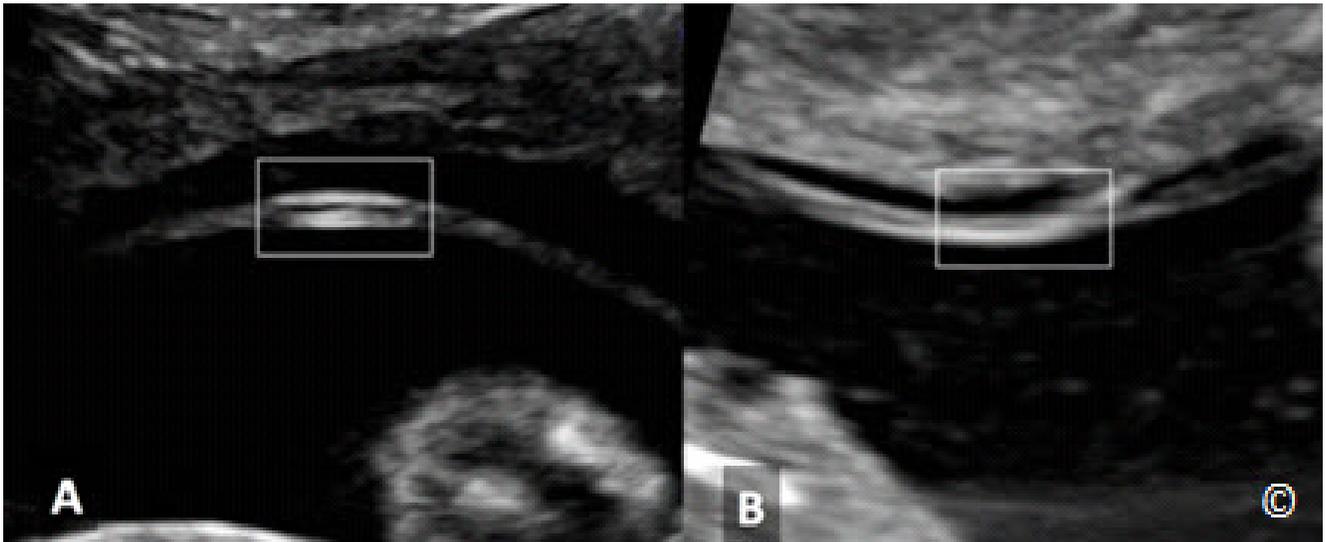
Figure 7.6: Number of layers within the dividing membrane as a predictor of chorionicity in twin gestation. Note the presence of 4 layers in a dichorionic twin gestation in A and 2 layers in a monochorionic twin gestation. See text for more details.

Figure 7.7: Dichorionic – diamniotic twin gestation (A and B) in the third trimester. Note the thick dividing membrane with a twin-peak sign (asterisk) at placental insertion. Also note the presence of fused placentas.

ULTRASOUND IN FOLLOW-UP OF TWIN GESTATIONS

Twins require heightened evaluation in the antepartum period in order to detect complications such as discordant growth, twin-twin transfusion syndrome, selective intrauterine fetal growth restriction, twin-reversed arterial perfusion and single fetal demise. Surveillance for monochorionic twinning should be performed more frequently given the associated risk involved with such pregnancies. Ultrasound frequency every 4 weeks is adequate to detect growth abnormalities in dichorionic twinning. In monochorionic twins, ultrasound examinations every 2 weeks, starting as early as 16 weeks gestation and until delivery should be considered (11, 12). Doppler ultrasound in twins is reserved for cases where fetal growth restriction is noted or there is twin growth discordance or twin-twin transfusion syndrome. Doppler ultrasound can also be used to evaluate for conditions associated with fetal anemia in twin pregnancies. **Table 7.4** and **7.5** provide the indication, timing and type of ultrasound exams recommended in dichorionic and monochorionic twin gestations respectively (11).

TABLE 7.4	Ultrasound in Dichorionic Twin Pregnancies; Modified with Permission from the American Institute of Ultrasound in Medicine (11)
Timing	**Indications**
First trimester (7-13 weeks)	Pregnancy dating
	Diagnosis of twins
	Determination of chorionicity
Second trimester (18-20 weeks)	Anatomic survey
	Placental evaluation
Follow-up (start at 24 weeks)	Every 4 weeks if uncomplicated
	More often for complicated twins

TABLE 7.5	Ultrasound in Monochorionic Twin Pregnancies; Modified with Permission from the American Institute of Ultrasound in Medicine (11)
Timing	**Indications**
First trimester (7-13 weeks)	Pregnancy dating
	Diagnosis of twins
	Determination of chorionicity
Follow-up (start at 16 weeks)	Every 2 weeks if uncomplicated
	More often for TTTS[*] and monoamniotic twins
Second trimester (18-20 weeks)	Anatomic survey
	Placental evaluation

* Twin–Twin Transfusion Syndrome

DISCORDANT TWINS

Discordance is the difference in weights between twin fetuses and is defined with the larger twin as the standard of growth. It is calculated by the following equation: (larger twin estimated weight-smaller twin estimated weight)/ larger twin estimated weight X 100. A 15-20% or more weight difference among twins is considered discordant (13). Twin-discordance is not a rare event as the likelihood of 20% twin discordance is about 16% in twin gestations (14). Discordant growth is associated with a multitude of problems including increased likelihood of anomalies, intrauterine growth restriction, preterm birth, infection in 1 fetus, admission to the NICU, stillbirth or death within 1 week of birth (13). Serial ultrasound evaluation is essential in twin pregnancies in order to enhance the diagnosis of twin-discordance and for stratification of risk. Once discordance is diagnosed, fetal surveillance should be performed given the associated increase in morbidity and mortality.

TWIN-TWIN TRANSFUSION SYNDROME

Twin-twin transfusion syndrome (TTTS), which complicates 10-20 % of monochorionic twin pregnancies, is believed to occur when vascular anastomosis exist in a monochorionic placenta with net blood flow going to one fetus at the expense of the other. The recipient twin-fetus is typically plethoric, larger in size and has polyhydramnios due to excess urination (**Figure 7.8 A**). The donor twin-fetus is anemic, smaller in size and has a "stuck" appearance due to oligohydramnios (**Figure 7.8 B**) with restricted movements (**Figure 7.9 A and B**). TTTS is commonly diagnosed in the second trimester of pregnancy and can progress quickly and lead to preterm labor and preterm rupture of membranes.
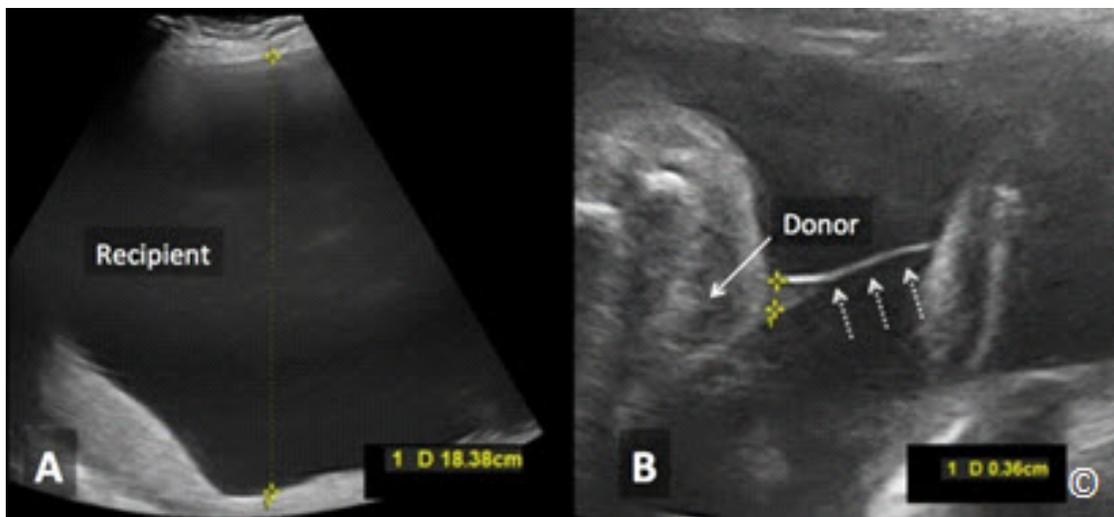
Figure 7.8: Twin-twin transfusion syndrome in a monochorionic twin gestation showing the presence of polyhydramnios in the recipient sac (A) and oligohydramnios in the donor sac (B). Note the wrapping of the amniotic membrane (arrows in B) around the body of the donor twin.
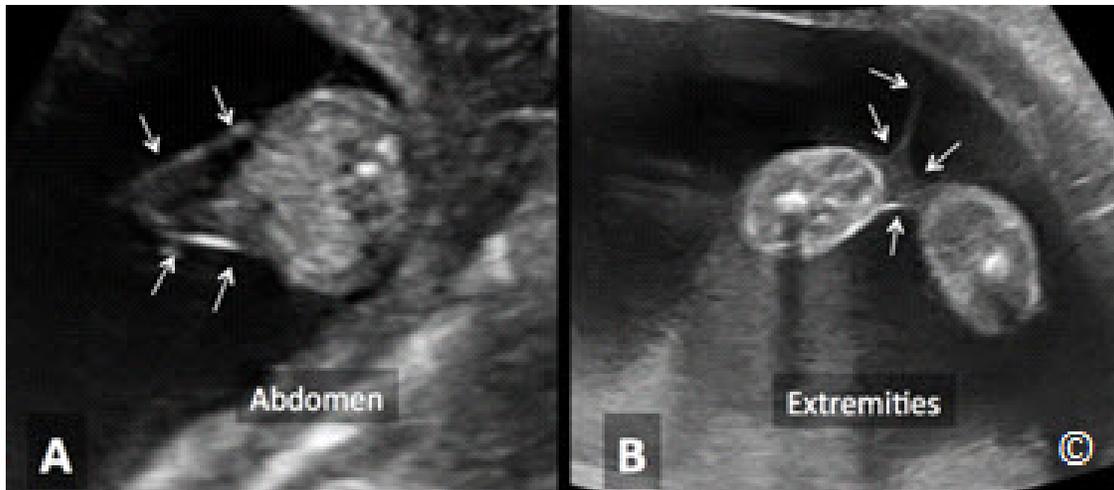
Figure 7.9: The donor twin in a monochorionic twin gestation with twin-twin transfusion syndrome (TTTS). Note the wrapping of the membrane (arrows) around the abdomen (A) and extremities (B) of the donor twin. This phenomenon results is a stuck twin syndrome, a common complication of TTTS.

Ultrasound is essential to the diagnosis and management of TTTS. Criteria for establishing the diagnosis of TTTS by ultrasound include a monochorionic placenta, polyhydramnios in one sac with a maximum vertical pocket of equal to or greater than 8 cm and oligohydramnios in the other sac with a maximum vertical pocket of less than 2 cm, in the absence of congenital abnormalities that may explain fluid and growth discrepancies. Concurrent confirmatory features include a small or non-visible bladder in the donor twin and an enlarged bladder in the recipient twin.

A staging mechanism for TTTS was established by Quintero (15) and is shown in **Table 7.6**.

Treatment of TTTS is in general stage dependent. In the presence of Quintero stage 2 or higher, laser of vascular anastomosis on the placental surface appears to be the best treatment option. Controversy still exists for treatment of stage 1, with serial reductive amniocentesis of the polyhydramnios sac or laser therapy, being two viable options. In low-resource settings where laser therapy is not available, treatment with serial reductive amniocentesis is deemed appropriate.

TABLE 7.6	**Quintero Staging System for Twin-Twin Transfusion Syndrome; Reproduced with Permission from Reference 15.**				
Stage	Polyhydramnios/ Oligohydramnios	Absent bladder in donor	Critically abnormal Doppler studies	Hydrops	Death of 1 twin
I	+	-	-	-	-
II	+	+	-	-	-
III	+	+	+	-	-
IV	+	+	+	+	-
V	+	+	+	+	+

MONOCHORIONIC-MONOAMNIOTIC TWINS

Monochorionic/monoamniotic twins (monoamniotic twins) account for about 1% of all monochorionic twins. Diagnosis is established when a monochorionic placenta is noted in a twin pregnancy in the absence of a dividing membrane. It is important to confirm this diagnosis after multiple sonographic evaluations and ensure that a stuck twin is excluded. Furthermore, monoamniotic twins tend to have placental cord insertions that are in close proximity. Monoamniotic twins are at significant risk of cord entanglement, which can be diagnosed by grey scale, color and pulsed Doppler evaluation. In our experience, cord entanglement is a common finding in monoamniotic pregnancies.

On grey scale, cord entanglement appears as a mass of cord between the two fetuses (**Figure 7.10**). Color Doppler will confirm that this mass is indeed entanglement of umbilical cords (**Figure 7.11**) and pulsed Doppler can confirm the diagnosis by documenting two distinct Doppler waveforms, confirming different fetal heart rate patterns (twin A and twin B), on one Doppler spectrum (**Figure 7.12**). In order to obtain these waveforms, open the Doppler gate wide, within the suspected cord entanglement region (**Figure 7.12**). Cord entanglement can be noted in the first trimester in monoamniotic twins and confirmed by pulsed Doppler (**Figure 7.13**). Most authorities suggest delivery by 34-35 weeks when cord entanglement is prenatally diagnosed in monoamniotic pregnancies and fetal surveillance with non-stress testing on a daily, or multiple times per week, frequency. The authors have correlated the presence of umbilical artery waveform notching on pulsed Doppler evaluation with cord compression (**Figure 7.14**): a feature that can be useful in the surveillance of monoamniotic twins with cord entanglements (16).
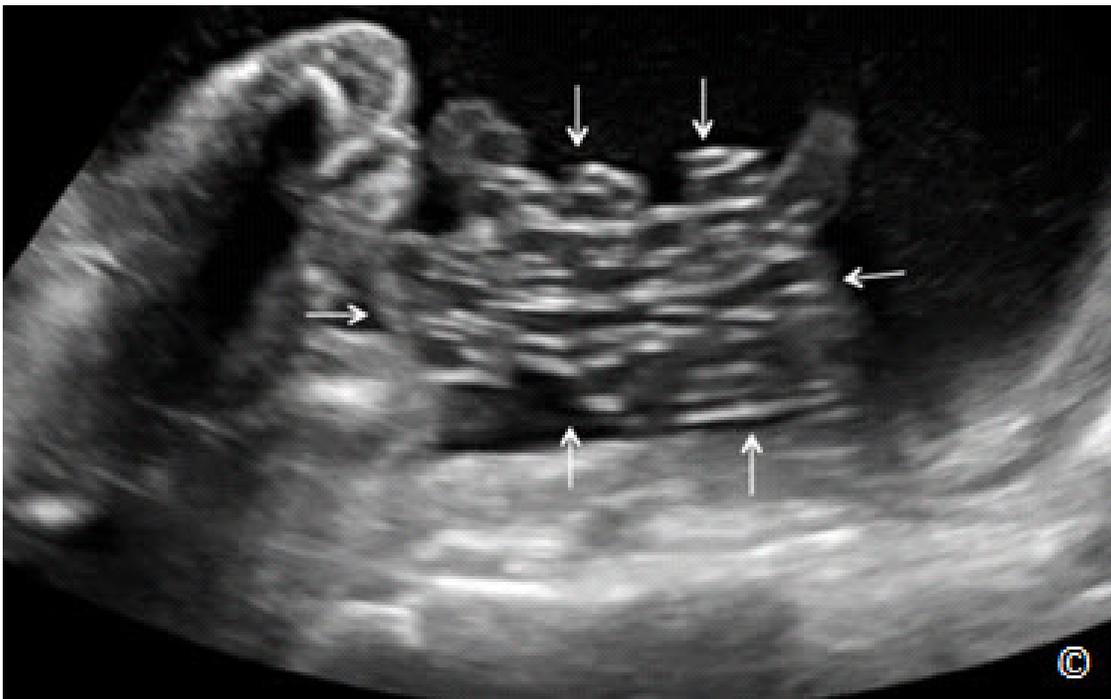
Figure 7.10: Monochorionic-monoamniotic twin gestation with cord entanglement seen on B-mode (grey scale). Note the presence of a mass of cords (arrows) between the 2 fetuses.

Figure 7.11: Monochorionic-monoamniotic twin gestation with cord entanglement seen on color Doppler mode (same fetus as in figure 7.10). Note the presence of a "mass of cords" between the 2 fetuses.
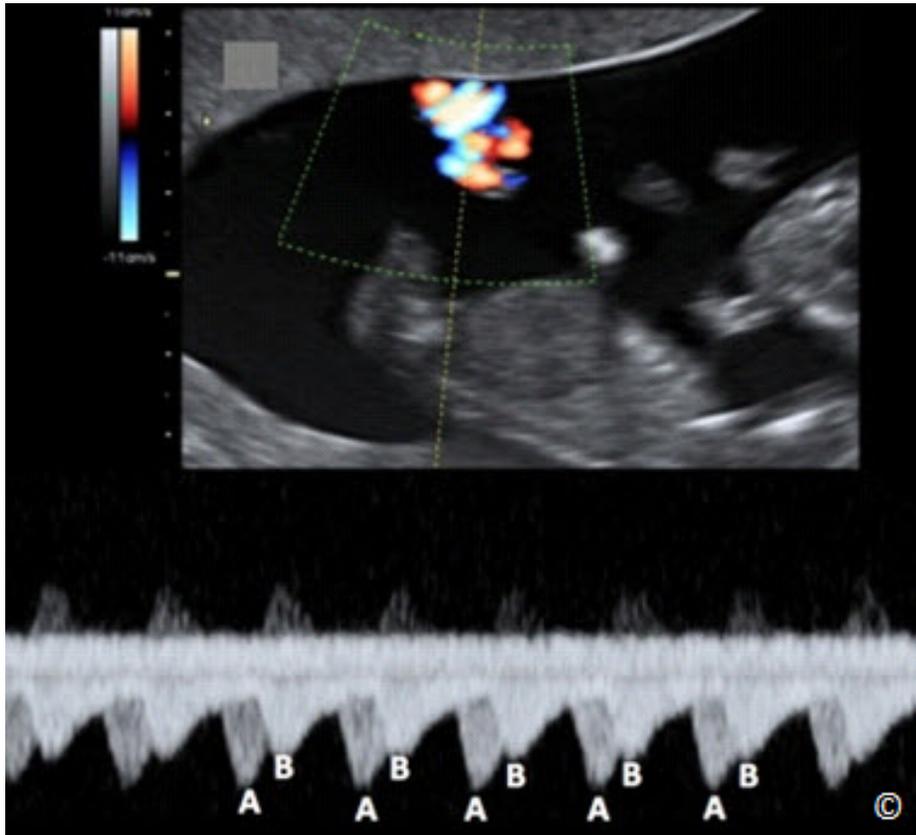

Figure 7.12: Monochorionic-monoamniotic twin gestation with cord entanglement seen on color and pulsed Doppler modes. Note the presence of 2 distinct Doppler waveforms (A and B) within the same Doppler spectrum.
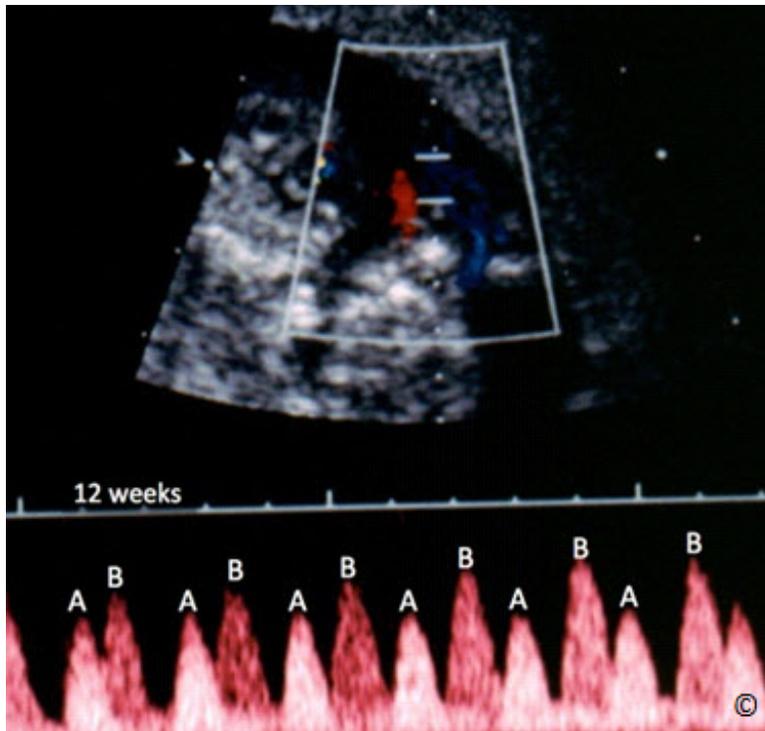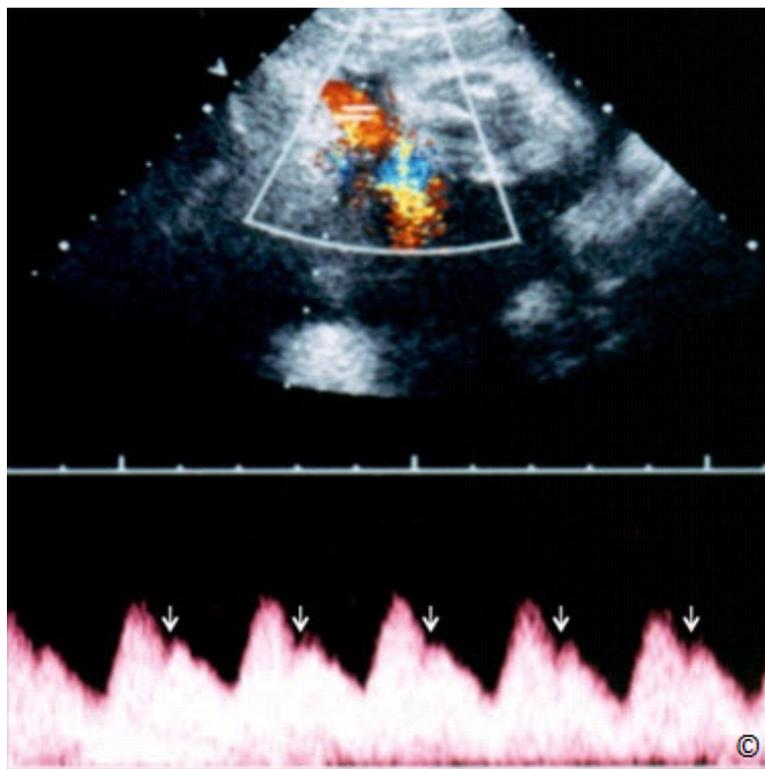
Figure 7.13: Monochorionic-monoamniotic twin gestation with cord entanglement seen on color and pulsed Doppler modes at 12 weeks gestation. Note the presence of 2 distinct Doppler waveforms (A and B) within the same Doppler spectrum.

Figure 7.14: Monochorionic-monoamniotic twin gestation with cord entanglement. Note the presence of umbilical artery Doppler waveforms notching (arrows), which suggests cord compression.

CONJOINED TWINS

Conjoined twins are very rare complications of monochorionic twinning which results from incomplete division of the fertilized egg between day 13 and 15 from conception. The incidence is around 1 in 50,000 births (17). The anatomic site of conjunction describes conjoined twins. Complex types are described by combination of forms. **Table 7.7** lists the five types of conjoined twins and their frequency.

TABLE 7.7	Types and Frequency of Conjoined Twins	
Type		**Frequency**
Craniopagus (head)		1-2 %
Thoracopagus (chest)		75 %
Omphalopagus (abdomen)		Rare
Pygopagus (rump)		20 %
Ischiopagus (pelvis)		5 %

Diagnosis of conjoined twins can be made in the first trimester by grey scale and color Doppler ultrasound (**Figure 4.23, Figures 7.15** and **7.16**). The prognosis is dependent on the degree and site of fusion and the joined organs. Extensive multidisciplinary counseling should be part of the prenatal management of conjoined twins.

Head Twin-B

Head Twin-A
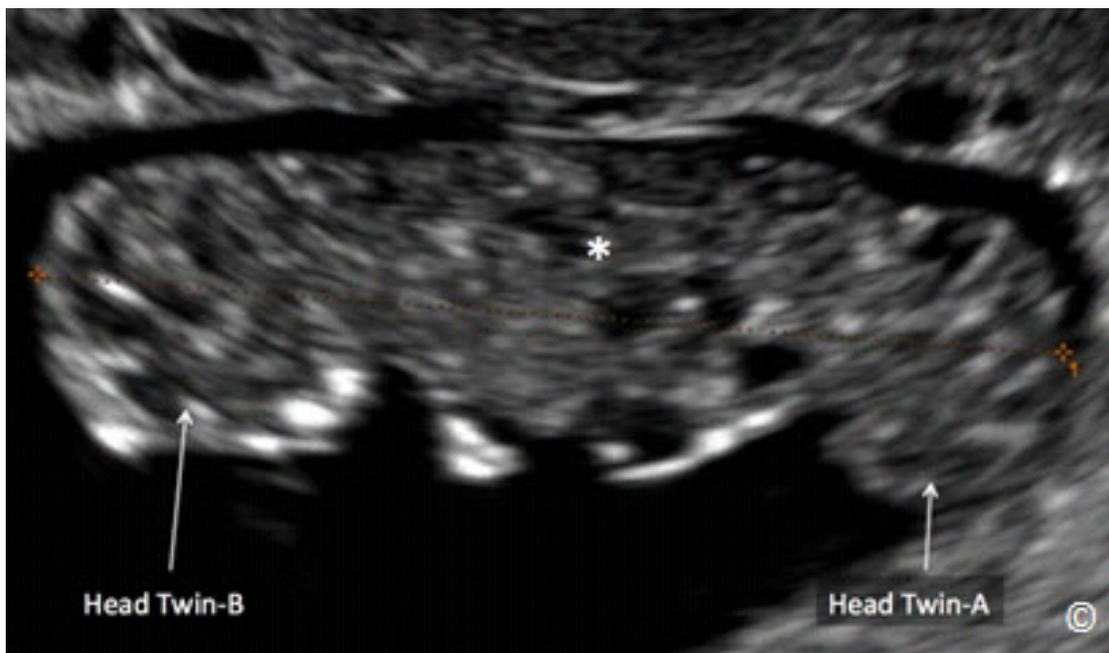
Figure 7.15: Conjoined twins noted on 2D – grey scale ultrasound at 9 weeks gestation. Note the fusion of twins in the pelvic area (asterisk). Cephalic regions of twins are labeled.
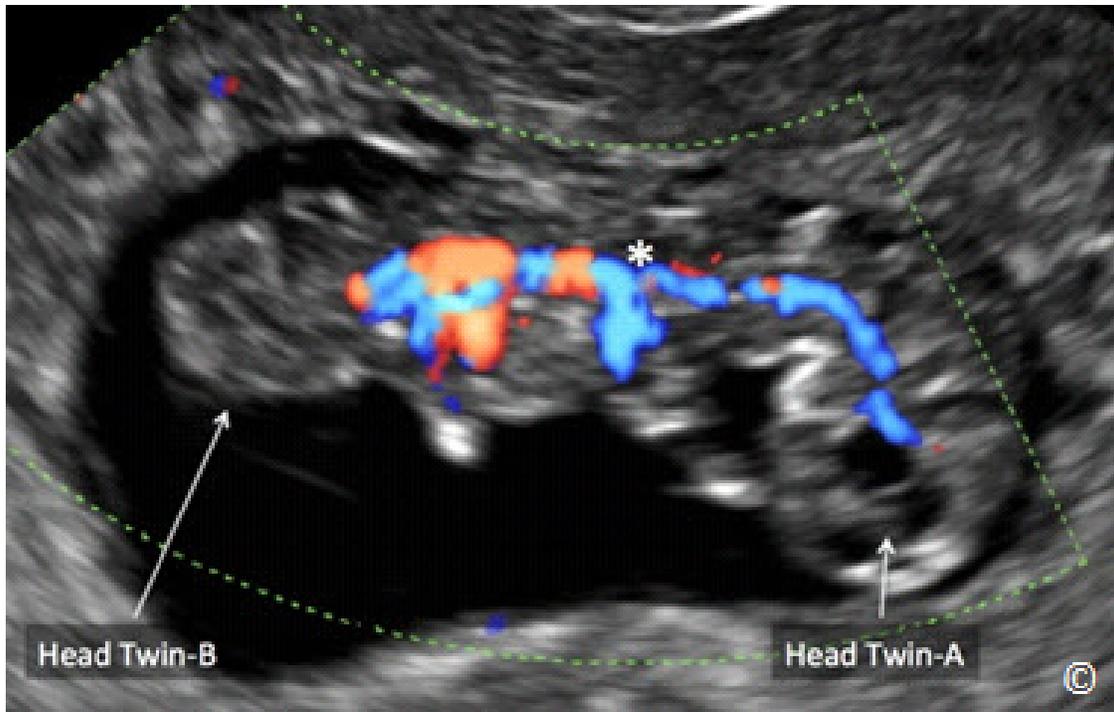
Figure 7.16: Conjoined twins noted on ultrasound at 9 weeks gestation (same twins as in figure 7.15) with color Doppler ultrasound confirming the vascular connectivity between the 2 embryos (asterisk). Color Doppler can be used to confirm the diagnosis of conjoined twins, and differentiate it from monoamniotic non-fused embryos that are closely positioned in the amniotic cavity. Cephalic regions of twins are labeled.

TWIN REVERSED ARTERIAL PERFUSION

Twin Reversed Arterial Perfusion (TRAP), known as acardiac twinning is a very rare condition characterized by monochorionic placentation and absence of a functioning heart in one fetus of a twin pregnancy (**Figure 7.17** and **7.18**). The normal fetus perfuses the acardiac mass by an arterial-to-arterial anastomosis on the placental surface. Typically, in normal conditions, the umbilical arteries carry blood from the fetus to the placenta. In TRAP, the anastomosis allows for reverse perfusion to the acardiac mass thus the acronym TRAP. The acardiac fetus commonly has multiple anatomic and growth abnormalities.
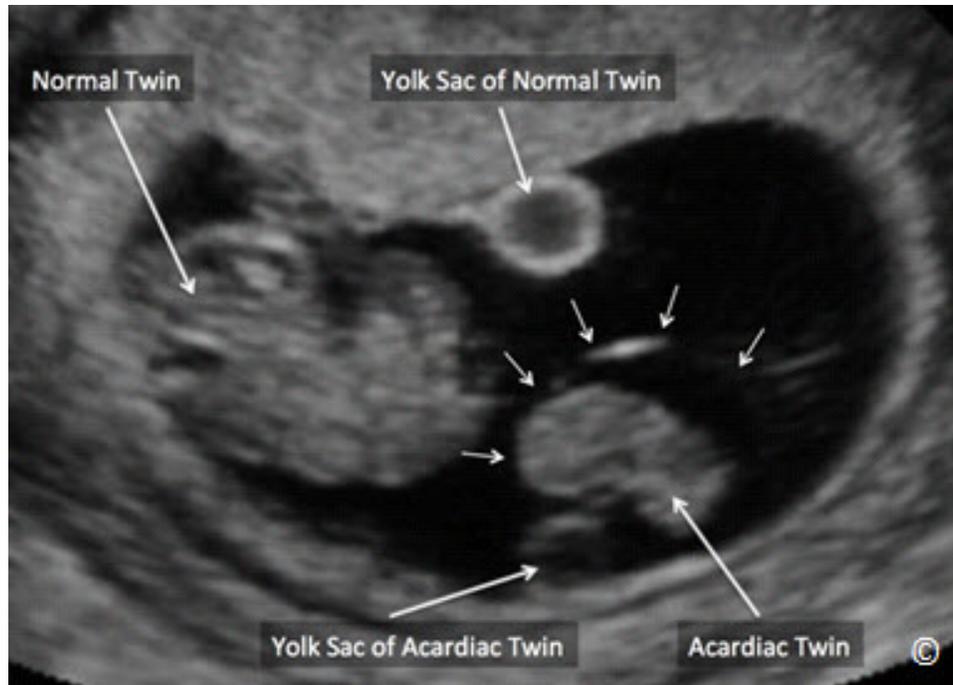
Figure 7.17: Grey scale ultrasound of a twin reversed arterial perfusion (TRAP) in a monochorionic twin at 9 weeks gestation. Note the presence of a mass of tissue (labeled as acardiac twin) with an amniotic membrane covering (small arrows) and a yolk sac (labeled as yolk sac of acardiac twin). The normal twin is seen (labeled as normal twin) with a yolk sac (labeled as yolk sac of normal twin).
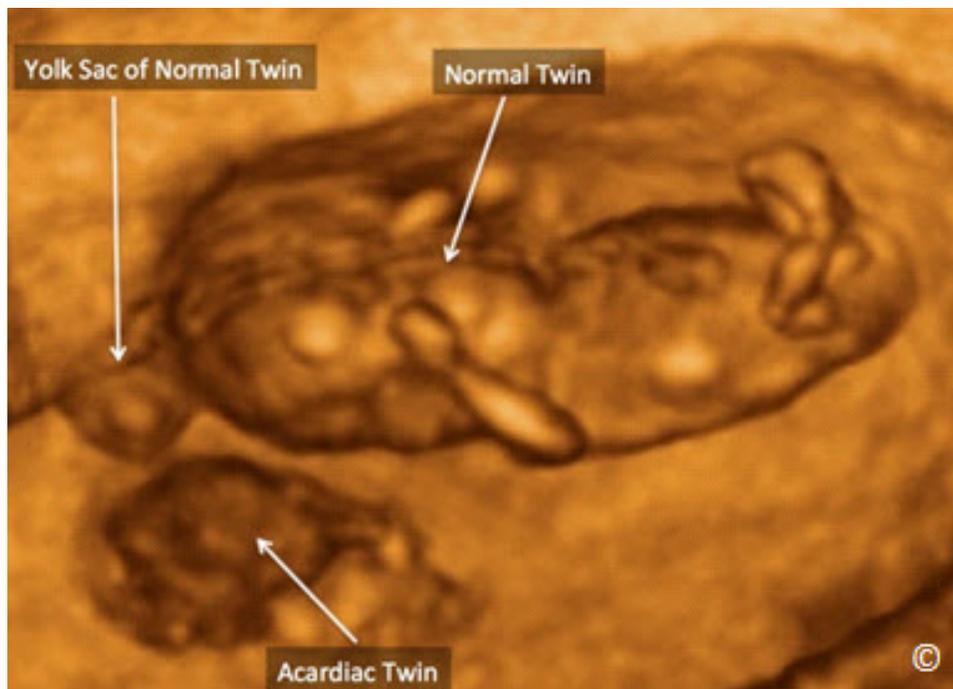
Figure 7.18: Three-dimensional ultrasound of a twin reversed arterial perfusion (TRAP) in a monochorionic twin at 9 weeks gestation (same as in **Figure 7.17**). Note the presence of a mass of tissue (labeled as acardiac twin) that is separate from the normal twin (labeled as normal twin). The yolk sac of the normal twin is seen (labeled as yolk sac of normal twin). The acardiac twin yolk sac is not clearly visible.

Given that the normal fetus has to perfuse his/her body and that of the acardiac mass, there is significant increase in cardiac workload and a risk for cardiac failure and hydrops. The overall perinatal mortality of the normal fetus in TRAP syndrome is in the range of 30 – 50 % (18, 19). Frequent echocardiographic evaluation of the normal twin in TRAP syndrome may help recognize cardiovascular stress and help guide management. Management options include expectant management, or cord coagulation of the acardiac twin. Bipolar cord coagulation of the acardiac twin appears to be the most feasible option for cord coagulation and is best performed before 24 weeks' gestation.

References:

1) Martin JA, Hamilton BE, Sutton PD, Ventura SJ, et al. Births: final data for 2002. Natl Vital Stat Rep 2003; 52(10): 1-102.
2) Jewell SE, Yip R. Increasing trends in plural births in the United States. Obstet Gynecol 1995; 85:229-32.
3) Martin JA, Hamilton BE, Ventura SJ, Osteman JK, et al. Births: final data for 2011. Natl Vital Stat Rep 2013; 62(1): 1-70.
4) Mathews TJ, MacDorman MF. Infant mortality statistics from the 2009 period linked birth/infant death data set. National vital statistics reports; vol 61 no 8. Hyattsville, MD: National Center for Health Statistics. 2013. Available from: http://www.cdc.gov/nchs/data/ nvsr/nvsr61/nvsr61_08.pdf.
5) Nylander PP. The factors that influence twinning rates. Acta Genet Med Gemellol (Roma) 1981;30:189
6) MacGillivray I. Epidemiology of twin pregnancy. Seminars Perinatol 1986; 10:4.
7) Bernirschke K. Multiple pregnancy (First of two parts). N Engl J Med 1973;288:1276
8) Monteagudo A, Timor-Tritsch IE, Sharma S. Early and simple determination of chorionic and amniotic type in multifetal gestations in the first fourteen weeks by high-frequency transvaginal ultrasonography. Am J Obstet Gynecol 1994; 170(3):824–9.
9) Winn HN, Gabrielli S, Reece EA, et al. Ultrasonographic criteria for the prenatal diagnosis of placental chorionicity in twin gestations. Am J Obstet Gynecol 1989; 161(6 Pt 1):1540–2.)
10) Finberg H. The ''twin peak'' sign: reliable evidence of dichorionic twining. J Ultrasound Med 1992; 11:571– 7.
11) Reddy UM, Abuhamad AZ, Levine D, Saade GR. Fetal Imaging Executive Summary of a Joint Eunice Kennedy Shriver National Institute of Child Health and Human Development, Society for Maternal-Fetal Medicine, American Institute of Ultrasound in Medicine, American College of Obstetricians and Gynecologists, American College of Radiology, Society for Pediatric Radiology, and Society of Radiologists in Ultrasound Fetal Imaging Workshop. J Ultrasound Med 2014; 33:745–757.

12) Society for Maternal-Fetal Medicine, Simpson LL. Twin-twin transfusion syndrome. Am J Obstet Gynecol 2013; 208(1):3-18.

13) American College of Obstetricians and Gynecologists. Multiple gestation: complicated twin, triplet and higher order multifetal pregnancy. ACOG practice bulletin no. 56. Washington, DC: The College; 2004 (reaffirmed 2009).

14) Miller J, Chauhan SP, Abuhamad AZ. Discordant twins, diagnosis, evaluation and management. Am J Obstet Gynecol 2012; FIND NUMBERS.

15) Quintero RA, Morales WJ, Allen MH, et al. Staging of twin-twin transfusion syndrome. J Perinatol 1999; 19(8 Pt 1):550 –5.

16) Abuhamad A, Mari G, Copel JC, Cantwell CJ, Sayed A, Evans AT: Umbilical artery flow velocity waveforms in Monoamniotic Twins with cord enlargement: Can it be used in pregnancy management. Obstet Gynecol 1995; 86:674-7.

17) Malone FD, D'Alton ME. Multiple gestations, clinical characteristics and management. In Creasy RK, Resnik R (eds): Maternal Fetal Medicine, ed 4, Philadelphia, WB Saunders, 2000, p595-615.

18) Moore TR, Gale S, Bernishke K. Perinatal outcome of forty nine pregnancies complicated by acardiac twinning. Am J Obstet Gynecol 1990; 163: 907-912.

19) Healy MG. Acardia: predictive risk factors for the co-twin's survival. Teratology 1994;50:205-213.

(section marker) **INTRODUCTION**

The placenta develops from the trophoblast cell layer of the blastocyst embryo at about 6 days from fertilization. With attachment of the blastocyst to the endometrial cavity, the trophoblastic cells differentiate into an inner layer; the cytotrophoblasts and an outer layer; the syncytiotrophoblasts. The syncytiotrophoblasts develop lacunae forming early intervillous spaces.

The placenta forms at the site of the chorion frondosum (the fetal portion of chorion) and the decidua basalis and is first recognized sonographically as a thickened echogenic region by about 9-10 weeks of gestation (**Figure 8.1**). Maternal blood flow is established within the placenta by 12 weeks of gestation (1). The placenta at term is about 20 cm in diameter with a volume of 400 to 600 ml (2). In general, measurement of the placenta in not obtained currently unless in rare pathologic conditions and thus assessment of the biometric dimensions of the placenta are infrequently performed on prenatal sonography today. The normal thickness of the placenta is correlated to gestational age with approximately 1 mm per weeks of gestation (3).
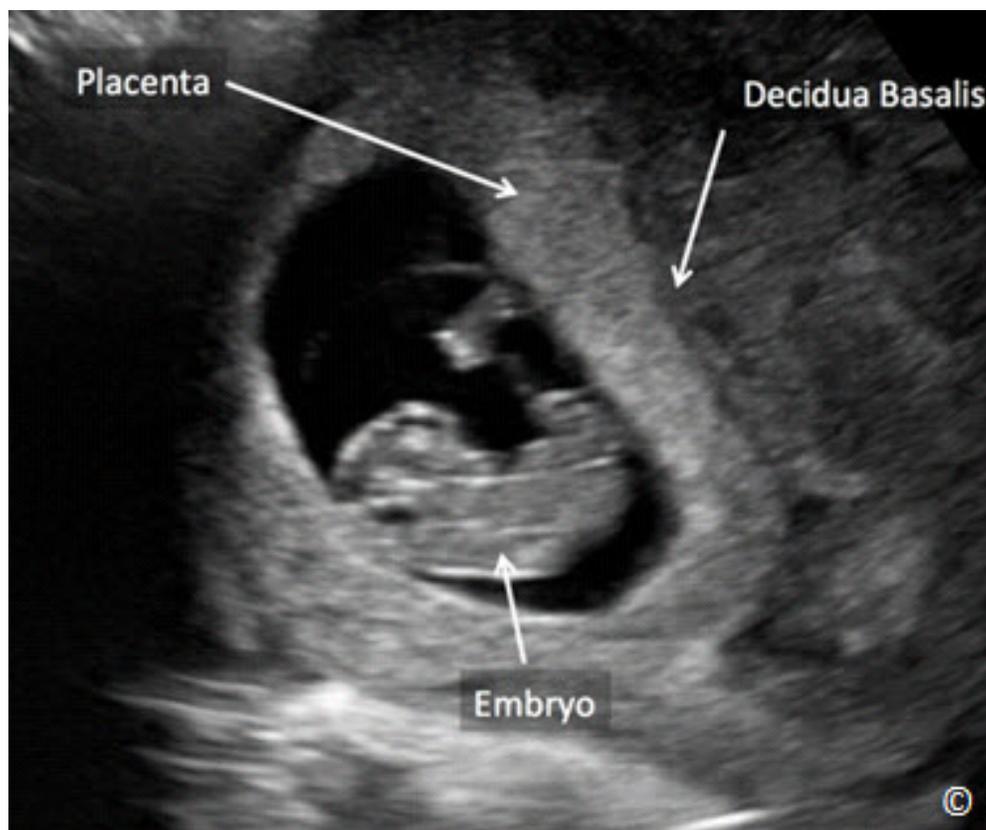
Figure 8.1: Ultrasound of an intrauterine pregnancy at 9 weeks showing the echogenic placenta (labeled). Note the decidua basalis (labeled) as a hypoechoic region behind the placenta. The embryo is also shown (labeled).

Placental localization by ultrasound is one of the six components of the standardized approach to the basic obstetric ultrasound examination and the technical detail of this examination is described in chapter 10. In this chapter, we will focus on the ultrasound diagnosis of placental abnormalities.

PLACENTA PREVIA

The term placenta previa describes a placenta that covers part or all of the internal cervical os. In normal pregnancy, the placenta implants in the upper uterine segment. In the case of placenta previa, the placenta is partially or totally implanted in the lower uterine segment.

Placenta previa is one of the most common causes of bleeding in the second and third trimester of pregnancy. The incidence of placenta previa in the United States at term is estimated at 4.8/1000 deliveries (4). Given that there is a positive association between placenta previa and multiparity, it is expected that the incidence of placenta previa is increased in countries with a high prevalence of multiparity. The classical presentation of placenta previa is painless vaginal bleeding in the late second and third trimester of pregnancy. Painful bleeding may occur in some pregnancies with placenta previa however due to the association with uterine contractions or placental separation (abruption). The first presentation of placenta previa maybe bleeding during labor which highlights the critical importance of prenatal diagnosis and a planned delivery by cesarean section if the placenta previa persists into the third trimester of pregnancy. Placenta previa is also associated with a higher incidence of fetal malpresentation, which by itself maybe a clue to the presence of a placental previa.

Placenta previa is more commonly seen in early gestation (**Figure 8.2**), and in many such cases, with advancing gestation and growth of the uterus, the placenta is lifted into the upper uterine segment. This mechanism of "placental shift/migration" is poorly understood but may be related to a preferential growth of the placental towards a better-vascularized upper endometrium (trophotropism).
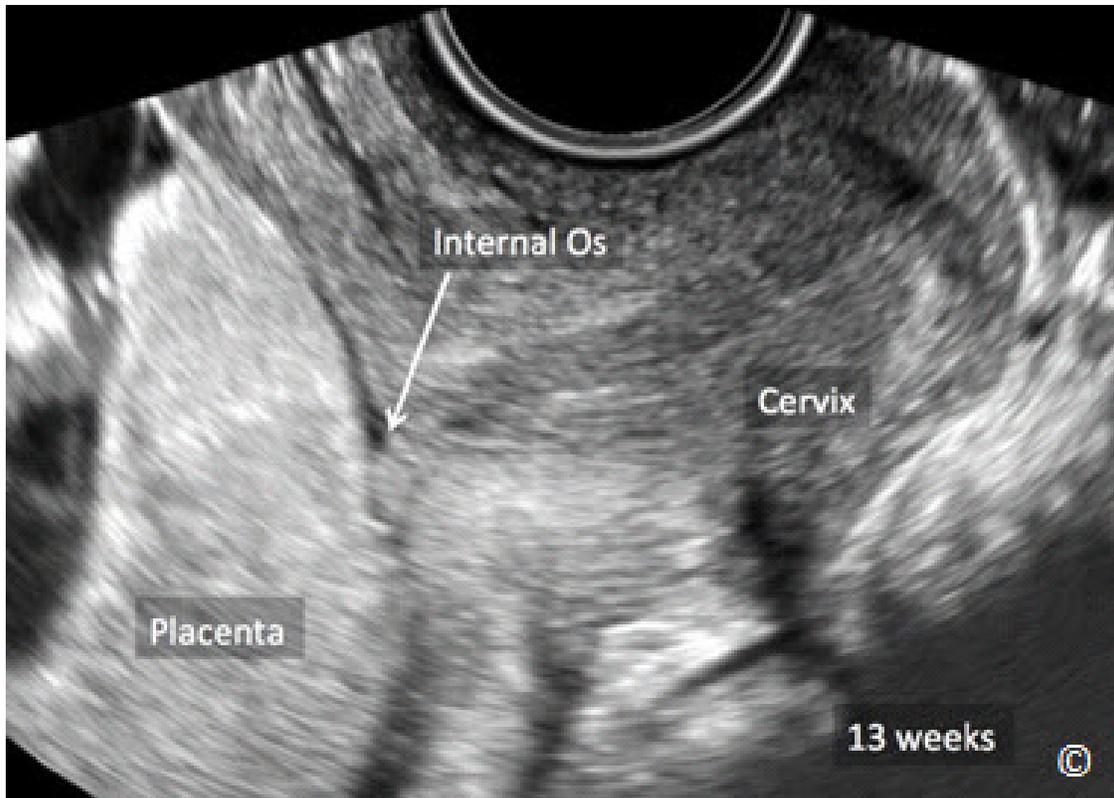
Figure 8.2: Ultrasound of an intrauterine pregnancy at 13 weeks. Note that the placenta (labeled) is covering the internal os of the cervix (labeled), representing a placenta previa.

Table 8.1 lists risk factors for placenta previa. An exponential increase in the incidence of placenta previa exists with increasing number of prior cesarean sections. The presence of four prior cesarean sections increases the incidence of placenta previa about 10 folds (5).

TABLE 8.1	Risk Factors for Placenta Previa
- History of prior cesarean delivery - Prior pregnancy termination(s) - Prior uterine surgery - Maternal smoking - Advanced maternal age - Multiparity - Cocaine use in mother - Multiple pregnancy	

The current terminology used to describe types of placenta previa has been somewhat confusing. Complete placenta previa describes a placenta that completely covers the internal os, a partial placenta previa describes a placenta that partially covers a dilated cervix and a marginal placenta previa describes a placenta where the edge reaches the internal cervical os. If the placental edge is a short distance away from the internal os, within a few cm(s), the term low-lying placenta is suggested, and the distance should be measured. Assessing a dilated cervix by ultrasound for the diagnosis of partial previa is difficult, if not impossible, and the distance used to designate a low-lying placenta has been variable in the literature. Recently, a multi-disciplinary consensus conference in the United States has suggested a simpler terminology of placenta previa that is more pertinent and clinically applicable (6). This new classification uses 3 terms only: placenta previa, low-lying placenta or normally implanted placenta (normal). The terms partial placenta previa and marginal placenta previa are eliminated. Other terms such as incomplete and total placenta previa should also be eliminated.

The new classification is as follows: for pregnancies at less than 16 weeks of gestation, diagnosis of placenta previa is overestimated. For pregnancies greater than 16 weeks, if the placental edge is ≥2 cm from the internal os, the placental location should be reported as normal. If the placental edge is < 2 cm from the internal os, but not covering the internal os, the placenta should be labeled as low-lying (**Figure 8.3**) and a follow-up ultrasound is recommended at 32 weeks. If the placental edge covers the internal cervical os, the placenta should be labeled as placenta previa (**Figure 8.4**) and a follow-up ultrasound is recommended at 32 weeks. At the follow-up ultrasound at 32 weeks, if the placental edge is still less than 2 cm from the internal cervical os (low-lying) or covering the cervical os (placenta previa), a follow-up transvaginal ultrasound is recommended at 36 weeks (6). These recommendations are for asymptomatic women and an earlier follow-up ultrasound may be indicated in the presence of bleeding. Because low-lying placenta or placenta previa detected in the mid second trimester that later resolves in pregnancy is associated with vasa previa, transvaginal ultrasound with color/pulsed Doppler in the third trimester (around 32 weeks) is recommended to rule-out vasa previa (**Figure 8.5**) (6). The transvaginal ultrasound should be used as the primary mode of imaging for the diagnosis of placenta previa as a full bladder and / or a uterine contraction of the lower uterine segment can potentially result in a false positive diagnosis of a placenta previa, when a transabdominal approach is used. The transvaginal approach allows for a clear evaluation of the internal cervical os and the exact anatomic relation of the placental edge to the cervix. Furthermore, color Doppler, when available, can assess the vascularity of the placenta, cervix and lower uterine segment and evaluate for the risk of accreta and bleeding at delivery (**Figure 8.6**). The safety of the transvaginal ultrasound approach in the assessment of placenta previa has been well established (7). This is due to the angle of the transvaginal transducer, which places it against the anterior lip of the cervix, unlike a digital examination, which typically introduces a finger

into the cervical canal. **Figure 8.7**, **8.8** and **8.9** show normal anterior, fundal and posterior placentas respectively.
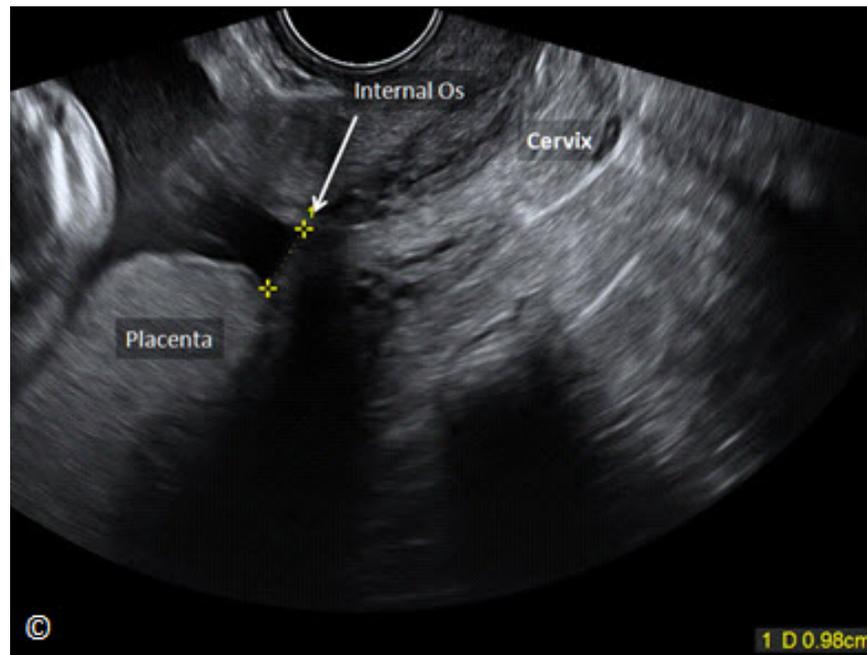

Figure 8.3: Transvaginal ultrasound in the third trimester showing a low-lying posterior placenta (labeled). Note that the lower edge of the placenta is about 0.9 cm from the cervical internal os (labeled). The cervix is also labeled for image orientation.
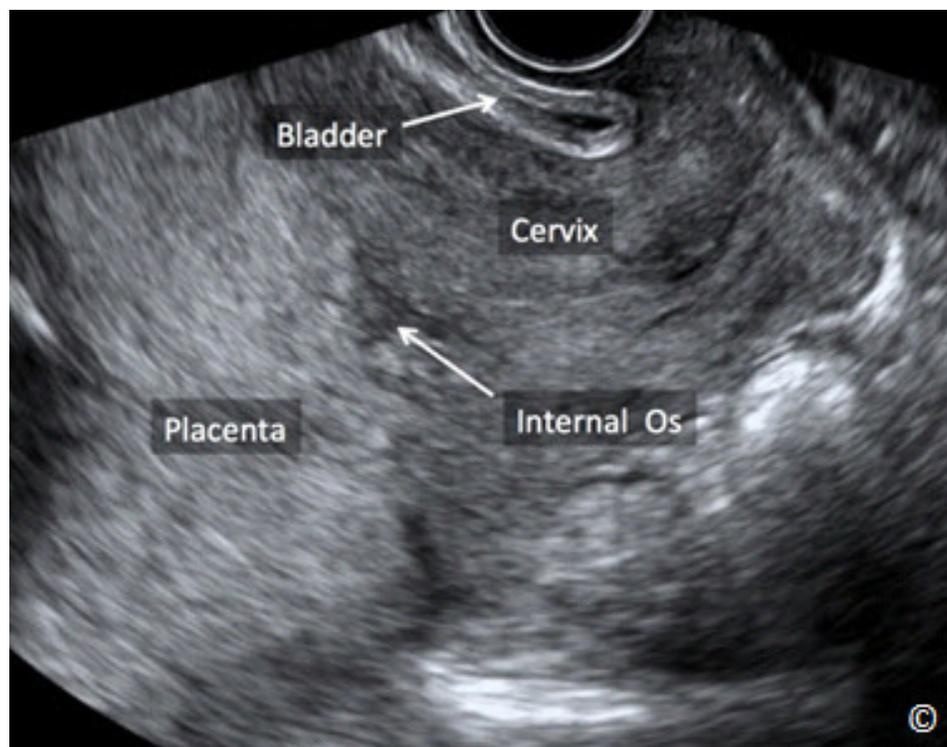

Figure 8.4: Transvaginal ultrasound in the third trimester showing a placenta previa. Note that the placenta (labeled) is covering the cervical internal os (labeled). The bladder is seen anteriorly (labeled). The cervix is also labeled for image orientation.
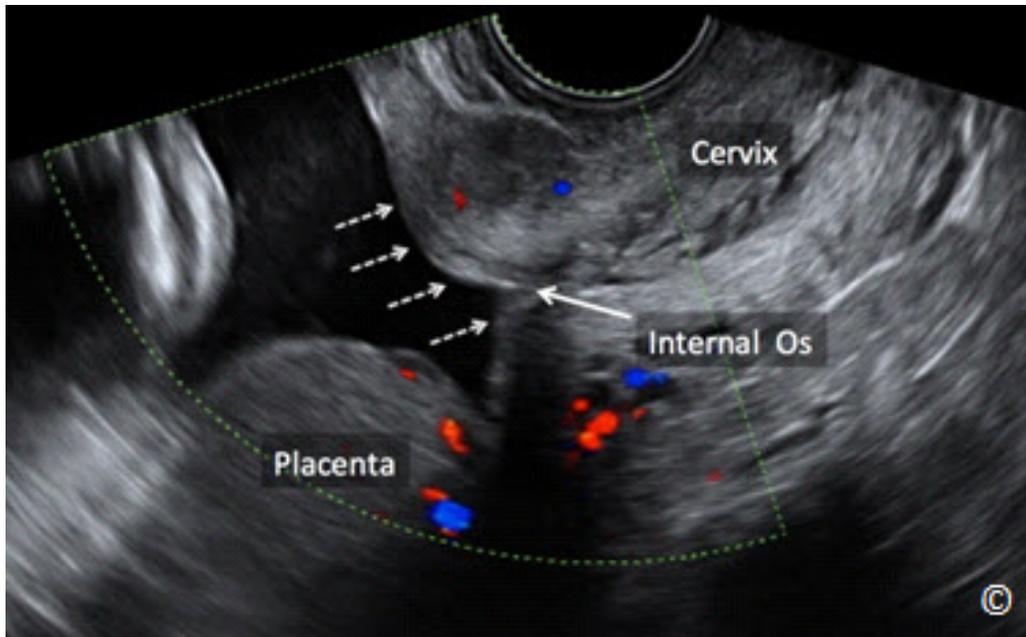
Figure 8.5: Transvaginal ultrasound with color Doppler at 32 weeks showing the absence of a vasa previa (dashed arrows) in a pregnancy that had a placenta previa in the second trimester. Note that the placenta is no longer covering the cervical internal os (labeled). The cervix and internal os are also labeled for image orientation.
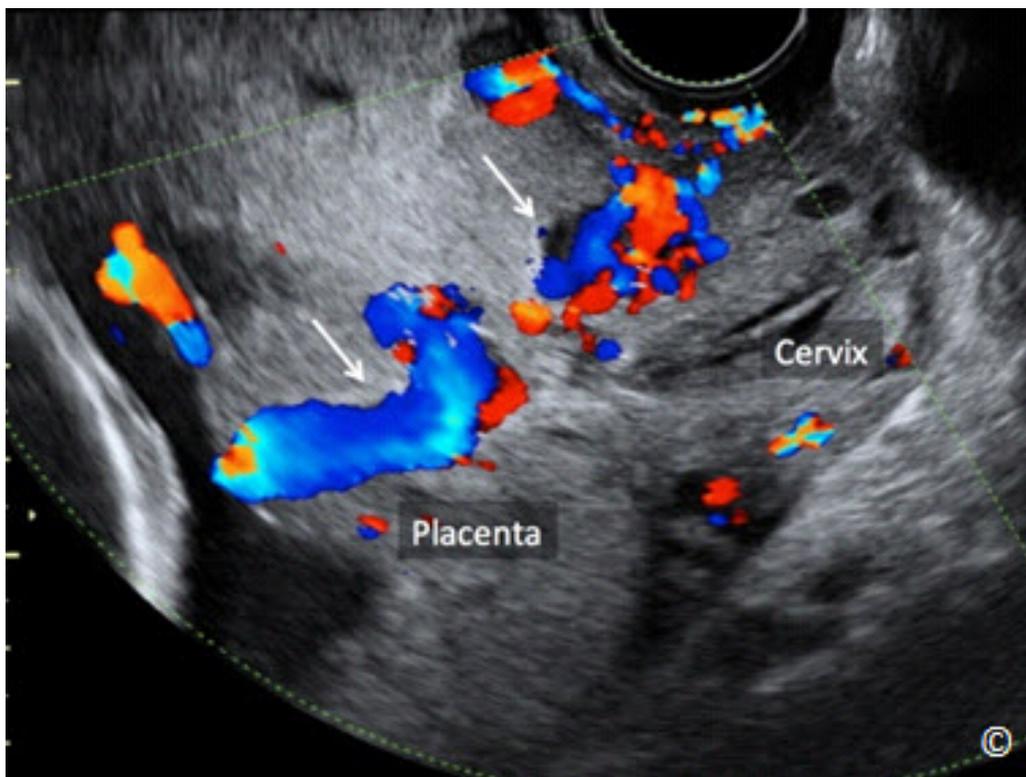
Figure 8.6: Transvaginal ultrasound with color Doppler in the third trimester in a patient with placenta previa and placenta accreta. Note the presence of increased vascularity in the placenta and cervix (labeled – arrows).
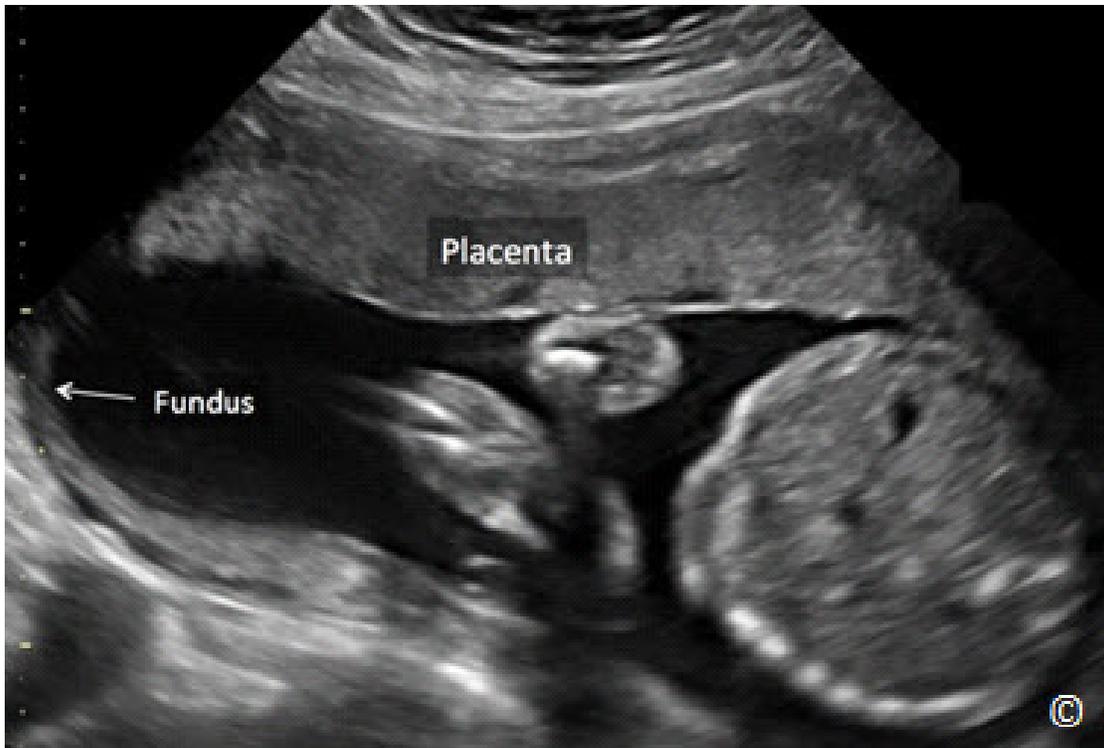
Figure 8.7: Transabdominal ultrasound in the second trimester in a sagittal orientation showing an anterior normal placenta (labeled). The uterine fundus is labeled for image orientation.
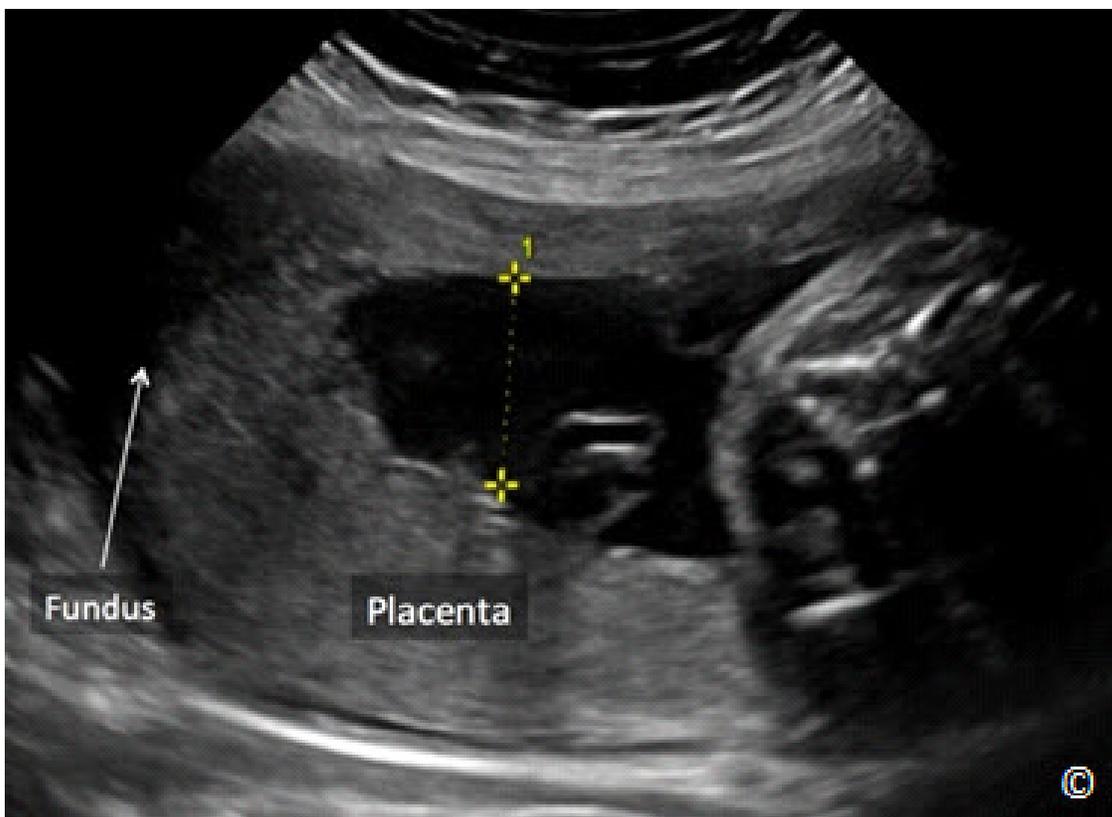
Figure 8.8: Transabdominal ultrasound in the second trimester in a sagittal orientation showing a fundal normal placenta (labeled). The uterine fundus is labeled for image orientation. In this figure, a vertical pocket of amniotic fluid is also measured.
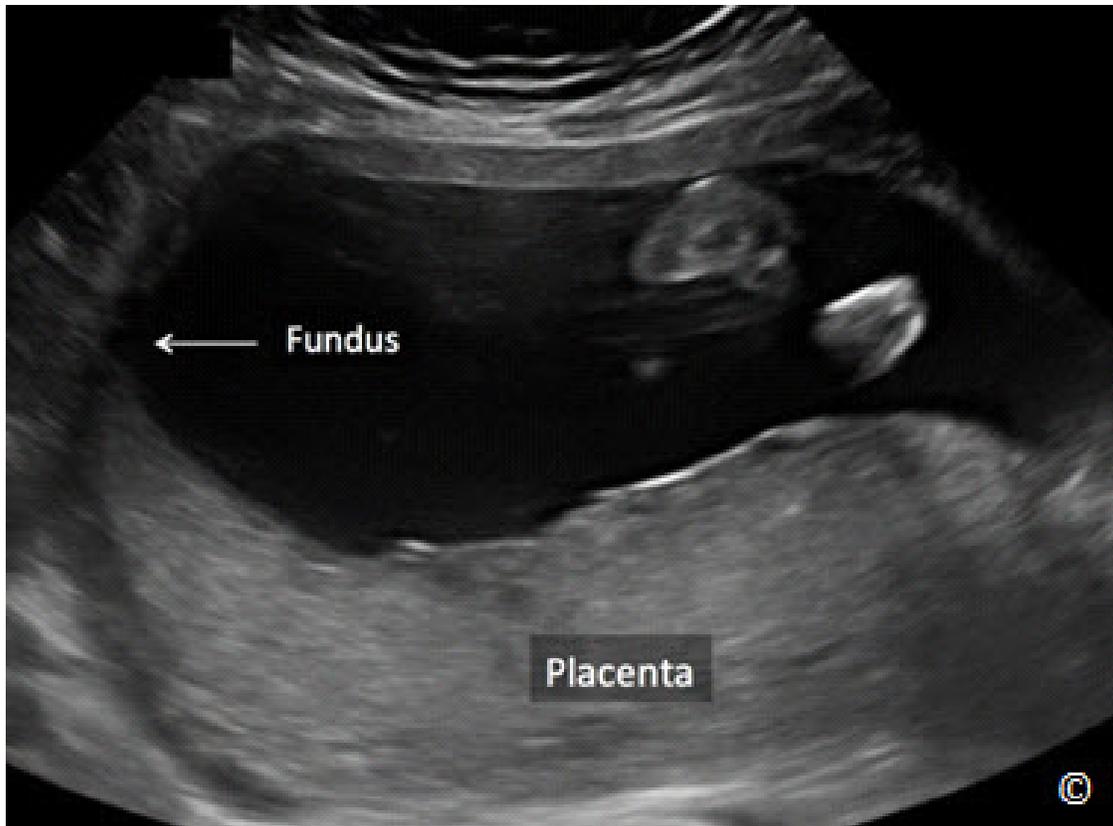
Figure 8.9: Transabdominal ultrasound in the second trimester in a sagittal orientation showing a posterior normal placenta (labeled). The uterine fundus is labeled for image orientation.

Table 8.2 describes the transvaginal ultrasound approach in the evaluation of the placenta when a placenta previa is suspected.

TABLE 8.2	Transvaginal Approach to the Evaluation of the Placenta

- Use the transvaginal transducer
- Ensure that the woman's urinary bladder is empty
- Insert the transvaginal transducer until you see the cervix, identify the internal cervical os
- Maintain sagittal orientation of the transvaginal transducer
- Ensure minimal pressure on the cervix
- Localize the lower placental edge and assess its relationship to the internal cervical os

VASA PREVIA

Vasa previa refers to the presence of fetal blood vessels between the presenting fetal parts and the cervix. The fetal blood vessels can run in the fetal membranes unprotected or the umbilical cord can be tethered to the membranes at the level of the cervical os.

The incidence of vasa previa is approximately 1 in 2500 deliveries (8). The implication of having fetal vessels in front of the fetal presenting part is potentially catastrophic in that should the membranes rupture, the fetal vessels are at risk of rupturing with resulting fetal exsanguination. When undiagnosed, vasa previa has an associated perinatal mortality of 60%, whereas 97 % of fetuses survive when the diagnosis is made prenatally (9).

Prenatal diagnosis relies on the transvaginal ultrasound approach. Vasa previa is diagnosed by ultrasound when color Doppler documents the presence of fetal vessels overlying the cervix (**Figure 8.10 A and B**). It is important to confirm by pulsed Doppler that the vascular flow is fetal in origin (**Figure 8.10 B**). On transvaginal grey-scale ultrasound evaluation of the cervix, the presence of echogenic lines along the amniotic sac and overlying the internal cervical os, should alert the examiner for the presence of a vasa previa (**Figure 8.11 A**). Once these echogenic lines are noted, the addition of color Doppler confirms that the echogenic lines are actually vessels running in fetal membranes (**Figure 8.11 B**). If the umbilical cord or umbilical vessels appear to be tethered to the membranes at the level of the internal os, or in the lower uterine segment along the cervix (**Figure 8.12 A and B**), a vasa previa should also be diagnosed. It is important to rule out a funic presentation by either asking the patient to move around and see if the umbilical cord moves in the process. Repeating the transvaginal ultrasound examination at a later date will also confirm this finding.
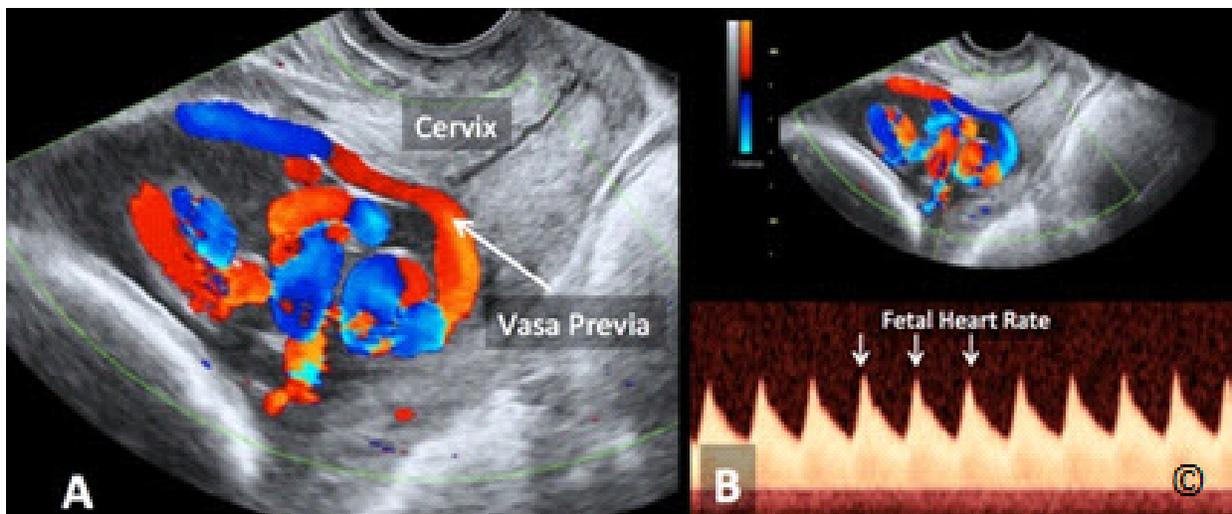

Figure 8.10 A and B: Transvaginal ultrasound in the third trimester in color (A) and Pulsed (B) Doppler in a fetus with vasa previa. Note that color Doppler (A) shows a vessel crossing in front of cervix (labeled as vasa previa) and pulsed Doppler (B) documents fetal heart rate in the vessel. The cervix is labeled in A.
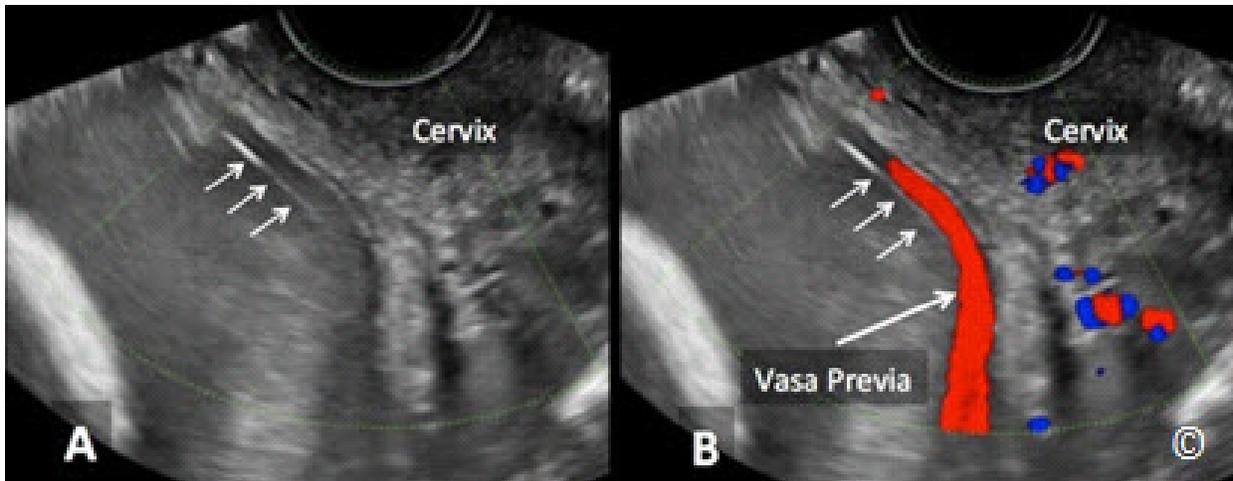
Figure 8.11 A and B: Transvaginal ultrasound in the second trimester in grey scale (A) showing an echogenic line (arrows) in front of the cervix (labeled). Color Doppler (B) confirms the presence of vasa previa. The presence of an echogenic line in front of the cervix may represent a vessel wall and should alert for the presence of vasa previa.
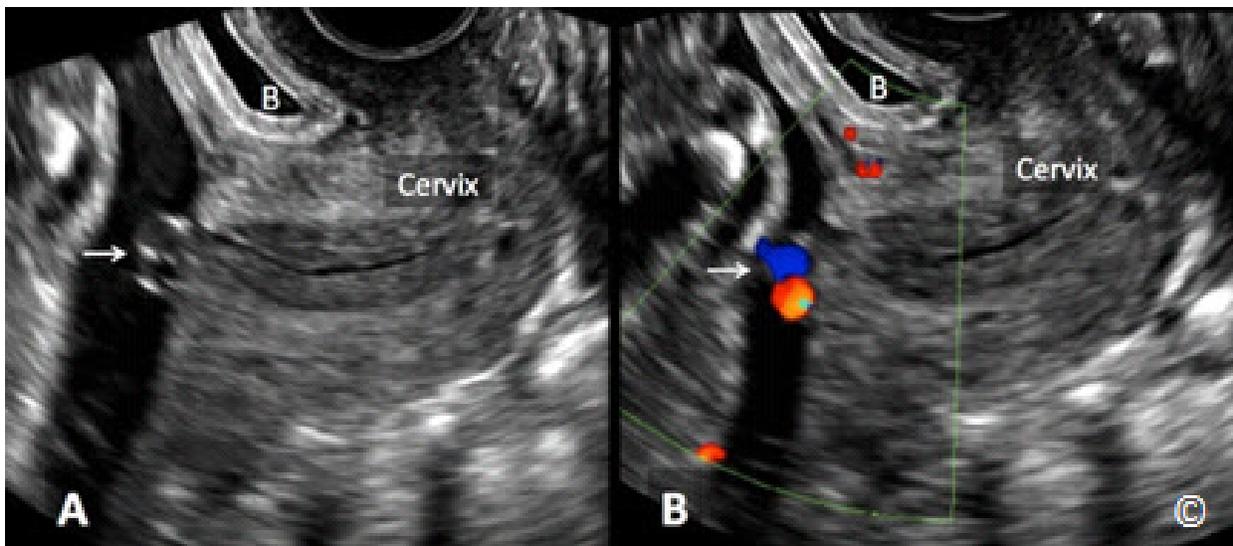

Figure 8.12 A and B: Transvaginal ultrasound in the late second trimester in grey scale (A) and color Doppler (B) showing a vasa previa involving a tethered umbilical cord (arrow) to the cervix (labeled). B = Bladder.

Risk factors for vasa previa are listed in **Table 8.3**. Of those listed, the presence of a second trimester low-lying placenta, or placenta previa is a significant risk factor for vasa previa (9), and thus a follow-up transvaginal ultrasound with color Doppler at 32 weeks is recommended to screen for vasa previa (6).

TABLE 8.3	Risk Factors for Vasa Previa

- Resolving second trimester low-lying placenta
- Resolving second trimester placenta previa
- Presence of accessory placental lobes (succensuriate lobe)
- Velamentous or marginal cord insertion
- Multiple pregnancies
- Echogenic line(s) seen along the amniotic sac overlying the internal os

Management of vasa previa relies on the prenatal diagnosis and a planned elective delivery by cesarean section before the beginning of labor. This is typically accomplished around 36-38 weeks. The balance of neonatal resuscitation capabilities with the risk of labor and rupture of membranes should be taken into account when vasa previa is diagnosed in low-resource settings. The status of the cervix and prior obstetric history may help in making such decision.

MORBIDLY ADHERENT PLACENTA

The term morbidly adherent placenta implies an abnormal implantation of the placenta into the uterine wall and this term has been used to describe placenta accreta, increta, and percreta. Placenta accreta is a placenta where the placental villi adhere directly to the myometrium, placenta increta is a placenta where the placental villi invade into the myometrium, and placenta percreta is a placenta where the placental villi invade through the myometrium and into the serosa. About 75% of morbidly adherent placentas are placenta accretas, 18% are placenta incretas, and 7% are placenta percretas (10). Placenta accretas can be subdivided into total placenta accreta, partial placenta accreta, or focal placenta accreta based upon the amount of placental tissue involved in their attachment to the myometrium. Pathogenesis of placenta accreta is not currently clear. It is theorized to result from abnormal vascularization resulting from the scaring process after surgery with secondary localized hypoxia, leading to both defective decidualization and excessive trophoblastic invasion (11, 12, 13). The presence of any type of placenta accreta can be catastrophic to the patient especially in a low-resource setting given the potential need for massive blood transfusion and possibly emergency hysterectomy. Prenatal diagnosis and a planned delivery are therefore essential for optimizing the maternal and neonatal outcome.

The overall incidence of placenta accreta is around 3 per 1000 deliveries and there has been a significant increase in the incidence of placenta accreta over the past several decades (14, 15). The main reason for this increase is the significant rise in cesarean section rates, as cesarean section and placenta previa are both known risk factors for placenta accreta (16) (**Graph 8.1**).

For instance, a patient with three prior cesarean sections, the presence of a placenta previa is associated with a 40% risk for placenta accreta (16) (**Graph 8.1**). It is of note that this association is directly related to the presence of a placenta previa. In this same patient, the risk for the presence of a placenta accreta decreases to less than 1% if there is no placenta previa in the at risk pregnancy (16) (**Graph 8.1**). Assessing for the presence of placenta previa is therefore critical in pregnant women with prior cesarean sections. As the number of previous cesarean sections increase, the risk for placenta accreta increase substantially in the presence of a placenta previa. Other risk factors for placenta accreta are listed in **Table 8.5**.
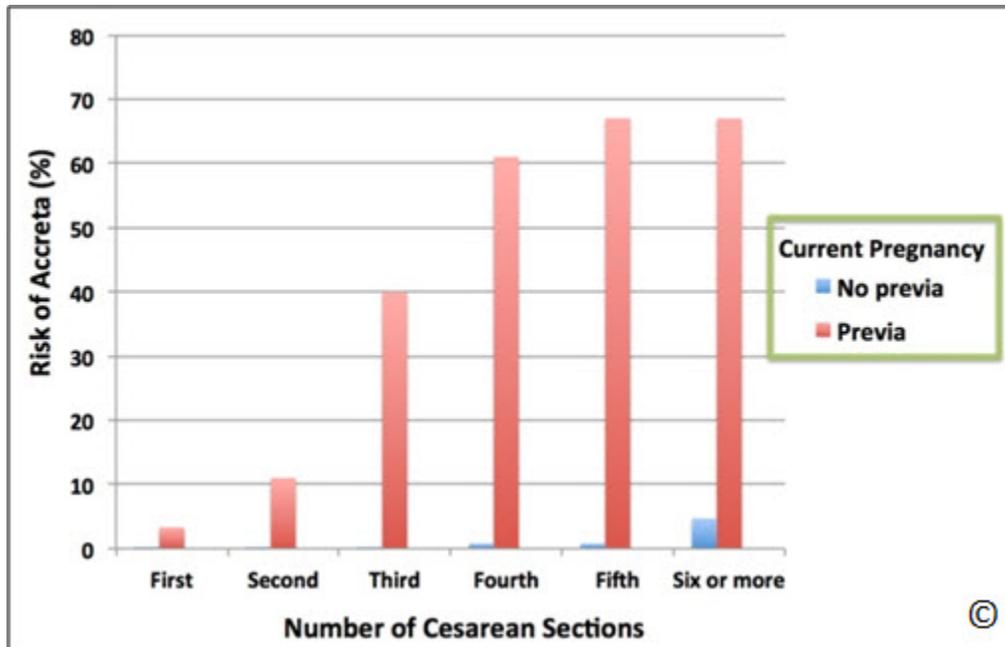
Graph 8.1: Risk for placenta accreta in pregnancies with and without a placenta previa and prior cesarean deliveries. Note that the risk of placenta accreta increases significantly as the number of prior cesarean deliveries increases in the presence of a placenta previa on ultrasound. When a placenta previa is not noted on ultrasound, the risk for placenta accreta remains small (< 1%), irrespective of the number of prior cesarean deliveries.

TABLE 8.5	Risk Factors for Placenta Accreta

- Placenta previa and prior cesarean section
- Advanced maternal age
- Multiparity
- Prior uterine surgery
- Prior uterine irradiation
- Endometrial ablation
- Asherman's syndrome
- Leiomyomas
- Uterine anomalies
- Hypertensive disorders in pregnancy
- Smoking

SONOGRAPHIC FINDINGS OF PLACENTA ACCRETA

First Trimester

A gestational sac that is implanted in the lower urine segment increases the risk for placenta accreta in pregnancy (**Figure 8.13**) (17). Other sonographic findings correlating first trimester ultrasound with placenta accreta include multiple irregular vascular spaces within the placental bed (18) (**Figure 8.14**). Cesarean section scar implantation of the gestational sac is a different entity than a low gestational sac implantation and is used to describe implantation of a gestational sac within a cesarean section scar. Ultrasound findings of cesarean section scar implantation include a gestational sac imbedded into the cesarean section scar at the level of the internal cervical os, at the base of the bladder (**Figure 8.15**). If untreated, cesarean section scar implantation may lead to significant placental abnormalities such as placenta accreta, percreta and increta. A preferred treatment option for cesarean scar implantation includes injection of the gestational sac with methotrexate under direct ultrasound guidance (**Figure 8.16**).

Figure 8.13: Transvaginal ultrasound in the first trimester showing a gestational sac (labeled) implantation in the lower uterine segment. This pregnancy progressed to a placenta percreta. Modified with permission from the American Institute of Ultrasound in Medicine (18).
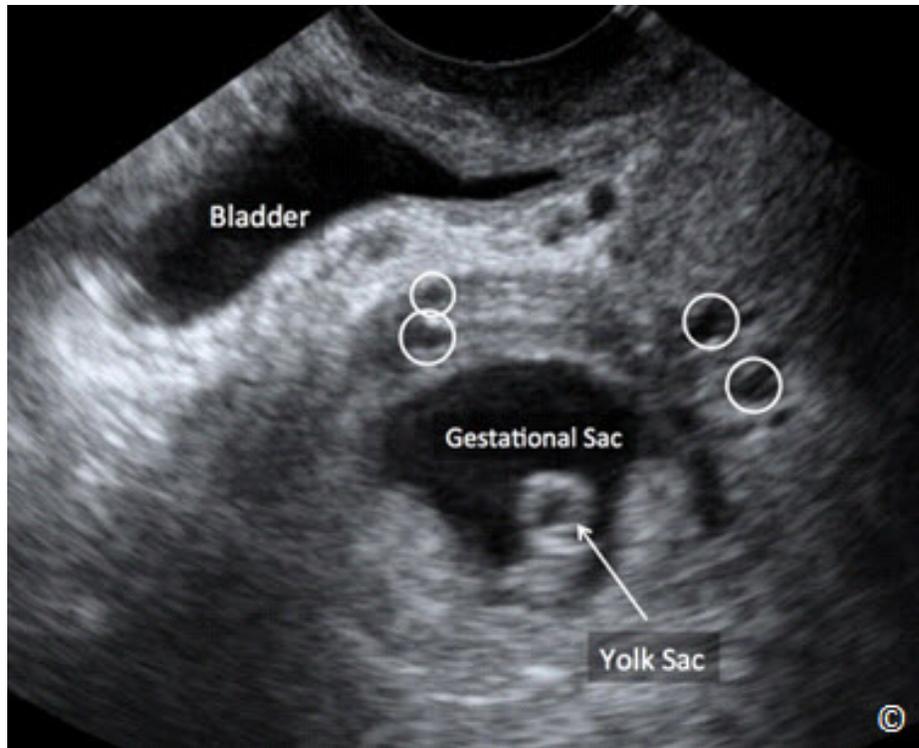
Figure 8.14: Transvaginal ultrasound in the first trimester in the same pregnancy as in figure 8.13. Note the presence of multiple irregular vascular spaces in and around the placenta (white circles). This pregnancy progressed to a placenta percreta. Modified with permission from the American Institute of Ultrasound in Medicine (18).
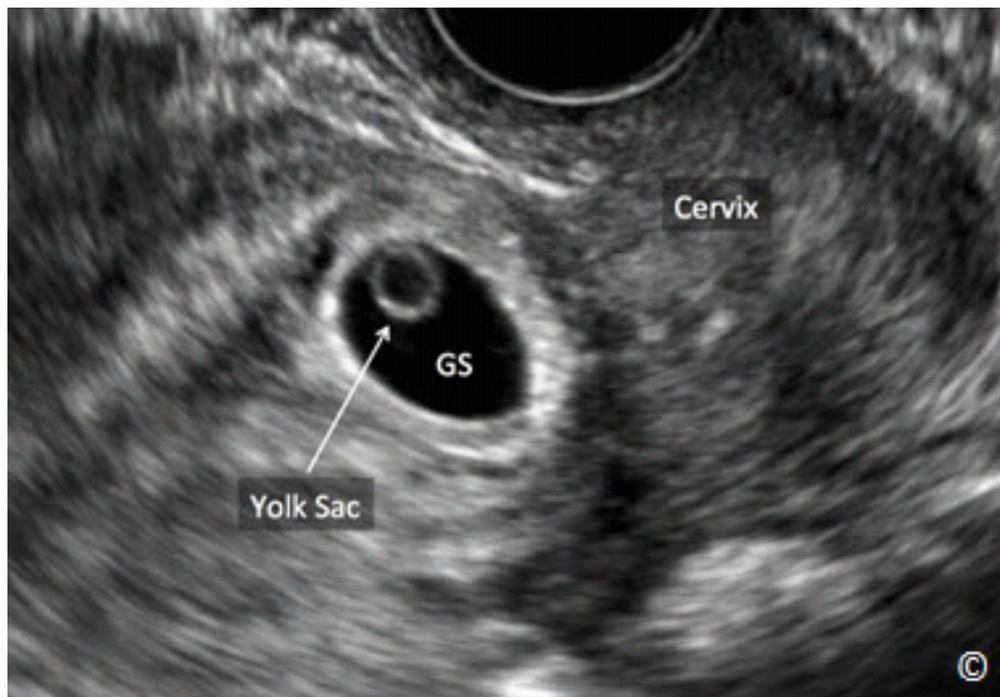

Figure 8.15: Transvaginal ultrasound of a cesarean section scar implantation of a gestational sac. Note that the gestational sac (GS) is imbedded into the cesarean section scar at the level of the internal cervical os (cervix). The yolk sac is labeled.
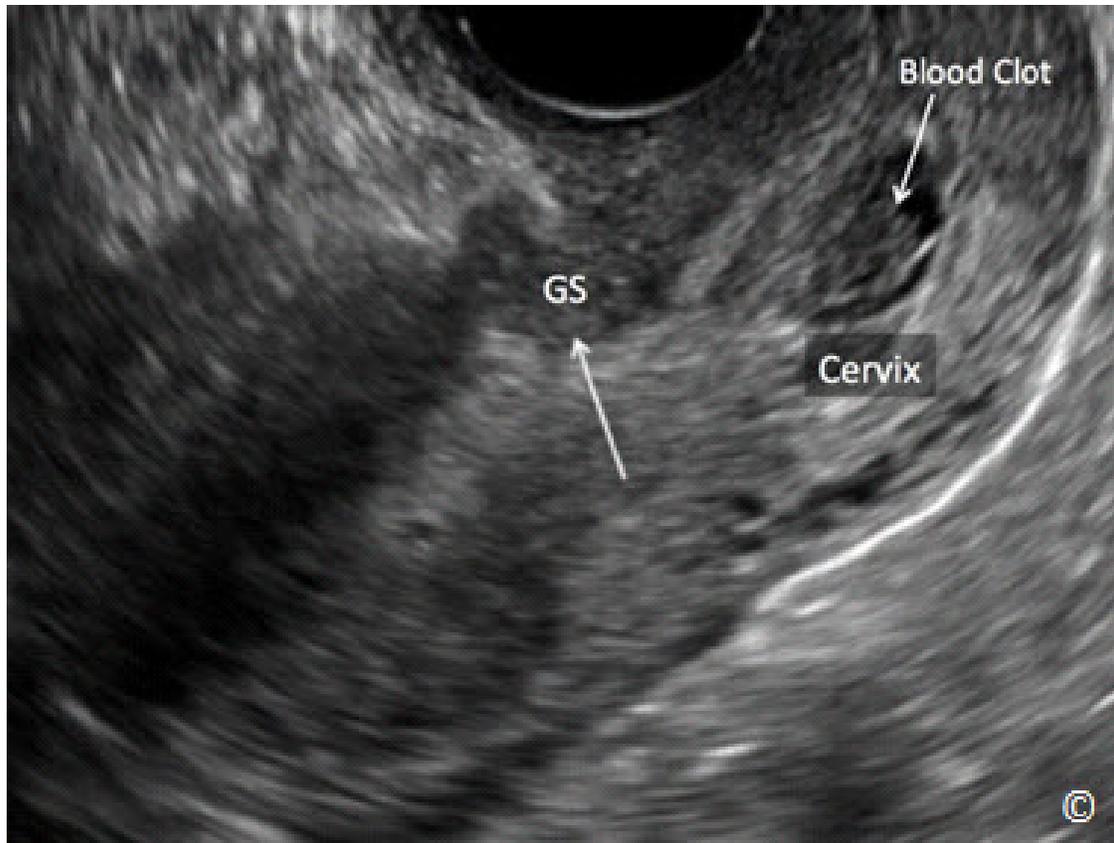
Figure 8.16: Transvaginal ultrasound of a cesarean section scar implantation of a gestational sac, 2 weeks following treatment with direct methotrexate injection under ultrasound guidance (same pregnancy as in figure 8.15). Note that the gestational sac (GS) has collapsed and a small blood clot (labeled) is noted in the cervical canal (cervix).

Second and Third Trimester

Multiple vascular lacunae within the placenta in the second trimester have been correlated with a high sensitivity (80-90%) and a low false positive rate for placenta accreta (19) (**Figure 8.17**). Placental lacunae in the second trimester appear to have the highest sensitivity and positive predictive value of other markers for placenta accreta (19). There are multiple sonographic markers that have been described in the late second and third trimester for placenta accreta. Loss of the normal hypoechoic retroplacental zone, also referred to as loss of the clear space between the placenta and the uterus, is one of those markers (20, 21) (**Figure 8.18 A and B**). This sonographic finding (loss of normal hypoechoic retroplacental zone) tends to have high false positive rate and should not be used alone as it is angle dependent and can be absent in normal anterior placentas (20 - 23).
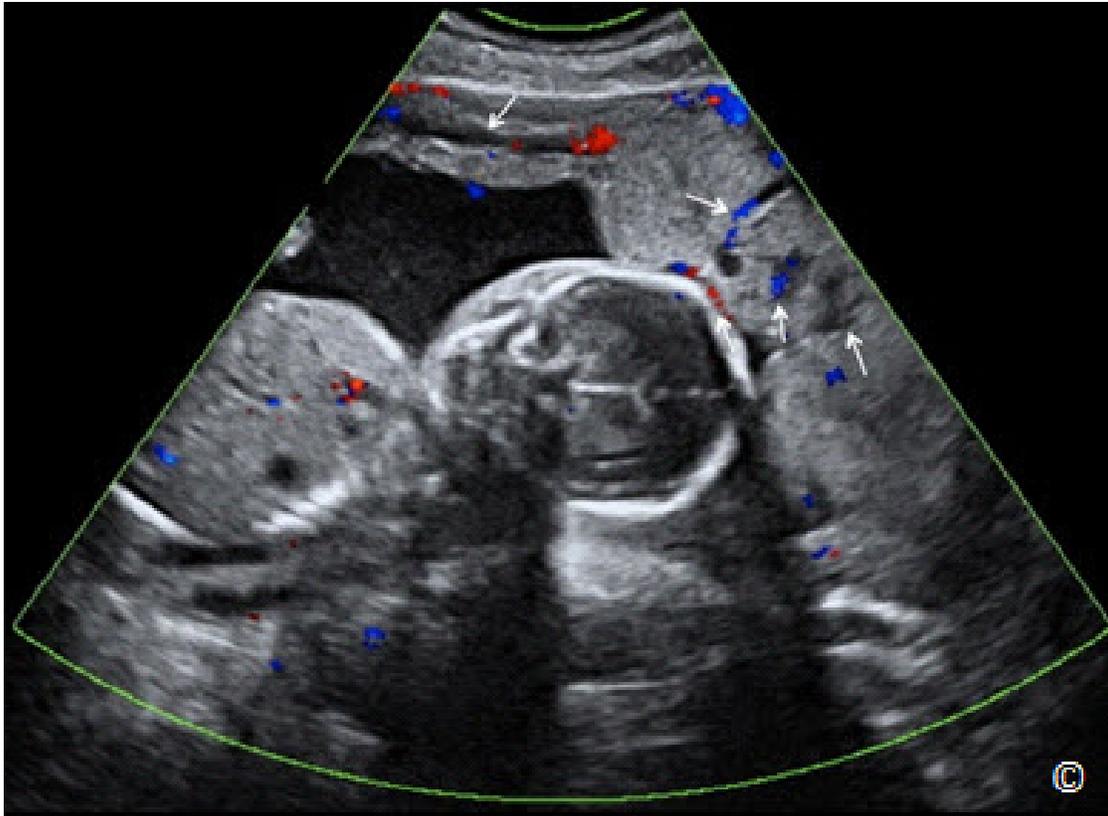
Figure 8.17: Transabdominal ultrasound at 18 weeks with color Doppler showing a placenta accreta. Note the presence of multiple vascular lacunae within the placenta (white arrows). Color Doppler shows blood flow within the lacunae.
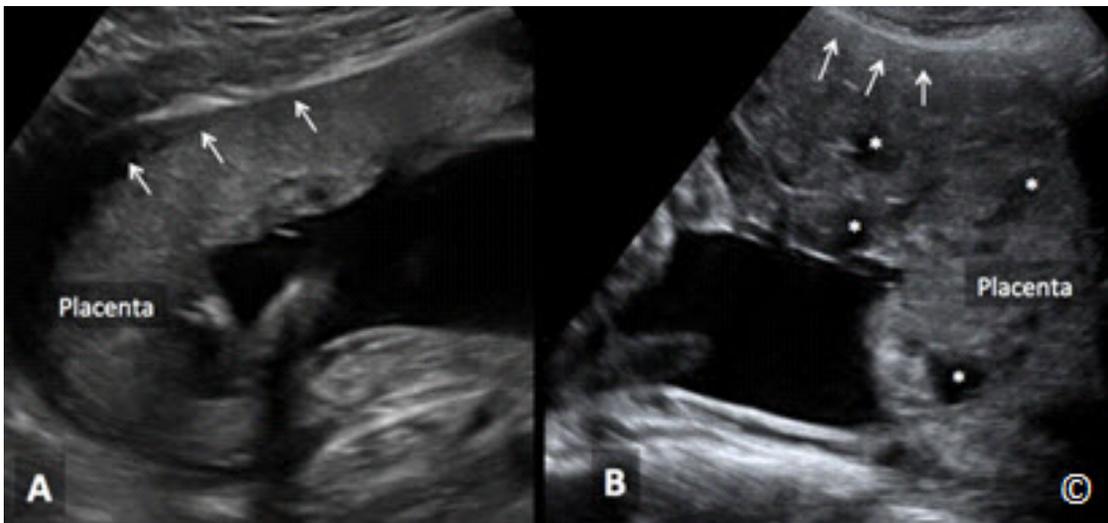

Figure 8.18 A and B: Transabdominal ultrasound showing a normal placenta in A with a normal hypoechoic retroplacental zone (arrows). Note the presence of a placenta accreta in B with loss of the normal hypoechoic retroplacental zone (arrows). The placenta in B also has multiple lacunae (small asterisks).

The presence of multiple vascular lacunae within the placenta, or "swiss-cheese appearance", is one of the most important sonographic finding of placenta accreta in the third trimester (**Figure 8.19** and **8.20 A and B**). The pathogenesis of this finding is probably related to placental tissue alterations resulting from long-term exposure to pulsatile blood flow (24, 25). The presence of multiple lacunaes, especially four or more has been correlated with a detection rate of 100% for placenta accreta. This marker also has low false positive rates, but it should be noted that placenta accretas have been reported with absent multiple vascular lacunaes.
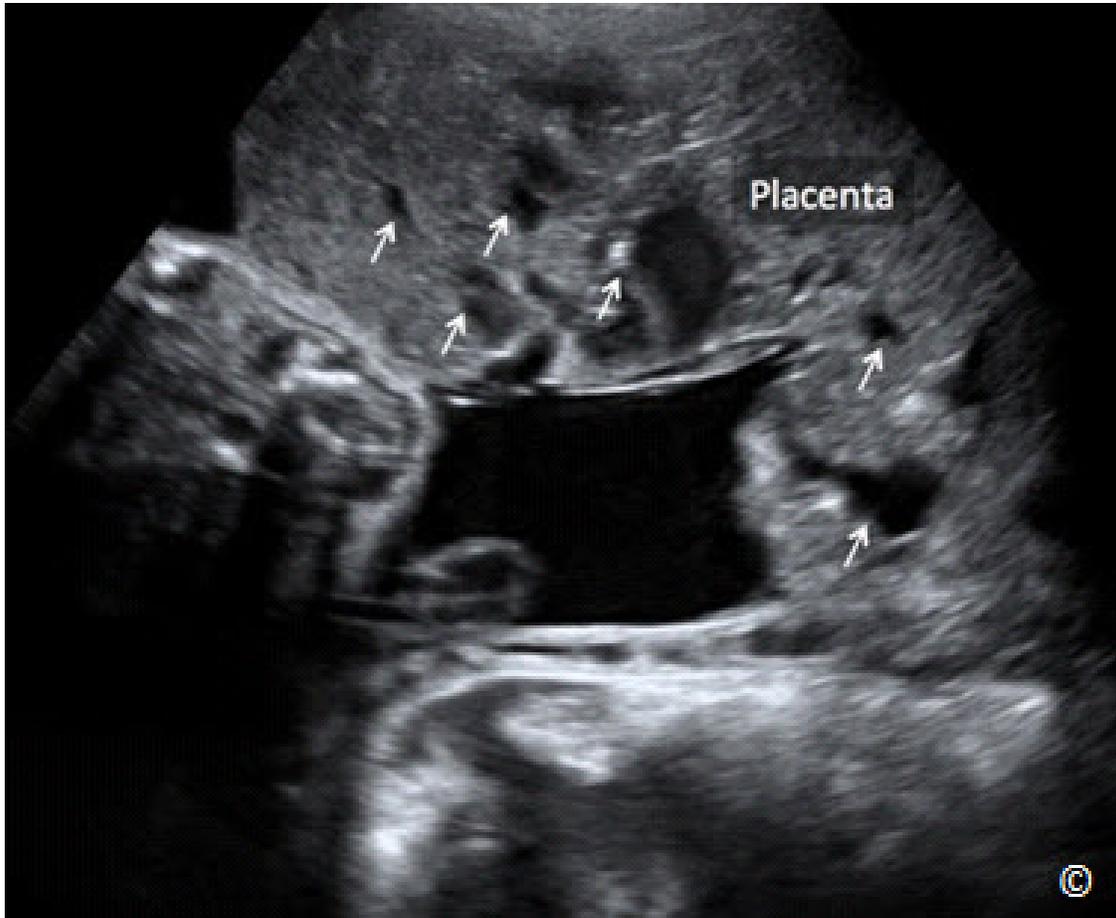
Figure 8.19: Transabdominal ultrasound in the third trimester showing a placenta accreta (labeled as placenta). Note the presence of multiple placental lacunae (arrows).
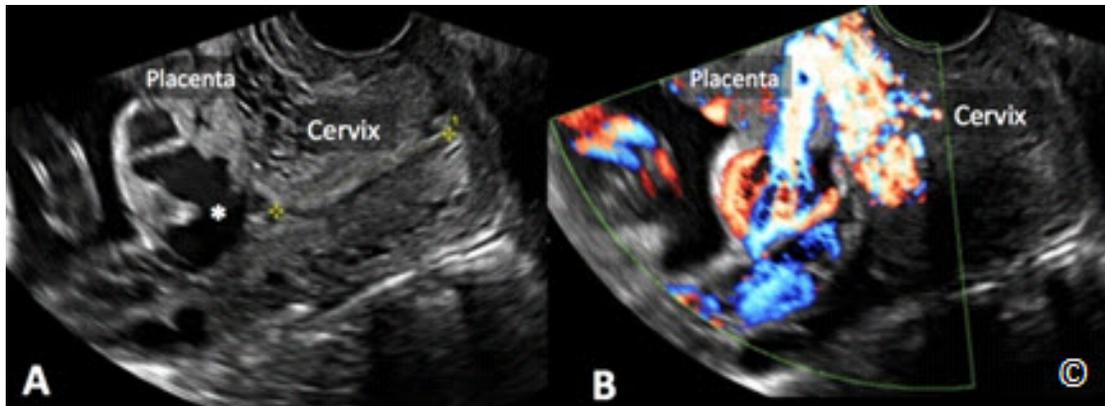
Figure 8.20 A and B: Transvaginal ultrasound in grey scale (A) and color Doppler (B) in a patient with placenta accreta. Note the presence of large placental lacunae (asterisk in A) and color Doppler showing extensive vascularity in B. Cervix and placenta are labeled.
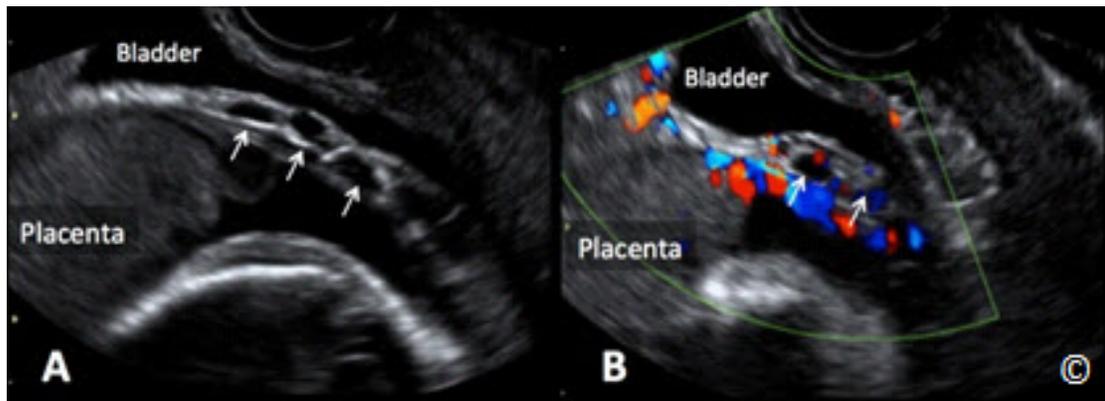

Figure 8.21 A and B: Transvaginal ultrasound in grey scale (A) and color Doppler (B) in a pregnancy with an anterior placenta accreta with abnormalities of the uterine serosa-bladder interface line. Note the presence of abnormal vascularity in the posterior wall of the bladder (A and B - arrows). Placenta and bladder are labeled.

Another important marker in the third trimester includes abnormality of the uterine serosa-bladder interface. This includes interruption of the line, thickening of the line, irregularity of the line, or increase line vascularity on a color Doppler (26, 27) (**Figure 8.21 A and B**). The normal uterine serosa-bladder interface is a thin line that is smooth with no irregularities or vascular signals. Other sonographic findings include extension of the villi into the myometrium, serosa, or bladder, retroplacental myometrial thickness of less than one millimeter, and turbulent blood flow through the lacunae on Doppler ultrasonography.

Overall, grey scale ultrasonography is a good tool for the prenatal diagnosis of placenta accreta in women at risk for this abnormality. Its sensitivity has been reported in the range of 77-87% with a specificity of 96-98%, a positive predictive value of 65-93% and a negative predictive value of 98%. It should be the primary tool for the diagnosis of placenta accreta and should be used exclusively in the great majority of cases. **Table 8.6** lists the diagnostic ultrasound findings in placenta accreta.

TABLE 8.6	Ultrasound Diagnostic Findings in Placenta Accreta

- Gestational sac implanted in the lower uterine segment
- Cesarean section scar implantation
- Multiple vascular lacunaes in the second trimester
- Loss of normal hypoechoic retroplacental zone
- Multiple vascular lacunaes in the third trimester
- Abnormality in uterine-serosa-bladder interface
- Retroplacental myometrial thickness of less than 1 millimeter
- Turbulent blood flow on color Doppler through the lacunae
- Extension of villi into myometrium, serosa or bladder

MRI FINDINGS IN PLACENTA ACCRETA

Although this represents an electronic book on obstetric and gynecologic ultrasound, we added this section on MRI findings in placenta accreta for completeness sake and to highlight the value of ultrasound as the primary modality for the diagnosis of placenta accreta. MRI findings that are suggestive of placenta accreta include the presence of uterine bulging, heterogeneous signal intensity within the placenta, dark intra-placental bands on T2-weighted images, abnormal placental vascularity, focal interruptions in the myometrial wall, tenting of the bladder, and direct visualization of the invasion of nearby organs (26, 28, 29). MRI should be reserved for cases in which ultrasound is non-diagnostic such as in obese patients with a posterior placenta. When ultrasound or MRI is used concomitantly on the same patients, the findings of the most aggressive diagnosis should be used in guiding management (30). The authors believe that transvaginal ultrasound is the optimum imaging modality for the assessment of placenta accreta and should be used exclusively in most cases.

COMPLICATIONS OF PLACENTA ACCRETA

Complications of placenta accreta are many and include damage to local organs, postoperative bleeding, amniotic fluid embolism, consumptive coagulopathy, transfusion-related complications, acute respiratory distress syndrome, postoperative thromboembolism, infectious morbidities, multi-system organ failure, and maternal death (31). Genital ureteral complications are common and include cystotomy in about 15% of cases and ureteral injury in about 2% of cases (16).

MANAGEMENT OF PLACENTA ACCRETA

Successful management of placenta accreta is dependent on its recognition prenatally and a planned delivery with the best available resources. When resources are limited such as in a low-resource (outreach) setting, the authors recommend the following management steps, which may help to optimize outcome of the mother and the newborn:

1) Ensure availability of blood ahead of scheduled surgery. The blood should be immediately available for transfusion in the operating room

2) Plan your surgery with a multidisciplinary team approach, even in low-resource settings. Ensure your best nursing team, anesthesiologist, surgeons and allied health care team are involved in the management of the patient.

3) Obtain consent for hysterectomy prior to initiating surgery.

4) Studies have shown that the optimum time for a planned delivery for a patient with placenta accreta is around 34-35 weeks following a course of corticosteroid injection (30). This optimizes outcome for the mother as 93% of patients with placenta accreta report hemorrhage after 35 weeks and this planned delivery has been shown to result in shorter operating room times, lower frequency of transfusions, and lower intensive care unit admission (31, 32). This decision needs to be balanced with the nursery capability in the low-resource settings as the risk-benefit analysis may shift based upon the newborn outcome.

5) Most favor general anesthesia as the anesthesia method of choice and preparation should include large bore intravenous access with central lines, compression stockings, padding and positioning to prevent nerve injury, and avoidance of hypothermia (33, 34).

6) Map the placental localization using ultrasound and plan the uterine incision to avoid entry through the placenta if possible. Use ultrasound intra-operatively directly on the uterus if needed. You can protect the abdominal probe with a sterile glove, use sterile gel on the uterus, (peritoneal fluid usually suffice), and scan the uterus directly to localize the placental upper edge and incise the uterus in such a way to avoid entry through the placenta. This will minimize bleeding while delivering the newborn and assessing for the next step.

7) If a decision is made to proceed with a hysterectomy, consider supra-cervical hysterectomy as an option. It requires less operative time and is associated with less bleeding. Proceed with cesarean hysterectomy while keeping the placenta attached. On occasions however, a supra-cervical hysterectomy may not control bleeding and a complete hysterectomy is needed.

8) Conservative management of placenta accreta has been reported. In a series reporting on conservative management of placenta accreta in 167 pregnancies where the placenta was left attached in the uterine cavity after delivery of the newborn, successful conservative management of such cases was achieved in 78 % with spontaneous resorption of the placenta in 75 % of pregnancies (35). Severe maternal morbidity was noted in 6 % of cases (35). This approach should be employed with caution and in select cases where the risk of the hysterectomy is deemed higher than conservative management, especially where resources such as blood replacement or expert pelvic surgery is limited. Note that consideration for broad-spectrum antibiotic coverage, and close follow-up should be considered if conservative management is chosen.

9) The use of compression sutures, such as the B-Lynch suture may be helpful in tamponading bleeding and has been used in cases of placenta accreta (36). The physicians caring for pregnancies with placenta accreta should familiarize themselves with these compression sutures prior to the cesarean delivery.

10) If blood is available and there is a need for massive transfusion of patients with placenta accreta when a hysterectomy is preformed, it is recommend that a balanced ratio (1 to 1 or 2 to 1) of packed red blood cells to fresh frozen plasma is achieved, as this approach has been shown to reduce morbidity and mortality. Careful monitoring of maternal electrolyte imbalance with massive transfusion should be undertaken.

The successful management of placenta accreta relies heavily on the prenatal diagnosis of this entity. It is thus critical to identify the at-risk pregnancy, recognize the diagnostic capabilities of ultrasound, and carefully prepare for the surgical management by ensuring that the most skilled multidisciplinary team is available. It is through this approach that the outcome is optimized for the mother and newborn.

PLACENTAL ABRUPTION

Placental abruption is defined by the presence of bleeding behind or within the placenta. The bleeding may track behind the membranes. The incidence of placental abruption is estimated around 0.5-1% (37), and the clinical presentation is that of painful bleeding with uterine contractions. Unlike placenta previa where the sensitivity for diagnosis by ultrasound is almost 100%, in placental abruption the sensitivity of ultrasound in visualizing hemorrhage is reported to be approximately 50% (38) and thus ultrasound cannot be relied upon for making such

diagnosis when patients are presenting with signs and symptoms suggestive of a placental abruption. Clinical judgment including history, physical exam, findings on the fetal monitor tracing (uterine contraction pattern) and laboratory evaluation should be relied upon primarily in making the diagnosis of abruption. Ultrasound assessment of the placenta is an adjunct test and may be helpful when a placental bleed is noted. A normal ultrasound examination does not rule-out a placental abruption.

Ultrasound findings in placental abruption will show a slightly hypoechoic mass either retroplacental or behind the membranes at the edge of the placenta that mimic an organized blood clot (**Figure 8.22**). Color Doppler will confirm the absence of capillary flow within the content of the blood clot on low velocity scale.
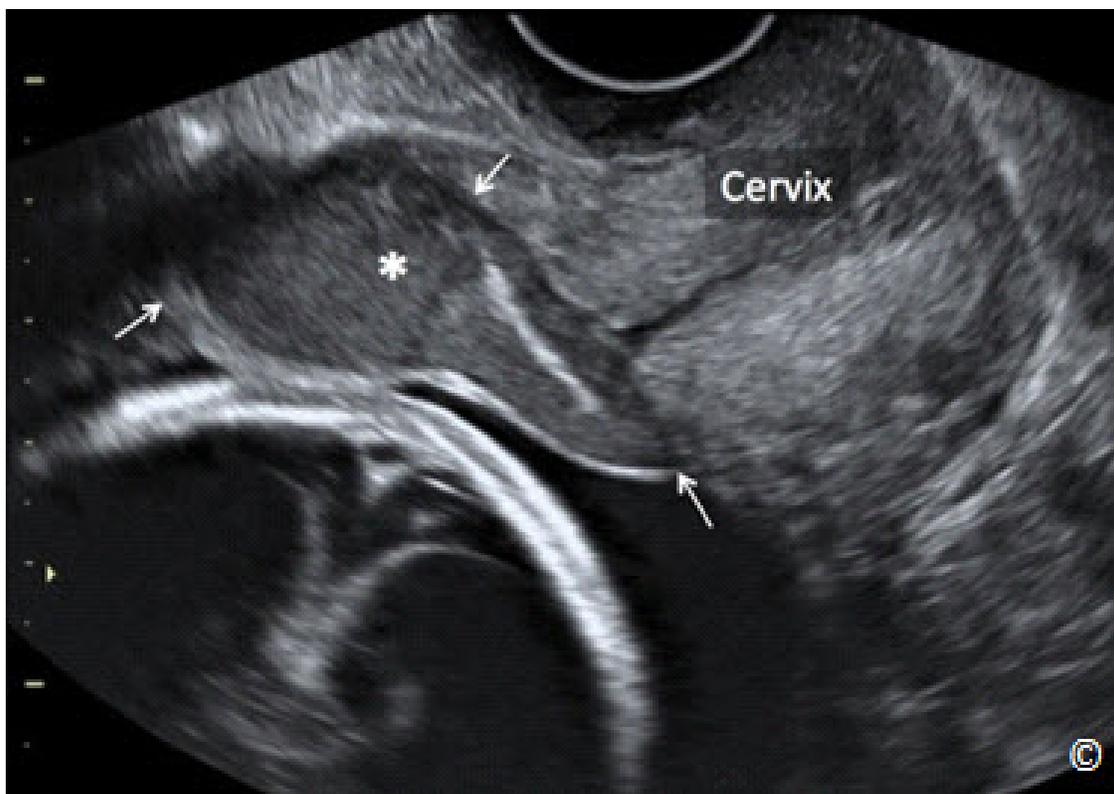
Figure 8.22: Transvaginal ultrasound of a pregnancy with a placental abruption. Note the presence of a blood clot (asterisk and arrows) behind the membranes and in front of cervix (labeled). Note that ultrasound can miss a placental abruption on many occasions – see text for details.

References:

1) Jaffe R, Jauniaux E, Hustin J: Maternal circulation in the first trimester human placenta – myth or reality? Am J Obstet Gynecol 176:695,1997.

2) Fox H: The development and structure of the placenta. In Fox H 9ed): Pathology of the Placenta, 2nd ed. London, WB Saunders Co. Ltd., 1997, pp1-41.

3) Tonsong T, Boonyanurak P: Placental thickness in the first half of pregnancy. J Clin Ultrasound 32:231, 2004.

4) Iyasu S, Saftlas AK, Rowley DL, Koonin LM, Lawson HW, Atrash HK. The epidemiology of placenta previa in the United States, 1979 through 1987. Am J Obstet Gynecol 93; 168:1424–9.

5) Ananth CV, Wilcox AJ, Savitz DA, Bowes WA Jr., Luther ER. Effect of maternal age and parity on the risk of uteroplacental bleeding disorders in pregnancy. Obstet Gynecol 1996;88:511–6.

6) Reddy UM, Abuhamad AZ, Levine D, Saade GR. Fetal Imaging Executive Summary of a Joint Eunice Kennedy Shriver National Institute of Child Health and Human Development, Society for Maternal-Fetal Medicine, American Institute of Ultrasound in Medicine, American College of Obstetricians and Gynecologists, American College of Radiology, Society for Pediatric Radiology, and Society of Radiologists in Ultrasound Fetal Imaging Workshop. J Ultrasound Med 2014; 33:745–757.

7) Timor-Tritsch IE, Yunis RA. Confirming the safety of transvaginal sonography in patients suspected of placenta previa. Obstet Gynecol 1993;81:742–4.

8) Oyelese KO, Turner M, Lees C, Campbell S. Vasa previa: an avoidable obstetric tragedy. Obstet Gynecol Surv 1999;54:138–45.

9) Francois K, Mayer S, Harris C, Perlow JH. Association of vasa previa at delivery with a history of second-trimester placenta previa. J Reprod Med 2003;48:771–4.

10) Miller, D., Chollet, J.A., Goodwin, T. M. (1997). Clinical risk factors for placenta previa–placenta accreta. *American Journal of Obstetrics and Gynecology, 177*(1): 210-214.

11) Wehrum, M.J., Buhimschi, I.A., Salafia, C., Thung, S. Bahtiyar, M.O., and Werner, E.F., et al. (2011). Accreta complicating complete placenta previa is characterized by reduced systemic levels of vascular endothelial growth factor and by epithelial-to-mesenchymal transition of the invasive trophoblast. *American Journal of Obstetrics and Gynecology, 204*(5): e1-411.

12) Tantbirojn, P., Crum, C. P., Parast, M. M. (2008). Pathophysiology of placenta accreta: the roll of deciduas and extravillous trophoblast. *Placenta, 29*(7): 639-45.

13) Strickland, S. Richards, W. G. (1992). Invasion of the trophoblast. *Cell, 71*: 355-7.

14) Belfort, M.A. (2010). Placenta accreta. *American Journal of Obstetrics and Gynecology, 203*(5): 430-9

15) Hull,A.D., Resnik, R. (2010). Placenta Accreta and Postpartum Hemorrhage. *Clinical Obstetrics and Gynecology, 53*(1): 228-36.

16) Silver, R. M., Landon, M. B., Rouse, D. J., Leveno, K. J., Spong, C. Y., Thom, E. A., et al. (2006). Maternal Morbidity Associated With Multiple Repeat Cesarean Deliveries. *Obstetrics & Gynecology, 107*(6): 1226-32.

17) Comstock, C.H., Wesley, L., Vettraino, I.M., Bronsteen, R.A. (2003). The Early Sonographic Appearance of Placenta Accreta. *The Journal of Ultrasound in Medicine, 22*(1): 19-23.

18) Berkley EM, Abuhamad AZ (2013). Prenatal diagnosis of placenta accreta: Is sonography all we need? *The Journal of Ultrasound in Medicine, 32*: 1345.

19) Comstock, C.H., Love, J.J., Bronsteen, R.A., Lee, W., Vettraino, I.M., Huang,R.R. (2004). Sonographic detection of placenta accreta in the second and third trimesters of pregnancy. *American Journal of Obstetrics and Gynecology, 190*(4): 1135-40.

20) Gielchinsky, Y., Mankuta, D., Rojansky, N. ,Laufer, N., Gielchinsky, I., Ezra, Y. (2004). Perinatal Outcome of Pregnancies Complicated by Placenta Accreta. *Obstetrics & Gynecology, 104*(3): 527-30.

21) Hudon, L., Belfort, M. A., Broome, D. R. (1998). Diagnosis and Management of Placenta Percreta: A Review. *Obstetrical & Gynecological Survey, 53*(8): 509-17.

22) Finberg, H.J., Williams, J.W. (1992). Placenta accreta: prospective sonographic diagnosis in patients with placenta previa and prior cesarean section. *Journal of Ultrasound in Medicine, 11*(7): 333-43.

23) Royal College of Obstetricians and Gynaecologists (RCOG), (2011). Placenta praevia, placenta praevia accreta and vasa praevia: diagnosis and management. *Royal College of Obstetricians and Gynaecologists (RCOG)*; 26. (Green-top guideline; no. 27).

24) Hull, A.D., Salerno, C.C., Saenz, C.C., Pretorius, D.H. (1999). Three-Dimensional Ultrasonography and Diagnosis of Placenta Percreta with Bladder Involvement. *Journal of Ultrasound in Medicine, 18*(12): 856-6.

25) Baughman, W.C., Corteville, J.E., Shah, R.R. (2008). Placenta Accreta: Spectrum of US and MR Imaging Findings. Radiographics, 28(7): 1905-16.

26) Comstock, C.H. (2005). Antenatal diagnosis of placenta accreta: a review. *Ultrasound in Obstetrics and Gynecology, 26*(1): 89-96.

27) Warshak, C. R., Eskander, R., Hull, A. D., Scioscia, A. L., Mattrey, R. F., Benirschke, K., et al. (2006). Accuracy of Ultrasonography and Magnetic Resonance Imaging in the Diagnosis of Placenta Accreta. *Obstetrics & Gynecology, 108*(3): 573-81.

28) Lax, A., Prince, M. R., Mennitt, K. W., Schweback, J. R., Budorick, N. E. (2007). The value of specific MRI features in the evaluation of suspected placental invasion. *Magnetic Resonance Imaging, 25*(1): 87-93.

29) Derman, A. Y., Nikac, V., Haberman, S., Zelenko, N., Opsha, O., Flyer, M. (2011). MRI of Placenta Accreta: A New Imaging Perspective. *American Journal of Roentgenology, 197*(6): 1514-21.

30) McLean, L. A., Heilbrun, M. E., Eller, A. G., Kennedy, A. M., Woodward, P. J. (2011). Assessing the Role of Magnetic Resonance Imaging in the Management of Gravid Patients at Risk for Placenta Accreta. *Academic Radiology, 18*(9): 1175-80.

31) O'Brien, J. M., Barton, J. R., Donaldson, E. S. (1996). The management of placenta percreta: Conservative and operative strategies. *American Journal of Obstetrics and Gynecology, 175*(6): 1632-8.

32) Robinson BK and Grobman WA (2010). Effectiveness of timing strategies for delivery of individuals with placenta previa and accrete. *Obstetrics & Gynecology 116;835-42*

33) Practice Guidelines for Obstetric Anesthesia (2007). *Anesthesiology, 106*(4): 843-63.

34) Kuczkowski, K. M. (2006). Anesthesia for the repeat cesarean section in the parturient with abnormal placentation: What does an obstetrician need to know? *Archives of Gynecology and Obstetrics, 273*(6): 319-21.

35) Sentilhes L, Ambroselli C, Kayem G, et al (2010). Maternal outcome after conservative treatment of placenta accrete. *Obstetrics & Gynecology 115;526-34*.

36) El-Hamamy E, Wright A, B-Lynch. The B-Lynch suture technique for postpartum hemorrhage: a decade of experience and outcome. J Obstet Gynaecol. 2009 May;29(4):278-83.

37) Abu-Heija A, al-Chalabi H, el-Iloubani N: Abruptio placentae: risk factors and perinatal outcome. J Obstet Gynaecol Res 24:141, 1998.

38) Sholl JS: Abruptio placentae; clinical management in nonacute cases. Am J Obstet Gynecol 156:40, 1987.

INTRODUCTION

The primary source of amniotic fluid in the second and third trimester of pregnancy is fetal urine. The source of amniotic fluid in the first trimester of pregnancy however, is still poorly understood. Studies using dye installation tests in the amniotic cavity have shown that amniotic fluid volume increase throughout gestation until about 39-40 weeks (1, 2).

Assessment of amniotic fluid volume is an essential part of the basic obstetric ultrasound examination. The two techniques that are most commonly proposed for the estimation of amniotic fluid include assessment of the single maximal vertical pocket of fluid or the amniotic fluid index. The single maximal vertical pocket (MVP) technique involves finding the single largest pocket of amniotic fluid on ultrasound, free of cord and fetal parts, and then measuring the greatest vertical dimension with the ultrasound transducer perpendicular to the floor (**Figures 9.1** and **9.2**). The amniotic fluid index (AFI) technique is based on the division of the uterus into 4 equal quadrants and measuring the deepest vertical pocket of fluid in each quadrant (same technique as for MVP) and then adding the four measurements together (**Figure 9.3**) (3, 4). Most sonologists and sonographers measure the MVP and AFI in amniotic fluid pockets that are at least 1 cm in width and free of cord and fetal parts.

Figure 9.1: Transducer orientation for the measurement of amniotic fluid. Note that the transducer is in sagittal orientation on the maternal abdomen and is maintained perpendicular to the floor while scanning.
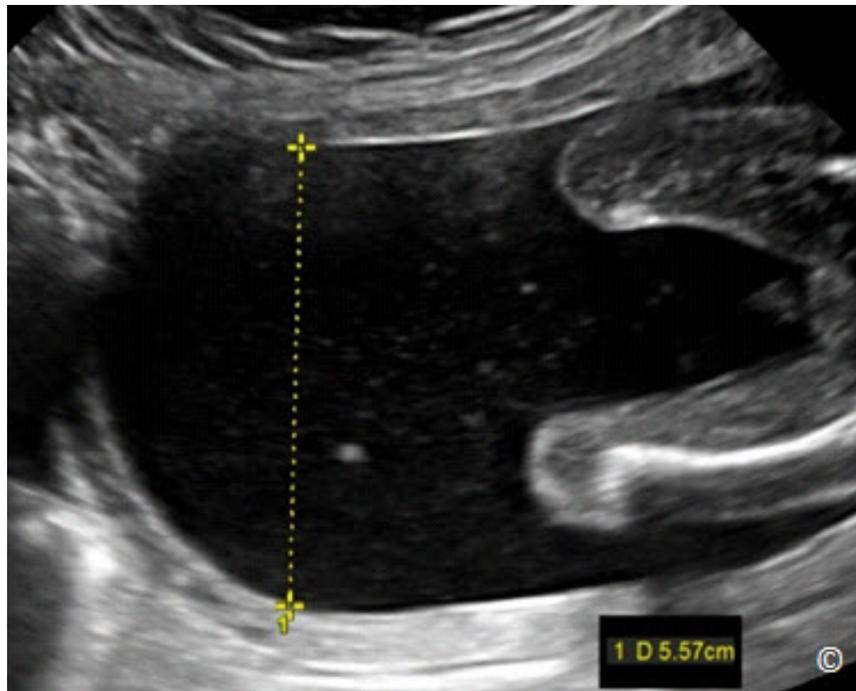
Figure 9.2: Maximal vertical pocket measurement of amniotic fluid. The quadrant in the uterus with most amniotic fluid is chosen and the deepest portion of that pocket is measured in a vertical line measurement (normal here at 5.5 cm). Note that the pocket is free of cord and fetal parts and is at least 1 cm in width.
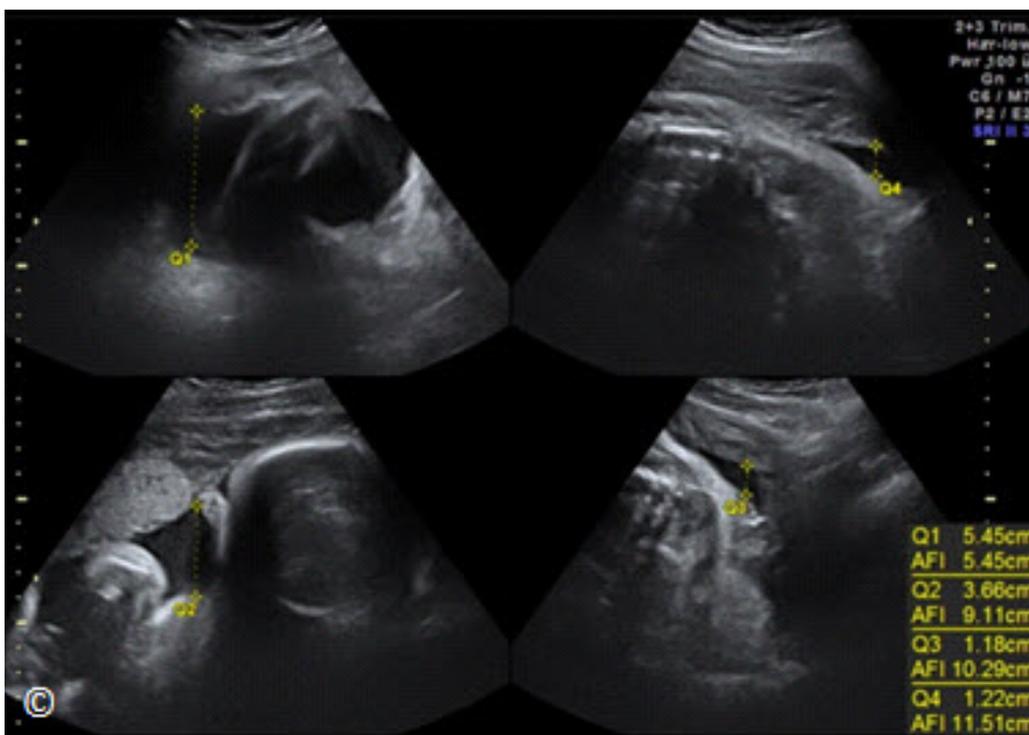
Figure 9.3: Measurement of amniotic fluid using the Amniotic Fluid Index (AFI) technique in a pregnancy with normal fluid. Note the measurements in four quadrants (Q) of the uterine cavity. AFI is determined by adding the four-quadrant measurements (normal range at 11.5 cm). See text for details.

OLIGOHYDRAMNIOS

The term oligohydramnios refers to decreased amniotic fluid volume relative to gestational age. **Table 9.1** lists the common causes of oligohydramnios. Oligohydramnios is described by a MVP of less than 2 cm (**Figure 9.4**), or an AFI of less than 5 cm. When no measurable pocket of amniotic fluid is noted in the uterine cavity, the term anhydramnios is used (**Figure 9.5**). Oligohydramnios has been linked to increased perinatal morbidity and mortality (5, 6). A corresponding corrected perinatal mortality rates of 109.4/1000, 37.74/1000 and 1.97/1000 were reported for MVP of < 1 cm, MVP between 1 - 2 cm, and MVP > 2 cm and < 8 cm respectively (6).

| TABLE 9.1	Common Causes of Oligohydramnios
	- Premature rupture of membranes - Genitourinary abnormalities - Uteroplacental insufficiency - Postdates pregnancies
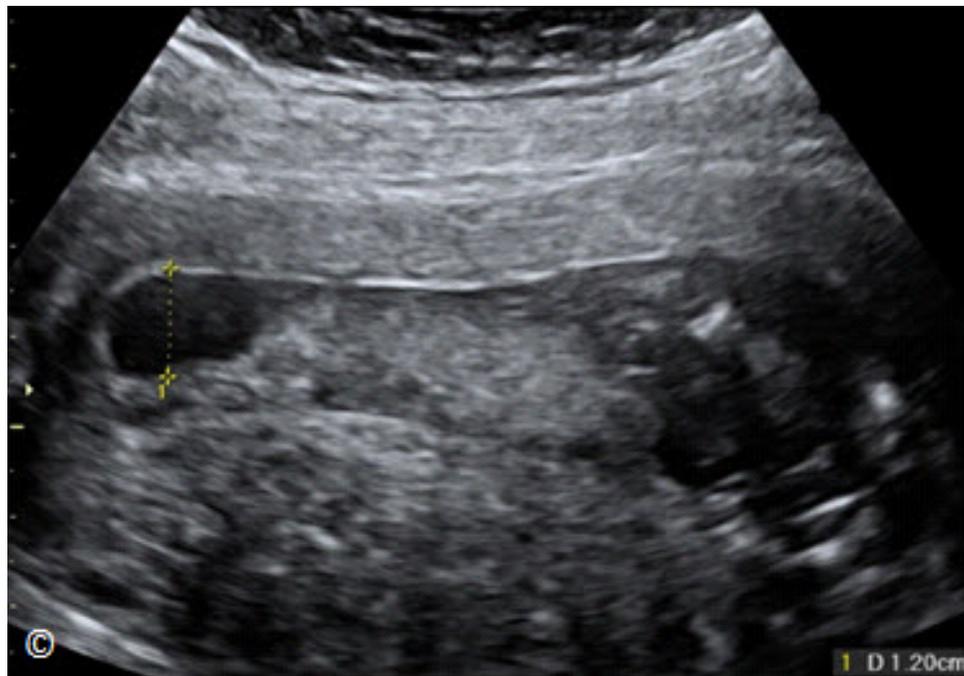
Figure 9.4: Oligohydramnios diagnosed by the Maximal Vertical Pocket (MVP) method. Note that the MVP measured 1.2 cm in this pregnancy.
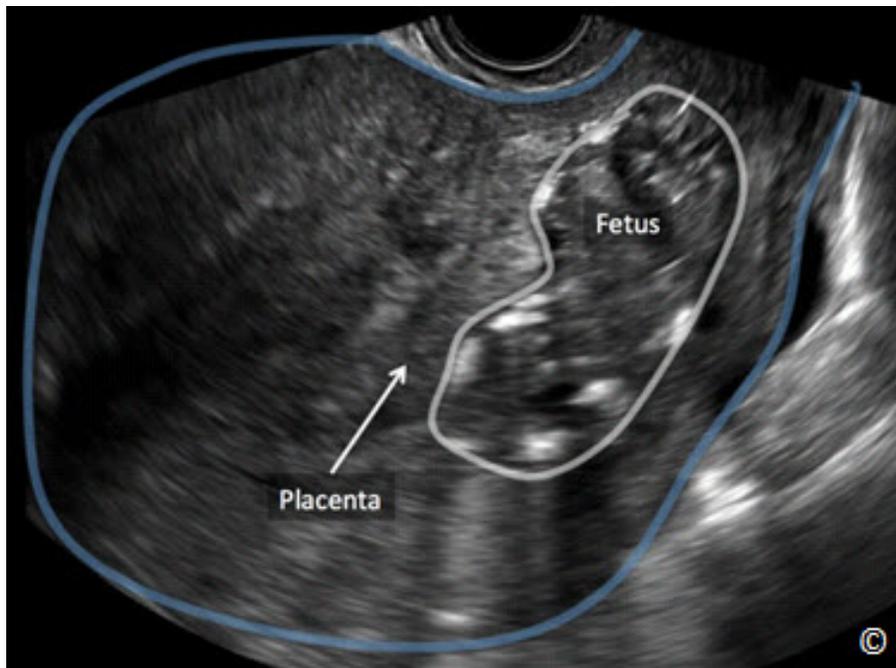
Figure 9.5: Anhydramnios in a fetus with bilateral renal agenesis. Note the total absence of amniotic fluid resulting in suboptimal ultrasound visualization. The white line is drawn around the fetus and the blue line is drawn around the uterus. The placenta is labeled.

The two described methods for the diagnosis of oligohydramnios, namely the MVP and AFI were compared in a Cochrane review (7). Five randomized trials with over 3000 pregnancies were analyzed. The AFI cut-off of oligohydramnios of < 5 cm was associated with more cases of diagnosed oligohydramnios (RR = 2.39), more induction of labor (RR = 1.92) and more emergent cesarean deliveries (RR = 1.46), with no effect on perinatal morbidity, including admission to the neonatal intensive care unit (7). Furthermore, assisted vaginal deliveries and the overall rate of cesarean deliveries were not different whether MVP or AFI was used (7). Given an increased in pregnancy intervention with no demonstrable perinatal benefit when oligohydramnios is defined by the AFI < 5 cm method, the authors of the Cochrane review and others have suggested that the MVP method is preferred over the AFI for amniotic fluid assessment in fetal surveillance (7, 8).

POLYHYDRAMNIOS

The term polyhydramnios refers to increased amniotic fluid volume relative to gestational age. **Table 9.2** lists the common causes of polyhydramnios. Polyhydramnios is defined by a MVP of equal to or greater than 8 cm (**Figure 9.6**), or an AFI equal to or greater than 24 cm (**Figure 9.7**). Idiopathic polyhydramnios, which occurs in 50 – 60 % of cases of polyhydramnios, has been

linked to fetal macrosomia and an increase in adverse pregnancy outcome (9). Polyhydramnios has also been associated with increased perinatal morbidity and mortality (10, 11).

TABLE 9.2	Common Causes of Polyhydramnios
- Gestational and pregestational diabetes - Isoimmunization - Fetal structural and chromosomal abnormalities - Fetal infections - Multiple pregnancies with Twin-Twin Transfusion Syndrome - Idiopathic	
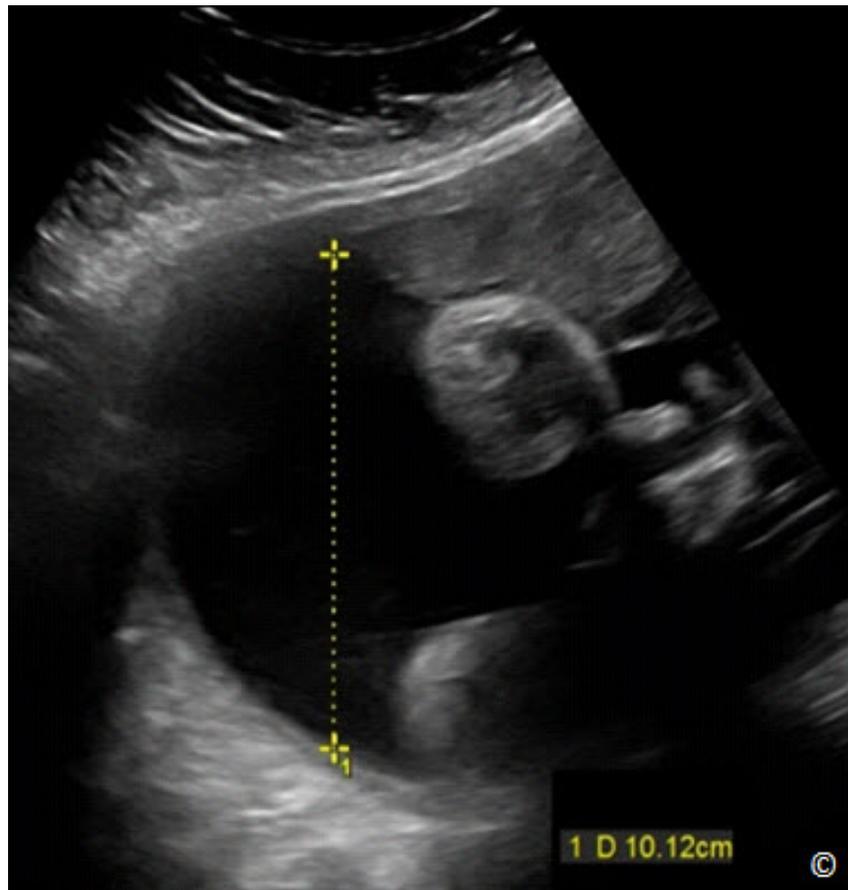
Figure 9.6: Polyhydramnios diagnosed by the Maximal Vertical Pocket (MVP) method. Note that the MVP measured 10.1 cm in this pregnancy.
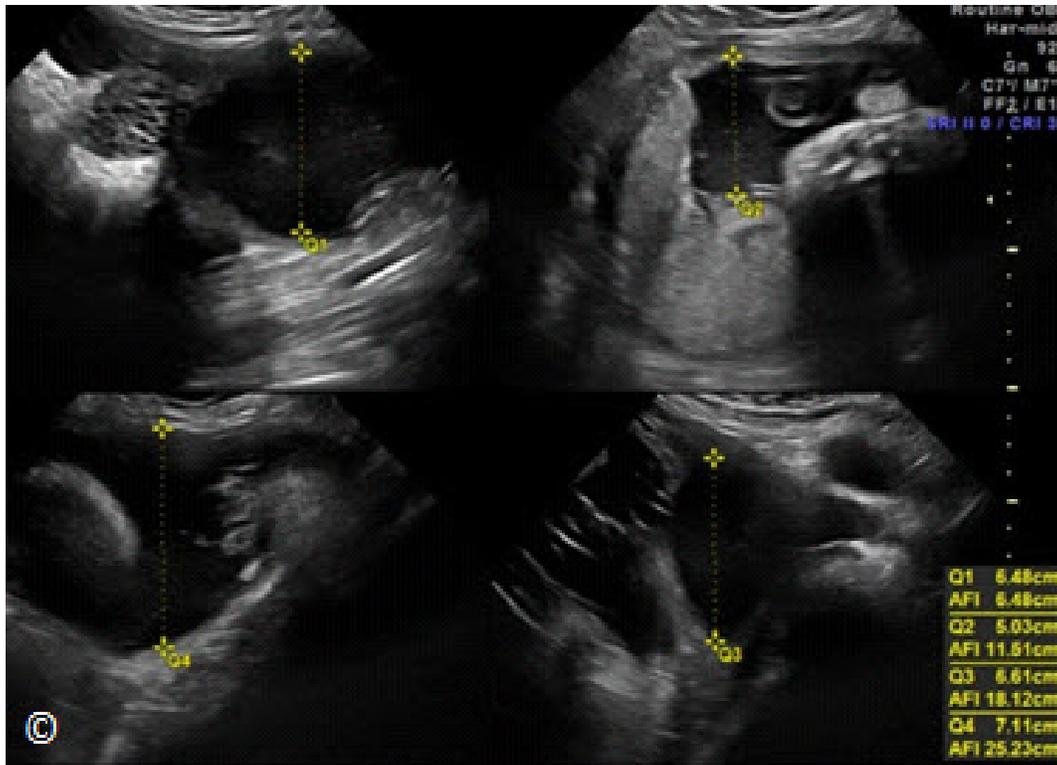
Figure 9.7: Polyhydramnios diagnosed by the Amniotic Fluid Index (AFI) method. Note that the AFI measured 25.2 cm in this pregnancy.

Given its simplicity, the authors recommend the MVP method for assessment of amniotic fluid. The choice of MVP for amniotic fluid assessment was also supported by a recent multi-society fetal imaging consensus workshop (12).

ULTRASOUND ESTIMATION OF AMNIOTIC VOLUME IN TWIN GESTATIONS

Both the MVP and AFI have been used to assess amniotic fluid volume in twin gestations (13). The AFI requires an understanding of the spatial relationship of the gestational sacs in order to allow for each twin's amniotic compartment to be divided into four quadrants. Given the technical difficulty involved in this process, especially in the third trimester when fetal crowding is common, the authors recommend the use of MVP of each twin's amniotic fluid compartment to assess the fluid volume (**Figure 9.8**). The MVP in the amniotic sac of each twin appears to remain relatively stable between 17 and 37 weeks' gestation, with a 2.5[th] percentile and 97.5[th] percentile at 2.3 and 7.6 cm, respectively (14). This data supports the use of cut-offs of 2 cm and 8 cm to define oligohydramnios and polyhydramnios in twin gestation respectively and these limits have been used in the diagnosis of twin-twin transfusion syndrome in monochorionic pregnancies (15).
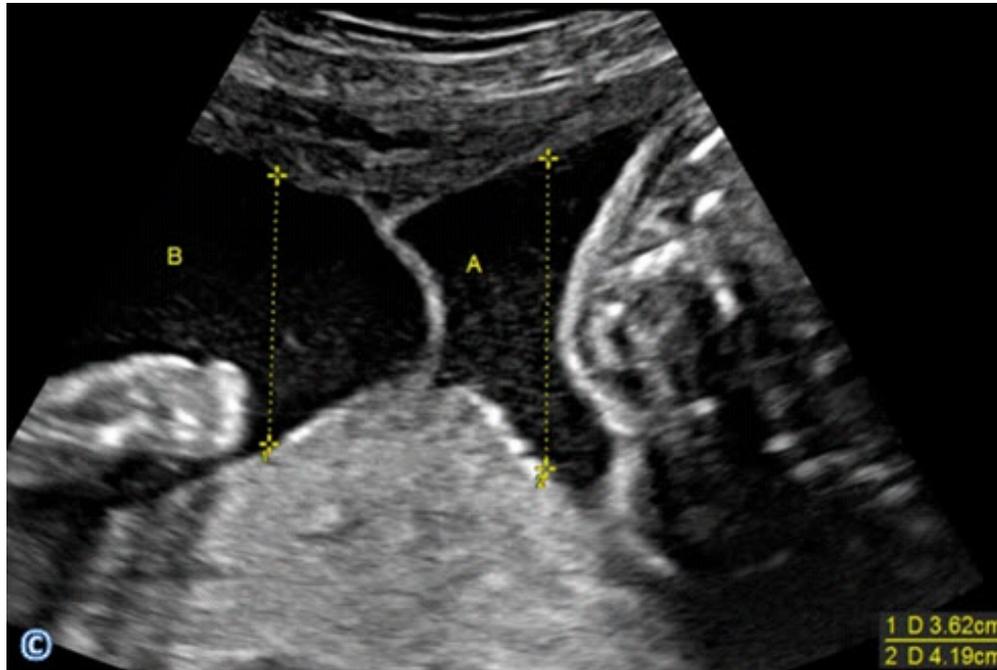
Figure 9.8: Amniotic fluid assessment in twin gestation using the Maximal Vertical Pocket (MVP) measurement in each gestational sac. Note that the MVP measured 4.1 cm in sac A and 3.6 cm in sac B.

References:

1) Magann EF, Bass JD, Chauhan SP, et al. Amniotic fluid volume in normal singleton pregnancies. Obstet Gynecol 1997;90:524-8.
2) Brace RA, Wolf EJ. Normal amniotic fluid volume changes throughout pregnancy. Am J Obstet Gynecol 1989;161:382-8.
3) Phelan JP, Ahn MO, Smith CV, et al. Amniotic fluid index measurements during pregnancy. J Reprod Med 1987;32:601-4.
4) Moore TR, Cayle JE. The amniotic fluid index in normal human pregnancy. Am J Obstet Gynecol 1990;162:1168-73.
5) Manning FA, Platt LD, Sipos L. Antepartum fetal evaluation: development of a fetal biophysical profile. Am J Obstet Gynecol 1980;136:787-95.
6) Scoring. IV. An analysis of perinatal morbidity and mortality. Am J Obstet Gynecol 1990;162:703-9.
7) The Cochrane Collaboration. Amniotic fluid index versus single deepest vertical pocket as a screening test for preventing adverse pregnancy outcome. 2009; Issue 3, pp 1 – 31)

8) Chauhan S, Doherty D, Magann E, Cahanding F, et al. Amniotic fluid index vs. single deepest pocket technique during modified biophysical profile: A randomized clinical trial. Am J Obstet Gynecol 2004;191:661-8.

9) Magann E, Chaudan S, Doherty D, Lutgendorf M, et al. A review of idiopathic hydramnios and pregnancy outcomes. Obstet Gynecol Surv. 2007 Dec;62(12):795-802.

10) Chamberlain PF, Manning FA, Morrison I, et al. Ultrasound evaluation of amniotic fluid volume. II. The relationship of increased amniotic fluid volume to perinatal outcome. Am J Obstet Gynecol 1984;150:250-4.

11) Pri-Paz S, Khalek N, Fuchs KM, et al. Maximal amniotic fluid index as a prognostic factor in pregnancies complicated by polyhydramnios. Ultrasound Obstet Gynecol 2012;39:648-53.

12) Reddy UM, Abuhamad AZ, Levine D, Saade GR. Fetal Imaging Executive Summary of a Joint Eunice Kennedy Shriver National Institute of Child Health and Human Development, Society for Maternal-Fetal Medicine, American Institute of Ultrasound in Medicine, American College of Obstetricians and Gynecologists, American College of Radiology, Society for Pediatric Radiology, and Society of Radiologists in Ultrasound Fetal Imaging Workshop. J Ultrasound Med 2014; 33:745–757.

13) Hill LM, Krohn M, Lazebnik N, et al. The amniotic fluid index in normal twin pregnancies. Am J Obstet Gynecol 2000;182:950-4.

14) Magann EF, Doherty DA, Ennen CS, et al. The ultrasound estimation of amniotic fluid volume in diamniotic twin pregnancies and prediction of peripartum outcomes. Am J Obstet Gynecol 2007;196:570 e1-6; discussion e6-8.

15) Quintero RA, Morales WJ, Allen MH, et al. Staging of twin-twin transfusion syndrome. J Perinatol 1999;19:550-5.

INTRODUCTION

We recommend a stepwise approach to the basic obstetric ultrasound examination in the second and third trimester of pregnancy, which applies a structured and standardized method of ultrasound examination that is simple to learn and is geared towards the identification of major findings, which have direct impact on the wellbeing of the mother and fetus. This stepwise approach includes six steps, which we believe should be part of the basic ultrasound examination in the second and third trimester of pregnancy. These six steps are designed to assess fetal presentation and lie, the presence of fetal cardiac activity, the number of fetuses within the uterus, the adequacy of the amniotic fluid, the localization of the placenta and pregnancy dating/estimation of fetal weight (**Table 10.1**). The term basic obstetric ultrasound has been used by various national and international organizations to define an ultrasound examination; the components of which include a review of fetal anatomy. The six steps described in this chapter are designed to identify risk factors in pregnancy, which require planning for prenatal care and delivery in a facility that is equipped and staffed to deal with these findings. **This approach is primarily intended for the low-resource (outreach) setting as the six steps described hereby are relatively easy to learn, do not require sophisticated equipment and can identify the "high-risk" pregnancy.** The inclusion of basic fetal anatomy is a step that requires more expertise and is generally not warranted in the initial introduction of ultrasound in the outreach settings, given the lack of resources to care for fetuses with major congenital malformations. This however does not preclude adding a step for major fetal malformations by ultrasound when the facility is capable of caring for neonates with these findings.

This chapter describes the sonographic approach that should be employed for each of the six steps of the basic ultrasound examination in the second and third trimester of pregnancy. Images and video clips are used to describe and illustrate each step.

TABLE 10.1	Stepwise Standardized Approach to the Basic Obstetric Ultrasound Examination in the Second and Third Trimester of Pregnancy
	- Fetal lie and presentation - Fetal cardiac activity - Number of fetuses in the uterus - Adequacy of amniotic fluid - Localization of the placenta - Fetal biometry

STEP ONE: FETAL LIE AND PRESENTATION IN THE UTERUS

The lie of the fetus in the uterus is defined by the orientation of the fetal spine to the maternal spine. A longitudinal lie is defined when the fetal spine is in parallel orientation to the maternal spine. A transverse lie is defined when the fetal spine is in a transverse orientation to the maternal spine, and an oblique fetal lie is defined when the fetal spine is in an oblique orientation to the maternal spine. Determining the lie of the fetus by ultrasound therefore requires obtaining a mid-sagittal plane of the fetal spine (**Figure 10.1**), which is a technically difficult plane to acquire for the novice ultrasound examiner. We therefore recommend that the fetal lie be inferred from determining the fetal presentation. If the fetal presentation is cephalic or breech, a technically easy step to determine by ultrasound, then a longitudinal fetal lie can be inferred. If neither a cephalic nor a breech presentation is noted in the lower uterine segment on ultrasound, an oblique or a transverse fetal lie should then be suspected and an attempt for a confirmation of such should be done by obtaining a mid-sagittal plane of the fetal spine (**Figure 10.1**) and assessing the orientation of the fetal spine to the maternal spine.
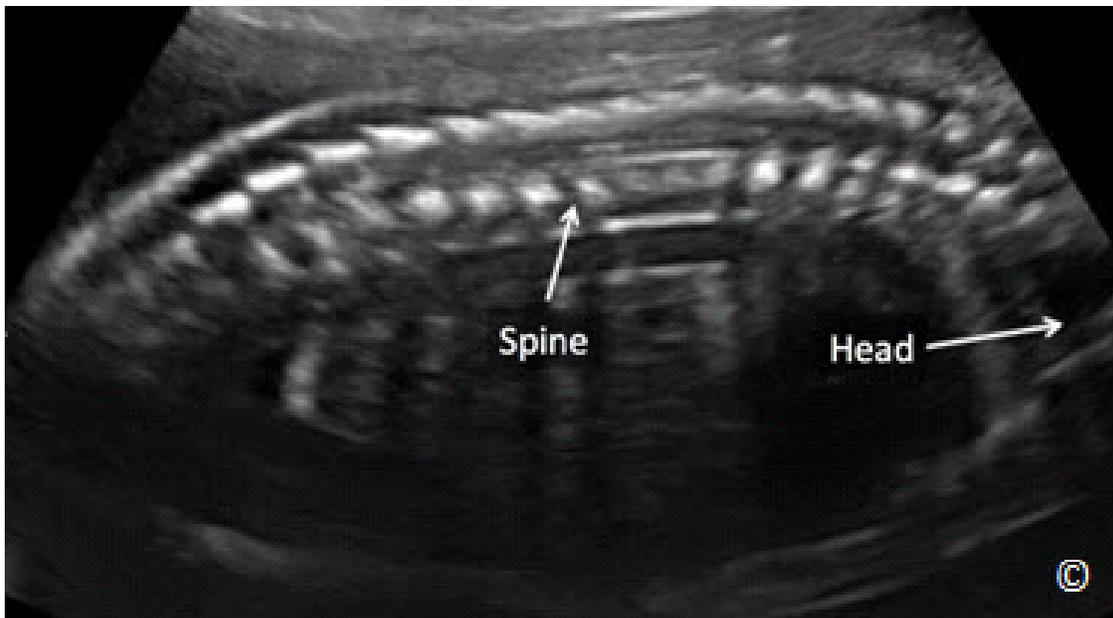
Figure 10.1: Mid-Sagittal view of the fetal spine (labeled) by ultrasound in the late second trimester of pregnancy. This plane is used to determine fetal lie in the uterus. The location of the fetal head is noted for orientation purposes. See text for details.

Step One-Technical Aspect of Determining Fetal Presentation in the Uterus

Place the transducer transversely in the lower abdomen just above the symphysis pubis as shown in **Figures 10.2** and **10.3**, and angle inferiorly towards the cervix as shown in **Clip 10.1**. The

presence of a fetal head on the ultrasound monitor confirms a cephalic presentation (**Figure 10.4**) and the presence of fetal buttocks confirms a breech presentation (**Figure 10.5**). Note that the presence of either a cephalic or a breech presentation implies a longitudinal lie of the fetus. If neither cephalic nor breech fetal parts are seen in the lower uterine segment on step one (**Figure 10.6**), further evaluation is needed to assess for an abnormal fetal lie. Note that the presence of a placenta previa is commonly associated with abnormal fetal presentation and lie.

Figure 10.2: Initial transducer placement for determining fetal presentation (step 1). Note the placement transversely in the lower abdomen just above the symphysis pubis. Uterine fundus is labeled. This picture is taken from the patient's left side.

Figure 10.3: Initial transducer placement for determining fetal presentation (step 1). Note the placement transversely in the lower abdomen just above the symphysis pubis. This represents the same transducer placement as in **Figure 10.2**, imaged from a different angle. Uterine fundus is labeled
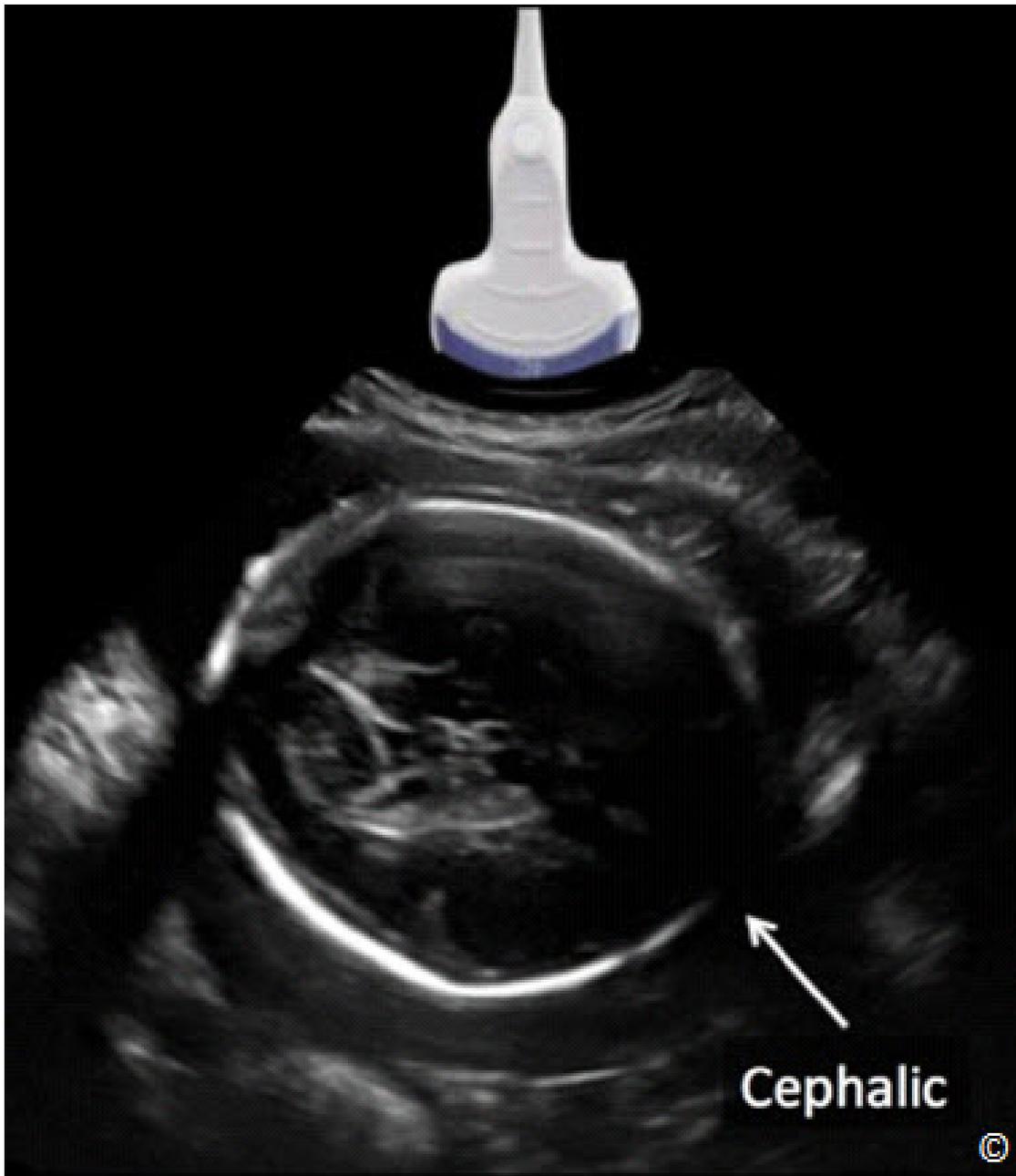
Figure 10.4: Step 1: determining fetal presentation. Note the transverse orientation of the transducer. This figure shows a cephalic presentation. See text for details.
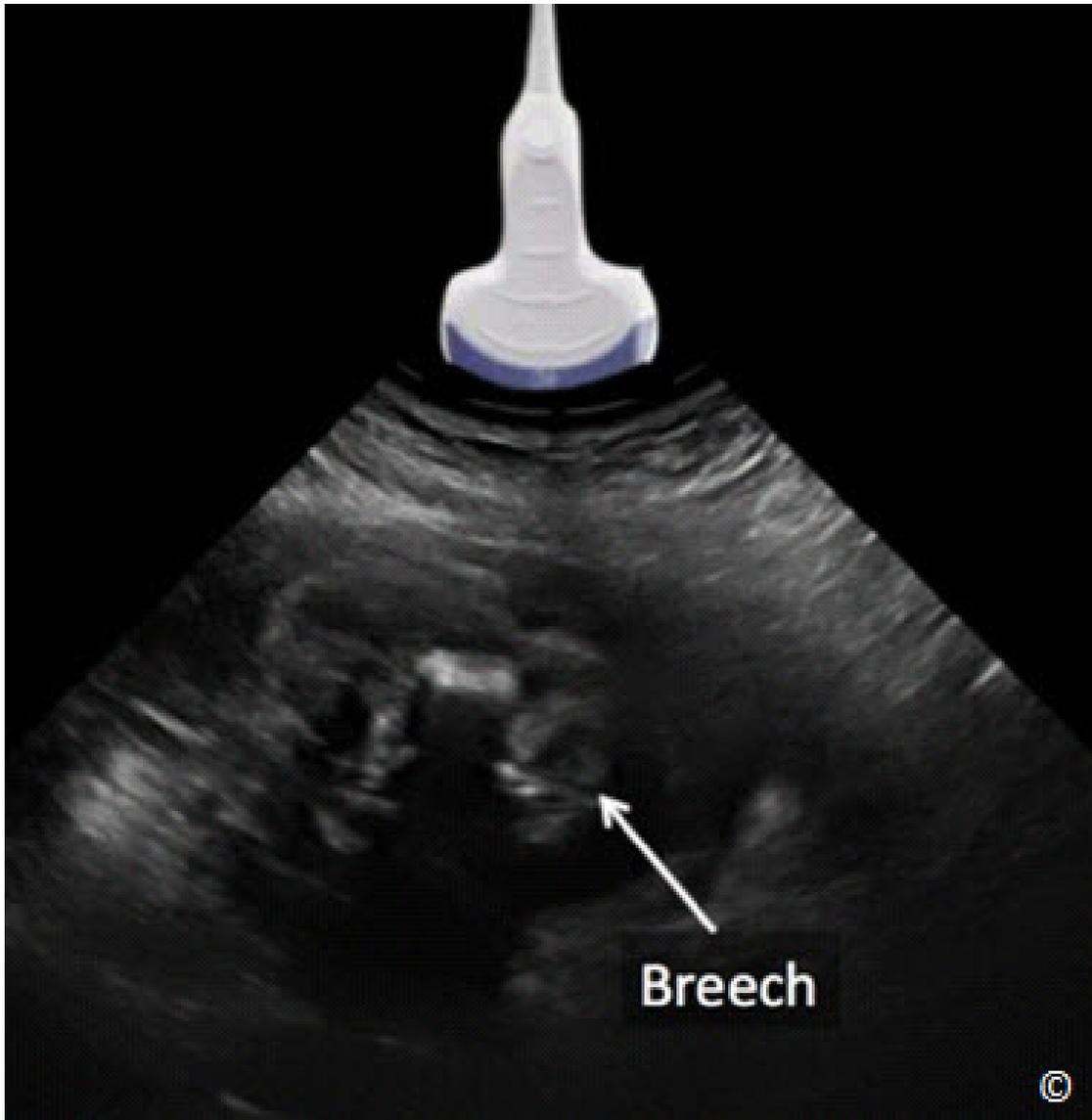
Figure 10.5: Step 1: determining fetal presentation. Note the transverse orientation of the transducer. This figure shows a breech presentation. See text for details.
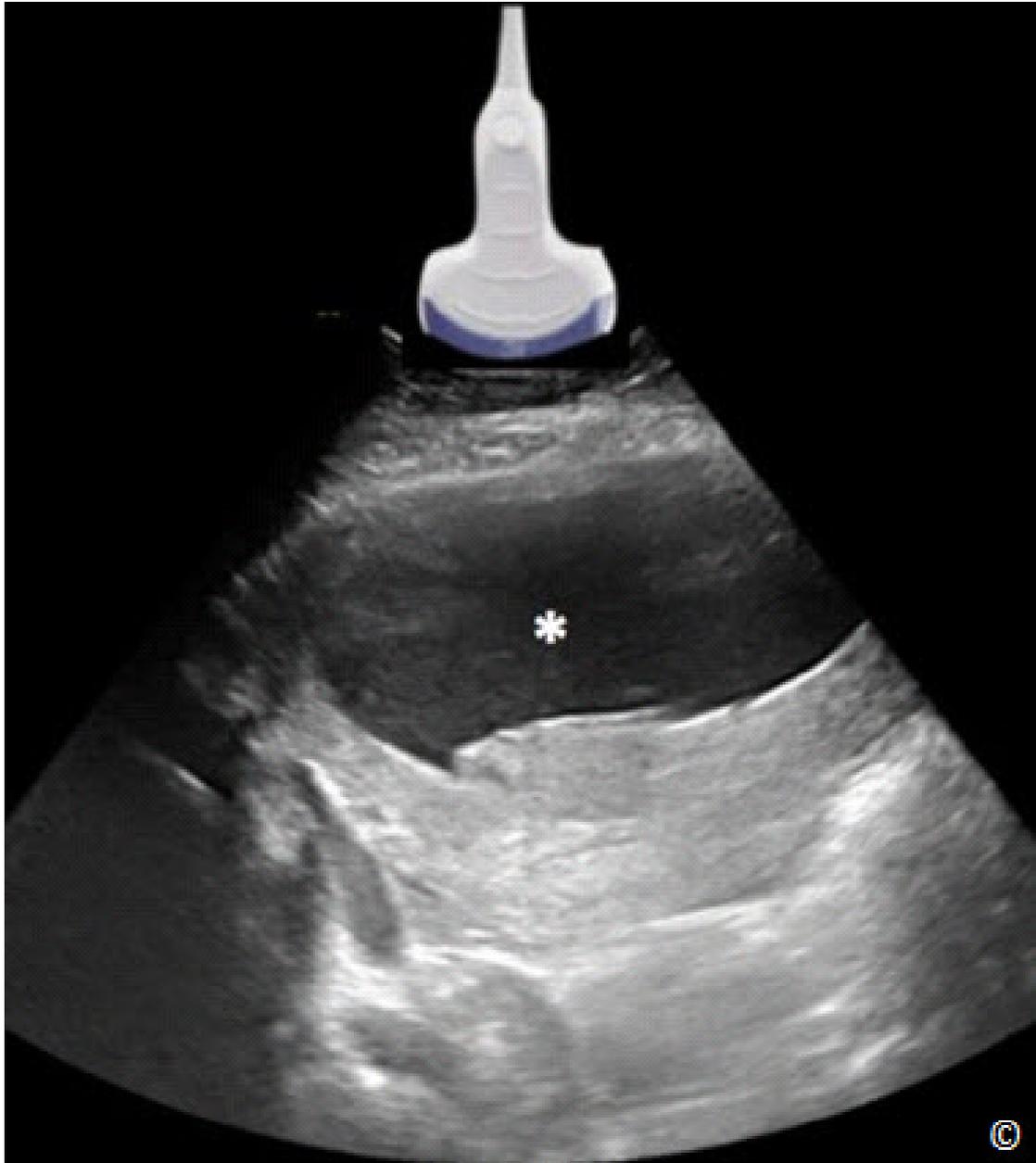
Figure 10.6: Step 1: determining fetal presentation. Note the transverse orientation of the transducer. This figure infers the presence of a transverse or oblique fetal lie given that no fetal presenting parts (asterisk) are noted. See text for details.

STEP TWO: FETAL CARDIAC ACTIVITY

Confirming fetal viability by noting the presence of fetal cardiac activity should be an essential component of the obstetric ultrasound examination and performed in the early steps of the examination. In the second and third trimester of pregnancy, this is easily accomplished by the visualization of the movements of the heart on ultrasound. Color Doppler, if available on the ultrasound equipment, can help in identifying the moving heart but is not an essential part of this step, as the heart motion can be easily imaged on real-time grey scale ultrasound. Documentation of fetal cardiac activity can be performed by saving a movie (cine-loop) clip of the moving heart on the hard drive of the ultrasound equipment or by using M-Mode. M-Mode, which stands for Motion mode, is an application that is available on most ultrasound equipment. When M-Mode is activated, a line appears on the ultrasound screen, which detects any motion along its path and can be moved by the track ball. By placing the M-Mode line across the cardiac chambers, motion of the cardiac chambers can thus be documented and a still image reflecting cardiac activity can be printed (**Figure 10.7**) and stored for documentation. See chapters 1 and 2 for more details.
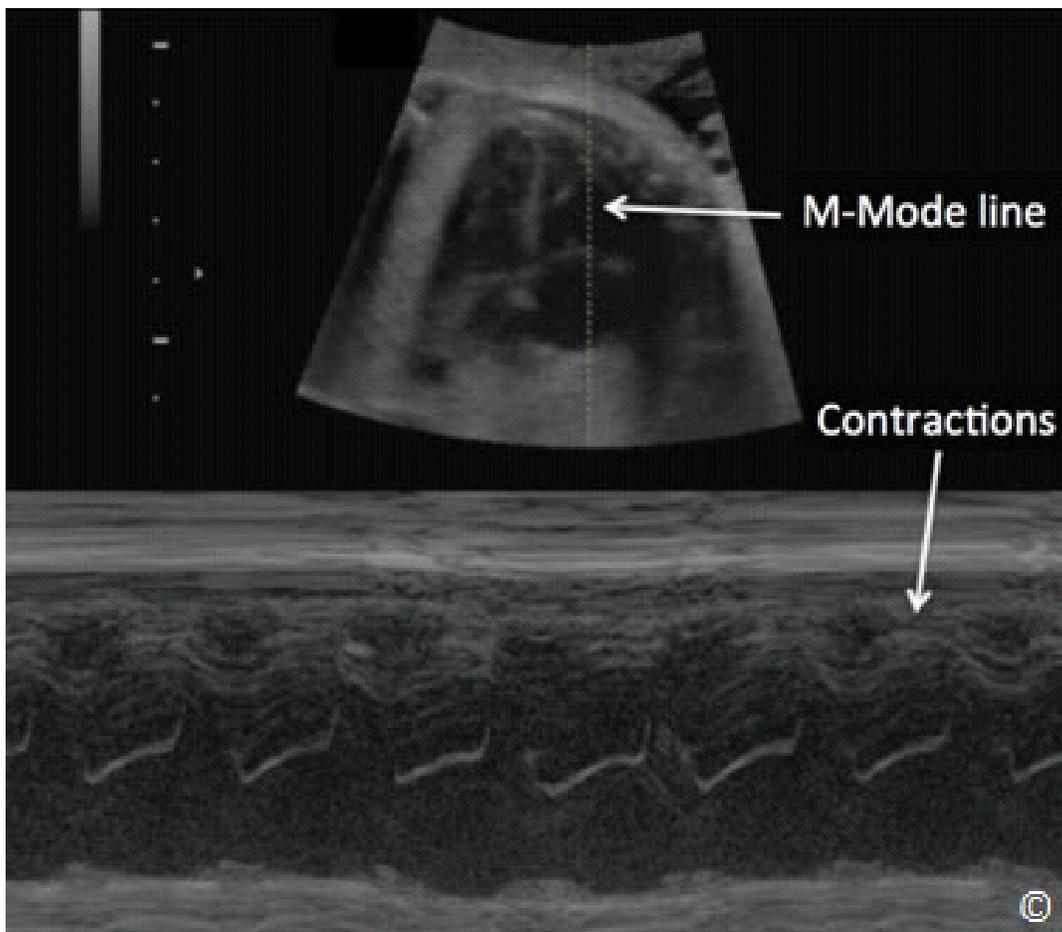
Figure 10.7: M-Mode documenting fetal cardiac activity in the second trimester of pregnancy. Note the M-Mode line (labeled) intersecting the cardiac chambers and note the presence of cardiac chamber contractions (labeled) in the tracing section. See text for details. Chapters 1 and 2 provide more information on M-Mode.

STEP TWO - TECHNICAL ASPECT OF DETERMINING FETAL CARDIAC ACTIVITY

Place the transducer transversely in the lower abdomen just above the symphysis pubis as shown in **Figures 10.1** and **10.2**, and slide superiorly in the mid-abdomen towards the umbilicus while maintaining the transverse orientation of the ultrasound transducer as shown in **Clip 10-2**. Fetal cardiac activity can be seen along the path of the transducer in the majority of ultrasound examinations. If fetal cardiac activity is not seen following the steps outlined here, slide the ultrasound transducer from the mid-abdomen to the right and/or the left lateral abdomen while maintaining the transverse orientation as shown in **Clip 10.3**. These steps show cardiac activity when present, in almost all fetal presentations.

STEP THREE-NUMBER OF FETUSES IN THE UTERUS

One of the most important benefits of ultrasound in obstetrics is in its ability to identify the presence of twins or higher order multiple pregnancy. Twin pregnancy is associated with an increased risk of preterm delivery, preeclampsia, abnormal labor and growth restriction (see chapter 7). By identifying twin pregnancy prenatally, pregnancy surveillance can be initiated and planning for delivery can be optimized which may significantly minimize the risk for pregnancy complications.

The diagnosis of a twin pregnancy in the second and third trimester is commonly first suspected when 2 fetal heads are seen in the uterine cavity during the ultrasound examination. Confirming the presence of twins is thus dependent on the identification of 2 separate fetal bodies within one uterus. A dividing membrane is seen when twin pregnancy is of the dichorionic-diamniotic or dichorionic-monoamniotic twin type. When two fetal heads are seen on ultrasound within the uterine cavity, the presence of a dividing membrane confirms the presence of a multiple pregnancy (**Figure 10.8**).
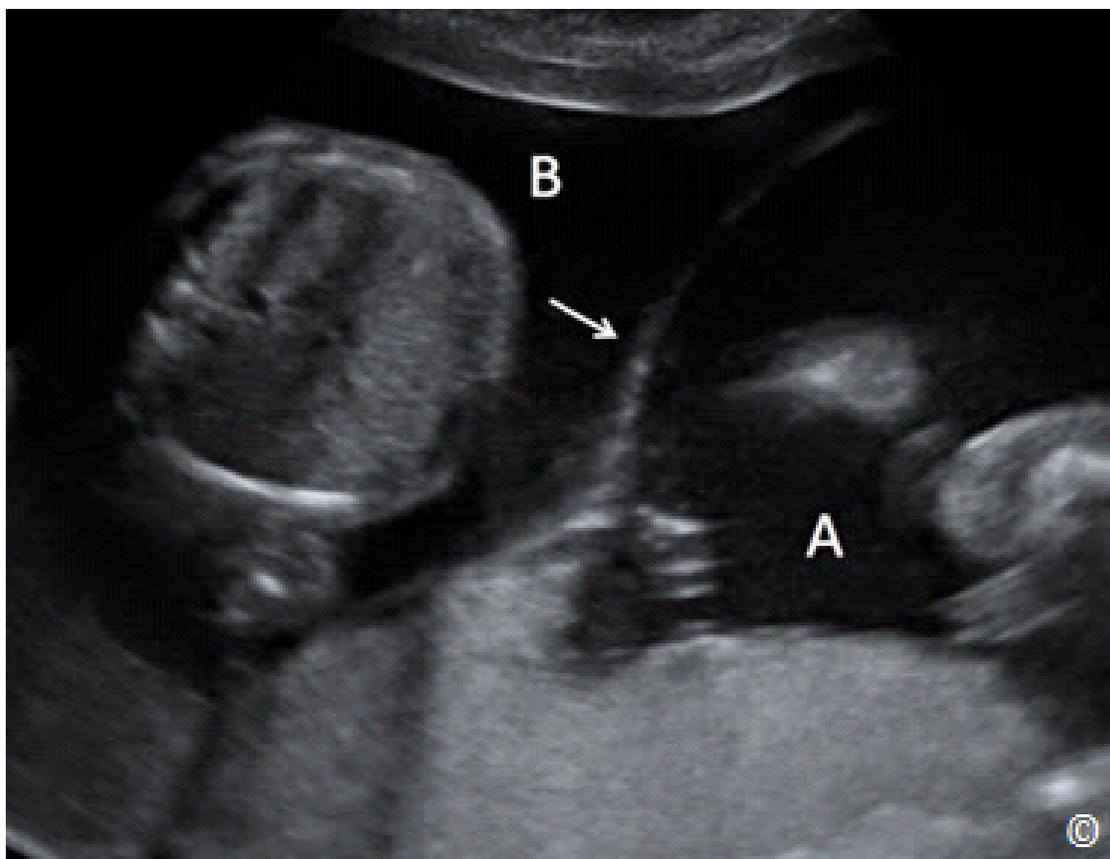
Figure 10.8: Transabdominal ultrasound of a twin pregnancy showing a thick dividing membrane (arrow) confirming the presence of twins. A and B denote the locations of gestational sacs for twin A and twin B respectively.

Step Three-Technical Aspect of Identifying the Number of Fetuses in the Uterus

The technical aspect of identifying the number of fetuses within a uterus is dependent upon mapping the entire uterine cavity by ultrasound in a systematic and standardized way, looking for the number of fetal heads (crania) within the uterus. If more than one fetal head is identified, confirmation of the presence of twins should then be performed. Mapping the uterus by ultrasound involves scanning the uterus in its entirety both in a longitudinal and transverse approach.

Technique for mapping the uterine cavity by ultrasound, searching for 2 fetal heads, involves imaging the uterine cavity from a transverse (part 1) and sagittal (part 2) orientations as follows: start by placing the transducer in a transverse orientation in the right lower abdomen as shown in **Figure 10.9** and slide the transducer superiorly towards the upper right abdomen while maintaining the transverse orientation (**Figure 10.10** and **Clip 10.4**). Repeat these steps in the mid and left abdomen in similar fashion as the right abdomen (**Figure 10.10** and **Clip 10.4**).

Place the transducer in a sagittal orientation in the right upper abdomen as shown in **Figure 10.11** and slide the transducer towards the left upper abdomen while maintaining the sagittal orientation as shown in **Figure 10.12** and **Clip 10.5**. Repeat these steps in the lower abdomen in similar fashion to the upper abdomen as shown in **Figure 10.12** and **Clip 10.5**. Look for the presence of more than one fetal head, which indicates the presence of a multiple pregnancy. When a false diagnosis of twins is made by ultrasound, a common source of error involves imaging a single fetal head from multiple angles. This error occurs when the ultrasound transducer is oblique and not maintained in a perpendicular orientation to the abdomen (floor) as shown in **Figures 10.9** to **10.12**. It is therefore important to maintain the ultrasound transducer in a perpendicular orientation to the floor while performing this technique. When the presence of a second fetus is suspected, provide confirmation of twin pregnancy by the identification of two separate bodies and a dividing membrane when present. Imaging both fetal heads or bodies in a single image when feasible, is proof of a twin pregnancy.

Figure 10.9: Initial transverse transducer placement for determining number of fetuses in uterine cavity (step 3-part 1). Note the transverse placement in the right lower abdomen. Uterine fundus is labeled.
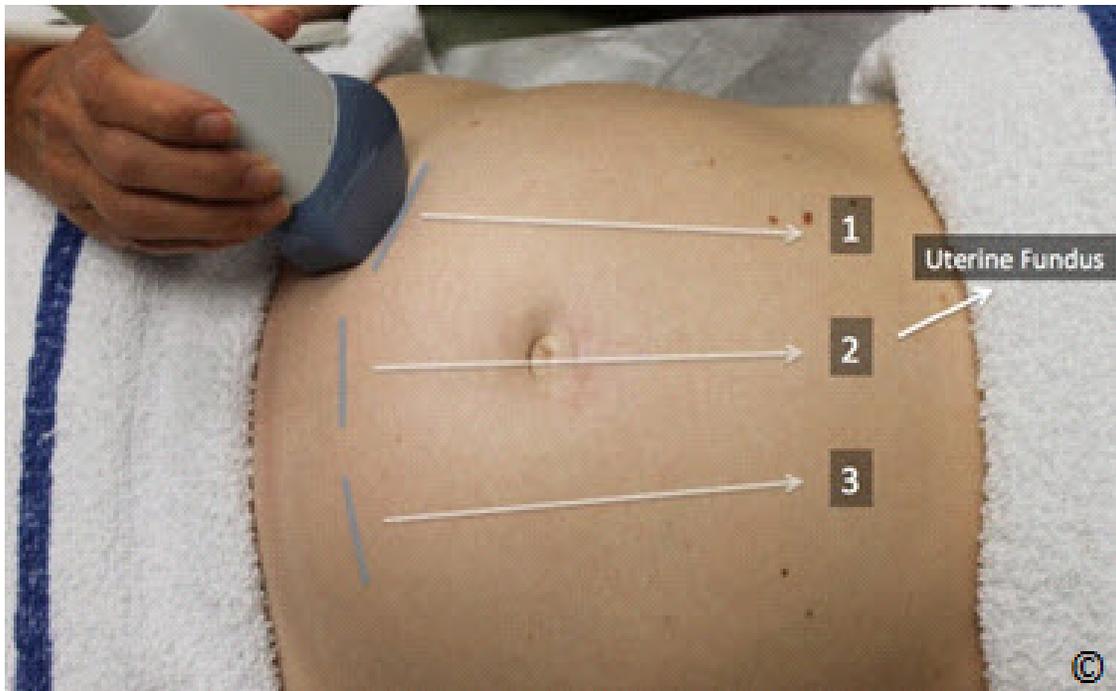
Figure 10.10: Transverse transducer movement for determining number of fetuses in uterine cavity (step 3- part 1). Note that the uterine cavity is scanned inferiorly to superiorly along tracks 1, 2 and 3, while maintaining the perpendicular orientation of the transducer to the floor. Uterine fundus is labeled.
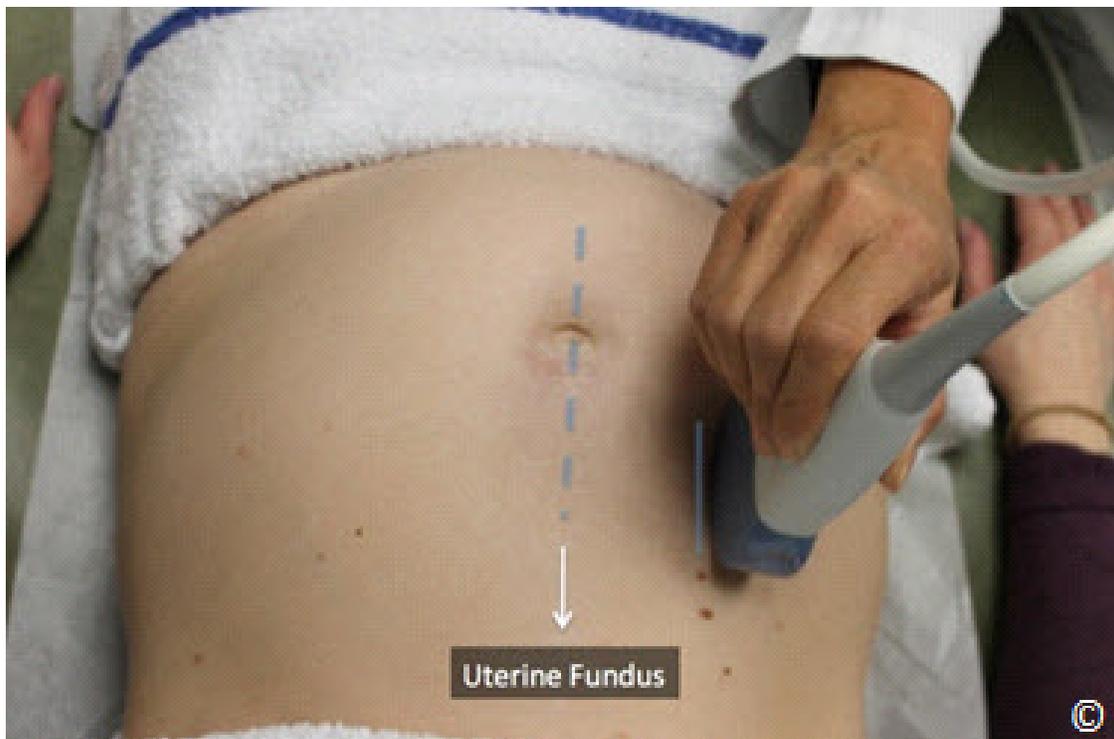
Figure 10.11: Initial sagittal transducer placement for determining number of fetuses in uterine cavity (step 3-part 2). Note the sagittal placement in the right upper abdomen and the perpendicular orientation of the transducer to the floor. Uterine fundus is labeled.
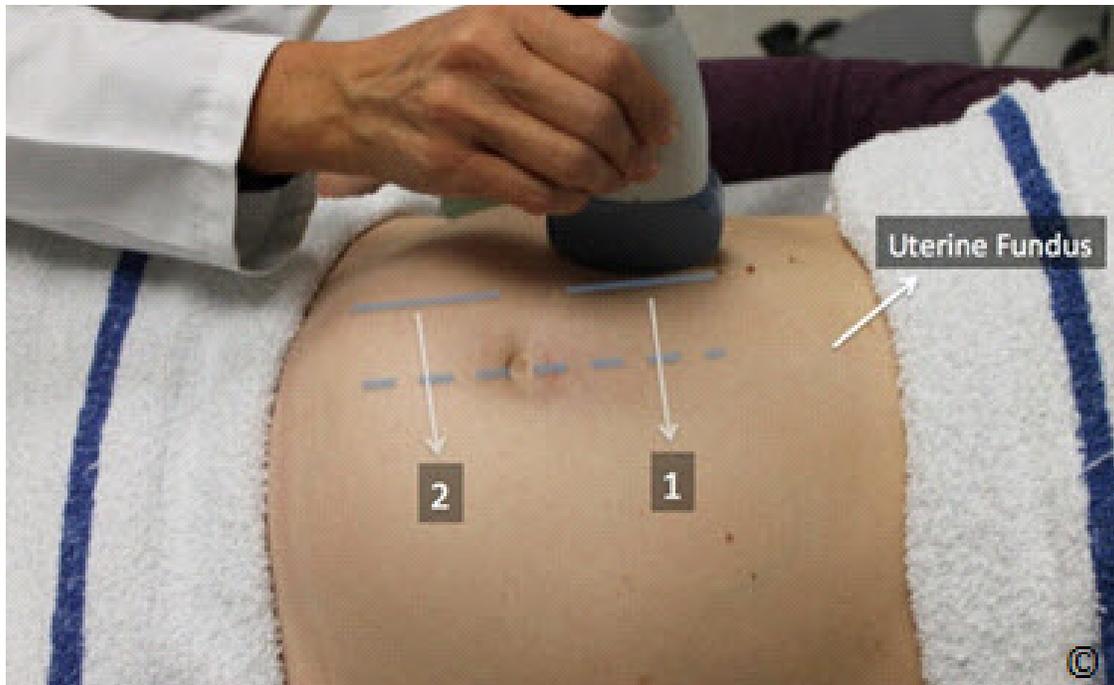
Figure 10.12: Sagittal transducer movement for determining number of fetuses in uterine cavity (step 3-part 2). Note that the uterine cavity is scanned from right to left along tracks 1 and 2 while maintaining the transducer perpendicular to the floor. Uterine fundus is labeled.

## Step Four: Placental Localization in the Uterus

The presence of abnormal placental implantation such as placenta previa increases the risk of maternal hemorrhage before, during and after delivery. Ultrasound is the most optimal imaging modality for the diagnosis of placental abnormalities and the diagnosis of placenta previa by ultrasound is one of the most important benefits of incorporating ultrasound in prenatal care. Detailed description of placenta previa and its associated pregnancy complications are outlined in chapter 8. This section deals with the technical aspect of placental localization by ultrasound.

Step Four-Technical Aspect of Placental Localization in the Uterus

Place the transducer in the sagittal orientation in the right upper abdomen, just above the uterine fundus and scan longitudinally towards the lower right abdomen as shown in (**Figure 10.13**). Repeat the same steps in the mid and left abdomen as shown in (**Figure 10.13** and **Clip 10.6**). It is important to start at the fundus of the uterus and ensure that you see the fundal contour of the uterus at the beginning of this step in order not to miss a fundal placenta. Look for the placenta on ultrasound and determine its location on the uterine wall. The placenta can be located in the fundal, anterior, posterior, right lateral, or left lateral uterine walls (**Figures 10.14 – 10.18** respectively). When the placenta is on the posterior uterine wall, shadowing may occur from the

fetus especially in the third trimester, which makes placental imaging suboptimal. This can be overcome by placing the transducer on the lateral aspect of the abdomen as shown in **Figures 10.19** and **10.20**. The lower placental edge should be assessed and its relationship to the lower uterine segment and the cervix should be evaluated and documented. If the lower placental edge is noted to be in the lower uterine segment (**Figure 10.21**) and suspected to be close to or covering the cervix, a transvaginal ultrasound is recommended in order to confirm the presence or absence of placenta previa. The diagnosis of a placenta previa is best performed by the transvaginal ultrasound approach.
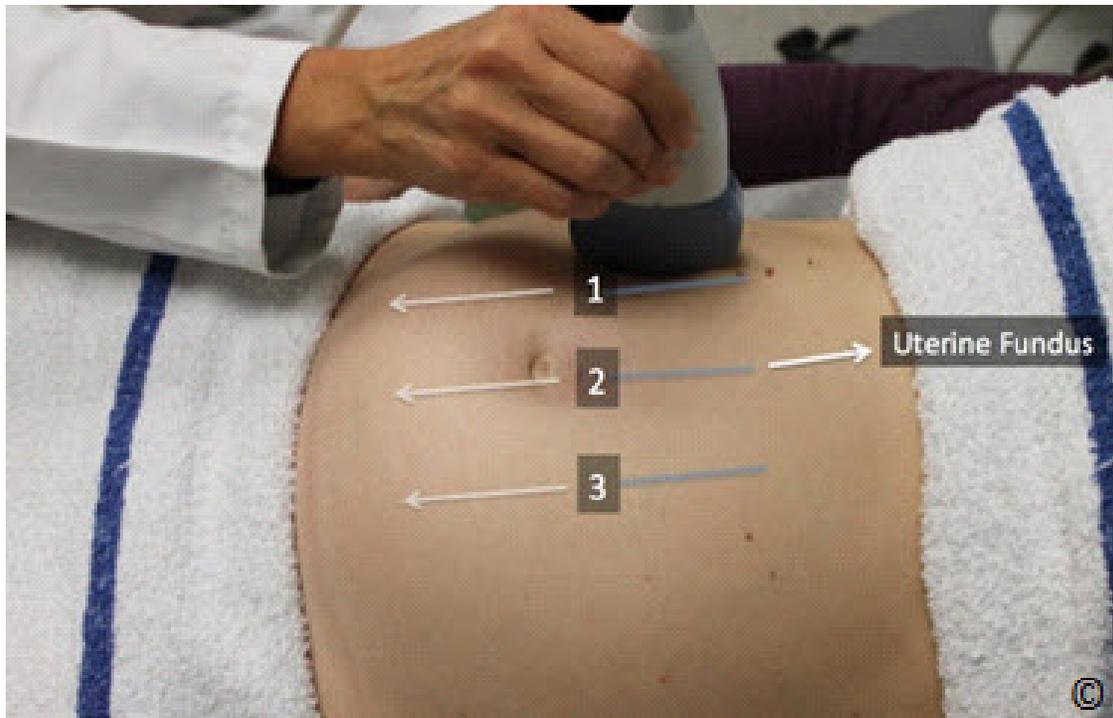
Figure 10.13: Sagittal transducer movement for determining placental localization (step 4). Note that the uterine cavity is scanned from superior (fundal region) to inferior along tracks 1, 2 and 3 while maintaining the transducer perpendicular to the floor. Uterine fundus is labeled.
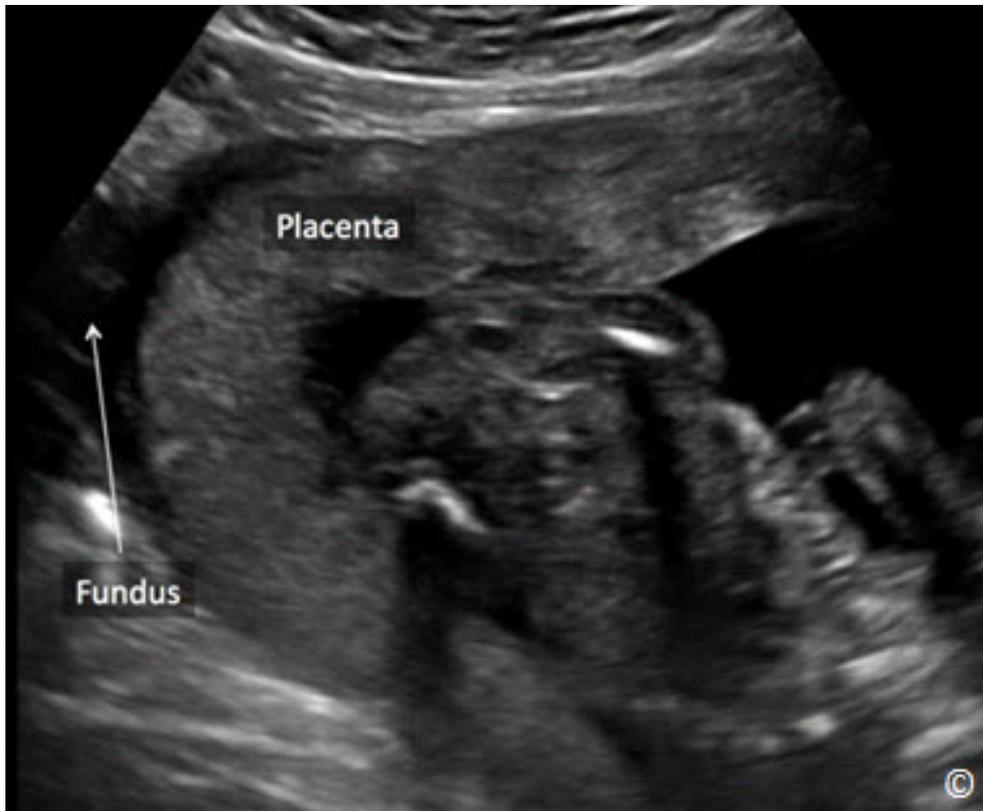
Figure 10.14: Fundal placenta (labeled) shown on ultrasound obtained from a sagittal view of the uterus. The uterine fundus is labeled. See text for details.
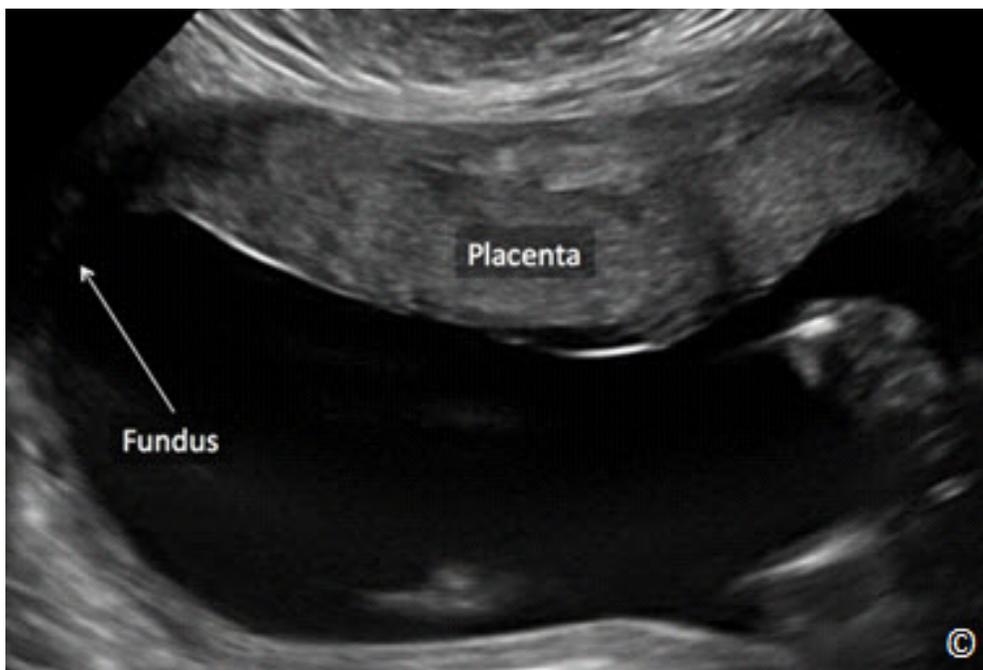
Figure 10.15: Anterior placenta (labeled) shown on ultrasound obtained from a sagittal view of the uterus. The uterine fundus is labeled. See text for details.
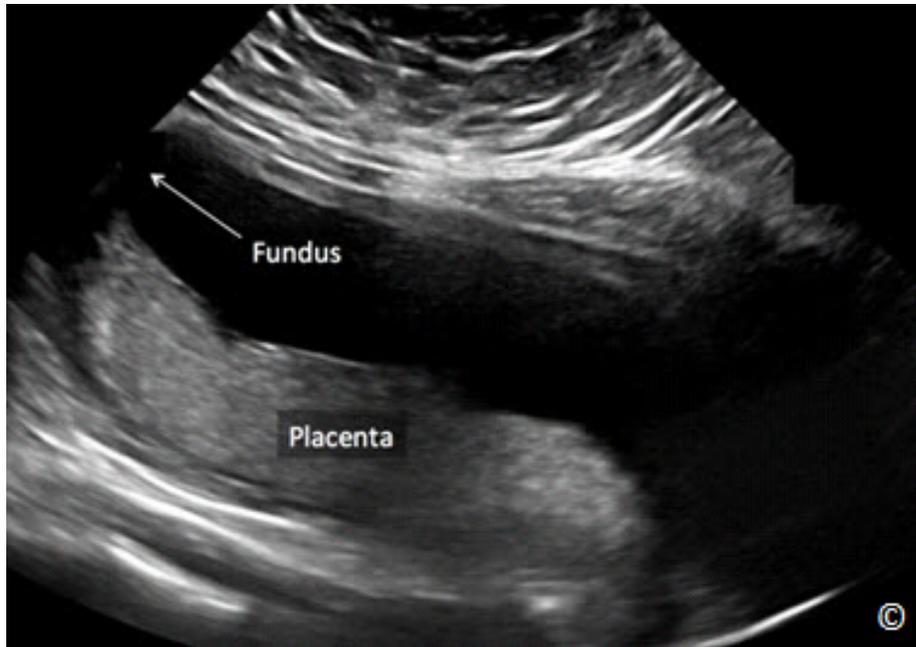
Figure 10.16: Posterior placenta (labeled) shown on ultrasound obtained from a sagittal view of the uterus. The uterine fundus is labeled. See text for details.
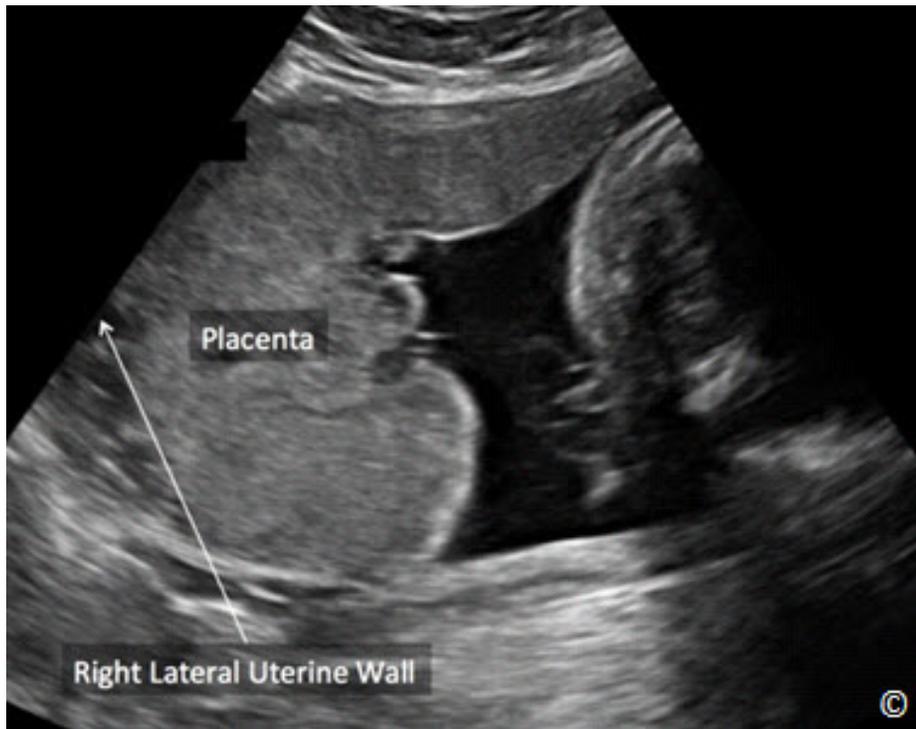
Figure 10.17: Right lateral placenta (labeled) shown on ultrasound obtained from a sagittal view of the uterus. Right lateral uterine wall is labeled. See text for details.

Figure 10.18: Left lateral placenta (labeled) shown on ultrasound obtained from a sagittal view of the uterus. Left lateral uterine wall is labeled. See text for details.

Figure 10.19: Ultrasound imaging of the uterus from the lateral aspect of the abdomen for placental localization in the third trimester when fetal shadowing obstructs view and the placenta is on the posterior uterine wall. The uterine fundus is labeled.

Figure 10.20: Ultrasound imaging of the uterus from the lateral aspect of the abdomen for placental localization in the third trimester when fetal shadowing obstructs view and the placenta is on the posterior uterine wall. Note the orientation of the transducer, almost lateral to the floor. This represents the same transducer placement as in figure 10.19, imaged from a different angle. The uterine fundus is labeled.
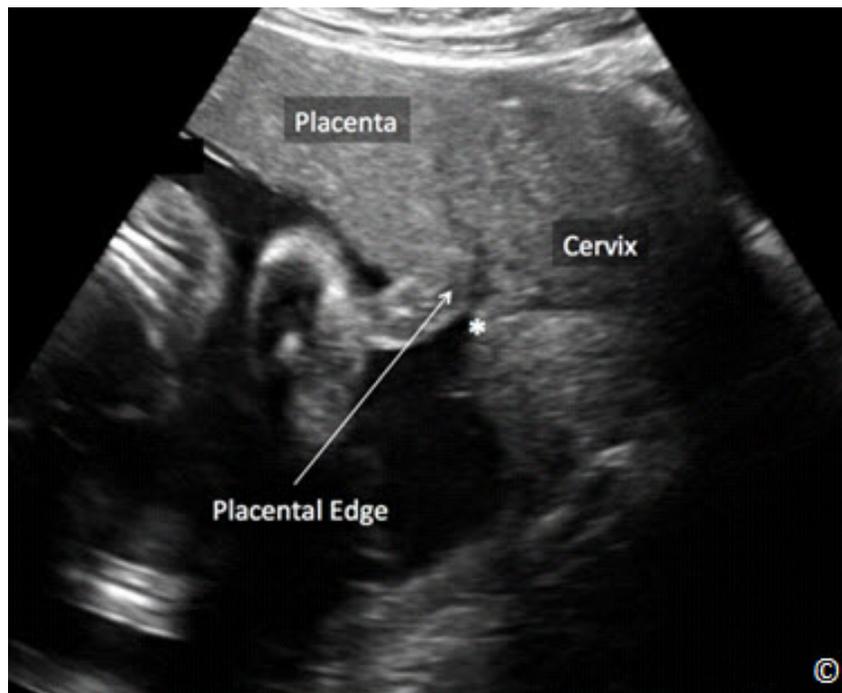
Figure 10.21: Placenta (labeled) shown on transabdominal sagittal ultrasound to be reaching the lower uterine segment, in close proximity to the cervical internal os (asterisk - labeled). A transvaginal ultrasound is indicated for accurate localization of placental edge. See text for details.

STEP FIVE: AMNIOTIC FLUID ESTIMATION

Estimation of amniotic fluid is an important part of the ultrasound examination. Several techniques for estimation of amniotic fluid have been proposed during the ultrasound examination including a subjective assessment, single deepest maximal vertical pocket (MVP) and amniotic fluid index (AFI). We recommend the use of the MVP technique as it is easy to learn and has been shown to have a lower false positive diagnosis for oligohydramnios in randomized studies (1). The term oligohydramnios (decreased amniotic fluid), which is defined by a MVP of less than 2 cm (**Figure 10.22**), is associated with genitourinary abnormalities in the fetus, premature rupture of the membranes, uteroplacental insufficiency and posterm pregnancy. Oligohydramnios has been linked to increased rates of perinatal morbidity and mortality (2). The term polyhydramnios or hydramnios (increased amniotic fluid), which is defined by a MVP of equal to or greater than 8 cm (**Figure 10.23**), is often idiopathic but can be associated with gestational diabetes, isoimmunization, fetal structural or chromosomal abnormalities or complicated multiple pregnancy. More discussion on ultrasound and amniotic fluid assessment is present in chapter 9.
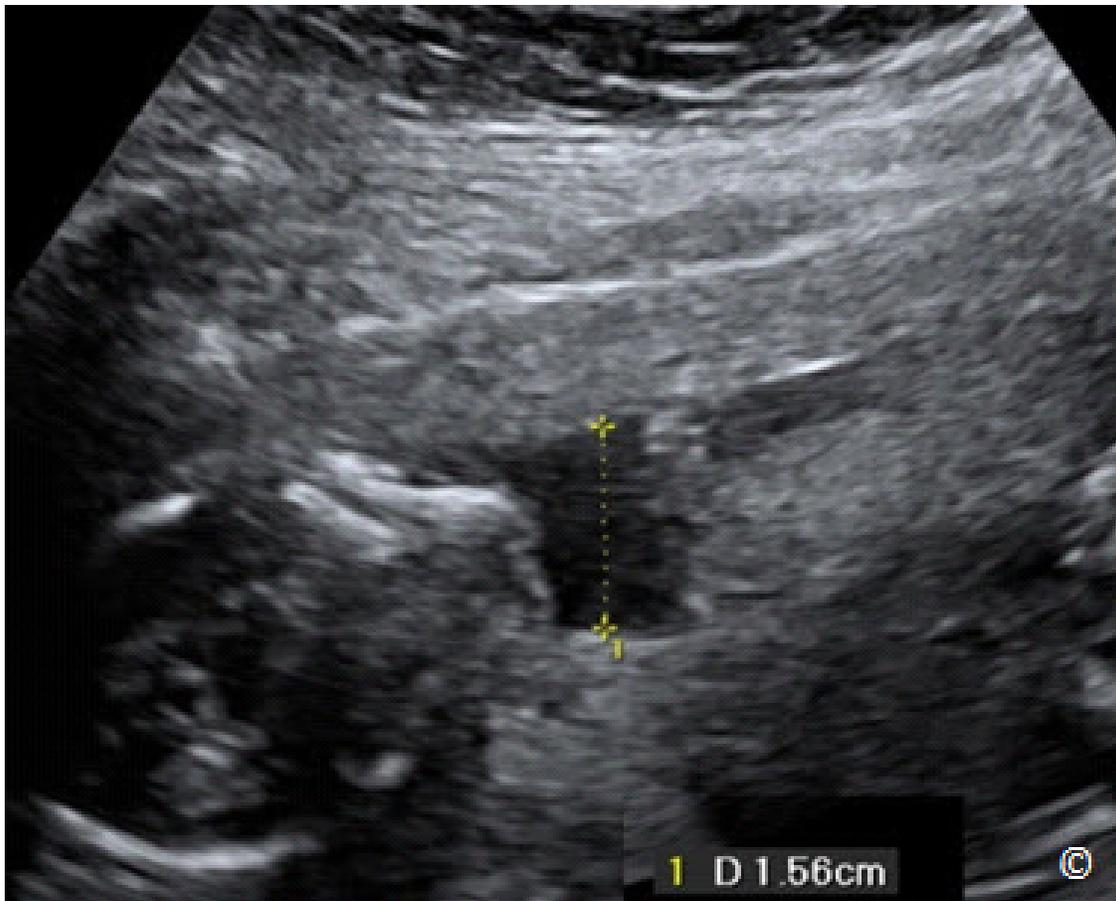
Figure 10.22: Oligohydramnios noted on ultrasound with a maximal vertical pocket (MVP) of 1.5 cm.
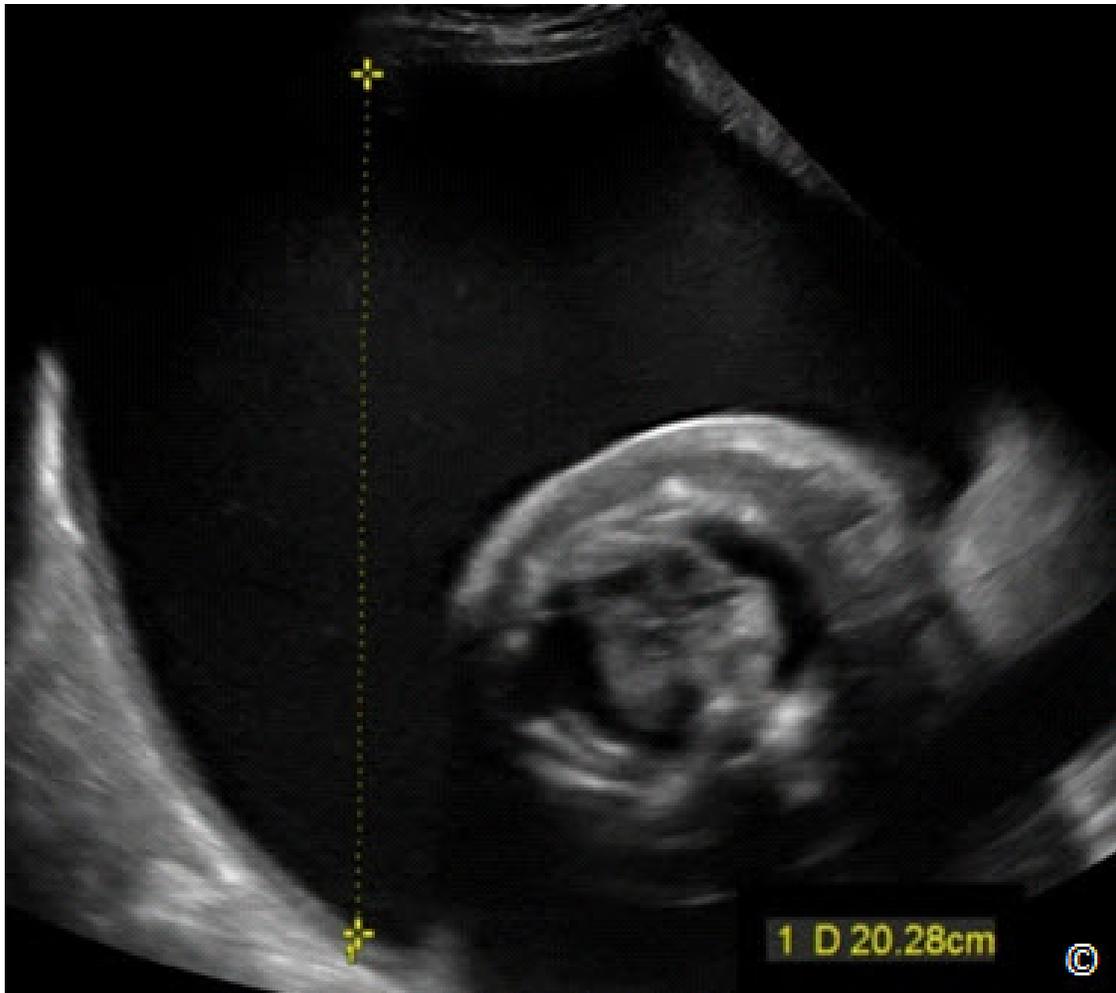
Figure 10.23: Polyhydramnios noted on ultrasound with a maximal vertical pocket (MVP) of 20.2 cm. Note the presence of fetal hydrops.

Step Five-Technical Aspect for Amniotic Fluid Estimation

The estimation of amniotic fluid using the MVP involves finding the single deepest pocket of amniotic fluid in the amniotic cavity on ultrasound examination, free of cord and fetal parts, and then measuring the greatest vertical dimension with the ultrasound transducer in sagittal orientation and perpendicular to the floor. In order to be a measurable pocket on ultrasound, the width of the pocket must be at least 1 cm.

This step requires mapping of the uterine cavity initially in order to identify the location of the MVP. Mapping of the uterus is performed by scanning the entire amniotic cavity with the transducer in sagittal orientation and perpendicular to the floor (**Figure 10.24** and **10.25** and **Clip 10.7**). When the deepest pocket is identified, measurement is performed by placing the calipers in a straight vertical line avoiding any cord or fetal parts in the image as shown in **Figure 10.22** and **10.23**.

Figure 10.24: Accurate transducer orientation for amniotic fluid measurement for the Amniotic Fluid Index (AFI) or the Maximal Vertical Pocket (MVP) methods. Note that the ultrasound transducer is in sagittal orientation and is perpendicular to the floor.
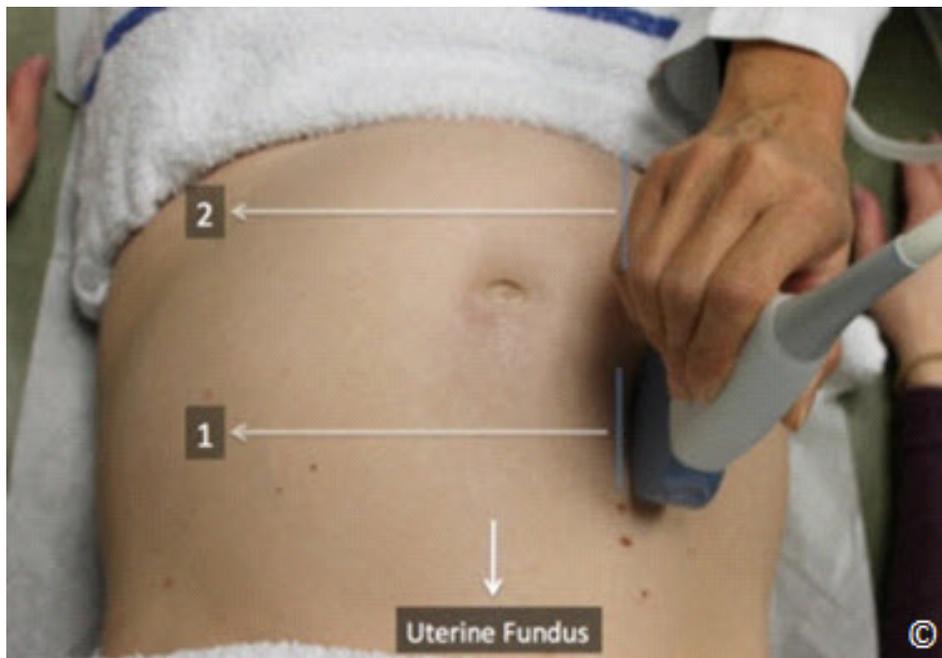
Figure 10.25: Sagittal transducer movement for amniotic fluid assessment (step 5). Note that the uterine cavity is scanned from right lateral to left lateral along tracks 1 and 2, while maintaining the transducer in sagittal orientation and perpendicular to the floor. Uterine fundus is labeled.

STEP SIX- FETAL BIOMETRY

The final step (step 6) in the basic obstetric ultrasound evaluation in the second and third trimester includes fetal biometric measurements. Fetal biometric measurements of the biparietal diameter, head circumference, abdominal circumference and femur length have been discussed in details in chapter 5 and 6, including estimation of fetal weight and the technical aspect of each measurement. The reader should review these chapters for more detailed information on this subject.

CLIP 10.1

CLIP 10.2

CLIP 10.3

CLIP 10.4

CLIP 10.5

CLIP 10.6

CLIP 10.7

References:

1) Chauhan S, Doherty D, Magann E, Cahanding F, et al. Amniotic fluid index vs. single deepest pocket technique during modified biophysical profile: A randomized clinical trial. Am J Obstet Gynecol 2004; 191:661-8.

2) The Cochrane Collaboration. Amniotic fluid index versus single deepest vertical pocket as a screening test for preventing adverse pregnancy outcome. 2009; Issue 3, pp (1 – 31).

INTRODUCTION

Ultrasound is the most optimal imaging modality for the evaluation of the uterus and should be used first when the patient's symptoms suggest the presence of uterine or other surrounding organ abnormalities. The approach to imaging the uterus by ultrasound can be accomplished by the transabdominal or the transvaginal route and is typically dictated by the type of uterine pathology being evaluated. With the exception of large uterine masses, such as uterine leiomyomas, which extend the uterus outside of the pelvis, the transvaginal approach, with its higher resolution and closer proximity to pelvic organs, is preferred, as it enhances the sonographic depiction of normal and abnormal uterine anatomy. Furthermore, the transvaginal transducer allows for direct contact with pelvic tissue and thus can elicit pain or discomfort during the ultrasound examination and thus correlate the patient's symptoms with the sonographic findings. When the transvaginal approach is not feasible, the transrectal or the translabial approach can be used. This chapter discusses and illustrates the sonographic features of the normal non-pregnant uterus and the most common uterine and endometrial malformations.

PREPARATION FOR THE EXAMINATION

Given that the majority of the ultrasound examinations to assess the uterus can be performed with the transvaginal approach, it is recommended that the patient present with an empty bladder. The patient is best placed in a dorsal lithotomy position, with the legs flexed and the perineum at the edge of table, which allows for manipulation of the transvaginal transducer. The transvaginal transducer is best introduced under real-time imaging, and the presence of a chaperone should be considered in accordance with local policies. When a transabdominal ultrasound is performed, the patient's bladder should be distended adequately to displace small bowel from the field of view. A written request for the ultrasound examination should be available and should provide sufficient clinical information to allow for the appropriate performance and interpretation of the examination (1). Refer to chapter 13 for more details on the technical aspects of the transvaginal ultrasound examination. Indications for the examination of the pelvis by ultrasound are listed in **Table 11.1**.

Table 11.1	Indication of Pelvic Sonography Include, but are not Limited to the Following: [Modified with permission from the American Institute of Ultrasound in Medicine (1)]

- Pelvic pain
- Dysmenorrhea (painful menses)
- Amenorrhea (absence of menses)
- Menorrhagia (excessive menstrual bleeding)
- Metrorrhagia (irregular uterine bleeding)
- Menometrorrhagia (excessive irregular uterine bleeding)
- Follow-up of a previously detected abnormality
- Evaluation, monitoring, and/or treatment of infertility patients
- Delayed menses, precocious puberty, or vaginal bleeding in a prepubertal child
- Postmenopausal bleeding
- Abnormal or technically limited manual pelvic examination
- Signs or symptoms of pelvic infection
- Further characterization of a pelvic abnormality noted on another imaging study
- Evaluation of congenital uterine anomalies
- Excessive bleeding, pain, or signs of infection after pelvic surgery, delivery, or abortion
- Localization of an intrauterine contraceptive device
- Screening for malignancy in patients at increased risk
- Urinary incontinence or pelvic organ prolapse
- Guidance for interventional or surgical procedures

SCANNING TECHNIQUES

The sonographic examination of the uterus by the transvaginal approach is typically initiated at the midsagittal plane. This view is obtained by introducing the transvaginal transducer into the upper vaginal fornix while maintaining the reference notch on the transducer at the 12 o'clock position (**Figure 11.1**). In this view, the uterine fundus, uterine isthmus and cervix is seen (**Figure 11.2**) and the uterine length is measured from the fundus to the external os (**Figure 11.2**). The depth (height) of the uterus (anteroposterior dimension) is measured in the same long-axis view from its anterior to posterior walls, perpendicular to the length (**Figure 11.2**). This midsagittal view also allows for assessment and measurement of the endometrium. The endometrium should be analyzed for thickness, focal abnormalities, and the presence of fluid in the endometrial cavity. Measurement of the endometrium should include the anterior and posterior portions while excluding any endometrial fluids (**Figure 11.3**). Accurate evaluation and measurement of the endometrium is important especially in the presence of uterine bleeding. When measuring endometrial thickness on ultrasound, it is critical to ensure that the uterus is in a mid-sagittal plane, the whole endometrial lining is seen from the fundal region to the endocervix, the thickest portion is measured and the image is clear and magnified (**Figure 11.3**). Rotating the

transducer 90 degrees counterclockwise (maintains correct orientation) allows for the display of the transaxial or transverse view of the uterus. The operator should fan the probe in the superior – inferior direction until the widest transverse view of the uterus is displayed (**Figure 11.4**). From this widest transverse view, the maximum width of the uterus is measured (**Figure 11.4**).

Figure 11.1: Initial step in the performance of the transvaginal ultrasound examination. Note that the transvaginal transducer is introduced into the vaginal canal with the transducer marker at the 12 o'clock position. A mannequin is used for demonstration.
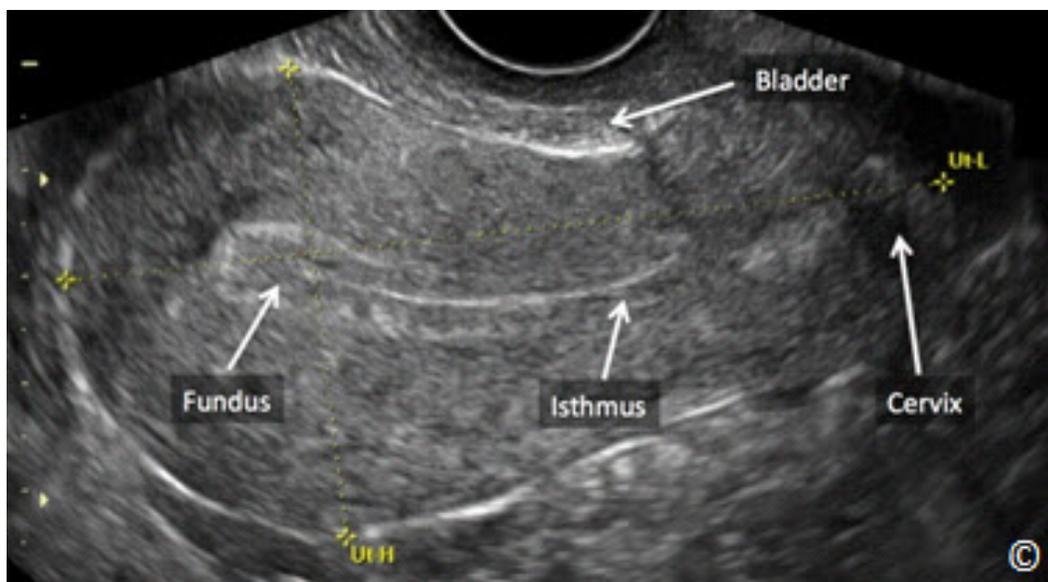
Figure 11.2: Midsagittal plane of the uterus showing the uterine fundus, isthmus, cervix and a collapsed bladder anteriorly (all labeled). In this plane uterine length (Ut-L) and height (Ut-H) are measured.
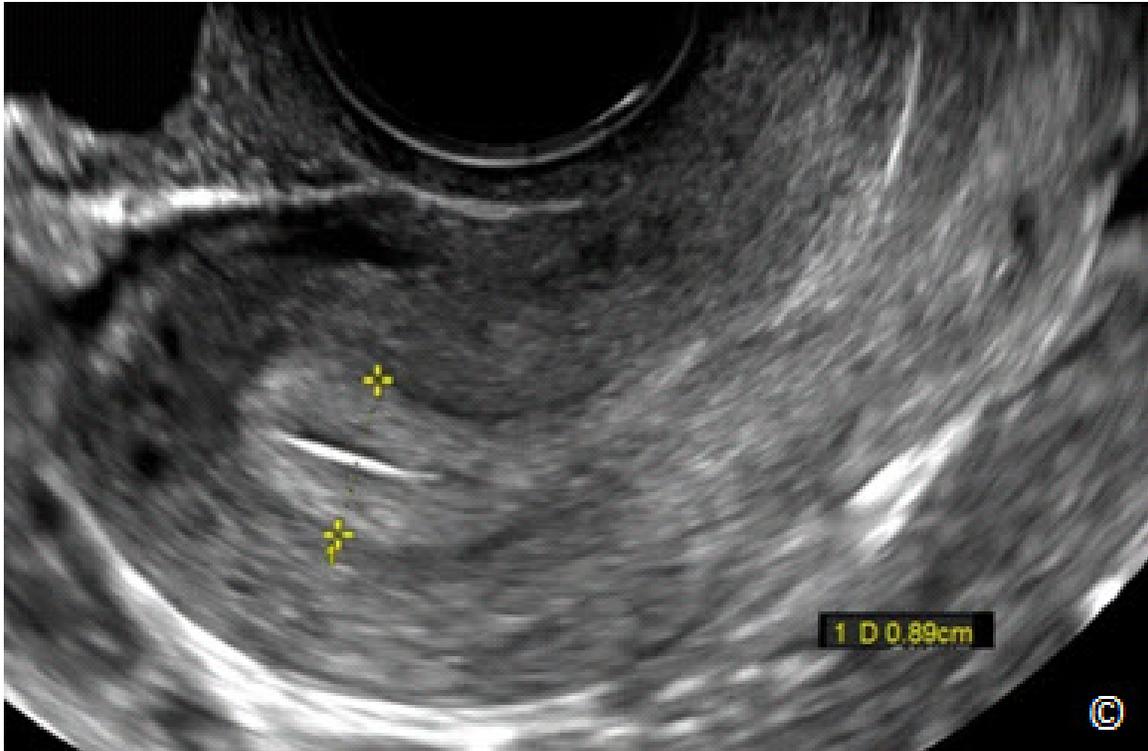
Figure 11.3: Endometrial thickness measurement. Note that the endometrial thickness is measured at its thickest portion and in a midsagittal plane of the uterus. See text for details.

Figure 11.4: Transverse plane of the uterus at its widest dimensions. In this plane uterine width (Ut-W) is measured.

During each ultrasound examination, the uterus should be evaluated for its dimensions (including the endometrium), shape and orientation. The presence of abnormalities involving the cervix, endometrium and myometrium should be evaluated and reported. Adjunct imaging modalities such as color and pulsed Doppler can occasionally help in the presence of abnormal findings. Applying gentle pressure on the transducer while using the other hand on the patient's abdomen to exert counter pressure may help to elicit symptoms in presence of endometritis, endometriosis and pelvic inflammatory disease. This maneuver may also allow assessing for uterine mobility, which is limited in presence of adhesions or scarring. Sonohysterography may be useful for the assessment of the endometrial cavity when an abnormality is suspected (2) (**Figure 11.5**). Sonohysterography (hydrosonography) is performed by inserting a thin, sterile, plastic catheter (insemination catheter or a small feeding tube), connected to a plastic syringe containing sterile saline, into the uterine cavity through the cervical canal (**Figure 11.6**). The author recommends performing the procedure during the proliferative phase of the menstrual cycle to avoid the risk of a pregnant uterus and to ensure a thin endometrium. Other recommendations for sonohysterography to consider include wiping the external cervical os with an aseptic solution before inserting the catheter to minimize the risk of infection and flushing the catheter with saline before insertion to avoid injecting air into the endometrial cavity, which may obscure visualization. The catheter can be inserted easily through the internal cervical os in most women but when cervical stenosis is encountered, the use of a tenaculum to straighten the cervix and a small uterine sound may help in widening the endocervical canal. Side effects of sonohysterography are rare and include around a 1% risk for endometritis and a 1-5 % risk for significant cramping or pain (3). Taking Ibuprofen orally, 1 hour before the procedure, may help to minimize uterine cramping.
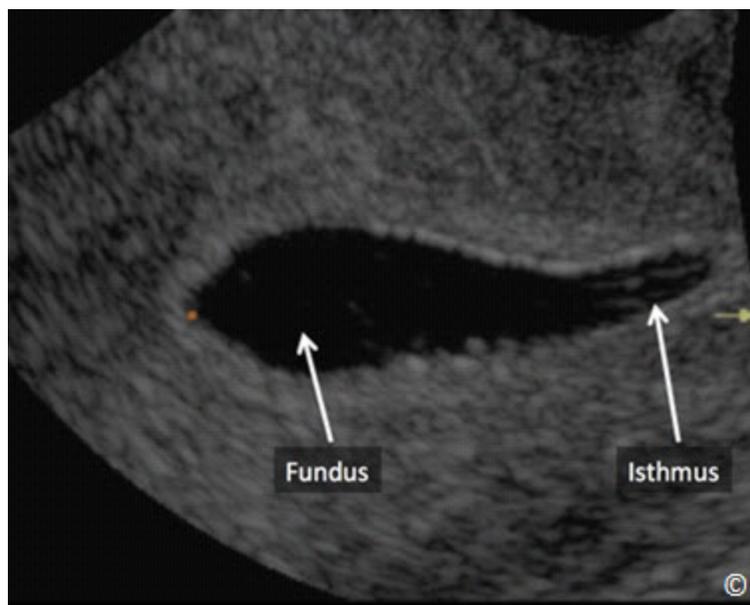
Figure 11.5: Sonohysterography of a normal endometrial cavity showing the fundus and isthmus (labeled).
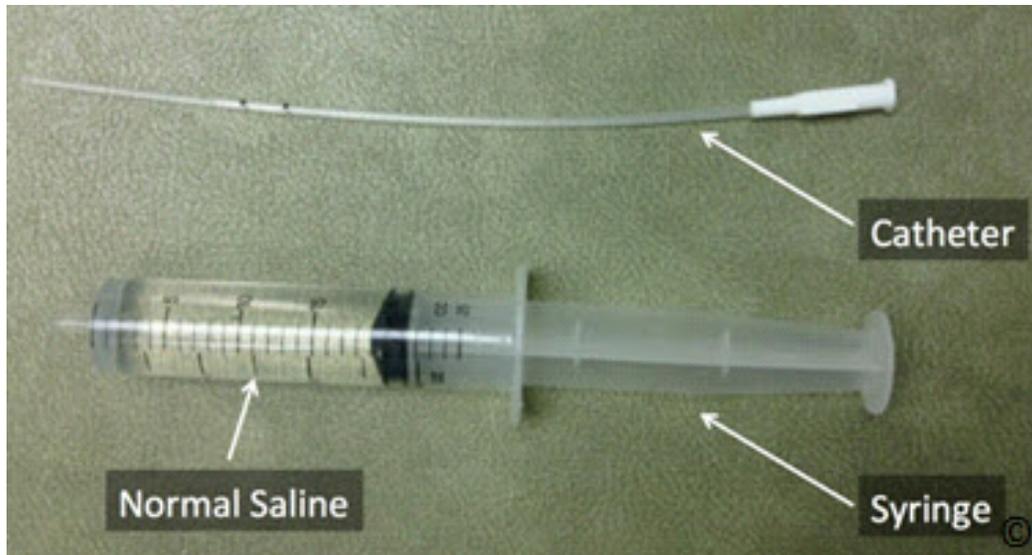
Figure 11.6: Supplies needed for sonohysterography include a syringe filled with sterile normal saline and a thin sterile plastic catheter (labeled). See text for details.

The technical aspect of obtaining the mid-coronal plane of the uterus on three-dimensional sonography will be discussed later in this chapter in the section on congenital mullerian malformations.

SONOGRAPHIC FEATURES OF THE NORMAL UTERUS

The uterus is primarily a muscular organ located in the true pelvis between the urinary bladder anteriorly and the rectosigmoid colon posteriorly. The space between the uterus and the rectosigmoid is the posterior cul-de-sac; the most dependent area in the peritoneal cavity where peritoneal fluid tends to accumulate. In the reproductive years, the endometrium is under the influence of sexual hormones and undergoes anatomic changes during the woman's menstrual cycle.

As described in the section on scanning techniques, the uterus is first imaged in its long axis on the midsagittal plane, which is obtained by visualizing the long axis of the echogenic endometrium. The midsagittal plane allows for the visualization of the uterine fundus, a significant section of the myometrium, the endometrium in sagittal section, the cervix in sagittal section, the cul-de-sac, the rectosigmoid and the bladder (**Figure 11.7**). Measuring the length, depth (height) and width of the uterus, as described in the prior section, should be part of the pelvic ultrasound examination. The length of a normal nulliparous uterus is 6 - 8.5 cm and in multiparous women it is 8 - 10.5 cm (4). The depth (height) of the normal uterus in nulliparous

women is 2 – 4 cm and in multiparous women it is 4 – 6 cm (4). The widest transverse plane of the uterus measures 3 – 5 cm in nulliparous and 4 – 6 cm in multiparous women (4).
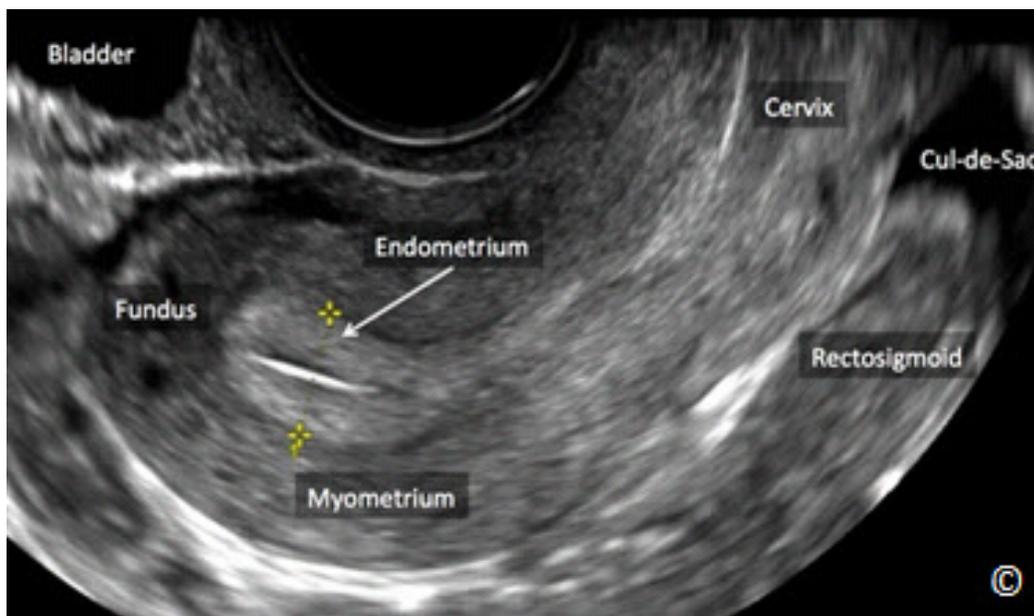
Figure 11.7: Midsagittal plane of the uterus showing the uterine fundus, the myometrium, the endometrium, the cervix, the cul-de-sac, the rectosigmoid and the bladder (all labeled). Note that the myometrium is less echogenic than the endometrium (labeled).

It is important to describe and report the orientation of the uterus as part of the ultrasound examination as this information is helpful if uterine instrumentation is required. The orientation of the uterus is described in the midsagittal plane and in relation to the supine body. Two terms are used to describe the orientation of the uterus in the pelvis; flexion and version. Flexion is the bending of the uterus on itself and thus the uterus is flexed when there is an angle in the midsagittal plane between the cervix/lower uterine (isthmus) segment and the fundal portion. An anteroflexed uterus is a uterus with an acute or obtuse angle (< 180 degrees) between the cervix/lower uterine (isthmus) segment and the fundus with the fundal portion close to the bladder (**Figure 11.8**). A retroflexed uterus is a uterus with a reflex angle (> 180 degrees) between the cervix/lower uterine (isthmus) segment and the fundus with the fundal portion close to the rectosigmoid (**Figure 11.9**). If there is no angulation between the cervix/lower segment (isthmus) and the uterine fundus, the uterus is described in terms of version. Version thus describes displacement of the entire uterus forwards or backwards. An anteverted uterus is a uterus where the fundal portion is close to the bladder (**Figure 11.10**) and a retroverted uterus is a uterus where the fundal region is close to the rectosigmoid (**Figure 11.11**).
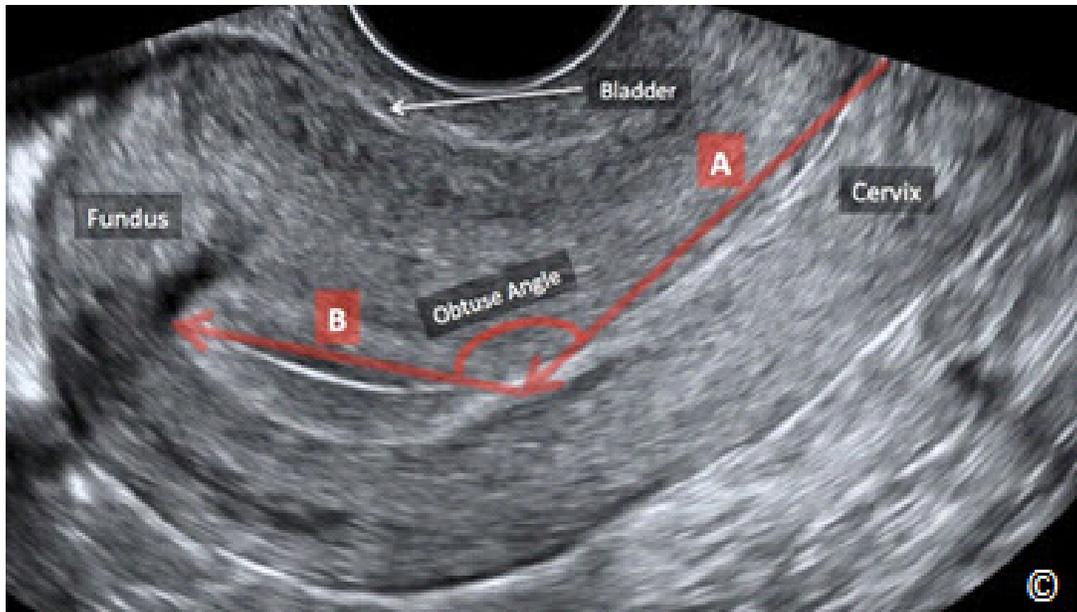
Figure 11.8: Transvaginal ultrasound of an anteroflexed uterus. Note the obtuse angle (< 180°) between the lower uterine segment (isthmus)/ cervix (A) and the fundal portion (B). The uterine fundus is close to the bladder (compressed - labeled).
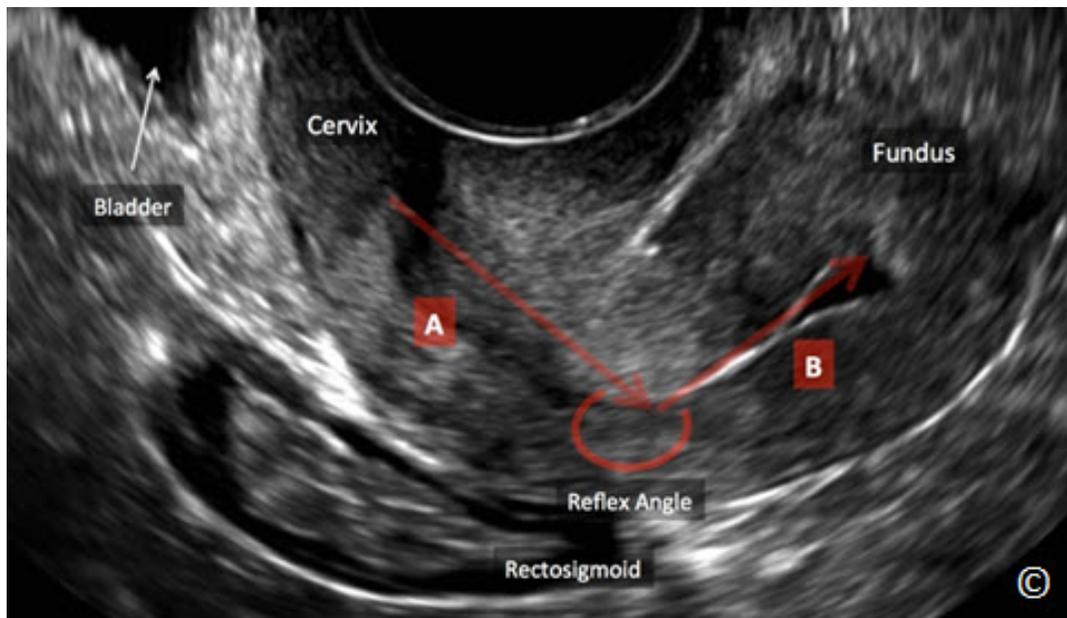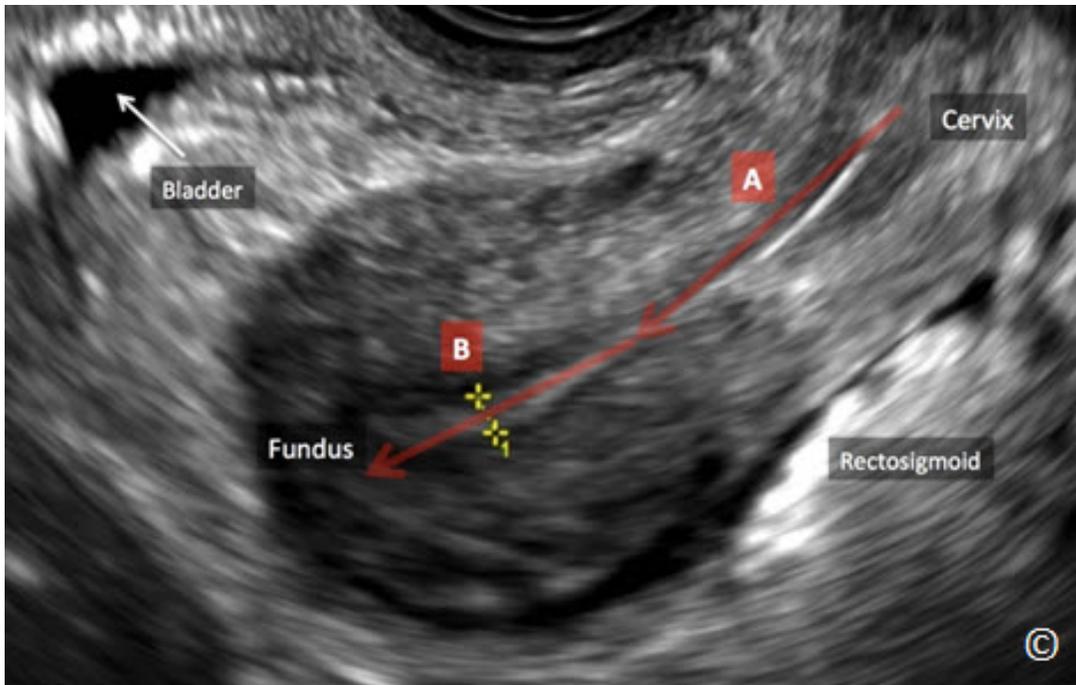

Figure 11.9: Transvaginal ultrasound of a retroflexed uterus. Note the reflex angle (> 180°) between the lower uterine segment (isthmus) / cervix (A) and the fundal portion (B). The uterine fundus is close to the rectosigmoid (labeled). Note location of bladder (labeled).

Figure 11.10: Transvaginal ultrasound of an anteverted uterus. Note the absence of angulation between the lower uterine segment (isthmus)/ cervix (A) and the fundal portion (B). The fundal portion is close to the bladder (labeled). Rectosigmoid is labeled.
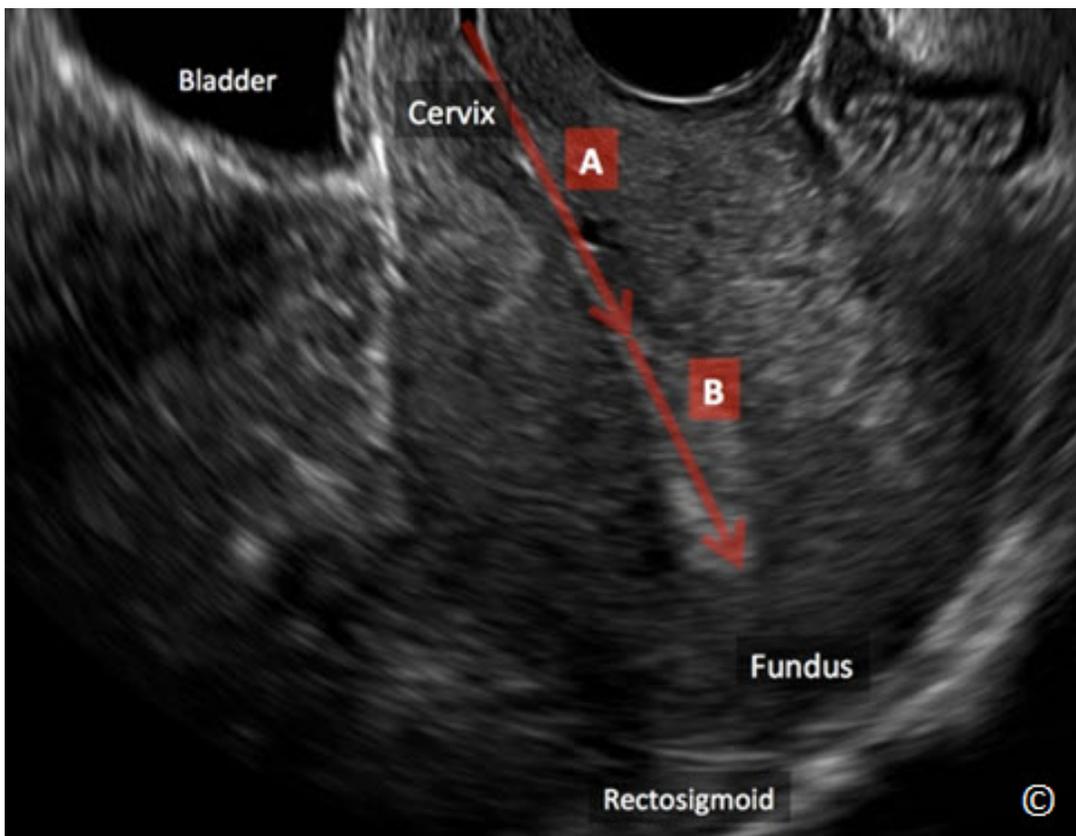
Figure 11.11: Transvaginal ultrasound of a retroverted uterus. Note the absence of angulation between the lower uterine segment (isthmus)/ cervix (A) and the fundal portion (B). The fundal portion is close to the rectosigmoid (labeled). Note the location of the bladder (labeled).

The myometrium is made of a homogeneous layer of smooth muscle and blood vessels. Sonographically the normal myometrium is less echogenic than the endometrium (**Figure 11.7**). The myometrium can be divided into three layers; the inner or junctional layer, which abuts the endometrium, is thin and hypoechoic, the middle layer is thick and homogeneous and an outer layer which is thin and hypoechoic (**Figure 11.12**). The arcuate vessels separate the middle from the outer myometrial layers.

The endometrium undergoes significant change during the menstrual cycle (5, 6) and anatomically is divided into the inner functional layer that sloughs during the menstrual cycle and the outer basal layer that abuts the myometrial junctional layer. Sonographically, in the immediate postmenstrual phase, the endometrium appears as a thin echogenic line and typically measures between 3 – 8 mm (Type A) (**Figure 11.13**). Under the influence of increasing estradiol hormone levels secreted by the growing ovarian follicles, endometrial proliferation occurs and endometrial thickening ensues. Sonographically, this is seen as thickening of the lining into the so-called trilaminar layer (Type B) with an anterior and posterior hypoechoic layer separated in the midline by an echogenic central line. During the late proliferative period and near the time of ovulation, endometrial lining is 8 to 12 mm in thickness with an accentuated trilaminar appearance (Type C), (**Figure 11.14**). The post ovulatory endometrial lining, under the influence of progesterone hormone, secreted by the corpus luteum, is characterized by loss of the trilaminar appearance and the development of a uniformly hyperechoic endometrium (Type D), (**Figure 11.15**).
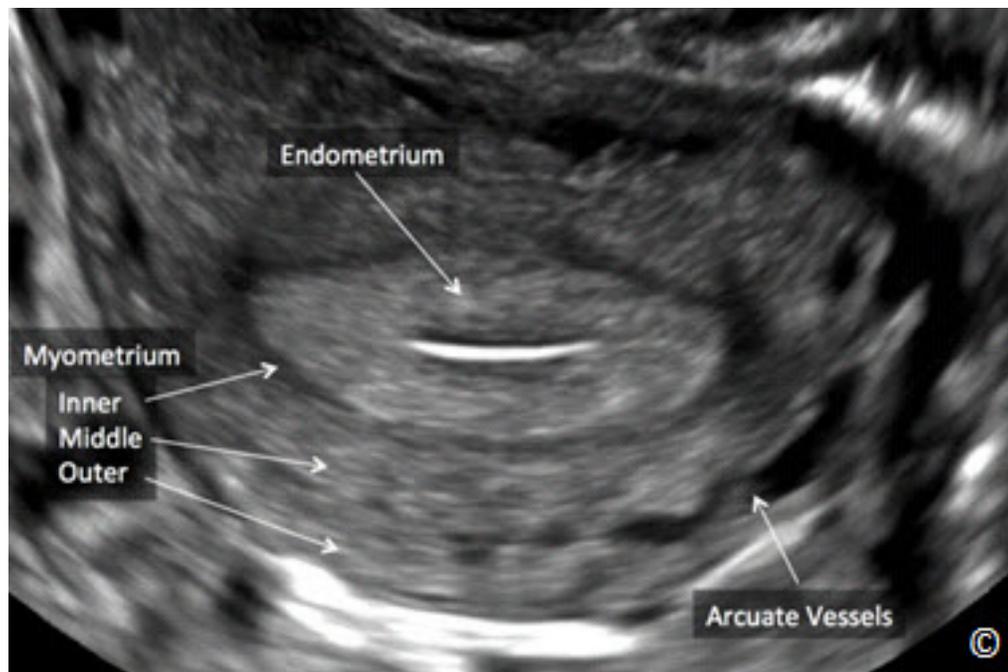

Figure 11.12: Transvaginal ultrasound of a transverse view of the uterus showing the three myometrial layers. Note the inner thin and hypoechoic layer that abuts the endometrium (labeled), the middle layer that is thick and homogeneous and the outer layer that is slightly less echogenic than the middle layer (labeled). Note that the arcuate vessels (labeled) separate the middle from the outer myometrial layers.
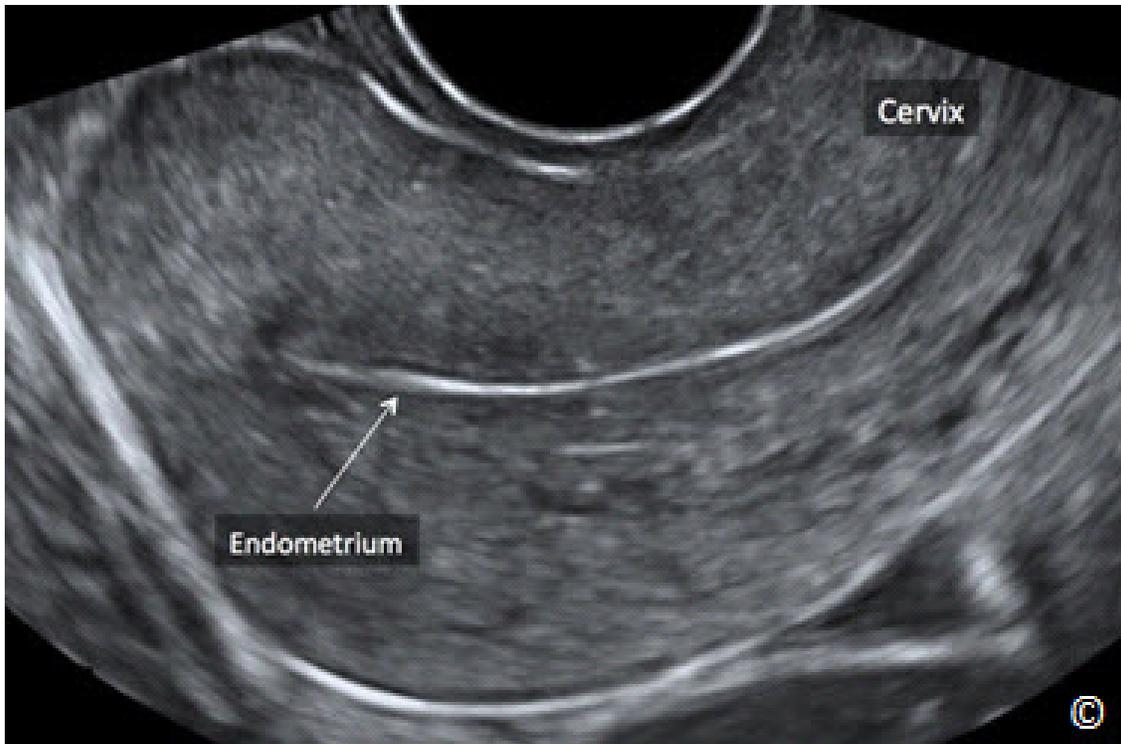
Figure 11.13: Transvaginal ultrasound of a sagittal view of the uterus in the immediate postmenstrual phase. Note the thin echogenic endometrium (labeled). Cervix is labeled for image orientation. Image is courtesy of Dr. Bernard Benoit.
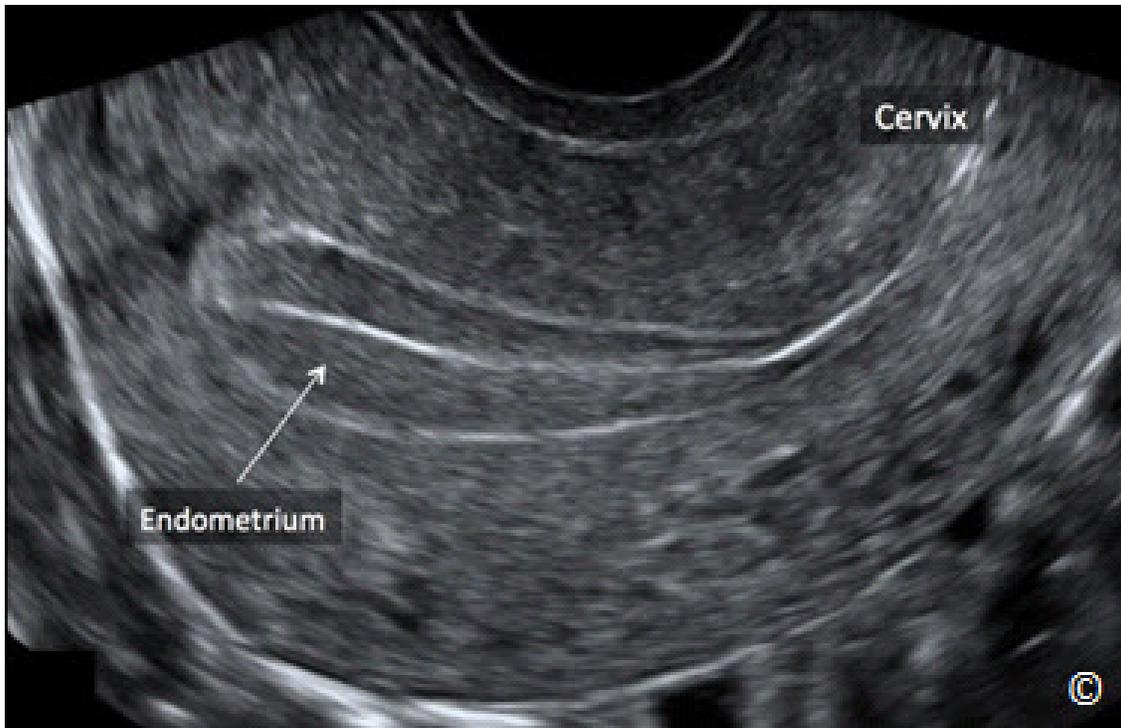

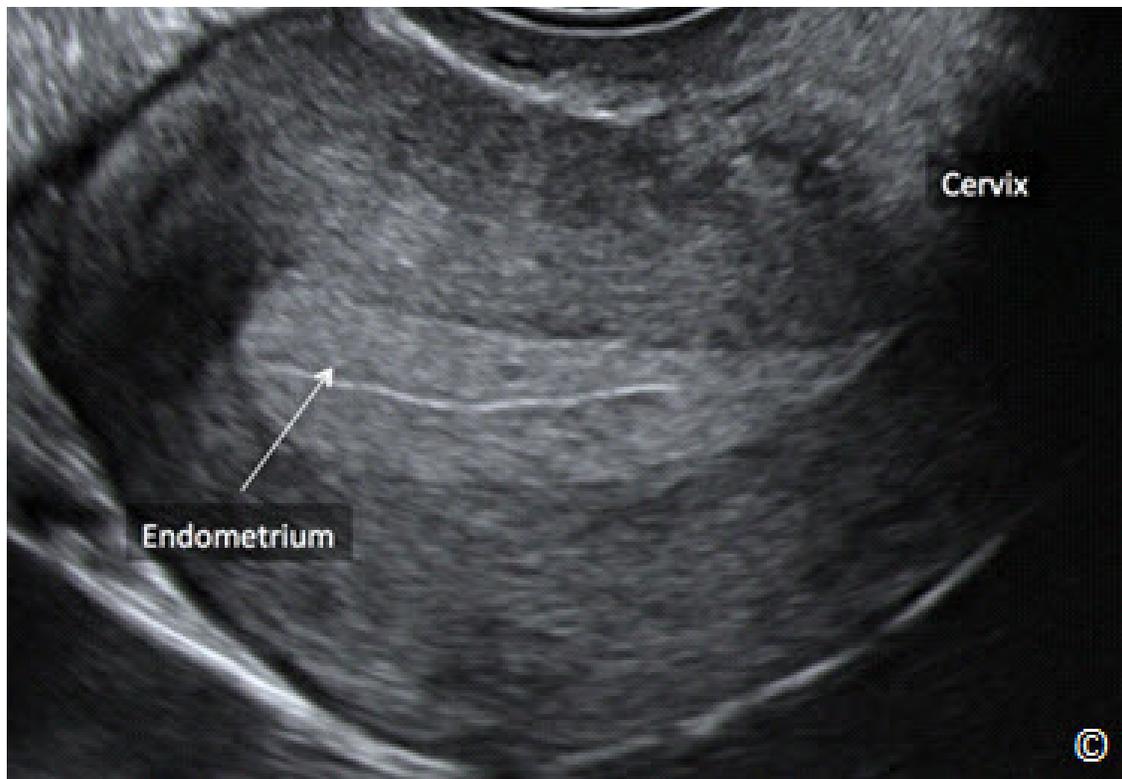**Figure 11.14**: Transvaginal ultrasound of a sagittal view of the uterus in the late proliferative, near ovulation phase of the menstrual cycle. Note the accentuated thick trilaminar endometrium (labeled). Cervix is labeled for image orientation. Image is courtesy of Dr. Bernard Benoit.

Figure 11.15: Transvaginal ultrasound of a sagittal view of the uterus in the post-ovulatory phase of the menstrual cycle. Note that the endometrium is uniformly hyperechoic with the loss of the trilaminar appearance (labeled). Cervix is labeled for image orientation. Image is courtesy of Dr. Bernard Benoit.

The cervix can be divided into the portio vaginalis or ectocervix, the endocervix and the endocervical canal. It is best imaged using the transvaginal approach. To fully display the cervix, the transvaginal transducer is rotated to the midsagittal position, and is pulled gently backward until the whole cervix comes into view. Applying transducer pressure should be avoided, as it will distort the cervix. Sonographically, the cervical stroma is of the same consistency as the myometrium, and is not affected by hormonal changes (7). Nabothian cysts can be occasionally seen within the cervical stroma (**Figure 11.16**).

Figure 11.16: Transvaginal ultrasound of the cervix in sagittal view. Note the presence of a Nabothian cyst (labeled), which typically presents as an anechoic cyst within the cervical stroma

ADENOMYOSIS

Adenomyosis is a common condition that predominantly affects women in the late reproductive years. It has been noted to occur in about 30% of the general female population and in up to 70% of hysterectomy specimens depending on the definition of the entity (8). Adenomyosis is defined by the presence of ectopic endometrial glands and stroma within the myometrium, which induces a hypertrophic and hyperplastic reaction in the surrounding myometrial tissue.

Most patients with adenomyosis are asymptomatic. Symptoms related to adenomyosis include dysmenorrhea, dyspareunia, chronic pelvic pain and menometrorrhagia. Adenomyosis presents most commonly as a diffuse disease involving the entire myometrium (**Figure 11.17**). Adenomyosis can also present in a focal area of the uterus, known as adenomyoma (**Figure 11.18**). Adenomyosis is occasionally associated with other uterine pathology such as leiomyoma and endometrial polyps. Clinical diagnosis of adenomyosis is difficult due to its vague presenting symptoms. A homogeneously enlarged (globular) uterus on pelvic examination is suggestive of the diagnosis (**Figure 11-17**).
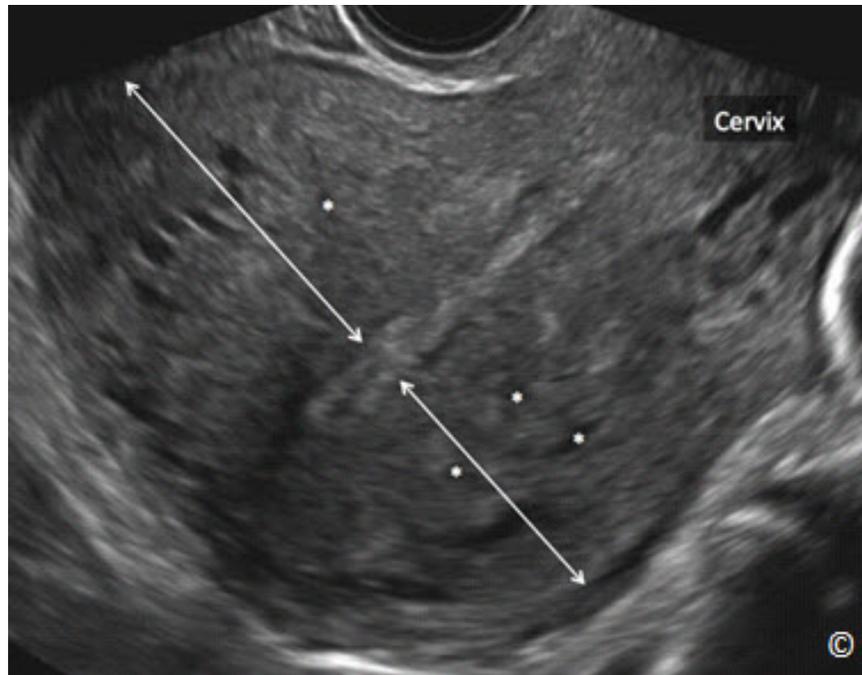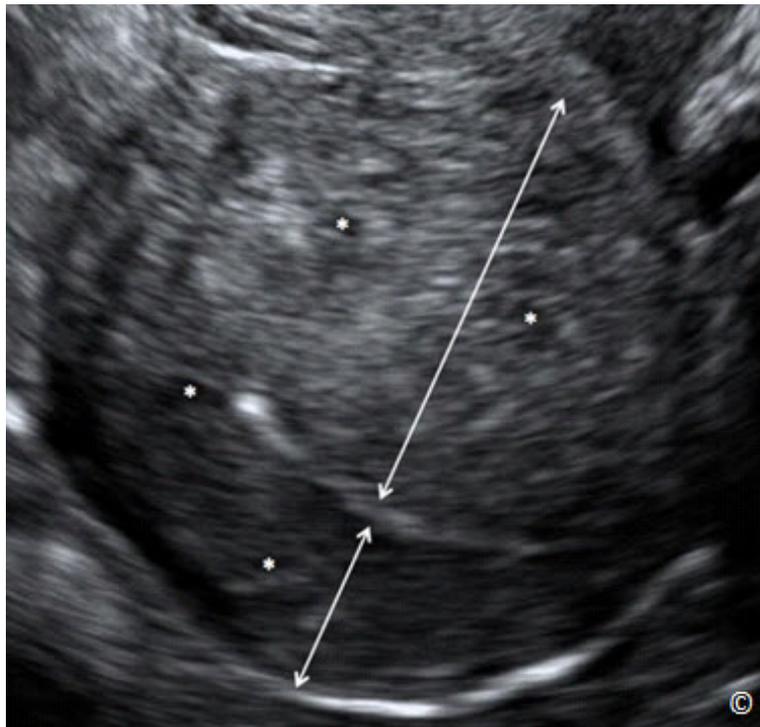
Figure 11.17: Transvaginal ultrasound of the uterus in sagittal view in the presence of diffuse adenomyosis. Note the globular enlargement of the uterus, the asymmetric anterior and posterior wall thickness (arrows) and the presence of multiple anechoic spaces within the myometrium (asterisks). The cervix is labeled for image orientation. See text and **Table 11.2** for more details.

Figure 11.18: Transvaginal ultrasound of the uterus in sagittal view in the presence of focal adenomyosis (arrows). Note the presence of multiple anechoic spaces (arrows) within the myometrium. See text and **Table 11.2** for more details. The cervix is labeled for image orientation. Image is courtesy of Dr. Bernard Benoit.

Ultrasound features of adenomyosis have been described in the literature (9) and are listed in **Table 11.2**. **Figures 11.17** to **11.19** show the common ultrasound features of adenomyosis. The diagnosis of adenomyosis by ultrasound is best performed by the transvaginal approach and its clinical implication is most significant in symptomatic women. On some occasions, differentiating adenomyosis from a leiomyoma may be difficult and color/pulsed Doppler may be helpful in that setting (10, 11).

TABLE 11.2	Ultrasound Findings in Adenomyosis
	- Globular enlargement of the uterus - Anechoic spaces in the myometrium - Asymmetric anterior and posterior uterine wall thickening - Subendometrial echogenic linear striations - Heterogeneous echo texture - Obscure endometrial-myometrial border - Thickening of the transition zone

Figure 11.19: Transvaginal ultrasound of the uterus in sagittal view in the presence of diffuse adenomyosis. Note the globular enlargement of the uterus, the asymmetric anterior and posterior wall thickness (arrows), the presence of multiple anechoic spaces within the myometrium (asterisks) and the heterogeneous echo texture. See text and **Table 11.2** for more details.

CONGENITAL UTERINE MALFORMATIONS

The true prevalence of female genital tract malformations is unknown (12), but can be up to 8-10% in women with recurrent pregnancy loss (13). Congenital uterine malformations are associated with an increased risk of infertility, miscarriage, premature birth, fetal loss, fetal malpresentation and cesarean sections (14, 15). Accurate diagnosis of the specific type of a uterine anomaly is of clinical importance as the prognosis and the need for surgical repair is dependent on this distinction. The American Fertility Society's classification (1988) consists of seven basic groups that are based on Mullerian development and its relationship to fertility: (1) agenesis and hypoplasias, (2) unicornuate uteri, (3) didelphys uteri, (4) bicornuate uteri, (5) septate uteri, (6) arcuate uteri and (7) anomalies related to diethylstilbestrol exposure syndrome (16). In this classification, additional findings referring to the vagina, cervix, fallopian tubes, ovaries and urinary system must be addressed separately.

Although transvaginal 2D sonography has been shown to be a good screening tool for the detection of uterine anomalies with a sensitivity as high as 90 % (17, 18), its ability is limited however to distinguish between different anomaly types with certainty (19). The development of three-dimensional (3D) ultrasound has permitted scanning of the uterus in coronal planes, which allows for accurate depiction of the endometrial and serosal fundus in such planes and thus allowed for accurate distinction between various types of uterine malformations (**Figure 11.20**). When the uterus is viewed in the midcoronal plane on 3D ultrasound, indentation in the serosal and endometrial fundus can be seen and measurement of the distance between the mid-fundus and a line connecting the two internal tubal ostia can be obtained (**Figure 11.21**). **Table 11.3** lists the criteria used by the authors for the classification of congenital uterine malformations by 3D ultrasound.
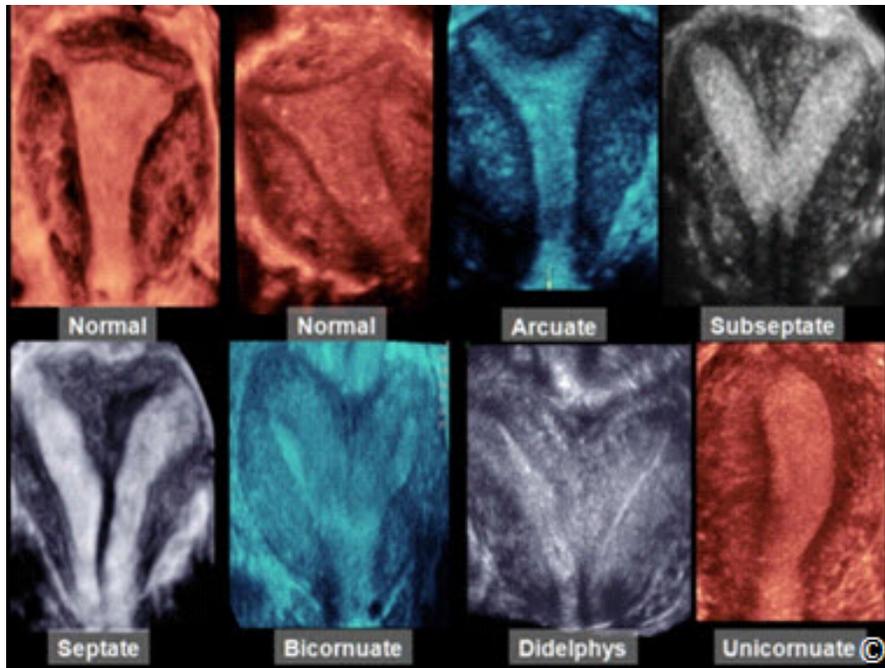
Figure 11.20: Midcoronal planes of uteri obtained from 3-D ultrasound volumes in normal and abnormal uterine abnormalities. Note the clear depiction of the serosal and endometrial fundi and lower-uterine segments, which allow for differentiation of various mullerian anomalies. See **Table 11.3** for details. Modified with permission from the American Institute of Ultrasound in Medicine (18).
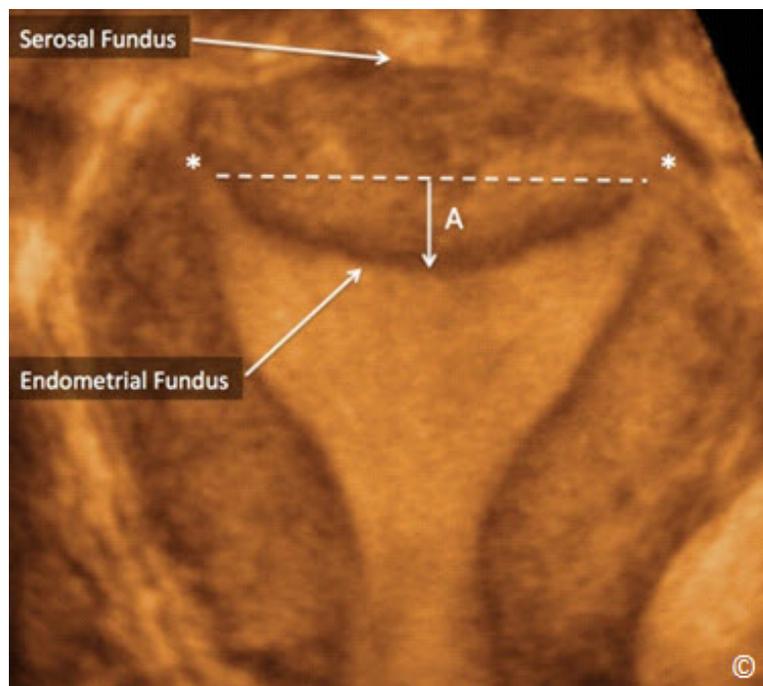

Figure 11.21: Midcoronal plane of the uterus obtained from a 3D ultrasound volume showing the serosal fundus (labeled), the endometrial fundus (labeled) and the location of the two internal tubal ostia (asterisks). Note that the indentation of the endometrial fundus (A) is measured as the distance from a line connecting the two tubal ostia (dashed line) to the mid-endometrial fundus (arrow-A). See **Table 11.3** for details. Image is courtesy of Dr. Bernard Benoit.

TABLE 11.3	Classification of Mullerian Malformations by 3D Ultrasound (Modified with Permission from Reference 20)	
Uterine Morphology	**Endometrial Fundus**	**Serosal Fundus**
Normal	Straight or Convex	Uniformly convex or with <10 mm indentation
Arcuate	Concave fundal indentation with central point of indentation at obtuse angel (>90°) – or indentation < 10 mm	Uniformly convex or with indentation <10 mm
Subseptate	Presence of septum, which does not extend to cervix, with central point of septum at an acute angle (<90°) – indentation > 10 mm	Uniformly convex or with indentation <10 mm
Septate	Presence of uterine septum that completely divides cavity from fundus to cervix	Uniformly convex or with indentation <10 mm
Bicornuate	Two well-formed uterine cornua – two cavities commonly communicate in isthmus / cervical region	Fundal indentation >10 mm dividing the two cornua
Didelphys	Two well-formed uterine cornua – two cavities that are wide apart and do not communicate	Fundal indentation >10 mm dividing the two cornua
Unicornuate with or without rudimentary horn	Single well-formed uterine cavity with a single interstitial portion of fallopian tube and concave fundal contour	Fundal indention >10 mm dividing the 2 cornua if rudimentary horn present

We have described an easy technique for the retrieval of the midcoronal plane from a 3D uterine volume (21). This standardized technique, termed, the Z-technique, is easy to learn, reduces operator dependency and enhances the diagnostic accuracy of 3D ultrasound in the detection of mullerian anomalies. **Table 11.4** and corresponding **Figures 11.22** to **11.26** details the sequence of steps for the display of the midcoronal plane of the uterus from a 3D volume using the Z-technique.

TABLE 11.4	The Z-Technique: Steps for the Retrieval of the Midcoronal Plane in a 3D Volume of the Uterus [Modified with Permission from the American Institute of Ultrasound in Medicine (21)].

Step 1. Place the reference/rotational point in the midlevel of the endometrial lining in the sagittal plane (**Figure 11.22**)

Step 2. Use the Z rotation to align the long axis of the endometrial lining along the horizontal axis in the sagittal plane of the uterus (**Figure 11.23**)

Step 3. Place the reference/rotational point in the midlevel of the endometrial lining in the transverse plane (**Figure 11.24**)

Step 4. Use the Z rotation to align the endometrial lining with the horizontal axis in the transverse plane of the uterus (**Figure 11.25**)

Step 5. After step 4, the midcoronal plane of the uterus will be displayed in plane C (**Figure 11.25**); apply Z rotation on plane C to display the midcoronal plane in the traditional orientation (**Figure 11.26**).
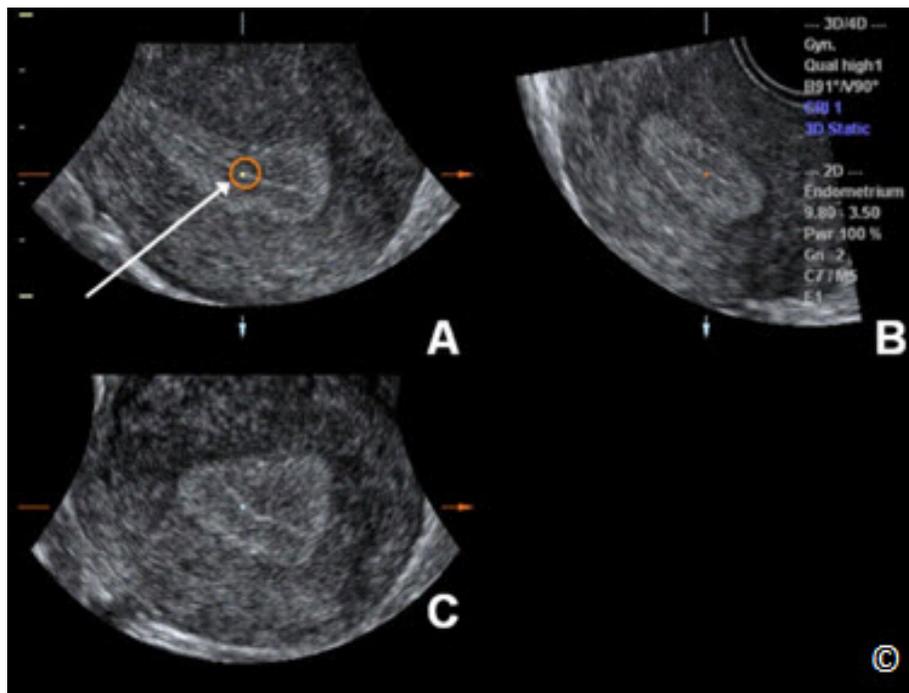
Figure 11.22: 3D volume of the uterus in multiplanar display. Plane A represents the reference plane (sagittal in this case) and B and C represent 2 orthogonal planes. The initial step in the Z-Technique involves placing the reference/rotational point in the midlevel of the endometrial lining in plane A (circle and arrow). Modified with permission from the American Institute of Ultrasound in Medicine (21).
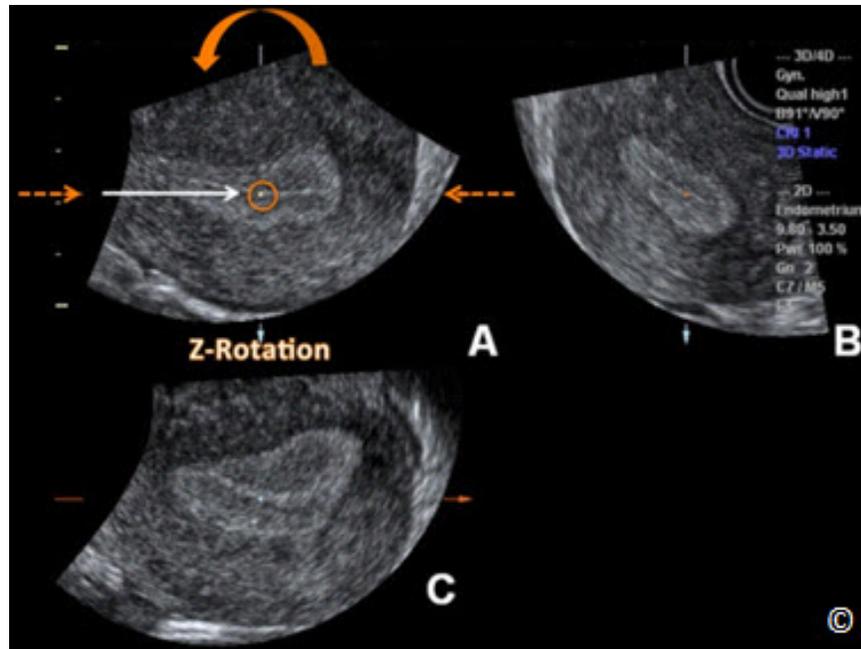
Figure 11.23: 3D volume of the uterus (same as in **Figure 11.22**) in multiplanar display. The second step in the Z-Technique involves aligning the long axis of the endometrial lining in plane A along the horizontal axis (dashed arrows) by rotating plane A along the Z-axis (curved arrow). The white arrow and circle shows the reference/rotational point. Modified with permission from the American Institute of Ultrasound in Medicine (21).
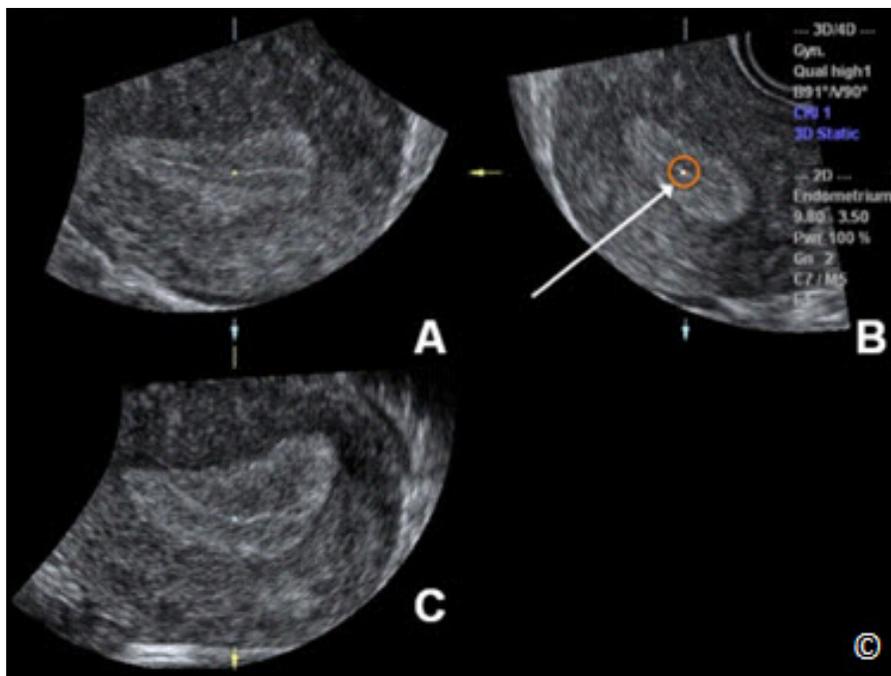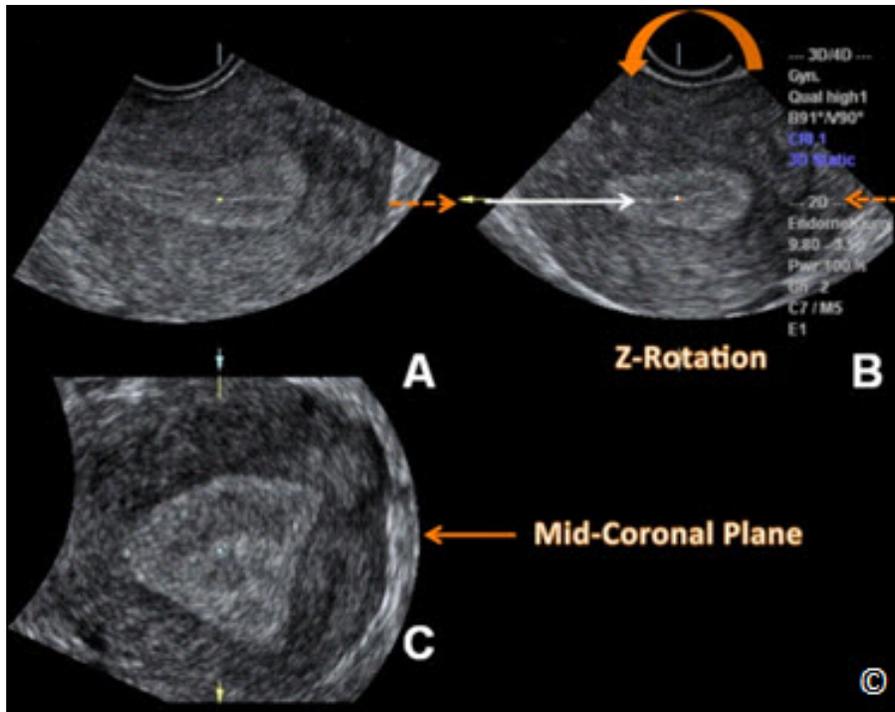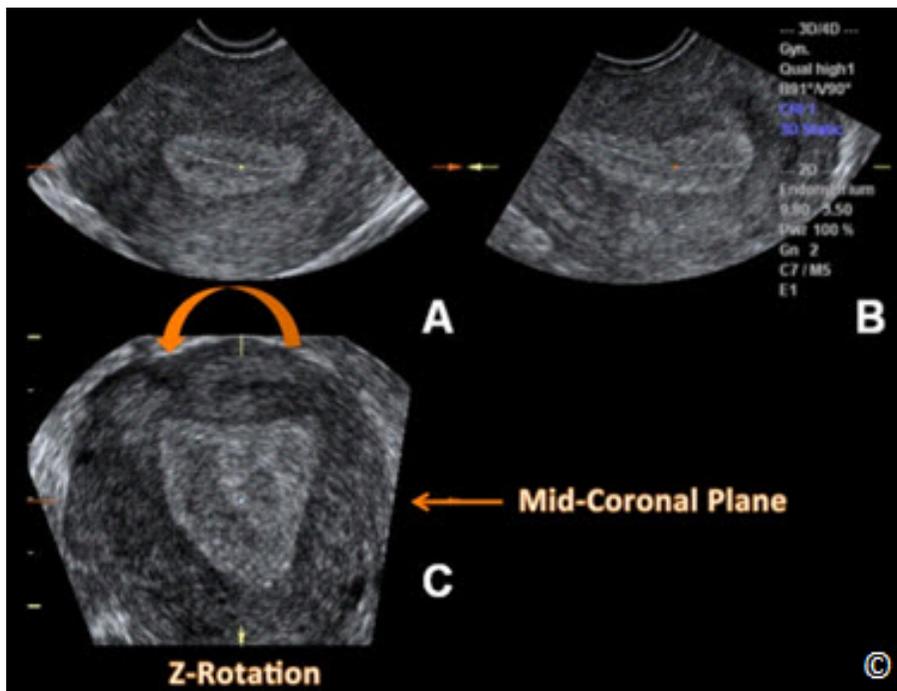

Figure 11.24: 3D volume of the uterus (same as in **Figure 11.22**) in multiplanar display. The third step in the Z-Technique involves placing the reference/rotational point in the midlevel of the endometrial lining in the transverse plane (plane B). The white arrow and circle shows the reference/rotational point in B. Modified with permission from the American Institute of Ultrasound in Medicine (21).

Figure 11.25: 3D volume of the uterus (same as in **Figure 11.22**) in multiplanar display. The fourth step in the Z-Technique involves aligning the long axis of the endometrial lining in plane B along the horizontal axis (dashed arrows) by rotating plane B along the Z-axis (curved arrow). Note that the mid-coronal plane is displayed in plane C. The white arrow shows the reference/rotational point in plane B. Modified with permission from the American Institute of Ultrasound in Medicine (21).

Figure 11.26: 3D volume of the uterus (same as in **Figure 11.22**) in multiplanar display. The final step (step 5) of the Z-technique involves applying Z rotation on plane C (curved arrow) to display the mid-coronal plane in the traditional orientation. Modified with permission from the American Institute of Ultrasound in Medicine (21).

Several authors have reported on the high accuracy of 3D ultrasound when comparing it with surgical findings in the diagnosis of uterine anomalies (22, 23). Furthermore, its accuracy compared to MRI has been established (24). We recommend 3D ultrasound as the modality of choice when evaluating a patient for a suspected uterine anomaly because of its relative low cost, lack of ionizing radiation or iodine contrast agents and excellent diagnostic capability, in addition to eliminating the need for laparoscopy in certain cases (25).

LEIOMYOMAS

Leiomyomas (fibroids) are the most common benign tumors encountered in gynecology as they are seen in about 20 – 30 % of women older than 35 years of age (26). By 50 years of age, about 70% of white women and more than 80% of black women will have had at least one leiomyoma with related significant symptoms in 15 to 30% of these women (26, 27). Histologically, leiomyomas consist of smooth muscle with varying amount of connective tissue and their growth is generally, estrogen dependent. The presence of leiomyosarcoma in a leiomyoma is rare and occurs in about 0.2% of cases. Leiomyomas are more prevalent in black women (26) and despite their estrogen dependency; only about 50 % show growth in association with pregnancy. In postmenopausal women, leiomyomas typically regress in size and are rarely of clinical concern. Leiomyomas have pseudocapsules, which are formed of compressed surrounding myometrium. Leiomyomas are usually multiple and most are asymptomatic and are discovered as palpable masses, or uterine enlargement, on routine gynecologic examination. On occasions, they are associated with abnormal uterine bleeding or pelvic pain.

Leiomyomas arise from the uterine myometrium and can occupy various anatomic positions within the uterus or surrounding structures. **Table 11.5** lists various types of leiomyomas in relation to their anatomic locations. The degree to which the leiomyoma projects into the endometrial cavity is of clinical importance as it helps to determine whether the leiomyoma can be resected hysteroscopically or not. In general, if the leiomyoma is protruding 50% or more into the endometrial cavity, hysteroscopic resection can be achieved. **Figure 11.27** is a schematic over an ultrasound image of various types of leiomyomas and **Figures 11.28** to **11.31** show various types of leiomyomas on ultrasound.

TABLE 11.5	Anatomic Locations of Leiomyomas (Figure 11.27)

- **Intramural:** The leiomyoma is within the myometrium with minimal or no bulging into the serosa or endometrium
- **Subserosal:** A significant portion of the leiomyoma is bulging into the serosal surface
- **Submucosal:** A significant portion of the leiomyoma is bulging into the endometrial cavity
- **Pedunculated:** The leiomyoma is exophytic and is attached to the uterus by a pedicle
- **Intracavitary:** The leiomyoma is within the endometrial cavity and is attached to the myometrium by a pedicle
- **Parasitic:** The leiomyoma is exophytic with blood supply obtained from an adjacent structure other than the uterus
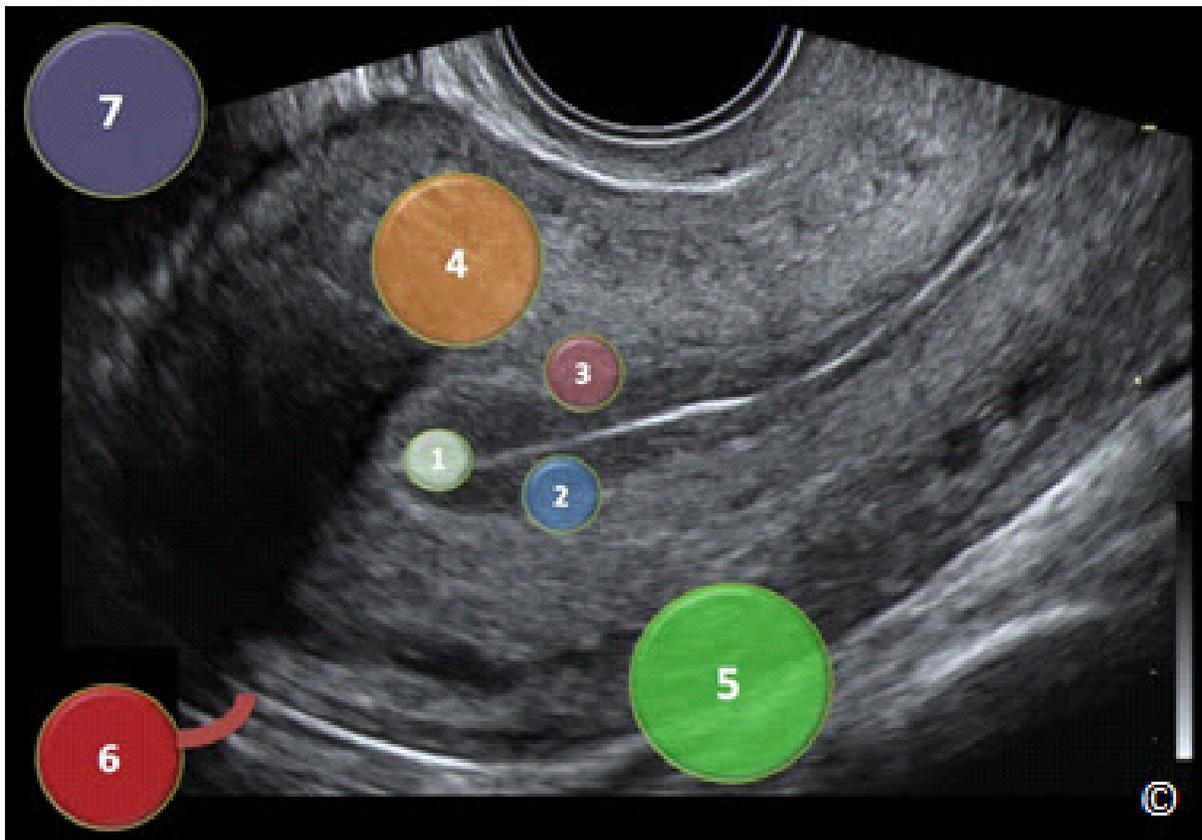
Figure 11.27: Transvaginal ultrasound of a midsagittal plane of the uterus with schematic overlay of leiomyomas to describe their anatomic locations. 1 = Intracavitary, 2 = Submucosal with > 50% into the endometrial cavity. 3 = Submucosal with < 50% into the endometrial cavity. 4 = Intramural. 5 = Subserosal. 6 = Pedunculated. 7 = Parasitic.
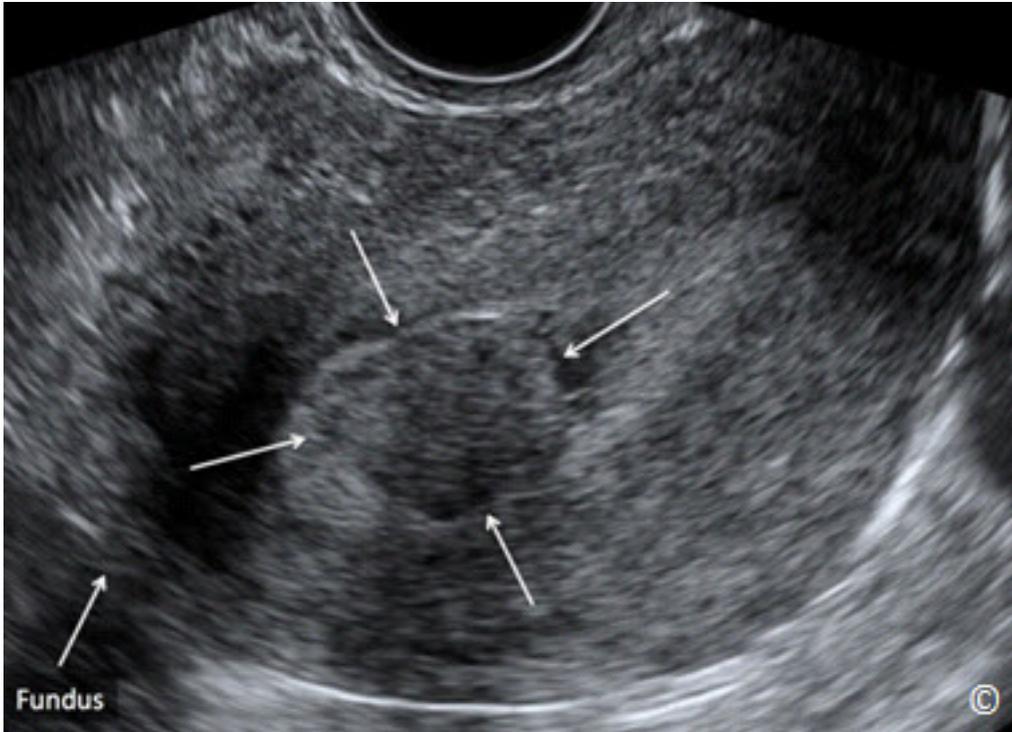
Figure 11.28: Transvaginal ultrasound of a midsagittal plane of the uterus showing a submucosal (intracavitary) leiomyoma (arrows). Uterine fundus is labeled for image orientation. See **Table 11.6** for sonographic features. Image is courtesy of Dr. Bernard Benoit.
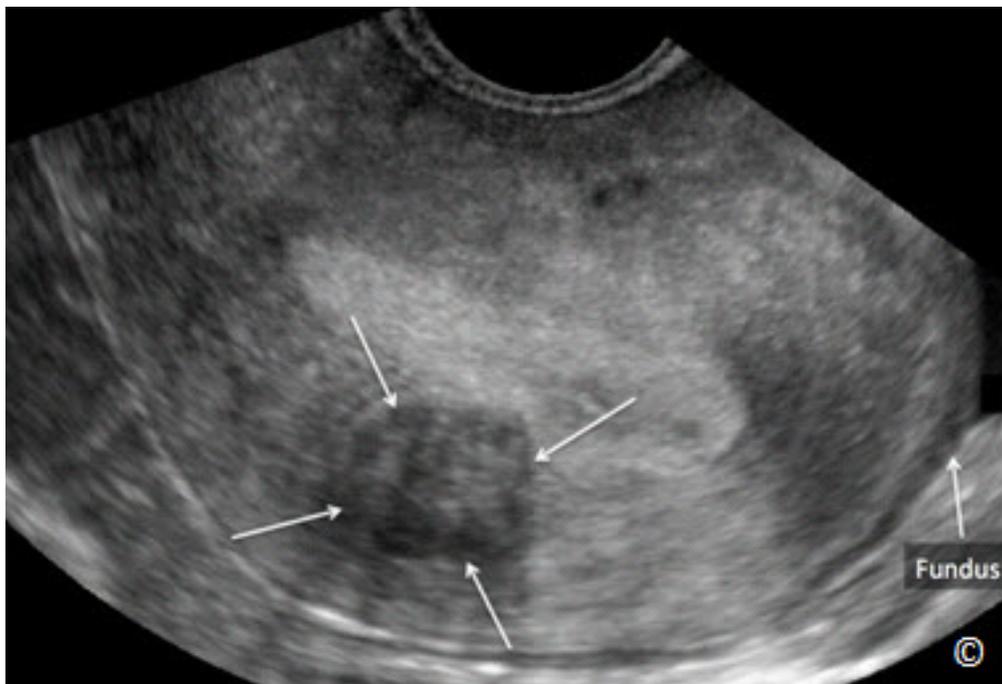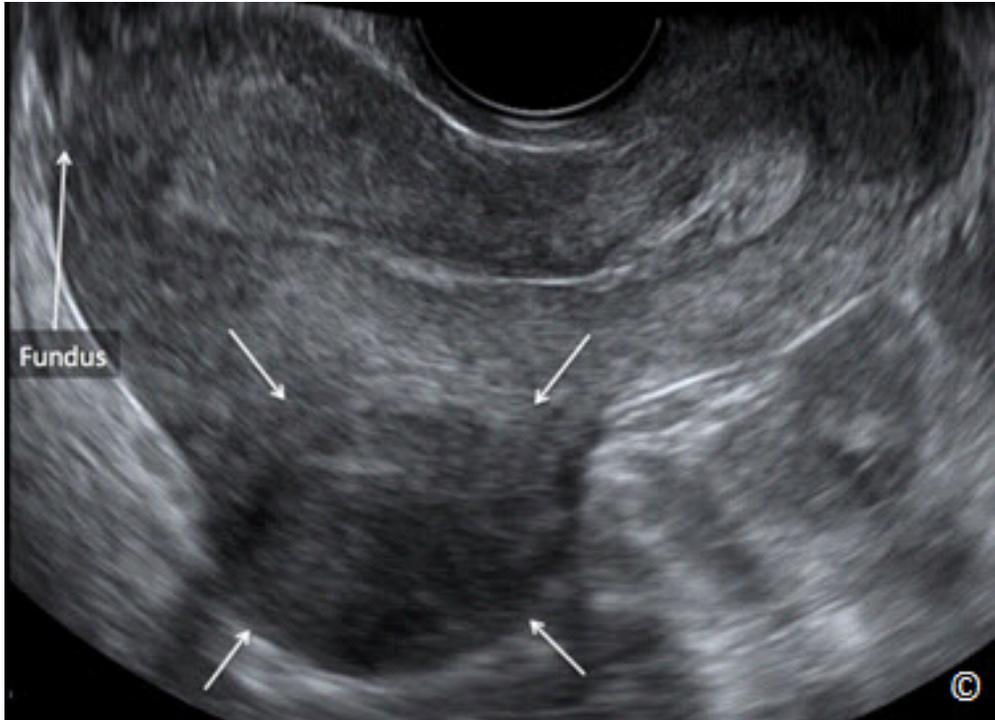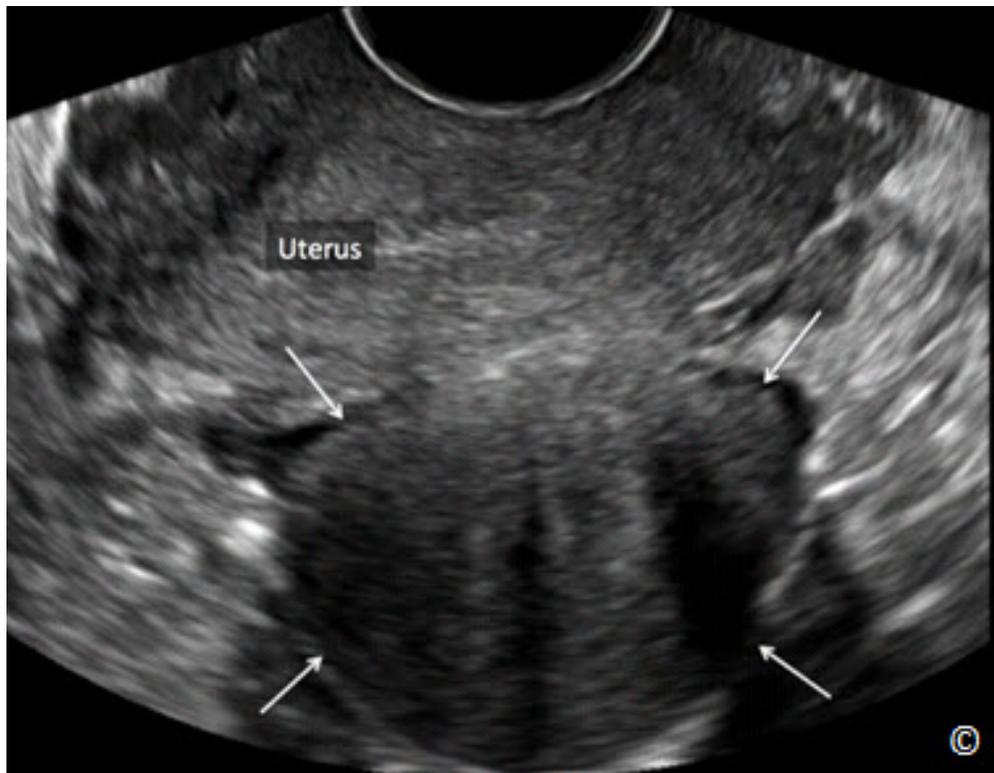

Figure 11.29: Transvaginal ultrasound of a midsagittal plane of the uterus showing an intramural leiomyoma (arrows). Uterine fundus is labeled for image orientation. See **Table 11.6** for sonographic features. Image is courtesy of Dr. Bernard Benoit.

Figure 11.30: Transvaginal ultrasound of a midsagittal plane of the uterus showing a subserosal leiomyoma (arrows). Uterine fundus is labeled for image orientation. See **Table 11.6** for sonographic features. Image is courtesy of Dr. Bernard Benoit.

Figure 11.31: Transvaginal ultrasound of a midsagittal plane of the uterus showing a pedunculated leiomyoma (arrows) in a posterior location to the uterus. Uterine fundus is labeled for image orientation. See **Table 11.6** for sonographic features.

The sonographic features of leiomyomas are listed in **Table 11.6** and the various types of leiomyoma's degeneration are listed in **Table 11.7**. Hyaline degeneration is the most common and appears as anechoic areas within the central portion of a leiomyoma (**Figure 11.32**).

TABLE 11.6	Sonographic Features of Leiomyomas

- Solid echogenic mass arising from the uterine myometrium
- Well defined contour (pseudocapsule)
- Whorled appearance due to smooth muscle and connective tissue arranged in a concentric pattern
- Significant attenuation of ultrasound beam
- Characteristic shadow pattern described as "venetian blind shadowing" (**Figure 11.33**)
- Minimal to moderate vascularity on color Doppler
- When pedunculated, the solid leiomyoma tends to move with the uterus and distinctly from the ovary (**Clip 11.1**)
- Color Doppler can on occasions identify a stalk and connect it to the uterus in pedunculated leiomyomas
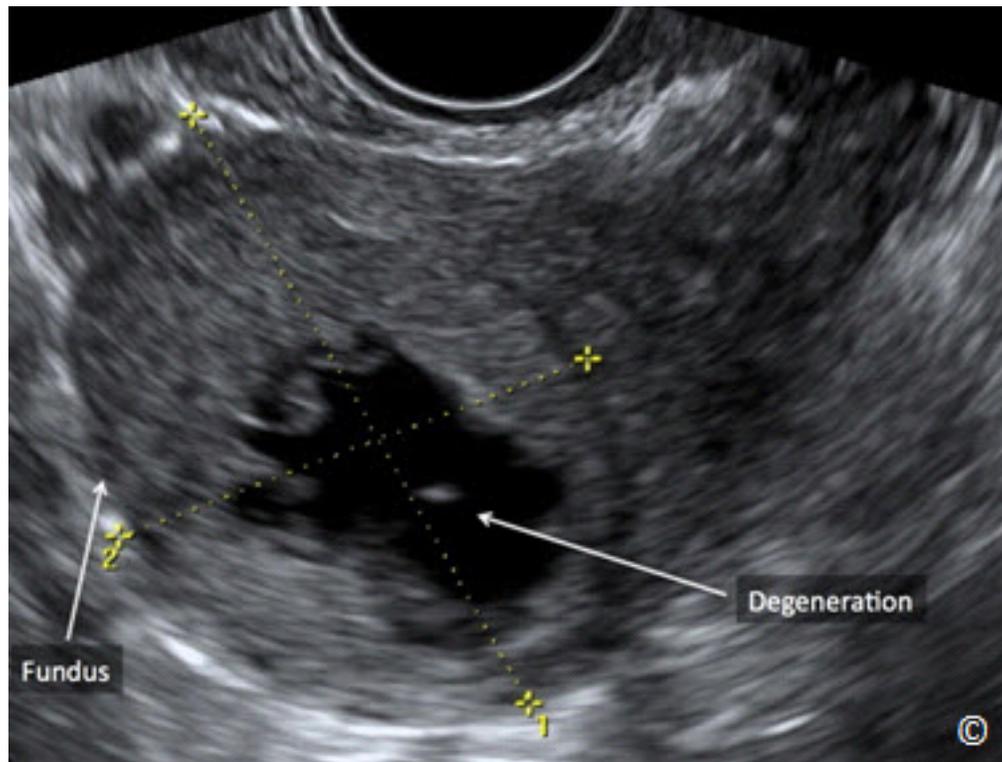
Figure 11.32: Transvaginal ultrasound showing a hyaline degeneration of an intramural leiomyoma (labeled). The uterine fundus is labeled for image orientation.
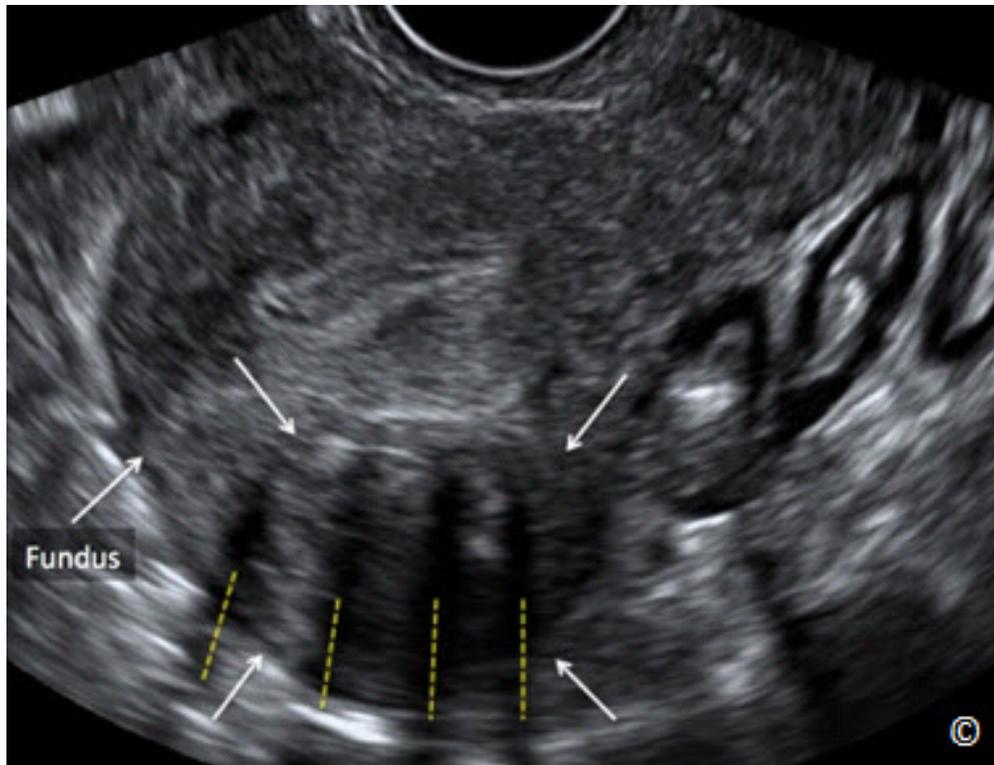
Figure 11.33: Transvaginal midsagittal plane of a uterus showing a subserosal leiomyoma (arrows). Note the typical leiomyoma shadowing described as "venetian blinds shadowing" (dashed lines). The uterine fundus is labeled for image orientation.

TABLE 11.7	Types of Leiomyoma Degeneration
- Atrophic - Hyaline - Carneous - Myxoid - Calcific - Cystic - Hemorrhagic	

ENDOMETRIAL ABNORMALITIES

Abnormal Uterine Bleeding:

Abnormal uterine bleeding (AUB) is a term that describes abnormal menstrual flow in women of reproductive age. AUB can be related to abnormal volume, duration, frequency and regularity of menstrual flow. In an effort to standardize diagnosis and management of AUB, the International

Federation of Gynecology and Obstetrics (FIGO) in 2011, introduced a new classification of AUB known by the acronym PALM-COEIN, which stands for polyps, adenomyosis, leiomyoma, malignancy (hyperplasia), coagulopathy, ovulatory dysfunction, endometrial iatrogenic and not yet classified (28). The American Congress of Obstetrics and Gynecology (ACOG) supported the adoption of this classification in the practice bulletin on diagnosis of AUB in reproductive age women (29). The term dysfunctional uterine bleeding, which has been commonly used to describe AUB, should be abandoned (28, 29).

The evaluation of women with AUB is beyond the scope of this textbook, but in general should include a history, physical examination, laboratory and imaging studies and endometrial sampling when indicated, based upon the age of symptomatic women. There is insufficient evidence to recommend the use of transvaginal ultrasound for endometrial thickness evaluation in AUB in women of reproductive age unless there are risk factors for endometrial carcinoma. Transvaginal ultrasonography is useful however as a screening test to assess the endometrial cavity for leiomyomas and polyps. In postmenopausal women, transvaginal ultrasound has the ability to exclude malignancy when the endometrial lining is uniform and is 4 mm or less. This is discussed in more details later in this chapter.

Endometrial Polyps and Submucosal Leiomyomas:

Common focal intracavitary endometrial lesions include polyps and submucosal leiomyomas as they account for 30% and 10% of causes of postmenopausal bleeding respectively (30). Sonohysterography has been shown to be a superior imaging modality in the evaluation of intracavitary endometrial lesions such as polyps (**Figure 11.34**) and leiomyomas, when compared to transvaginal ultrasound alone (31). The efficacy of sonohysterography in the diagnosis of endometrial polyps and submucosal leiomyomas has been shown to be equal to hysteroscopy in some series (32).
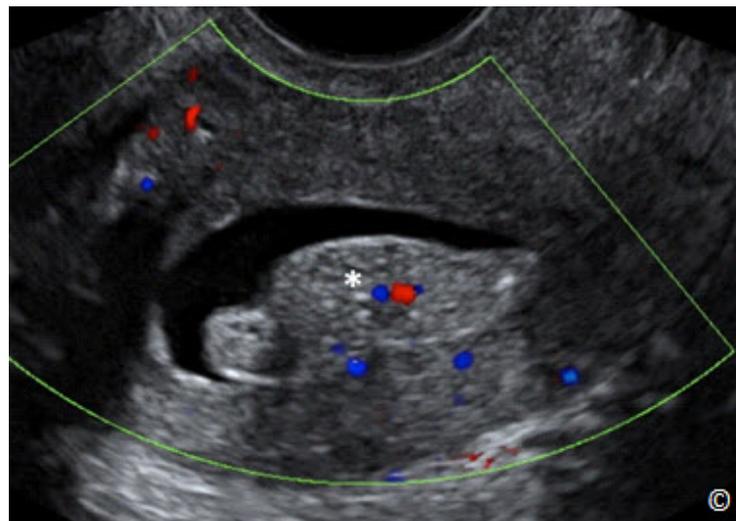

Figure 11.34: Transvaginal sonohysterography with color Doppler of a midsagittal plane of the uterus showing an endometrial polyp (asterisk). Note the increased echogenicity of the polyp as compared to myometrial tissue.

Endometrial polyps appear on sonohysterography as more echogenic than the surrounding myometrium, completely contained within the endometrial cavity with no extension into the myometrium, homogeneous in echo texture with a narrow base of attachment to the underlying myometrium (**Figure 11.34**). Color Doppler may demonstrate a vascular pedicle at the base of the polyp in most cases (**Figure 11.35** and **11.36**). Cystic changes within a polyp are occasionally seen and polyps can also be seen in the isthmic portion of the cavity (**Figure 11.36**) and endocervical canal. Submucosal leiomyomas appear on sonohysterography as less echogenic than the surrounding endometrium, broad-based and lift the surrounding endometrium as they project to varying degrees into the cavity (**Figure 11.37**). Given that submucosal leiomyomas arise from the subendometrial myometrium, a portion of the leiomyoma extends into the myometrium: a differentiating feature from an endometrial polyp. Submucosal leiomyomas tend to shadow the ultrasound beam, another important distinctive feature from endometrial polyps (**Figure 11.37**). **Table 11.7** lists differentiating features of polyps and submucosal leiomyomas. The degree to which the submucosal leiomyoma projects into the endometrial cavity is of clinical relevance. Extension of a leiomyoma by more than 50% of its surface into the cavity allows for possible hysteroscopic resection.
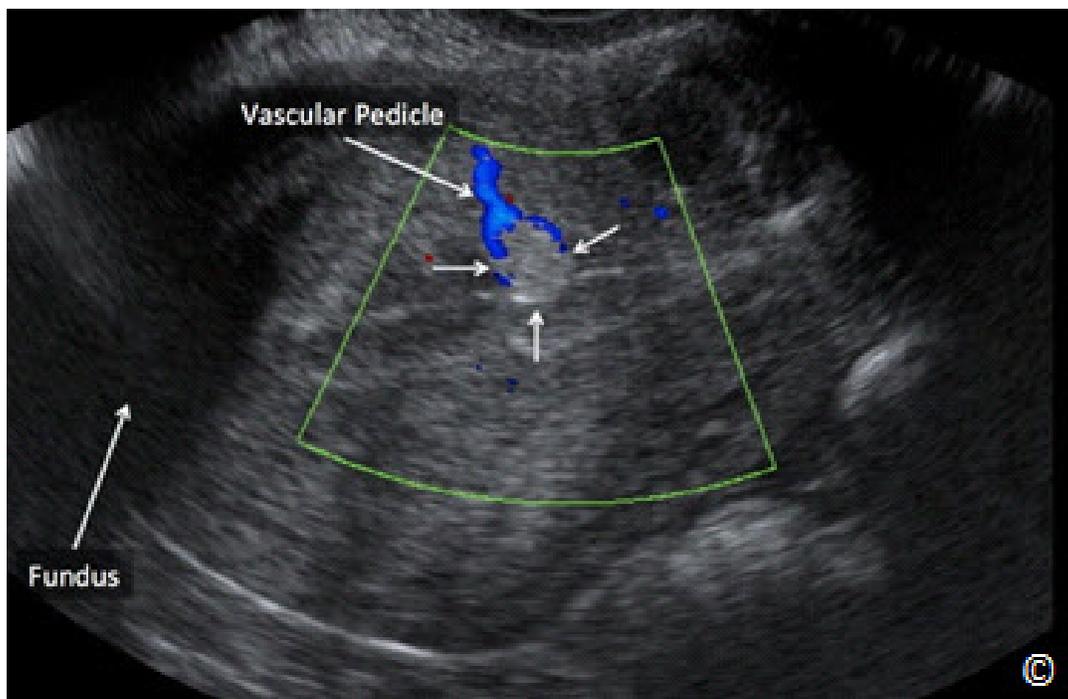

Figure 11.35: Transvaginal ultrasound with color Doppler of a midsagittal plane of the uterus showing a small endometrial polyp (arrows). Note the increased echogenicity of the polyp as compared to myometrial tissue and a vascular pedicle noted on color Doppler. The uterine fundus is labeled for image orientation.
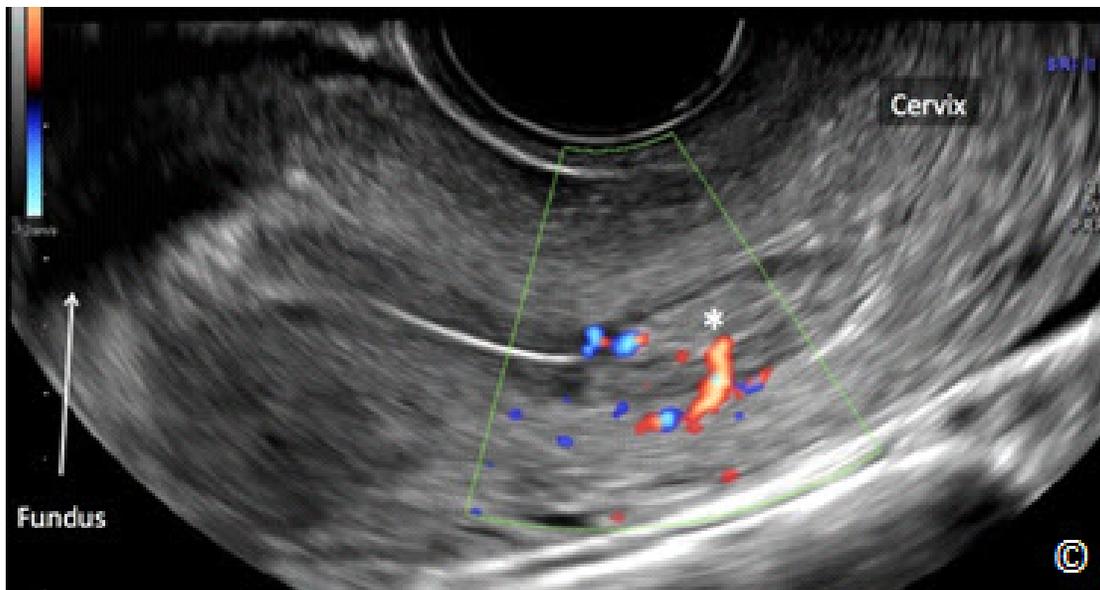
Figure 11.36: Transvaginal ultrasound with color Doppler of a midsagittal plane of the uterus showing an endometrial polyp (asterisk) in the isthmic portion of the endometrial cavity. Note the presence of a vascular pedicle on color Doppler. The uterine fundus is labeled for image orientation.
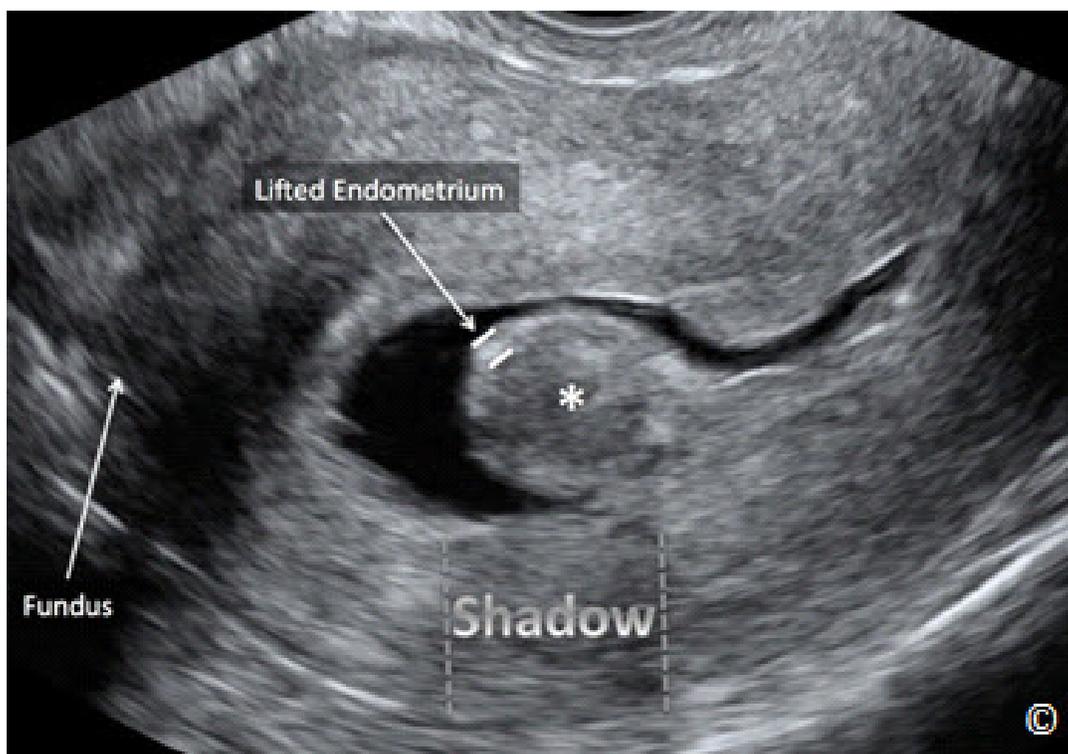

Figure 11.37: Transvaginal sonohysterography of a midsagittal plane of the uterus showing a submucosal leiomyoma (asterisk). Note that the echogenicity of the leiomyoma is comparable to that of the myometrium. The lifted endometrium (labeled – equal sign) is noted surrounding the leiomyoma in the endometrial cavity. Also note the shadowing (shadow – dashed lines) from the leiomyoma. The uterine fundus is labeled for image orientation. Image is courtesy of Dr. Bernard Benoit.

TABLE 11.7	Differentiating Sonographic Features of Endometrial Polyps and Submucosal Leiomyomas

- Polyp are contained within the endometrial cavity whereas Leiomyomas extend into the myometrium
- Echogenicity of polyps is similar to endometrial lining whereas echogenicity of leiomyomas is similar to myometrium (less)
- Polyps tend to have a visible vascular pedicle on color Doppler and are homogeneous in echotexture
- Leiomyomas lift the endometrial lining
- Leiomyomas tend to shadow the ultrasound beam

Endometrial Adhesions and Retained Products of Conception:

Other endometrial pathology amenable to diagnosis by sonohysterography includes intrauterine adhesions, and retained products of conception. Intrauterine adhesions are clearly visible on sonohysterography as thick or thin echogenic bands that attach to the endometrial walls (**Figure 11.38**). Sonohysterography is the best imaging modality for the detection of intrauterine adhesions (33) and should be considered in patients with prior intrauterine instrumentation. Retained products of conception appear as an echogenic mass within the endometrial cavity (**Figure 11.39**). They are typically seen in women following an abortion, a miscarriage or a delivery.
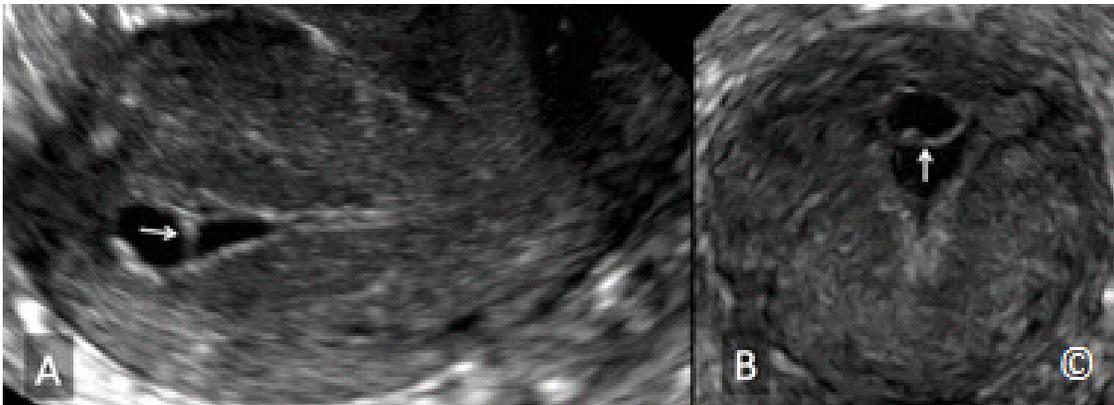

Figure 11.38: Transvaginal sonohysterography in a patient with suspected endometrial adhesions. Note the presence of a thin reflective membrane in the sagittal (arrow in A) and coronal (arrow in B) plane. These planes were obtained from a 3D volume.

Figure 11.39: Transvaginal sonohysterography of the uterus in sagittal plane showing an echogenic mass (arrows) suggestive of retained products of conception. This patient had a complicated delivery 5 weeks prior.

Endometrial Hyperplasia and Cancer:

Endometrial cancer is the most common gynecologic cancer in the United States, with vaginal bleeding being the most common presenting symptom (34, 35). When postmenopausal women present with vaginal bleeding, a systemic approach should be performed to rule-out endometrial cancer or hyperplasia. An endometrial thickness that is 4 mm or less on a transvaginal ultrasound in women presenting with postmenopausal bleeding, practically excludes endometrial cancer and further endometrial evaluation is not warranted. Transvaginal ultrasound is therefore a reasonable first approach to the evaluation and management of postmenopausal bleeding. If the endometrial thickness is greater than 4 mm, further evaluation is needed with endometrial sampling, sonohysterography or hysteroscopy. If endometrial sampling has been performed first and insufficient tissue was obtained for diagnosis, a transvaginal ultrasound can be performed and if it shows an endometrial thickness of 4 mm or less, no further evaluation is needed (36). The significance of an endometrial thickness of greater than 4 mm in asymptomatic women is unclear and should not prompt further work-up unless the patient is at a significantly increased risk for endometrial cancer (37). It is important to note that endometrial thickness should only be measured when a midsagittal plane of the uterus is obtained with clear depiction of the endometrial thickness from the fundal to the uterine isthmic / cervical area (**Figure 11.13**). If such a plane cannot be obtained, or visualization of the endometrial thickness is unclear,

transvaginal ultrasound cannot be used in the evaluation of women with postmenopausal bleeding and alternate methods should be obtained. The validity of transvaginal ultrasound as a screening tool for endometrial cancer has not been established and thus it should not be used for this clinical indication.

Endometrial hyperplasia can be diffuse or focal. Diffuse endometrial hyperplasia will appear on sonohysterography as thickening of the endometrium. Focal endometrial hyperplasia on the other hand is seen as a broad-based echogenic mass that does not distort the endometrial-myometrial junction. Differentiating focal endometrial hyperplasia from an endometrial polyp can at times be difficult. Endometrial cancer has similar sonographic characteristics to endometrial hyperplasia or an enlarged polyp, with the exception of myometrial invasion, which can be occasionally visible on ultrasound. **Figures 11.40** to **11.42** represent transvaginal ultrasounds of endometrial and uterine cancers.
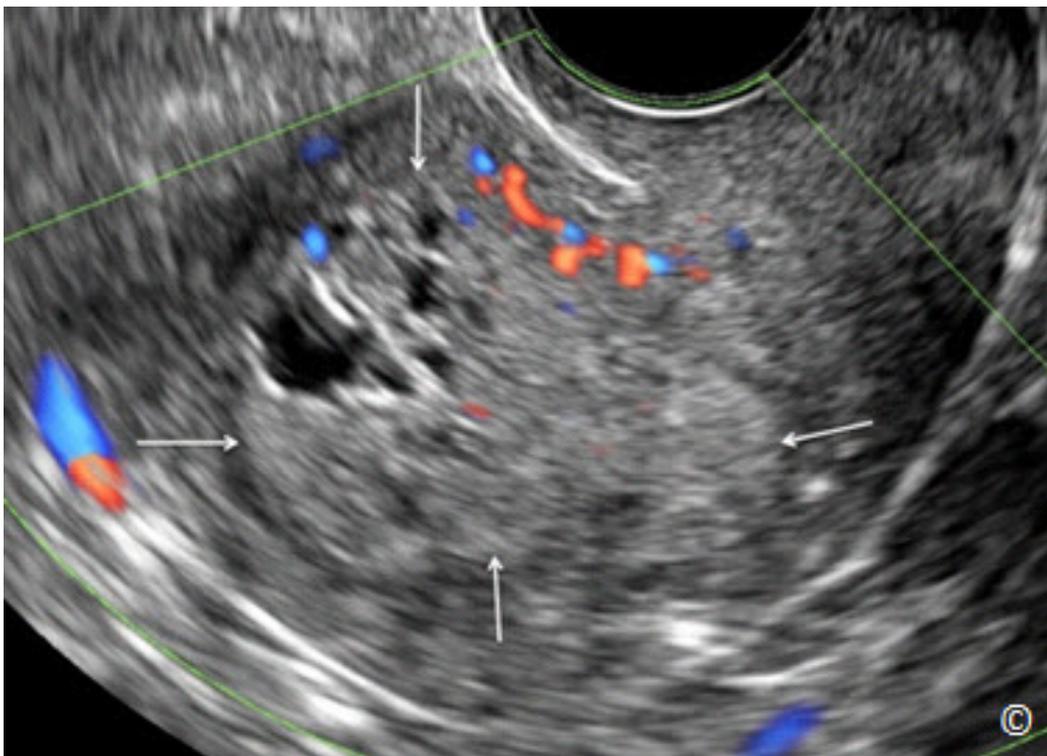
Figure 11.40: Transvaginal ultrasound of a sagittal plane of the uterus in a woman with endometrial cancer. Note the enlarged, heterogeneous and thickened endometrium (arrows).

Figure 11.41: Transvaginal sonohysterography of a sagittal plane of the uterus in a woman with endometrial cancer. Note the multiple papillary projections (arrows) in the endometrial cavity.
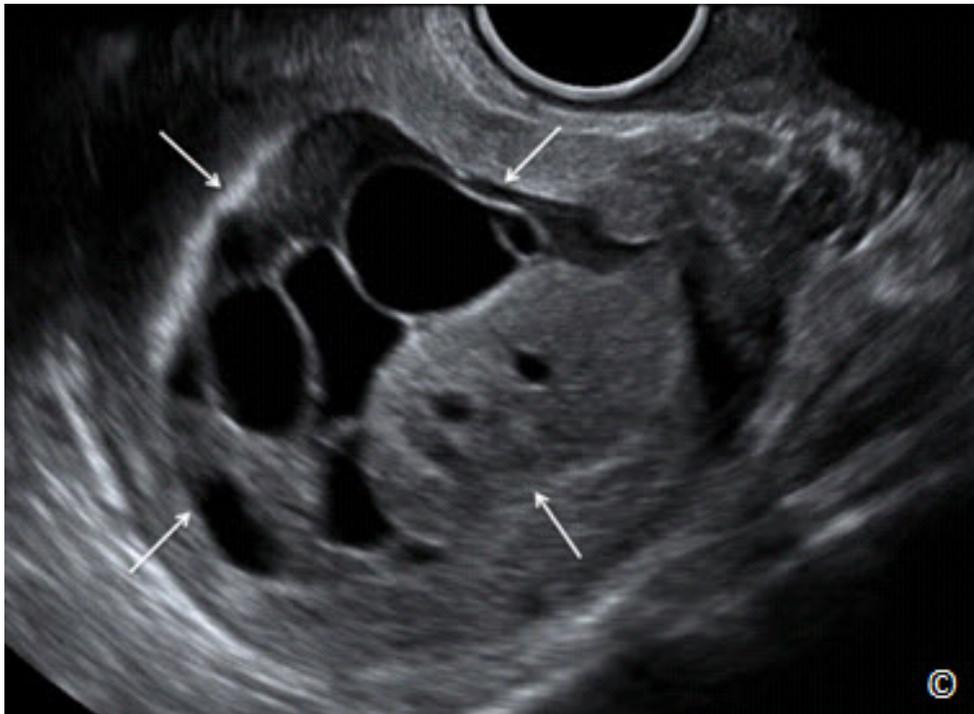

Figure 11.42: Transvaginal ultrasound of a parasagittal plane of the uterus in a patient presenting with a uterine mass. Note the presence of a complex mass (arrows), which was a uterine stromal sarcoma on pathologic evaluation.

Arteriovenous Malformations:

Uterine arteriovenous malformations (AVM) are rare and represent direct communications between the arterial and venous system. They typically arise following instrumentation of the endometrial cavity, commonly in association with pregnancy loss or delivery. On occasions, they are associated with malignancies, infections or retained products of conception in molar pregnancies (38, 39). AVM can also be congenital in nature and as such, they are less common and symptomatic than the acquired variety (40).

The most common clinical presentation of AVM is heavy vaginal bleeding in patients who had instrumentation of the endometrial cavity following a pregnancy. Other less common symptoms include pelvic pain and dyspareunia. The diagnosis of AVM is best achieved by a transvaginal ultrasound with color and pulsed Doppler. On grey scale ultrasound, AVM are seen as anechoic spaces within the uterus, with irregular contour, typically located within the myometrium near its junction with the endometrium (**Figure 11.43**). Color Doppler shows turbulent flow within the anechoic spaces with aliasing (**Figure 11.44**), and pulsed Doppler demonstrates high-velocity, low impedance flow patterns (**Figure 11.45**). Color and pulsed Doppler is helpful in confirming the presence of AVM and also in differentiating AVM from pseudoaneurysms. Pseudoaneuryms, which can also occur following instrumentation of the uterine cavity, have swirling arterial blood in them with high-velocity and high impedance blood flow patterns on color and pulsed Doppler evaluation (41).
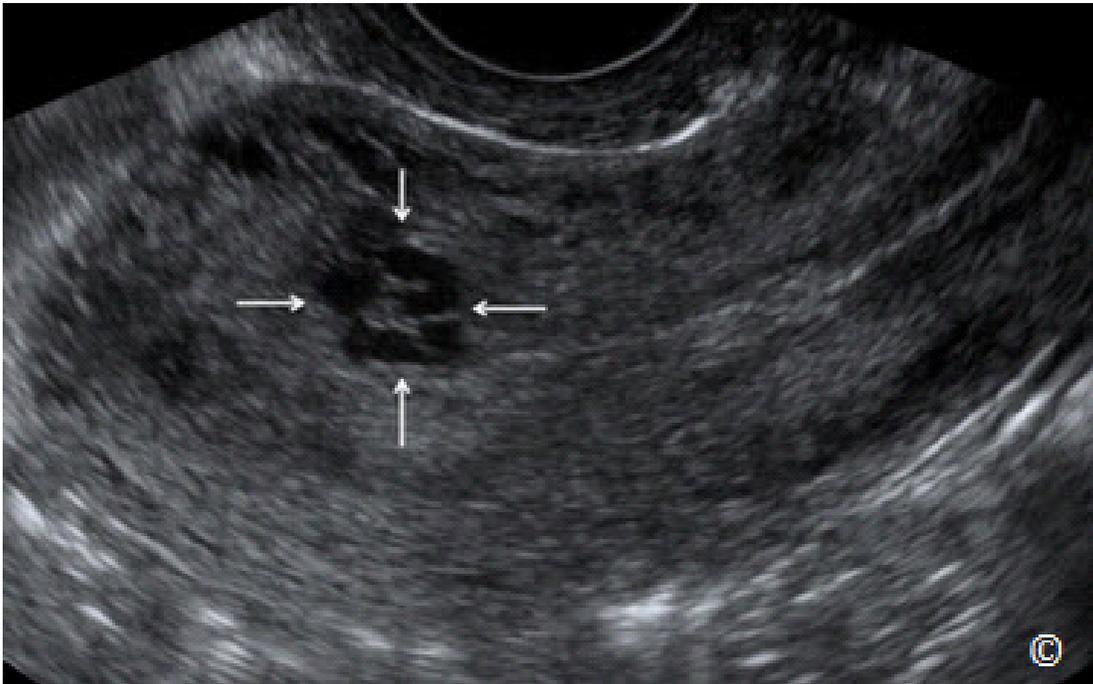

Figure 11.43: Transvaginal ultrasound of a sagittal plane of the uterus showing an arterio-venous malformation (AVM) (arrows). Note the sonographic appearance of AVM as anechoic spaces, with irregular contour, located within the myometrium near its junction with the endometrium.
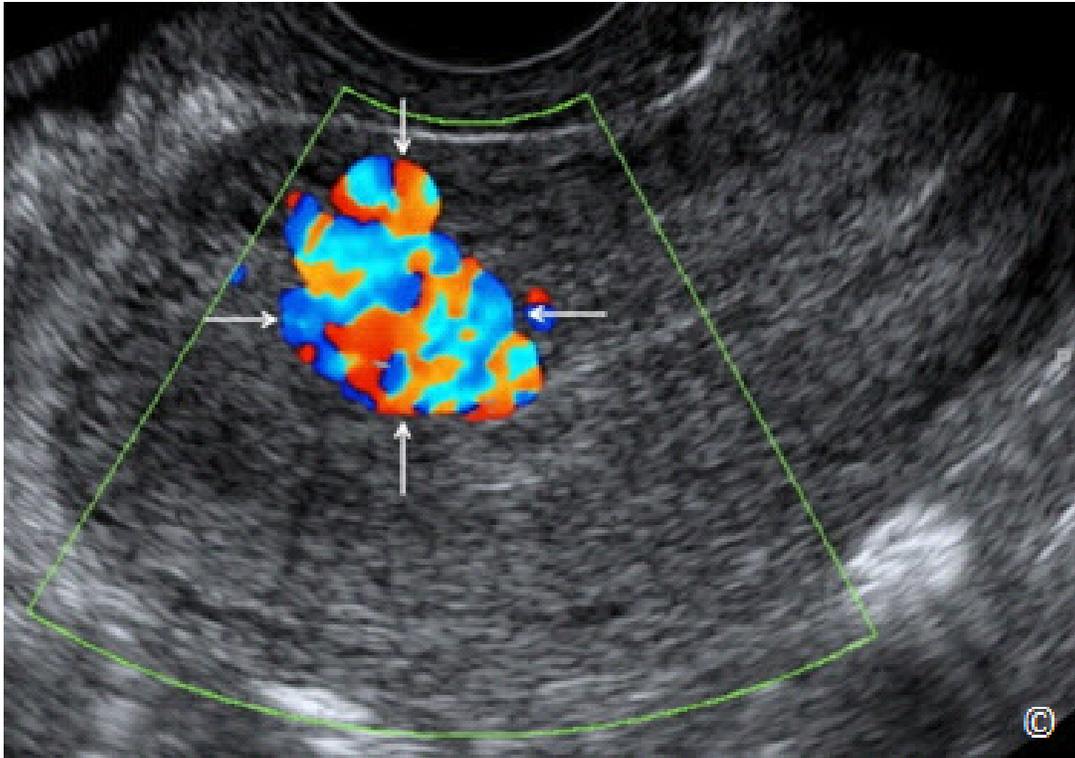
Figure 11.44: Transvaginal ultrasound with color Doppler of a sagittal plane of the uterus showing the same arterio-venous malformation (AVM) (arrows) as that in **Figure 11.43.** Note the presence of blood flow within the AVM with turbulence and aliasing.
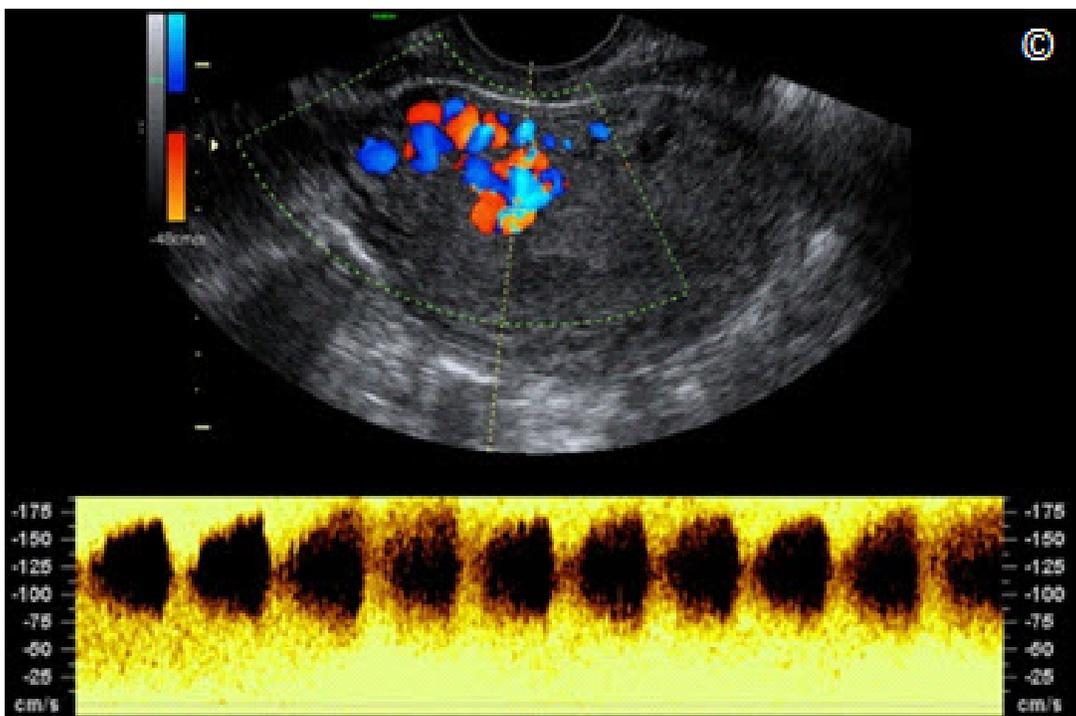

Figure 11.45: Transvaginal ultrasound with color and pulsed Doppler of a sagittal plane of the uterus showing the same arterio-venous malformation (AVM) (arrows) as that in figure 11.43. Note the pulsed Doppler waveforms showing low-impedance, high velocity (100 cm/sec) flow.

Management of AVM should include a conservative approach following diagnosis, assuming that the bleeding is not very heavy and the patient is not significantly anemic. Our experience and that of others suggest resolution of AVM in a significant number of women with conservative management over a 2-5 months period (42). Transcatheter arterial embolization is the preferred method of treatment if conservative management fails, or bleeding is very heavy. Transcatheter arterial embolization has a reported success rate of 50 – 70 % (43). Long-term prognosis is good for women with AVM that regressed following conservative management or with arterial embolization with reports of successful pregnancies (44).

Copyrighted-Ultrasound in Obstetrics & Gynecology: A Practical Approach
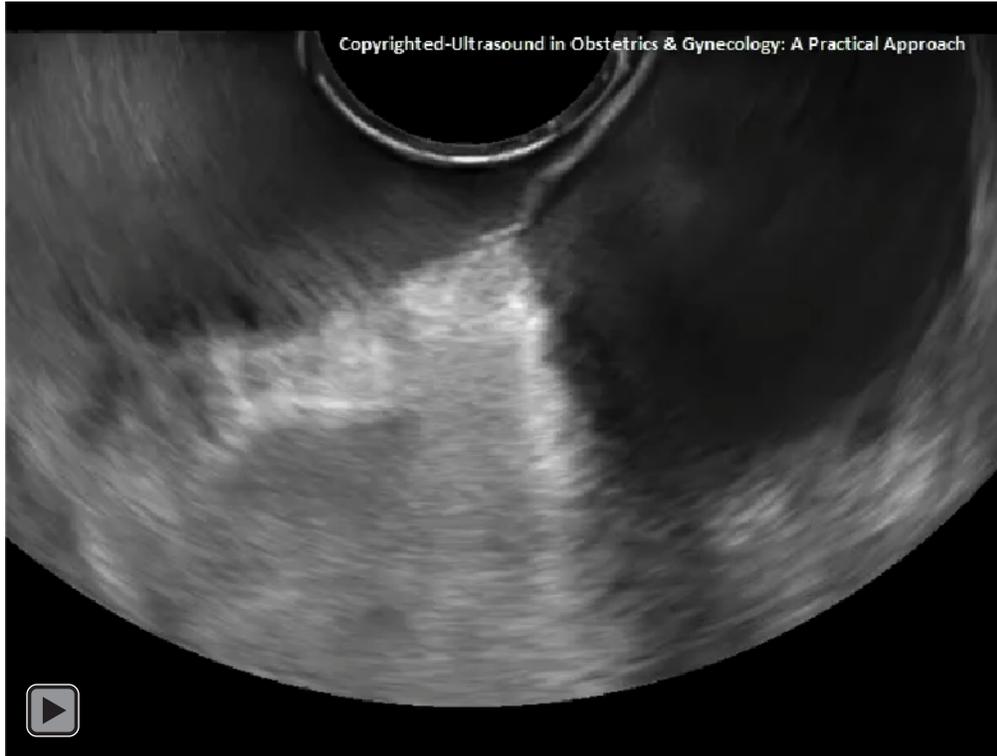
References:

1) AIUM practice guideline for the performance of pelvic ultrasound examinations. American Institute of Ultrasound in Medicine. J Ultrasound Med. 2010; 29 (1):166-72.
2) AIUM practice guideline for ultrasonography in reproductive medicine. American Institute of Ultrasound in Medicine; Society for Reproductive Endocrinology and Infertility; American Society of Reproductive Medicine. J Ultrasound Med. 2009;28(1):128-37.
3) Bonnamy L, Marret H, Perrotin F, Body G, Berger C, Lansac J. Sonohysterography: a prospective survey of results and complications in 81 patients. Eur J Obstet Gynecol Reprod Biol 2002;102:42-47.
4) Merz E, Miric-Tesanic D, Bahlmann F, Weber G, Wellek S. Sonographic size of uterus and ovaries in pre- and postmenopausal women. Ultrasound Obstet Gynecol. 1996;7(1):38-42.
5) Fleischer AC, Kalemeris GC, Entman SS. Sonographic depiction of the endometrium during normal cycles. Ultrasound Med Biol. 1986;12(4):271-7.
6) Santolaya-Forgas J. Physiology of the menstrual cycle by ultrasonography. J Ultrasound Med. 1992;11(4):139-42.
7) Duijkers IJ, Klipping C. Ultrasonographic assessment of endocervix and cervical mucus in ovulatory menstrual cycles. Eur J Obstet Gynecol Reprod Biol. 2000;93(1):13-7.
8) R Azziz. Adenomyosis: current perspectives. Obstet Gynecol Clin North Am 1989;16:221-35.
9) Sakhel K, Abuhamad A. Sonography of Adenomyosis. J Ultrasound Med 2012 May;31(5):805-8.
10) Botsis D, Kassanos D, Antoniou G, Pyrgiotis E, Karakitsos P, Kalogirou D. Adenomyoma and leiomyoma: differential diagnosis with transvaginal sonography. J Clin Ultrasound. 1998;26(1):21-5.
11) Chiang CH, Chang MY, Hsu JJ. Tumor vascular pattern and blood flow impedance in the differential diagnosis of leiomyoma and adenomyosis by color Doppler sonography. *J Assist Reprod Genet*. 1999;16(5):268-75.
12) Acien P, Acien M, Sanchez-Ferrer ML. Complex malformations of the female genital tract. New types and revision of classification. Hum Reprod 2004; 19:2377-2384
13) Raga F, Bauset C, Remohi J, Bonilla-Musoles F, Simon C, Pellicer A. Reproductive impact of congenital Mullerian anomalies. Hum Reprod 1997;12(10):2277-2281
14) Rock JA and Schlaff WD. The obstetric consequences of uterovaginal anomalies. Fertil Steril 1985; 43:681
15) Ludmir J, Samuels P, Brooks S. Pregnancy outcome of patients with uncorrected uterine anomalies managed in a high risk obstetric setting. Obstet Gynecol 1990; 75:906
16) The American Fertility Society. The American Fertility Society classifications on adnexal adhesions, distal tubal occlusion, tubal occlusion secondary to tubal ligation, tubal

pregnancies, Mullerian anomalies and intrauterine adhesions. Fertil Steril 1988;49:944-955.

17) Pellerito JS, McCarthy SM, Doyle MB, Glickman MG, DeCherney AH. Diagnosis of uterine anomalies: relative accuracy of MR imaging, endovaginal ultrasound, and hysterosalpingography. Radiology 1992; 183:795-800.

18) Bocca SM, Abuhamad AZ. Use of 3-dimensional sonography to assess uterine anomalies. J Ultrasound in Medicine 2013;32:1.

19) Randolph J, Ying Y, Maier D, Schmidt C, Riddick D. Comparison of real time ultrasonography, hysterosalpingography, and laparoscopy/hysteroscopy in the evaluation of uterine abnormalities and tubal patency. Fertil Steril 1986; 5:828-832.

20) Salim R, Woelfer B, Backos M, Regan L, Jurkovic D. Reproducibility of three-dimensional ultrasound diagnosis of congenital uterine anomalies. Ultrasound Obstet Gynecol 2003; 21:578–582.

21) Abuhamad A, Singleton S, Zhao Y, Bocca S. The Z technique: an easy approach to the display of the mid-coronal plane of the uterus in volume sonography. J Ultrasound Med 2006; 25:607-612.

22) Deutch T, Bocca S, Oehninger S, et al. Magnetic resonance imaging versus three-dimensional transvaginal ultrasound for the diagnosis of Mullerian anomalies. Fertil Steril 2006;86:S308

23) Bocca S, Abuhamad A. Use of 3-Dimensional Sonography to Assess Uterine Anomalies. J Ultrasound Med 2013;32:1-6.

24) Deutch TD, Abuhamad AZ. The role of 3-dimensional ultrasonography and magnetic resonance imaging tin the diagnosis of mullerian duct anomalies: a review of the literature. J Ultrasound Med 2008;27(3):413-23.

25) Bocca SM, Oehninger S, Stadtmauer L, Agard J, Duran H, Sarhan A, Horton S, Abuhamad A. Prospective study to evaluate the costs, accuracy, risks and benefits of 3D ultrasound compared to other imaging modalities in women with intrauterine lesions. J Ultrasound Med 2012;31:81-85.

26) Baird DD, Dunson DB, Hill MC, Cousins D, Schectman JM. High cumulative incidence of uterine leiomyoma in black and white women: ultrasound evidence. Am J Obstet Gynecol 2003;188:100-7.

27) Catherino WH, Parrott E, Segars J. Proceedings from the National Institute of Child Health and Human Development conference on the Uterine Fibroid Research Update Workshop. Fertil Steril 2011;95:9-12

28) Munro MG, Critchley HO, Broder MS, Fraser IS. FIGO classification system (PALM-COEIN) for causes of abnormal uterine bleeding in nongravid women of reproductive age. FIGO Working Group on Menstrual Disorders. Int J Gynaecol Obstet 2011;113:3–13.

29) ACOG Practice Bulletin on Diagnosis of Abnormal Uterine Bleeding in Reproductive-Aged Women. Number 128, July 2012.

30) N O'Connoll LP, Fries MH, Aeringue E, Brehm W. Triage of abnormal postmenopausal bleeding: a comparison of endometrial biopsy and transvaginal sonohysterography versus fractional curettage with hysteroscopy. Am J Obstet Gynecol 1998;178:956-61.

31) Schwarzler P, Concin H, Bosch H, Berlinger A, Wohlgenannt K, Collins WP, et al. An evaluation of sonohysterography and diagnostic hysteroscopy for the assessment of

32) Kelekci S, Kaya E, Alan M, Alan Y, Bilge U, Mollamahmutoglu L. Comparison of transvaginal sonography, saline infusion sonography, and office hysteronscopy in reproductive-aged women with or without abnormal uterine bleeding. Fertil Steril 2005;84:682–6.

33) Soares SR, Barbosa dos Reis MM, Camargos AF, Diagnostic accuracy of sonohysterography, transvaginal sonography, and hysterosalpingography in patients with uterine cavity diseases. Fertil Steril 2000;73:406-11.

34) American Cancer Society: Cancer Facts and Figures 2008. Atlanta, Georgia ACS: 2008. www.cancer.org/STT/2008CAFFFinalSecured.pdf

35) Goldstein RB, Bree RL, Benson CB, Benacerraf BR, Bloss JD, Carlos R et al. Evaluation of the woman with postmenopausal bleeding. Society of Radiologists in Ultrasound-Sponsored consensus conference statement. J Ultrasound Med 2001;20:1025-36

36) Bakour SH, Khan KS, Gupta JK. Controlled analysis of factors associated with insufficient samples on outpatient endometrial biopsy. BJOG 2000; 107:1312-4.

37) Fleischer AC, Wheeler JE, Lindsay I, Hendrix SL, Grabill S, Kravitz B. An assessment of the value of ultrasonographic screening for endometrial disease in postmenopausal women without symptoms. A J Obstet Gynecol 2001; 184:70-5.

38) Kwon JH, Kim GS. Obstetric iatrogenic arterial injuries of the uterus: diagnosis with US and treatment with transcatheter arterial embolization. Radiographics 2002; 22:35–46.

39) Yahi-Mountasser H, Collinet P, Nayama M, Boukerrou M, Robert Y, Deruelle P. Les malformations artério-veineuses intra-utérines. À propos de 4 cas. J Gynecol Obstet Biol Reprod (Paris) 2006; 35:614–20.

40) Bauer V, Briex M, De Meeus JB, Drouineau J, Ferrie JC, Magnin G. Malformation artérioveineuse congénitale de l'artère iliaque interne découverte au cours de la grossesse. J Gynecol Obstet Biol Reprod (Paris) 1993; 22:312–6.

41) S. Sanguin, S. Lanta-Delmas, A. Le Blanche, E. Grardel-Chambenoit, P. Merviel, J. Gondry, R. Fauvet. Diagnostic et traitement des malformations artério-veineuses utérines (MAVU) en 2011

42) Timmerman D, Van Den Bosch T, Peeraer K, Debrouwere E, Van Schoubroeck D, Stockx L, et al. Vascular malformations in the uterus: ultrasonographic diagnosis and conservative management. Eur J Obstet Gynecol Reprod Biol 2000; 92:171–8.

43) Kwon JH, Kim GS,: Obstetric iatrogenic arterial injuries of the uterus: Diagnosis with US and treatment with transcatheter arterial embolization. Radiographics 2002;22:35.

44) Delotte J, Chevallier P, Benoit B, Castillon JM, Bongain A. Pregnancy after embolization therapy for uterine arteriovenous malformation. Fertil Steril 2006;85:228.

INTRODUCTION

Ultrasound is the preferred imaging modality for the assessment of the pelvis and in particular the uterus and the ovaries for the presence of pathology. Advantages that ultrasound has over other imaging modalities, such as Computed Tomography and Magnetic Resonance Imaging, are obvious and includes the lower cost of ultrasound, its bedside portability, and the ability of the transvaginal ultrasound transducer to obtain high resolution images which allow for outstanding detailed anatomic evaluation of the pelvic organs. Furthermore, the transvaginal ultrasound transducer can be used by the examiner as an extension of the gynecologic examination and thus can help in correlating the patient's symptoms with the exact anatomic location on ultrasound. The use of color and pulsed Doppler can also be added to assess the vascularity of tissue, which may help in the characterization of some adnexal masses. The presence of an abnormal adnexal mass should be evaluated by ultrasound in details. The relationship of the adnexal mass to the ovary and or the uterus should be assessed and the possibility of malignancy should be evaluated.

THE NORMAL OVARY

The most optimal approach to assess the ovaries on ultrasound is the transvaginal approach using the transvaginal ultrasound transducer as it allows for the best resolution of morphologic details. The transvaginal approach is best performed with an empty bladder. The transabdominal approach, which should be reserved for situations where the transvaginal approach is not feasible, is a limited approach to the evaluation of the ovaries due to the lower resolution of the abdominal ultrasound transducers and the presence of bowel loops, which often shadow the ovaries in the pelvis.

The normal ovary is relatively easy to detect in the reproductive years. The presence of ovarian follicles **(Figure 12.1)**, or a corpus luteum, serves to differentiate the ovary from surrounding tissue in the pelvis on ultrasound. The normal ovary's typical anatomic location in the pelvis is lateral to the broad ligament and overlying the hypogastric vein (**Figure 12.2**). Bowel peristalsis helps to differentiate between moveable structures and the static ovary. The authors recommend the following steps for the localization of the normal ovaries by transvaginal ultrasound:
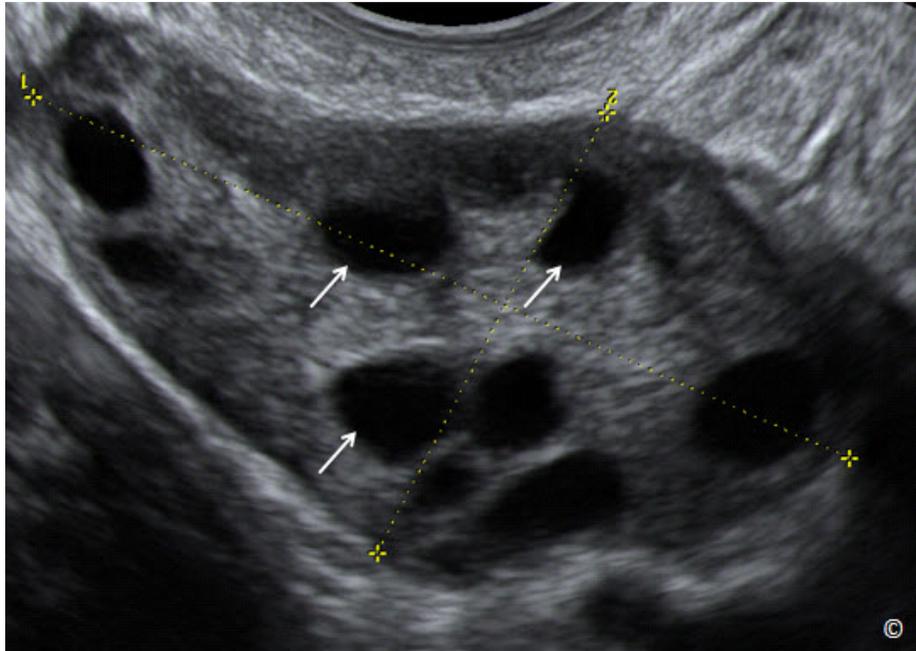
Figure 12.1: Transvaginal ultrasound of a normal ovary. Note the presence of multiple ovarian follicles (arrows) that help to differentiate the ovary from surrounding tissue. Image is courtesy of Dr. Bernard Benoit.
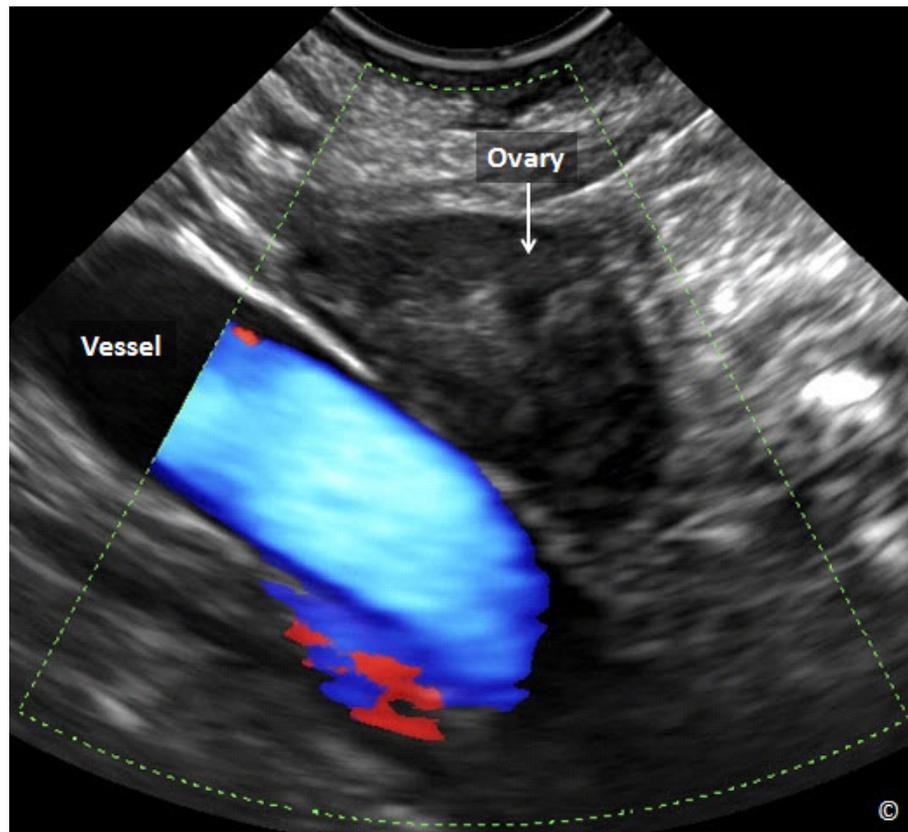

Figure 12.2: Transvaginal ultrasound of a normal ovary (labeled). Note the anatomic location of the ovary, overlying the hypogastric vein (labeled as vessel).

Step One: Insert the transvaginal transducer and obtain a mid-sagittal plane of the uterus (**Figure 12.3**).
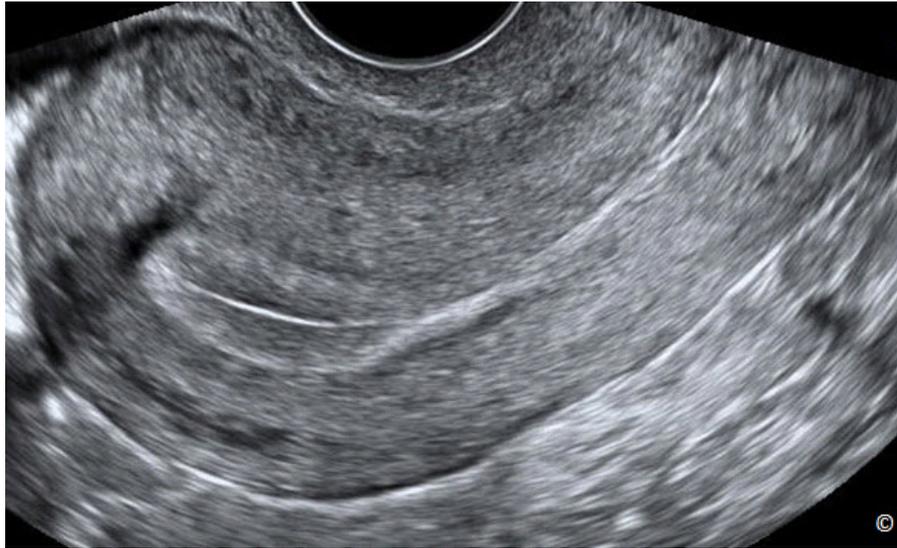
Figure 12.3: Transvaginal ultrasound of the mid-sagittal plane of the uterus. For more details on ultrasound imaging of the uterus, refer to chapter 11.

Step Two: Rotate the transvaginal transducer ninety degrees and obtain a transverse plane of the uterus at the level of the fundus (**Figure 12.4**). Ensure that the transverse plane is at the level of the fundus and not at the uterine isthmus.
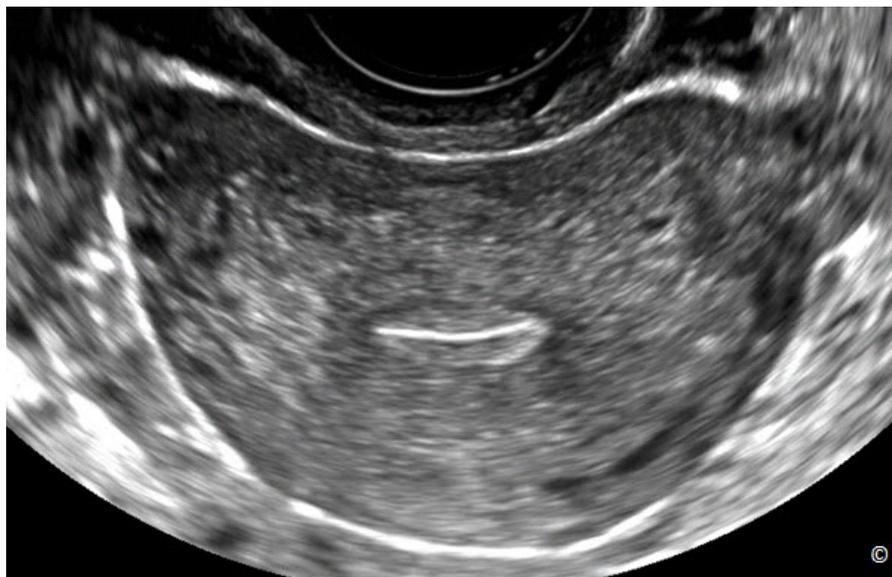
Figure 12.4: Transvaginal ultrasound of the transverse plane of the uterus, obtained by rotating the transducer 90 degrees from the midsagittal plane (see **Figure 12.3**). For more details on ultrasound imaging of the uterus, refer to Chapter 11.

Step Three: While maintaining the transverse orientation, angle your probe towards the right side of the patient, looking for the right ovary – (the handle of the transducer should get close or touch the patient's left inner thigh). Follow the right ovarian ligament as it commonly leads you to the anatomic location of the right ovary (**Figures 12.5** and **12.6**). The right ovary should come into view overlying the right hypogastric vein (**Figure 12.2**). Repeat the same maneuver for the left side. **Clip 12.1** shows a movie of these suggested steps.
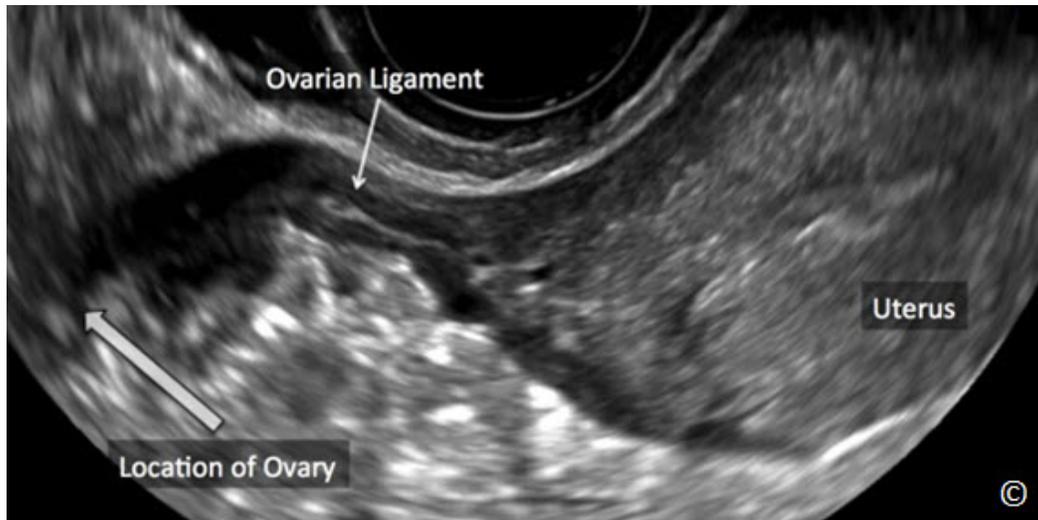
Figure 12.5: Transvaginal ultrasound of the uterus in transverse orientation looking for the right ovary. Note that if you follow the ovarian ligament (labeled), this commonly leads you to the ipsilateral ovary.

The size of the normal ovary varies slightly with the time of the menstrual cycle as well as the woman's age. The ovary should be measured on ultrasound in 3 dimensions; width, length and depth on views obtained in 2 orthogonal planes (**Figure 12.7 A** and **B**). The ovary appears ovoid (like a chicken egg) in shape and typically contains numerous follicles especially in the reproductive years (see **Figure 12.1**). The ovaries may not be identifiable in some women. This occurs most frequently prior to puberty, after menopause, or in the presence of large uterine fibroids, which shadow the adnexal regions. If a woman has undergone hysterectomy, the ovaries are typically more difficult to image by ultrasound because the bowel fills the space left by the removal of the uterus, and makes ultrasound imaging less optimal. The normal fallopian tubes are not commonly identified as separate structures on ultrasound unless they have pathology.
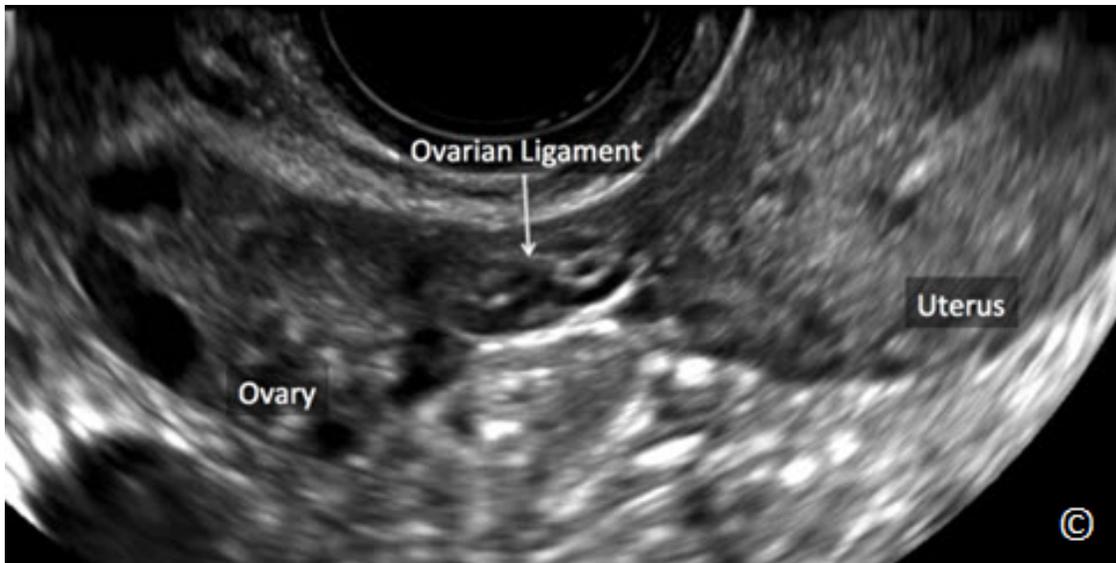
Figure 12.6: Transvaginal ultrasound of the uterus in transverse orientation showing the ovarian ligament and the ovary. Note the relationship between the transverse plane of the uterus (uterus), the ovarian ligament and the ovary (both labeled). By following the ovarian ligament, the ovary can commonly be seen. See text for details.
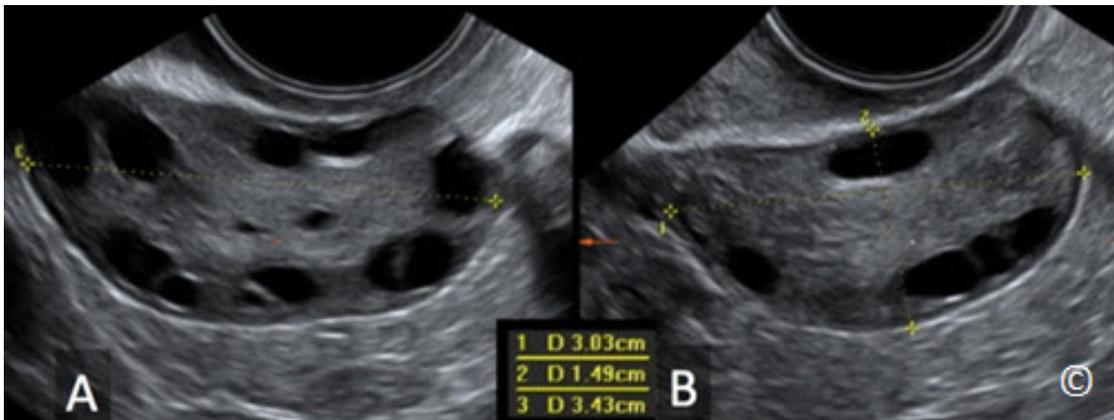

Figure 12.7 A and B: Transvaginal ultrasound showing the measurement of an ovary in its 3 dimensions; length in A and width (measurement 1 on figure B) and depth (measurement 2 on figure B). Figures A and B are orthogonal planes. Image is courtesy of Dr. Bernard Benoit.

Table 12.1 lists benign adnexal masses that are commonly encountered in women of reproductive age. Detailed sonographic characteristics of these masses are discussed in the following sections.

TABLE 12.1	Common Benign Adnexal Masses in Reproductive Age Group
- Simple Cyst - Endometrioma - Pedunculated leiomyoma - Tubo-ovarian Abscess	- Hemorrhagic Cyst - Dermoid Cyst - Hydrosalpinx - Peritoneal Inclusion Cyst

SIMPLE CYST

Characteristics of a simple ovarian cyst on ultrasound include a thin well-rounded capsule with smooth wall and excellent sound transmission (**Figure 12.8**). There should be no internal irregularities on the capsule wall and no internal papillary projections (**Figure 12.8**). The cyst content should be anechoic with no reflection of echo, which typically suggests clarity of the fluid (**Figure 12.8**). The presence of recognized ovarian tissue on ultrasound in the capsule of the cyst is a normal finding (**Figure 12.8**). The presence of septations or papillary projections within a cyst (**Figure 12.9**) may represent signs of malignancy and thus should warrant a referral to an experienced sonographer or sonologist for further evaluation of the adnexae.
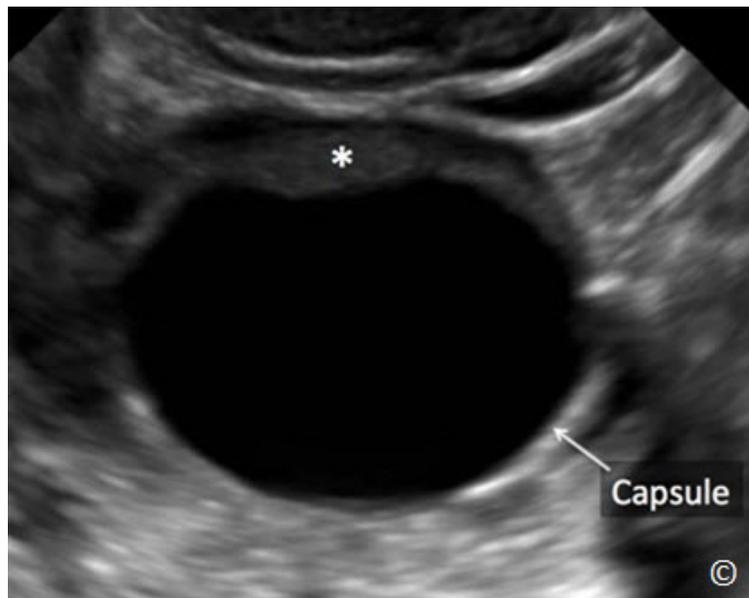

Figure 12.8: Transvaginal ultrasound of a simple ovarian cyst. Note the presence of a thin round, smooth capsule (labeled) with no papillary projections and with excellent sound transmission. Note the presence of ovarian tissue (asterisk).
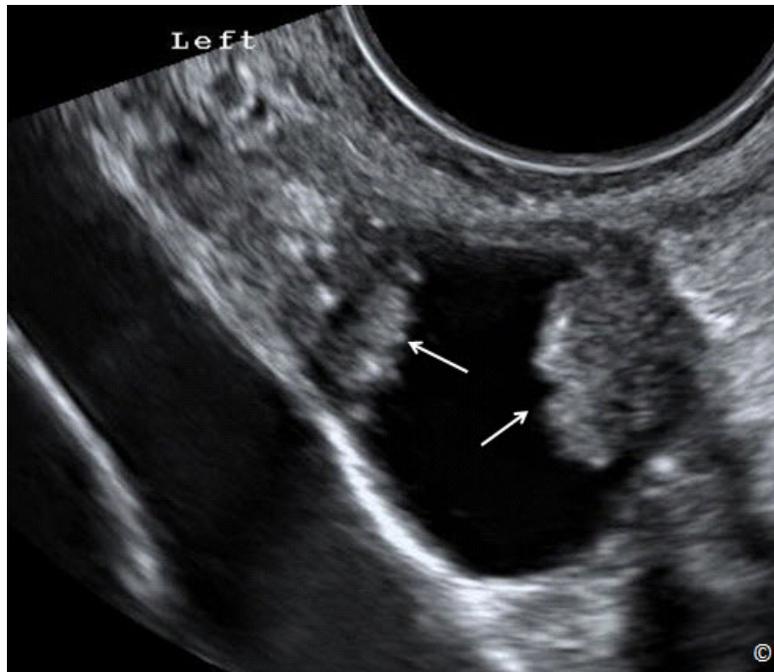
Figure 12.9: Transvaginal ultrasound of a left adnexal mass. Note the presence of papillary projections (arrows), which may suggest the presence of malignancy and thus requires referral to experienced sonography.

HEMORRHAGIC CYST

Hemorrhagic cyst, also commonly referred to as hemorrhagic corpus luteum, results from bleeding inside an ovarian cyst. The event is typically noticeable by the woman and is described as an acute pain in the right or left lower quadrant of the abdomen. The hemorrhagic cyst typically goes through a temporal pattern of clot formation within the cyst, clot lysis, clot retraction and clot resolution. The sonographic appearance of the hemorrhagic cyst is thus dependent on the stage of evolution of the cyst's content. Given that hemorrhagic cysts present in symptomatic women and that the sonographic appearance on ultrasound resembles a "solid appearing adnexal mass" at some phases of development, it is a common reasons for unnecessary pelvic surgery.

In its early stages, hemorrhagic cysts appear as solid masses with smooth thin walls and excellent sound transmission (**Figure 12.10**). The cyst content has variable echogenicity with characteristic thin linear reticular strands (**Figure 12-10**). Upon follow-up, blood clot retracts within the hemorrhagic cyst and a fluid layer develops within the cyst itself, resulting in another sonographic characteristic of a hemorrhagic cyst (**Figure 12.11**). At a point of clot retraction, the clot may appear like a papillary projection within the cyst (**Figure 12.12**). It is important to make

the distinction between a retracted blood clot and a papillary projection resulting from a malignant growth. We propose several differentiating features:
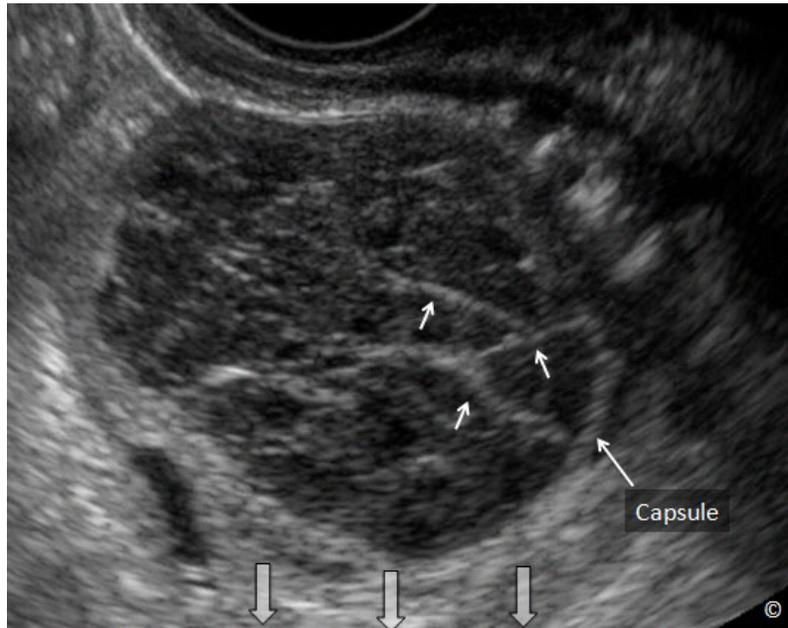

Figure 12.10: Transvaginal ultrasound of a hemorrhagic cyst. Note the solid appearance with smooth capsule (labeled) and excellent sound transmission (big arrows). Note the variable echogenicity and the characteristic thin linear reticular strands (small arrows).

Figure 12.11: Transvaginal ultrasound follow-up of the hemorrhagic cyst in figure 12.10. Note the retraction of the blood clot (asterisk) with the development of a fluid layer.
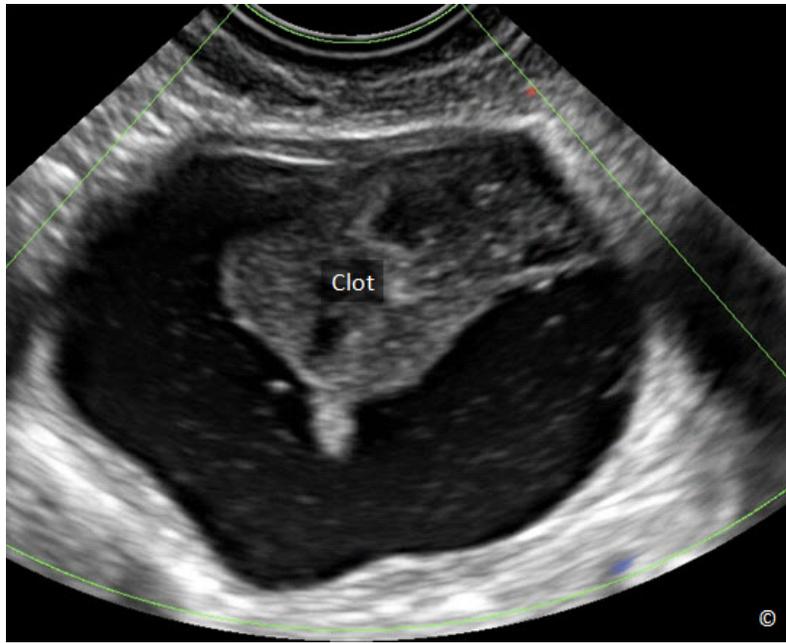
Figure 12.12: Transvaginal ultrasound of a hemorrhagic cyst with blood retraction. Note the appearance of the retracted blood clot (labeled), similar to a papillary projection. Read text for differentiating features between a retracted clot and a papillary projection.

1) A blood clot within an ovary (hemorrhagic cyst) should never have any capillary flow within it on color Doppler sonography. We therefore recommend the placement of color Doppler sonography (using low velocity scale, around 5-10 cm/sec and low filter settings) on all adnexal masses to assess for capillary flow. The absence of capillary flow within an adnexal mass with the sonographic appearance of a hemorrhagic cyst confirms its diagnosis (**Figure 12.13**). The presence of capillary flow within the content of an adnexal mass (**Figure 12.14**) on the other hand, is not compatible with a hemorrhagic cyst and should be referred to expert sonography for further evaluation.
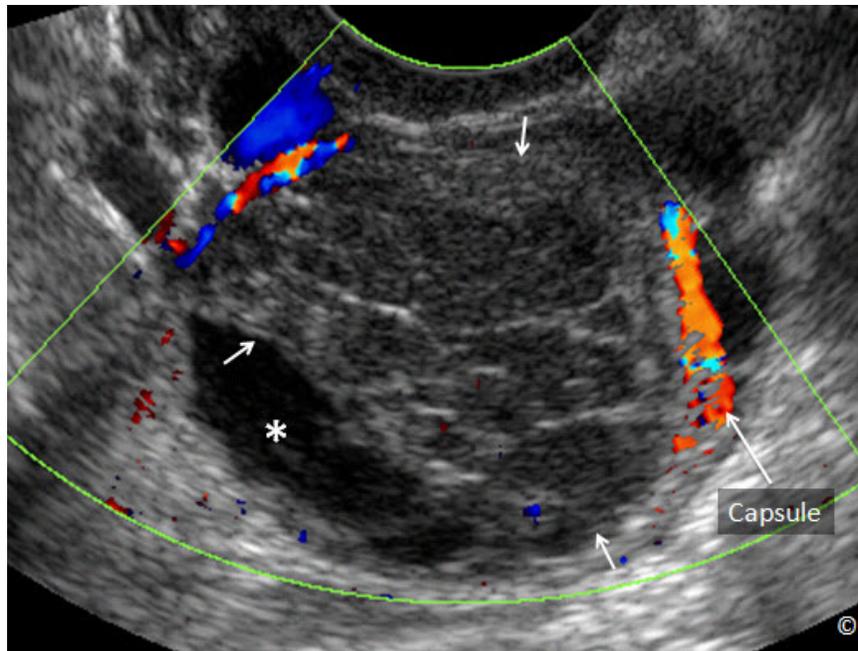
Figure 12.13: Transvaginal ultrasound with color Doppler of the hemorrhagic cyst in figure 12.11. Note the retraction of the blood clot (asterisk) with the development of a fluid layer. Color Doppler shows vascular flow in the capsule (labeled) but none within the blood clot (arrows).
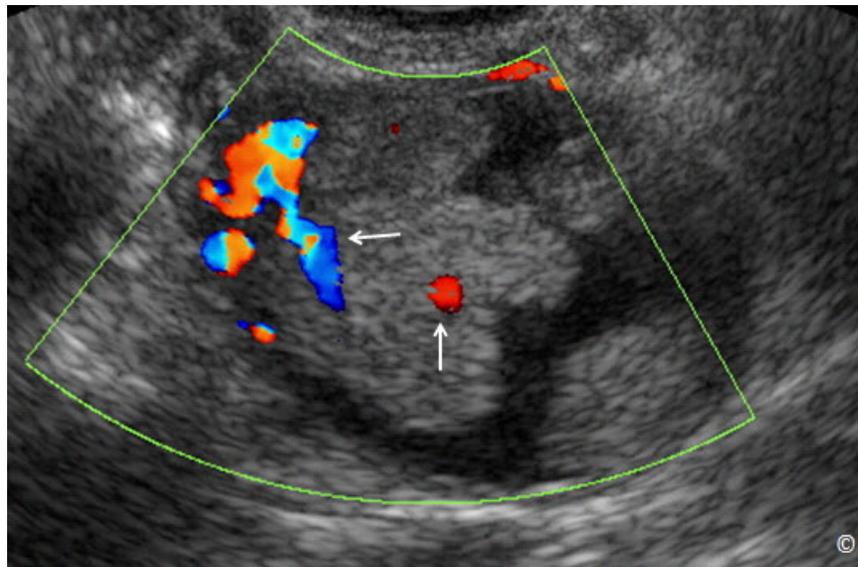

Figure 12.14: Transvaginal ultrasound with color Doppler of an ovarian cancer. Note the presence of multiple papillary projections. Color Doppler shows vascular flow within the papillary projections (arrows).

2) A blood clot within a hemorrhagic cyst tends to jiggle when probed by the transvaginal ultrasound transducer (**Clip 12.2**). Use this technique to confirm the content of a hemorrhagic cyst.

3) Blood clots within hemorrhagic cysts also tend to have broad bases (**Figure 12.12**) and the content tends to shift with patient repositioning.

4) The blood clot retraction typically results in a single mass of clotted blood within the cyst (**Figure 12.12**). The presence of multiple papillary projections (**Figure 12.14**) within a cyst therefore is more compatible with a neoplastic process.

5) Follow-up examination is also one of the most important tools to help in the differentiation. Given the important temporal change of hemorrhagic cysts; a follow-up ultrasound examination within 4-6 weeks should help in differentiating a hemorrhagic cyst from a borderline or malignant tumor. Hemorrhagic cysts tend to resolve and regress with time whereas solid adnexal masses of malignant origin tend to grow. **Table 12.2** lists the characteristics of a hemorrhagic ovarian cyst.

TABLE 12.2	Characteristics of an Ovarian Hemorrhagic Cyst

- Excellent sound transmission
- Thin Reticular lacy pattern
- Temporal changes
- Solid – Fluid level
- Jiggles when probed
- Absence of vascular signals on low-velocity color Doppler
- Single mass of clotted blood when retracted
- Follow-up shows resolution

ENDOMETRIOMAS

Endometriomas are thin walled "solid" appearing ovarian masses that are typically unilocular and have a characteristic "ground glass" appearance (**Figure 12.15**). They are commonly homogeneous and have low-level echoes with excellent sound transmission (**Figure 12.16**). Hyperechoic foci are commonly seen within endometriomas and are sometimes referred to as calcific stippling (**Figure 12.17**). Unlike hemorrhagic cysts, the sonographic appearance of endometriomas tends to remain stable over time. An endometrioma should not have any blood vessels within its content. The application of color Doppler at low velocity scales, around 5-10 cm / sec with low filter settings, for the demonstration of absence of vascularity within the endometrioma, is therefore an essential component of the diagnosis (**Figure 12.15** and **12.18**). The presence of vascularity on color Doppler in the setting of an endometrioma-like mass

(**Figure 12.19**) should raise suspicion for malignancy (endometrioid tumor) and a referral to expert sonography should be immediately performed. **Table 12.3** lists the sonographic characteristics of endometriomas.
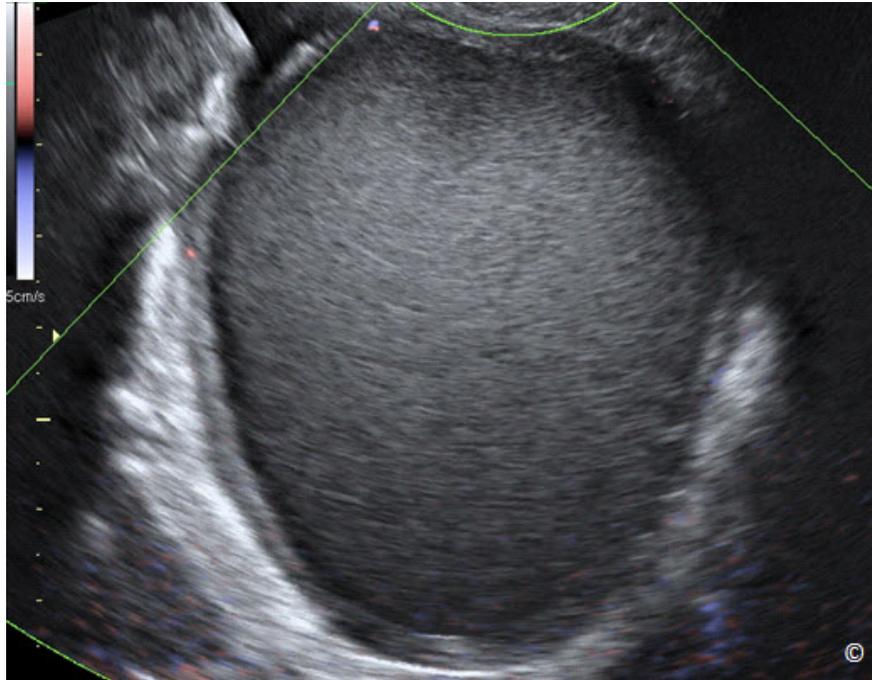

Figure 12.15: Transvaginal ultrasound with color Doppler of an endometrioma showing a unilocular mass with ground glass appearance. Note the absence of vascularity within the content of the mass on low velocity scale (5 cm/sec) color Doppler.
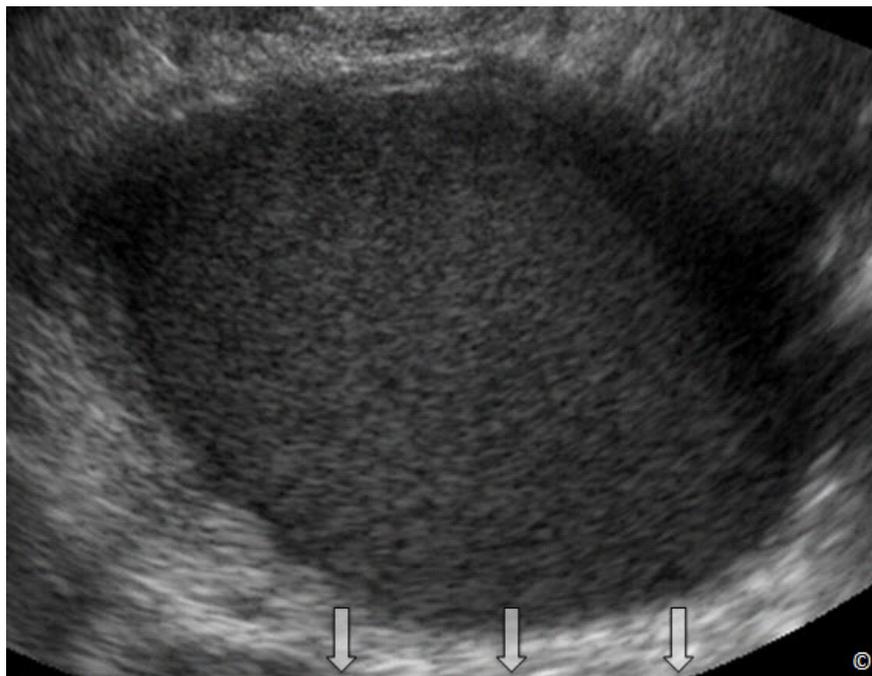

Figure 12.16: Transvaginal ultrasound of an endometrioma showing a unilocular mass with ground glass appearance and excellent sound transmission (arrows).
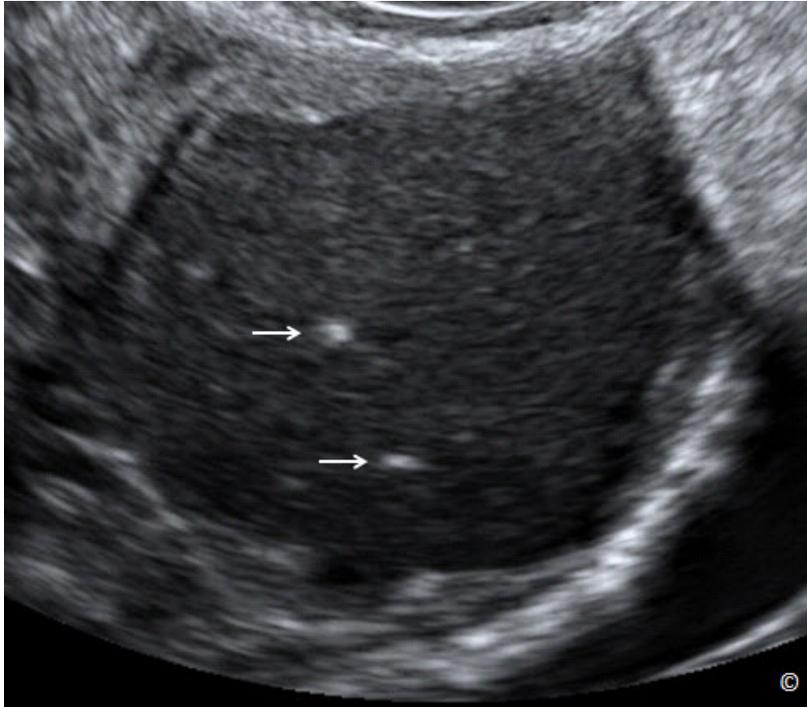
Figure 12.17: Transvaginal ultrasound of an endometrioma showing a unilocular mass with ground glass appearance. Note the presence of hyperechoic foci (arrows) that are also referred to as calcific stippling.
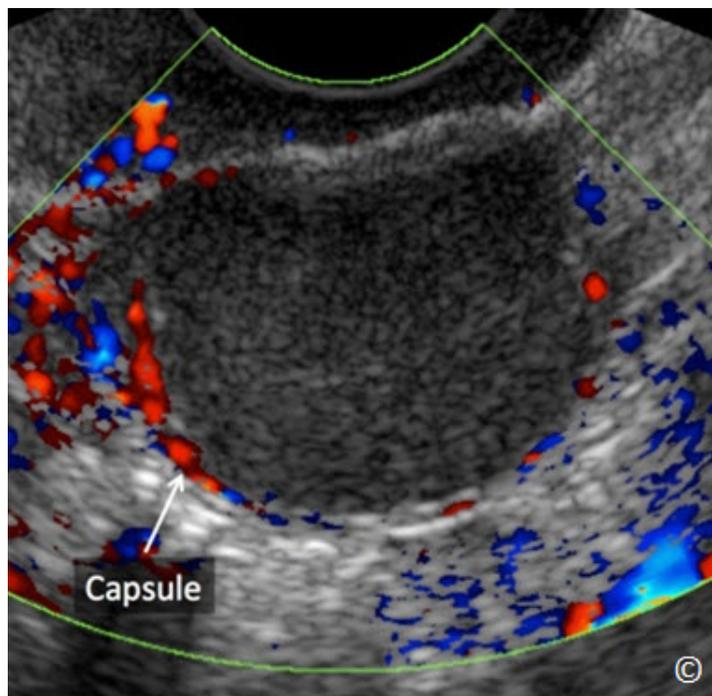

Figure 12.18: Transvaginal ultrasound with color Doppler of an endometrioma showing the absence of vascularity within the content of the mass on low-velocity color Doppler. Vascular flow can be demonstrated in the capsule (labeled).
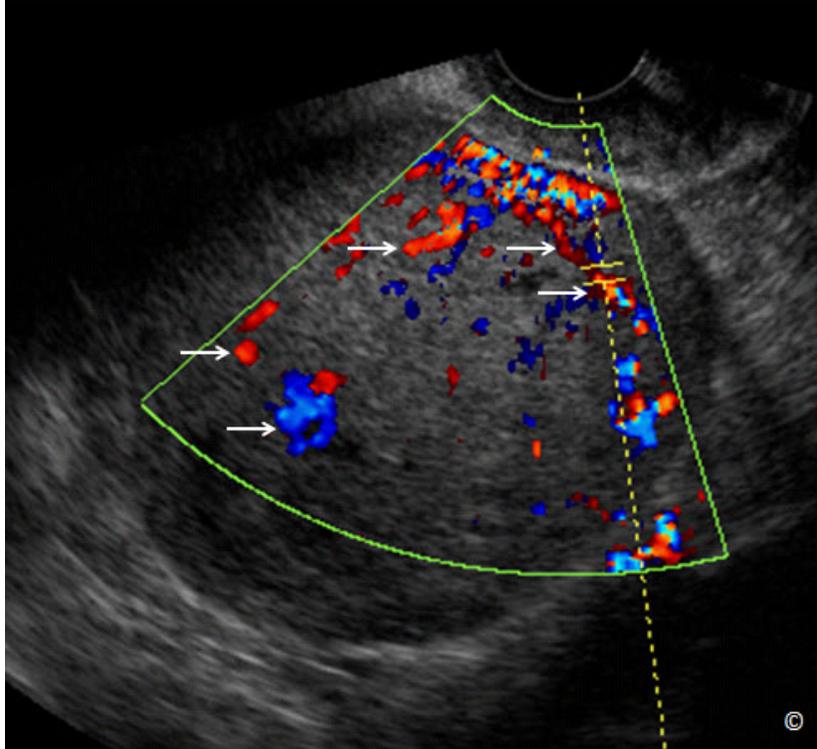
Figure 12.19: Transvaginal ultrasound with color Doppler of a solid mass that appeared similar to an endometrioma on grey scale imaging. Note the presence of extensive vascularity within the solid component (arrows). Pathologic examination revealed an endometrioid ovarian cancer.

TABLE 12.3	Sonographic Characteristics of Endometriomas

- Excellent sound transmission
- Homogeneous, ground glass appearance
- Typically unilocular
- No or minimal temporal changes
- Hyperechoic foci
- Absence of vascular signals on low-velocity, low-filter color Doppler settings

DERMOID CYST (MATURE CYSTIC TERATOMA)

Dermoid cysts, or mature cystic teratomas, originate from the ovarian germ cells. They affect younger age groups than epithelial tumors, are slow growing and are bilateral in about 10 % of cases. The most common sonographic appearance of a dermoid cyst is a complex, cystic and solid mass, with echogenic internal content that shadows extensively resulting in a "tip of the iceberg" effect (**Figure 12.20**). Characteristic features on ultrasound include a white echogenic "ball" which typically corresponds to the sebum and hair content of the dermoid, long and short echogenic linear strands which correspond to the hair in the fluid content of the cystic components, and significant attenuation of sound (**Figure 12.21 A and B**). The white echogenic ball is referred to as the Rokitansky nodule or dermoid plug (**Figure 12.21 A and B**). Dermoid cysts may be small and located within the ovary (**Figure 12.22**) or may assume different shapes and sizes (**Figure 12.23 A and B**). They tend to be located superiorly in the pelvis and thus on occasions may be outside the reach of the transvaginal transducer. The presence of excessive papillary projections within a dermoid cyst, in addition to the presence of vascularity on color Doppler evaluation, (**Figure 12.24**) should raise the suspicion for the presence of immature or neuronal elements within and thus appropriate referrals should be made. **Table 12.4** lists the sonographic characteristics of dermoid cysts.
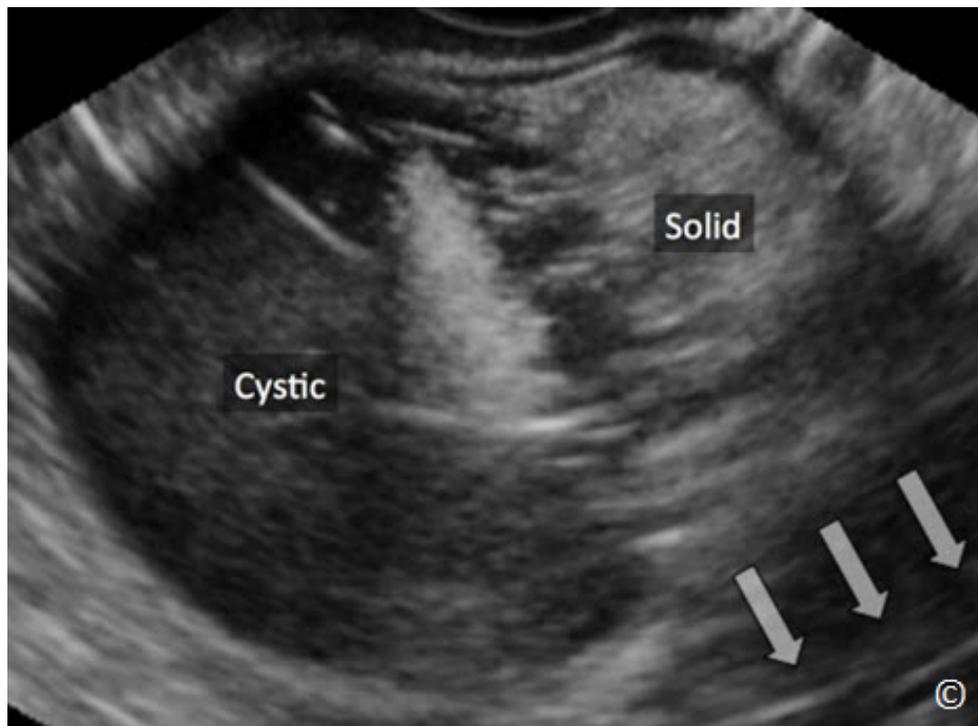

Figure 12.20: Transvaginal ultrasound of a dermoid cyst. Note the complex, cystic and solid content (labeled) with extensive shadowing (arrows). This has been compared to the "tip of the iceberg". See text for details
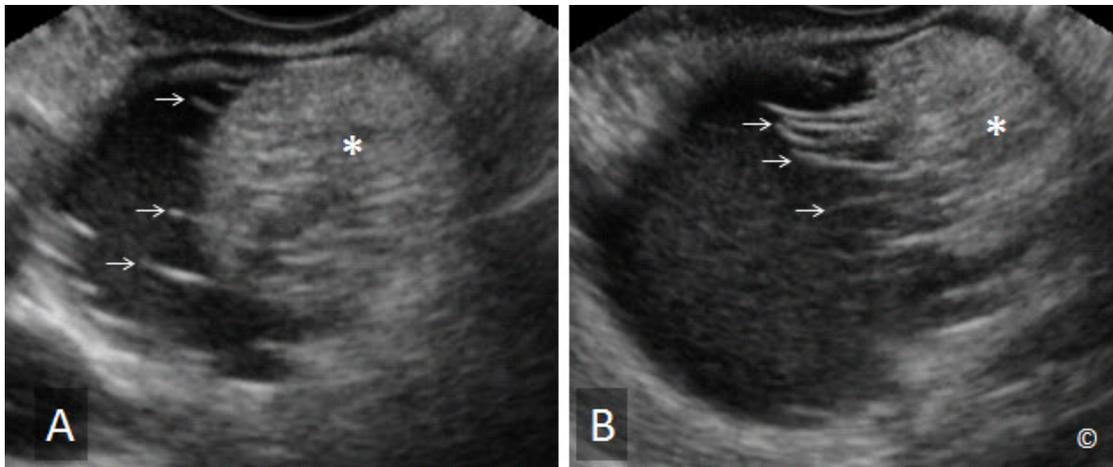
Figure 12.21 A and B: Transvaginal ultrasound of dermoid cyst A and B. Note the white echogenic "ball" (Rokitansky nodule) in A and B (asterisk). Note the long and short echogenic linear strands, which correspond to the hair content (arrows).
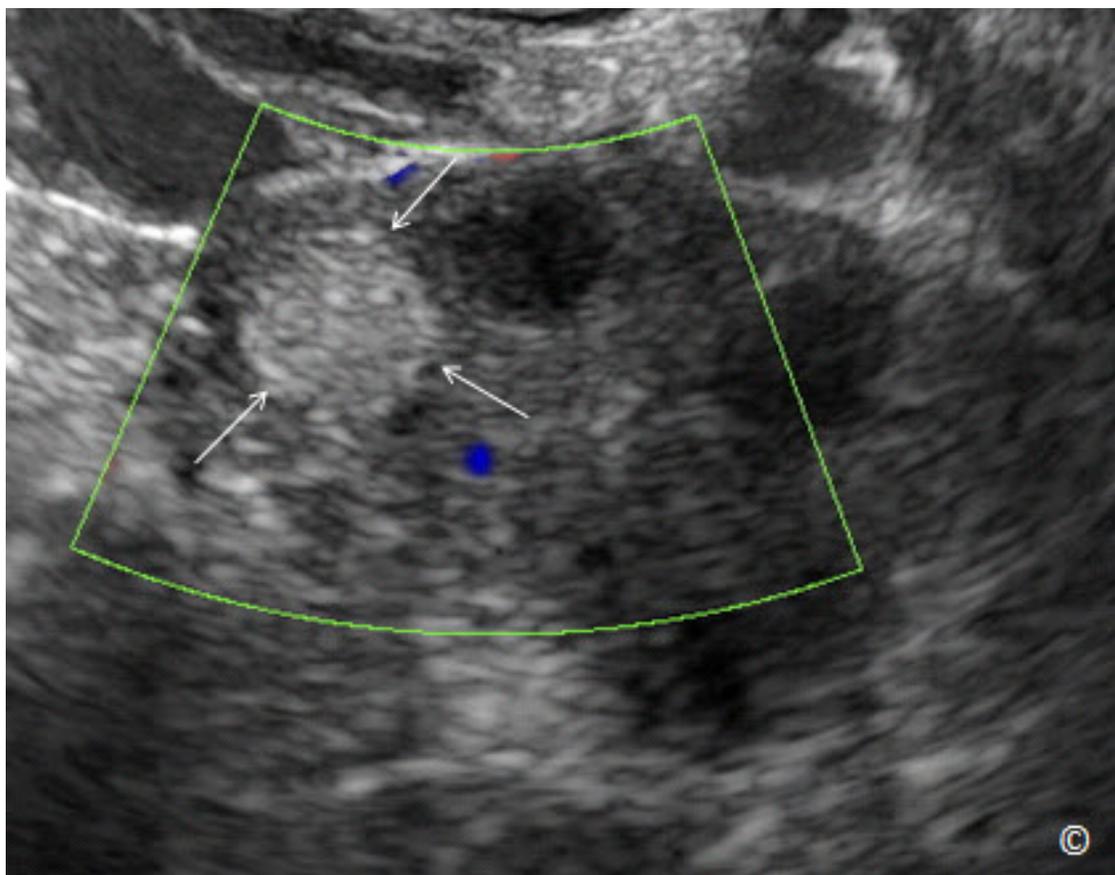

Figure 12.22: Transvaginal ultrasound with color Doppler of a small dermoid (arrows), located within the ovary.
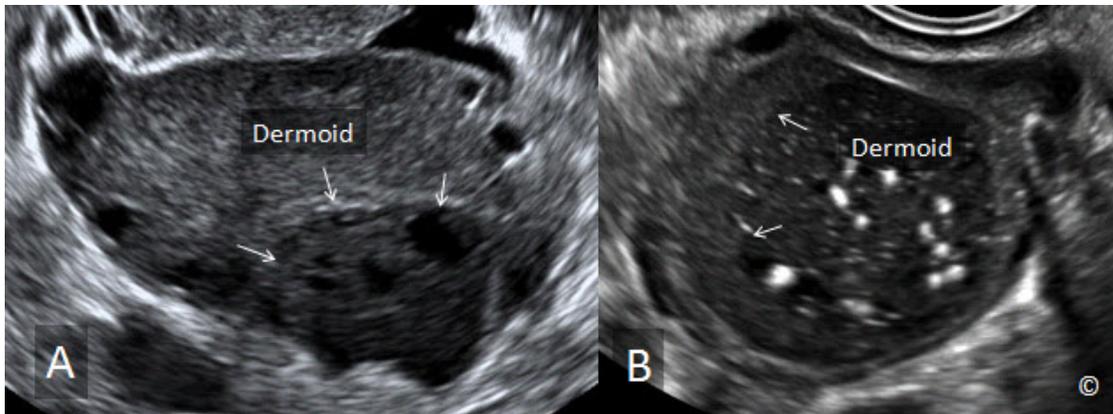
Figure 12.23 A and B: Transvaginal ultrasound of dermoid cysts in A and B. The dermoid cysts are labeled in A and B. The arrows point to normal ovarian tissue. In B, the dermoid is cystic with echogenic foci corresponding to the fat content within the fluid.
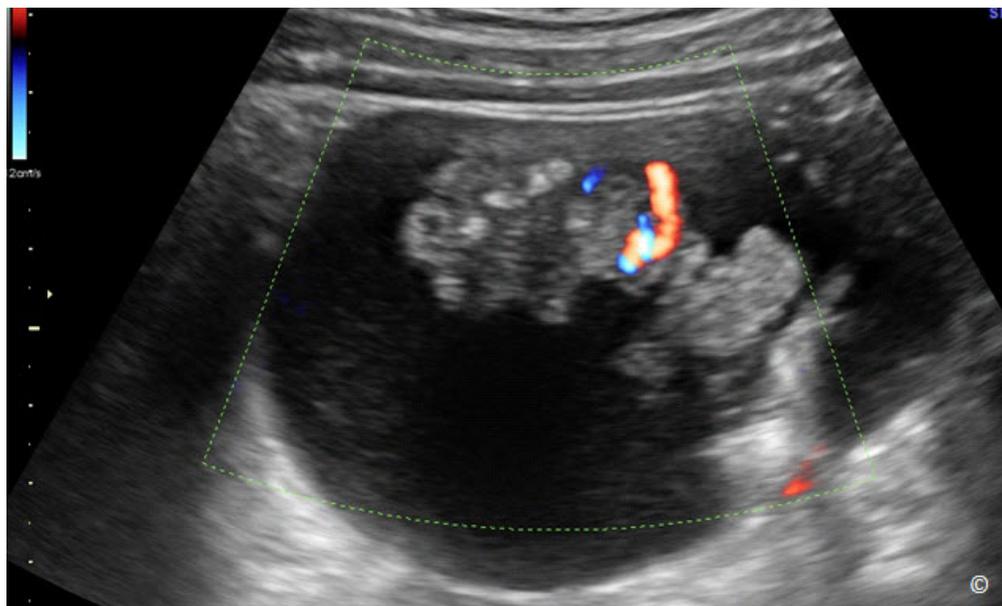

Figure 12.24: Transvaginal ultrasound with color Doppler of an immature teratoma with neuronal elements. Note the presence of papillary projections with vascularity noted on color Doppler.

TABLE 12.4	Sonographic Characteristics of Dermoid Cysts
- Poor sound transmission (tip of iceberg effect) - Complex, solid tumors, heterogeneous content - White echogenic ball (Rokitansky nodule) - Thin linear strands - Superior location in pelvis - Absence of vascular signals on low-velocity, low-filter, color Doppler settings	

PEDUNCULATED LEIOMYOMA – OVARIAN FIBROMA

Pedunculated leiomyomas are included in this chapter as they typically present as solid adnexal masses with extensive shadowing (**Figure 12.25**) and are commonly associated with a vascular pedicle that can be traced by color Doppler to the uterus. They are commonly round or oval with a regular striped echogenicity. Leiomyomas display a characteristic shadow pattern of the ultrasound beam described as "venetian blinds shadowing" (blinds that are partially open with the sun rays coming through) (**Figure 12.25**). This shadowing pattern is present in most leiomyomas and helps differentiate leiomyomas from other solid tumors. Identifying a separate normal ovary in the adnexal region, when a pedunculated leiomyoma is suspected, helps in confirming the diagnosis. The ovary should be freely movable and separate from the pedunculated leiomyoma thus insuring that the leiomyoma and the ovary are not anatomically attached (**Clip 11.1**). **Table 12.5** lists the sonographic characteristics of pedunculated leiomyomas. For more detailed discussion on leiomyomas, please refer to chapter 11.

An ovarian fibroma is a solid tumor that arises from the ovary and it shares several of the sonographic characteristics of a pedunculated leiomyoma (**Figure 12.26**). The ovarian fibroma however is an ovarian tumor and thus is not freely movable in the adnexa as it is attached to the ovary (**Clip 12.3**).
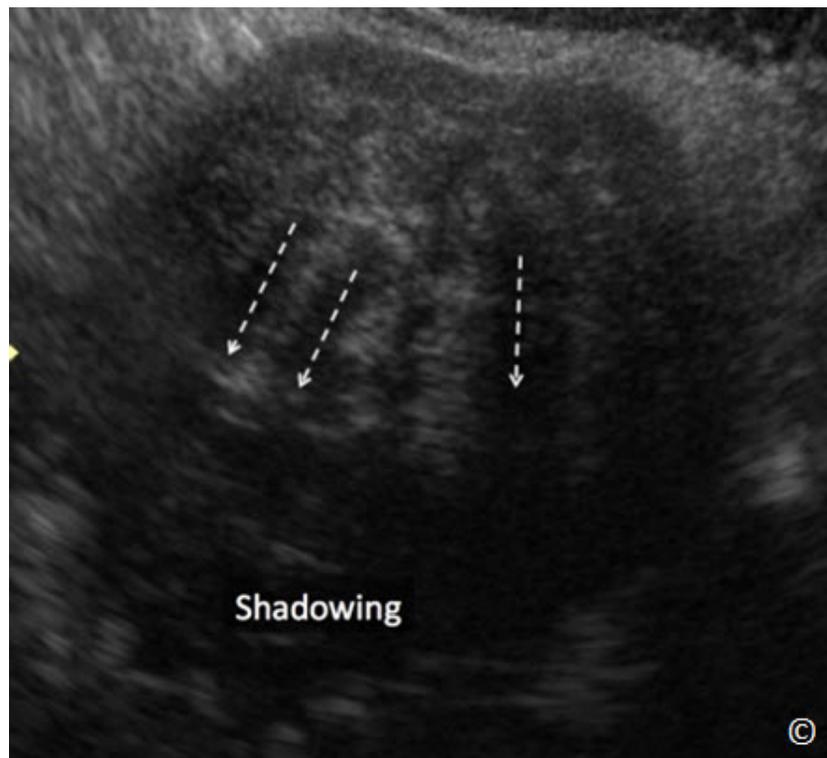

Figure 12.25: Transvaginal ultrasound of a pedunculated leiomyoma with the characteristic "venetian blinds shadowing" (dashed arrows). Note the extensive shadowing (labeled) on the posterior aspect of the leiomyoma.
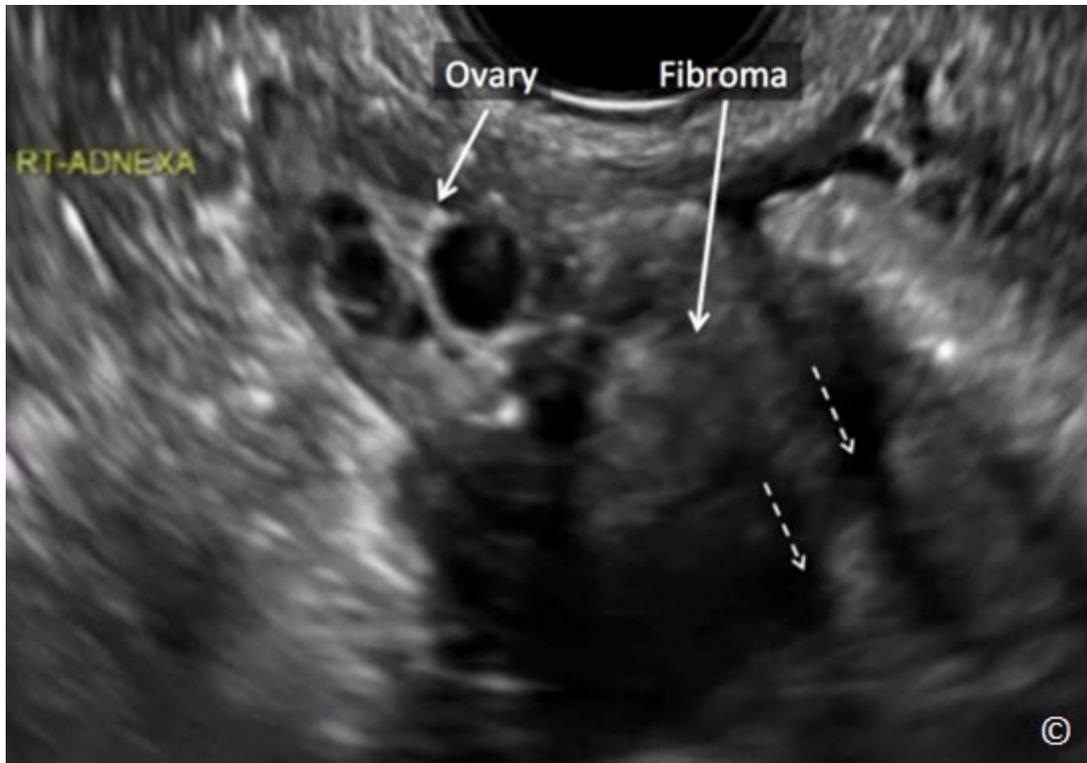
Figure 12.26: Transvaginal ultrasound of an ovarian fibroma. Note the characteristic "venetian blinds shadowing" (dashed arrows). The fibroma is attached to the ovary and does not move freely in the adnexa. See **Clip 12-3** for details.

TABLE 12.5	Sonographic Characteristics of Pedunculated Leiomyomas

- Poor sound transmission
- Solid tumors, regular striped echogenicity
- Vascular pedicle to the uterus
- "Venetian blinds shadowing"
- Separate freely movable ovary

HYDROSALPINX

The normal fallopian tube is rarely seen on transvaginal ultrasound. When the tube is filled with fluid however, it is easily seen as a fluid-filled sausage-shaped structure, with thin walls, incomplete septations (**Figure 12.27**), and a cogwheel appearance on cross section. There is lack of peristalsis, a feature that differentiates the elongated fluid filled structure from bowel. Furthermore, the hydrosalpinx, with its elongated sausage-shaped structure tends to taper near its uterine origin. The presence of a tubular structure filled with clear fluid in the adnexal region

should raise suspicion for a hydrosalpinx, especially when a separate ovary is seen. Hydrosalpinges are typically asymptomatic and are commonly seen in postmenopausal women. If the diagnosis of a hydrosalpinx is entertained, a follow-up ultrasound is helpful, as it typically shows no sonographic change in appearance. The application of three-dimensional ultrasound in inverse mode, if available, can confirm the diagnosis (**Figure 12.28**). **Table 12.6** lists the sonographic characteristics of a hydrosalpinx.
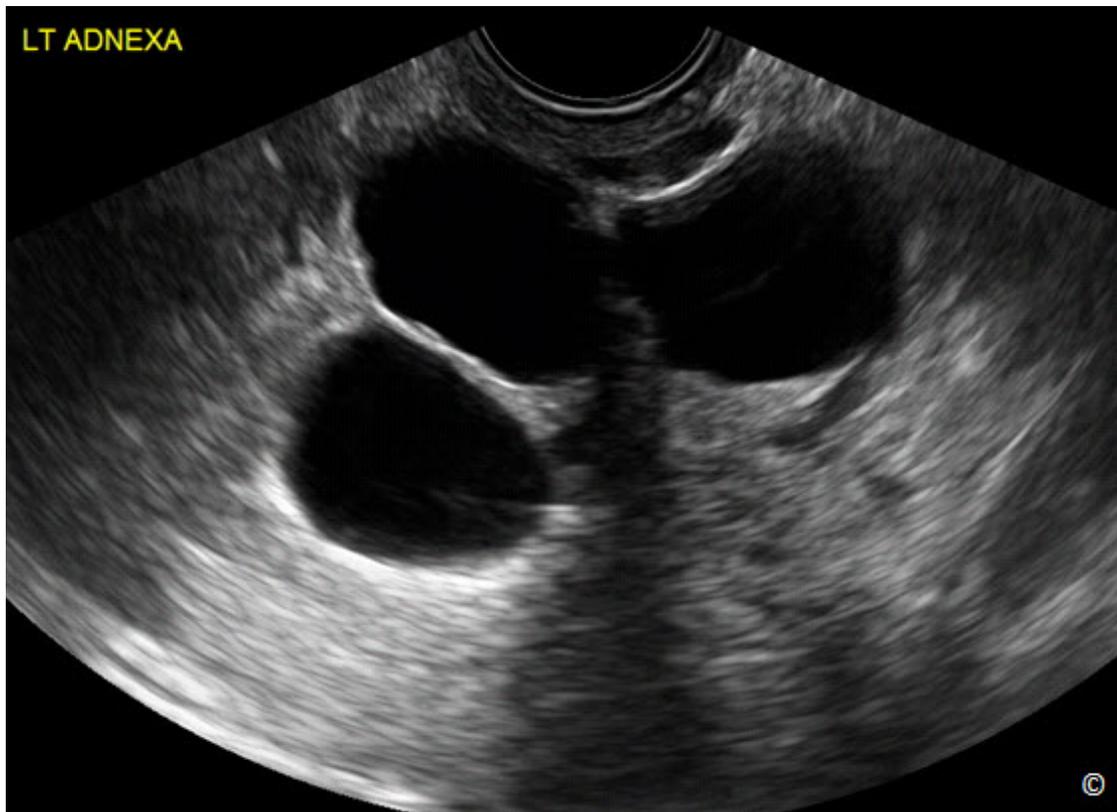

Figure 12.27: Transvaginal ultrasound of a hydrosalpinx. Note the presence of a tubular structure with thin walls and multiple septations.
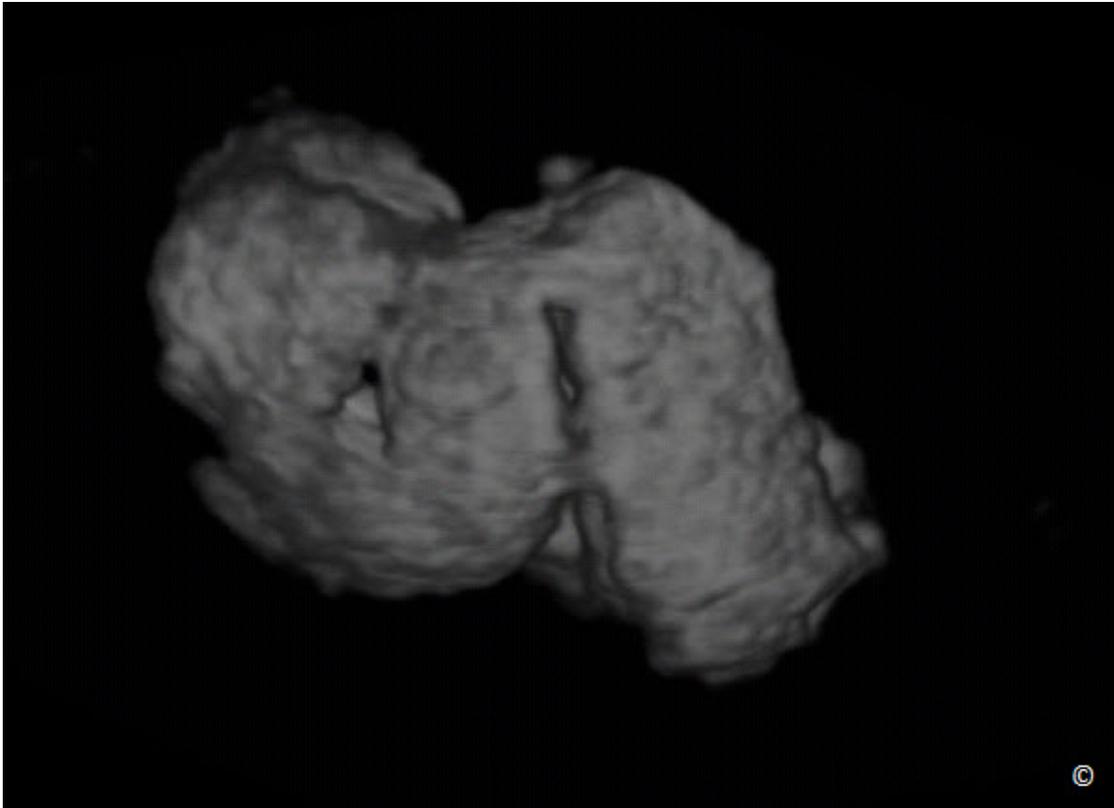
Figure 12.28: Three-dimensional ultrasound in inverse mode of the cystic mass in figure 12.26. Note the display on 3D of a folded tubular structure confirming the diagnosis of hydrosalpinx.

TABLE 12.6	Sonographic Characteristics of Hydrosalpinges

- Fluid filled, sausage shaped structure
- Structure tapers near the uterine origin
- Thin walls
- Multiple and incomplete septations
- Absence of peristalsis
- Cogwheel appearance on cross section

TUBO-OVARIAN ABSCESS

A tubo-ovarian abscess occurs when an ascending infection involves the tube and ovary as part of an acute process. Women are typically symptomatic with fever and pelvic pain and tenderness, but on occasions tubo-ovarian abscesses may be silent. The ultrasound characteristics include a multilocular mass with thick walls and thick incomplete septae that are filled with an

echogenic fluid of ground glass appearance (**Figure 12.29**). The fluid content derives from the inflammatory process. The sonographic appearance may be similar to endometriomas, but endometriomas are more commonly unilocular in asymptomatic women and do not have incomplete septations. Differentiating a tubo-ovarian abscess from other pelvic abscesses may be difficult. The involvement of the ovary in the process is helpful in that differentiation. **Table 12.7** lists the sonographic characteristics of tubo-ovarian abscesses.
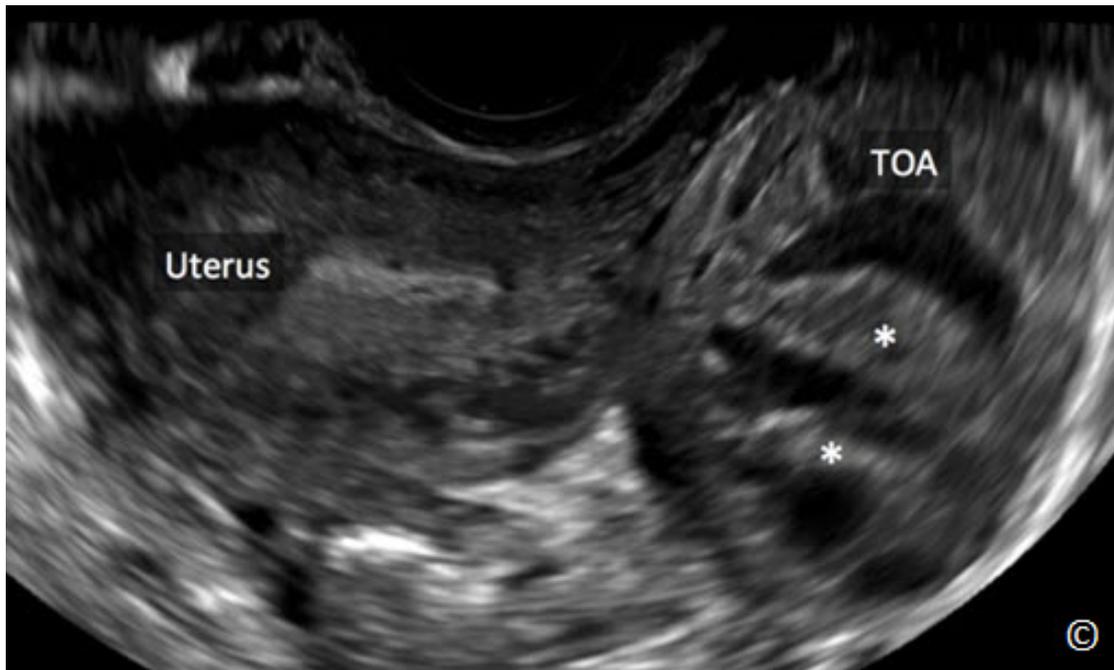

Figure 12.29: Transvaginal ultrasound of a tubo-ovarian abscess (TOA). Note the ovoid shape of the TOA, with thickened walls and septations (asterisks). The uterus (labeled) is noted adjacent to the TOA.

TABLE 12.7	Sonographic Characteristics of Tubo-Ovarian Abscesses
- Multilocular mass with thick walls - Thick incomplete septae - Fluid content is echogenic, with ground-glass appearance - Involvement of the ovary	

PERITONEAL INCLUSION CYSTS

Peritoneal inclusion cysts also referred to, as pseudocysts are cystic structures within the pelvis that entraps peritoneal fluid. These cysts primarily occur following pelvic surgery or infection

and result from pelvic adhesions that entrap fluid. Ultrasound characteristics include multiple primarily thin (**Clip 12.4**), but occasionally thick septations that attach to pelvic organs such as the uterus, bowel and ovaries (**Figure 12.30**). The fluid content is typically clear and normal looking ovaries can be seen on occasions, which confirm the diagnosis (**Figure 12.30**). Peritoneal inclusion cysts are typically asymptomatic and women are commonly referred with the finding of a septated pelvic mass diagnosed on CT scan or Magnetic Resonance Imaging (MRI). Inquiring about the patient's surgical history is important, as pelvic adhesion from prior pelvic surgery is an etiological factor for peritoneal inclusion cysts. **Table 12.8** lists the sonographic characteristics of peritoneal inclusion cysts.
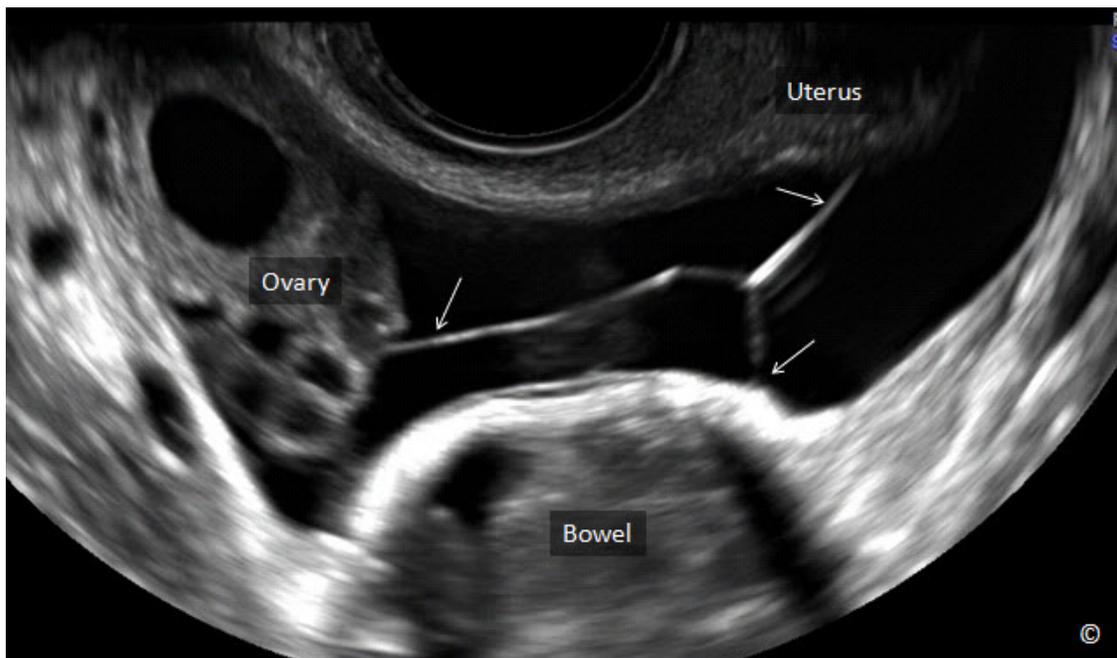

Figure 12.30: Transvaginal ultrasound of peritoneal inclusion cysts. Note the presence of multiple primarily thin septations (arrows) that entrap fluid and attach to pelvic organs such as the uterus, bowel and ovary (labeled).

TABLE 12.8	Sonographic Characteristics of Peritoneal Inclusion Cysts
	- Multiple primarily thin septations
	- Septations attach to pelvic organs
	- Fluid within the cysts is primarily clear
	- Normal looking ovaries can be occasionally seen

THE POLYCYSTIC OVARY

Polycystic ovary syndrome is a metabolic disorder that is characterized by menstrual disorders, such as anovulation, hyperandrogenism, infertility and a spectrum of metabolic abnormalities. The presence of polycystic ovaries, unilaterally or bilaterally, is part of the polycystic ovary syndrome but having polycystic ovaries is not a requirement for diagnosis. The morphologic criteria for the diagnosis of polycystic ovaries have changed throughout the years. Since 2003, most investigators have used a threshold of 12 follicles (measuring 2-9 mm in diameter) per ovary, with increased stromal echogenicity. An increase in ovarian volume at greater or equal to 10 ml has also been suggested. Recent data suggest a follicular number per ovary of 25 or greater for the diagnosis of polycystic ovaries when transvaginal ultrasound is used (1) (**Figure 12.31**). If transvaginal ultrasound is not available and transabdominal ultrasound is used, an ovarian volume of 10 ml or greater is then recommended for diagnosis (1). Finally, the finding of polycystic ovaries in ovulatory women not showing clinical or biochemical androgen excess may be inconsequential, even though there is a suggestion that this may represent the milder end of the polycystic ovary syndrome spectrum.
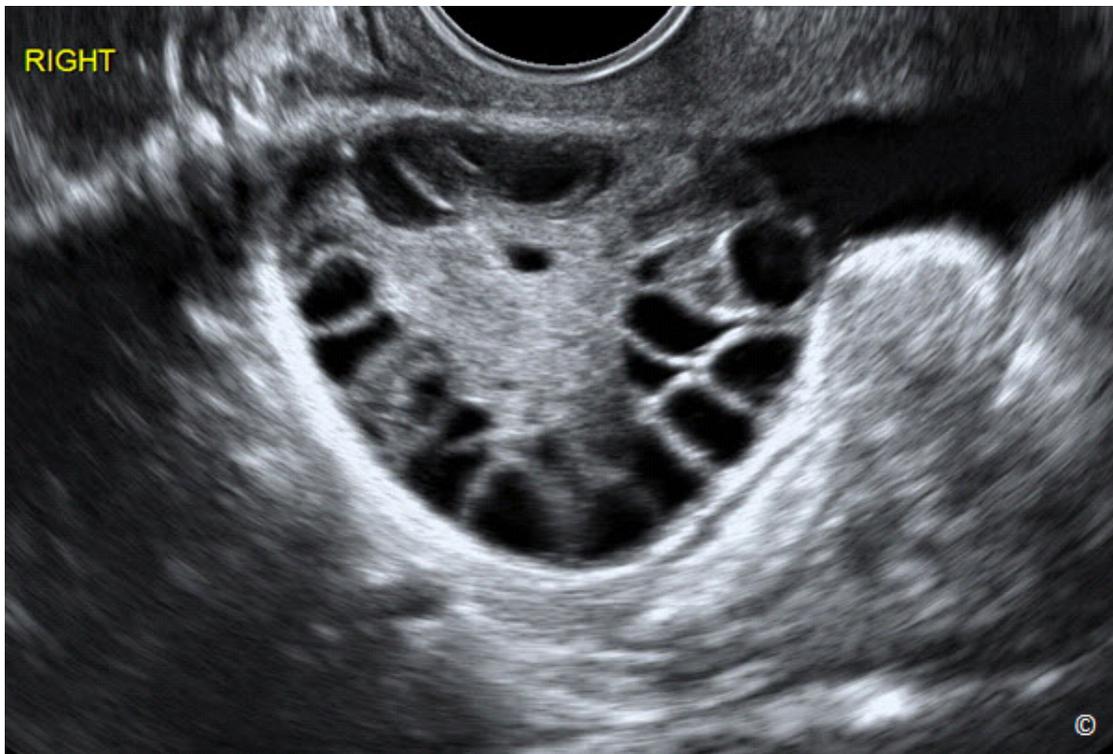

Figure 12.31: Transvaginal ultrasound of a polycystic ovary. The ovary is more spherical in shape and has an increased number of follicles that are situated in the periphery of the ovary. Note also the presence of increased stromal echogenicity.

BORDERLINE AND MALIGNANT ADNEXAL MASSES

Ultrasound evaluation of adnexal masses is primarily performed to differentiate benign from malignant lesions. Several common benign adnexal masses have sonographic characteristics (**Tables 12.1** to **12.8**) that allow the examiner to make the diagnosis with near certainty. Borderline and malignant adnexal masses also have certain characteristics that allow for a high index of suspicion. Sonographic characteristics of malignant adnexal masses are listed in **Table 12.9** and include irregularities in the capsule, thick septations, solid papillary projections (2) and vascularity seen on color Doppler evaluation. Purely cystic masses that are unilocular or even multilocular are overall benign with the exception of a large number of septae, which correlates with borderline mucinous tumors.

TABLE 12.9	Sonographic Characteristics of Borderline and Malignant Adnexal Masses
	- Irregularities in capsule and content - Thick septations - Solid content - Papillary projections - Vascularity on color Doppler

The use of pulsed Doppler in the evaluation of adnexal masses has been shown to be inaccurate due to high degree of overlap between benign and malignant masses, especially in premenopausal women (3). In postmenopausal women where ovarian angiogenesis is nonexistent, pulsed Doppler evaluation, looking for low impedance circulation and timed-average maximum velocity, has some predictive value (4). In the authors' experience, pattern recognition of grey scale ultrasound is still the most important in differentiating benign from malignant masses and the use of color and pulsed Doppler are adjuncts to grey scale evaluation. **Figures 12.32** to **12.36** show some borderline and malignant adnexal masses.
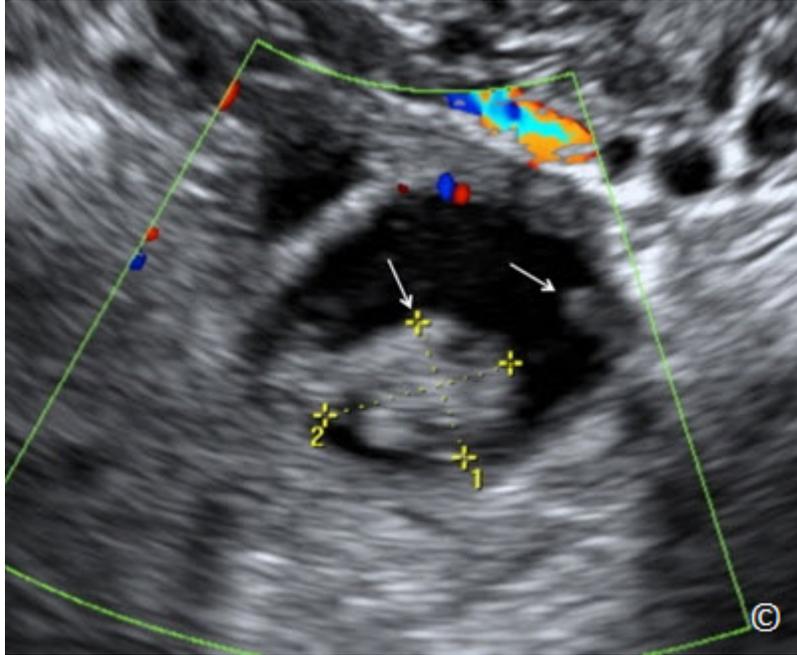
Figure 12.32: Transvaginal ultrasound of a borderline serous cystadenocarcinoma. Note the presence of papillary projections (arrows) in a small cystic mass.
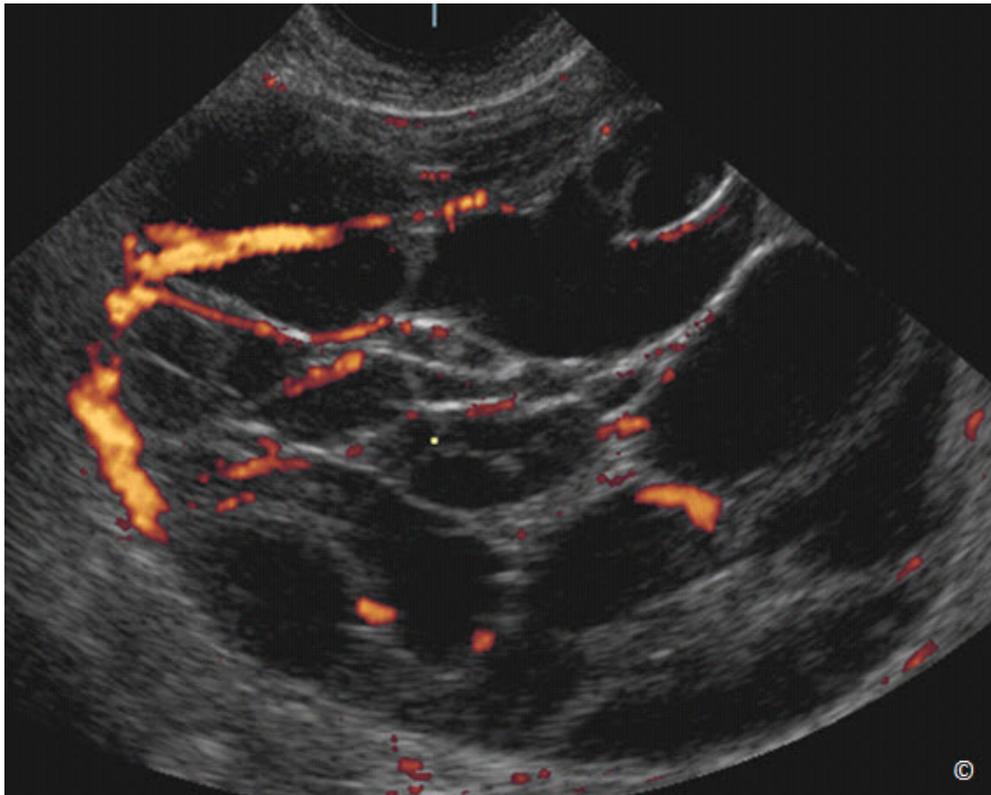

Figure 12.33: Transvaginal ultrasound with high definition color of a borderline mucinous cystadenocarcinoma. Note the presence of multiple thick septations with vascularity noted on high definition color Doppler.

Figure 12.34 A and B: Transvaginal ultrasound of serous cystadenocarcinoma of the ovary. Note the presence of multiple papillary projections in A (arrows) and in B, color and pulsed Doppler shows vascularity within the papillary projections.

Figure 12.35 A and B: Transvaginal ultrasound of an endometrioid carcinoma of the ovary. Note the presence of a solid mass with thick septations in A and vascularity with low impedance flow in B on color and pulsed Doppler ultrasound.
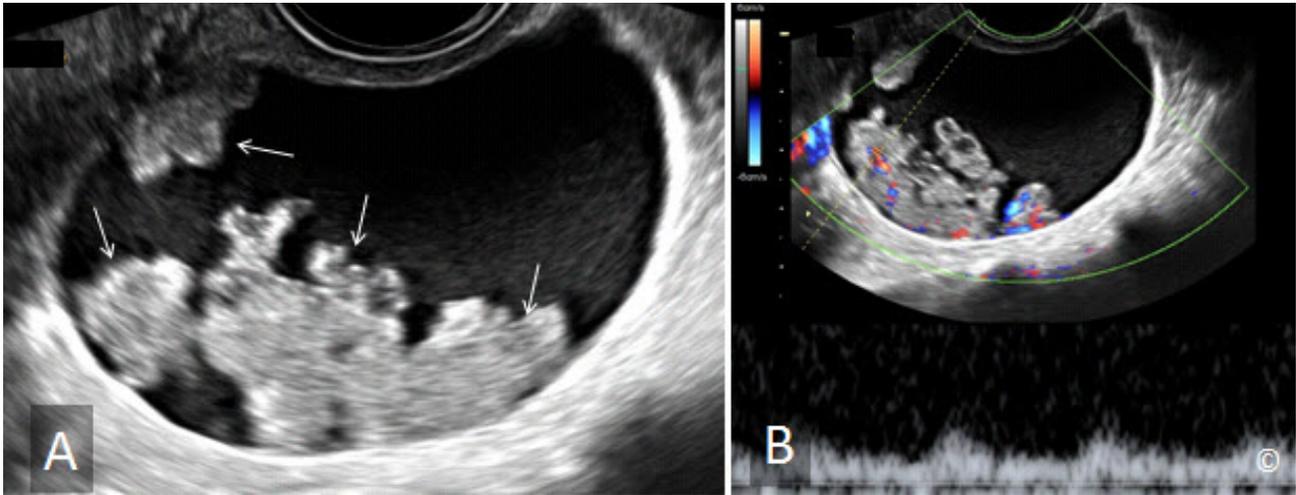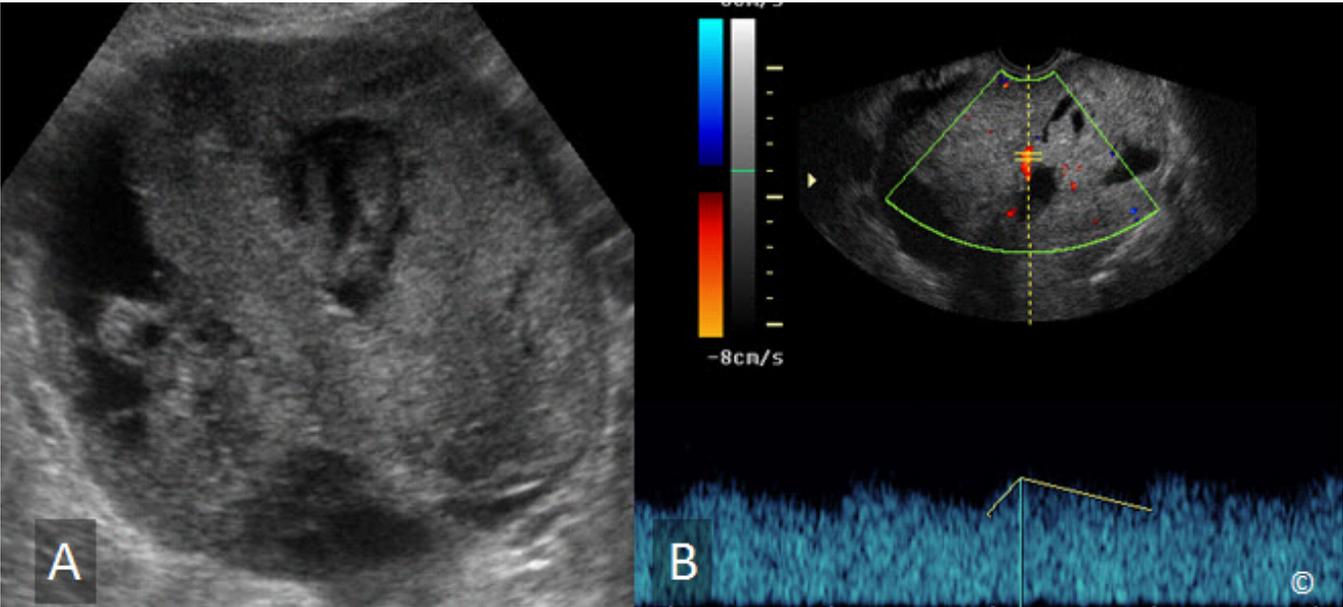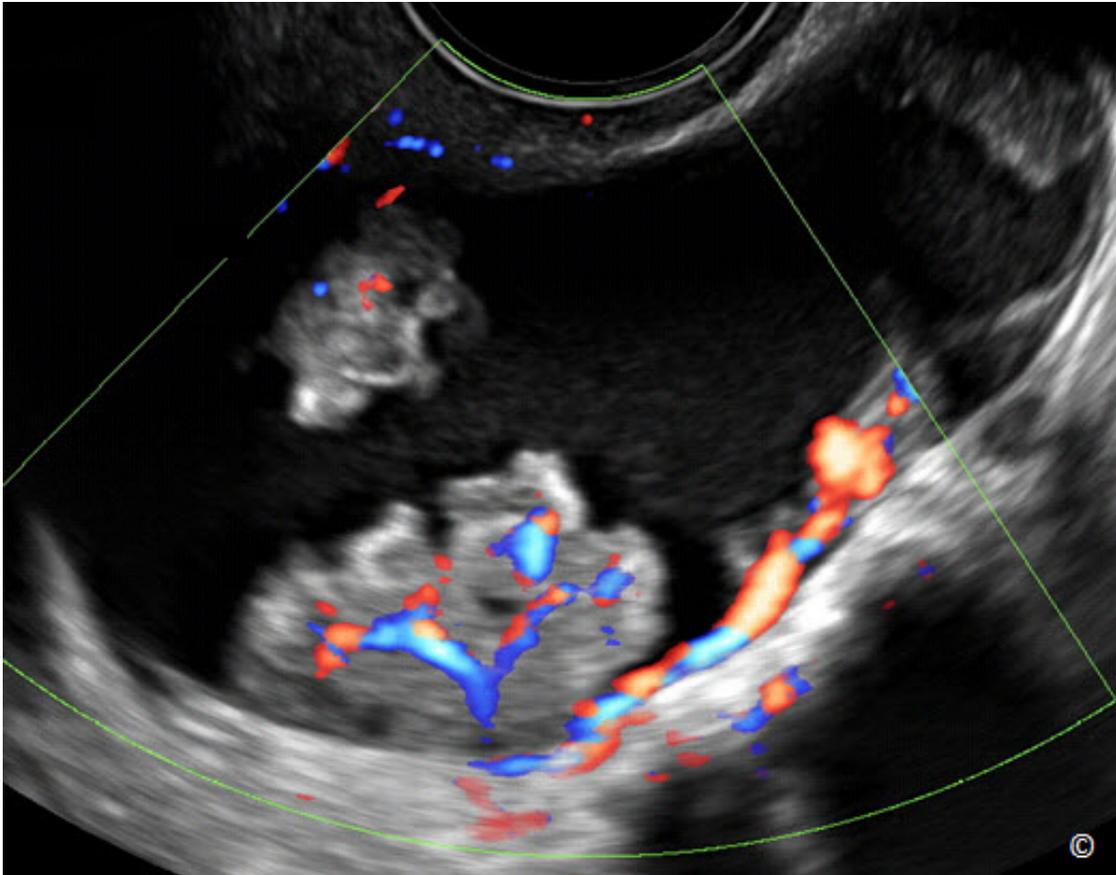
Figure 12.36: Transvaginal ultrasound of a serous cystadenocarcinoma of the ovary. Note the presence of papillary projections with vascularity noted on color Doppler.

ADNEXAL TORSION

Patients presenting with an adnexal torsion are typically symptomatic with acute pelvic pain and tenderness. It is a common gynecologic presentation in the emergency department. Although there are sonographic signs suggestive of the presence of adnexal torsion, ultrasound is not diagnostic of such entity and a high suspicion should occur based upon the presenting symptoms of the patient. Torsion results in obstruction of lymphatic and venous drainage of the ovary and tube and thus is commonly associated with an enlarged, edematous adnexal mass. Hemorrhagic infarction may occur and result in the presence of fluid with varying degrees of echogenicity. Color and Doppler ultrasound does not confirm or rule out the diagnosis, as significant variations with vascular occlusions exist. Intraperitoneal fluid may be present and is thought to result from transudate from the capsule of the ovary with lymphatic and venous obstruction. **Table 12.10** lists the sonographic characteristics of adnexal torsion.

TABLE 12.10	Sonographic Characteristics of Adnexal Torsion

- Enlarged edematous adnexal mass
- Cystic areas within the mass with varying degrees of echogenicity
- Tender mass on probing with the transvaginal transducer

PREDICTION MODELS FOR OVARIAN CANCER

Several models have been developed to characterize adnexal masses on ultrasound in order to improve differentiation between benign and malignant tumors (5-7). One of the most widely used classification method is that by the International Ovarian Tumor Analysis (IOTA) (8). IOTA is a collaborative that standardized the approach to the ultrasound description of adnexal pathology (8). A prospectively collected large database tested prediction models like the IOTA risk of malignancy index (RMI) and showed excellent consistency and predictability of malignant pathology. Their test performance almost matches subjective assessment by experienced examiners, which is accepted to be the best way to classify adnexal masses prior to surgery. Simple rules, many of which have been discussed in this chapter, can be applied to classify tumors into benign or malignant (**Figure 12.37**). Alternatively, a logistic regression model can be adopted for that purpose. For more information on the IOTA classification, the readers are encouraged to review reference 8 in this chapter. Acquiring the expertise in the subjective ultrasound evaluation of adnexal masses, on the other hand, provides excellent differentiation between benign and malignant adnexal pathology.
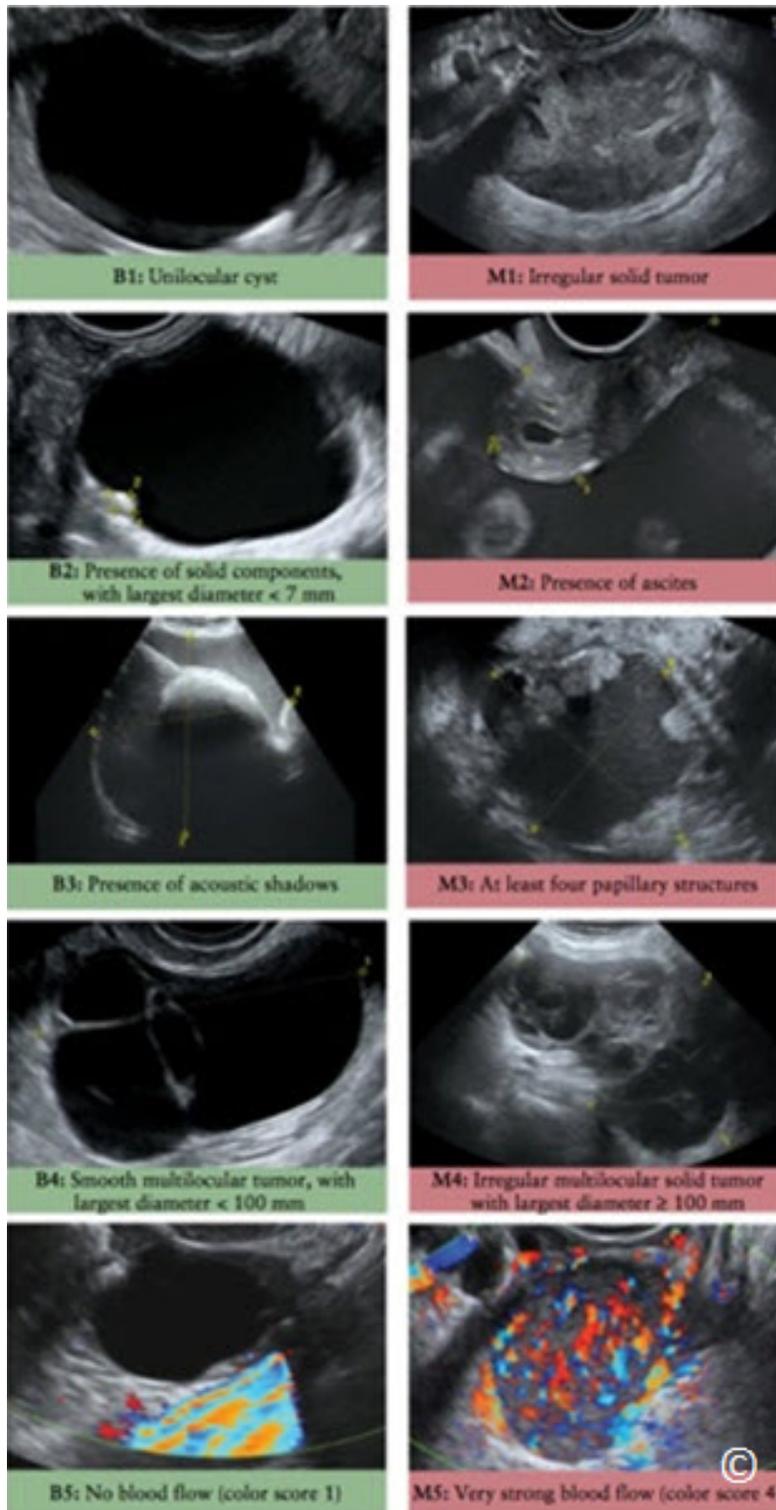
Figure 12.37: Ultrasound features used in the International Ovarian Tumor Analysis (IOTA) simple rules, illustrated by ultrasound images. B1–B5, benign features; M1–M5, malignant features. Reproduced with permission from reference 8.

CLIP 12.1

CLIP 12.2

CLIP 12.3

CLIP 12.4

References:

1) Dewailly D, Lujan ME, Carmina E, Cedars MI, Laven J, Norman RJ, Escobar Morreale HF. Definition and significance of polycystic ovarian morphology: a task force report from the Androgen Excess and Polycystic Ovary Syndrome Society. Hum Reprod Update. 2013 Dec 16. [Epub ahead of print]

2) Granberg S, Wikland M, Jansson I. Macroscopic characterization of ovarian tumors and the relation to the histological diagnosis: criteria to be used for ultrasound evaluation. Gynecol Oncol 1989;35:139

3) Tekay A, Jouppila P. Controversies in assessment of ovarian tumors with transvaginal color Doppler ultrasound. Acta Obstet Gynecol Scand 1996;75:316

4) Fleisher AC, Brader KR. Sonographic depiction of ovarian vascularity and flow: current improvements and future applications. JUM 2001; 20:241.

5) Mol BW, Boll D, De Kanter M, Heintz AP, Sijmons EA, Oei SG, Bal H, Bro¨lmann HA. Distinguishing the benign and malignant adnexal mass: an external validation of prognostic models. *Gynecol Oncol* 2001; **80**: 162 – 167.

6) Ferrazzi E, Zanetta G, Dordoni D, Berlanda N, Mezzopane R, Lissoni AA. Transvaginal ultrasonographic characterization of ovarian masses: comparison of five scoring systems in a multicenter study. *Ultrasound Obstet Gynecol* 1997; **10**: 192 – 197.

7) Aslam N, Banerjee S, Carr JV, Savvas M, Hooper R, Jurkovic D. Prospective evaluation of logistic regression models for the diagnosis of ovarian cancer. *Obstet Gynecol* 2000; 96: 75 – 80.

8) Kaijser J., Bourne T, Valentin L, Sayasneh S, Van Holsbeke C, Vergote I, Testa AC, Franchi D, Van Calster B and Timmerman D. Improving strategies for diagnosing ovarian cancer: a summary of the International Ovarian Tumor Analysis (IOTA) studies. *Ultrasound Obstet Gynecol* 2013; 41: 9–20.

INTRODUCTION

Ectopic pregnancy is the leading cause of pregnancy-related deaths during the first trimester (1). The incidence of ectopic pregnancy has been on the increase over the past several decades (2) and it continues to contribute significantly to maternal morbidity and mortality, especially in the developing world (3).

RISK FACTORS

Several risk factors for ectopic pregnancy exist (4) and are listed in **Table 13.1**. History of tubal surgery such as prior tubal sterilization or prior tubal surgery for ectopic pregnancy are amongst the most common risk factors and thus should heighten alertness for the presence of an ectopic pregnancy in symptomatic patients. Other risk factors include pelvic inflammatory disease, female infertility and use of an intra-uterine device.

TABLE 13.1	Risk Factors for Ectopic Pregnancy
- History of tubal surgery - History of prior ectopic pregnancy - Use of Intrauterine Device - History of infertility	

CLINICAL SYMPTOMS

Ectopic pregnancy should be considered when a patient presents with pain and/or vaginal bleeding in the setting of a positive pregnancy test. The presence of an adnexal mass on physical examination should also initiate an ectopic pregnancy work-up, when a positive pregnancy test is present. Clinical symptoms are not specific for ectopic pregnancy and should not be used solely for diagnosis. The location of the pain may vary (5) and the clinical triad of pain, bleeding and adnexal mass is present in less than half of patients with ectopic pregnancy (6).

ANATOMIC LOCATION OF ECTOPIC PREGNANCY

Most ectopic pregnancies are located along the course of the fallopian tube, with the ampullary and isthmic sections of the tube accounting for the largest proportions of ectopic pregnancies (**Figure 13.1**). Other rare tubal locations include the fimbrial end of the tube or the interstitial (cornual) end of the tube (**Figure 13.1**). The interstitial or cornual ectopic pregnancy deserves special mention, as ectopic pregnancies in this location typically present at a more advanced stage in gestation and are commonly associated with severe hemorrhage and maternal shock at the time of presentation. Cornual ectopic pregnancies are also more difficult to diagnose by ultrasound as they mimic a normal intrauterine gestation, especially when they present at an advanced stage. **Figure 13.2** and **13.3** show cornual ectopic pregnancies in the early part of the first trimester and **Figures 13.4** and **13.5** show cornual ectopic pregnancies at more advanced gestations. Cervical ectopic pregnancies occur in less than 1 % of all ectopic pregnancies and are typically diagnosed by transvaginal ultrasound (**Figure 13.6**). Cervical ectopic pregnancies are best treated with either intramuscular or direct injection, into the gestational sac, of methotrexate or potassium chloride (into gestational sac) under ultrasound guidance, especially when preservation of fertility is desired. Conservative management, following injection of methotrexate or potassium chloride into the gestational sac, is desired, as long as the patient is not bleeding excessively, as most injected cervical ectopic pregnancies will spontaneously resolve. In low-resource settings where treatment options are limited, cervical ectopic pregnancy with heavy vaginal bleeding can be temporarily managed (tamponade) with placement of a cervical cerclage when technically feasible or by inserting compression (30 cc) Foley balloon-catheter(s) into the cervical canal.
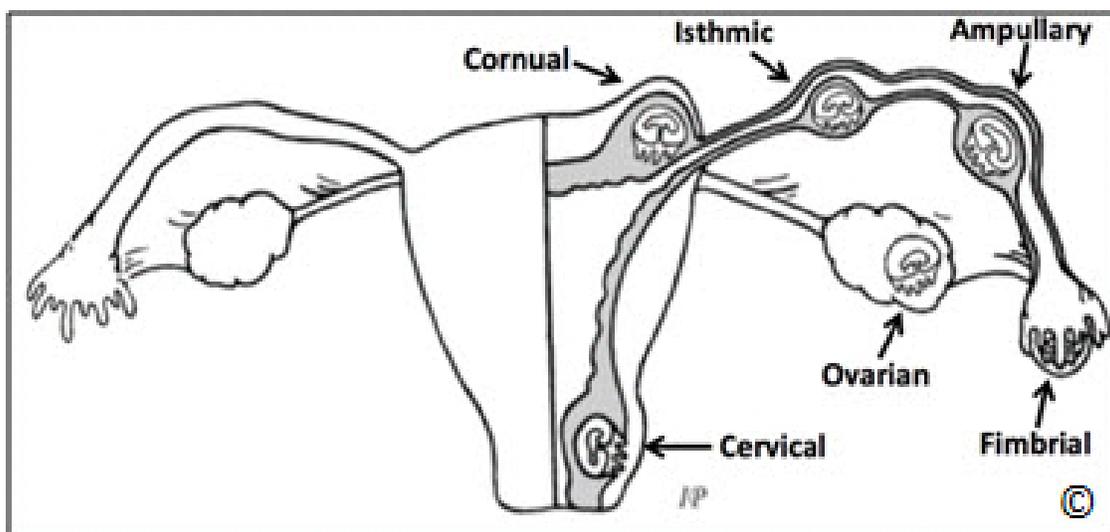

Figure 13.1: Locations of ectopic pregnancies in the pelvis. Most ectopic pregnancies are located along the course of the fallopian tube, with the ampullary and isthmic sections accounting for the largest proportions. Abdominal pregnancy is not depicted in this sketch. Sketch is courtesy of Dr. Igor Palahnuk.
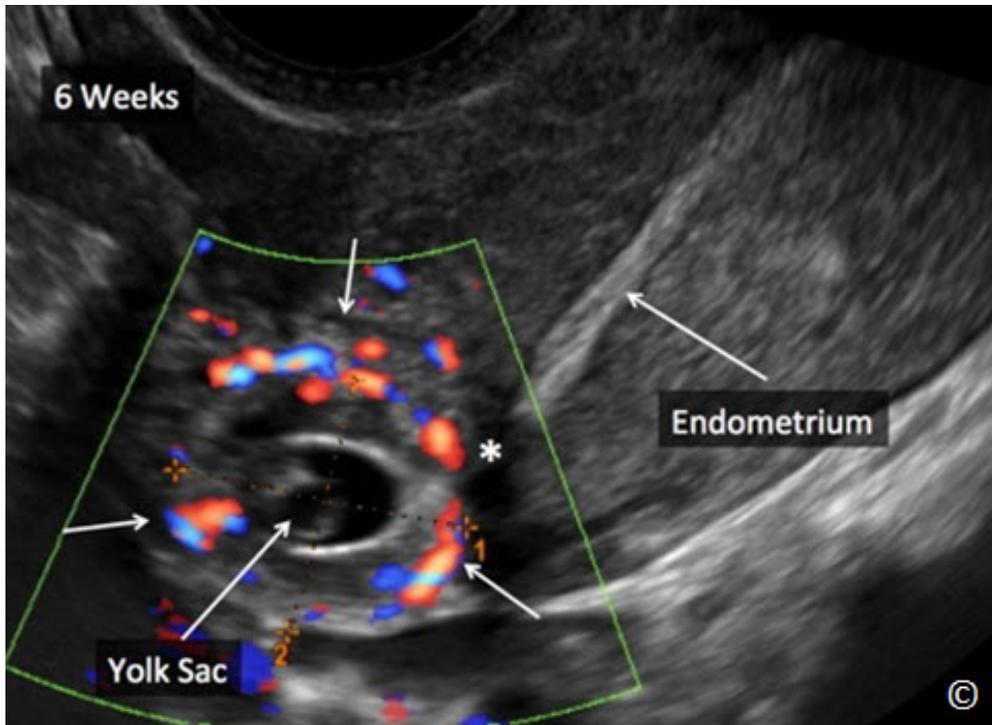
Figure 13.2: Grey scale and color Doppler ultrasound of a cornual ectopic pregnancy at 6 weeks' gestation (arrows). Note that the endometrial echo (labeled as endometrium) is distinctly separate from the cornual ectopic pregnancy (asterisk). Note the yolk sac within the ectopic pregnancy (labeled).
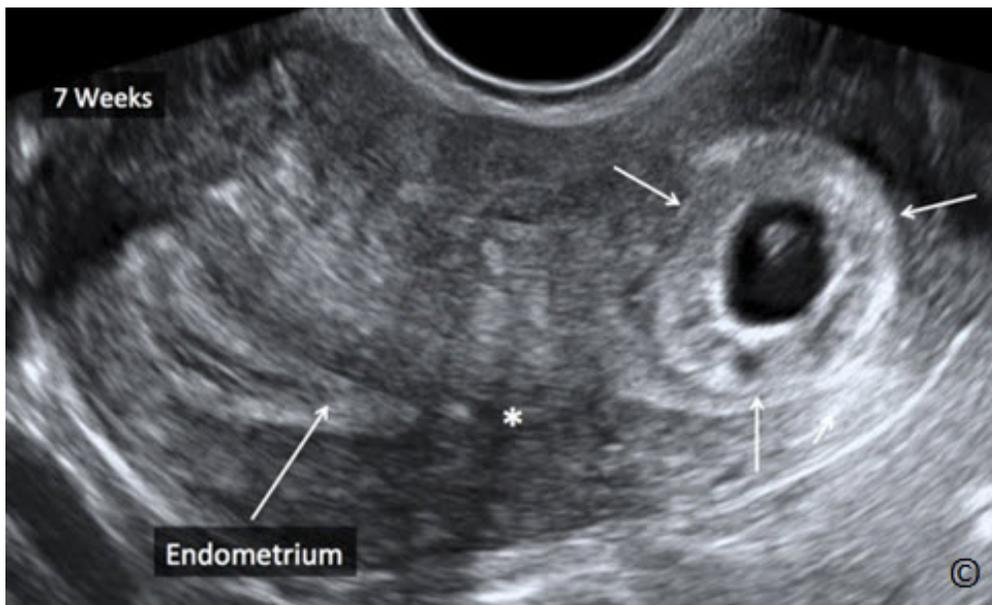

Figure 13.3: Grey scale ultrasound of a cornual ectopic pregnancy at 7 weeks' gestation (arrows). Note that the endometrial echo (labeled endometrium) is distinctly separate from the cornual ectopic pregnancy (asterisk).

Figure 13.4: Transvaginal ultrasound of a transverse plane of the upper uterus showing a cornual ectopic pregnancy (white arrows) at 9 weeks' gestation. Note that the endometrial echo (labeled as endometrium) is distinctly separate from the cornual ectopic pregnancy (asterisk). The ectopic sac is bulging on the serosal aspect of the uterus (red arrow heads).

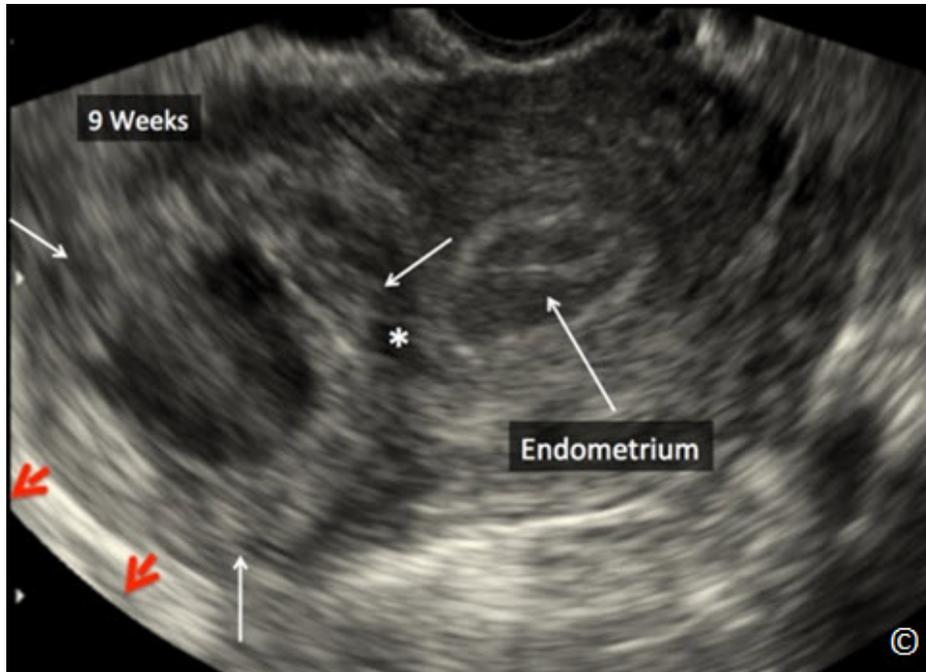**Figure 13.5**: Transvaginal ultrasound of an oblique plane of the upper uterus showing a cornual ectopic pregnancy (arrows) at 13 weeks' gestation. Note the size of the cornual pregnancy (labeled) that may be mistaken for an intrauterine gestation. The uterus is labeled in yellow.

Figure 13.6: Transvaginal ultrasound of a sagittal plane of the uterus showing a cervical ectopic pregnancy (arrows). The uterine fundus and cervix are labeled for image orientation.

Implantation of a gestational sac in a cesarean section scar is referred to as cesarean scar implantation and is technically not an ectopic pregnancy as the gestational sac is within the uterine cavity. Cesarean scar implantation can lead, later in gestation, to severe placental abnormalities, such as placenta accreta, or rupture of the gestational sac (7, 8). The diagnosis of a cesarean section scar implantation is performed when a gestational sac is noted by ultrasound to be located in the lower uterine segment, in or near, a cesarean section scar, in a patient with a prior cesarean section. Magnification of the ultrasound image may help confirm the diagnosis (**Figure 13.7** and **13.8**). Similar to cervical ectopic pregnancy, treatment of cesarean section scar implantation is best achieved by direct injection of methotrexate or potassium chloride into the gestational sac, under ultrasound guidance (**Figure 13.9 A and B**).

Figure 13.7: Transvaginal ultrasound in grey scale of a sagittal plane of the uterus showing a cesarean scar implantation of a gestational sac (arrows). The cervix is labeled for image orientation.
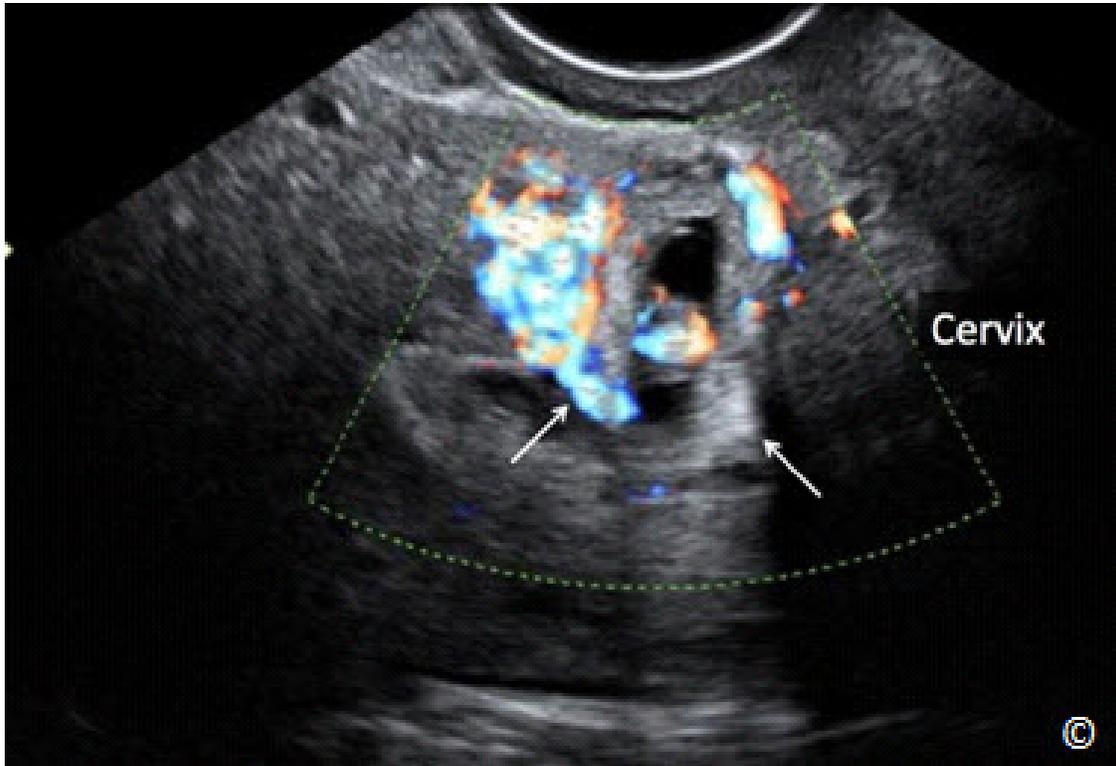

Figure 13.8: Transvaginal ultrasound in color Doppler of a sagittal plane of the uterus showing a cesarean scar implantation of a gestational sac (arrows – same as in figure 13.7). Note the increased vascularity on color Doppler of the gestational sac. The cervix is labeled for image orientation.
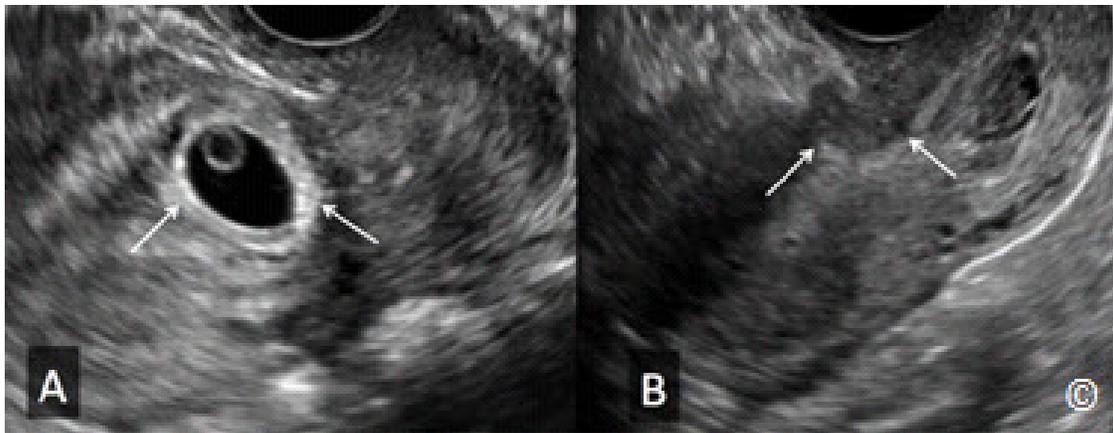
Figure 13.9 A and B: Transvaginal ultrasound of a sagittal plane of the uterus showing in (A) a cesarean scar implantation (arrows). The figure B shows the same cesarean scar implantation (arrows) two weeks after direct methotrexate injection. Note the significant resolution.

■ STEP-WISE ULTRASOUND APPROACH TO THE DIAGNOSIS OF ECTOPIC PREGNANCY

This section describes the step-wise approach to the work-up of a woman presenting with clinical symptoms suggestive of the presence of an ectopic pregnancy. Before this stepwise approach is initiated, it is important to note that taking a detailed history and performing a physical examination are essential components of the care of the woman and thus should be part of the initial evaluation. A differential diagnosis should then be formulated as new information and diagnostic tests are being gathered. **Table 13.2** lists a typical differential diagnosis for a woman presenting with lower abdominal pain and vaginal bleeding.

TABLE 13.2	**Differential Diagnosis of a Woman Presenting in the Reproductive Age Group with Lower Abdominal Pain and Vaginal Bleeding**
	- Normal pregnancy - Threatened or impending miscarriage - Ectopic pregnancy - Symptomatic ovarian mass (hemorrhagic cyst, dermoid, torsion) - Pelvic inflammatory disease - Dysfunctional uterine bleeding - Gastrointestinal origin - Urinary origin

Obtaining a pregnancy test should be one of the first diagnostic tests to be performed. A negative pregnancy test practically rules out a live ectopic pregnancy, assuming that the pregnancy test that is available has sufficient sensitivity to detect human chorionic gonadotropin (HCG) levels commensurate with early pregnancy. A positive pregnancy test establishes pregnancy but does not indicate the location of the gestational sac, or the viability of the pregnancy. Please note that chronic ectopic pregnancies may coexist with low HCG levels and are typically associated with chronic pelvic pain. **Figures 13.10** and **13.11** show a chronic ectopic pregnancy with an HCG level of 22 IU / ml. The patient presented with a pelvic mass and chronic right pelvic pain.
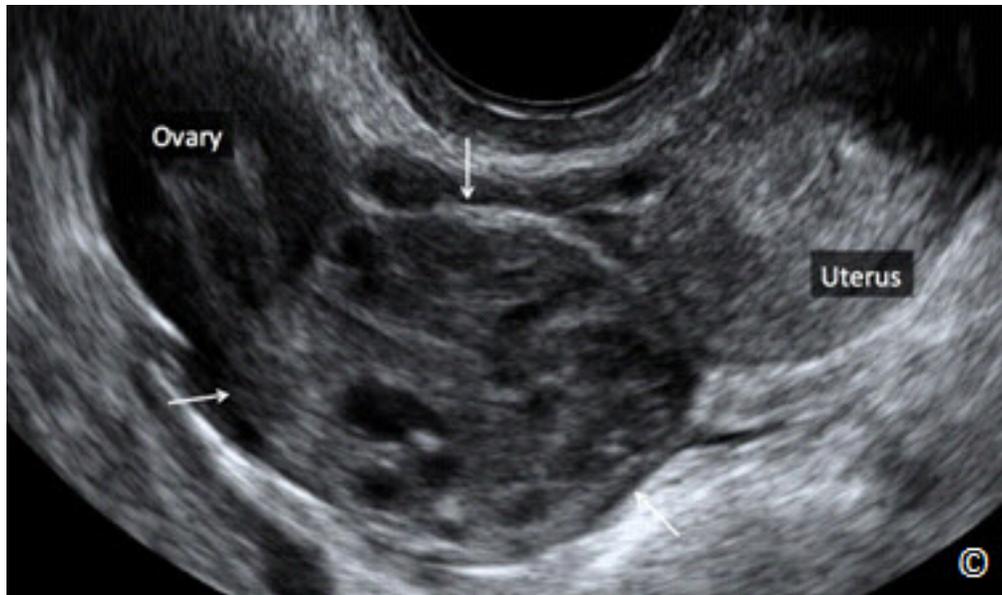
Figure 13.10: Transvaginal ultrasound showing a chronic ectopic pregnancy (arrows- confirmed on pathology) in a woman who presented with chronic pelvic pain. HCG levels were 22 IU/ml. A separate ovary was noted (labeled). The uterus (labeled) is seen adjacent to the chronic ectopic.
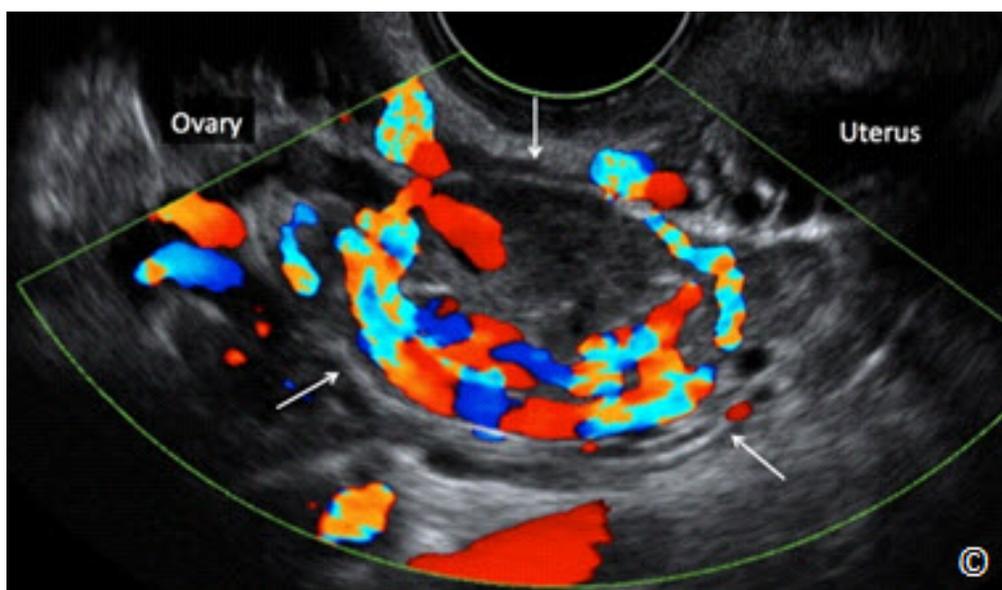

Figure 13.11: Transvaginal ultrasound with color Doppler in the same woman as in figure 13.10 showing significant vascularity of the chronic ectopic pregnancy (arrows)

Given that this textbook represents a basic approach to the use of ultrasound in obstetrics and gynecology, we will not expand on the relationship of the serum HCG level with the sonographic appearance of the gestational sac in the uterus. Suffice it to say that there is a relationship between rising HCG levels and normal intrauterine pregnancies. In general, normal pregnancies will show a doubling of the HCG level every 2-3 days (9). This rule however is not exclusive as 1 in 5 ectopic pregnancies will show this rise in HCG levels (9) and thus HCG levels should not be used alone in excluding an ectopic pregnancy.

The stepwise ultrasound approach hereby described should be initiated if the pregnancy test is positive.

This stepwise approach is performed by the transvaginal ultrasound:

Step one:

Assess the endometrial cavity for the presence of a gestational sac:

The presence of a gestational sac in the endometrial cavity (**Figure 13.12**) practically rules out an ectopic pregnancy. Note that on very rare occasions, a heterotopic pregnancy can occur (a concurrent intrauterine and an extrauterine pregnancy) (**Figure 13.13**) – (**Clip 13.1**). The incidence of a heterotopic pregnancy in a natural pregnancy is around 1 in 7000 pregnancies. Heterotopic pregnancies are more common in pregnancies of assisted reproduction (**Figure 13.14**).

The gestational sac of a normal pregnancy on ultrasound, which appears between the 4th and the 5th menstrual week, corresponds to the chorionic cavity of the embryo (**Figure 13.12**). The yolk sac is the first structure to appear on ultrasound within the gestational sac and is typically first seen at the 5th menstrual week (**Figure 13.15**), followed by the amnion between the 5th and the 6th week and the embryo by the 6th menstrual week (**Figure 13.16**). The normal intrauterine gestational sac has a distinctive ultrasound appearance, with a thick rim of echogenic tissue (**Figure 13.17**). This echogenic rim differentiates the gestational sac from blood or fluid collection within the endometrial cavity. Blood or fluid collection within the endometrial cavity is commonly called pseudosac (**Figure 13-18 A and B**). The term pseudosac is used in relation to the presence of an ectopic pregnancy. For more discussion on the first trimester, please refer to chapter 4.

If a gestational sac is seen within the endometrial cavity, complete the ultrasound examination by evaluating the adnexal regions and the cul-de-sac. Go to step 2, if no gestational sac is seen in the endometrial cavity.

Figure 13.12: Transvaginal ultrasound of a sagittal plane of the uterus showing a gestational sac (labeled) at about 5 weeks' gestation. The presence of an intrauterine gestational sac practically rules out an ectopic pregnancy with some exceptions. See text for details.
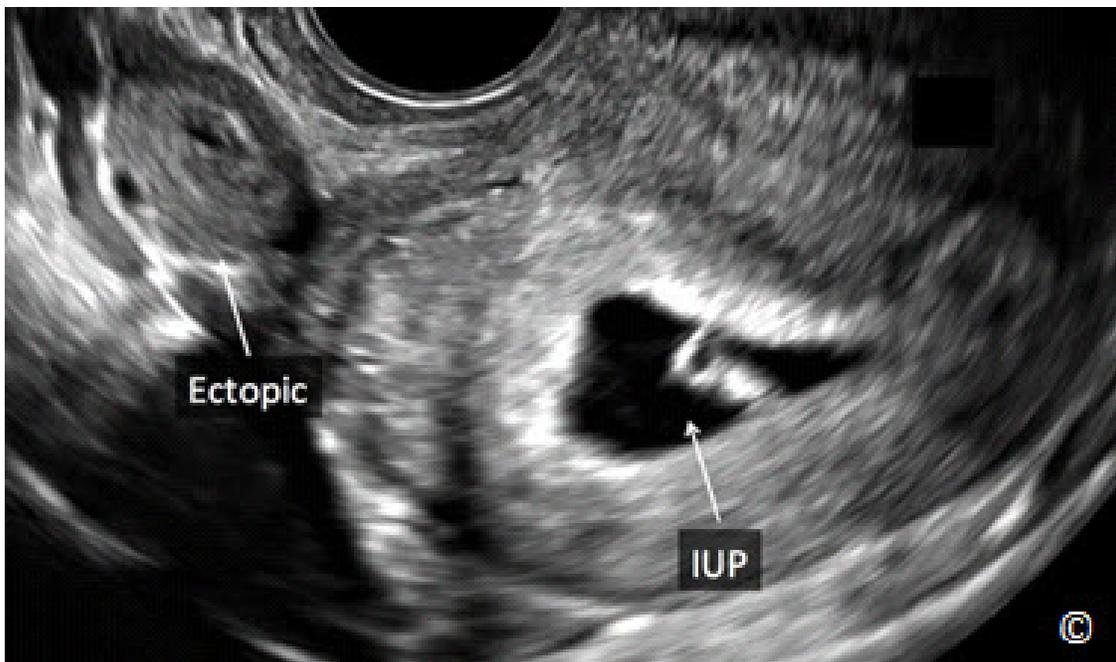

Figure 13.13: Transvaginal ultrasound of a heterotopic pregnancy at 6 week's gestation. Note the presence of an intrauterine pregnancy (IUP) and a tubal ectopic pregnancy (labeled) in the adnexa.
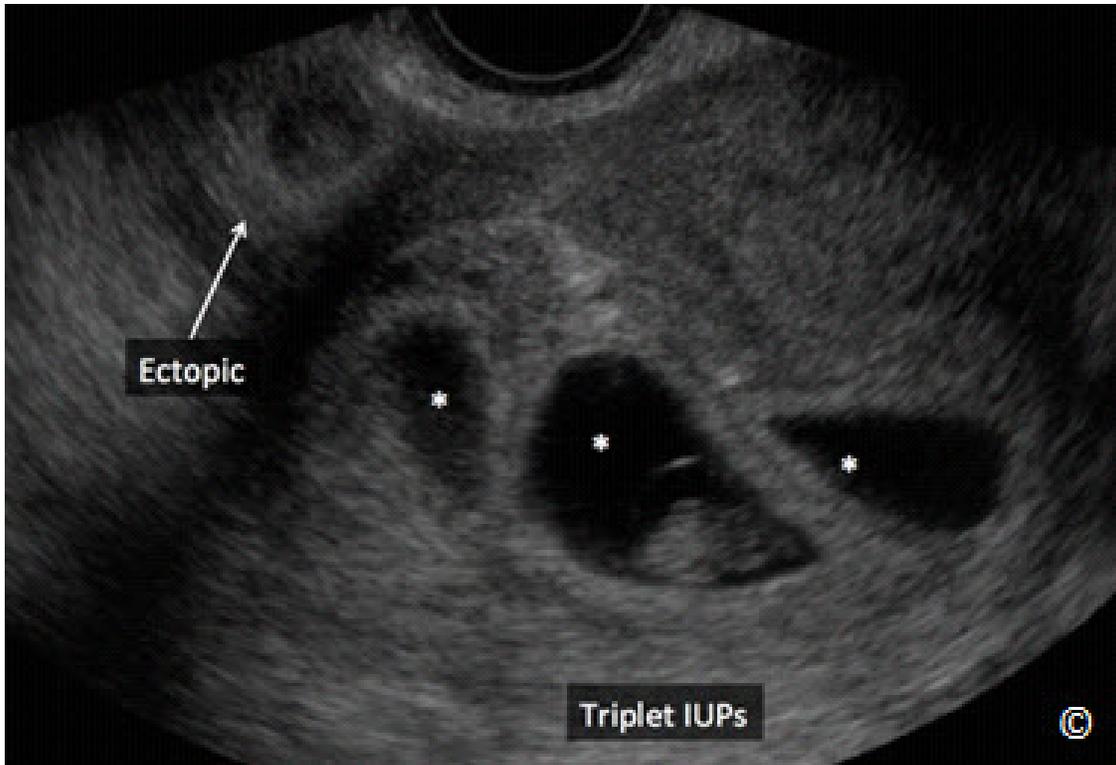
Figure 13.14: Transvaginal ultrasound of a heterotopic pregnancy at 7 week's gestation. Note the presence of a triplet intrauterine pregnancy (asterisks - Triplet IUPs) and a tubal ectopic pregnancy (labeled) in the adnexa. This pregnancy was conceived by assisted reproduction.

Figure 13.15: Transvaginal ultrasound of a sagittal plane of the uterus showing a gestational sac at 5 weeks' gestation with a yolk sac (labeled). Note that the yolk sac is the first structure to appear within the gestational sac and is typically first seen at the 5th menstrual week.
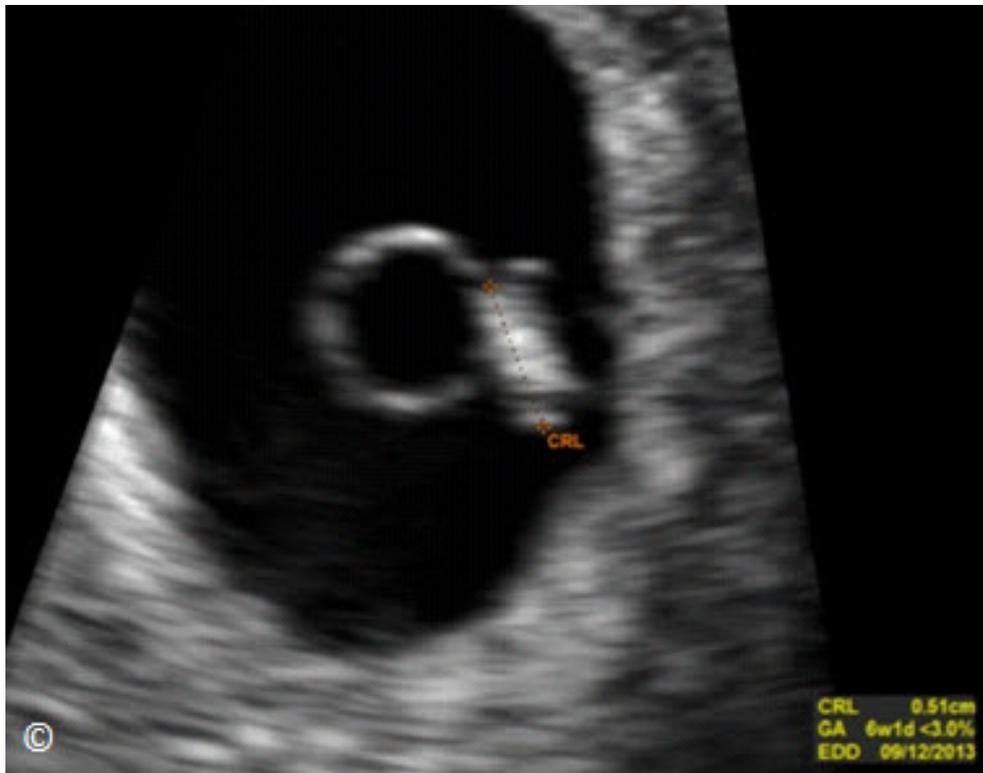
Figure 13.16: Transvaginal ultrasound of a gestational sac at 6 weeks' gestation showing an embryo (measured). The yolk sac (not labeled) is seen next to the embryo. CRL = crown rump length, GA = gestational age and EDD = estimated date of delivery.

Figure 13.17: Transvaginal ultrasound of a sagittal plane of the uterus with a normal gestational sac (labeled) at 5 weeks' gestation. Note the echogenic rim surrounding the gestational sac (dashed circle).
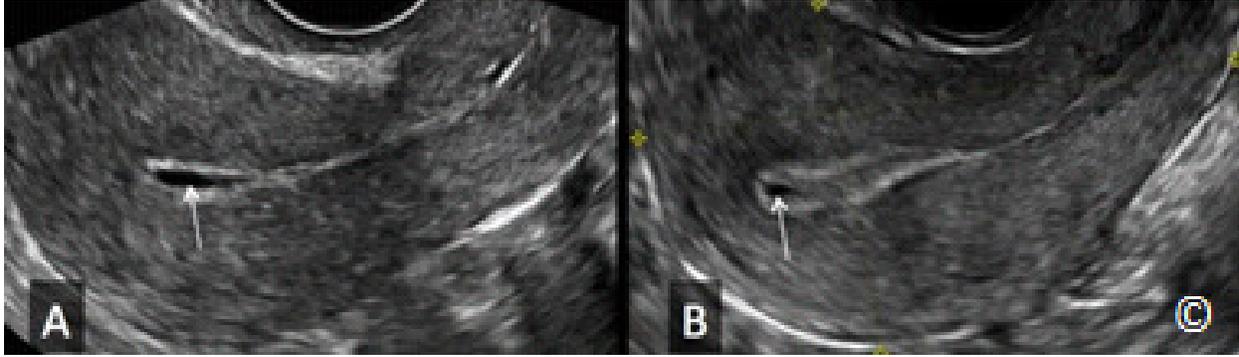
Figure 13.18 A and B: Transvaginal ultrasound of sagittal planes of two uteri (A) and (B) with endometrial fluid (arrows) in the setting of suspected ectopic pregnancies. The term pseudosac is used when endometrial fluid is noted in association with an ectopic pregnancy.

Step Two:

Assess the cul-de-sac for the presence of fluid:

The presence of fluid in the cul-de-sac is an important part of this evaluation as it may suggest the presence of blood from a ruptured ectopic pregnancy or a ruptured ovarian cyst. The cul-de-sac can be assessed for fluid or blood on ultrasound by imaging the space posterior to the cervix and the lower uterine segment in a sagittal plane of the uterus and cervix using the transvaginal approach (**Figure 13.19**). Low-velocity color Doppler, if available, can be used to confirm the absence of vascular flow within the blood clots. It is important to note that the mere presence of fluid in the cul-de-sac in a patient with a suspected ectopic pregnancy should be concerning for the possibility of intra-abdominal bleeding and this information should be considered in the overall management of the patient. If fluid is noted in the cul-de-sac region in significant quantity, assessing the regions in the upper gutters of the abdomen is important as the presence of fluid in those locations will confirm that a significant amount of free fluid is present in the abdomen and pelvis and will raise the suspicion for significant intra-peritoneal bleeding. It is also important to note that the presence of fluid in the cul-de-sac in small amount is a normal finding and is part of the normal physiologic changes of the menstrual cycle.

Figure 13.19: Transvaginal ultrasound of a sagittal plane of the uterus in a patient with a ruptured ectopic pregnancy. Note the presence of free fluid in the cul-de-sac and surrounding the uterus (asterisks). A blood clot (labeled) is also noted in the cul-de-sac. In this image, the endometrial thickness is also measured (yellow calipers).

Step 3:

Assess the Adnexal Region for the Ectopic Gestational Sac:

The third step in the ultrasound examination of the pelvis includes a thorough evaluation of both adnexal regions in transverse and sagittal scanning planes. This evaluation should include assessment of the ovaries and the surrounding anatomic regions, looking for fluid, blood and for the ectopic gestational sac. The ectopic gestational sac, when present in the adnexal region, is commonly in the fallopian tube. It is typically round in shape and has an echogenic ring and an anechoic center (**Figure 13.20 A and B**). Commonly, the patient's symptoms correlate with the location of the ectopic pregnancy in the pelvis but with noted exceptions. It is also important not to confuse an ectopic gestational sac with a corpus luteum (**Figure 13.21**), which is commonly located on the same side ovary. **Table 13.3** shows differentiating characteristics of the corpus luteum from the ectopic gestational sac. **Figures 13.22** and **13.23** show tubal ectopic pregnancies on ultrasound. Color Doppler is not helpful in the differential diagnosis given the overlap with corpus luteum flow and the varying degrees of blood flow patterns in ectopic pregnancies. **Figure 13.24 A-C** shows varying degrees of blood flow on color Doppler in three different ectopic pregnancies.
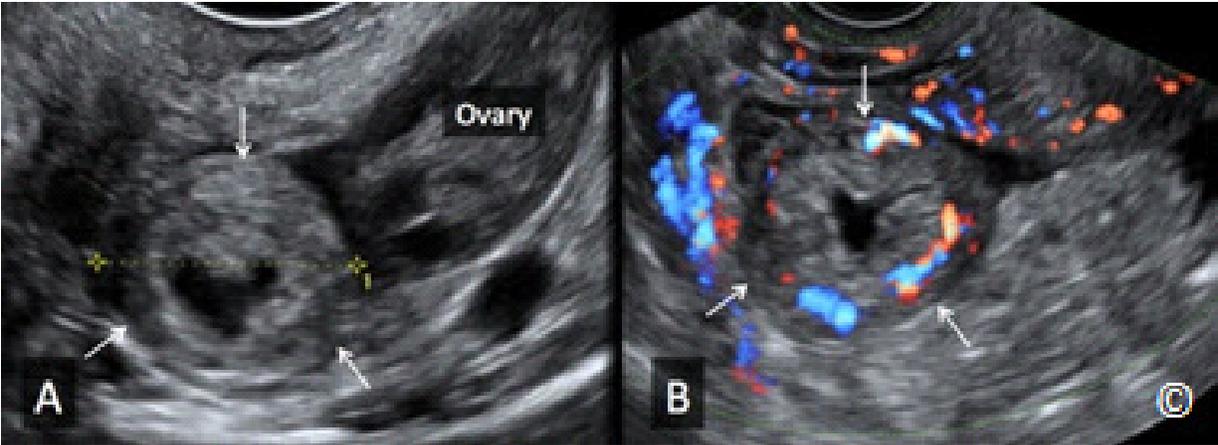
Figure 13.20 A and B: Tubal ectopic pregnancies in A and B (arrows) imaged on transvaginal ultrasound. Note the echogenic ring and the anechoic center (doughnut-like appearance) in both ectopic pregnancies. Color Doppler in B shows moderate ectopic sac vascularity. The ovary is seen (labeled) in A.
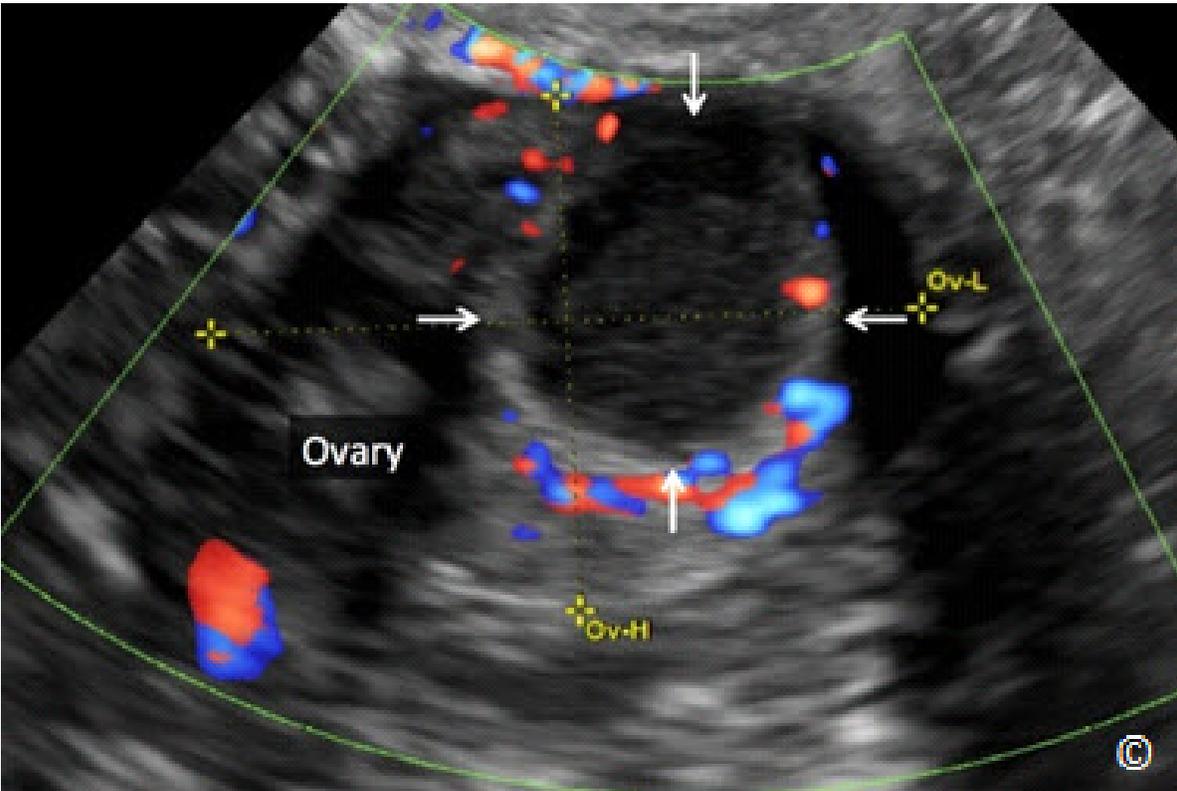
Figure 13.21: Transvaginal ultrasound in grey scale and color Doppler of a corpus luteum (arrows) within the ovary (labeled). See **Table 13.3** for differentiating features from an ectopic pregnancy.

TABLE 13.3	Differentiating Features of a Corpus Luteum From an Ectopic Pregnancy

- Corpus luteum is located within the ovary
- Corpus luteum is surrounded by normal ovarian tissue
- Corpus luteum moves with the ovary with manipulation
- Corpus luteum typically does not have a thick echogenic ring
- Color Doppler and pulsed Doppler cannot differentiate between the two entities
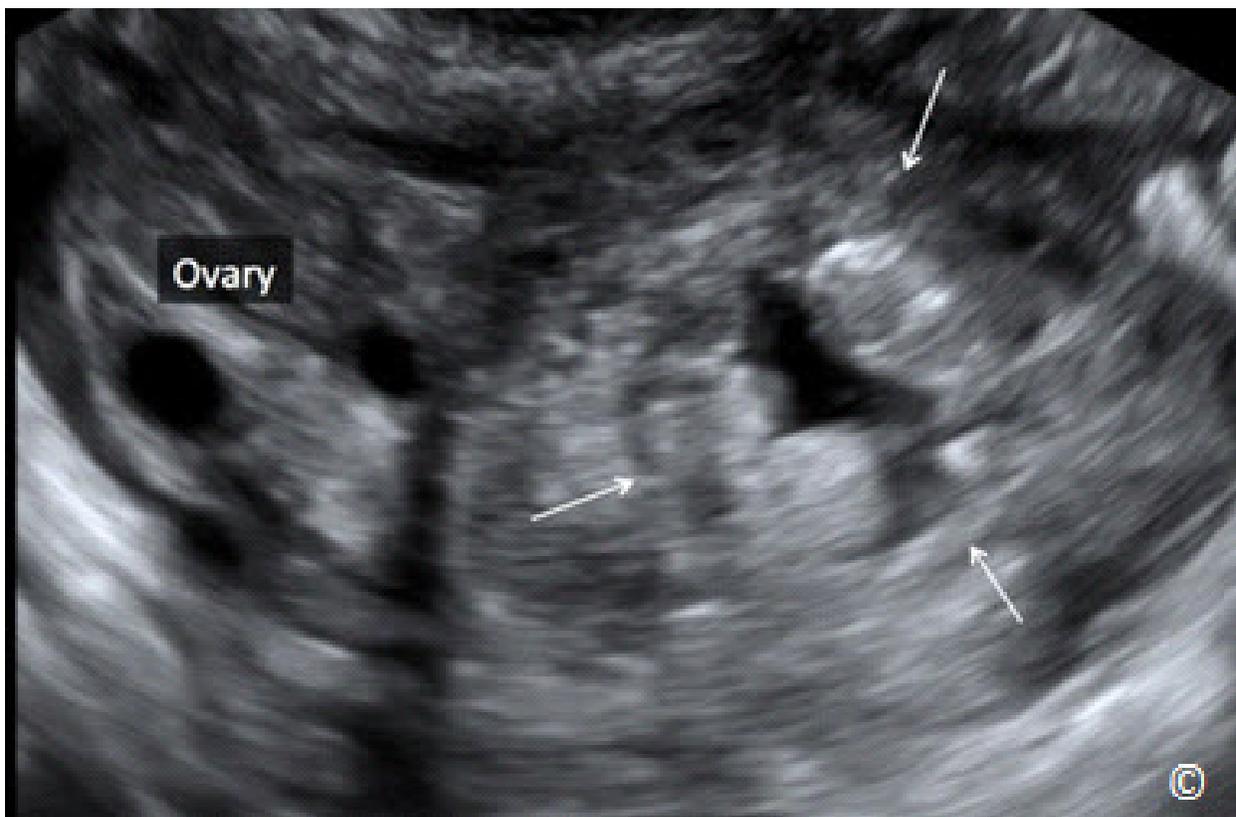
Figure 13.22: Transvaginal ultrasound showing a tubal ectopic pregnancy (arrows). Note the separation of the ectopic sac from the ovary (labeled). The ectopic sac has echogenic borders and an anechoic center (doughnut-like appearance).
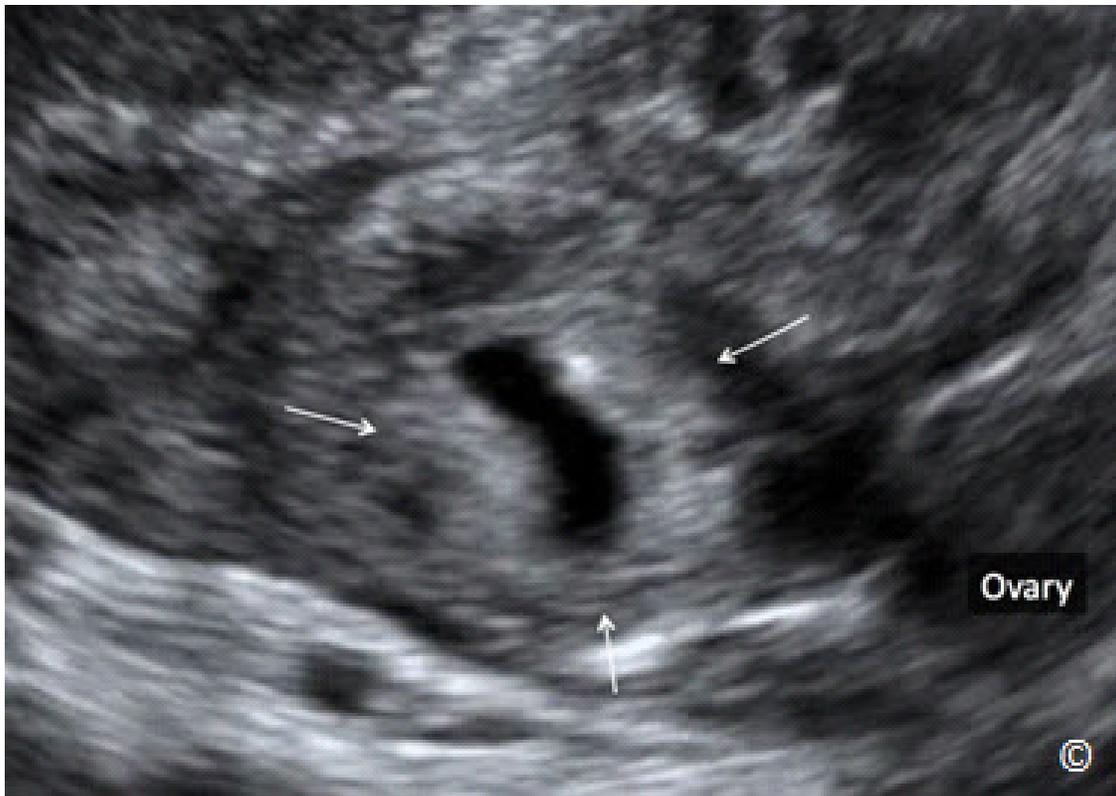
Figure 13.23: Transvaginal ultrasound showing a tubal ectopic pregnancy (arrows). Note the echogenic thick borders and an anechoic center (doughnut-like appearance). The ovary is labeled and is typically lateral to the ectopic gestation.
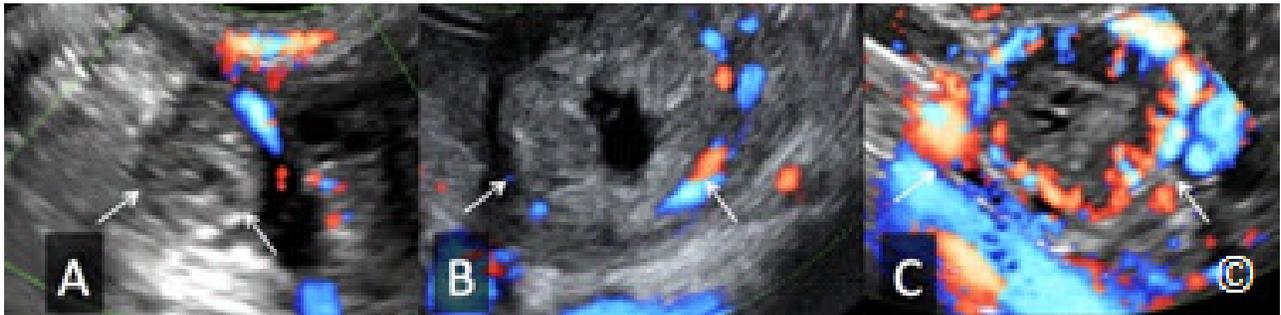

Figure 13.24 A, B, and C: Tubal ectopic pregnancies in A, B and C (arrows) imaged on transvaginal ultrasound with color Doppler at similar velocity scale and filter set-up. Note the varying degrees of vascularity between ectopic pregnancies with minimal to absent in A, moderate in B and excessive in C. Color Doppler is not a helpful differentiating feature of ectopic pregnancy.

The presence of an ectopic gestational sac in the adnexa that is distinctly separate from the ovary in a woman presenting with symptoms suggestive of an ectopic pregnancy, especially in the absence of an intra-uterine gestational sac, establishes the diagnosis of an ectopic pregnancy. The additional presence of fluid in the cul-de-sac confirms the diagnosis. When ultrasound findings are not diagnostic of ectopic pregnancy, it is important to consider all findings and make a judgment based upon available information. Given that significant change in the normal gestation occurs in the first trimester in a short time-frame, a follow-up ultrasound within a short period of time such as in 3 to 4 days when the woman's medical condition is stable and compliance is adequate, may help clarify the diagnosis. If the woman's condition is unstable, intervention is warranted irrespective of the ultrasound findings.

A rare presentation of an ectopic pregnancy is the abdominal pregnancy. Abdominal pregnancy can be associated with significant morbidity, especially if the pregnancy is allowed to grow. Placental insertion on the bowels or pelvic vasculature can result in significant bleeding if removal is attempted. If an advanced abdominal pregnancy is encountered, it is prudent to remove the fetus but keep the placenta in situ to avoid massive bleeding. **Figures 13.25** and **13.26** show an abdominal pregnancy at 14 weeks gestation in the right adnexa. The patient presented with lower abdominal pain. This abdominal ectopic pregnancy was treated with direct injection of potassium chloride and methotrexate into the gestational sac under transvaginal ultrasound guidance. No further intervention was needed and the woman's symptoms improved immediately following this procedure.

Figure 13.25 A and B: Transvaginal ultrasound of an abdominal ectopic pregnancy at 14 weeks gestation in the right pelvis. Figure 13.25-A shows a sagittal view of the uterus with pelvic free fluid (asterisks). Figure 13.25-B shows the abdominal pregnancy (arrows) in the right pelvis.

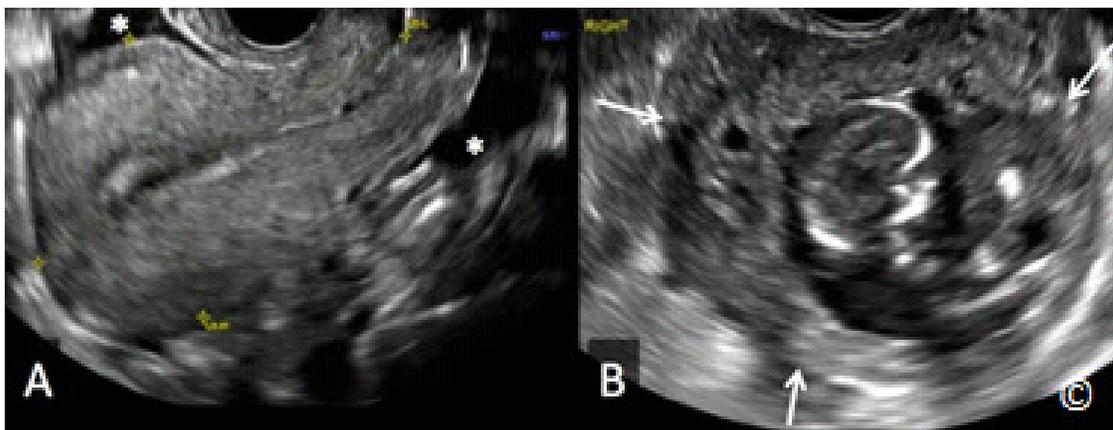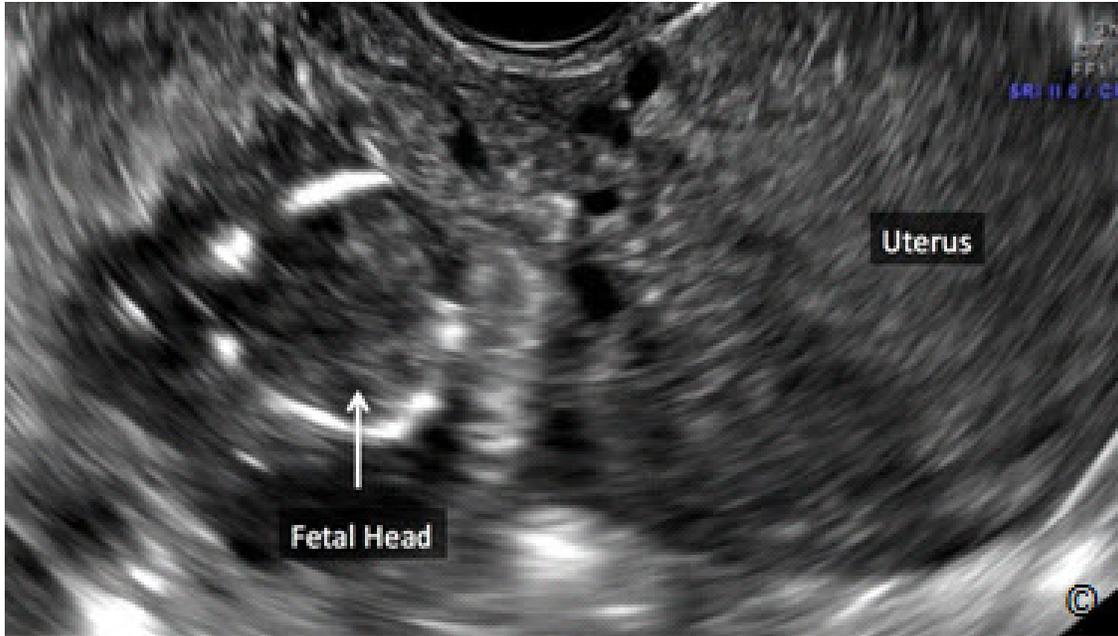**Figure 13.26**: Transvaginal ultrasound of an abdominal ectopic pregnancy at 14 weeks gestation in the right pelvis (same as in figure 13.25) following direct injection of potassium chloride and methotrexate. The uterus (labeled) is seen separate from the ectopic pregnancy. The macerated fetal head is labeled.

Copyrighted-Ultrasound in Obstetrics & Gynecology: A Practical Approach

References:

1) Nederlof KP, Lawson HW, Saftlas AF, Atrash HK, Finch EL. Ectopic pregnancy surveillance, United
2) States, 1970–1987. In: CDC Surveillance Summaries. MMWR 1990; 39(no. SS-4):9–17.
3) Ectopic pregnancy – United States, 1990-1992.MMWR Morb Mortal Wkly Rep 44:46, 1995.
4) Goyaux N, Leke R, Keita N, Thonneau P. Ectopic pregnancy in African developing countries. Acta Obstet Gynecol Scand 2003; 82(4):305-12.
5) Pisarka M, Carson SA, Buster JE. Ectopic pregnancy. Lancet 1998;351:1115
6) Breen JL. A 21 year survey of 654 ectopic pregnancies. Am J Obstet Gynecol 1970;106:1004
7) Schwartz RO, Di Pietro DL. Beta-HCG as a diagnostic aid for suspected ectopic pregnancy. Obstet Gynecol 1980; 56:197.
8) Unforeseen consequences of the increasing rate of cesarean deliveries: early placenta accreta and cesarean scar pregnancy. A review. Timor-Tritsch IE, Monteagudo A. Am J Obstet Gynecol. 2012 Jul;207(1):14-29
9) The diagnosis, treatment, and follow-up of cesarean scar pregnancy. Timor-Tritsch IE, Monteagudo A, Santos R, Tsymbal T, Pineda G, Arslan AA. Am J Obstet Gynecol. 2012 Jul;207(1):44.e1-13
10) Discriminatory HCG zone; its use in the sonographic evaluation of ectopic pregnancy. Kadar N, DeVore G, Romero R. Obstet Gynecol 1981; 58:156-161.

INTRODUCTION

The stepwise standardized approach to the basic ultrasound examination of the female pelvis applies a structured and standardized method of ultrasound examination which is simple to learn and complies with existing guidelines for the performance of the gynecologic examination (1). This stepwise approach is comprised of five steps that are geared towards the identification of pelvic abnormalities and comprise the basic gynecologic ultrasound examination. The five steps are designed to assess the bladder, uterus and cervix, the cul-de-sac, the adnexae and surrounding structures. This chapter describes the sonographic approach that is employed for each of the five steps and uses images and video clips to illustrate each step. Evaluation of the female pelvis by ultrasound is best achieved by the transvaginal approach, using a transvaginal transducer. This chapter will focus on this approach. When the transvaginal approach is not feasible, the transrectal approach is preferred and is usually well tolerated. The presence of a large pelvic mass that expands outside of the range of the transvaginal transducer necessitates a complementary abdominal approach for comprehensive assessment.

STEP ONE: PREPARING AND INTRODUCING THE TRANSVAGINAL TRANSDUCER

The transvaginal transducer is an endocavitary transducer that is designed to fit into small spaces. It is shaped like a long cylinder with a handle and has a small footprint at its tip that transmits and receives sound waves from the end of the transducer (**Figure 14.1**). The frequency range of a transvaginal transducer is typically in the 5-12 MHZ and given this high resolution, effective imaging to a 7-10 cm range can generally be achieved. The transvaginal transducer is made of a probe, or a transducer head, a connecting cable and a connector, or a device that connects the transducer to the ultrasound machine (**Figure 14.2**). The transvaginal transducer has a marker, such as a notch, a dot or a light that is typically located on the dorsal aspect, next to the handle of the probe (**Figure 14.1**). The transducer marker helps to identify the transducer orientation. For more information on the transvaginal transducer and its function please review chapters 1 and 2.

Figure 14.1: Transvaginal ultrasound transducer: note its shape like a long cylinder with a handle (labeled) and has a small footprint (labeled) at its tip that transmits and receives sound waves. The image also shows the transducer marker (labeled).
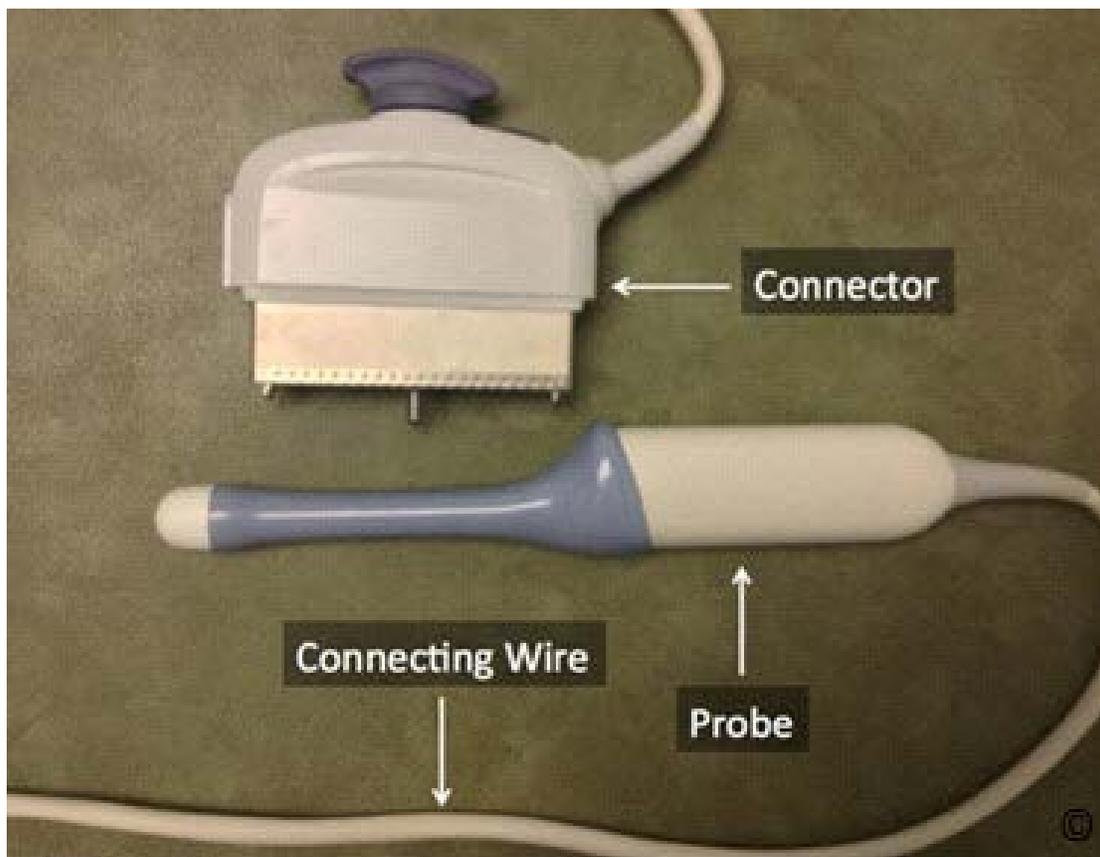

Figure 14.2: Transvaginal ultrasound transducer: Note its components that include the probe (see figure 14.1), a connecting wire (cable) and a connector (labeled). See text for details.

It is optimal to perform the transvaginal ultrasound on a gynecologic examination table. This table is equipped with 2 footrests, which allows the patient to assume the lithotomy position for convenient transvaginal scanning. The gynecologic examination table also has a retractable leg support, which makes the transabdominal sonographic examination more comfortable (**Figure 3.2** in Chapter 3). If a gynecologic examination table is not available, an elevation below the woman's pelvis will enable the downward tilt of the transvaginal transducer handle (**Figure 3.3** in Chapter 3).

Step One: Technical Aspects: Preparing and Introducing the Transvaginal Transducer

The woman's demographic data, her last menstrual period and other important pertinent observations should be recorded before the transvaginal ultrasound examination is initiated. When preparing a transvaginal transducer for use in an ultrasound examination of the pelvis, gel should be placed in a protective cover, such as a condom or the digit of a surgical rubber glove, and the transducer should be inserted in the protective cover in order to prevent microbial contamination. It is easier to place the gel in the condom rather than on the tip of the transducer, however if you are using the digit of a glove, placing the gel on the tip of the transducer will minimize air entrapment. The condoms or gloves must be clean but need not be sterile. Gel is also applied to the outside of the protective cover, at the transducer tip, to facilitate transmission of ultrasound waves given that sound waves do not transmit well in air. Before starting the preparation, it is recommended to inquire about the woman's allergy to latex in order to avoid its exposure. In the presence of latex allergy, latex free condoms/gloves should be employed.

The woman's bladder should be emptied. The operator performing the transvaginal ultrasound examination should wear a glove and hold the transducer is such a way to secure the protective cover in place (**Figure 14.3**). The woman should be informed that the transvaginal transducer is about to be inserted in her vaginal canal. The transvaginal transducer is then inserted into the lower vaginal canal under direct vision, with the transducer marker at the 12 o'clock position (**Figure 14.4**). The transducer should be advanced gently into the vaginal canal while maintaining this orientation. The authors recommend that the transvaginal transducer is pointed slightly downward towards the rectum while it is being gently advanced into the vaginal canal in order to minimize discomfort generated from the sensitive urethral region. The operator should advance the transvaginal transducer into the vaginal canal under real-time ultrasound and not in the freeze mode. This allows for the identification on the ultrasound monitor of the cervix or the vaginal fornix. Once the apex of the vagina is reached and seen on the ultrasound monitor, the transducer should be withdrawn slightly to reduce pressure on the cervix and the uterine isthmus and minimize distortion of uterine orientation. This maneuver of minimizing pressure on the vaginal apex with the transvaginal transducer will also minimize woman's discomfort. The small footprint region of the transvaginal transducer needs to remain in contact with the vaginal

mucosa in order to transmit and receive ultrasound waves. In a symptomatic woman, the transducer can be used to probe (transducer palpation) any pelvic organ seen on the monitor and thus try to elicit the symptom (pain) that the woman may have, by using the contralateral hand to apply gentle pressure from the abdomen, in similar fashion to the bimanual vaginal examination. This maneuver may localize the source of the woman's symptom. **Table 14.1** lists the various ways that the transducer can be manipulated during the transvaginal ultrasound examination.
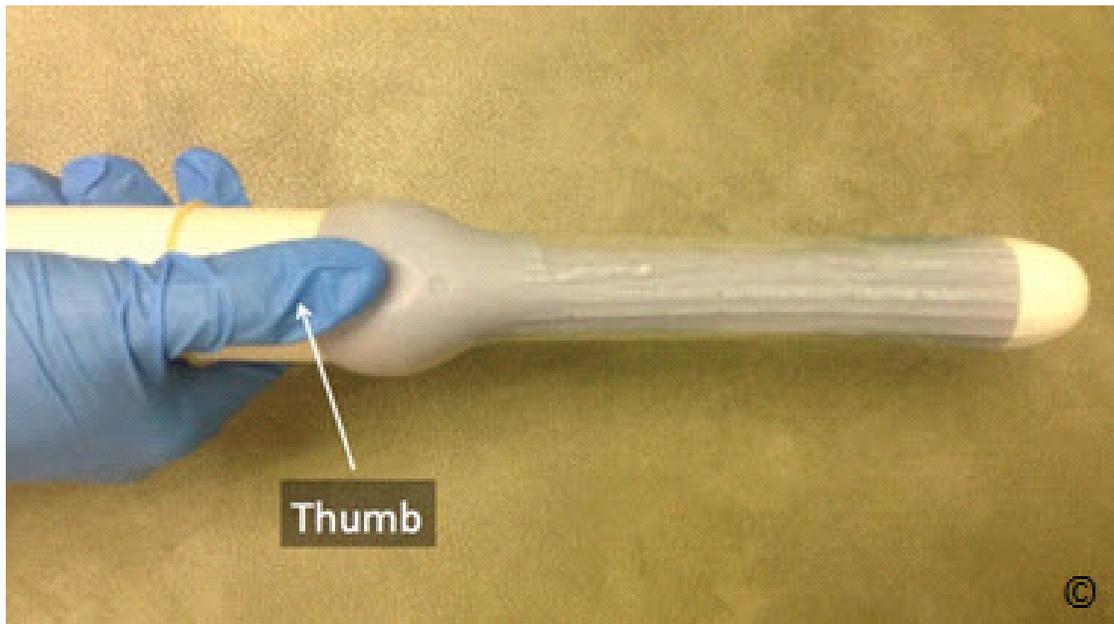
Figure 14.3: Note the preferred way to hold the transvaginal transducer during the ultrasound examination. The probe should rest in the palm of the operators scanning hand protected by a glove with the thumb on the transducer's marker, securing the protective cover in place.

Figure 14.4: This image shows the orientation of the transvaginal transducer during insertion into the lower vaginal canal. The transducer marker (labeled) is kept at the 12 o'clock position during gentle insertion under direct vision and in real-time ultrasound mode. A mannequin is used for this demonstration.

TABLE 14.1	Manipulation of the Transducer During the Transvaginal Ultrasound Examination

1) Tilting (angling) the shaft of the transducer in an inferior to superior, or left to right orientation
2) Advancing or retracting the transducer in the vaginal canal
3) Rotating the transducer around its longitudinal axis

STEP TWO: THE SAGITTAL PLANE OF THE UTERUS

The midsagittal plane of the uterus is the first plane imaged when the transvaginal transducer is introduced with the marker at the 12 o'clock position (**Figure 14.4**). In this plane, you can see the upper vaginal canal, the bladder, the cervix, the isthmus, the fundal region of the uterus and the cul-de-sac (**Figure 14.5**). The display on the monitor for the sagittal plane of the uterus shows the bladder on the upper left side of the screen with the external cervical os pointing toward the right side of the screen (**Figure 14.5**). If the uterus is anteverted or anteroflexed, the uterine fundus appears on the same side of the urinary bladder. If the uterus is retroverted or retroflexed, the uterine fundus points toward the opposite side of the bladder. There is currently no international consensus on the display of organs in the transvaginal ultrasound examination. In the United States and other countries around the world, the image is displayed as shown in **Figure 14.5**. Some colleagues display the transvaginal ultrasound image with the tip of the ultrasound transducer at the bottom of the image (**Figure 14.6**). Irrespective of the display, the ultrasound examiners should familiarize themselves with pelvic anatomy. Chapter 11 presents more details on uterine orientation in the pelvis.
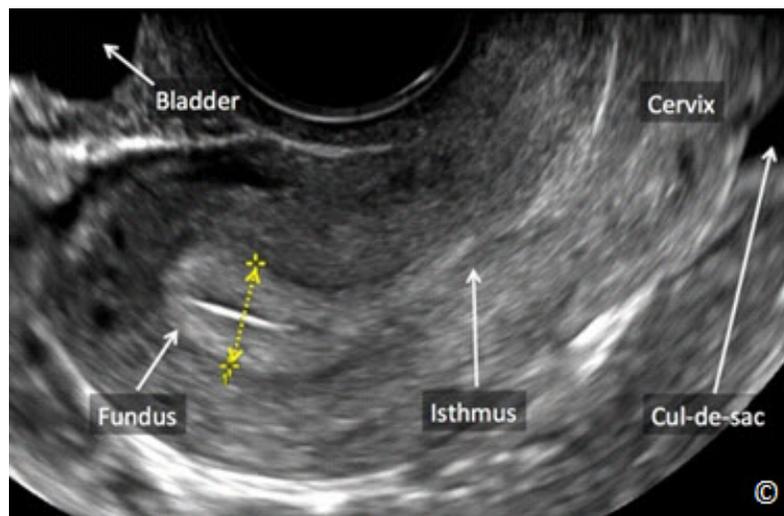

Figure 14.5: Transvaginal ultrasound of the midsagittal plane of an anteroflexed uterus showing the bladder in the left upper image, the fundus close to the bladder, the isthmus and the cervix in the right upper image. In this image, the endometrial thickness is measured (yellow double arrow and calipers). The cul-de-sac is also labeled and shows pelvic fluid.
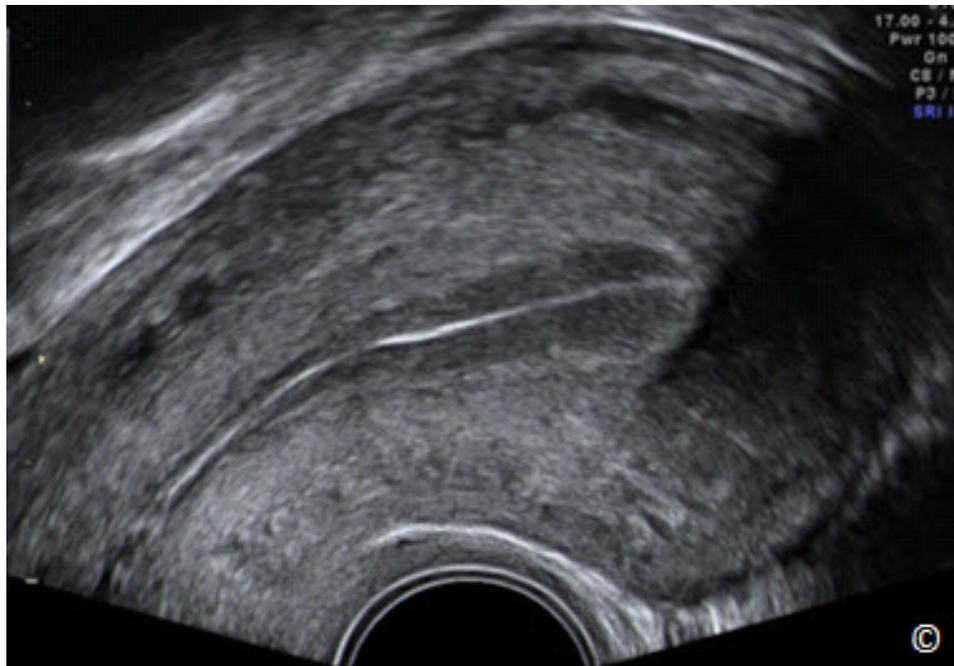
Figure 14.6: Transvaginal ultrasound of the sagittal plane of the uterus displayed with the tip of the transducer at the bottom of the image. See text for details. Image is courtesy of Dr. Bernard Benoit.

The midsagittal plane is also used to measure the uterine length from the fundus to the cervical external os and the depth of the uterus (anteroposterior dimension), which is a perpendicular diameter to the length, at the widest dimension (**Figure 14.7**). This midsagittal view also allows for the assessment and measurement of the endometrium. The endometrium is measured in an anteroposterior fashion at the widest location (**Figure 14.5**). When measuring endometrial thickness on ultrasound, it is critical to ensure that the uterus is in a mid-sagittal plane, the whole endometrial lining is seen from the fundal region to the endocervix, the image is clear and magnified and the thickest portion of the endometrium is measured (**Figure 14.5**).
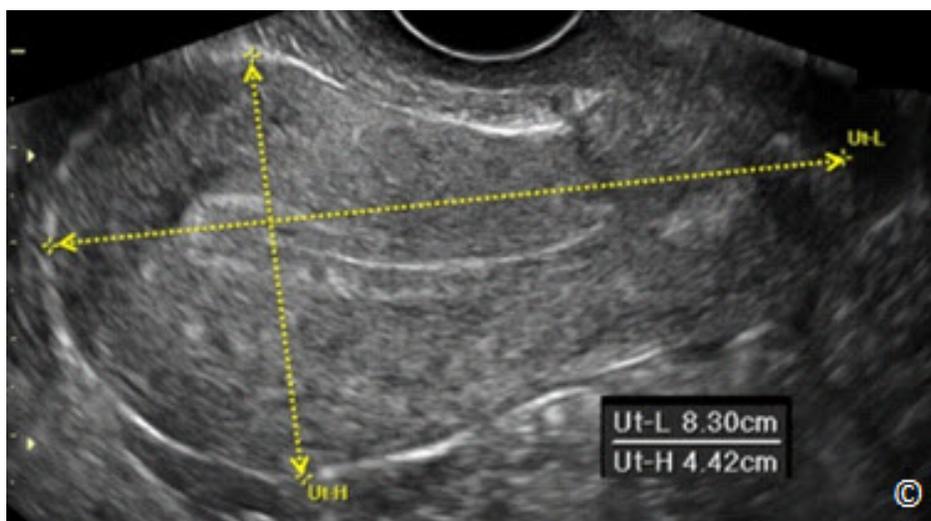

Figure 14.7: Transvaginal ultrasound of a midsagittal plane of the uterus showing measurements of uterine length (Ut-L) and height (Ut-H).

Step Two: Technical Aspects: Obtaining the Sagittal Plane of the Uterus

The sagittal or longitudinal plane of the uterus is obtained when the transvaginal ultrasound transducer is introduced into the upper vaginal canal with the marker at the 12 o'clock position. Slight manipulation of the transducer is sometimes required with an inferior–superior or right-left angling in order to get the midsagittal plane of the uterus as some uteri are slightly shifted to the right or left of the midline or rotated along the long axis of the body (2).

If the midsagittal plane appears to be significantly shifted to the right or the left of the midline, consideration should be given for evaluation of a unicornuate uterus with 3D ultrasonography (**Figure 11.20** in Chapter 11). Once the midsagittal plane of the uterus is identified, reduce the depth and sector width to ensure that the uterus is magnified for optimal visualization (**Figure 14.5** and **14.7**).

STEP THREE: THE TRANSVERSE PLANE OF THE UTERUS

The transverse or axial plane of the uterus demonstrates the width of the uterus and is a good plane to assess the myometrium (**Figure 14.8**). In this plane, the maximum width of the uterus is measured at the widest section (**Figure 14.8**). The endometrial lining should not be measured from this plane. This transverse plane of the uterus however is important in the evaluation of the endometrium at the fundal region, which helps in the identification of mullerian malformations. The presence of 2 endometrial echoes at the fundal region of the uterus, rather than a single one, suggests the presence of 2 endometrial cavities in the fundal region which may indicate the presence of a uterine septum, a bicornuate uterus or uterine didelphys (**Figure 14.9**). Differentiating between various types of mullerian anomalies requires a coronal plane of the uterus, which is obtained by 3D ultrasound or Magnetic Resonance Imaging (see chapter 11 for details).
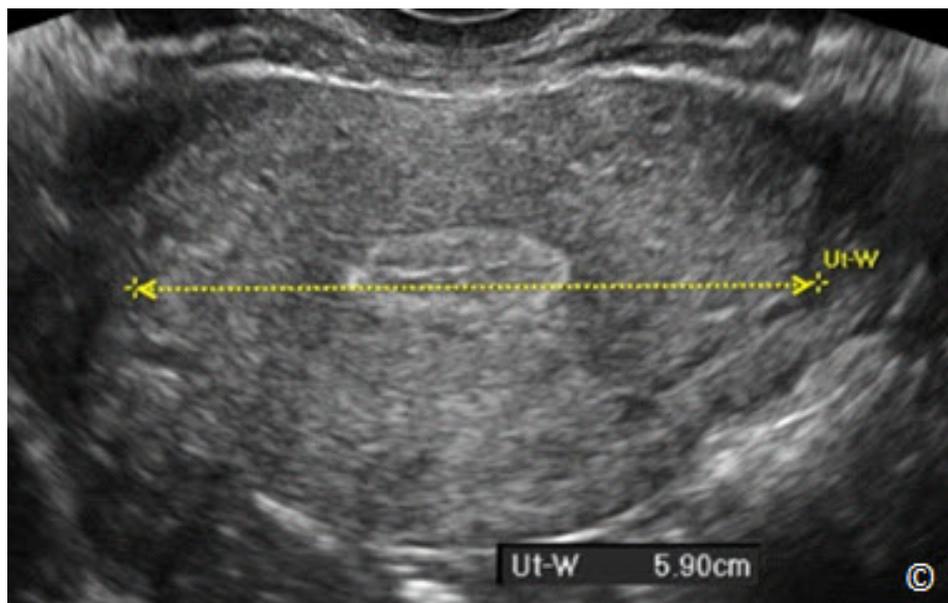

Figure 14.8: Transvaginal ultrasound of a transverse plane of the uterus at its widest dimension showing the measurement of uterine width (Ut-W).
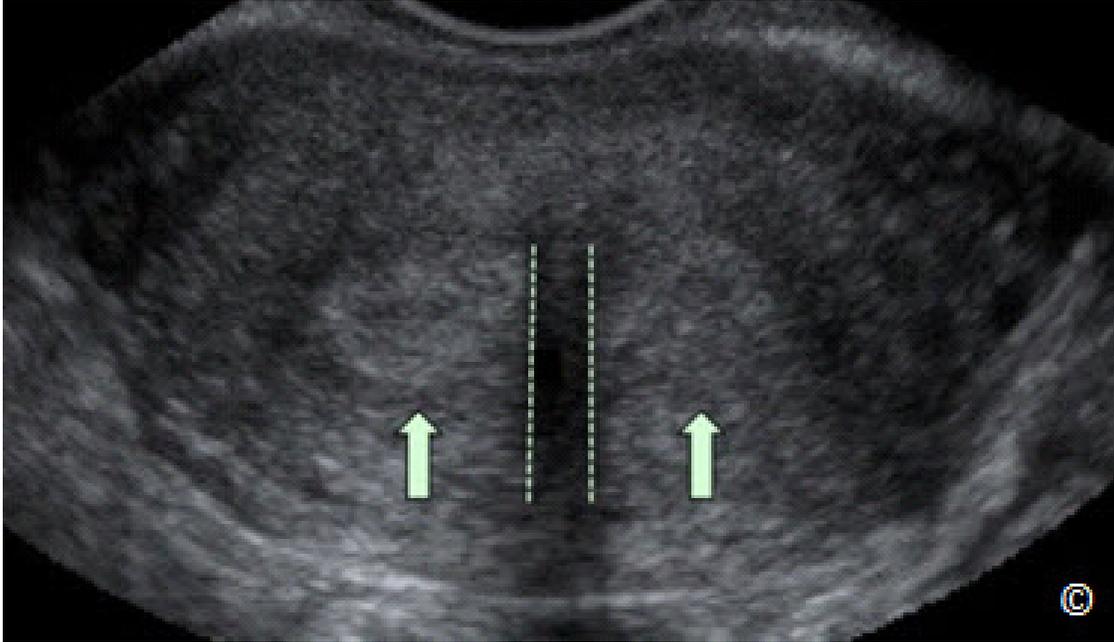
Figure 14.9: Transvaginal ultrasound of a transverse plane of the uterus showing 2 separate endometrial echoes (arrows). A coronal plane of the uterus, which can be obtained by 3D ultrasound or Magnetic Resonance Imaging, can determine the type of mullerian abnormality.

Step Three: Technical Aspects: Obtaining the Transverse Plane of the Uterus

The transverse plan of the uterus is obtained by rotating the transducer along its long axis 90 degrees counterclockwise from the midsagittal plane of the uterus. When the transverse plane is imaged, a superior-inferior movement (angling) of the tip of the transducer allows for the evaluation of the uterus in transverse view from the cervical/isthmic region into the fundus. As you perform this maneuver, freeze the screen at the widest segment, and use this plane for measurement. Although you can get the midsagittal plane of the uterus by either a clockwise or a counterclockwise rotation from the midsagittal plane, counterclockwise rotation will ensure that the transducer marker is on the patient's right side, which maintains appropriate orientation.

STEP FOUR: THE RIGHT AND LEFT ADNEXAE

Imaging of each adnexa includes an evaluation of the ovary, the fallopian tube and any other abnormality of surrounding structures. The normal fallopian tube is not easily seen on ultrasound. When the tube is filled with fluid, or thickened due to inflammation, it is then typically seen in a medial location to the ovary.

The normal ovary is relatively easy to detect in the reproductive years. The presence of ovarian follicles, or a corpus luteum, serves to differentiate the ovary from surrounding tissue in the

adnexa on ultrasound (**Figure 14.10**). The normal ovary in typically located lateral to the broad ligament and overlying the hypogastric vein (**Figure 14.10**). Bowel peristalsis helps to differentiate between moveable structures and the static ovary.
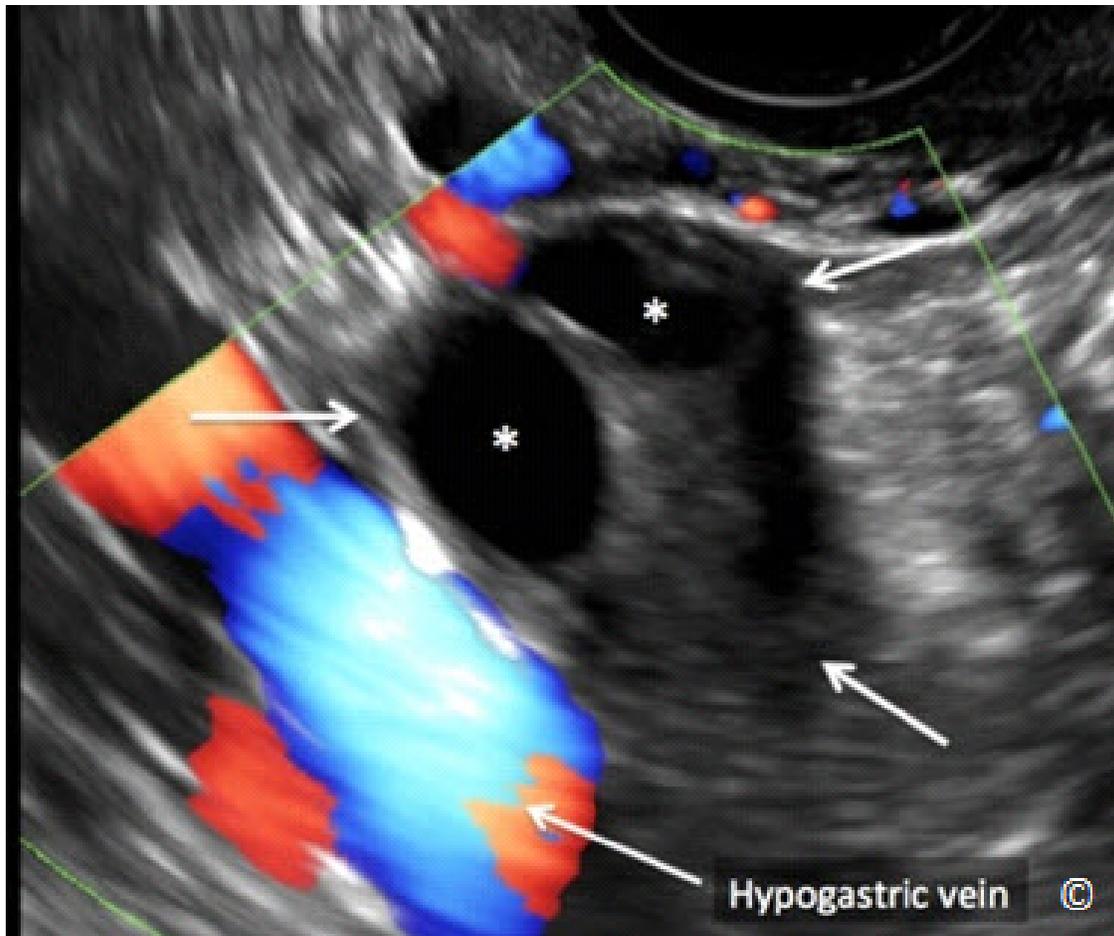
Figure 14.10: Transvaginal ultrasound of the ovary (arrows) in the adnexa overlying the hypogastric vein (labeled). Note that the ovarian tissue is slightly less echogenic than the surrounding tissue and can be noted by the presence of ovarian follicles (asterisks).

The size of the normal ovary varies slightly with the time of the menstrual cycle as well as the woman's age. The ovary should be measured on ultrasound in 3 dimensions; width, length and depth, on views obtained in 2 orthogonal planes (See **Figure 12.6**). The ovary appears ovoid (like a chicken egg) in shape and typically contains numerous follicles especially in the reproductive years. Refer to chapter 12 for more details on the ultrasound evaluation of the ovary.

Step Four: Technical Aspects: Imaging the Right and Left Ovary

The transverse plane of the uterus, at its widest dimension, typically displays the ovarian ligaments on the right and left side as thin hypoechoic curvy lines (**Figure 14.11**). To image the right ovary, start with the transverse plane at its widest dimension of the uterus and angle the transvaginal transducer towards the right iliac crest of the woman (handle of the probe almost touching the woman's left inner thigh) (**Figure 14.12**). Follow the right ovarian ligament as it commonly leads toward the right ovary (**Clip 12.1**). The right ovary will come into view overlying the right hypogastric vein (**Figure 14.10**). Repeat the same maneuver on the opposite side to image the left ovary. On occasions, the operator needs both hands, one to manipulate the transvaginal probe and the second to place it on the abdominal wall and facilitate the mobilization of the pelvic structures. **Figure 14.13** is an extended view of the transverse pelvis on transvaginal ultrasound showing the uterus, ovaries, tubo-ovarian ligaments and hypogastric vessels.
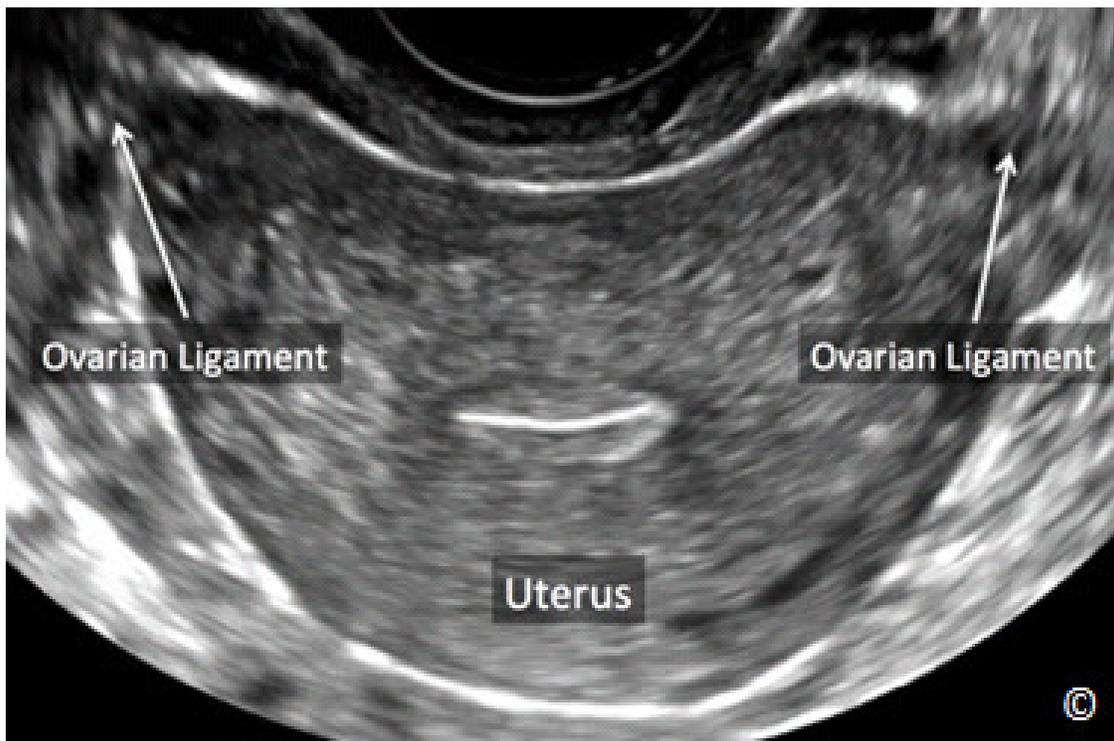
Figure 14.11: Transvaginal ultrasound of a transverse plane of the uterus (labeled) showing the ovarian ligaments (labeled) as thin hypoechoic curvy lines.

Figure 14.12: Transvaginal ultrasound of the same uterus as in figure 14.11 with the transducer angled to the adnexal region. By following the ovarian ligament (labeled), the ipsilateral ovary can be commonly seen.

Figure 14.13: Transvaginal ultrasound in extended transverse view of the pelvis showing the uterus (labeled), right and left ovaries (labeled), ovarian ligaments (blue arrows) and the right and left hypogastric veins (asterisks).

Once one ovary is identified on transvaginal ultrasound, identifying the contralateral ovary can be commonly achieved by fanning the probe to the opposite side of 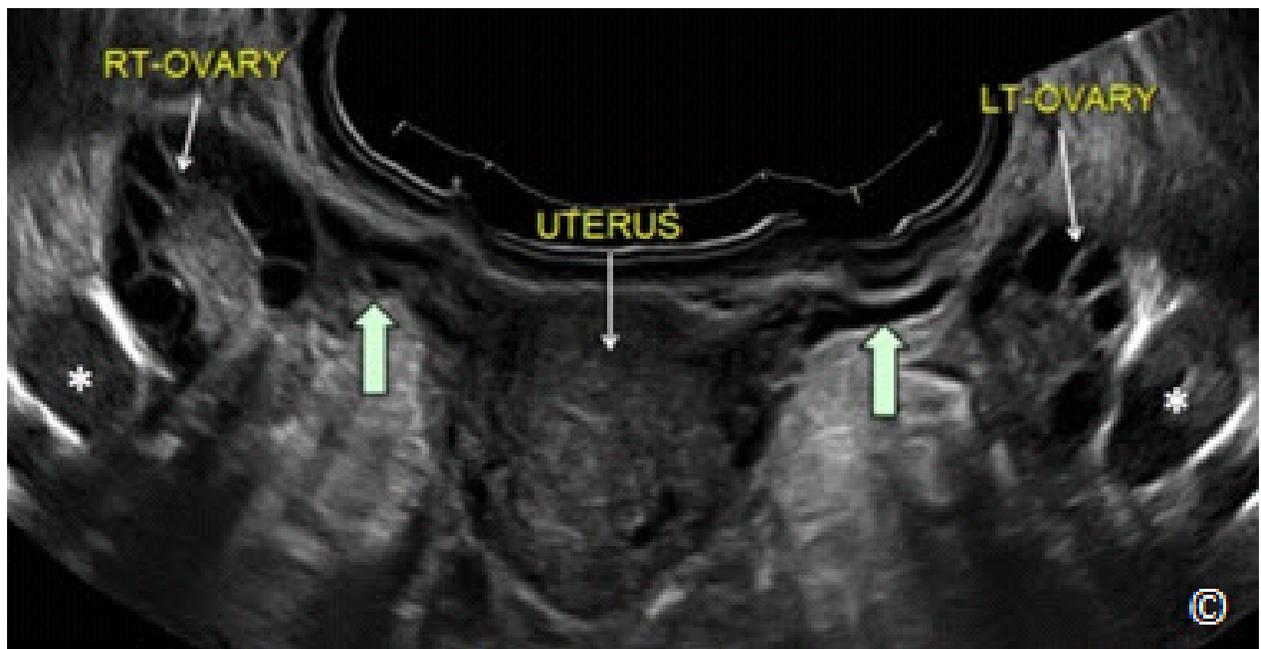the pelvis at equidistance from the mid-transverse plane of the uterus. Normal ovaries tend to be positioned in the same anatomic location, on either side of the uterus.

The ovaries may not be identifiable in some women. This occurs most frequently prior to puberty, after menopause, or in the presence of large uterine fibroids, which shadow the adnexal regions. Also, it is common occurrence that the left ovary is shadowed by the colo-rectal content. In this case, pelvic pressure by the contralateral hand towards the left iliac fossa may help in locating the ovary. Along the same line, if a patient has undergone hysterectomy, the ovaries are typically more difficult to image by ultrasound because the bowel fill the space left by the removal of the uterus, and make ultrasound imaging less optimal. In women who had prior vaginal hysterectomy, the ovaries are commonly located around the vaginal cuff, and in women who had laparoscopic hysterectomy; the ovaries are commonly located next to the lateral pelvic walls. On rare occasions, filling the bladder may help to localize the ovaries in these conditions.

STEP FIVE - WITHDRAWAL OF THE TRANSVAGINAL TRANSDUCER

Once the ultrasound examination is completed, the transvaginal transducer can be gently withdrawn from the vaginal canal. It is recommended that the operator holds the transducer is such a way to secure the protective cover in place as the transducer is being withdrawn from the vaginal canal (**Figure 14.4**). This maneuver will minimize dislodging the protective cover and exposing the patient to the bare transducer. The protective cover can be removed after the transducer is outside of the vaginal canal and disposed off in appropriate containers.

Protocols for ultrasound transducer cleaning should be adhered to in order to reduce the spread of infectious agents. The transvaginal transducer should be wiped clean between patients and disinfection should be performed according to national or manufacturer guidelines (3). It is safer to wipe the transducer in the freeze mode in order to protect the array within.

Documentation of the ultrasound examination and description of ultrasound abnormalities in the pelvis are discussed in details in separate chapters.

References:

1) AIUM practice guidelines for the performance of pelvic ultrasound examinations, revised 2009. http://www.aium.org/resources/guidelines/pelvic.pdf.

2) Sakhel K, Sinkovskaya E, Horton S, Beydoun H, Chauhan SP, Abuhamad AZ. Orientation of the uterine fundus in reference to the longitudinal axis of the body: a 3-dimensional sonographic study. J Ultrasound Med. 2014 Feb; 33(2):323-8.

3) AIUM Official Statement: Guidelines for Cleaning and Preparing Endocavitary Ultrasound Transducers Between Patients, approved 2003. http://www.aium.org/officialStatements/27

INTRODUCTION

Writing the ultrasound report is an important and essential part of the ultrasound examination as it documents and records the study findings for the woman, for healthcare providers and other interested parties. The ultrasound report becomes part of the patient's medical record and is a permanent documentation of the ultrasound examination. National and international ultrasound societies have recommended that a permanent record of the ultrasound examination and its interpretation be generated. Images both normal and abnormal should be recorded in a retrievable format and that retention of such images and the report should be consistent both with clinical needs and with relevant legal and local health care facility requirements. The ultrasound report is therefore a way to communicate your findings to others and should be performed after each ultrasound examination.

COMPONENTS OF THE ULTRASOUND REPORT

Patient Characteristics

Patient characteristics and identifiers, such as her name, identification numbers, age or preferably date of birth, gravity and parity and date of last menstrual period are important components of the ultrasound report and should be included in its top section and easily identified. Patient identification numbers vary and may be assigned at the institution as medical record numbers and may not be essential in the low-resource (outreach) setting as long as the woman's date of birth or other identifier is available that can help in differentiating patients. Information with regards to the referring healthcare worker or clinic should also be included. Patient characteristics are needed for all reports being obstetrics or gynecology.

Indication for the Ultrasound Examination

An indication for the ultrasound examination should be entered in the report. Various indications for ultrasound examination in obstetrics and gynecology have been presented in previous chapters. Knowing the indication for the ultrasound examination is important as it may focus the examination on a target organ after the components of the ultrasound examination have been completed and may raise awareness for the presence of abnormalities. The readers should refer to previous chapters in this book for ultrasound study indications.

Obstetrics

The obstetric ultrasound report should include 3 essential components: basic information about the pregnancy, fetal biometric measurements and fetal anatomic details. Basic information about the pregnancy includes viability of the fetus, whether the gestational sac is intrauterine, the number of fetuses, the location of the placenta, ruling out a placenta previa, the assessment of the amniotic fluid and the presentation and lie of the fetus. Fetal biometric measurements should include the gestational sac if an embryo is not visualized, a crown-rump length up to 13 6/7 weeks of gestation, biparietal diameter, head circumference, abdominal circumference and femur length after 13 6/7 weeks of gestation. **Table 15.1** lists biometric measurements that should be included in a basic obstetric report (see chapters 4, 5 and 6 for more details). Fetal anatomy that needs to be listed in the obstetric report is based upon the type of ultrasound examination and the setting under which the ultrasound examination is performed. National and international societies have developed lists of fetal anatomy as part of the basic and detailed (advanced-targeted) obstetric ultrasound examination (1 - 4) (see chapters 5 and 6 for more details). In the low-resource (outreach) setting, the level of training of the ultrasound examiner and the availability of postnatal resources dictate the complexity of the ultrasound examination. As described in chapter 10, the basic six steps for the performance of the obstetric ultrasound examination can provide sufficient information to identify the high-risk pregnancy in low-resource settings.

TABLE 15.1	Biometric Measurements of the Basic Obstetric Ultrasound Examination
- Mean sac diameter (if no embryo is seen) - Crown-Rump Length (up to 13 6/7 weeks gestation) - Biparietal Diameter (after 13 6/7 weeks gestation) - Head Circumference (after 13 6/7 weeks gestation) - Abdominal Circumference (after 13 6/7 weeks gestation) - Femur Length (after 13 6/7 weeks gestation)	

A statement regarding the estimated date of delivery should be made and whether the final due date is changed based upon the ultrasound derived biometric criteria or the final due date will be unchanged and kept based upon the woman's last menstrual period. Furthermore, an estimated fetal weight should be derived and entered in the report for all obstetric examinations performed at or beyond 24-28 weeks of gestation.

Gynecology

The gynecologic ultrasound examination is intended to assess the pelvic organs including the uterus, both ovaries and the cul-de-sac. Biometric measurement of the uterus includes its length, height and width, and the endometrial thickness measured in a sagittal plane. Each ovary should

be measured in its length, height and width and the cul-de-sac should be evaluated for the presence of fluid or other abnormalities. The presence of any abnormality such as uterine fibroid or adnexal mass should be described in details in its anatomic location and ultrasound characteristic and measured in three dimensions. Chapter 14 describes a standardized approach to the performance of the gynecologic ultrasound examination.

Final Diagnosis and Follow-up

After describing the above findings for both the obstetric and the gynecologic report, a section summarizing the final diagnosis should be entered along with comments about the ultrasound findings. A follow-up plan should be provided as part of the ultrasound report. The presence of significant pathology such as major fetal malformation, an ectopic pregnancy or suspected ovarian cancer should be communicated to the referring healthcare provider immediately at the conclusion of the ultrasound examination.

References:

1) American Institute of Ultrasound in Medicine practice guidelines on the performance of the obstetric ultrasound examination, 2013.
2) http://www.aium.org/resources/guidelines/obstetric.pdf
3) Wax, J, Minkoff H, Johnson A, Coleman B, Levine D, Helfgott, A, O'Keeffe D, Henningsen, C and Benson C. Consensus Report on the Detailed Fetal Anatomic Ultrasound Examination: Indications, Components, and Qualifications. JUM, 2014:33; 189-195.
4) Salomon LJ, Alfirevic Z, Berghalla C, Bilardo C, Hernandez-Andrade E, Johnsen SL< Kalache K, Leung KY, Malinger G, Munoz H, Prefumo F, Toi A, Lee W. Practice guidelines for performance of the routine mid-trimester fetal ultrasound scan. Ultrasound Obstet Gynecol 2011:37; 116-126.
5) ISUOG Practice Guidelines: Performance of first-trimester fetal ultrasound scan. Ultrasound Obstet Gynecol 2013; 41: 102-113